MAMMALS OF THE RIO JURUÁ AND THE EVOLUTIONARY AND ECOLOGICAL DIVERSIFICATION OF AMAZONIA

Authors: PATTON, JAMES L., DA SILVA, MARIA NAZARETH F., and MALCOLM, JAY R.

Source: Bulletin of the American Museum of Natural History, 2000(244) : 1-306

Published By: American Museum of Natural History

URL: https://doi.org/10.1206/0003-0090(2000)244<0001:MOTRJA>2.0.CO;2

MAMMALS OF THE RIO JURUÁ AND THE EVOLUTIONARY AND ECOLOGICAL DIVERSIFICATION OF AMAZONIA

JAMES L. PATTON

Museum of Vertebrate Zoology, University of California, Berkeley, CA 94720 USA

MARIA NAZARETH F. DA SILVA

Instituto Nacional de Pesquisas da Amazônia, C.P. 478, Manaus, AM 69083, Brazil

JAY R. MALCOLM

Faculty of Forestry, University of Toronto, Toronto, Ontario, Canada M5S 3B3

BULLETIN OF THE AMERICAN MUSEUM OF NATURAL HISTORY

Number 244, 306 pages, 172 figures, 85 tables, 3 appendices

Issued January 25, 2000

Price: $30.00 a copy

ISSN 0003-0090

CONTENTS

ABSTRACT

We describe the nonvolant mammal fauna of the Rio Juruá of the western Amazon of Brazil, based on collections made during a year-long survey of the river. We, along with our colleagues Drs. Claude Gascon and Carlos Peres, designed the field project to examine the effects of the river on the differentiation among terrestrial vertebrates (mammals, birds, and amphibians and reptiles) at both the community and population levels. This monograph examines only the patterns of geographic variation and community structure of the small-bodied mammals. Species inventories were made at 16 primary trapping localities divided into eight pairs of cross-river sites, with two pairs in each of four regions from near the mouth to the headwaters of the Rio Juruá. A total of 81 species of nonvolant mammals were obtained, including nine new to science. Four of these are described herein; the others have been described elsewhere. We used a standardized trapping protocol to assess community structure at each of the 16 localities that included terrestrial and canopy trap stations in floodplain (*várzea*) and upland (*terra firme*) forest formations. Supplemental trapping was done in secondary habitats at all sites. We describe these sites, the trap effort expended, and the placement of trap stations relative to local habitats. We also describe each species of marsupial, sciurid rodent, murid rodent, and echimyid rodent encountered; comment on their systematics; and summarize aspects of habitat use, life history, geographic distribution, and geographic differentiation based on morphological and molecular traits. We examine patterns of differentiation in the mitochondrial cytochrome-b gene for samples of 41 of the 45 species of marsupials and rodents obtained within the Rio Juruá Basin, and discuss these patterns from the perspective of the entire Amazon and, in some cases, the Mata Atlântica of coastal Brazil. We also examine patterns of community organization within the Rio Juruá basin and throughout Amazonia, drawing attention to the geographic distribution of what appear to be major faunal units that are independent of habitat differences. Finally, we use principles of phylogeography to analyze patterns of geographic differentiation among the nonvolant mammals with regard to the Riverine Barrier Hypothesis. We show that, while there are few examples of taxa for which the Rio Juruá is apparently a barrier, most taxa either are largely undifferentiated throughout the basin or are sharply divided into reciprocally monophyletic mtDNA haplotype clades separable into upriver and downriver units. We argue that the concordance in the geographic placement of clade boundaries suggests a common history; moreover, both the age of these clades and their geographic position in relation to underlying geological features suggest that landform evolution has been an important, but underappreciated component of diversification within western Amazonia.

RESUMEN

En este trabajo describimos la fauna de mamíferos no voladores del Río Juruá de la Amazonía Occidental de Brasil, basándonos en colecciones hechas durante un reconocimiento del Río de un año de duración. El proyecto de campo se diseñó para examinar los efectos del Río en la estructura de los vertebrados terrestres; esta muestra incluye mamíferos, tanto a nivel de comunidades como en los patrones de diferenciación geográfica de especies individuales. Hicimos inventarios de especies en 16 sitios de captura principales divididos en ocho pares de lugares a ambos lados del Río, con dos pares de sitios en cada una de cuatro regiones, desde cerca de la desembocadura hasta la cabecera del Río Juruá. Obtuvimos un total de 81 especies de mamíferos no voladores, incluyendo nueve especies nuevas para la ciencia. Describimos aquí cuatro de estas especies, puesto que las otras ya han sido descritas en otros trabajos. Utilizamos una metodología de captura estandarizada para evaluar la estructura de la comunidad en cada uno de 16 sitios que incluyeron estaciones de captura en tierra y en árboles en bosques de áreas planas inundables (várzea) y de tierras altas (terra firme). Hicimos recolecciones suplementarias en hábitats secundarios en todos los sitios. Describimos estos lugares, el esfuerzo llevado a cabo y la colocación de estaciones de captura en relación a hábitats individuales. También describimos cada especie de marsupial y de roedor múrido y equimídido que encontramos; comentamos sobre su sistemática; y resumimos aspectos de uso del hábitat, historia de vida, distribución geográfica y diferenciación geográfica, basándonos en caracteres morfológicos y moleculares. Examinamos los patrones de diferenciación en el gene mitocon-

drial citocromo-b para representantes de 41 de las 45 especies de marsupiales y roedores que coleccionamos dentro de la cuenca del Río Juruá y discutimos estos patrones desde una perspectiva común para toda la Amazonía, incluyendo en algunos casos el bosque de la zona costera Atlántica de Brasil. Luego examinamos los patrones de organización de comunidades dentro de la cuenca del Río Juruá y a través de toda la Amazonía, y recalcamos la distribución geográfica de las que parecen ser unidades faunísticas principales que no están relacionadas con diferencias entre los hábitats. Finalmente, usamos principios de filogeografía para analizar los patrones de diferenciación geográfica entre los mamíferos no voladores en el marco de la Hipótesis de la Barrera de Río. A pesar de que hay algunos taxones para los cuales el Río Juruá aparentemente constituye una barrera para la dispersión, demostramos que la mayoría de los taxones no está diferenciada en unidades geográficas a lo largo de la cuenca, o está marcadamente dividida en unidades de haplotipos de AND mitocondrial recíprocamente monofiléticas que son separables en unidades correspondientes a las partes altas y bajas del Río. La concordancia en la ubicación de los límites de grupos monofiléticos (‘‘clades’’) sugiere que estos grupos comparten una historia común; mantenemos también que la edad de estos grupos monofiléticos, así como su posición geográfica en relación con características geológicas fundamentales, indica que la evolución de la fisiogeografía ha sido un componente importante de la diversificación en la Amazonía Occidental que hasta ahora ha sido poco apreciado.

RESUMO

Nesse estudo descreve-se a fauna de mamíferos não-voadores do Rio Juruá, situado a oeste da Amazônia brasileira, por meio das coletas realizadas ao longo desse rio durante levantamento de aproximadamente um ano. Os trabalhos de campo foram planejados para examinar os efeitos do rio na estrutura dos vertebrados terrestres, inclusive dos mamíferos, tanto no que se refere às comunidades quanto aos padrões de diferenciação geográfica para espécies individuais. Dezesseis sítios de coleta primários foram inventariados segundo desenho experimental constituido por dois pares de sítios situados em margens opostas, em cada uma das quatro regiões distribuidas das proximidades da foz até a região da cabeceira do rio. Um total de 81 espécies foram obtidas, e inclui nove espécies novas para a ciência. Quarto delas estão descritas neste estudo; as outras encontram-se descritas em outros trabalhos. A estrutura das comunidades foi determinada a partir de um protocolo de amostragem padronizado para cada um dos 16 sítios que incluia estações de captura, com armadilhas terrestres e arbóreas, nas matas de várzea e de terra firme. Capturas adicionais foram realizadas em habitats considerados secundários em todos os sítios de amostragem. Descrevem-se esses sítios, o esforço de amostragem e a localização das estações de captura correspondentes aos habitats locais. Também descreve-se cada uma das espécies de marsupiais e de roedores murídeos e equimídeos encontradas, comenta-se sobre sua sistemática, e sumarizam-se aspectos relativos ao uso de habitat, história natural, distribuição geográfica, e diferenciação geográfica baseada em caracteres morfológicos e moleculares. A variação nas sequências do gene mitocondrial citocromo-b foi examinada para amostras de 41 das 45 espécies de marsupiais e roedores obtidas. Para cada um dos táxons, cujas amostras eram suficientes, examinaram-se os padrões de diferenciação na bacia do Rio Juruá, e discutiram-se esses padrões para toda a Amazônia e, em alguns casos, incluiu-se também a Mata Atlântica. Posteriormente, examinaram-se os padrões de organização das comunidades na bacia do Rio Juruá e em toda a Amazônia, chamando atenção sobre a distribuição geográfica do que aparentemente representam unidades faunística maiores, independentes das diferenças no habitat. Retorna-se, então, ao objetivo original e utilizam-se os princípios filogeográficos para analisar os padrões geográficos de diferenciação entre os mamíferos não-voadores com referência à Hipótese dos Rios. Mostra-se que embora para alguns táxons o Rio Juruá funcione como barreira, a maioria dos táxons ou é largamente indiferenciada em toda a bacia ou marcadamente dividida em clades de haplotipos monofiléticos separáveis em duas unidades distintas, uma rio-acima e outra rio-abaixo. Argumenta-se que essa concordância na localização geográfica dos limites dos clados indicam uma história comum e, tanto a idade desses clados quanto suas posições geográficas em relação às estruturas geológicas subjacentes sugerem que a evolução das paisagens tem sido um componente importante, embora desconsiderado dos processos de diversificação no oeste da Amazônia.

INTRODUCTION

The Amazonian morphoclimatic domain (as defined by Ab'Saber, 1977) covers approximately 7 million km^2. Substantial heterogeneity in features of the soil, relief, drainage, vegetation, and climate characterizes the lowland forests below 400 m elevation over this enormous area. Here, species richness is high, both in terms of the total number of species and the number existing in sympatry (Cody, 1996).

Knowledge of the distribution and systematics of Amazonian mammals, especially nonprimates, is generally inadequate. This message is present in most recent syntheses dealing with this fauna (Voss and Emmons, 1996; Emmons and Feer, 1997; Patton et al., 1997; da Silva and Patton, 1998). Despite the paucity of information, and a few dissenting voices (e.g., Mares, 1992), most workers agree that ''. . . the mammalian faunas of western Amazonia are the most diverse of any in the Americas and perhaps in the world'' (Voss and Emmons, 1996: 1). However, adequate inventories are available for only eight localities throughout greater Amazonia, a pitifully small number. The data we provide below for the Rio Juruá basin will help fill the great void that exists in our knowledge base for Amazonian mammals, their ecologies, distributions, and evolutionary histories.

This monograph serves two major purposes. First, it summarizes the patterns of ecological and geographic distribution and differentiation of species of small-bodied, nonvolant terrestrial and arboreal mammals of the Rio Juruá, a major tributary of the Rio Amazonas-Solimões entering on its south bank in western Brazil. Most emphasis is given to marsupials and to murid and echimyid rodents, the most diverse groups characterizing these forests, and groups for which our trapping program (described below) was specifically designed to examine. We chose the Rio Juruá basin for study for several reasons. For one, its biota has received only the most cursory attention during past biological investigations of the Amazon Basin. Several reports of the mammals of the area have been published, but all contain only short species lists from very few localities in the central part of the river, and none provide data on natural history or ecological distribution (Ihering, 1904; Olalla, 1938; Vieira, 1948; Carvalho, 1957; Patterson, 1992). There are few collections of mammals available from the entire region delimited by the Peruvian border on the west, the Rio Solimões to the north, and the Rio Madeira to the south and southeast, an area of some 875,000 km^2. Secondly, the Rio Juruá is one of the major tributaries of the Amazon, extending nearly 1000 km from its headwaters in the Cordillera Divisor on the border between Perú and Brazil to its confluence with the Amazon. As such, the river could represent a substantive barrier to small mammal distribution and thus be a good candidate for the examination of riverine barriers in general. Thirdly, the Rio Juruá, or at least its basin, has been identified as an avian contact zone (Haffer, 1974) and as a presumptive zone of rapid environmental transition (Brown, 1982; Endler, 1982). Both suggestions support a potential role of the Rio Juruá, and other rivers, in the overall biological diversification of Amazonia. Fourthly, the Rio Juruá basin is also part of one of the Global 200 ecoregions identified by Olson and Dinerstein (1998; Region 10, Neotropical moist broadleaf forest) as among the world's most valuable biologically. And, importantly, this is a region still regarded as relatively stable or intact so that the patterns of structure and diversity uncovered will represent relatively nonimpacted, and thus historically complete, communities.

Our second major purpose is to integrate the patterns of distribution and differentiation of the nonvolant small mammals of the Rio Juruá into the broader area of Amazonia. To do this, we provide data on genetic differentiation for those taxa for which sufficient information is available, using sequence diversity of the mitochondrial cytochrome-b gene. We use these data to illustrate common geographic patterns among delineated lineages, to evaluate some of the models that have been proposed as general explanations for patterns of Amazonian faunal and floral diversity, and to identify geographic areas in critical need for additional sampling. Since the overall study was initiated to examine

riverine effects on the terrestrial vertebrate fauna of the Rio Juruá, we examine and evaluate this model explicitly in light of patterns of both population and species differentiation and ecological distribution.

We have organized this monograph in the following manner. First, we introduce the Rio Juruá basin, focusing on our field sites distributed from the river's mouth to its headwaters. Sample sites, and the trapping design at each, were chosen both to provide suitable comparisons among sites and to permit examination of the relationship of the river and its forest types to patterns of differentiation of both small mammal communities and individual taxa within the Rio Juruá basin. As is described in detail below, we established eight cross-river pairs of sample sites, themselves organized in groups of pairs distributed at somewhat equal intervals from near the mouth to the river's headwaters. Both upland, nonseasonally flooded forest (terra firme) and the seasonally flooded (várzea) margins of the river were specifically included in our sampling protocol. We then present accounts for most of the small-bodied nonvolant mammals, specifically marsupials and sciurid, murid, and echimyid rodents. In so doing, we comment on their systematics and distribution both within the Rio Juruá basin and throughout Amazonia, where appropriate. We do this, in part, to provide a more general guide to the identification of small mammals from the western Amazon. We exclude xenarthrans, large caviomorph rodents, carnivores, or ungulates from these accounts, because relatively few individuals were obtained or seen and because our trapping program was not designed to routinely assess their presence. Standardized censuses of the primate communities were accomplished at all sites; these data have been published separately by Peres (1993, 1997). Next, we examine the adequacy of our inventory efforts and discuss local and broader patterns of mammalian diversity and species turnover. Finally, we summarize the patterns found at the community level and from the comparative phylogeography of specific taxa, and discuss aspects of the historical biogeography of Amazonian mammals within and beyond the Rio Juruá basin.

MATERIALS AND METHODS

SPECIMENS AND ABBREVIATIONS: Vouchers were taken from all specimens collected on all trap lines, including the standardized plots and all supplemental trap efforts. Specimens were prepared as either standard skins with accompanying skulls, as skins with skulls and partial skeletons, as complete skeletons, as skins with skulls with bodies in fluid (preserved in 10% formalin and maintained in 70% ethanol), or as fluids with or without the skulls removed and subsequently cleaned. The collection totals nearly 3000 specimens, and will be eventually divided equally between the Museu Paraense Emílio Goeldi in Belém (MPEG), the Instituto Nacional de Pesquisas da Amazônia in Manaus (INPA), or the Museum of Vertebrate Zoology, University of California, Berkeley (MVZ). Specimens from new taxa that have already been described (e.g., Patton and da Silva, 1995; da Silva, 1998), or that are described herein, have already been cataloged into these collections; where so, those catalog numbers are indicated in the accounts below. All primate specimens have already been cataloged at MPEG (Peres, 1993). Otherwise, the field catalog numbers of members of the expedition are utilized to identify individual vouchers, as follows:

DMN	Field numbers of Dalton Novaes, then an undergraduate student at the Universidade de São Paulo, São Paulo, Brazil
JLP	Field numbers of James L. Patton
JUR	Field numbers of Jay R. Malcolm
MNFS	Field numbers of Maria Nazareth F. Da Silva

In addition to our specimens from the Rio Juruá, we also report on sequences or karyotypes of other specimens collected elsewhere within Amazonia and provided by other individuals and institutions. These are identified in the text, tables, and figures by museum abbreviation and catalog number for specimens already cataloged in specified repositories. However, some of these specimens either have yet to be cataloged in a recognized collection or we have been unable to obtain collection catalog numbers. These specimens are identified by the collector and his or her field numbers. The following are abbreviations of these institutions or

individuals. In the latter case, the museum repository where the specimens will eventually be cataloged is indicated:

ALG	Field numbers of Alfred L. Gardner—specimens deposited at the National Museum of Natural History, Smithsonian Institution, Washington D.C. (USNM), or Museo Biológica Universidad Central de Venezuela, Caracas (MBUCV)
AMNH	American Museum of Natural History, New York
BMNH	British Museum (Natural History), London
CM	Carnegie Museum of Natural History, Pittsburgh
CS	Field numbers of Raquel Moura and Maria Nazareth da Silva—specimens deposited in Instituto Nacional de Pesquisas da Amazônia, Manaus (INPA)
EDH	Field numbers of Erica D. Hingst—specimens to be deposited in the Museu Nacional, Rio de Janeiro (MN)
INPA	Instituto Nacional de Pesquisas da Amazônia
KU	University of Kansas Museum of Natural History, Lawrence
LPC	Field numbers of Leonora P. Costa—specimens to be deposited either in the Museum of Vertebrate Zoology, University of California (MVZ) or Universidade Federal de Minas Gerais, Belo Horizonte (UFMN)
LHE	Field numbers of Louise H. Emmons—specimens deposited at the National Museum of Natural History, Smithsonian Institution, Washington, D.C. (USNM), Colección Boliviana de Fauna, La Paz, Bolivia (CBF), Museo de Historia Natural, Universidad Mayor de San Marcos, Lima, Perú (MHN), or Museu de Zoologia, Universidade de São Paulo, São Paulo, Brazil (MZUSP)
MAM	Field numbers of Meika A. Mustrangi—specimens deposited in the Museu de Zoologia, Universidade de São Paulo, São Paulo, Brazil (MZUSP)
MDC	Field numbers of Michael D. Carleton—specimens deposited at the National Museum of Natural History, Smithsonian Institution, Washington, D.C. (USNM), or Museu de Zoologia, Universidade de São Paulo, São Paulo, Brazil (MZUSP)
ML	Field numbers of Márcia Lara—specimens deposited in the Museu Nacional, Rio de Janeiro (MN)
MN	Museu National, Rio de Janeiro
MNHN	Muséum National d'Histoire Naturelle, Paris, France
MNU	Tissue collection numbers of François Catzeflis, Université de Montpellier, Montpellier, France
MPEG	Museu Paraense Emílio Goeldi, Belém
MSB	Museum of Southwestern Biology, University of New Mexico
MZUSP	Museu de Zoologia, Universidade de São Paulo, São Paulo
ROM	Royal Ontario Museum, Toronto
TTS	Field numbers of Teresa Tarifa S.—specimens deposited in the Colección Boliviana de Fauna, La Paz, Bolivia (CBF)
TTU	The Museum, Texas Tech University, Lubbock
UMMZ	University of Michigan Museum of Zoology, Ann Arbor
USNM	National Museum of Natural History, Smithsonian Institution, Washington, D.C.
VPT	Field numbers of Victor Pacheco T., Museo de Historia Natural, Universidad Mayor de San Marcos, Lima Perú (MHN)
YL	Field numbers of Yuri R. Leite—specimens to be deposited either in the Museum of Vertebrate Zoology, University of California (MVZ) or Universidade Federal de Minas Gerais, Belo Horizonte (UFMN)

Measurements: External measurements were taken from dead individuals prior to specimen preparation and recorded both in field journals and on specimen labels, as follows:

TOL	Total length, from tip of nose to tip of terminal tail vertebra
TAL	Tail length, from dorsal flexure at base of the tail to tip of last vertebra
HF	Hind foot length, from proximal margin of calcaneus to tip of longest claw
E	Ear height, from notch to top of pinna

Cranial dimensions were taken with digital calipers to the nearest 0.01 mm. These measurements are summarized for samples of all taxa in the accounts below, as are statistical comparisons between related taxa based on

univariate and multivariate methodologies. Capitalized color terms, when used, are from Ridgway (1912).

Marsupials: We recorded either 13 or 15 cranial measurements from each marsupial from the following list:

CIL	Condyloincisive length, from the anterior face of the upper incisors to the posterior margin of the occipital condyles
ZB	Zygomatic breadth, greatest breadth across the zygomatic arches
BB	Braincase breadth, greatest breadth above the squamosal root of the zygomatic arch
MB	Mastoid breadth, breadth of skull across the mastoid bones
IOC	Least interorbital constriction, minimal breadth across the roof of the skull above the orbits, taken anterior to the postorbital processes for those taxa with such structures (= IOC-1)
IOC2	Least interorbital constriction, taken posterior to the postorbital processes
RL	Rostral length, from the anterior margin of the orbit to the midline tip of the nasal bones
NL	Length of the nasal bones, midline distance from anterior tip to posterior margins of nasals
RW	Rostral width, width of the rostrum at the level of the canines
C-M4	Maxillary toothrow length, from the anterior face of the canine to the posterior margin of M4
M1-M4	Molar toothrow length, taken on the labial margin of the toothrow from M1 to M4
PL	Palatal length, midline distance from the posterior margins of the first upper incisor to the posterior margin of the hard palate
PW	Palatal width, width of palate taken across the lateral margins of third molars
OCB	Occipital condyle breadth, breadth across the outside margins of the occipital condyles
BOL	Basioccipital length, distance from anterior margin of foramen magnum to basioccipital-basisphenoid suture
CD	Cranial depth, vertical distance between ventral margins of bullae and top of cranium

The assignment of individuals to age classes generally followed the scheme of tooth eruption and wear defined for *Didelphis* by Gardner (1982). Data are summarized only for adult specimens in which the fourth molars are fully erupted.

Murid Rodents: We took the same set of 20 cranial measurements on all murid rodents, as follows:

CIL	Condyloincisive length, from the anterior margins of the upper incisors to the posterior margins of the occipital condyles
ZB	Zygomatic breadth, greatest breadth across the zygomatic arches
MB	Mastoid breadth, greatest width across the mastoid processes
IOC	Interorbital constriction, least distance across roof of skull between the orbits
RL	Rostral length, diagonal measurement taken from anterior margin of orbit to anterior margins of nasal bones
NL	Nasal length, maximum midline length of nasal bones
RW-1	Rostral width-1, taken across outside margins of the nasolacrymal capsule
RW-2	Rostral width-2, taken at premaxilla-maxilla suture
OL	Orbital length, taken diagonally from anterior to posteriormost margins of orbit
D	Diastemal length, from the posterior face of the upper incisor to the anterior edge of M1
MTRL	Molar toothrow length, crown length of maxillary toothrow
IFL	Incisive foramen length, length of maximal opening of incisive foramen
PBL	Palatal bridge length, from the posterior margin of upper incisors to anterior margin of mesopterygoid fossa
AW	Alveolar width, outside distance across the alveolae of first upper molars
OCB	Occipital condyle breadth, outside distance between occipital condyles
BOL	Basioccipital length, distance from anterior margin of foramen magnum to basioccipital-basisphenoid suture
MPFL	Mesopterygoid fossa length, midline distance from anterior margin to posterior tip of hamular processes
MPFW	Mesopterygoid fossa width, maximal width taken at suture of palatine and pterygoid bones
ZPL	Zygomatic plate length, taken at midheight from anterior to posterior margins of plate
CD	Cranial depth, vertical distance from plane determined by incisor tips and bullae and top of cranial vault

All specimens were placed into age categories based on molar eruption and wear patterns similar to those used by Myers and Carleton (1981) for *Oligoryzomys*: Age 1—third molars not fully erupted; Age 2—third molars erupted but with no observable wear; Age 3—limited to moderate wear on first and second molars, limited wear on 3rd; Age 4—all three molars well worn, but with cusps and flexi still visible; Age 5—most surface features of all molars obliterated. Only individuals of age classes 3 through 5 were considered ''adults'' and were used in statistical summaries and comparisons.

Echimyid rodents: We took 20 or 21 cranial measurements from all echimyid rodents, generally following the illustrations or descriptions in Patton and Rogers (1983), Patton and Emmons (1985), and da Silva (1998), as follows:

CIL Condyloincisive length, midline distance from anterior face of upper incisors to posterior margins of occipital condyles

ZB Zygomatic breadth, maximum width across outside margins of zygomatic arches

MB Mastoid breadth, distance across cranium at mastoid processes

IOC Interorbital constriction, least distance across top of skull between the orbits

RL Rostral length, taken from anterior margin of orbit to tip of nasal bones

NL Nasal length, midline distance from tip to base of nasal bones

RW-1 Rostral width, taken across outside margins of nasolacrymal capsule

RW-2 Rostral width, taken at premaxillary-maxillary suture

RD Rostral depth, minimal depth of the rostrum between incisor and M1

OL Orbital length, internal distance between anterior and posterior margins of orbit

D Diastemal length, midline distance between posterior margins of upper incisors and anterior edge of PM4

MTRL Maxillary toothrow length, distance between anterior edge of alveolus of PM4 and posterior edge of alveolus of M3

IFL Incisive foramen length, maximal distance of opening of incisive foramen

PL Palatal length A of Patton and Rogers (1983), midline distance between posterior margins of upper incisors to anterior margin of mesopterygoid fossa

BUL Bullar length, maximal distance from anterior to posterior edges of tympanic bulla

AW Alveolar width, distance across palate taken at outside margin of alveolus of PM4

OCB Occipital condyle breadth, taken across outside margins of occipital condyles

MPFL Mesopterygoid fossa length, maximum midline length from anterior margin to posterior extensions of hamular processes

MPFW Mesopterygoid fossa width, maximum width taken at the suture between palatine and pterygoid bones

CD Cranial depth, vertical distance from ventral margin of bulla to top of cranium.

CDM Cranial depth at M1 (taken only for species of *Proechimys*).

We based age categories of *Proechimys* on the toothwear sequence established by Patton and Rogers (1983). Young individuals are those of age classes 1 through 5 that have undeveloped M3 and juvenile pelage; subadults are those of age classes 6 and 7 with erupted but unworn M3 and a mixture of both juvenile and adult pelage; and adults are those individuals of age classes 8 through 10 that have all four cheekteeth erupted and worn, as well as complete adult pelage. Only individuals of age classes 8 to 10 were used in statistical summaries and in comparisons of species or populations within them.

STATISTICAL ANALYSES: All statistical analyses were performed with one of three commercially available programs for the personal computer. Univariate summaries of morphometric variables were performed primarily with StatView (version 4.5) on a Macintosh PowerPC 8500. Principal components analysis and discriminant function analyses designed to compare samples pooled by locality for given species were performed with either StatView or Statistica, also written for the Macintosh PowerPC. Nongeographic variation (due to sex and age, as estimated from toothwear categories) was examined for some taxa where sample sizes were sufficiently large for individual localities. Analyses of these taxa were based on two-way analysis of variance (ANOVA, random-effects model to accommodate for unequal sample sizes), and utilized the StatView pro-

gram. Univariate comparison between sexes or among populations or species used one-way ANOVAs, again with a random-effects model. Variance components analysis, based on a nested ANOVA and random-effects model (with locality, sex, and ''age'' as successive strata), was employed to examine the proportion of total variation in mensural characters due to these characters, for those species where adequate samples were available. This analysis employed the VARCOMP and NESTED routines in SAS (version 6.04), using an MS-DOS personal computer (SAS Institute, 1988). Finally, for comparisons between geographic samples of single taxa we generally used Thorpe's (1983, 1987; see also Thorpe and Baez, 1987) multiple groups principal components analysis. These also employed routines from the SAS statistical program, and followed procedures outlined in Patton and Smith (1990). All multivariate analyses used $\log_{10}$ transformations of cranial variables.

KARYOTYPE ANALYSES: We made chromosome preparations in the field using a slightly modified version of Patton's (1967) colchicine-hypotonic salt and Carnoy's fixative protocol and a hand-driven centrifuge. Cell suspensions were stored in the field at ambient temperature in 5 cc screw-cap cryogenic vials, and transported to the laboratory in Berkeley where they have been maintained at $-5°C$. Slides were prepared months to years following collection and by both the flame-dry and air-dry techniques. These were stained with Wright's stain and examined and photographed under oil immersion using bright-field optics. Definitions of the chromosome categories ''metacentric,'' ''submetacentric,'' ''subtelocentric,'' and ''acrocentric'' are given in Patton (1967).

MOLECULAR ANALYSES: Measures of genetic diversity within populations and comparisons of genetic divergence among samples for selected taxa were made from mitochondrial DNA (mtDNA) cytochrome-b sequences. The amount of sequence available varied from the initial 450 base pairs (bp) to 801 bp, depending upon the genus. Methods of extraction of DNA, amplification by the polymerase chain reaction of both double- and single-strand products, and sequencing are detailed in Smith and Patton (1991, 1993), da Silva and Patton (1993), and Patton et al. (1994). We obtained sequences either by manual sequencing or by use of an ABI Prism 377 automatic sequencer. Sequencing protocols are given in the previous citations, or followed recommendations from the manufacturer. We have not submitted the entire set of sequences for each taxon examined herein to GenBank. Instead, we will provide Nexus files of sequences for any taxon to any investigator upon request, either to J. L. Patton (e-mail address: patton@uclink4.berkeley.edu).

Calculations of sequence divergence (in percent) using the Kimura two-parameter algorithm (Kimura, 1980), as well as numbers of transition and transversion differences by codon position, and the proportions of each base at each codon position were obtained from MEGA, version 1.02 (Kumar et al., 1993). Relationships among haplotypes representative of populations and taxa were examined by maximum parsimony using PAUP, version 4.0b1 or earlier versions (Swofford, 1998). The search option employed (heuristic, branch-and-bound, or exhaustive) depended on the size of the data file. All analyses were performed with stepwise addition of 10 random replicates (following Maddison, 1991), and are generally reported as the strict consensus tree derived from all minimal-length trees obtained. The strength of internal nodes was gauged by bootstrap analysis, with 1000 replicates. Although the exact statistical interpretation of bootstrap results remains to be determined, a rule of thumb is that internal tree branches that have $> 70\%$ bootstrap support are likely to be correct at the 95% level (Hillis and Bull, 1993). In some cases, matrices of Kimura two-parameter distances were analyzed using the neighbor-joining algorithm, in either PAUP or PHYLIP, version 3.5c (Felsenstein, 1993).

REPRODUCTIVE ANALYSES: We ascertained the reproductive condition of both sexes for most specimens of each species by autopsy during specimen preparation in the field. For male rodents, we recorded information on testis position (scrotal or not scrotal), testis size (length by width), greatest length of the vesicular glands, and degree of visibility of the tubules in the cauda epididymis. Since scrotal males of various rodent species often

withdraw their testes when stressed (such as during trapping and handling), we relied on the combination of testis and vesicular dimensions and the visibility of epididymal tubules to distinguish between nonreproductive and reproductive individuals. Plots of mean testis versus mean vesicular length split by epididymal tubules grouped as 'visible' or 'nonvisible' routinely divided samples into males with both small testes and vesicular glands and nonvisible tubules from those with large testes, large vesicular glands, and visible tubules. We considered the former group nonreproductive and the latter reproductive. The dimensions dividing these conditions for different species are given under their respective accounts, below. For female rodents, we considered the following categories: (1) nulliparous—individuals with nonvascularized, thin, and threadlike uteri, generally with no evidence of ripe follicles on the surface of the ovary, and with tiny mammary nipples; (2) parous but nonreproductive—females with a swollen and vascularized uteri, obvious placental scars, enlarged and visible nipples, and/or ovaries with corpora; (3) pregnant; (4) lactating—milk that can be expressed from nipples by palpation; or (5) pregnant and lactating. Litter size is based on fetal counts, although the number of placental scars visible in each uterine horn was also recorded. In general, these two indicators of litter size were concordant. Reproductive condition for marsupials was more subjective, especially for males for which we simply recorded testis size and color. Adult males typically have black or bluish-colored testes; juveniles are white or cream. Reproductively active females either had attached young or exhibited a distinct rusty-orange mammary area; juvenile females lacked that latter coloration.

ACKNOWLEDGMENTS

The research reported herein was undertaken as part of the Projeto Juruá, a joint effort by the authors and Drs. Claude Gascon and Carlos A. Peres, under the auspices of Dr. J. Márcio Ayres of the Museu Emílio Goeldi in Belém who served as project coordinator, and the Conselho Nacional de Desenvolvimento Científico e Tecnológico (CNPq) and Instituto Brasileiro do Meio Ambiente e dos Recursos Naturais Renovavais (IBAMA). Field support for the mammal part of the project was provided by Dalton Novaes, Alexandre Percequillo, Pedro Develey, Antonio Pinheiro, Osmar and Lincoln Pereira da Cunha, Carol Patton, and Justina Ray. Help in laboratory phases was provided by Leonora P. Costa, Luis Fernando Garcia, Márcia C. Lara, Yuri R. Leite, Marjorie D. Matocq, Meika A. Mustrangi, Manuel Ruedi, Margaret F. Smith, and Andrea Swei. Guy G. Musser and Robert S. Voss (American Museum of Natural History), Michael D. Carleton (National Museum of Natural History), and Alfred L. Gardner (USGS Patuxent Wildlife Research Center) permitted our access to their respective collections and shared their vast knowledge of Neotropical small mammals; to them we are especially grateful. Louise H. Emmons (National Museum of Natural History) similarly shared her extensive experiences throughout Amazonia, generously made available her notes, photographs, and karyotypes of various echimyid rodents for our use, and collected the tissue samples from many of the specimens outside of the Rio Juruá that we have analyzed. Her generosity in sharing both information and primary data (e.g., specimens of all kinds) represents the optimal level of scientific collegiality. Bruce D. Patterson (Field Museum of Natural History) made available specimens from the Royal Natural History Museum, Stockholm, collected from the Rio Juruá by A. M. Olalla. Eric Brothers (American Museum of Natural History) kindly provided a xerox copy of Christopher Tribe's PhD thesis on *Rhipidomys*. Javier Rodríguez-Robles translated the abstract into Spanish. We are also grateful to Robert M. Timm (University of Kansas), Mark D. Engstrom (Royal Ontario Museum), Robert J. Baker (Texas Tech University), Terry L. Yates and William L. Gannon (University of New Mexico), Al Gardner, Louise Emmons, and Jeremy E. Jacobs (National Museum of Natural History), Rui Cerqueira, Erika Hingst, and Vera Vidigal (Universdidade Federal do Rio de Janeiro), Yatiyo Yonenaga-Yassuda (Universidade do São Paulo), and François Catzeflis (Université Montpelier II, France) for making tissue samples

from their own work available to us for analysis. Specimens examined from the Parque Nacional do Jaú were collected with the aid of Leonora P. Costa, Yuri R. Leite, and Vera Vidigal. Paula Jenkins (British Museum) graciously facilitated the loan of a fragment of the skin of a specimen of the type series of *Neacomys tenuipes* for DNA extraction. Michael Carleton, Louise Emmons, Al Gardner, Guy Musser, and Rob Voss reviewed all, or part, of the manuscript in its various drafts, and combined to improved greatly both the prose and scientific content, although they should not be held responsible for the final effort. Lea Boyd helped in the organization and curation of the specimens collected, with the skulls and skeletons professionally prepared by Robert E. Jones and Ward Russell in record time. Karen Klitz drew some of the figures of specimens, and Jim Hendel photographed the skins and most of the skulls and generated black-and-white prints of habitats from color slides. Financial support for fieldwork was provided by the Wildlife Conservation Society, National Geographic Society, and Museum of Vertebrate Zoology; laboratory work was supported by grants from the National Science Foundation to J. L. Patton. During the fieldwork and for a period thereafter, M. N. F. da Silva was supported by a fellowship from the Conselho Nacional de Desenvolvimento Científico e Tecnológico (CNPq), and J. R. Malcolm was supported by a fellowship from the National Science and Engineering Research Council of Canada. The Museum of Vertebrate Zoology (MVZ) and the Instituto Nacional de Pesquisas da Amazônia (INPA) provided logistical and other support. Finally, we are extremely grateful to the peoples of the Rio Juruá for their warm hospitality throughout our year-long expedition, especially for allowing us to intrude into their daily lives. This study could not have been accomplished without their complete support.

THE FIELD SITES

LOCALITIES

The Rio Juruá is the third largest whitewater river of Amazonia, excepting the Amazon-Solimões proper, ranking in size behind only the Rio Madeira and Rio Purus (Ayres and Clutton-Brock, 1992). The river has its origin in the Cordillera Divisor along the Perú-Brazil border, and it courses a linear distance of nearly 1000 km with elevations grading from about 250 to 65 m above sea level. The annual discharge is approximately 10^{12} m^3 (Gibbs, 1967). The gentle slope of the basin coupled with heavy discharge results in a sinuous and dynamic channel braiding through the floodplain. The actual length of the river doubles if measured along the midchannel. The annual water level in the mid to lower reaches of the river varies by 8 to 12 m in amplitude between dry and wet seasons. Floods may increase water levels by 15 m in the headwaters, although these occur only on an irregular basis, not annually. This fluviodynamic state produces a floodplain belt that broadens extensively from headwaters to mouth. The floodplain consists of a complex forest mosaic interspersed with abandoned channels (oxbow lakes), swales, erosional riverbanks, and strips of colonizing and successional vegetation in young landforms. Extensive descriptions of the Rio Juruá and its basin, including geology, geomorphology, soils, and vegetation, can be found in volume 15 of the Projeto RadamBrasil series (1977).

We sampled at 16 primary localities between August 1991 and June 1992, numbered sequentially from the headwaters to the mouth of the Rio Juruá (see map, fig. 1). Peres (1997) gives brief descriptions of some of these, and we provide more expanded descriptions of the habitats and trapping programs at each locality below. We group the localities into four regions, each with two pairs of cross-river sites: Headwaters (localities **1**--**4**), Upper Central (localities **5**–**8**), Lower Central (localities **9**–**12**), and Mouth (localities **13**–**16**). All right-bank localities have odd numbers; those from the left bank have even numbers. We designate primary localities as those where standardized canopy and terrestrial trap stations were established. We also briefly visited a few other localities,

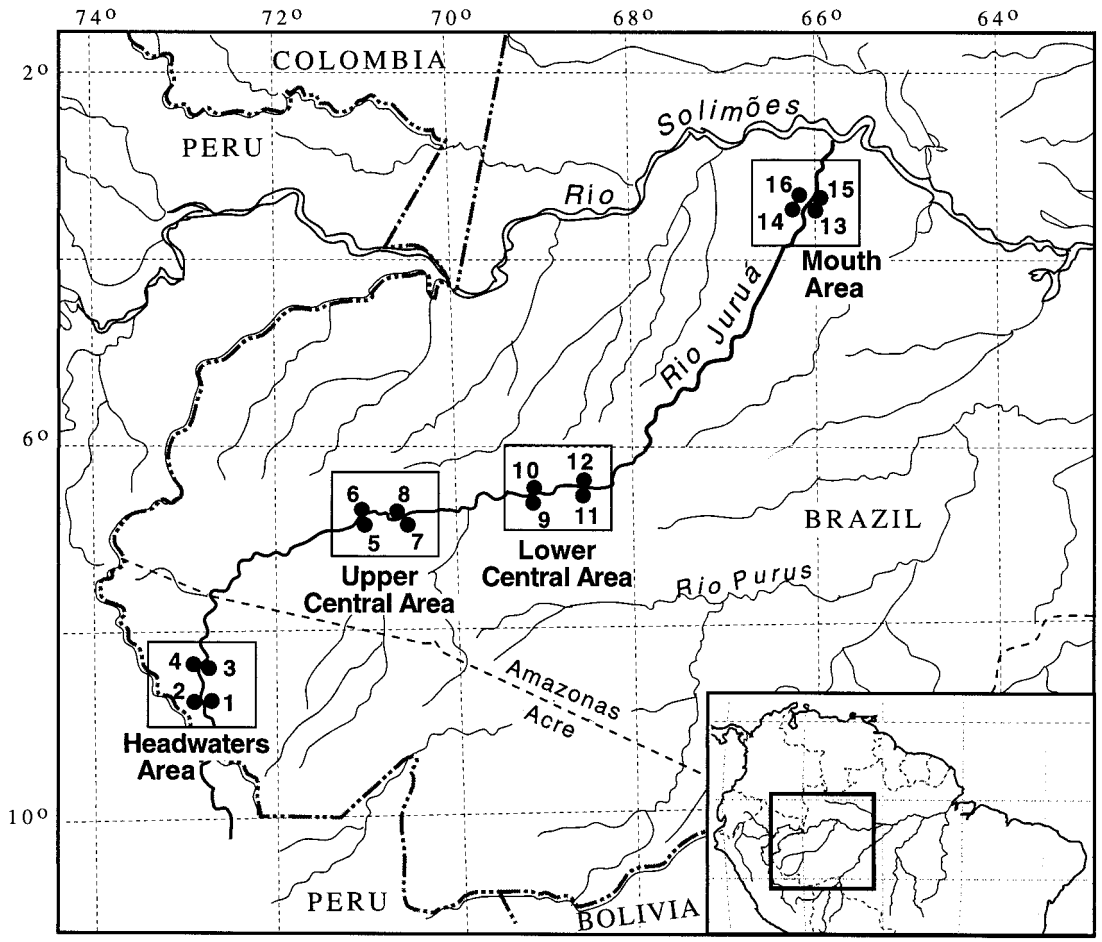

Fig. 1. Map of the Rio Juruá basin indicating position of the sixteen primary sample localities, as grouped into the four regional units (Headwaters, Upper Central, Lower Central, and Mouth areas).

labeled by lower case letters, but usually for no more than a single night. We use the primary localities for all riverine comparisons; the others provide supplemental records only. Each of the eight opposite-bank pairs of sites was visited for an approximately 3-week period, with trap lines on both sides run nearly simultaneously. The two central regions were sampled in the months of August through November, which is during the annual dry season; the Headwaters and Mouth regions were sampled over the months of February through May, in the rainy season. Table 1 provides a matrix of straight-line geographic distances (in kilometers) between all sample sites.

GAZETTEER

Listed below are each of our 16 primary (designated by numbers and highlighted in bold) and secondary localities (designated by letters) visited along the Rio Juruá, as well as inclusive dates when collections were made. Detailed descriptions of each locality, including habitats present, trap lines, types of traps used, and so forth are given in the descriptions beyond. All localities (primary and secondary) are mapped in figures 18, 23, 28, and 33; photographs of some sites are provided in figures 2 through 8. Localities from outside of the Rio Juruá for which specimens have been examined for cytochrome-b se-

TABLE 1
Matrix of Straight-Line Distances (in kilometers) Between Primary Sample Localities from the Four Regions Along the Rio Juruá (see map, fig. 1, and text)
Distances between regions were determined from a 1:2,000,000 RadamBrasil map; those within regions were taken from 1:250,000 RadamBrasil maps.

	Distance (km)																
Loc.	1	2	3	4	5	6	7	8	9	9a	10	11	12	13	14	15	16
1	0.0																
2	3.0	0.0															
3	35.0	35.0	0.0														
4	33.8	33.8	2.0	0.0													
5	300.0	300.0	276.0	276.0	0.0												
6	300.0	300.0	276.0	276.0	1.5	0.0											
7	300.0	300.0	276.0	276.0	11.3	10.3	0.0										
8	300.0	300.0	276.0	276.0	9.8	9.0	3.8	0.0									
9	488.0	488.0	472.0	472.0	220.0	220.0	216.0	216.0	0.0								
9a	488.0	488.0	472.0	472.0	220.0	220.0	216.0	216.0	4.8	0.0							
10	488.0	488.0	472.0	472.0	220.0	220.0	216.0	216.0	0.8	4.5	0.0						
11	580.0	580.0	492.0	492.0	238.0	238.0	234.0	234.0	19.8	19.0	20.0	0.0					
12	580.0	580.0	492.0	492.0	238.0	238.0	234.0	234.0	20.3	19.5	20.0	0.8	0.0				
13	962.0	962.0	940.0	940.0	666.0	666.0	662.0	662.0	488.0	488.0	488.0	468.0	468.0	0.0			
14	954.0	954.0	932.0	932.0	658.0	658.0	654.0	654.0	482.0	482.0	482.0	462.0	462.0	25.8	0.0		
15	962.0	962.0	940.0	940.0	666.0	666.0	662.0	662.0	488.0	488.0	488.0	468.0	468.0	1.3	27.0	0.0	
16	954.0	954.0	932.0	932.0	658.0	658.0	654.0	654.0	482.0	482.0	482.0	462.0	462.0	25.0	0.8	26.3	0.0

quences are specified in the tabular materials associated with each taxon and analysis, in the accounts below.

Estado do Acre

1. **Igarapé Porongaba**, right bank Rio Juruá 8°40′S, 72°47′W. 14 February to 3 March 1992.
2. **Opposite Igarapé Porongaba**, left bank Rio Juruá 8°40′S, 72°47′W. 14 February to 3 March 1992
   a. Flora (= Fazenda Santa Fé), left bank Rio Juruá 8°36′S, 72°51′W. 7–14 February 1992.
   b. Ocidente, right bank Rio Juruá 8°34′S, 72°48′W. 7–14 February 1992.
   c. opposite Ocidente, left bank Rio Juruá 8°34′S , 72°48′W. 7–14 February 1992.
3. **Nova Vida**, right bank Rio Juruá 8°22′S, 72°49′W. 5–27 March 1992.
4. **Sobral**, left bank Rio Juruá 8°22′S, 72°49′W. 5–27 March 1992.

Estado do Amazonas

   d. São José, right bank Rio Juruá 6°46′S, 70°52′W. 23 September 1991.
5. **Sacado**, right bank Rio Juruá 6°45′S, 70°51′W. 12 September to 8 October 1991.
6. **Seringal Condor**, left bank Rio Juruá 6°45′S, 70°51′W. 12 September to 8 October 1991.
   e. Opposite Condor, right bank Rio Juruá 6°45′S, 70°51′W. 2–4 October 1991.
   f. Colocação Sabiá, left bank Rio Juruá 6°47′S, 70°49′W. 25–26 September 1991
7. **Penedo**, right bank Rio Juruá 6°50′S, 70°45′W. 21 August to 9 September 1991.
8. **Igarapé Nova Empresa**, left bank Rio Juruá 6°48′S, 70°44′W. 21 August to 9 September 1991.
   g. near União, right bank Rio Juruá 6°50′S, 70°30′W. 19 August 1991.
   h. Caioá, right bank Rio Juruá 6°44′S, 70°13′W. 18 August 1991.
   i. near Miranda, left bank Rio Juruá 6°45′S, 70°00′W. 17 August 1991.
   j. Eirunepé, left bank Rio Juruá 6°38′S, 69°52′W. 16 August 1991.

k. Seringal Três Unidos, right bank Rio Juruá 6°37′S, 69°33′W. 14 August 1991.
l. 7.5 km W Providência, right bank Rio Juruá 6°34′S, 68°59′W. 13 August 1991.
m. Seringal Petrópolis, right bank Rio Juruá 6°35′S, 68°56′W. 15 November 1991.

9. **Altamira**, right bank Rio Juruá 6°35′S, 68°54′W. 7–24 November 1991.

9a. **Boa Esperança**, right bank Rio Juruá 6°32′S, 68°55′W. 7–24 November 1991.

10. **Opposite Altamira**, left bank Rio Juruá 6°35′S, 68°56′W. 7–24 November 1991.

11. **Jainu**, right bank Rio Juruá 6°28′S, 68°46′W. 14 October to 6 November 1991.

12. **Barro Vermelho**, left bank Rio Juruá 6°28′S, 68°46′W. 14 October to 6 November 1991.
n. Itamarati, left bank Rio Juruá 6°28′S, 68°15′W. 11 August 1991.

13. **Ilha Paxiuba**, right bank Rio Juruá 3°19′S, 66°00′W. 2–19 May 1992.

14. **Colocação Vira-Volta**, left bank Rio Juruá on Igarapé Arabidi, affluent of Paraná Breu 3°17′S, 66°14′W. 21 May to 10 June 1992.
o. Lago Três Unidos, left bank Rio Juruá on Igarapé Arabidi, afluent of Paraná Breu 3°16′S, 66°13′W. 21 May to 10 June 1992.

15. **Lago Vai-Quem-Quer**, right bank Rio Juruá 3°19′S, 66°01′W. 2–19 May 1992.

16. **Ilhazinha**, left bank Rio Juruá on Igarapé Arabidi, afluent of Paraná Breu 3°17′S, 66°14′W. 21 May to 10 June 1992.

HABITATS

The general and simple distinction between seasonally inundated floodplain, or várzea forests and the nonflooded upland, or terra firme forests (following Pires and Prance, 1985) has given way more recently to a much greater appreciation of, and classification system for, lowland Amazonian forest diversity that reflects differences in land forms, soil characteristics, and even local topography (see Daly and Prance [1989] for historical summary of phytogeography of Amazonia, and Tuomisto et al. [1994] and Puhakka and Kalliola [1995] for more recent delineations of forest types). Silva et al. (1992) provide a partial description of the forest formations of the Rio Juruá, and Campbell et al. (1992) compare the plant community structure of seasonally inundated (várzea) forests in the upper parts of the basin. Although we recognize the substantial degree of heterogeneity in lowland forest formations, we established our sampling program around the simplified recognition of terra firme and várzea. The topographic distinction between upland and floodplain forest was clear at all sites, with terra firme sites on relatively hilly, dissected terrain and várzea sites nearly flat. Sites in upland forest were chosen so that they could be easily accessed from the river; that is, where the river actually or nearly reached the edge of terra firme forest. Usually, the terra firme we censused abutted adjacent várzea, although at one site (Igarapé Porongaba, locality **1**) terra firme was separated from the várzea edge by low-lying bamboo forest (*tabôca*) nearly 2 km wide. We avoided swamps, streams, and secondary forests in the placement of the terra firme sites, and the beginning of each standardized trap line (see below) began at least 150 m from the edge of the forest.

In the várzea, we censused areas of mature forest that had large-diameter trees and that were physiognomically similar to the terra firme. Based on descriptions of floodplain forests along the Río Manu in southeastern Perú (Foster, 1990; Terborgh and Petren, 1991; see also Worbes et al., 1992), these forests are probably $>$ 300 years old. We avoided setting traps close to young successional forests (such as *Cecropia* stands), areas that flooded deeply ($>$ 3 m), vine (liana) forests (Bodmer, 1990), and second growth forests. Traps were in most cases at least 100 m from early successional habitats along the channel margin, and, except at sites close to the river mouth (see below), they were at least 150 m from terra firme forest. We also avoided the inner (concave) margins of meander loops in minimize any possible ‘‘pen-

Fig. 2. View of the Rio Juruá at Seringal Condor (locality **6**) in the Upper Central Region, looking south towards the right bank. The photograph was taken in September 1991, during the dry season. An extensive sand bar covered with grass is exposed, behind which is a thick stand of *Cecropia* some 50 m in depth before the edge of várzea forest is encountered. The beach grass is a seasonally ephemeral community, but is the primary habitat of *Oligoryzomys microtis*. The Rio Juruá is approximately 30 m wide at this point. Photograph by J. L. Patton.

insular'' effect on small mammal communities.

We placed standardized trap plots at each of the eight pairs of cross-river primary sites sampled (fig. 1). A brief characterization of most of our sites is given in Peres (1997); a more detailed description is given in the section below. Although we sampled both upland and floodplain forests on the same side of the river at some localities, usually only one forest type was accessible on a given side. Additional habitats sampled included (1) the beach grass (*capim*) community that lines the exposed sediment banks during the low water season (fig. 2); (2) the narrow band of dense *Cecropia*, typically found just behind the grass at the edge of várzea forest (fig. 2); (3) mixtures of grasses and short (less than 3 m) shrubs that bordered pastures or stream edges through open disturbed areas (fig. 7); (4) locally flooded grasslands (*campos inundáveis*; fig. 7); and low-relief areas within the forest (*baixios*) dominated by palm or *Heliconia* thickets; (5) active garden plots, comprised primarily of banana, manioc, and/or melons (fig. 8); (6) human-disturbed second growth, such as fallow, abandoned garden plots or areas where trees had been felled (termed *capoeira*); and (7) second-growth forest that represented successional stages following wind blow-downs or other types of natural disturbances. Views of the Rio Juruá during both the dry and rainy seasons, that is, at low and high water levels, are given in figs. 2 and 3. The terra firme habitat at Seringal Condor (locality **6**) is shown in fig. 4, and várzea during both dry (Barro Vermelho, locality **12**) and wet (Colocação Vira-Volta, locality **14**) seasons in figs. 5 and 6.

Fig. 3. View of the Rio Juruá at Sobral (locality **4**) in the Headwaters Region, looking east towards the right bank. The photograph was taken in March 1992, during the height of the rainy season. Note the lack of an exposed beach covered with grass, as in fig. 2, above; rather, the river meets, and sometimes penetrates, the edge of a narrow band of *Cecropia* with várzea forest just behind. The Rio Juruá is approximately 25 m wide at this point. Photograph by J. L. Patton.

HABITAT STRUCTURE

Structural differences between forests can have important implications for small mammals, and the organization of mammal com munities may reflect the vertical structure of the forest in which these communities exist (Malcolm, 1995). Consequently, we made an effort to compare terra firme and várzea forests with respect to both structure and floristics, as we were interested in comparing communities of terra firme and várzea forests in the absence of significant variation in habitat structure. To assess the consistency of habitat structure across our chosen sites, we focused on three types of data: understory density, vertical stratification of foliage, and the point-quadrat samples of trees greater than 10 cm diameter at breast height (DBH). These variables were examined at all standardized trap plots established in each forest type at each pair of opposite-bank localities (see fig. 1 and descriptions below).

METHODS: Understory density was measured on three of the traplines at each site by use of a 2.5 m pole, banded in 10 cm intervals. At each trap station, the pole was positioned 20 m into the forest at a point perpendicular to the trail, and the density of the understory was quantified by counting the number of bands that were at least partially obstructed by vegetation. In addition to comparing average understory density between the two forest types, we compared the average understory density calculated both within traplines (small-scale variability) and among traplines (large-scale variability).

Fig. 4. View of the interior of terra firme forest at Seringal Condor (locality **6**) in the Upper Central Region of the Rio Juruá. Note the thick understory and relatively closed canopy. Photograph by M.N.F. da Silva in September 1991.

We examined the vertical stratification of foliage along a transect 5 m parallel to each trapline at 5 m intervals. We made a vertical sighting into the canopy, using a 2.5 m pole, and scored vegetation thickness into six height intervals along the sighting: 0–2, 2–5, 5–10, 10–20, 20–30, and 30–40 m (see Malcolm, 1995). Height estimation was periodically checked with a range finder. We estimated the proportion of the interval covered by foliage to the nearest 25%. After multiplying the number of meters in the interval by the estimated foliage cover, we recorded these values as foliage thickness.

Finally, in the Lower Central Region, we also used the point-quadrat method to census trees with diameters of greater than 10 cm. We examined 600 trees in each forest type on each side of the river. Data collected included the diameter of the tree at breast height (DBH), its family, and its common name. In some cases, common names identified particular species; in others, these represented broader taxonomic units.

PATTERNS: Average understory density varied more from site to site in floodplain forests than in upland, terra firme forests, as did within-transect variance (fig. 9). Várzea sites in the central reaches of the river experienced more frequent and deeper flooding than sites in the headwaters, and as a result, had a more open understory. Understory density was similar between the two forest types in the Mouth Region, in part because the várzea sites sampled bordered terra firme and flooded only infrequently. We could not sample true floodplain forest because it was under water at the time we worked these sites (May–June). There was little evidence that the correlation between average understory density and within-trapline or among-trapline variability varied between forest types (fig. 9).

Structurally, the canopies of the two forest types were also quite similar (fig. 10), again indicating that we were generally successful in holding forest structure constant for community comparisons. In both, the canopy reached its greatest development in the 10–20 m interval. There was some indication that the várzea forests, on average, had a slightly lower canopy than terra firme forest. The vegetation was less dense at 10–20 m, but more dense as 5–10 m. Distributions of tree diameters in the two forest types also supported our impression of general structural similarity between them. Both forests were dominated by trees of small diameter, and large trees were approximately equally abundant (fig. 11). Total basal area was variable and not consistently higher in either várzea or terra firme forests.

However, in contrast to general structural similarity, the two forest types differed floristically. We ranked the 34 most abundant tree families at the two upland forest sites visited in the Lower Central Region and compared these rankings to the corresponding abundance in the two floodplain forests (fig. 12). The pattern of rank abundance differed greatly between the two; some families

Fig. 5. View of the interior of várzea forest at Barro Vermelho (locality **12**) in the Lower Central Region of the Rio Juruá. The photograph was taken in October 1991 during the dry season. Note the open forest with extensive leaf litter but few understory plants. Photograph by J. L. Patton.

common in terra firme forest were rare in the várzea, or vice versa. We found these same differences at the lower taxonomic level using common names. The ten most common taxa in upland forest were not necessarily common in the várzea, nor was the reverse true (fig. 13). We also obtained evidence of a major difference in floristic diversity between the two forest types within the Lower Central Region. We recorded 227 taxa (by common name) in terra firme but only 142 in the várzea. In the former, 50% of the 1200 trees counted were in 23 taxa, whereas in the latter, 50% of the trees represented only 12 taxa. A similar pattern of lower species diversity in floodplain versus upland forests has been reported for many taxa, including plants (Dumont et al., 1990; Klinge et al., 1990), termites (Martius, 1994), and ants (Wilson, 1987; Majer and Delabie, 1994).

SAMPLE DESIGN AND EFFORT

Each of the eight paired cross-river sample sites was comprised minimally of a set of terra firme standardized trap lines on one side and a várzea set on the opposite. This design resulted from the sinuous nature of the river—where a bend would abut against a high bank with terra firme forest on one side, the opposite bank always consisted of an extensive várzea floodplain (views in figs. 2 and 3). Because of this limitation, each of the two pairs of sites within a sample region specifically contained a set of terra firme lines on only one side of the river. However, because we set up two pairs, the result was one set of terra firme lines on opposite sides. At some pairs of opposite-bank sites, we established várzea standardized lines on both sides of the river. Secondary trap lines were also established at most sites; these were designed specifically to sample habitat types (e.g., *pantanos*, *campos inundáveis*, and *Cecropia* riverine edge) not available at either the terra firme or várzea standardized plots. Such secondary trap lines were grossly uneven in effort, both in the number of traps per line and the number of nights maintained.

Fig. 6. View of the edge of flooded várzea forest at Colocação Vira-Volta (locality **14**) in the Mouth Region of the Rio Juruá. The photograph was taken by M. N. F. da Silva in early June 1992, during the end of the high-water season.

At all sites in both upland and terra firme forest, we cut a central trail perpendicular to the edge of the river and established five or six 280 m long trails perpendicular to the central trail and spaced at 150 m intervals. The area covered was, thus, approximately 170 hectares. When we trapped in the floodplain forest on both sides of the river at a particular pair of sites, we established only two or three parallel trails per side. Traplines were established along each parallel trail and consisted of 15 trap-stations spaced at 20 m intervals, with the first line inland at least 100 m from early successional habitats along the river edge. Trap-station design followed Malcolm (1991a). Traps were placed in the most likely microhabitat within 2 to 4 m of the station marker. All lines had terrestrial trap stations, each with a single folding Sherman live trap (8 × 8 × 23 cm) and Tomahawk live trap (model number 203; 14 × 14 × 40 cm). We used two trap sizes to lessen biases to particular size classes of mammals. In addition, three of the lines also had canopy platform trap stations (as described by Malcolm, 1991a) above each terrestrial station point; each with a Sherman trap placed on top of a Tomahawk trap (fig. 14). Canopy trap height, measured with a rangefinder to the nearest 0.1 m, averaged 11.9 m in terra firme forest (n = 345, standard error = 0.13, range = 6.6–19.2 m) and 10.3 m in várzea forest (n = 375, standard error = 0.13, range = 2.5–20.7 m). Pulleys were used to raise and lower the traps and were attached to wood or plastic (PVC) frames that were transported between sites. There were, thus, 150 terrestrial and 90 canopy traps on each standardized plot. Terrestrial traps were left open for a minimum of seven consecutive nights (1050 ''trap nights'' per locality) and canopy traps for 12 consecutive nights (1080 ''trap nights'' per locality). We left canopy traps open longer because we hoped to partly compensate for the higher sampling variability among sites in the canopy sample due to

Fig. 7. View of pasture and inundated grassland at Penedo (locality 7) in the Upper Central Region of the Rio Juruá. The dense grassy area in the foreground that is crossed by wooden planks is partly flooded. Both *Holochilus sciureus* and *Nectomys apicalis* were obtained here. Photograph by J. L. Patton in early September 1991.

fewer trap-stations per site and overall lower capture success in the canopy. All individual lines were uniquely identified, as were trap stations along each line, and all specimens collected were recorded as to line, trap station, and trap type. For bait, we used ripe plantains and a mixture of ground peanuts, whole oats, vegetable oil, and honey. Canopy traps in addition had a small cloth sack filled with raisins and the peanut mixture, which served as a long-term bait source (Malcolm, 1991a). Terrestrial traps were rebaited daily, whereas canopy traps were rebaited only when they had a capture or were otherwise disarmed.

Our goal was to maintain the same standardized trap design and effort at all sites, both terra firme and várzea. However, several problems limited our ability to standardize everything in such an explicit fashion. For example, it was not always possible to establish a rectangular array of five parallel lines due to local aspects of topography or differences in forest structure. Moreover, since we wanted to place all standardized lines only in undisturbed forest, we were often forced to modify the placement of trap lines to avoid disturbed habitats. Finally, in some regions (e.g., Lower Central), we sampled várzea on both sides of the river at each site. Because of equipment and time limitations, this resulted in a reduced trap line design at these localities. We also lost a considerable amount of equipment when our boat sank in the upper Rio Juruá on February 3, 1992 (figs. 15 and 16). This required a shift in total trap effort in the Headwaters and Mouth regions, in comparison to that in the central regions.

Table 2 summarizes trap effort, by trap

Fig. 8. View of a fallow garden at Penedo (locality **7**) in the Upper Central Region of the Rio Juruá. *Didelphis marsupialis*, *Oryzomys perenensis*, and *Proechimys cuvieri* were especially common in this habitat. Photograph by J. L. Patton in late August 1991.

type and habitat, for each of the 16 individual localities sampled.

LOCALITY DESCRIPTIONS

Headwaters Region (fig. 17; RadamBrasil 1:250,000 Folha Porto Walter, SC.18-X-B, 1977).

Sample sites within this region are midway along the river between Porto Walter and Taumaturgo in the state of Acre. The primary sites at Igarapé Porongaba are approximately 35 straight-line km upriver from Sobral and Nova Vida. The communities of Flora (locality ''a'') and Ocidente (locality ''b'') are between these primary sites (fig. 17). The river is narrow (less than 40 m wide) throughout most of the area, and it lacks the large sweeping meanders characteristic of many stretches downriver. Narrow várzea, always less than 3 km wide, is present along both sides. However, locals report that flooding occurs only periodically, on an approximately 5-year cycle rather than annually. Consequently, the várzea habitat is quite different than that of all downriver sites, characterized by an extensive and dense understory. In general, there is, and has been, a heavier impact by colonists in the upper reaches of the Rio Juruá than in the central or lower regions. This is evident both by the increased number of settlements and individual houses located along the river margin, but also by the second-growth nature of much of the forest adjacent to the river edge, even well away from current human occupation sites.

Localities **1** (Porongaba) and **2** (opposite Porongaba). Porongaba is the name given to a small stream (*igarapé*) in an uninhabited area located on the right bank of the Rio Juruá at approximately 8°40′S, 72°47′W, upriver from the small community of Flora (also called Fazenda Santa Fé). Camp was established on the bluff overlooking the river in disturbed second growth forest (*capoeira*)

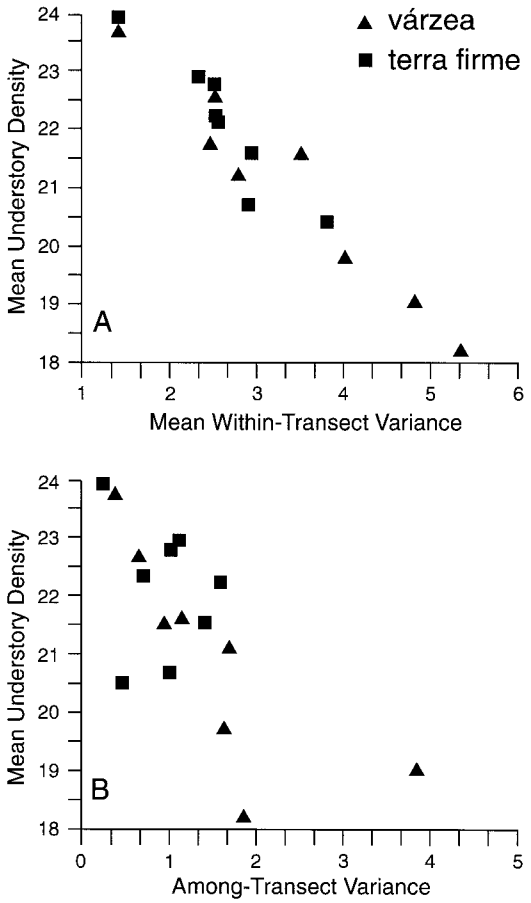

Fig. 9. Average understory density plotted against mean within-transect variance **(A)** or mean among-transect variance **(B)**. At each site, understory density was measured at 15 points spaced at 20 m intervals along each of three parallel 280 m transects.

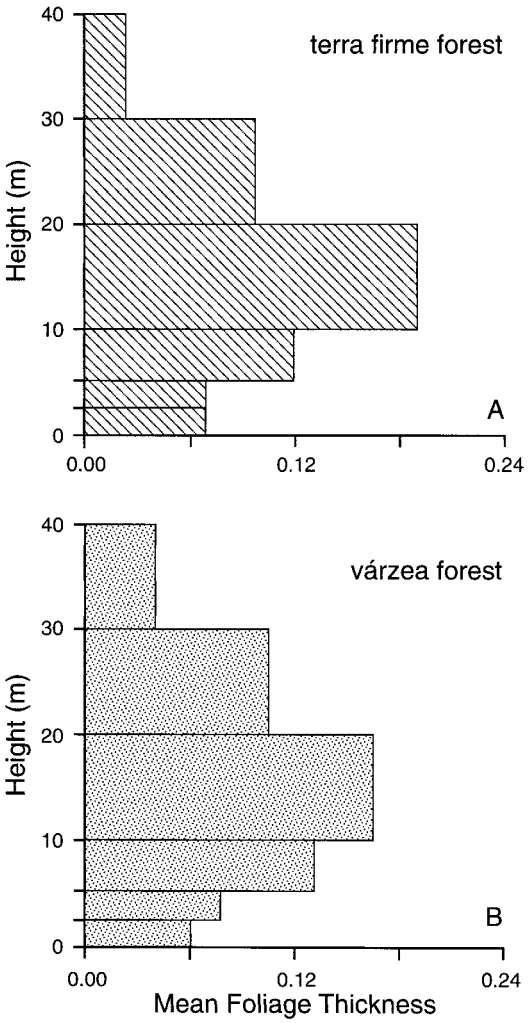

Fig. 10. Average foliage density at six height intervals averaged across eight sites in upland, terra firme forest **(A)** and eight sites in floodplain, várzea forest **(B)**. At each site, foliage thickness was measured at 57 points at 5 m intervals on each of three parallel transects.

about 10 to 40 years old and adjacent to a large area of bamboo (*tabôca*) that was regrowing following a major flowering about 5 to 7 years previously (fig. 18). Terra firme forest was located approximately 3 km inland from the river's edge. Two Tomahawk trap lines were established in the *capoeira* (lines 1 and 2) and a second placed in the *tabôca* (line P). These were run periodically, but for a total of only 5 nights each (table 2). Standardized trap plots were placed in terra firme forest, approximately 2.6 km from the river on the right bank. Five lines were comprised of terrestrial stations (F, and H through K); two with canopy platforms (N and O). A second standardized plot was located in várzea forest directly across from camp on the left bank of the Rio Juruá (fig. 19). This was comprised again of five lines of terrestrial stations (A through E) and two of canopy platforms (L and M). The first trap line began at 180 m inland from the water's edge. Locals call the habitat *restinga alta*, meaning ''high várzea.'' Two of the lines (A and B) were dominated by a dense area of *Heliconia*, indicative of low and wet soils but

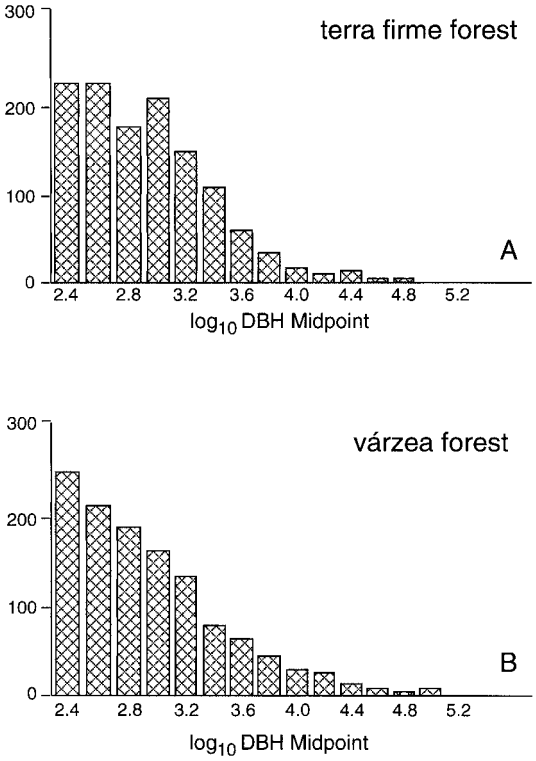

Fig. 11. Log_{10}DBH (diameter in cm at breast height) distribution of **(A)** 1200 trees in terra firme forest (600 on each side of the Rio Juruá) and **(B)** 1200 trees in várzea forest (600 on each side of the river).

not long-term inundation. We were at this site for 18 days during the rainy season, from February 14 to March 3, 1992.

Localities **3** (Nova Vida) and **4** (Sobral). Sobral was a single family site with a small saw mill on the left bank of the Rio Juruá at 8°22′S, 72°49′W (fig. 10); a photograph of the river taken from Sobral and looking across to Nova Vida is given in fig. 3. The locality is identified as Nova Vida on the Projeto RadamBrasil map (Folha Porto Walter, SC.18-X-B, 1977), but locals place Nova Vida on the right bank, opposite Sobral. The left side of the river exhibits considerable topographic relief, with relatively steep-sided hills 30 or more m in height. The area immediately adjacent to the river at this site has been cleared for pasture (fig. 20). Several small streams entered the river at points though the pasture and adjacent second growth *capoeira* forest. Camp was established in an abandoned house at the edge of *capoeira*. The standardized terra firme trap line began approximately 450 m to the west-northwest of camp following an established trail and bordering a large area of 10–30 year old capoeira (fig. 21). All five lines had terrestrial stations (A through E), and three had canopy platforms (K through M). In addition, nonstandardized Tomahawk live trap lines were run along the shrub border of the pasture, in an abandoned garden, and inside the second-growth forest; one Victor rat trap line was established along a trail in *capoeira* and second-growth forest. Nova Vida was located directly opposite Sobral on the right bank. The line began approximately 315 m from the water's edge, with five lines placed in a decidedly nonparallel fashion due to exigencies of local topography and habitat (fig. 21). Five terrestrial (F through J) and three canopy lines (N–P) were established. We worked at this site from March 5 to March 27, 1992.

Upper Central Region (fig. 22; RadamBrasil 1:250,000 Folha Itaquaí, SB.19-Y-A, 1978).

This region is about 300 km downriver by air from the Headwaters region (fig. 1). The two pairs of sites from this region are more than 10 km apart by air, and were chosen because they are the only sites where terra firme is adjacent to the left and right banks, respectively. Sacado (locality **5**) and Condor (**6**) are essentially opposite one another, but the downriver várzea site of Nova Empresa (**8**) was located about 1.5 km upriver from its paired terra firme site at Penedo (**7**).

Localities **5** (Sacado) and **6** (Condor). Seringal Condor is on the left bank of the Rio Juruá at approximately 6°45′S, 70°51′W (fig. 23). At the time of our visit (September 12 through October 8, 1991) the area was unoccupied, except for a single caretaker. The river meander on the left side cuts directly to terra firme, with a high (about 30 m) bluff overlooking the river (fig. 2). The right bank slopes gently, with an exposed sandbar dominated by coarse grasses at the river's edge grading into *Cecropia* and eventually várzea forest 100 or more m inland. Open pasture grazed by cattle characterizes the immediate

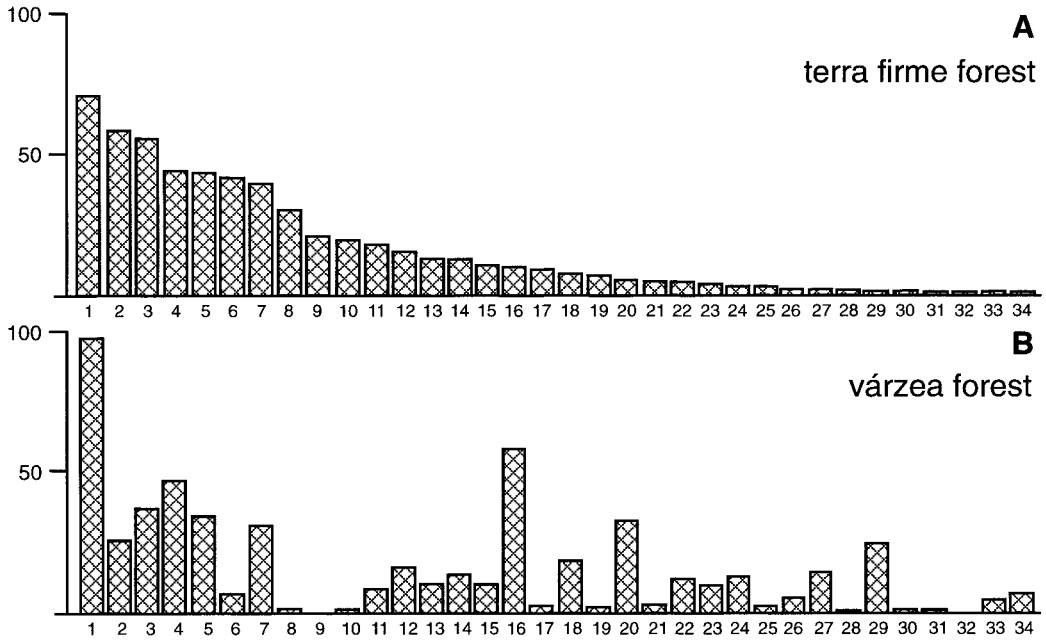

Fig. 12. Rank abundance of the 34 most common tree families in **(A)** terra firme forest and their corresponding abundances in **(B)** várzea forest (n = 1200 trees in each). Families: 1, Leguminosae; 2, Moraceae; 3, Lecythidaceae; 4, Sapotaceae; 5, Myristicaceae; 6, Palmae; 7, Chrysobalanaceae; 8, Burseraceae; 9, Musaceae; 10, Violaceae; 11, Lauraceae; 12, Euphorbiaceae; 13, Sterculiaceae; 14, Elaeocarpaceae; 15, Humiriaceae; 16, Annonaceae; 17, Vochysiaceae; 18, Meliaceae; 19, Ochinaceae; 20, Rubiaceae; 21, Melastomataceae; 22, Guttiferae; 23, Apocynaceae; 24, Malpighiaceae; 25, Combretaceae; 26, Tiliaceae; 27, Nyctaginaceae; 28, Celastraceae; 29, Myrtaceae; 30, Anacardiaceae; 31, Sapindaceae; 32, Simaroubaceae; 33, Bombacaeae; and 34, Olacaceae.

area on the left bank. A small stream (*igarapé*) with steep banks and bordered by a narrow, short-stature riparian community cuts northwest through the pasture, to enter the forest about 400 m from the river's edge. Downriver, a high bluff drops abruptly to a narrow zone of várzea forest. Upriver is an extensive exposed sandbar, covered with grasses and a small patch under cultivation that abuts a tract of várzea forest. We established five terrestrial (lines C through G) and three canopy platform (M–O) standardized lines in undisturbed, terra firme forest approximately 1 km to the north of the river's edge. The habitat along these lines is illustrated in fig. 4, and the trap lines are mapped in fig. 24. The area exhibits considerable topographic relief, with steeply rising ridges dissected by small streams.

We placed the várzea standardized lines on the right bank, about 1000 m upriver from Condor. The layout was the same as for the terra firme design, with five terrestrial (H through L) and three canopy lines (J–L; fig. 24). The first line began 120 m from the river's edge, extending about 70 m into the forest to near the edge of an oxbow lake.

In addition to the standardized lines, we had secondary lines of live traps in várzea forest on the left bank slightly downriver from the pasture of Seringal Condor. Also, we put three snap trap lines, run for several days each, in the pasture and grass edges on the Condor side of the river as well as in the thicket along the small *igarapé*. Finally, we placed a line of Victor snap traps on the right bank of the river directly opposite Seringal Condor within the grass and *Cecropia* that occurred along the river's margin (fig. 23 and table 2).

Localities **7** (Penedo) and **8** (Nova Empresa). Located approximately 12 km by air downriver from Condor and Sacado, these two localities are themselves separated by

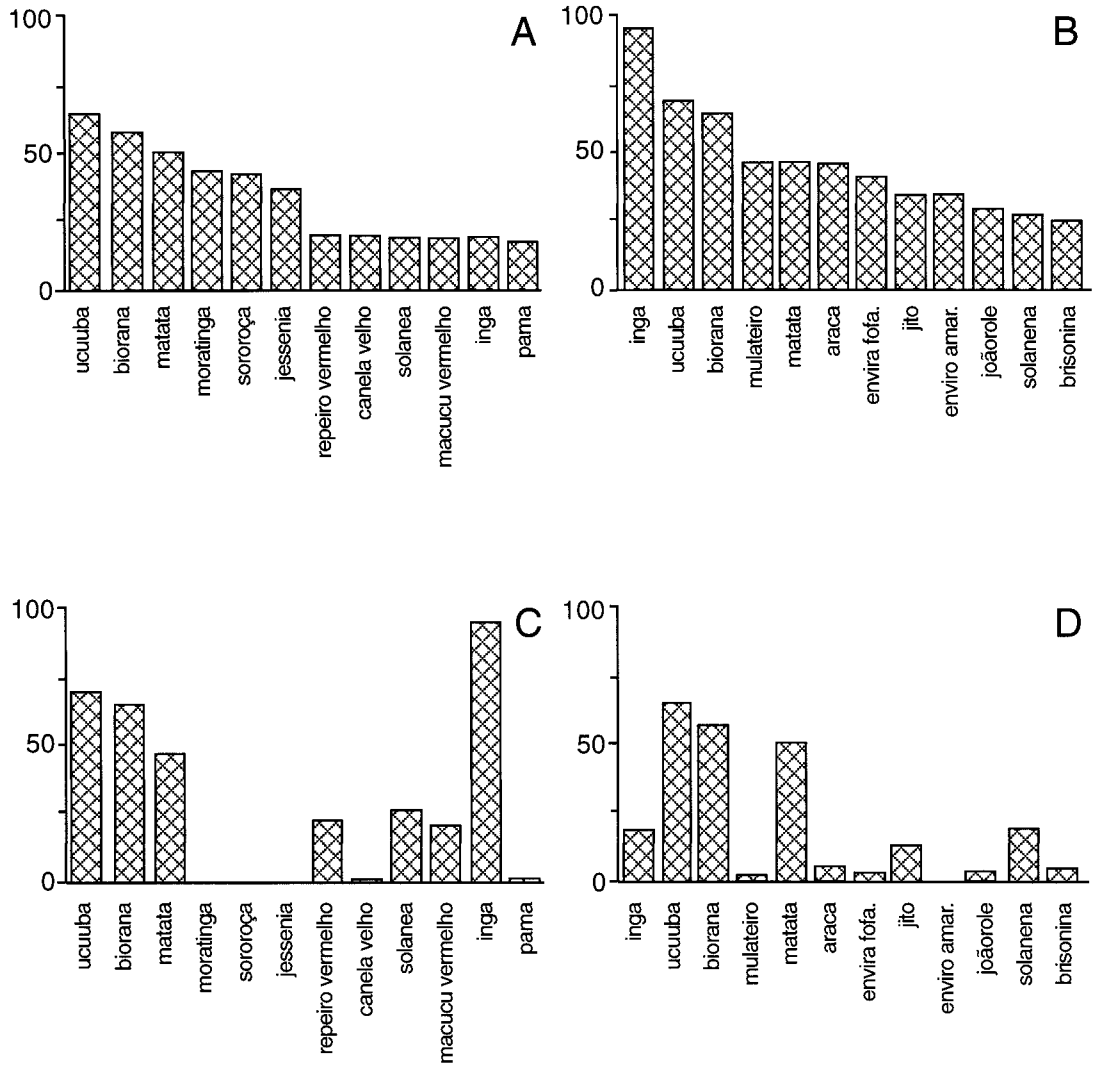

Fig. 13. Rank abundances of the 10 most common trees (as identified by local common name) by forest type: **A**, terra firme forest; **B**, várzea forest; **C**, terra firme forest trees in várzea forest; and **D**, várzea forest trees in terra firme forest. Six hundred trees were censused in each forest type on each side of the river. Data from Lower Central Region sites only.

1.5–2 km along the river. Penedo is on the right bank of the Rio Juruá, at approximately 6°50′S, 70°45′W, a point where a large meander of the river abuts terra firme (fig. 25). Two families lived at the site at the time of our visit (August 21 to September 9, 1991). A high, extensive sandbar separates a narrow, elongated lake from the river's edge, beyond which the land slopes through inundated grass and forest to cleared pasture, old garden plots, second-growth forest, and, eventually, to terra firme forest (fig. 7). People have used the area for an extended period, and a Kulina indigenous reserve is located a short distance to the southeast. The topography on the right side of the Rio Juruá through this central section of the river is one of low, sloping relief; it differs markedly from the high relief of terra firme sites on the left bank of the river. We placed the standardized trap lines (fig. 26) in terra firme forest approximately 1 km from the river's edge.

Fig. 14. A Malcolm-style (Malcolm, 1992) canopy platform operated by a pulley and line system and carrying a Sherman live trap placed on top of a Tomahawk live trap. Photograph than by M. N. F. da Silva in September 1991 at Seringal Condor (locality **6**).

Seven roughly parallel trap lines were in this plot; the first two had Victor rat traps that we ran for only three days total. The terrestrial lines were H through L; canopy lines were S through U (fig. 26). We placed additional trap lines of Victor rat traps in the other major microhabitats. Four of these were in the grass and shrubs atop the large sand hill fronting the river; one was in flooded forest to the immediate south of the small lake; and one line was run for three nights in the inundated grassland (fig. 7). Finally, we also ran lines of Tomahawk live traps in the flooded forest fronting the small lake and in an abandoned banana garden at the edge of second-growth forest (fig. 8).

Because of the large meander that abutted the terra firme at Penedo, a very narrow peninsula of várzea forest occurred on the opposite side of the river. Concerned for peninsular effects, we placed the várzea standardized line at Igarapé Nova Empresa, located on the left bank at approximately 6°48′S, 70°44′W, about 2 km upriver from Penedo (fig. 22). The actual physical conformation of the lines was modified to accommodate the presence of a small *igarapé* on the west and a large expanse of low stature, second-growth forest to the east (fig. 26). The habitat was otherwise undisturbed várzea, with large emergent trees and a very open understory. Here we established five terrestrial (M–R) and three canopy (V–X) lines. The first line began about 230 m in from the river edge, 150 m from the edge of the forest, with the last line ending at the 980 m mark.

Lower Central Region (fig. 27;
RadamBrasil 1:250,000 Folha Rio Xeruã,
SB.19-Z-A, 1978).

Located approximately 216 airline km downriver from Penedo, this region similarly consists of two pairs of opposite-bank localities. Altamira (locality **9**) is a terra firme site

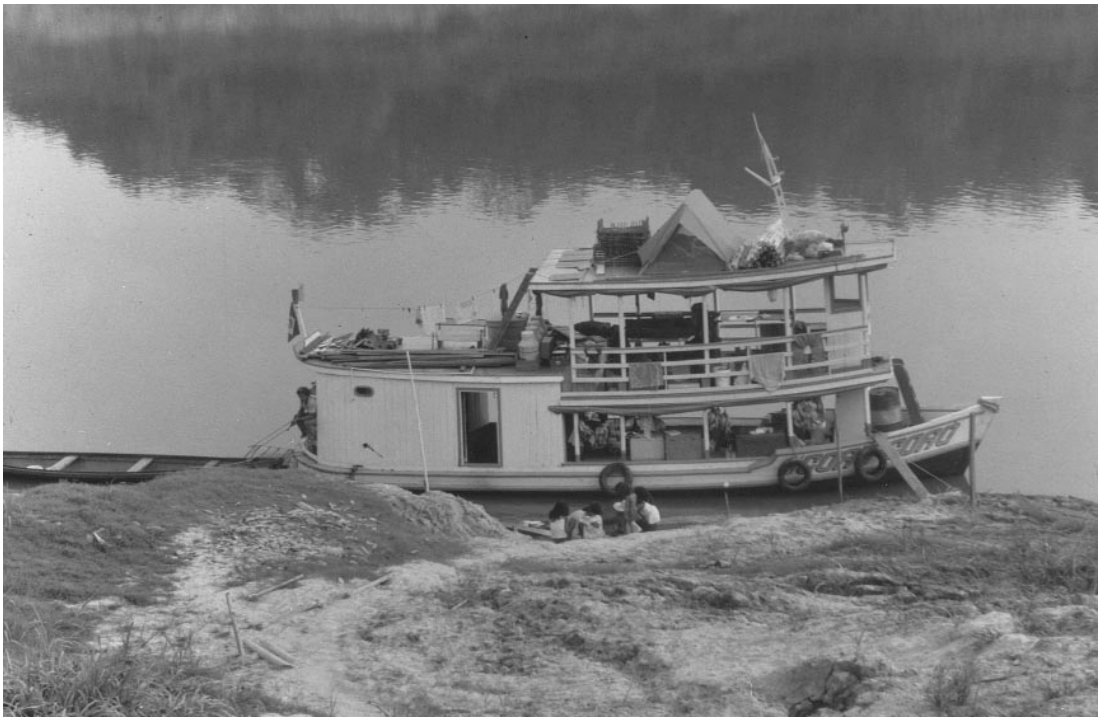

Fig. 15. Our ''research'' vessel, the *Coró-Coró*, a 13-m boat powered by a 25-hp inboard motor and purchased in Manacaparú, near Manaus. Photograph taken by J. L. Patton at Gregorio, near the mouth of the Rio Gregorio in the central Rio Juruá, August 1991.

on the right bank of the river, facing a várzea site (locality **10**; called ''opposite Altamira'') on the left bank immediately opposite. We placed a second várzea line on the left bank at Boa Esperança, at a distance about 4.5 km upriver from Altamira. Jainu (locality **11**), a várzea site on the right back, and Barro Vermelho (locality **12**), a terra firme site on the left bank, occur approximately 20 km (airline) further downriver.

Localities **9** (Altamira) and **10** (opposite Altamira). Altamira is a small community of several families, with their houses and a large cleared garden area on a bluff above the river, at coordinates 6°35′S, 68°54′W (fig. 28). We built a camp adjacent to a small stream in the narrow strip of várzea forest, inland of an exposed expanse of grass bordering the river. The area slopes gently from the river's edge, except around the house and garden, which are elevated some 30 m above the water. Our standardized trap lines were close to the edge of the terra firme, approximately 500 m inland from the river (fig. 29). An extensive area of low ground (*baixios*), dominated by small palms and clearly seasonally inundated, extended along the western edge of the lines. This resulted in the first line being displaced slightly in relation to the other four. This design contained five terrestrial (A–E) and three canopy (L–N) lines. The várzea standardized plot was on the left bank of the river directly opposite our campsite (fig. 29). Except for a narrow border of grass on the exposed sand beach, the forest is undisturbed and extends nearly to the water's edge. This plot contained three terrestrial (F–H) and two canopy (O, P) lines, the first of which began 120 m from the water. Six additional live trap or snap trap terrestrial lines were established in secondary habitats, four on the right bank and two on the left (fig. 28). In order to sample várzea in a standardized fashion on both sides of the river, we also established a standardized trap plot at Boa Esperança (locality **9a**), about 4.5 km upriver from Altamira (6°32′S, 68°55′W). This site contained two parallel lines, each

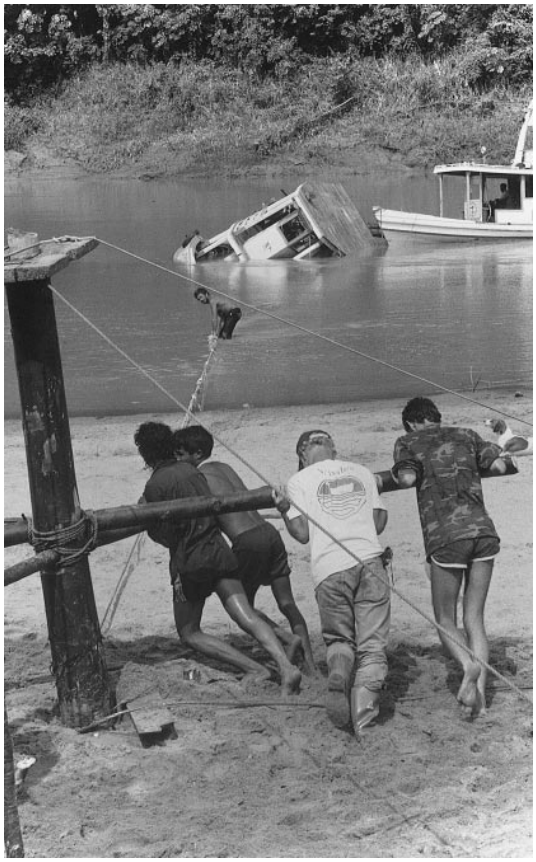

Fig. 16. Attempt to salvage the *Coró-Coró* after it sank following a collision with a submerged log on February 3, 1992, approximately 2 km below the community of Ocidente (locality **b**), in the headwaters of the Rio Juruá. Photograph taken by M. N. F. da Silva.

with both terrestrial (J, I) and canopy (Q, R) stations (fig. 29). We visited this set of sites from November 7 through November 24, 1991.

Localities **11** (Jainu) and **12** (Barro Vermelho). At approximately 6°28′S, 68°46′W, this pair of localities is some 20 airline km downriver from Altamira (fig. 27). Barro Vermelho (''red mud'') is so named because of the very high, exposed red-clay bluff on the left side of the river. The RadamBrasil maps show Jainu to be at this location, but locals apply this name to a small *igarapé* on the right bank of the river. Two families were living at Barro Vermelho at the time of our visit, from 14 October through 6 November, 1991. The immediate area adjacent to the edge of the river had been cleared, with an expanse of coarse and deep grass surrounding several mature banana trees, active garden plots of banana, melons, and other produce, and a large freshly-cleared and burned plot (fig. 30). The ground along the river upstream from the houses sloped sharply to near the level of the river, with mature várzea forest extending to the west and northwest. Second-growth terra firme forest occurred immediately behind (north) of the dwellings, and mature terra firme forest was about 250 m inland. We established a camp inside but close to the edge of the terra firme forest. Our terra firme standardized line began about 150 m from camp, at a straight-line distance of approximately 350 m from the river's edge. As with all left bank terra firme sites in the central portion of the Rio Juruá, this is an area of relatively sharp relief, with steep-sided slopes coursing down to narrow streams. We used an available trail that went along a ridge to establish the five parallel standardized trapping lines (fig. 31). As with other terra firme sites, this plot contained five lines of terrestrial trap stations (F–J), three of which also had canopy platforms (O–Q). Besides the standardized lines, we also established either Tomahawk, Sherman, or Victor rat trap secondary lines in the old and new garden plots and grassland bordering the river margin. We also established a várzea standardized plot on the left bank of the river, about 250 m upriver from Barro Vermelho (fig. 5). This plot had two lines, both with terrestrial (A, B) and canopy stations (T, U; fig. 31). A secondary line of Victor rat traps was also placed in this forest. Finally, we placed a line of 45 stations, each with a Sherman and Tomahawk live trap, in várzea forest approximately 500 m upriver from this site.

On the right bank of the river, we placed our standardized várzea line inland approximately 150 m from the edge of the river (fig. 31). At this time of year, the river border had about 20 m of exposed grass and small shrubs, followed by nearly 30 m of *Cecropia* before várzea forest was encountered. The standardized plot consisted of three parallel lines, all of which had terrestrial stations (C–E) and two of which also had canopy platforms (R, S). In addition, we placed a line

TABLE 2

Trap Effort, Trap Type, Habitat, and Placement at Each of 16 Primary Sampling Localities on the Rio Juruá

Locality numbers refer to those in the map, figure 1.

Locality	Trap line	Trap type	Habitat[a]	Placement	Effort[b]
Porongaba-R	standardized	Tomahawk	terra firme	terrestrial	735
(locality **1**)	standardized	Sherman	terra firme	terrestrial	735
	standardized	Tomahawk	terra firme	canopy	390
	standardized	Sherman	terra firme	canopy	390
	other[c]	Tomahawk	*taboca*	terrestrial	104
	other[c]	Tomahawk	*taboca*	canopy	88
	other[c]	Sherman	*taboca*	terrestrial	296
	other[c]	Sherman	*taboca*	canopy	232
	other[c]	Sherman	grass	terrestrial	80
				TOTAL	3050
Porongaba-L	standardized	Tomahawk	várzea	terrestrial	600
(locality **2**)	standardized	Sherman	várzea	terrestrial	600
	standardized	Tomahawk	várzea	canopy	360
	standardized	Sherman	várzea	canopy	360
				TOTAL	1920
Nova Vida	standardized	Tomahawk	várzea	terrestrial	600
(locality **3**)	standardized	Sherman	várzea	terrestrial	600
	standardized	Tomahawk	várzea	canopy	600
	standardized	Sherman	várzea	canopy	600
				TOTAL	2400
Sobral	standardized	Tomahawk	terra firme	terrestrial	570
(locality **4**)	standardized	Sherman	terra firme	terrestrial	570
	standardized	Tomahawk	terra firme	canopy	615
	standardized	Sherman	terra firme	canopy	615
	other[c]	Tomahawk	várzea	terrestrial	105
	other[c]	Sherman	várzea	terrestrial	105
	other[c]	Sherman	*capoeira*	terrestrial	210
	other[c]	Sherman	*capoeira*	canopy	210
				TOTAL	3000
Sacado	standardized	Tomahawk	várzea	terrestrial	525
(locality **5**)	standardized	Sherman	várzea	terrestrial	525
	standardized	Tomahawk	várzea	canopy	630
	standardized	Sherman	várzea	canopy	630
	other[c]	Victor rat	grass	terrestrial	120
				TOTAL	2310
Condor	standardized	Tomahawk	terra firme	terrestrial	585
(locality **6**)	standardized	Sherman	terra firme	terrestrial	585
	standardized	Tomahawk	terra firme	canopy	690
	standardized	Sherman	terra firme	canopy	690
	other[c]	Tomahawk	terra firme	terrestrial	500
	other[c]	Tomahawk	várzea	terrestrial	195
	other[c]	Sherman	grass/shrubs	terrestrial	820
	other[c]	Victor rat	grass/shrubs	terrestrial	322
				TOTAL	4387

TABLE 2
(Continued)

Locality	Trap line	Trap type	Habitat[a]	Placement	Effort[b]
Penedo	standardized	Tomahawk	terra firme	terrestrial	675
(locality **7**)	standardized	Sherman	terra firme	terrestrial	675
	standardized	Tomahawk	terra firme	canopy	495
	standardized	Sherman	terra firme	canopy	495
	other[c]	Tomahawk	grass/shrubs	terrestrial	107
	other[c]	Sherman	grass/shrubs	terrestrial	330
	other[c]	Victor rat	grass/shrubs	terrestrial	257
				TOTAL	3034
Nova Empresa	standardized	Tomahawk	várzea	terrestrial	525
(locality **8**)	standardized	Sherman	várzea	terrestrial	525
	standardized	Tomahawk	várzea	canopy	488
	standardized	Sherman	várzea	canopy	488
				TOTAL	2026
Altamira	standardized	Tomahawk	terra firme	terrestrial	735
(locality **9**)	standardized	Sherman	terra firme	terrestrial	735
	standardized	Tomahawk	terra firme	canopy	585
	standardized	Sherman	terra firme	canopy	585
	other[c]	Tomahawk	várzea	terrestrial	90
	other[c]	Sherman	garden	terrestrial	192
	other[c]	Victor rat	garden	terrestrial	52
	other[c]	Victor rat	terra firme	terrestrial	141
	other[c]	Victor rat	terra firme	canopy	141
				TOTAL	3256
Boa Esperança	standardized	Tomahawk	várzea	terrestrial	210
(locality **9a**)	standardized	Sherman	várzea	terrestrial	210
	standardized	Tomahawk	várzea	canopy	405
	standardized	Sherman	várzea	canopy	405
				TOTAL	1230
Opposite Altamira	standardized	Tomahawk	várzea	terrestrial	405
(locality **10**)	standardized	Sherman	várzea	terrestrial	405
	standardized	Tomahawk	várzea	canopy	405
	standardized	Sherman	várzea	canopy	405
	other[c]	Tomahawk	grass	terrestrial	16
	other[c]	Sherman	grass	terrestrial	59
				TOTAL	1695
Jainu	standardized	Tomahawk	várzea	terrestrial	450
(locality **11**)	standardized	Sherman	várzea	terrestrial	450
	standardized	Tomahawk	várzea	canopy	420
	standardized	Sherman	várzea	canopy	420
	other[c]	Tomahawk	várzea	terrestrial	180
	other[c]	Sherman	várzea	terrestrial	180
	other[c]	Sherman	grass	terrestrial	54
	other[c]	Victor rat	várzea	terrestrial	192
	other[c]	Sherman	garden	terrestrial	90
				TOTAL	2436
Barro Vermelho	standardized	Tomahawk	terra firme	terrestrial	750
(locality **12**)	standardized	Sherman	terra firme	terrestrial	750
	standardized	Tomahawk	terra firme	canopy	735

TABLE 2
(Continued)

Locality	Trap line	Trap type	Habitat[a]	Placement	Effort[b]
Barro Vermelho	standardized	Sherman	terra firme	canopy	735
(locality **12**)	standardized	Tomahawk	várzea	terrestrial	360
(continued)	standardized	Sherman	várzea	terrestrial	360
	standardized	Tomahawk	várzea	canopy	390
	standardized	Sherman	várzea	canopy	390
	other[c]	Tomahawk	grass/shrub	terrestrial	168
	other[c]	Sherman	grass	terrestrial	334
	other[c]	Victor rat	terra firme	terrestrial	192
	other[c]	Victor rat	terra firme	canopy	192
	other[c]	Victor rat	garden	terrestrial	182
				TOTAL	5538
Ilha Paxiuba	standardized	Tomahawk	várzea	terrestrial	240
(locality **13**)	standardized	Sherman	várzea	terrestrial	240
	standardized	Tomahawk	várzea	canopy	390
	standardized	Sherman	várzea	canopy	390
				TOTAL	1260
Vira-Volta	standardized	Tomahawk	terra firme	terrestrial	525
(locality **14**)	standardized	Sherman	terra firme	terrestrial	525
	standardized	Tomahawk	terra firme	canopy	630
	standardized	Sherman	terra firme	canopy	630
	standardized	Tomahawk	*igapó* edge	terrestrial	315
	standardized	Sherman	*igapó* edge	terrestrial	315
	standardized	Tomahawk	*igapó* edge	canopy	180
	standardized	Sherman	*igapó* edge	canopy	180
				TOTAL	3300
Vai-Quem-Quer	standardized	Tomahawk	terra firme	terrestrial	525
(locality **15**)	standardized	Sherman	terra firme	terrestrial	525
	standardized	Tomahawk	terra firme	canopy	630
	standardized	Sherman	terra firme	canopy	630
	standardized	Tomahawk	*igapó* edge	terrestrial	315
	standardized	Sherman	*igapó* edge	terrestrial	315
	standardized	Tomahawk	*igapó* edge	canopy	210
	standardized	Sherman	*igapó* edge	canopy	210
	other[c]	Sherman	terra firme	terrestrial	180
	other[c]	Sherman	terra firme	canopy	180
				TOTAL	3720
Ilhazinha	standardized	Tomahawk	*igapó* edge	terrestrial	210
(locality **16**)	standardized	Sherman	*igapó* edge	terrestrial	210
	standardized	Tomahawk	*igapó* edge	canopy	420
	standardized	Sherman	*igapó* edge	canopy	420
				TOTAL	1260
				GRAND TOTAL	45,822

[a] Habitat: includes terra firme and várzea forest, "*taboca*" (dead but regrowing bamboo stands), grass stands bordering the river on seasonally exposed sand bars, "*capoeira*" (second growth forest due either to natural or human-caused disturbance), and localized active garden plots. "*Igapó* edge" refers to the edge of várzea forest at the time of annual inundation.

[b] (Trap) effort: the number of each type of trap set each 24-hour period (trap "night"); in general, traps were baited in the morning and checked again the following morning.

[c] Other (trap line): all trap lines exclusive of the standardized lines placed in either terra firme or várzea forest.

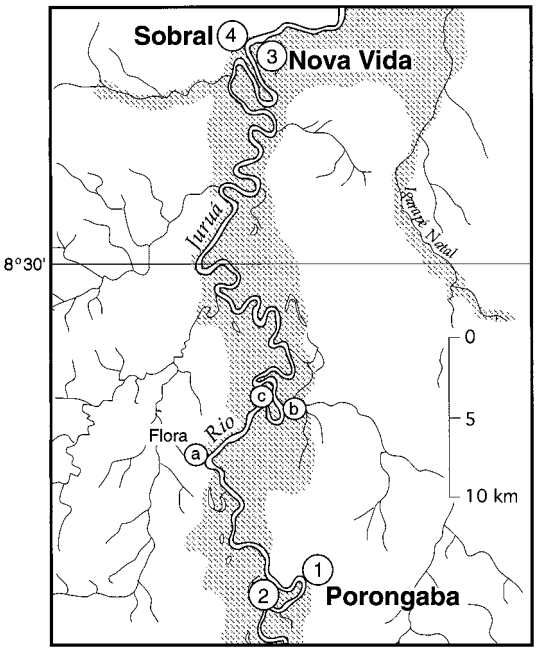

Fig. 17. Headwaters Regional Area of the Rio Juruá in the state of Acre, Brazil. Primary sample localities are designated by numbers, secondary sites by lower-case letters (see text for precise locality information). Hatching bordering the river indicates the extent of várzea forest, although this forest type does not flood annually here, but only on about a five year, or longer, schedule. Redrawn directly from RadamBrasil 1: 250,000 series, Folha Porto Walter (SC.18-X-B), 1977.

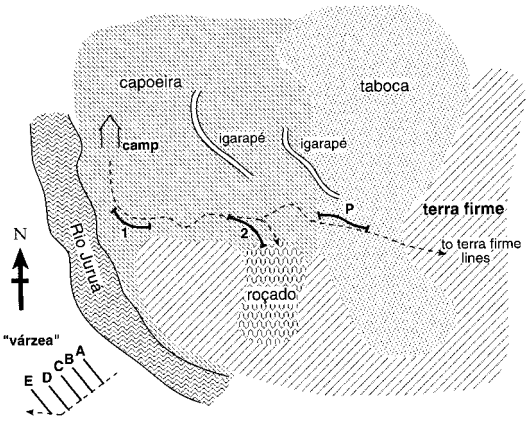

Fig. 18. Detailed map of the Rio Juruá at Igarapé Porongaba (localities **1** and **2**), illustrating position of camp relative to major habitat types, secondary trap lines (bold numbered lines) and placement of *t*erra firme and várzea standardized lines. *Capoeira* is secondary regrowth of human disturbed forest; *tabôca* is regrown bamboo forest following a major bloom approximately 5–7 years previous to our sampling; *roçado* is active garden plots (see text for further details). Not drawn to scale.

of 48 Victor snap traps along the central trail interior from the last standard line, 30 Sherman live traps in the grass along the edge of the river near the entrance to the standardized trail system, 30 Tomahawk and Sherman live traps in várzea forest about a kilometer downriver, and 30 Sherman traps in a garden of melons on the exposed beach about 750 m downriver.

Mouth Region (fig. 32; RadamBrasil 1: 250,000 Folha Juruá, SA.19-Z-D, 1977).

This region is near the confluence of the Rio Juruá and the Rio Solimões, below the small communities of Juruá and Alto Planeta on the right bank of the river, approximately 465 km downriver by air from the Lower Central Region. We worked here in the months of May and June, when water levels were near their maximum and, thus, when the várzea was inundated (fig. 6). Consequently, trap sites were limited to terra firme habitats and the edge of várzea. Extensive terrestrial trapping within the interior of várzea forest was not possible. The two members of sample sites on each side are closely adjacent to each other. Due to the extreme width of the várzea forest in the region (up to 20 km), the opposite-side trap sites are nearly 25 km apart. These localities are grouped into same-side pairs in the descriptions that follow.

Localities **13** (Ilha Paxiuba) and **15** (Vai-Quem-Quer). These two localities are located on opposite sides of Lago Vai-Quem-Quer on the right bank of the Rio Juruá, at 3°19′S, 66°00′W (fig. 32). We worked here from May 2 through May 19, 1992. Extensive várzea forest borders the lake on the east side, with terra firme on elevated ground away from this habitat. We placed our five parallel lines that formed the terra firme standardized plot approximately 900 m from the edge of the várzea north of camp (fig. 33). All lines contained terrestrial stations (A–E) and three also

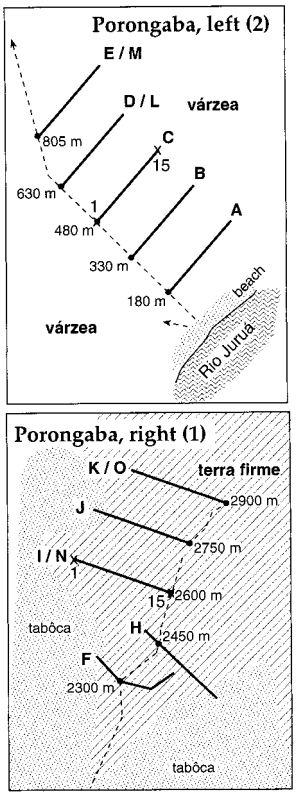

Fig. 19. Details of the placement of the standardized sample lines in the várzea forest on the left bank opposite Porongaba (locality **2**) and in the terra firme forest at Igarapé Porongaba, right bank (locality **1**). Distances (in meters) from the edge of the river are noted.

had canopy ones (F–H). In addition, we set three lines along the edge of the várzea forest, but on higher ground. According to locals, this area is not flooded, even at the height of the high water seasons, and there were no signs of flooding during our visit. Each of these secondary lines had 15 terrestrial stations of traps (I–K), with a Tomahawk and Sherman at each station; one line (J/P) also had a set of 15 canopy platforms, again each with a Tomahawk and Sherman live trap.

Ilha Paxiuba, at 3°19′S, 66°00′W, is on the west side of Lago Vai-Quem-Quer, opposite the site we call by that name (fig. 32). This is a small ''island'' of forest (termed *restinga alta*) above water, approximately 3.2 hectares in extent and bordered to the east by extensive inundated várzea at the time of our visit

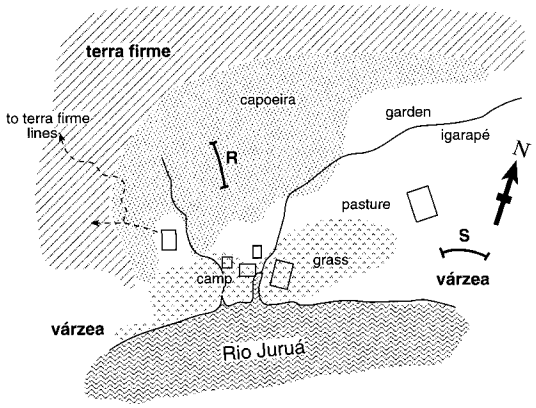

Fig. 20. Detailed map of the Rio Juruá at Sobral (locality **4**), indicating the position of camp relative to major habitat types, secondary trap lines (bold letters) and placement of terra firme and várzea standardized lines (see text for further details). Nova Vida (locality **3**) was directly across the river. Not drawn to scale.

(fig. 33). It floods only at very high water; the last time in local memory was 10 years previously, in 1982. Rising water during our visit encroached along its eastern margin to the edge of one trap line (M/Q). This patch is about 100 m from the edge of terra firme forest to the west. We placed two standardized lines along the edge of this forest patch, each with 15 terrestrial (M, N) and canopy (Q, R) stations consisting of a Tomahawk and Sherman trap (fig. 33).

Localities **14** (Colocação Vira-Volta) and **16** (Ilhazinha). This pair of localities is almost 26 km due west of Vai-Quem-Quer on the left margin of the Rio Juruá floodplain on the Igarapé Arabidi, a small tributary of the Paraná Breu, at approximately 3°17′S 66°14′W (fig. 32). There are two large oxbow lakes in the immediate vicinity, Lago São Raimundão and Lago Três Unidos, and a few singlefamily plots. The sites are at the margins of large tracts of várzea forest, which was still flooded at the time of our visit from May 21 to June 10, 1992. Our camp was on the left bank of a small *igarapé* that joins Igarapé Arabidi to Lago São Raimundão. The standardized trap plot was in terra firme forest, with the beginning of the main trail approximately 125 m inland from the várzea margin of Lago São Raimundão and about 900 m north of camp (fig. 34). This plot contained the usual five

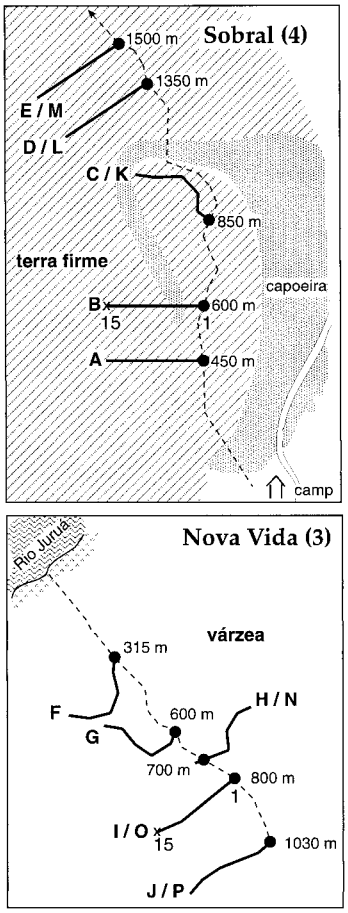

Fig. 21. Details of the placement of the standardized sample lines in the terra firme forest on the left bank at Sobral (locality **4**) and in várzea forest at Nova Vida, right bank (locality **3**). Distances (in meters) from the edge of the river are noted.

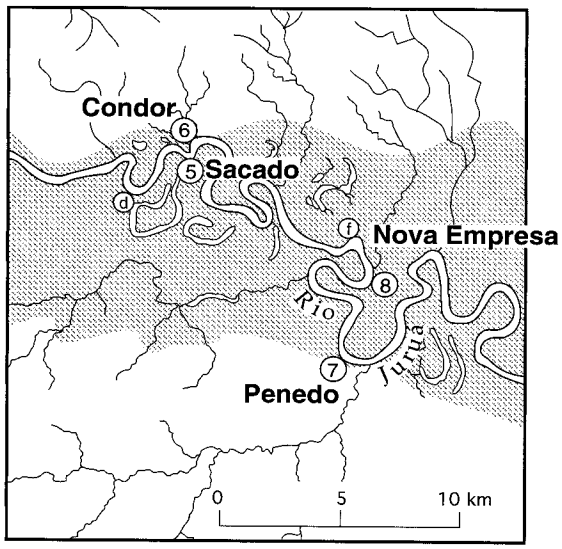

Fig. 22. Upper Central Regional Area of the Rio Juruá in the state of Amazonas, Brazil. The four primary sample localities are indicated by numbers (see text for precise locality information). Hatching bordering the river indicates the extent of várzea forest, which floods annually. Redrawn directly from RadamBrasil 1:250,000 series, Folha Rio Itaguaí (SB.19-Y-A), 1978.

parallel lines of 15 trap stations each; lines A through E were terrestrial with F, G, and H containing canopy platforms. Beyond the last line was an extensive area of blowdown caused by high winds in 1991. Three secondary lines (K–M) were set along the margins of the várzea, again with 15 stations with a Tomahawk and Sherman live trap at each; one of these (R) also had an equal number of canopy platforms.

Ilhazinha is a small island of terra firme forest, approximately 2.8 hectares in size and located between Igarapé Arabidi and Lago São Raimundão (lower right corner of upper map in fig. 34). We placed two lines along the margins of the island (bottom, fig. 34). Both had terrestrial and canopy stations with a Tomahawk and Sherman live trap at each station.

TRAP EFFORT AND SUCCESS

Nearly 46,000 ''trap nights'' of effort were collectively expended during the 10 months of fieldwork at the 16 primary localities (see table 2), including the two traps set at each standardized terrestrial and canopy station. These yielded approximately 2850 captures. During the length of the study, therefore, total trap return averaged about 5.9%, although there was considerable variation across all sites and time periods (table 3, fig. 35). Trap success was highest at Penedo (locality **7**; 12.2%) and Nova Empresa (locality **8**; 11.4%) and lowest at Boa Esperança (locality **9a**; 2.4%) and Vai-Quem-Quer (locality **15**; 2.7%). These data are pooled across all habitats and trap types for each locality.

In general, comparisons between paired terra firme or várzea localities sampled simul-

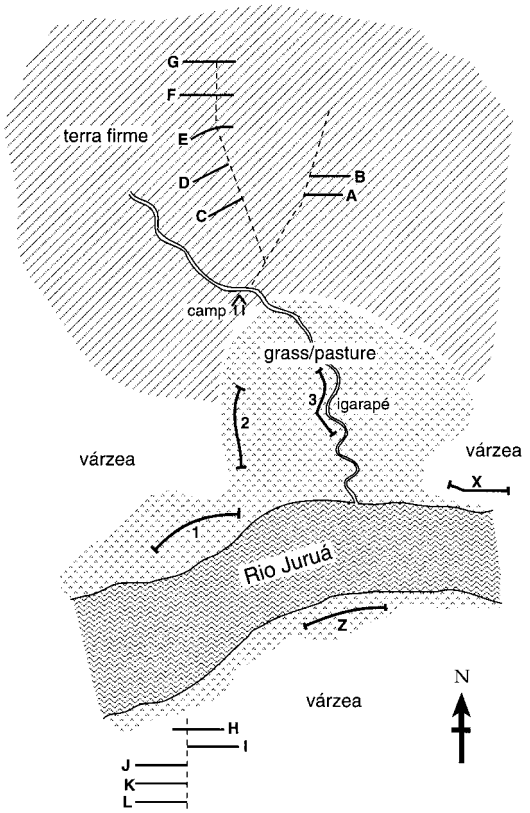

Fig. 23. Detailed map of the Rio Juruá at Sacado and Seringal Condor (localities **5** and **6**), illustrating position of camp relative to major habitat types, secondary trap lines (bold numbered and lettered lines) and placement of terra firme and várzea standardized lines (see text for further details). Not drawn to scale.

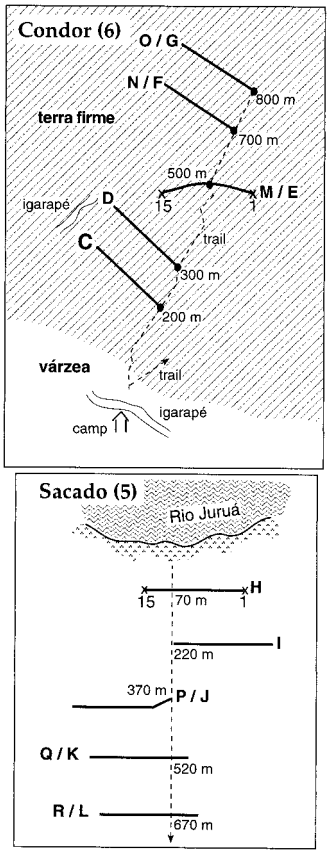

Fig. 24. Details of the placement of the standardized sample lines in the terra firme forest on the left bank at Seringal Condor (locality **6**) and in the várzea forest at Sacado, right bank (locality **5**). Distances (in meters) from the edge of the river are noted.

taneously indicated equivalent trap success (table 3; fig. 35). There is, however, an apparent seasonal pattern in trap success (fig. 35), with a high in August-September at the beginning of the dry, or low-water season, and lower success at the end of the dry season and during the rainy season. This seasonal shift presumably reflects corresponding shifts in population densities. However, any pattern of seasonal changes must be viewed with caution, since the successive monthly samples were not longitudinal from within single areas but came from separate localities spread over 1000 km along the river. Such an analysis thus lacks the proper experimental design to correctly address the question of seasonal variation.

We compared trap success between the generalized habitats of terra firme and várzea by restricting analyses to data from the standardized lines (table 4). The pooled average success for the terra firme was greater than that in the várzea (6.23% versus 5.57%), but not statistically so (one-way ANOVA, $F_{1,15} = 0.320$, $p = 0.5801$). However, there were clear differences between successes within both habitat types and trap position, either terrestrial or canopy (table 4). On average, terrestrial traps were six to seven times more successful than their canopy counterparts, whether based on comparisons between lines for each standardized site or pooled across all sites.

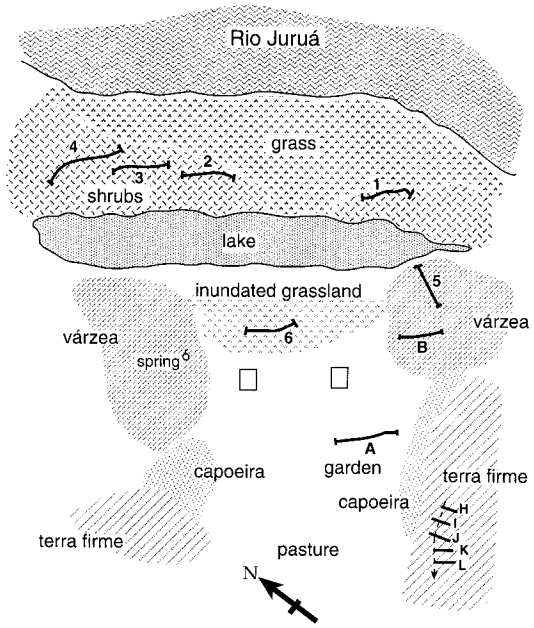

Fig. 25. Detailed map of the Rio Juruá at Penedo (locality **7**), illustrating major habitat types, secondary trap lines (bold numbered and lettered lines) and placement of terra firme standardized lines (see text for further details). Not drawn to scale. The várzea standard lines were placed at Igarapé Nova Empresa (locality **8**), on the left bank approximately 1.5 to 2 km upriver.

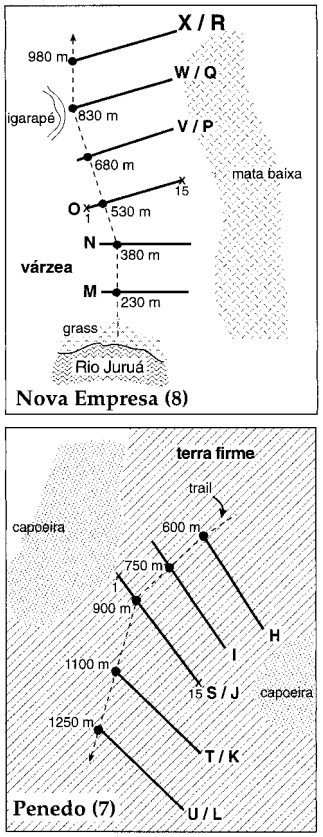

Fig. 26. Details of the placement of the standardized sample lines in the várzea forest on the left bank at Igarapé Nova Empresa (locality **8**) and in the terra firme forest at Penedo, right bank (locality **7**). *Mata baixa* is low-stature forest growing in an area with prolonged annual inundation. Distances (in meters) from the edge of the river are noted.

Although there was no difference in overall trap success for comparable lines between terra firme and várzea, there was a general, although not consistent, difference in temporal success in specific comparisons. For these we restricted data to the terrestrial record only, as the number of canopy captures was limited at most localities. The number of captures decreased throughout the seven-day sampling period in both habitats at all sites. This is not surprising, since we removed all individuals captured each day. However, the rate of loss is twice as great, on average, in várzea sites than in terra firme sites (2.2 individuals per day versus 1.1, respectively). This difference is not statistically significant, largely because of the few comparisons, but the trend is apparent. However, slopes based on the regression of number of captures per day against successive days during sampling periods exhibited a significant decrease in captures over time in four of the six várzea comparisons (Nova Vida, locality **3**; Sacado, locality **5**; Nova Empresa, locality **8**; and Boa Esperança and opposite Altamira combined, localities **9a** and **10**; no true várzea was sampled from the Mouth Region, which was visited during the high-water season) but only in two of the eight terra firme comparisons (Altamira, locality **9**, and Vira-Volta, locality **14**). In general, therefore, although the total numbers of individuals taken in the two major habitat types at each site were the same, the trap success was more even across the sampling period in the terra firme but decreased more sharply with time in the várzea. This pattern is readily apparent in compari-

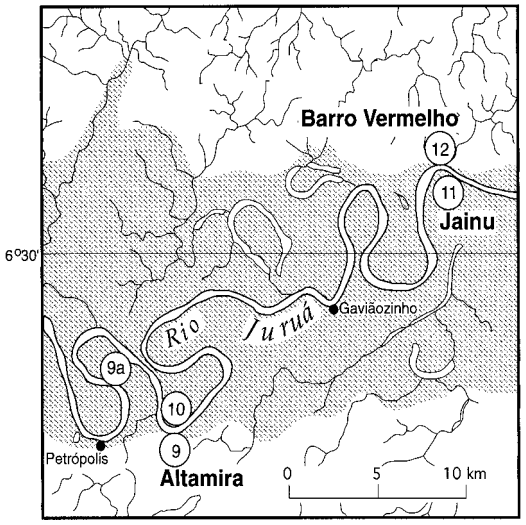

Fig. 27. Lower Central Regional Area of the Rio Juruá in the state of Amazonas, Brazil. The five primary sample localities are indicated by numbers (see text for precise locality information). Hatching bordering the river indicates the extent of várzea forest, which floods annually. Redrawn directly from RadamBrasil 1:250,000 series, Folha Rio Xeruã (SB.19-Z-A), 1978.

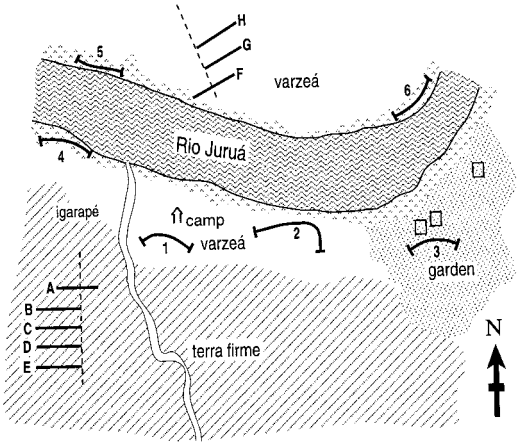

Fig. 28. Detailed map of the Rio Juruá at Altamira, illustrating position of camp relative to major habitat types, secondary trap lines (bold numbered and lettered lines) and placement of terra firme standardized line at Altamira itself (locality **9**) and the adjacent várzea site across the river (locality **10**). The standardized várzea site at Boa Esperança (locality **9a**) is located approximately 4.5 km upriver from Altamira (fig. 27). Not drawn to scale.

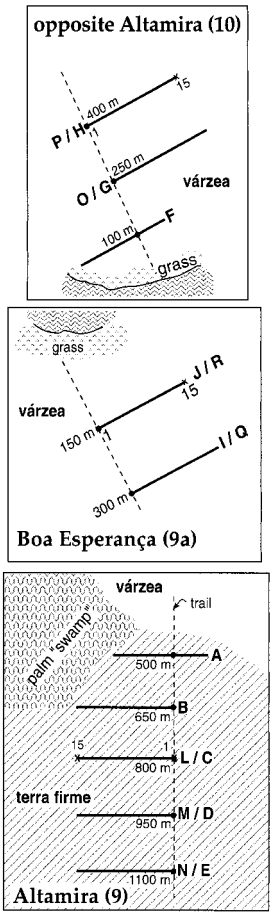

Fig. 29. Details of the placement of the standardized sample lines in várzea forest on the left bank (opposite Altamira [locality **10**]) and right bank (Boa Esperança [locality **9a**]) and in terra firme forest on the right bank (Altamira [locality **9**]). Distances (in meters) from the edge of the river are noted.

sons between temporal trap success at the paired terra firme site of Penedo (locality **7**) and várzea site of Nova Empresa (locality **8**), where our total sample sizes are the largest obtained in each habitat (table 3). These sites exhibit dramatically different temporal profiles of captures over their respective sampling periods (fig. 36). At Penedo there is a statistically stable number of successive captures over the sampling period (slope = −0.429, not significantly different from a slope of 0 by *t*-test [$t = -0.474$, $p = 0.6552$]), with an average loss rate, therefore,

of fewer than 0.5 individuals per day. On the other hand, Nova Empresa exhibited a dramatic temporal decrease in captures of more than 6.6 specimens per day over the sample period (slope = −6.643, significantly less than 0 by *t*-test [$t = -5.513$, $p = 0.0002$). Reasons for these differences are not readily apparent, but likely involve phenological differences in the vegetation of both habitats relative to food production, potential life history characteristics of the rodent and marsupial species within them, or only simple differences in the sizes of home ranges in upland versus floodplain forests.

ESTIMATES OF SPECIES RICHNESS

An important question to ask is whether the trap effort at individual sites was sufficient to sample adequately the true diversity of species of small mammals in both the terrestrial and canopy communities. This question is often addressed simply by plotting the cumulative number of species encountered at a given site against the time period of sample effort (e.g., Woodman et al., 1995). However, the documentation of local species richness by this means is fraught with a number of difficulties, not the least of which is the degree of constancy of effort over the sampling period, complications of ad hoc collecting as opposed to standardized effort, uneven distribution and trappability of individual species, and other factors inherent in both the sampling methodology and the fauna itself. Voss and Emmons (1996) and Simmons and Voss (1998) provide excellent reviews of these, and other difficulties, and Colwell and Coddington (1994) discuss estimation procedures for local richness and for extrapolating species accumulation curves.

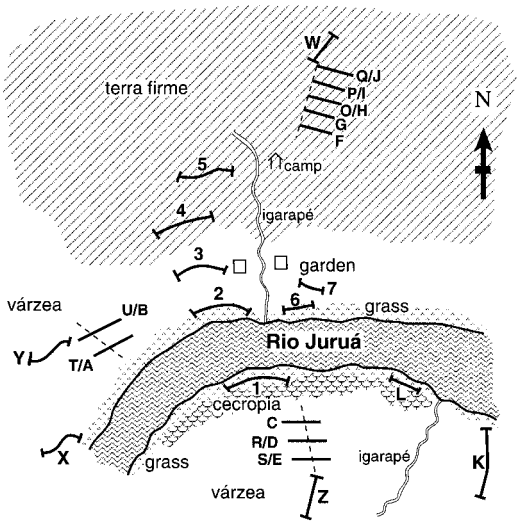

Fig. 30. Detailed map of the Rio Juruá at Jainu and Barro Vermelho (localities **11** and **12**), illustrating position of camp relative to major habitat types, secondary trap lines (bold numbered and lettered lines) and placement of terra firme and várzea standardized lines (see text for further details). Not drawn to scale.

Our own sampling efforts at each site included both that on standardized plots in terra firme and várzea forest, with generally the same trap design and effort at all localities, as well as opportunistic trapping in other local habitats. Combining data of both types would necessarily confound possible comparisons between sites, since the total sampling effort was not equivalent. Similarly, the number of specimens actually obtained at each site varied considerably (table 3), so that construction of accumulation curves may also be compromised by failure to trap many individuals, particularly toward the end of a given sampling period. Following the arguments of Voss and Emmons (1996) and the example of Simmons and Voss (1998), we plot the cumulative number of species as a function of the number of captures, rather than the temporal duration of trapping (fig. 37). We provide data only for the two sites for which we had the highest sampling success (table 3): the terra firme plot at Penedo (locality **7**) and the várzea plot on the opposite side of the river at Nova Empresa (locality **8**); see the map, fig. 22. We also include data only for the standardized trap plots, treating the terrestrial (8 days) and canopy (11 days) sampling efforts separately. Species numbers reflect those of marsupials and both murid and echimyid rodents, as no other kind of mammals were obtained in these traps (with the exception of a single kinkajou [*Potos flavus*], which is excluded from the data presented). Although all complications enumerated by Voss and Emmons (1996) are not completely removed, the two sets of graphs (fig. 37) show patterns similar to those observed at other

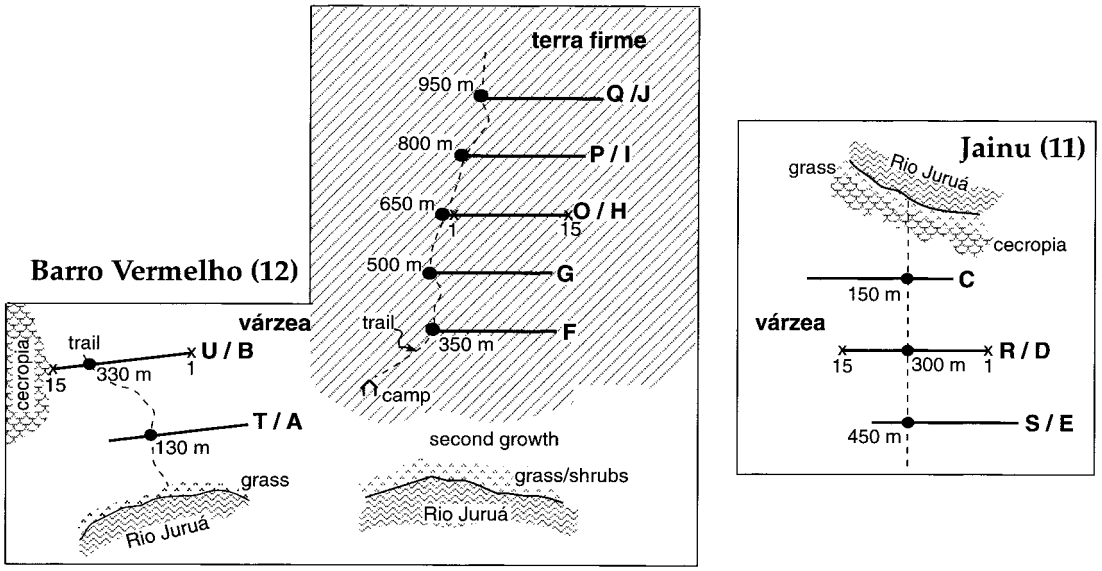

Fig. 31. Details of the placement of the standardized sample lines in the várzea forest at Jainu, right bank (locality **11**) and in both várzea and terra firme forest on the left bank at Barro Vermelho (locality **12**). Distances (in meters) from the edge of the river are noted.

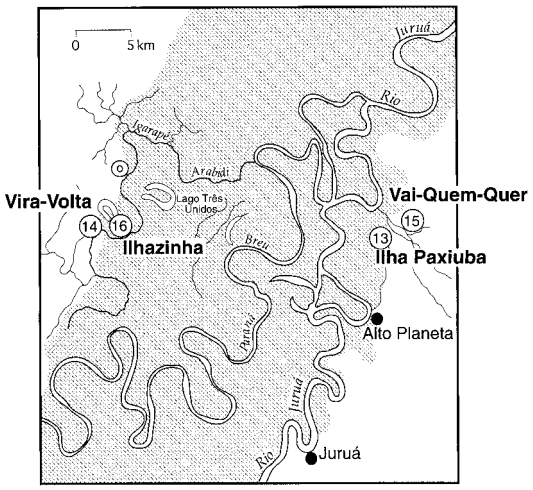

Fig. 32. Mouth Regional Area of the Rio Juruá in the state of Amazonas, Brazil. The four primary sample localities are indicated by numbers; the single secondary locality by letter (see text for precise locality information). Diagonal hatching along sides of the river indicates the extent of várzea forest, which floods annually. Redrawn directly from RadamBrasil 1:250,000 series, Folha Juruá (SA.19-Z-D), 1977.

sites within Amazonia. More detailed comparisons that consider all data from the Rio Juruá will be presented separately. Data from Penedo and Nova Empresa are also comparable to each other since both were trapped simultaneously and with nearly the same the trap effort (table 2).

A larger number of species characterizes the terrestrial terra firme plot as opposed to its canopy counterpart as well as both terrestrial and canopy components from várzea forest (fig. 37). There are more than twice the number of terrestrial terra firme species as those obtained in the canopy platform traps (14 versus 6 species, respectively), although this observation must be tempered by differences in the area sampled (five parallel lines as opposed to three) as well as by the number of available traps (table 2). The number of species obtained in the várzea at Nova Empresa is the same (7 species) on the ground and in the trees, although the particular species differed considerably between trap positions (appendices A and B). The first sample day obtained a substantial proportion of the species eventually collected in the várzea (5 of 7 terrestrial species; 3 of 7 canopy ones). Here as well, apparent saturation of

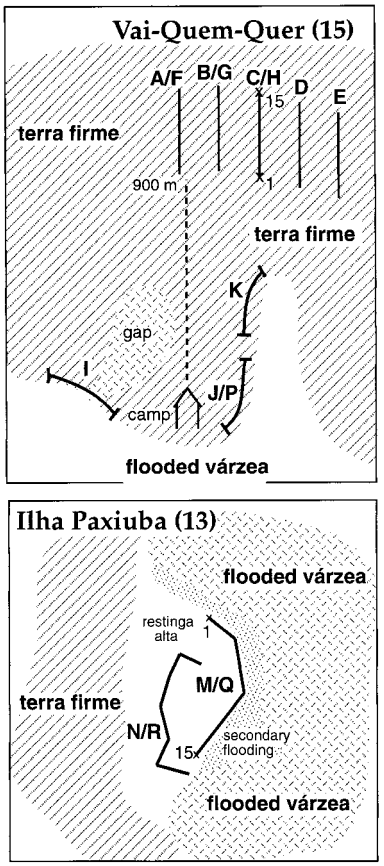

Fig. 33. Detailed maps of the Rio Juruá on the right bank at Vai-Quem-Quer and Ilha Paxiuba (localities **15** and **13**), illustrating position of camp relative to major habitat types, secondary trap lines (bold numbered lines) and placement of standardized lines (see text for further details). Not drawn to scale.

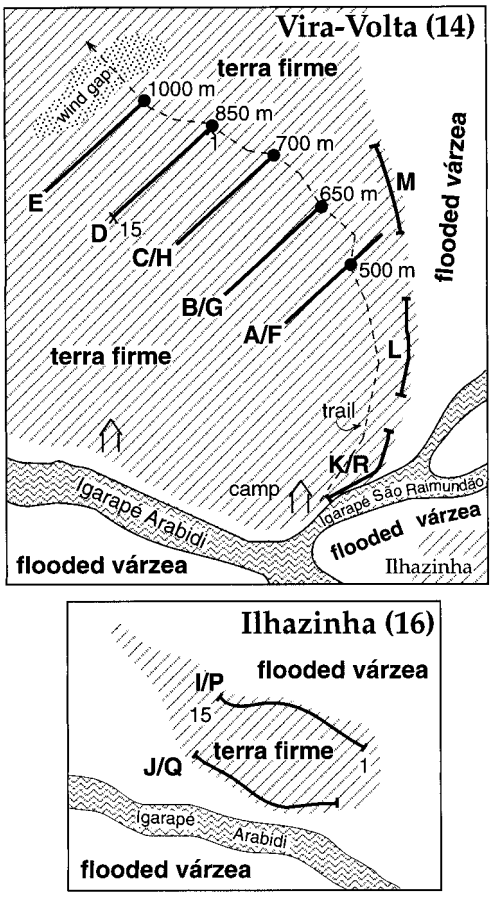

Fig. 34. Detailed maps of the Rio Juruá on the left bank at Colocação Vira-Volta and Ilhazinha (localities **14** and **16**), illustrating position of camp relative to major habitat types, secondary trap lines (bold numbered and lettered lines) and placement of terra firme and várzea standardized lines (see text for further details). Not drawn to scale.

canopy species numbers was achieved relatively quickly (by day 4, at less than half the total number of canopy captures for arboreal species). For the terrestrial community in the várzea, however, the final two species were not added until about 60% (*Philander opossum*) or 85% (*Marmosops neblina*) of all individual captures had been made. Only single individuals of these two species were obtained (appendix B). In the terra firme plot at Penedo, on the other hand, there was a rather gradual increase in new species obtained on the ground as the number of captures increased (fig. 37), with the final species (*Monodelphis emiliae*) added on the eighth (last) day of trapping. The few canopy species (6) were trapped quickly, as no new species were added after day 5 of the 11-day trapping period. The limited number of total canopy captures (21), however, precludes much confidence in a true estimation of species abundances for the canopy environment.

As will be discussed below, the pool of arboreal marsupial and murid and echimyid rodent species collected at both Penedo and Nova Empresa is reasonably complete relative to what was both found at other localities and might be expected for this region of Amazo-

TABLE 3
Trap Effort and Success by Locality
Number of specimens obtained, trap "nights,"and average trap success for each of the 16 primary sample localities along the Rio Juruá.

Locality	Habitat[a]	# specimens	# trap nights	% success
Porongaba, R (locality **1**)	terra firme	237	3050	7.77
Porongaba, L (locality **2**)	várzea	109	1920	5.68
Nova Vida (locality **3**)	várzea	138	2400	5.75
Sobral (locality **4**)	terra firme	161	3000	5.37
Sacado (locality **5**)	várzea	173	2310	7.49
Condor (locality **6**)	terra firme	248	4387	5.65
Penedo (locality **7**)	terra firme	371	3034	12.23
Nova Empresa (locality **8**)	várzea	230	2026	11.35
Altamira (locality **9**)	terra firme	220	3256	6.76
Boa Esperança (locality **9a**)	várzea	30	1230	2.44
Opposite Altamira (locality **10**)	várzea	59	1695	3.48
Jainu (locality **11**)	várzea	101	2436	4.15
Barro Vermelho (locality **12**)	terra firme	226	5538	4.08
Ilha Paxiuba (locality **13**)	várzea	57	1260	4.52
Vira Volta (locality **14**)	terra firme	196	3300	5.94
Vai-Quem-Quer (locality **15**)	terra firme	101	3720	2.72
Ilhazinha (locality **16**)	várzea	66	1260	5.24

[a] Major habitat at each locality; data summarized for all habitat types.

nia, based on other site inventories in western Amazonia (listings in Voss and Emmons, 1996). The terrestrial assemblage in the várzea forest at Nova Empresa also includes most of those species found elsewhere within the Rio Juruá in that forest type (appendices A and B), so that the effort expended there was reasonably effective in sampling the likely pool of available species. However, for the terrestrial assemblage in terra firme forest, the accumulation curves in fig. 37 suggest that additional species might well be expected on the standardized lines at Penedo. Certainly, ad hoc sampling elsewhere at Penedo yielded species not encountered on the standardized lines (appendix A). Moreover, terrestrial terra firme species found at localities both up- and downriver from Penedo, but not at this locality, are likely present as well. Nevertheless, our standardized trapping effort (both number of stations [= traps] and time) apparently did a reasonably adequate job of sampling both the terrestrial and arboreal marsupial and rodent faunas.

We will present a detailed comparison of species abundance and richness at all terra

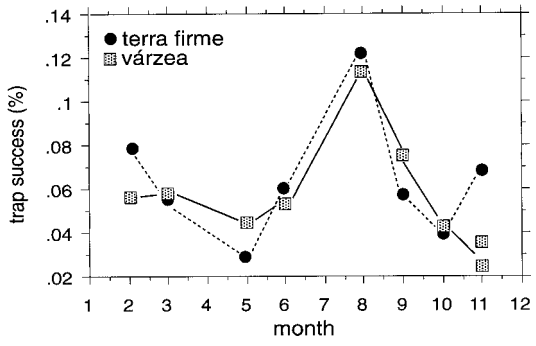

Fig. 35. Monthly patterns of trap success (number of captures relative to total number of trap "nights") for both terra firme (solid circles) and várzea (stippled squares) forest localities. Each monthly sample is at a different pair of cross-river localities (see text).

TABLE 4
Percent Trap Success on Standardized Trap Lines
Values are given as mean ± standard error, with range.

	Terrestrial		Canopy	
Habitat	Mean ± SE	Range	Mean ± SE	Range
Terra firme	7.86 ± 1.20	3.3–14.1	1.13 ± 0.30	0.4–2.6
Várzea	7.92 ± 1.40	3.1–17.2	1.83 ± 0.40	0.6–4.6

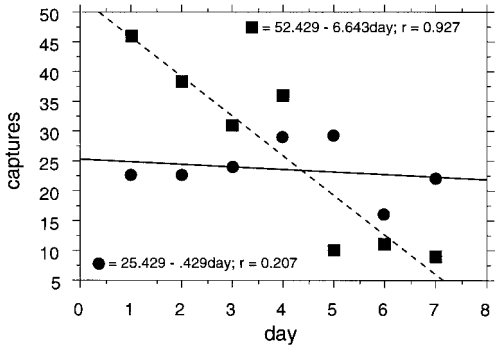

Fig. 36. Number of captures relative to the seven-day trap period for the standardized terra firme (solid circles) and várzea (solid squares) lines at Penedo (locality **7**) and Nova Empresa (locality 8) sites, respectively. Regression equations for each relationship are given.

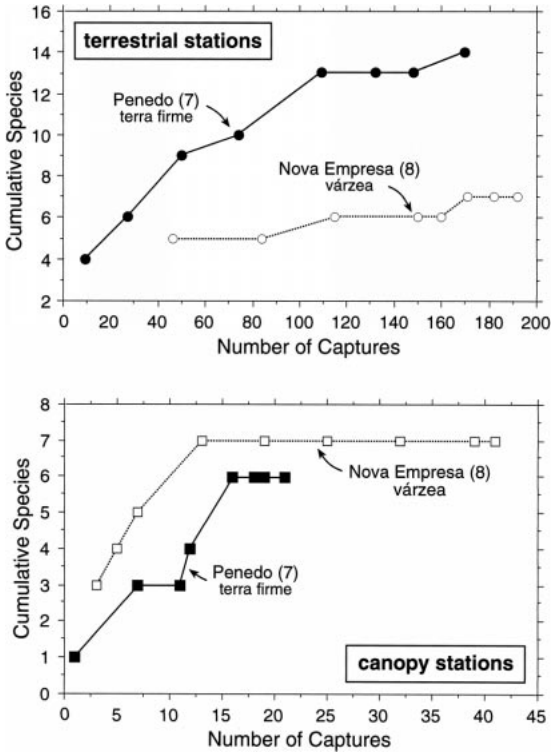

Fig. 37. Plots of cumulative numbers of species captured on the standardized terrestrial (above) and canopy (below) trap lines at the terra firme site of Penedo (locality **7**; solid circles and squares, respectively) and várzea site of Nova Empresa (locality **8**; open circles and squares). The terrestrial lines were sampled for 8 continuous days and the canopy platforms were sampled for 11. The numbers of traps available in each habitat and on both the ground and in the canopy over the sampling period at both localities are given in table 2.

firme and várzea sites elsewhere. The two forest types throughout the river basin generally had similar overall terrestrial abundances, but floodplain sites had significantly lower terrestrial richness, thus mirroring the comparisons between the paired sites at Penedo (locality **7**) and Nova Empresa (locality **8**) that we presented above. In contrast, várzea sites had significantly greater canopy abundance and richness than did upland forest sites. We attribute the lower terrestrial richness in the várzea to the harsh conditions for terrestrial organisms during periodic flooding. Presumably, the arboreal faunas experience the effects of flooding only indirectly, and hence any seasonal impacts are reduced. The relatively high abundance and richness of the canopy fauna in the várzea may reflect the richer soils and hence greater resource productivity.

SPECIES ACCOUNTS

The accounts below summarize the taxonomy, local distribution, habitat range, and other attributes of those taxa of small, nonvolant mammals encountered during our trapping efforts along the Rio Juruá. We restrict these accounts to marsupials and sciurid, murid, and echimyid rodents, for which our sampling methods secured the numbers of specimens adequate to judge both morphological and molecular variation and various habitat and life history parameters. Other nonvolant taxa collected or seen are listed in the species lists for each sampled locality (appendices A and B). Because the taxonomy of many of these animals is poorly understood at present (see Voss and Emmons, 1996; Emmons and Feer, 1997; Patton et al., 1997), we also describe phylogeographic pat-

terns for many taxa not just within the Rio Juruá basin but more globally across Amazonia. Finally, we describe four new species uncovered by our analyses; five other taxa obtained on this expedition have been described elsewhere (Patton and da Silva, 1995; da Silva, 1998).

The arrangement of families, genera, and species generally follows the taxonomic accounts given in Wilson and Reeder (1993), specifically that of Gardner (1993) for marsupials, Hoffmann et al. (1993) for sciurid rodents, Musser and Carleton (1993) for murid rodents, and Woods (1993) for histricognath rodents. The original citation for each species is not included in the References section, unless cited in the body of the text for other reasons. Type localities given in quotation marks are those of the original publication, followed by specific emendations or restrictions given by subsequent authors. Where the original citation was not available to us, we follow Gardner (1993), Hoffmann et al. (1993), Musser and Carleton (1993), and Woods (1993) in the designation of type localities, other than for taxa described more recently. No attempt has been made to provide subspecies identifications or to list synonyms. The latter can be found generally in the synoptic accounts cited immediately above. Where we differ in nomenclature, determination of species boundaries, or other taxonomic issues from these, or other authors, we document our decisions as appropriate below.

In addition to nomenclatural details, we summarize information on geographic and habitat range, reproduction, and karyotype (if available) for each species. For selected groups, details of the morphological features that distinguish similar species are provided, with illustrations to make comparisons easier, and analyses of populational and geographic variation in morphometric traits are summarized. We also provide, where we have data, a phylogeographic perspective for many taxa based on our on-going analyses of comparative sequence variation in the mitochondrial cytochrome-b gene (see, for example, da Silva and Patton, 1993, 1998; Patton et al., 1994, 1996a, Patton and da Silva, 1997). Finally, specimens collected and examined are listed by locality for each species. Localities are always listed from upriver to downriver, generally following decreasing longitude, and from right bank to left bank. All 16 primary localities are keyed by number to the map, fig. 1, and the list in the section above on Field Sites; lettered secondary localities are identified in the individual maps for each section along the river (figs. 17, 22, 27, and 32). This same scheme has been used in other papers (Patton et al., 1994, 1996a; da Silva and Patton, 1997).

Data are summarized in the species accounts below only for marsupials and sciurid, murid, and echimyid rodents. Few specimens of other taxa were obtained. All nonvolant taxa for which specimens were obtained, or, in the case of primates, where species were identified by sight, are listed in appendix C.

ORDER DIDELPHIMORPHIA
DIDELPHIDAE GRAY, 1821

Thirteen species of marsupials were recorded along the length of the Rio Juruá. This number is equivalent to the known marsupial fauna of Manu National Park in southeastern Perú (Pacheco et al., 1993; Voss and Emmons, 1996). The maximum number of species found at any given site was eight (Penedo, locality **7**; see discussion below and appendices A and B). This is two fewer than the number recorded sympatrically at either Manu National Park or Cusco Amazónico in southeastern Perú (Pacheco et al., 1993; Voss and Emmons, 1996; Woodman et al., 1991). Although the species list for the Juruá basin is impressive, taxa are missing that are likely present along the river. Included among these probable species are the water opossum *Chironectes minimus*, the arboreal opossums *Caluromysiops irrupta* and *Glironia venusta*, and small murine opossums of the genus *Gracilinanus* (see Gardner and Creighton, 1989; Hershkovitz, 1992). Patterson (1992) recorded *Gracilinanus emiliae* (Thomas) from the central Rio Juruá at Igarapé Grande (near Eirunepé), but these specimens were apparently misidentified and are actually juvenile *Marmosa lepida* (Robert S. Voss, personal commun.).

SUBFAMILY DIDELPHIDAE GRAY, 1821

DIDELPHIS LINNAEUS, 1758

Common opossums

Didelphis marsupialis Linnaeus, 1758

TYPE LOCALITY: "America"; restricted to Surinam by Thomas (1911).

DESCRIPTION: This is the largest species of didelphid marsupial in the region, with weights often over one kg. Individuals of black-color phase were present at all localities and were numerically dominant over those of the white phase at the four localities where both color morphs were recorded (the terra firme sites of Sobral, Penedo, Altamira, and Ilhazinha—localities **4**, **7**, **9**, and **16**, respectively). As a genus, *Didelphis* needs no comparison to any other marsupial wherever it occurs in tropical or subtropical forests, as it is readily separable from all other taxa. This is the largest marsupial in the community, lacking spots above the eyes, with long, coarse guard hairs covering dense underfur, and a very characteristic musky odor that marks the animal's presence even when not seen. However, species identifications can sometimes be problematic, especially in areas of near or actual sympatry between *D. marsupialis* and *D. aurita* in southeastern Brazil (Cerqueira, 1985) or between *D. marsupialis* and *D. albiventris* in the Guianan region (Catzeflis et al., 1997; Lavergne et al., 1997). Selected measurements (mean and range) for 14 adult specimens, separated by sex, are given in table 5. Since only a single adult male was obtained, we are unable to assess the degree of sexual dimorphism present, nor are we able to assess variation due to age. Both sexual dimorphism and age contribute signficiantly to variation among individuals in mensural characters in *Didelphis* (Gardner, 1973).

MOLECULAR PHYLOGEOGRAPHY: We have examined variation in the mtDNA cytochrome-b gene (the initial 660 bp) for 21 individuals from 13 localities within the Rio Juruá basin as well as from other localities throughout Amazonia (fig. 38; table 6). Sequence variation is relatively slight, as *D. aurita* from the Mata Atlântica of coastal Brazil and *D. marsupialis* from Central and South America differ by only 2.9%. These species of *Didelphis* are, however, reciprocally monophyletic with regard to their mtDNA haplotypes, with bootstrap values of 81 and 79 supporting each, respectively (fig. 39). Moreover, despite the low level of overall sequence divergence within *D. marsupialis*, some phylogeographic structure is present within this species across its sampled range. All haplotypes from the Rio Juruá form a monophyletic assemblage, with bootstrap support of 81%; these differ among themselves by an average of only 0.304%. Similarly, haplotypes from central Amazonia north of the Rio Solimões (Rio Jaú and left [= east] bank of Rio Negro) are monophyletic, with 82% bootstrap support. These are more different among themselves, with an average Kimura two-parameter distance of 1.112%, but the variation does not separate into differences between samples on opposite sides of the Rio Negro. Finally, there is a series of samples from the upper Rio Negro, eastern Ecuador, and Guyana, each of which are monophyletic unto themselves, but for which there is no clear geographic set of hierarchical relationships apparent, even in

TABLE 5
Selected External and Cranial Dimensions of Adult *Didelphis marsupialis*
Measurements (mm) are given as mean ± standard error, with range and sample size.

Variable	Males (n = 1)	Females (n = 13)	
		Mean ± SE	Range
TOL	732	752.1 ± 18.3	655–904
TAL	379	391.2 ± 8.6	348–472
HF	57	59.0 ± 0.9	51–66
E	50	51.4 ± 0.7	49–56
CIL	86.25	90.27 ± 1.83	82.44–103.59
ZB	44.56	45.41 ± 0.93	41.41–50.05
BB	22.54	24.01 ± 0.49	21.22–27.33
IOC-1	16.56	18.09 ± 0.47	15.81–21.29
IOC-2	11.23	11.76 ± 0.16	10.73–12.68
RL	35.24	35.10 ± 0.91	30.95–41.41
NL	43.26	43.18 ± 1.13	38.47–52.17
RW	15.59	16.05 ± 0.34	14.33–18.29
C–M4	38.29	39.03 ± 0.49	36.51–41.47
M1–M4	18.76	18.88 ± 0.20	18.11–20.14
PL	55.42	55.99 ± 1.30	47.19–63.61
PW	28.14	29.37 ± 0.35	27.95–31.37
OCB	24.98	27.08 ± 0.59	24.28–30.70
BOL	8.39	9.47 ± 0.21	8.65–11.50
CD	20.86	21.80 ± 0.37	20.02–23.80

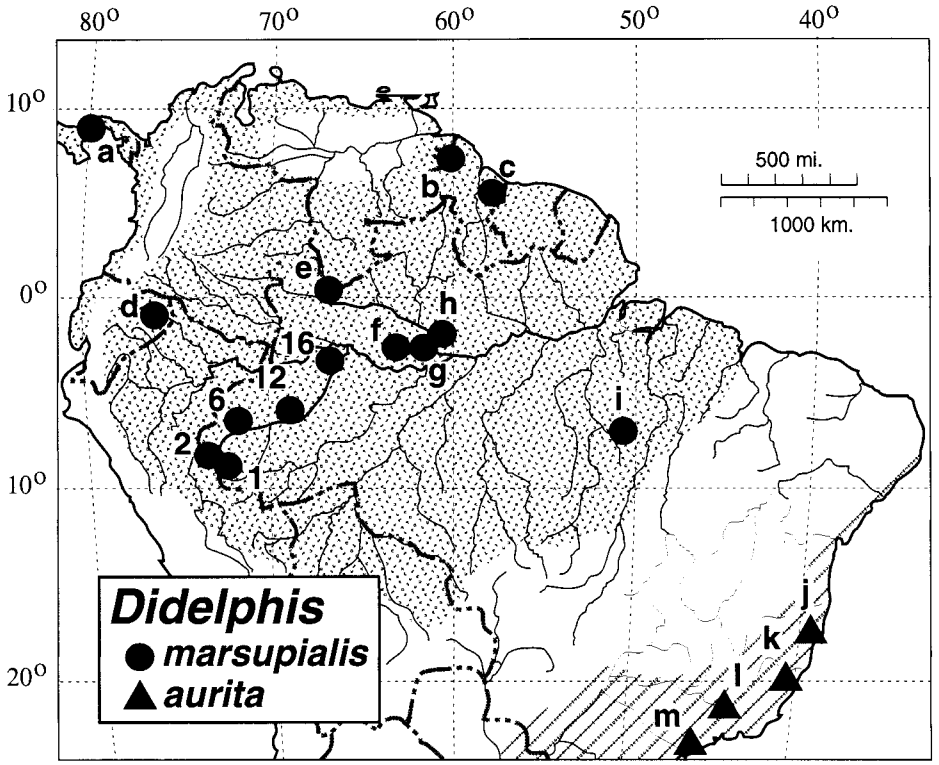

Fig. 38. Map of localities for which 660 bp of cytochrome-b gene sequences are available for the common opossums, *Didelphis marsupialis* and *D. aurita*. Localities are identified as in the tree, fig. 39, and provenance data are listed in table 6.

comparison to haplotypes from southern Central America (Costa Rica and Panamá) or from the southeastern Brazilian Amazon (Carajás, Estado do Pará). Consequently, while the level of sequence divergence within *D. marsupialis* is quite minimal, especially in comparison to that in other marsupials (see other accounts, below), there is some phylogeographic structure across its sampled range. It is unclear whether the low level of sequence divergence within *Didelphis* reflects a relative recency in the evolution of its member species, or simply slower rates of molecular evolution. In either case, the relatively high levels of similarity among haplotypes of specific phylogeographic regions cannot be assumed to result from differences in population structure (e.g., higher gene flow rates), despite the fact that *Didelphis* is often characterized as a nearly nomadic small mammal with large home ranges and great individual movement distances (Gardner, 1982).

DISTRIBUTION AND HABITAT: This species was taken at 10 of the 16 primary sample sites and in each of the four regional areas, from the headwaters to the mouth of the Rio Juruá (appendix A). At mid and lower river localities, we found *D. marsupialis* only in mature or second growth terra firme forest, in disturbed garden plots, or in traps placed in the ecotone between terra firme and *igapó* forest. At the headwaters localities, specimens were taken in both nonflooded and locally inundated river-edge forest. This appears to be primarily an upland, nonflooded forest taxon, that inhabits a wide range of usable microhabitats, including secondary growth indicative of heavy disturbance by humans. Nearly all specimens were taken in traps placed on the ground, although several individuals were seen and shot as they

TABLE 6
Haplotypes, Voucher Numbers, and Localities for Taxa of Common Opossums, Genus *Didelphis*
Individual haplotypes listed from top to bottom in the tree, figure 39, with the catalog numbers of their respective voucher specimens for which 660-bp haplotypes of the mitochondrial DNA cytochrome-b gene are available. Localities are identified as in the map, figure 38.

Haplotype	Voucher no.	Locality
Didelphis aurita		
1	EDH 29	Fazenda Beijo Grande, 12 km S & 1.1 km E Itabuna, Bahia, Brazil (j)
2	EDH 39	Mata da Caixa D'Agua, 1.7 km W Santa Tereza, Espirito Santo, Brazil (k)
3	ML 123	Mata da Caixa D'Agua, 1.7 km W Santa Tereza, Espirito Santo, Brazil (k)
4	MAM 234	Fazenda Guaricana, Guaratuba, Morretes, Paraná, Brazil (m)
5	MAM 238	Fazenda Intervales, Base Saibadela, Sete Barros, São Paulo, Brazil (l)
6	MAM 239	Fazenda Intervales, Base Saibadela, Sete Barros, São Paulo, Brazil (l)
Didelphis marsupialis		
7	ROM 97295	Wigdale House, Monteverde, Puntarenas, Costa Rica (not mapped)
8	USNM 578958	Isla Popa, 1 km E Sumwood Channel, Bocas del Toro, Panamá (a)
9	USNM 578138	Punta Alegre, Peninsula Valiente, Bocas del Toro, Panamá (a)
10	ROM 100358	Mapenna Creek, ca. 6 km from Corentyne River, East Berbice-Corentyne, Guyana (c)
11	ROM 101023	Baramita, Barima-Waini, Guyana (b)
12	ROM 101050	Baramita, Barima-Waini, Guyana (b)
13	CS 1	Floresta Nacional Tapirapé-Aquiri, Município de Marabá, Pará, Brazil, 5°48'05"S, 50°30'54"W (i)
14	ROM 104372	Parque Nacional Yasuni, 20 km S Pompeya Sur, Napo, Ecuador (d)
15	ROM 104533	Parque Nacional Yasuni, 20 km S Pompeya Sur, Napo, Ecuador (d)
16	JUR 468	Ilhazinha, left bank Rio Juruá on Igarapé Arabidi, affluent of Paraná Breu, Amazonas, Brazil (locality **16**)
17	MNFS 1160	opposite Igarapá Porongaba, left bank Rio Juruá, Acre, Brazil (locality **2**)
18	MNFS 1190	Igarapé Porongaba, right bank Rio Juruá, Acre, Brazil (locality **1**)
19	JLP 15654	Seringal Condor, left bank Rio Juruá, Amazonas, Brazil (locality **6**)
20	JLP 15751	Barro Vermelho, left bank Rio Juruá, Amazonas, Brazil (locality **12**)
21	INPA 2518	Estrada Picarreira, right bank Rio Cauaburi, Parque Nacional do Pico da Neblina, Amazonas, Brazil (e)
22	INPA 2523	Estrada Picarreira, right bank Rio Cauaburi, Parque Nacional do Pico da Neblina, Amazonas, Brazil (e)
23	JLP 16750	right bank Rio Jau above mouth, Amazonas, Brazil (g)
24	MNFS 1984	Tambor, left bank Rio Jau, Amazonas, Brazil (f)
25	JLP 16782	Lago Meduiním, left bank Rio Negro, Amazonas, Brazil (h)
26	JLP 16792	Lago Meduiním, left bank Rio Negro, Amazonas, Brazil (h)
27	JLP 16759	right bank Rio Jau above mouth, Amazonas, Brazil (g)

climbed in trees or vine tangles less than 2 m off the ground and five specimens were taken in canopy traps at heights above 10 m (Penedo, locality **7**; Vira-Volta, locality **14**; and Ilhazinha, locality **16**).

REPRODUCTION: Harder (1992) presents a brief summary of the literature on reproduction in *Didelphis* species. Among our specimens, all females of age class 3 or greater (from Gardner, 1982; age approximately 7–11 months, see also Tyndale-Biscoe and MacKenzie, 1976) were either parous (as judged by the orange color of the pouch region) or with pouch young; one of two females younger than age 3 showed signs of reproductive activity; and all females of age class 2 or less were nulliparous. For males, maximal testis size (length > 15 mm) was found in all specimens of age class 2 and older. Females with pouch young were taken in all months of our trapping effort, including August, September, October, November, February, March, and June. These data suggest that reproduction can occur in all months of the year, during both wet and dry seasons. Year-round reproduction also characterizes

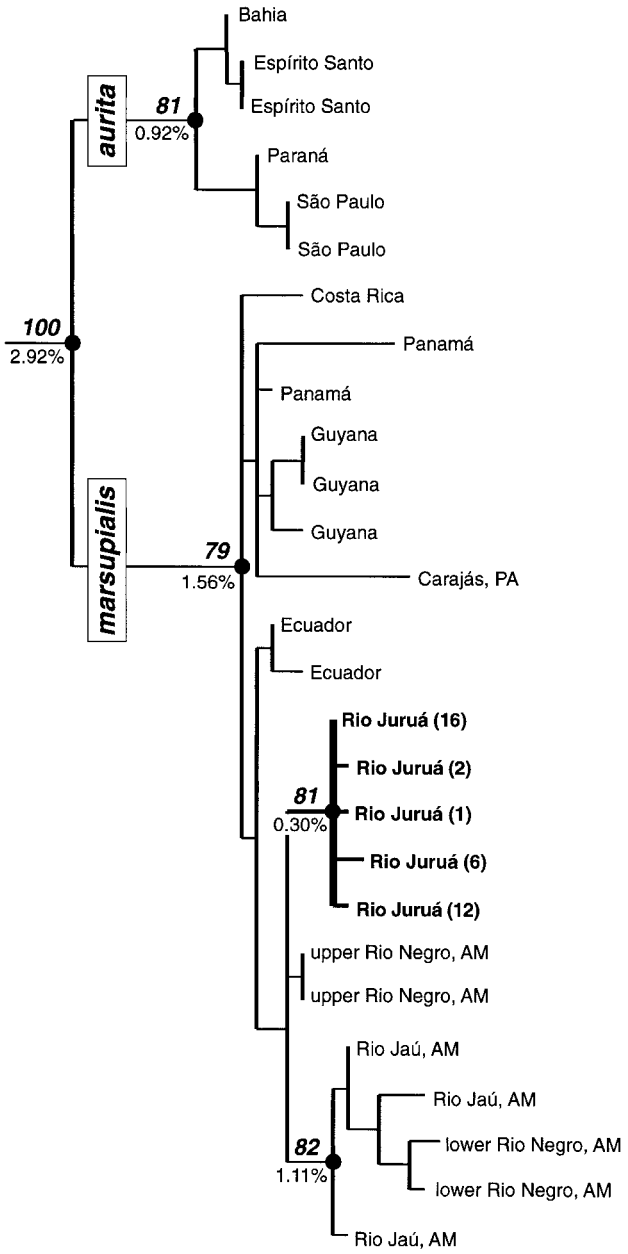

Fig. 39. Majority-rule consensus tree of 605 equally minimal length maximum parsimony trees for cytochrome-b haplotypes of the opossums, *Didelphis marsupialis* from Amazonia and *D. aurita* from the Atlantic Forest. Data are the initial 660 bp of sequence. Branch lengths are proportional to the number of character changes. Haplotypes for specimens from the Rio Juruá are identified by heavy lines and bold type; localities for all specimens are listed in table 6. The tree is rooted by comparison to sequences of *D. virginiana* and *Philander opossum*. Tree length = 75 steps; CI = 0.800, RI = 0.807. Bold numbers at internal nodes are bootstrap values, based on 1000 iterations; percentages are average Kimura two-parameter distances.

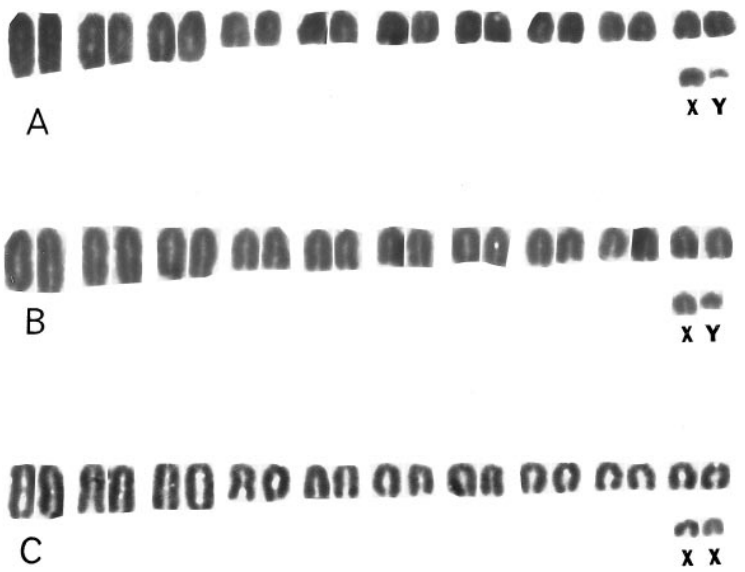

Fig. 40. Chromosome complements of three species of didelphid marsupials from the Rio Juruá with 2n = 22 karyotypes. **A**, *Didelphis marsupialis*, MNFS 1035, locality **5**; **B**, *Philander opossum*, MNFS 623, locality **9**; **C**, *Philander mcilhennyi*, MNFS 1435, locality **7**.

populations in primary rainforest in French Guiana (Catzeflis et al., 1997), but contrasts with the llanos (''plains'') of eastern Colombia that are highly affected by seasonal changes and where reproduction was limited to the dry season (January through August; Tyndale-Biscoe and MacKenzie, 1976). Litter size averaged 5.1 (range 4–7, n = 9). This value is within the range of litter sizes reported from other localities in South America (Colombia, 4.5 [Tyndale-Biscoe and MacKenzie, 1976]; and French Guiana, 4.7 to 6.5 [Catzeflis et al., 1997; Charles-Dominique, 1983; Julien-Laferrière and Atramentowicz, 1990]).

KARYOTYPE: 2n = 22, FN = 20 (fig. 40A). The autosomal complement as well as both X- and Y-chromosomes are acrocentric and graded by size (see Gardner, 1973; Reig et al., 1977; Palma and Yates, 1996). We karyotyped four specimens from two separate localities (MNFS 372, 396, 437, 1035).

SPECIMENS EXAMINED (n = 39): (**1**) 1m, 1f — MNFS 1160, 1190; (**2**) 2f — MNFS 1182–1183; (b) 1m — MNFS 1003; (**c**) 1m — MNFS 1035; (**3**) 1m, 4f — MNFS 1515–1517, 1639, JUR 203; (**4**) 1f — MNFS 1452; (**6**) 1f — JLP 15654; (**7**) 2m, 5f — MNFS 372, 396, 413, 429, 437–438, JLP 15354; (**9a**) 1m — MNFS 931; (**9**) 2m, 7f — JLP 15939, 15990, 15999–16000, 16020, 16044, 16070, 16075–16076; (**11**) 1m — JLP 15751; (**12**) 1m, 1f — MNFS 683, JLP 15798; (**13**) 1m — JUR 467; (**15**) 1m, 4f — JUR 468, 508, 521, 549, 560);.

MARMOSA GRAY, 1821

Murine mouse opossums

Marmosa murina (Linnaeus, 1758)

TYPE LOCALITY: ''Asia, America''; restricted to Surinam by Thomas (1911).

DESCRIPTION: A broadly distributed species, this small-bodied murine opossum is medium chestnut brown above and yellowish buff below. The pale hairs of the venter are restricted to the midline, and bordered by broad lateral bands of gray-based fur (fig. 41, right). The tail has large, diamond-shaped scales arranged in bands around the tail. Tail hairs are very small, nonpigmented and less than the length of a single scale. The skull has distinctly flared supraorbital ledges, with a sharp-pointed post-orbital process especially developed in older individuals. The auditory bullae have a uniquely globular alisphenoid portion without separate anterior struts

Fig. 41. Ventral color patterns of (from left to right) *Marmosops noctivagus* (JLP 15306, Penedo [locality **7**]); *Marmosops impavidus* (JLP 15633, Condor [locality **6**]; *Marmosops impavidus* (MNFS 760, Barro Vermelho [locality **12**]); *Marmosops neblina* (JLP 15450, Nova Empresa [locality **8**]); *Marmosops neblina* (MNFS 1067, Igarapé Porongaba [locality **1**]); and *Marmosa murina* (MNFS 746, Barro Vermelho [locality **12**]).

(the bullar types found in the five long-tailed murine opossum genera that Tate [1933] included within his concept of the genus *Marmosa* [*Thylamys, Gracilinanus*, *Marmosops*, *Marmosa*, and *Micoureus*] are illustrated in Reig et al., 1987).

COMPARISONS: This species of murine opossum is readily distinguished from sympatric *Micoureus demerarae* and *M. regina* by its smaller size, lack of dense, woolly pelage, and more gracile skull. Both genera have supraorbital processes, although these are distinctly better developed in *Micoureus*, and both possess a rounded alisphenoid portion of the bullae lacking anterior struts. *Marmosa murina* can be confused with same-sized and likely sympatric species of *Marmosops*, but can be distinguished by a combination of both external and cranial details. For example, in ventral coloration, particularly with regard to the band of gray-based hairs lateral to the pale medial portion, the specimens of *M. murina* are quite similar to *Marmosops impavidus* and *Marmosops neblina* (see below). The coloration of *M. murina* from the Rio Juruá is similar to that of *M. noctivagus*, but the former is more chestnut, less gray-brown in color, and the fur of the venter is yellowish-buff as opposed to having nearly white hairs. *Marmosa murina* also differs from all species of *Marmosops* in having prominent supraorbital ledges on the skull and in lacking anterior buttressing on the alisphenoid portion of the bullae. Finally, *Marmosa murina* can be distinguished from *Marmosops* by its large di-

amond-shaped tail scales arranged in bands, rather than small scales arranged spirally around the tail, with very small and nonpigmented hairs less than the length of a single scale. In *Marmosops*, the medial hair of each scale triplet is enlarged, petiolate, and is visually black in color, especially in live or fluid preserved individuals.

DISTRIBUTION AND HABITAT: The species was recorded only in the Lower Central and Mouth regions along the river, where it was taken in traps placed on the ground in terra firme forest, or at the interface between terra firme and local *igapó* forest. Since it is found throughout eastern and southeastern lowland Perú (Voss and Emmons, 1996) and eastern Bolivia (Anderson, 1997), however, *M. murina* is likely to be found along the entire Rio Juruá.

REPRODUCTION: Two specimens were parous females of age class 5 (based on Gardner's [1982] scheme for *Didelphis*), one each caught in October and May. Neither had attached young nor showed overt signs of lactation.

COMMENTS: This species is present at all thoroughly worked sites within Amazonia, including eastern and southern Perú, central and eastern Brazil, and the Guianan lowlands (local faunal reports in Voss and Emmons, 1996). We obtained only three specimens in over 49,000 total trap nights (table 2). Similar capture rates were found during long-term studies in southeastern Perú (Woodman et al., 1991, 1995) and north of Manaus in the central Amazon (Malcolm, 1991a, b), and the species has been taken at only one site within the very large and moderately thoroughly sampled Manu Biosphere Reserve (Pacheco et al., 1993). These few published studies thus suggest that *M. murina* is either generally rare within Amazonia, or does not readily go to traps. Pine (1973), however, recorded the species as ''common'' in eastern Amazonia, but did not record trap records or effort, and Louise H. Emmons (personal commun.) found it to be quite common, even if patchily distributed, in secondary areas (as along roadside brush) in the Manu Biosphere in Perú.

SPECIMENS EXAMINED (n = 3): (**9**) 1m — JUR 202; (**12**) 1f — MNFS 746; (**13**) 1f — JUR 450.

MARMOSOPS (MATSCHIE, 1916)

Slender mouse opossums

The slender mouse opossums are small to very small-bodied, pale reddish to dark brown opossums usually common in the lower reaches of locally inundated areas, such as *Heliconia* thickets, within either terra firme or várzea forests (Emmons and Feer, 1997). The genus can be distinguished from other small murine opossums by the combination of short and straight hair, very small tail scales arranged in spirals and with an enlarged and dark medial hair associated with each scale, and an alisphenoid portion of the auditory bullae with a distinct anterior spine, or buttress (see Gardner and Creighton, 1989).

Three species are usually recognized within the mammalian fauna of Amazonia (Gardner, 1993). These include the relatively large-bodied *M. noctivagus* (Tschudi) with a near-white venter that generally lacks lateral gray-based fur incursions; *M. impavidus* (Tschudi), somewhat smaller and with lateral gray-based incursions extending onto the venter; and the diminutive *M. parvidens* (Tate), also with lateral gray-based incursions. Mustrangi and Patton (1997), in their review of the Mata Atlântica members of the genus, provided sequence data from the cytochrome-b gene for several specimens of Amazonian taxa, including individuals from the Rio Juruá. Their data clearly delineated four sharply defined monophyletic clades within that drainage and, moreover, suggested that geographic samples allocated to different subspecies of *M. parvidens* were sufficiently distinct to justify their elevation to species status.

We have added a few additional specimens to the cytochrome-b data of Mustrangi and Patton (1997), and obtained sequence from all specimens of *Marmosops* trapped by us along the Rio Juruá (fig. 42, table 7). Based on a phylogenetic analysis of the sequence data (fig. 43), four species are recognizable within the Rio Juruá basin: the three identified above along with *M. neblina* Gardner, described originally as a subspecies of *M. impavidus*. Below we characterize each of these four species and, we hope, provide a

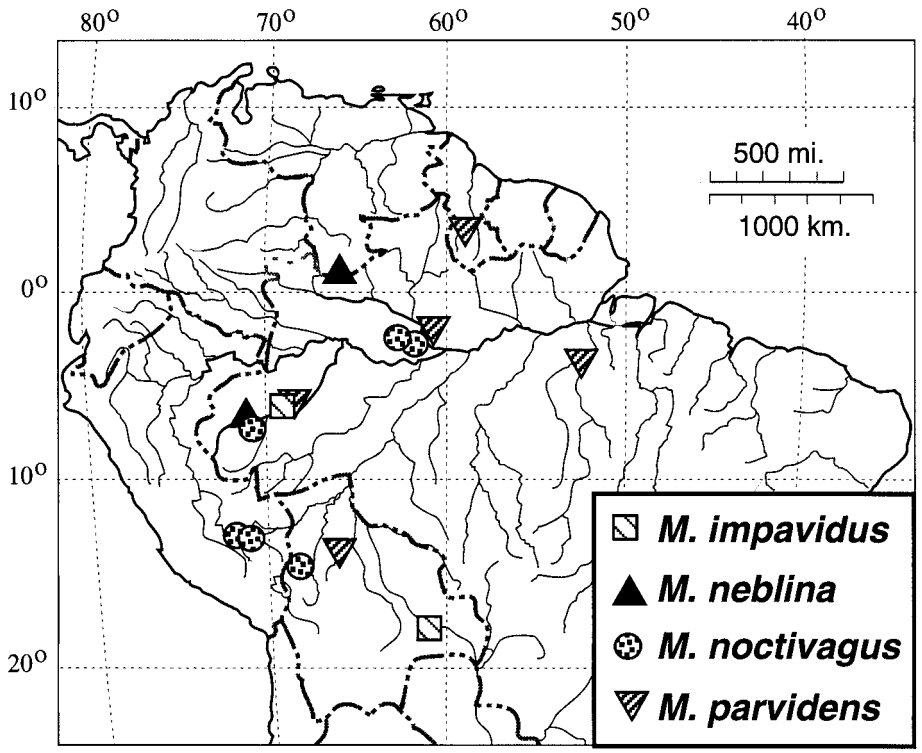

Fig. 42. Map of localities for which 630 bp of cytochrome-b gene sequences are available for the slender mouse opossums, genus *Marmosops*, from Amazonia (modified from Mustrangi and Patton, 1997). Provenance data are listed in table 7.

stimulus for others to undertake a proper review of this difficult genus.

The four species form a size-graded series, with *Marmosops noctivagus* larger in most external and all cranial dimensions than either *M. neblina* or *M. impavidus*, which in turn are larger in these same dimensions than *M. parvidens* (table 8). The degree of size difference is significant in nearly all pairwise comparisons for all measurements (table 9), with the exception of the comparison between *impavidus* and *neblina*. These two species can be distinguished by color and color pattern, as well as by qualitative craniodental features, but not by any quantitative variable.

Our samples of each species are inadequate for extensive statistical comparisons. For example, only one adult *M. neblina* was available. However, the four species generally share the same proportionality of cranial dimensions. That is, mensurally they differ mostly in size, not in differences in characters relative to overall size. This is readily apparent in the relationship of most cranial variables relative to condyloincisive length, a univariate measure of overall size (fig. 44). Both length (e.g., rostral length, fig. 44A) and width (e.g., palatal breadth, fig. 44B) measurements scale the same for all four species. Even the length of the maxillary tooth row (canine to molar 4) shows a similar pattern with overall size (fig. 44C), a result of increased spacing of the premolars with continued growth. However, the molar toothrow series is more fixed in size, with three nonoverlapping size classes among the four taxa; only *impavidus* and *neblina* are inseparable (fig. 44D).

Specimens of *M. impavidus* and *M. neblina* from the Rio Juruá differ by the same general qualitative craniodental differences identified by Gardner (1989) in his original description of *neblina*. He compared the type series of *neblina* (from Cerro de la Neblina on the Venezuelan-Brazilian border) with

TABLE 7
Haplotypes, Voucher Numbers, and Localities for Taxa of Slender Mouse Opossums, Genus *Marmosops*
Individual haplotypes listed from top to bottom in the tree, figure 43, with the catalog numbers of their respective voucher specimens, and localities (identified as in the map, fig. 42) for which 630-bp haplotypes of the mitochondrial DNA cytochrome-b gene are available.

Haplotype	Voucher no.	Locality
Marmosops neblina		
1	JLP 15450	Igarapé Nova Empresa, left bank Rio Juruá, Amazonas, Brazil (locality **8**)
2	USNM 560732	Cerro de la Neblina, camp VII, Amazonas, Venezuela
Marmosops impavidus		
3	MNFS 760	Barro Vermelho, left bank Rio Juruá, Amazonas, Brazil (locality **12**)
4	MSB 58511	Tita, Santa Cruz, Bolivia
Marmosops noctivagus		
5	MVZ 173930	2 km NE Amaybamba, Lucumayo Valley, Cusco, Perú
6	MVZ 171408	72 km NE Paucartambo, Cusco, Perú
7	LC 147	Macaco, left bank Rio Jaú, Amazonas, Brazil
8	YL 141	Macaco, left bank Rio Jaú, Amazonas, Brazil
9	MNFS 1982	Tambor, left bank Rio Jaú, Amazonas, Brazil
10	MNFS 2025	Tambor, left bank Rio Jaú, Amazonas, Brazil
11	MNFS 381	Penedo, right bank Rio Juruá, Amazonas, Brazil (locality **7**)
12	AMNH 268936	Chijchijpa, Río Yarisa, La Paz, Bolivia
Marmosops parvidens		
13	ROM 97938	Karanambo, upper Rupununi River, ca. 45 km N Kanuku Mtns., Upper Takutu–Upper Essequibo, Guyana
14	USNM 549294	52 km SSE Altamira, east bank Rio Xingu, Pará, Brazil
15	MNFS 2113	Lago Meduinim, left bank Rio Negro, Amazonas, Brazil
16	JLP 15826	Barro Vermelho, left bank Rio Juruá, Amazonas, Brazil (locality **12**)
17	AMNH 268398	La Reserva, La Paz, Bolivia

specimens of *impavidus* from elsewhere in Venezuela, as well as Panamá, Colombia, and Ecuador. He noted that *neblina* has fewer and smaller palatine vacuities, straighter dorsal profile of the rostrum (as opposed to distinctly depressed both interorbitally and on the anterior rostrum above the premaxilla), and lower premolars that are more bladelike with less of a tendency to have anterior accessory cuspulids. He also noted that *neblina* differs in both the size and shape of the upper molars, with the labial surface of M3 with shallow (as opposed to deep) indentations and the labial margin between the paracone and metacone both forming a smooth arc in occlusal view rather than being V-shaped and with the presence of accessory cusps. We record no difference in molar size, but the other differences between these two species are apparent in our specimens. In the accounts of each species below, we provide other differences between *impavidus* and *neblina*, as well as between these and other species of *Marmosops* from the Rio Juruá basin.

Marmosops impavidus (Tschudi, 1844)

TYPE LOCALITY: "Der mittleren und tiefen Waldregion"; interpreted by Cabrera (1957: 16) as "Montaña de Vitoc, cerca de Chanchamayo," Departamento de Junín, Perú.

DESCRIPTION: This is a moderate-sized murine opossum averaging 279 mm in total length, 32.6 mm in condylo-incisive length of the skull, and 41 g in weight when fully adult (all four molars fully erupted). The dorsal coloration is rich grayish-brown (Snuff-Brown to Saccardo's Brown; Ridgway, 1912). The tail is dark but with a tendency to become paler distally in most specimens. Fur of the venter is creamy white along the midline bordered by a distinct but narrow band of gray-based, silver-tipped hairs, which typically constrict the white in the ab-

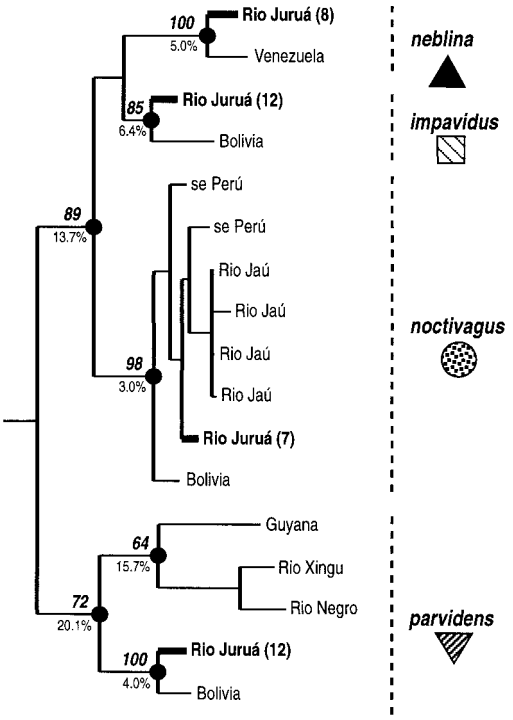

Fig. 43. Strict consensus of four equally minimum-length maximum parsimony trees for cytochrome-b haplotypes of Amazonian slender mouse opossums, *Marmosops*. Data are the initial 630 bp of sequence; the tree is rooted by comparison to species of *Marmosa* (data from Patton et al., 1996); branch lengths are proportional to the number of character changes. Specific localities and specimen voucher numbers are listed in table 7. Haplotypes for specimens from the Rio Juruá are identified by heavy lines and bold type; numbers refer to the specific locality as identified in the text and the map, fig. 1. Bold numbers at internal nodes are bootstrap values, based on 1000 iterations; percentages are average Kimura two-parameter distances. Data are given only for nodes with bootstrap values > 50. Tree length = 530 steps; CI = 0.545; RI = 0.669.

dominal and inguinal region (fig. 41, second and third from left); the width of the self-colored portion in the abdominal region is > 15 mm. The skull is delicate, with large anterior and posterior palatal vacuities (fig. 45), and the interorbital region bears supraorbital ledges that are only weakly evident in young animals but become increasingly apparent in older-age individuals. In the oldest animals, these ledges are weakly V-shaped, more so than in any other species from the Rio Juruá (fig. 46). The anterior opening of the infraorbital foramen lies dorsal to the anterior root of PM4. The maxillary toothrow averages 13.5 mm; upper M1-M4 molar series length averages 6.7 mm. The canine appears proportionately long and narrow, with its width at the base about 55% its length in unworn specimens.

COMPARISONS: Intermediate in overall size between the larger *M. noctivagus* and the smaller *M. parvidens* (see table 8), *M. impavidus* is readily distinguished from these two species by the white venter bordered by a narrow but distinct band of gray-based, silver-tipped hairs (as in *M. parvidens*) instead of a broad white venter lacking the border (as in *M. noctivagus*; fig. 41); dorsal coloration is similar to but darker and grayer than that of *M. noctivagus*; it lacks clearly developed supraorbital beading (in older individuals) present in *M. noctivagus*, but does have weakly developed ledges (fig. 46), as opposed to the lack of any beading in *M. parvidens*; relatively long and narrow canines in comparison to those of *M. noctivagus*; presence of posterior palatal vacuities, as in *M. noctivagus*, but which are lacking in *M. parvidens*. Compared with *M. neblina*, *M. impavidus* differs in its brighter dorsal coloration and broader white ventral area with narrower and less obvious lateral bands of gray-based hairs (fig. 41). It has less swollen paroccipital processes, more swollen mastoid processes, somewhat more well-developed supraorbital ledges (fig. 46), and somewhat longer and narrower upper canines. All palatal vacuities are larger with the posterior ones placed more distally on the palate (fig. 45). The two also differ in those qualitative features noted by Gardner (1989), but cannot be distinguished from each other on the basis of external or cranial dimensions (tables 8, 9).

DISTRIBUTION AND HABITAT: Despite the limited number of individuals, this species was taken at scattered localities in each of the four sample regions along the Rio Juruá (Headwaters, Upper and Lower Central, and Mouth). All individuals were taken in undisturbed or second-growth terra firme forest. Three were taken at heights of 1.5 to 2 m; the remainder were taken on the ground.

TABLE 8
Selected External and Cranial Dimensions of Four Species of Slender Mouse Opossums, Genus *Marmosops*, from the Rio Juruá
Measurements (mm) are given as mean ± standard error, with range and sample size. Individuals are pooled across all localities along the river.

	M. noctivagus			*M. impavidus*		
Variable	Mean ± SE	Range	n	Mean ± SE	Range	n
TOL	321.1 ± 6.0	272–348	14	283.0 ± 12.55	249–315	5
TAL	183.6 ± 3.7	154–202	14	167.4 ± 5.31	152–180	5
HF	20.0 ± 0.5	17–23	14	18.8 ± 0.49	17–22	5
E	22.8 ± 0.5	19–25	14	20.8 ± 0.58	20–23	5
CIL	37.19 ± 0.53	32.77–39.63	14	32.88 ± 0.74	29.76–35.22	6
ZB	19.12 ± 0.22	17.00–20.52	16	17.16 ± 0.53	15.30–19.55	7
BB	13.04 ± 0.09	12.04–13.50	16	12.08 ± 0.09	11.73–12.40	7
IOC	6.39 ± 0.06	5.97–6.95	16	5.73 ± 0.11	5.35–6.23	7
RL	14.77 ± 0.21	12.77–16.00	16	12.95 ± 0.33	11.67–13.89	6
NL	17.60 ± 0.26	15.17–19.00	16	15.09 ± 0.53	12.91–16.91	6
RW	5.85 ± 0.11	5.03–6.66	16	5.30 ± 0.25	4.46–6.30	7
C–M4	15.69 ± 0.14	14.87–16.46	16	13.58 ± 0.25	12.61–14.35	7
M1–M4	7.74 ± 0.04	7.48–8.15	16	6.71 ± 0.11	6.32–7.11	7
PW	11.31 ± 0.12	10.30–11.86	16	9.80 ± 0.22	9.14–10.83	7
OCB	7.77 ± 0.04	7.44–8.08	14	7.15 ± 0.16	6.63–7.76	6
BOL	4.66 ± 0.08	4.11–5.18	14	4.14 ± 0.15	3.60–4.73	6
CD	11.07 ± 0.08	10.69–11.63	16	10.66 ± 0.11	10.37–11.08	7

	M. neblina			*M. parvidens*		
Variable	Mean ± SE	Range	n	Mean ± SE	Range	n
TOL	278.5 ± 20.5	258–299	2	218	—	1
TAL	157.5 ± 12.5	145–170	2	130	—	1
HF	18.5 ± 1.5	17–20	2	18	—	1
E	21.0 ± 1.0	20–22	2	18	—	1
CIL	32.5 ± 1.97	30.53–34.47	2	25.87 ± 0.98	24.89–26.84	2
ZB	17.04 ± 0.72	16.06–18.44	3	13.66 ± 0.22	13.23–13.90	3
BB	12.30 ± 0.16	12.11–12.62	3	10.16 ± 0.11	9.99–10.36	3
IOC	5.93 ± 0.18	5.60–6.21	3	5.28 ± 0.16	4.99–5.53	3
RL	12.79 ± 0.20	12.31–12.90	3	10.56 ± 0.22	10.13–10.84	3
NL	14.83 ± 0.44	13.94–15.32	3	11.45 ± 0.40	10.91–12.24	3
RW	5.17 ± 0.20	4.92–5.57	3	4.11 ± 0.15	3.86–4.39	3
C–M4	13.82 ± 0.31	12.70–13.74	3	10.81 ± 0.14	10.53–10.97	3
M1–M4	6.61 ± 0.14	6.33–6.79	3	5.62 ± 0.11	5.411–5.78	3
PW	9.74 ± 0.30	9.29–10.30	3	7.87 ± 0.24	7.40–8.19	3
OCB	7.43 ± 0.26	7.17–7.69	2	5.91 ± 0.07	5.84–5.98	2
BOL	4.21 ± 0.10	3.81–4.61	2	3.34 ± 0.08	3.24–2.43	2
CD	10.56 ± 0.23	10.32–11.02	3	8.43 ± 0.10	8.27–8.60	3

None were collected in the canopy platform traps.

REPRODUCTION: All adult females (M1–M4 fully erupted) collected in the Headwaters (locality **1**) and Mouth regions (locality **14**) during the wet season were parous, with clearly evident discolored orange inguinal areas and enlarged nipples, although none had attached young. The one female taken during the dry season (November, at Altamira, locality **9**) was a juvenile. These data suggest that *M. impavidus* breeds during the wet season, but whether breeding extends into or through the dry season is unknown.

KARYOTYPE: 2n = 14, FN = 24 (fig. 47A). Chromosomal preparations are available from two specimens (MNFS 1191 and 1779). All members of this genus apparently have

the same diploid number and similar autosomal and sex-chromosome complements, although there appears to be slight differences in centromere position in some of the smaller autosomal elements and in the size of the Y-chromosome (Reig et al., 1977; Palma and Yates, 1996; Svartman, 1998) The autosomal complement of *M. impavidus* is comprised of four pairs of large meta- and submetacentrics and two pairs of small biarmed autosomes, one of which is clearly metacentric and the other subtelocentric. The X-chromosome is a small metacentric, smaller than the smallest autosome, and the Y is a somewhat smaller acrocentric.

SPECIMENS EXAMINED (n = 11): (**1**) 2m, 2f — MNFS 1191, 1235, 1319, 1366; (**6**) 1 m — JLP 15633; (**9**) 1 m — JUR 197; (**12**) 1 m — MNFS 760; (**14**) 2m, 2f — MNFS 1686, 1757, 1779, JUR 550.

Marmosops neblina Gardner 1990

TYPE LOCALITY: ''Camp VII (00°50′40′′N, 65°58′10′′W), 1800 m, Cerro de la Neblina, Territorio Federal Amazonas, Venezuela.''

DESCRIPTION: This is a medium-sized, dark brown mouse opossum. The single adult male weighed 44 grams with a total length of 299 mm, the condylo-incisive length of the skull 34.5 mm, maxillary toothrow 13.7 mm, and molar toothrow 6.7 mm (table 8). The dorsum is a uniform Mummy Brown (Ridgway, 1912) in color from forehead to furred base of tail. The tail is uniformly and darkly colored to its tip. The whitish ventral hair covers the throat and upper chest, but is restricted to the midline through the abdominal and inguinal regions by broad lateral bands of gray-based, silver-tipped fur (fig. 41, second and third from right). The whitish portion in the abdominal region is less than 1 cm wide. The skull is delicate, with a relatively smooth interorbital region, with beading only weakly developed even in old adults (fig. 46); the palate has both enlarged anterior and posterior vacuities (fig. 45); the mastoid processes are small; and the paroccipital processes are distinctly enlarged. The upper canine is relatively stout, with the width at its base averaging 61% of its length in unworn specimens. Our specimens match those of the type series of *M. neblina*, as detailed by Gardner (1989) in his original description, in external color and color pattern, particularly in the narrow mid-ventral white stripe bordered laterally by broad areas of darker pelage with pale-tipped hairs. Our specimens also possess the markedly developed accessory cusps between the paracone and metacone on the third upper molars and, therefore, the shallowly concave labial outline detailed in Gardner's diagnosis (1989: 414).

TABLE 9
Statistical Significance of Mensural Variables of *Marmosops* Species from the Rio Juruá
Based on one-way ANOVA[a]; ns = $p > 0.05$; * $p < 0.05$; ** $p < 0.01$; *** $p < 0.001$.

	Species comparison		
Variable	*noctivagus* vs. *impavidus*	*impavidus* vs. *neblina*	*impavidus* vs. *parvidens*
TOL	**	ns	ns
TAL	**	ns	ns
HF	ns	ns	ns
E	*	ns	ns
CIL	***	ns	***
ZB	***	ns	***
BB	***	ns	***
IOC-1	***	ns	ns
RL	***	ns	***
NL	***	ns	***
RW	**	ns	***
C–M4	***	ns	***
M1–M4	***	ns	***
PW	***	ns	***
OCB	***	ns	***
BOL	***	ns	***
CD	***	ns	***

[a] Sample sizes precluded the determination of the degree of sexual dimorphism in all species except *M. noctivagus*. For that taxon, only three characters (TOL, RL, and NL) exhibited significant dimorphism, but with *p*-values between 0.01 and 0.05.

COMPARISONS: This species can be distinguished from *M. noctivagus* and *M. parvidens* in the same way as can *M. impavidus*, with the exception that the interorbital region of *M. neblina* is even smoother with weaker supraorbital beading. For differences between *M. neblina* and *M. impavidus*, see the section above for *M. impavidus*.

COMMENTS: As suggested in the analyses presented by Mustrangi and Patton (1997), we recognize *N. neblina* as a species separate from *M. impavidus*. With available samples,

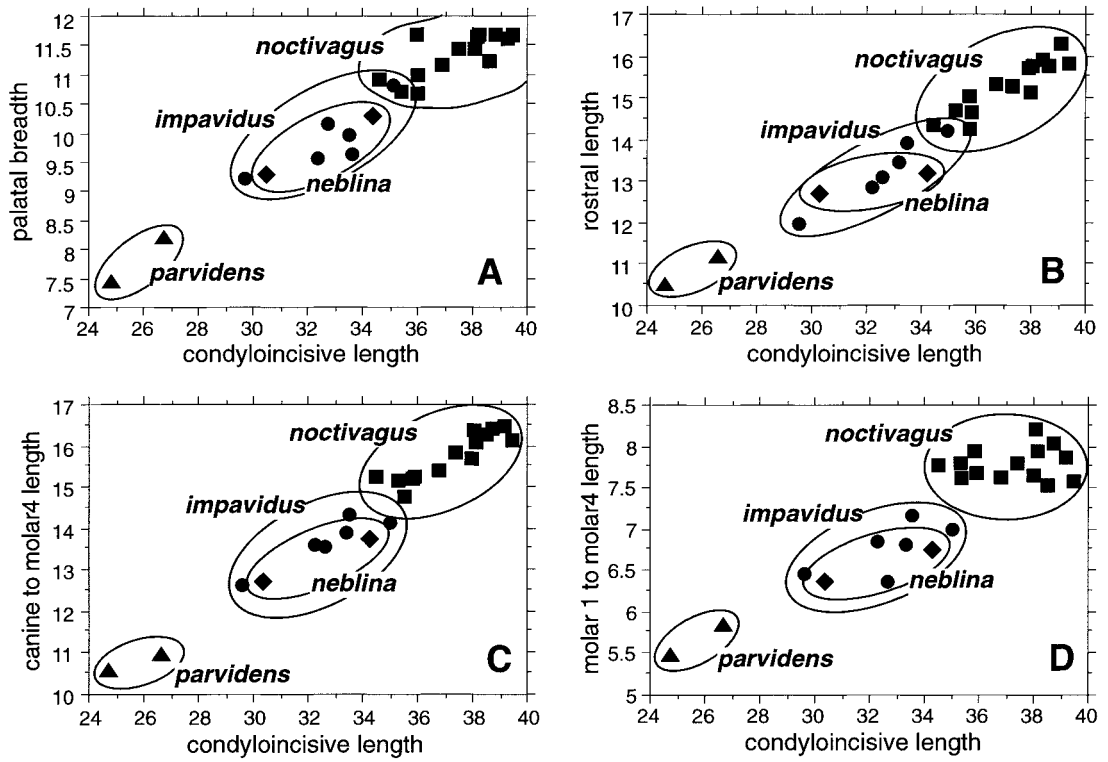

Fig. 44. Bivariate plots of four cranial measurements against condyloincisive length, a univariate measure of overall size, in four species of slender mouse opossums from the Rio Juruá: **A**, palatal breadth; **B**, rostral length; **C**, maxillary toothrow length (canine to M4); and **D**, molar toothrow length (M1 to M4). Squares = *M. noctivagus*; diamonds = *M. neblina*; circles = *M. impavidus*; and triangles = *M. parvidens*.

although the two species are apparently close phyletic relatives (fig. 43), they are sympatric at two localities and are readily separable by the morphological characters listed above.

DISTRIBUTION AND HABITAT: This taxon is known from a few localities in the Headwaters, Upper, and Lower Central regions of the Rio Juruá, all from várzea forest or disturbed river-edge areas. Two specimens were taken at approximately 1.5 m; the remainder were taken in traps placed on the ground. Single specimens of both *M. neblina* and *M. impavidus* were obtained at Igarapé Porongaba (locality **1**) and Altamira (locality **9**), where they were segregated by habitat in both cases.

REPRODUCTION: Specimens were collected in both wet and dry seasons. These include mostly juvenile or subadult individuals (with an incompletely erupted molar series), suggesting that breeding occurs throughout the year. The single adult female (Nova Empresa, locality **8**) showed no signs of recent past breeding activity.

KARYOTYPE: 2n = 14, FN = 24 (fig. 47B). Chromosomal data are available from two individuals (JLP 15215, from locality h; and MNFS 703, locality **11**). The karyotype appears identical to that described above for *M. impavidus*.

SPECIMENS EXAMINED (n = 11): (**1**) 1f — MNFS 1067; (**c**) 1m — MNFS 994; (**3**) 2 m — MNFS 1637, JUR 210; (**8**) 1m — JLP 15450; (h) 1f — JLP 15215; (**9**) 1f — JLP 16052; (**10**) 1m — MNFS 943; (**11**) 1m, 2 f — MNFS 703, 718–719.

Marmosops noctivagus (Tschudi, 1844)

TYPE LOCALITY: ''Der mittleren und tiefen Waldregion''; restricted by Tate (1933) to

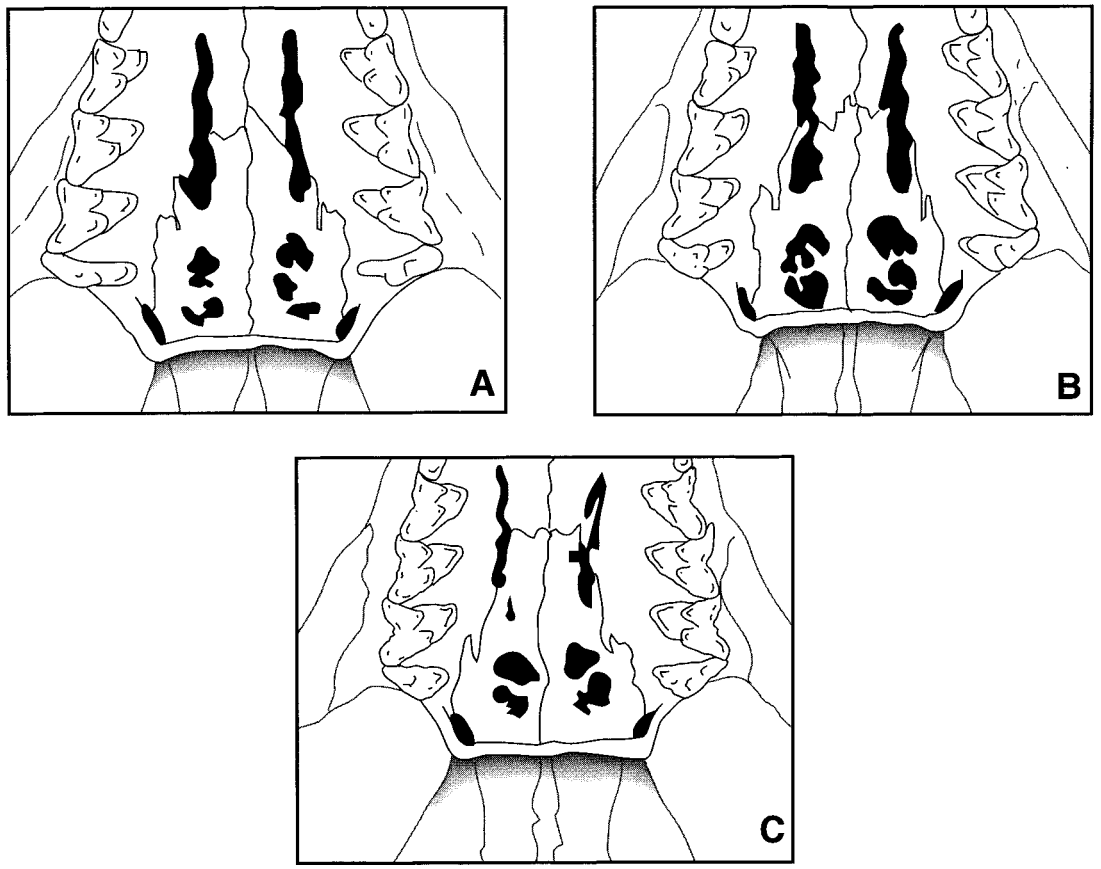

Fig. 45. Palatal views of: **A**, *Marmosops noctivagus* (JLP 15306, Penedo [locality **7**]); **B**, *Marmosops impavidus* (MNFS 760, Barro Vermelho [locality **12**]); and **C**, *Marmosops neblina* (JLP 15450, Nova Empresa [locality **8**]). All specimens are drawn to the same scale.

Montaña de Vitoc, near Chanchamayo, Río Perené drainage, Departamento de Junín, Perú.

DESCRIPTION: This is the largest of the four species of *Marmosops* recorded from the Rio Juruá drainage, averaging 321.1 mm in total length, 37.2 mm in condyloincisive length of the skull, and 54 g in weight (table 8). The dorsal color is paler, more orangish-red-brown than that of either *M. neblina* or *M. parvidens*, but similar to that of *M. impavidus*, ranging from Cinnamon-Brown to Dresden Brown (Ridgway, 1912). The venter is broadly white to cream from chin to inguinal region, either without a lateral band of gray-based hairs separating it from the sides and back or, if present, the band is narrow and confined to the abdominal region (fig. 41, left). The skull of *noctivagus* is large, with well-developed anterior and posterior pairs of palatal vacuities (fig. 45) and well-developed supraorbital beading that forms clearly evident ledges with small postorbital processes in older individuals (fig. 46). The anterior opening of the infraorbital foramen is positioned above the posterior root of PM4. The maxillary toothrow averages 15.7 mm in length, the upper molar series 7.7 mm. The upper canine is relatively short and stout, with the width at the base averaging 65.5% of its length.

COMPARISONS: *Marmosops noctivagus* can be readily distinguished from *M. neblina* by its larger size, brighter dorsal pelage, pure white venter without a lateral border of gray-based hairs (fig. 41), larger molar series and individual teeth, and well-developed supraorbital beading with ledges clearly evident in

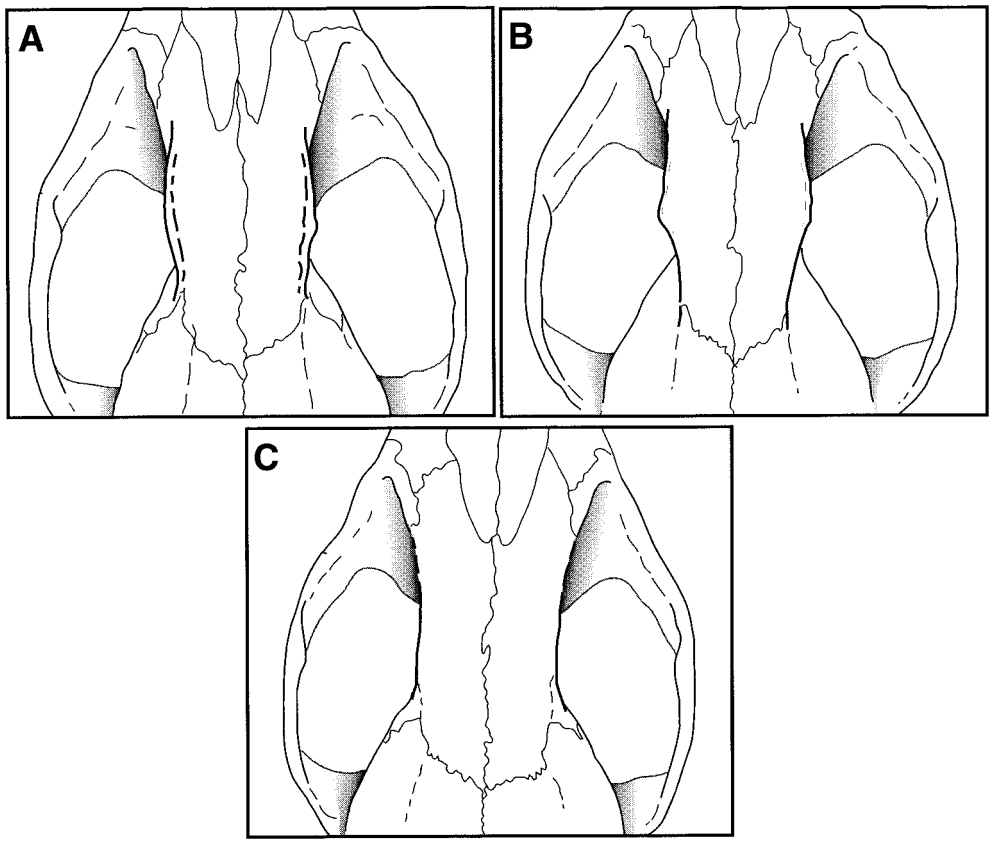

Fig. 46. Views of the interorbital region of crania of same-age specimens of: **A**, *Marmosops noctivagus* (JLP 15306, Penedo [locality **7**]); **B**, *Marmosops impavidus* (MNFS 760, Barro Vermelho [locality **12**]); and **C**, *Marmosops neblina* (JLP 15450, Nova Empresa [locality **8**]). All specimens are drawn to the same scale.

older individuals (fig. 46); it differs from *M. impavidus* in the same set of characters, with the exception that the dorsal color of both is quite similar. The large size, supraorbital beading, and presence of posterior palatal vacuities easily distinguish *M. noctivagus* from *M. parvidens*.

DISTRIBUTION AND HABITAT: This species was found in all four sampling areas along the Rio Juruá except the Lower Central Region. It was very common at Penedo (locality **7**) where 18 specimens were obtained, mostly in terra firme forest but also in second-growth. One specimen was shot at a height of about 10 m, two were shot at heights of about 2 m, with all others either trapped or shot while on the ground. Specimens from the Headwaters Region came from both terra firme and várzea forest (localities 1 versus 2 and 3); all those from the Upper Central or Mouth regions were taken in terra firme communities.

REPRODUCTION: We found no females with attached young. Specimens taken at localities in the Headwaters Region were collected in the rainy season and were all either juveniles or nulliparous adult females. Only one of the 11 adults (M1–M4 fully erupted) collected at Penedo (locality **7**) during the height of the dry season in August showed evidence of prior suckling in the form of the discolored orange inguinal region and evident nipples.

KARYOTYPE: 2n = 14, FN = 24 (fig. 47C). Karyotypic data are available from four individuals (MNFS 369, 381, JLP 15566, 15676). The autosomal complement consists of four pairs of large meta- and submetacentric and two pairs of small metacentric ele-

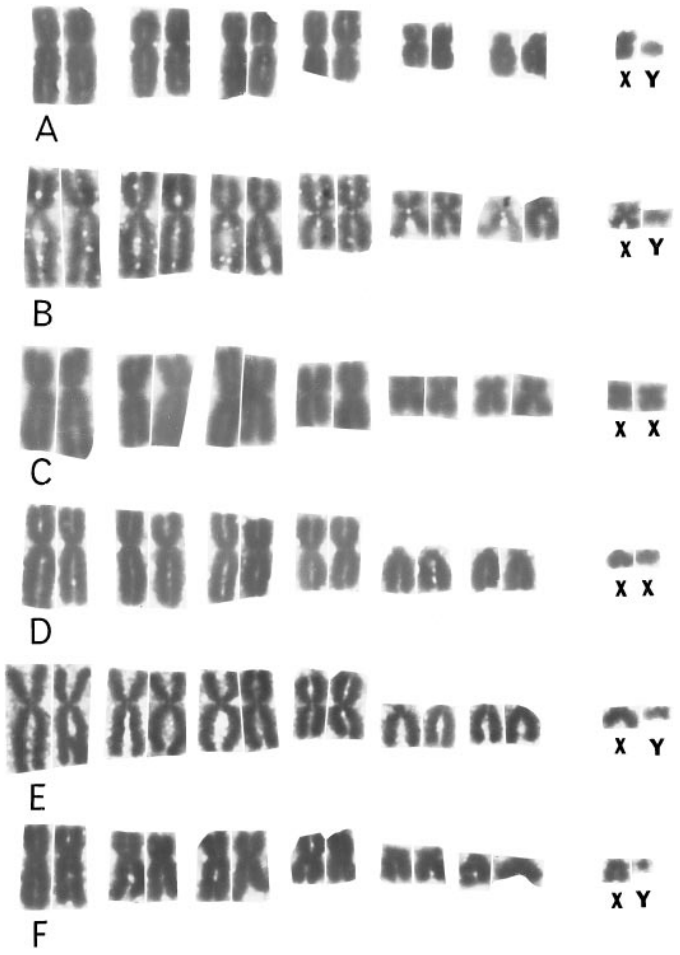

Fig. 47. Chromosome complements of five species of didelphid marsupials from the Rio Juruá with 2n = 14 karyotypes. **A**, *Marmosops impavidus* (MNFS 1191, Igarapé Porongaba [locality **1**]); **B**, *Marmosops neblina* (MNFS 703, Barro Vermelho [locality **12**]); **C**, *Marmosops noctivagus* (JLP 15676, Condor [locality **6**]); **D**, *Metachirus nudicaudatus* (JUR 399, Vai-Quem-Quer [locality **15**]); **E**, *Micoureus regina* [MNFS 1417, Igarapé Porongaba [locality **1**]); **F**, and *Caluromys lanatus* (MNFS 796, Barro Vermelho [locality **12**]).

ments; X-chromosome is a small metacentric, and the Y is an even smaller metacentric. This karyotype appears to differ from that of *M. impavidus* and *M. neblina* by two, versus one, small pairs of metacentric autosomes. Specimens from the Rio Juruá have the same karyotype as do those from eastern Perú (Reig et al., 1977) and Bolivia (Palma and Yates, 1996).

SPECIMENS EXAMINED (n = 40): (**1**) 3m, 1f — MNFS 1065, 1066, 1384, 1403; (**2**) 1f — MNFS 1184; (**3**) 4m — MNFS 1577, 1598, 1674, JUR 226; (**6**) 3f — JLP 15566, 15601, 15676; (**7**) 9m, 10f, 1 unknown — MNFS 336, 360–361, 369, 371, 381, 398, 403, 414–418, 495, 522, JLP 15253, 15306, 15313, 15353, 15360; (**15**) 5m, 3f — JUR 251, 283, 315–317, 331, 348, 397.

Marmosops parvidens (Tate, 1931)

TYPE LOCALITY: ''Hyde Park, 30 miles up the Demarara River, British Guiana, alt. 20 feet,'' East Demerara–West Coast Berbice, Guyana.

DESCRIPTION: This is the smallest species

in the Amazon region, with a total length of 218 mm, condyloincisive length of the skull not exceeding 25.9 mm, and adult weight less than 25 g. The molar teeth are small (mean maxillary toothrow length = 10.8 mm; M1–M4 length = 5.6 mm; table 8), the interorbital region is smooth and rounded in transverse section, with virtually no hint of supraorbital beading even in the oldest individuals. The palate lacks posterior vacuities, and the anterior pair are greatly reduced in size in comparison to the condition in the other three species. The coloration above is dark grayish-brown (Mummy Brown; Ridgway, 1912) as in *M. neblina*; below the venter is white along the midline with wide marginal bands of gray-based and silver-tipped hairs constricting the medial white, especially in the abdominal and inguinal region.

COMPARISONS: This species is readily distinguishable by its overall small size, lack of supraorbital beading even in old adult individuals, and lack of posterior palatal vacuities. It is similar in general coloration above and below with *M. neblina*, and indeed it looks like a miniature version of this species such that live specimens could be readily confused.

DISTRIBUTION AND HABITAT: We collected this species only at localities in our Lower Central and Mouth sampling regions along the Rio Juruá (fig. 1), where it was always found in terra firme forest, two individuals on the ground and four at heights of 1.5 to 2 m.

REPRODUCTION: We caught this species only in the months of October, April, May, and June. The three juveniles were collected at the end of the wet season in May and June; no adult females were found with attached young.

COMMENTS: The molecular data summarized in fig. 43 and evidence for sympatry in French Guiana of recognizable morphological entities (Robert S. Voss, personal commun.) underscore the composite nature of *M. parvidens* sensu Pine (1981). Since the type locality for *M. parvidens* is on the coast in Guyana, it is likely that another species name should be applied to our specimens from the Rio Juruá. We defer from making such a decision here, however, as we have not had the opportunity to examine specimens of appropriate candidate taxa.

SPECIMENS EXAMINED (n = 7): (**12**) 1m — JLP 15826; (**13**) 1m — JUR 476; (**14**) 1f, 2m — JUR 435–437; (**15**) 1f — JUR 381; (**16**) 1f — MNFS 1757.

METACHIRUS BURMEISTER, 1854

Brown four-eyed opossum

There is a single species in this genus as currently understood (Cabrera, 1957; Hall, 1981; Gardner, 1993). Over most of the Amazon Basin, *M. nudicaudatus* lacks any conspicuous phenotypic geographic differentiation, with color and color pattern and general size rather uniform among specimens we have examined from lowland tropical forests from Perú to eastern Brazil. Cabrera (1957) lists eight subspecies, three within Amazonia, with the nominate form in the Guianas and eastern Brazil. The species, however, has never been revised, and there are good series of specimens in existing collections that would make this possible.

Our limited sequence data from the mitochondrial cytochrome-b gene document deep divergences across the range of the species. We have examined 26 individuals from 20 localities, including specimens from western, central, and southeastern Amazonia, French Guiana, and the Mata Atlântica of coastal southeastern Brazil (fig. 48; table 10). Four reciprocally monophyletic clades are evident among this assemblage (fig. 49). Three clades are strongly supported phygeographic units with bootstrap values above 70%. These include samples from southwestern Amazonia (Rio Juruá and upper Rio Urucu in Brazil), northwestern and central Amazonia (northern Perú and Rio Jaú northwest of Manaus in Brazil), and the Mata Atlântica, each of which are comprised of closely related haplotypes with maximum levels of within-clade divergence of 2%. The fourth clade is comprised of a set of rather divergent individual haplotypes from the left (= east) bank of the Rio Negro north of Manaus in central Brazil, French Guiana, and southern Estado do Pará (fig. 49). The divergence between these three haplotypes is quite large (averaging 11.8%) and the bootstrap value is

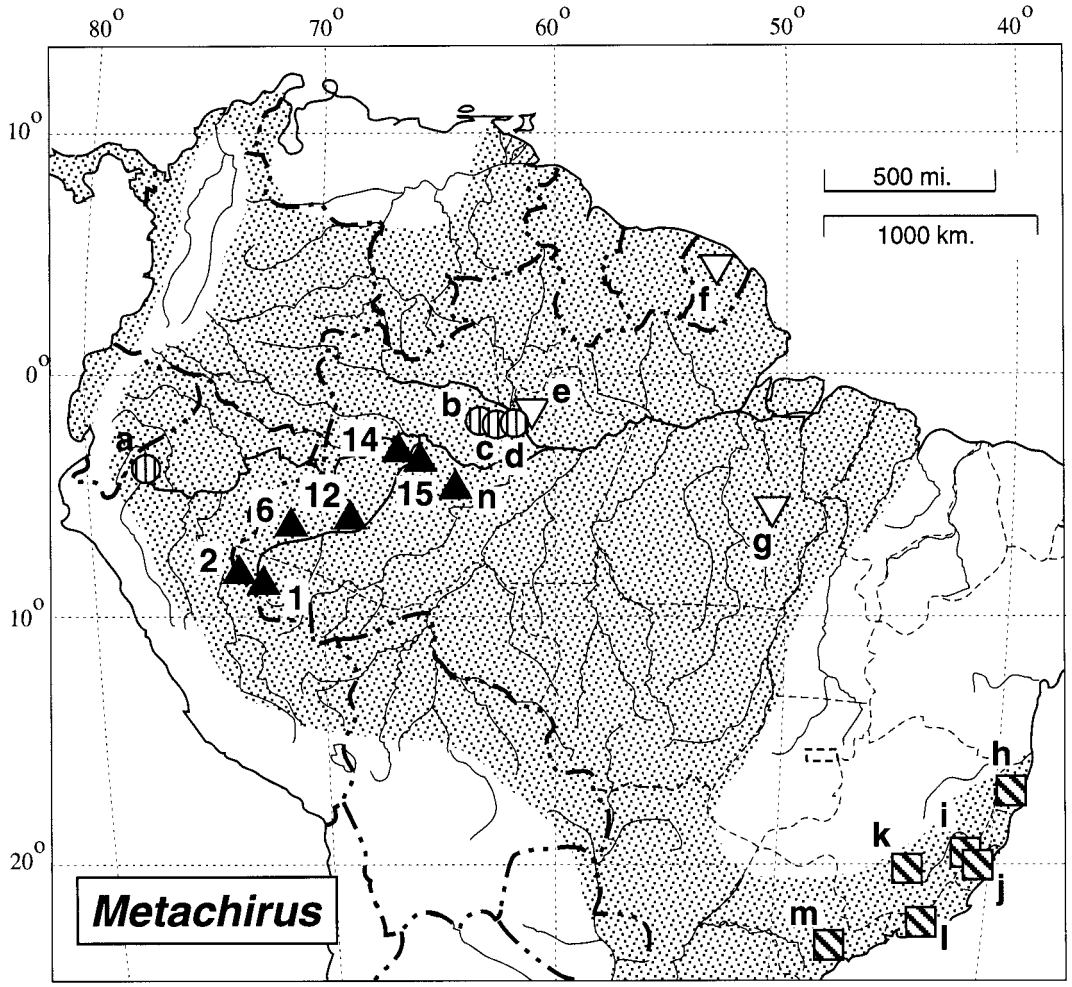

Fig. 48. Map of sample localities of the brown four-eyed opossum *Metachirus nudicaudatus* from which individuals have been examined for sequence variation in the mtDNA cytochrome-b gene. Symbols are keyed to the reciprocally monophyletic clades identified in the maximum parsimony tree, fig. 49. Provenance data are given in table 10.

low (58%). These three haplotypes sharply diverge from all others, including those from western and central Amazonia and the Mata Atlântica, differing by nearly 14% (fig. 49). Within Amazonia, samples from north of the Solimões-Amazonas axis (northern Perú and Rio Jaú in central Brazil) differ from those to the south in the Rio Juruá basin and adjacent upper Rio Urucu by an average of 8.5%. Finally, samples from the Mata Atlântica in the states of Minas Gerais, Espírito Santo, Bahia, Rio de Janeiro, and São Paulo link phylogenetically with those from the southwestern Amazon, with the difference between these two groups averaging only 4.8%. *Metachirus* is one of the few examples where Amazonian regional clades are not monophyletic relative to those of the Mata Atlântica (see discussion below, and da Silva and Patton, 1998). Finally, both the degree of sequence divergence observed and the strong regional pattern of monophyly suggest that the brown four-eyed opossum might be a composite of several separate species. Clearly, this is another taxon ripe for critical systematic study.

TABLE 10
Haplotypes, Map Localities, and Voucher Numbers for Specimens of *Metachirus nudicaudatus*
Individual haplotypes listed from top to bottom in the tree, figure 49, with the catalog numbers of their respective voucher specimens, and localities (identified as in the map, fig. 47) for which 450-bp haplotypes of the mitochondrial DNA cytochrome-b gene are available.

Haplotype	Voucher no.	Locality
1	ML 88	Fazenda Esmeralda, 30 km E & 4 km N Rio Casca, Minas Gerais, Brazil (locality k)
2	ML 114	Estação Biológica de Santa Lúcia, 8.2 km E Santa Tereza, Espírito Santo, Brazil (locality i)
3	MAM 193	Aracruz, Santa Cruz, Espírito Santo, Brazil (locality j)
4	MAM 246	Fazenda Intervales, Base Saibadela, Sete Barros, São Paulo, Brazil (locality m)
5	MAM 187	Cia. Mineradoras Brasileiras Reunidas, Ibicui, Mangaratiba, Rio de Janeiro, Brazil (locality l)
6	ML 89	Fazenda Esmeralda, 30 km E & 4 km N Rio Casca, Minas Gerais, Brazil (locality k)
7	EDH 23	Fazenda Beijo Grande, 12 km S & 1.1 km E Itabuna, Bahia, Brazil (locality h)
8	MNFS 757	Barro Vermelho, left bank Rio Juruá, Amazonas, Brazil (locality **12**)
9	JUR 399	Vai-Quem-Quer, right bank Rio Juruá, Amazonas, Brazil (locality **13**)
10	JUR 433	Colocação Vira-Volta, left bank Rio Juruá, Amazonas, Brazil (locality **14**)
11	MNFS 40	alto Rio Urucu, Tefé, Amazonas, Brazil (locality n)
12	MNFS 91	alto Rio Urucu, Tefé, Amazonas, Brazil (locality n)
13	MNFS 1356	Igarapé Porongaba, right bank Rio Juruá, Acre, Brazil (locality **1**)
14	MNFS 1394	opposite Igarapé Porongaba, left bank Rio Juruá, Acre, Brazil (locality **2**)
15	JLP 15542	Seringal Condor, left bank Rio Juruá, Amazonas, Brazil (locality **6**)
16	LC 124	Macaco, left bank Rio Jaú, Amazonas, Brazil (locality c)
17	YL 116	Macaco, left bank Rio Jaú, Amazonas, Brazil (locality c)
18	YL 120	Macaco, left bank Rio Jaú, Amazonas, Brazil (locality c)
19	MNFS 1981	Tambor, left bank Rio Jaú, Amazonas, Brazil (locality b)
20	JLP 16768	above mouth, right bank Rio Jaú, Amazonas, Brazil (locality d)
21	MNFS 2000	Tambor, left bank Rio Jaú, Amazonas, Brazil (locality b)
22	MVZ 153289	Huampami, Río Cenepa, Amazonas, Perú (locality a)
23	MVZ 153290	Huampami, Río Cenepa, Amazonas, Perú (locality a)
24	JLP 16789	Lago Meduiním, left bank Rio Negro, Amazonas, Brazil (locality e)
25	CS 83	Floresta Nacional Tapirapé-Aquiri, Município de Marabá, Pará, Brazil, 5°48'05"S, 50°30'54"W (locality g)
26	MNU 051	Sinnamary River, French Guiana (locality f)

Metachirus nudicaudatus
(Desmarest, 1817)

TYPE LOCALITY: "Cayenne," French Guiana.

DESCRIPTION: This is a terrestrial species that is readily distinguishable from all other sympatric marsupials by a combination of its moderate size, light yellow- to reddish-brown dorsal coloration with creamy-white spots over the eyes, venter from chin to tail a uniform pinkish yellow, naked tail with only a very minimally furred base, long and rather narrow hind feet, lack of a pouch in adult females, and skull with rounded interorbital region without supraorbital ledges or postorbital processes. Sexual dimorphism is slight to nonexistent within our limited sample, but it is present in six of 19 characters (TOL, HF, CIL, ZB, RW, and CD; all at $p < 0.05$, based on one-way ANOVA; table 11). Selected external and cranial measurements for adult individuals of both sexes are given in table 11.

DISTRIBUTION AND HABITAT: We took *M. nudicaudatus* only in the middle and lower reaches of the Rio Juruá, and always on the ground in terra firme forest. However, in the Headwaters localities we found individuals in terra firme as well as in "várzea" forest, which in this region is narrowly distributed along parts of the river and is probably only inundated in extreme years.

REPRODUCTION: The species appears to breed throughout the year as parous females

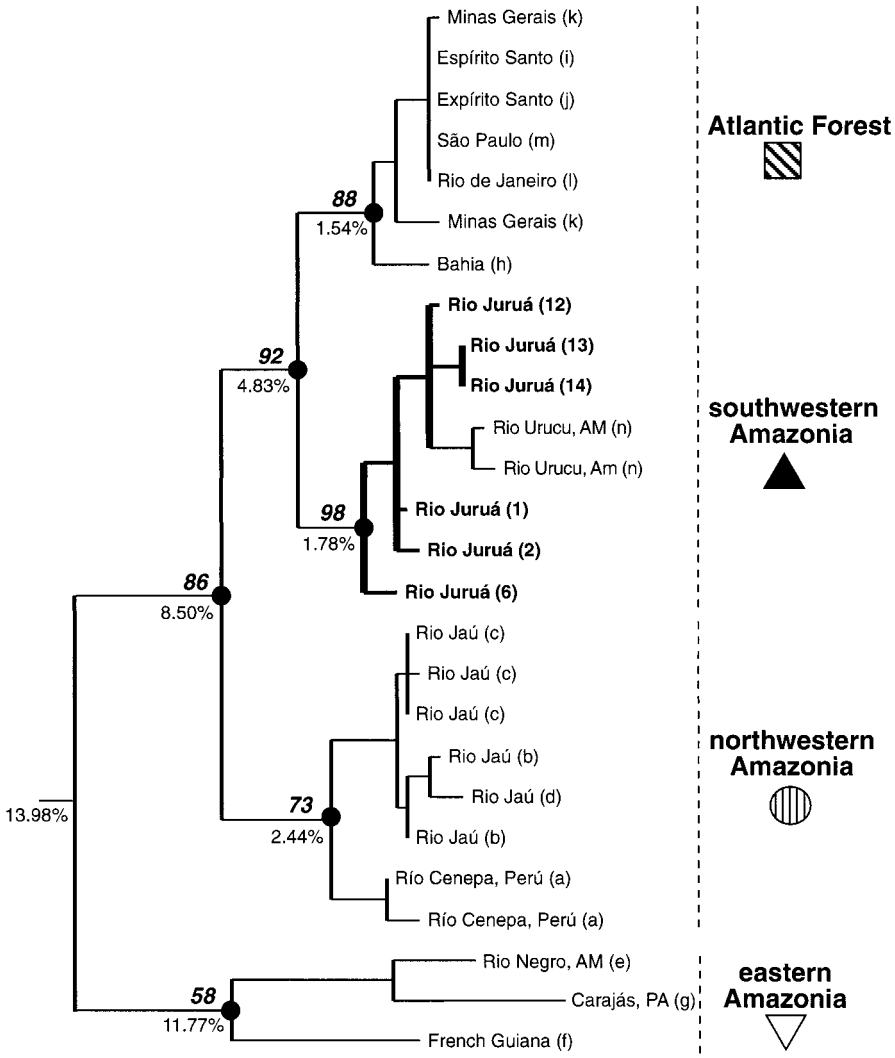

Fig. 49. Strict consensus tree of two minimum-length parsimony trees of the brown four-eyed opossum, *Metachirus nudicaudatus*, based on the initial 450 bp of the mtDNA cytochrome-b gene, and rooted by comparison to sequences from *Didelphis* and *Philander*. Branch lengths are proportional to the number of character changes. Regional reciprocally monophyletic clades are identified, and keyed to the localities mapped in fig. 48. Haplotypes for specimens from the Rio Juruá are identified by heavy lines and bold type; numbers refer to the specific locality as identified in the text and the map, fig. 1. Bold numbers at internal nodes are bootstrap values, based on 1000 iterations; percentages are average Kimura two-parameter distances. Individual haplotypes are identified by general locality, except for those from the Rio Juruá, which are identified by specimen and locality numbers (see table 10). Tree length = 215 steps; CI = 0.730; RI = 0.842.

with attached young were collected during the rainy season months of February, March, April, and May and during the dry season months of August and September. Very young aged individuals (age class 1 and 2 for *Didelphis*, Gardner, 1982) were taken at nearly all localities during the months from February to November. The modal number of attached young was 8 (range 6–9, n = 7).

KARYOTYPE: 2n = 14, FN = 20 (fig. 47D). The autosomal complement consists of four pairs of large metacentric and submetacentric

TABLE 11
Selected External and Cranial Dimensions of Adult *Metachirus nudicaudatus*
Measurements (mm) are given as mean ± standard error, with range and sample size. Individuals are pooled across all localities along the river. Differences between the sexes are noted (ns = $p > 0.05$; * $p < 0.05$; ** $p < 0.01$; *** $p < 0.001$).

	Males				Females		
Variable	Mean ± SE	Range	n	*p*	Mean ± SE	Range	n
TOL	582.3 ± 8.29	553–606	6	*	549.0 ± 7.19	512–587	11
TAL	319.7 ± 7.13	297–342	6	ns	304.27 ± 4.51	273–325	11
HF	45.8 ± 0.40	45–47	6	***	42.4 ± 0.45	41–46	12
E	35.7 ± 0.88	33–39	6	ns	35.1 ± 0.60	32–39	12
CIL	57.80 ± 1.01	54.58–60.90	5	*	55.09 ± 0.62	51.96–59.69	12
ZB	29.65 ± 0.61	27.39–31.67	6	**	27.54 ± 0.30	26.39–29.74	12
BB	17.93 ± 0.19	17.21–18.61	6	ns	17.59 ± 0.14	16.98–18.45	12
IOC-1	12.03 ± 0.19	11.39–12.57	6	ns	11.55 ± 0.18	5.35–6.23	12
IOC-2	9.33 ± 0.14	8.75–9.75	6	ns	9.05 ± 0.09	8.52–9.64	12
RL	24.02 ± 0.62	22.83–26.23	5	ns	22.83 ± 0.28	21.20–24.61	12
NL	29.02 ± 0.95	26.74–32.53	5	ns	28.02 ± 0.56	25.01–31.06	12
RW	9.84 ± 0.15	9.32–10.22	6	*	9.12 ± 0.18	8.27–10.22	12
C–M4	24.16 ± 0.33	23.66–25.81	6	ns	23.85 ± 0.24	22.35–25.32	12
M1–M4	11.67 ± 0.15	11.19–12.31	6	ns	11.52 ± 0.10	10.97–11.91	12
PL	32.92 ± 0.70	30.71–35.41	6	ns	31.98 ± 0.35	30.47–34.18	12
PW	17.74 ± 0.18	17.29–18.24	6	ns	17.50 ± 0.15	16.56–16.48	12
OCB	26.43 ± 0.14	25.24–27.93	6	ns	26.01 ± 0.16	24.87–27.44	12
BOL	7.22 ± 0.06	7.09–7.44	5	ns	6.71 ± 0.19	5.82–7.97	12
CD	15.47 ± 0.23	14.59–16.11	6	**	14.63 ± 0.13	14.12–15.59	12

elements and two pairs of medium acrocentrics. The X-chromosome is a small acrocentric and the Y is an even smaller acrocentric. This karyotype has been described and figured by Reig et al. (1977), Palma and Yates (1996), and Svartman (1998). Chromosomal preparations are available from four individuals (MNFS 366, 380, 1038, and 1104).

SPECIMENS EXAMINED (n = 44): (**1**) 1m, 3f — MNFS 1068, 1104, 1117, 1234; (**2**) 1f — MNFS 1394; (**a**) 1m — MNFS 1006; (**c**) 1m — MNFS 1038; (**3**) 1f — MNFS 1578; (**4**) 2m, 5f — MNFS 1479, 1529, 1659, JUR 211, 220 225, 244; (**6**) 2m, 3f — JLP 15542, 15567, 15569, 15620, 15661; (**7**) 2m, 9f — MNFS 366, 370, 380, 393-395, 400, 474, JLP 15305, 15340, 15359; (**9**) 2f — JLP 16042–16043; (**12**) 1m, 1f — MNFS 757–758; (**13**) 1m — JUR 292; (**14**) 4m, 2f — JUR 433, 466, 470, 495–496, 505; (**15**) 1m, 1f — JUR 352, 399.

MICOUREUS LESSON, 1842

Woolly mouse opossums

The woolly mouse opossums are arboreal, omnivorous, and common members of the Neotropical forest marsupial assemblage. The genus is widely distributed, ranging from Belize to northern Argentina, and from the lowland Amazonian to middle elevation elfin forests on both Andean slopes (Emmons and Feer, 1997). The number of species recognized in the genus is in flux, as adequate geographic analyses that can identify species boundaries have yet to be performed. For example, Gardner (1993) recognizes four species and Emmons and Feer (1997) five. Both sets of authors record three species within Amazonia: *constantinae* Thomas, 1904, from western Brazil and southeastern Bolivia, *regina* Thomas, 1898, in extreme western Amazonia, and *demerarae* Thomas, 1905, throughout Amazonia from western Brazil to the Guianan region and south to the Mata Atlântica of coastal Brazil. The widespread *M. demerarae*, however, exhibits considerable variation in coloration and other pelage characteristics, especially in the degree of the furred tail-base, and is likely to be composite (see immediately below). Its relationship to *M. constantinae*, for example, needs clarification (contrast map in Emmons and Feer

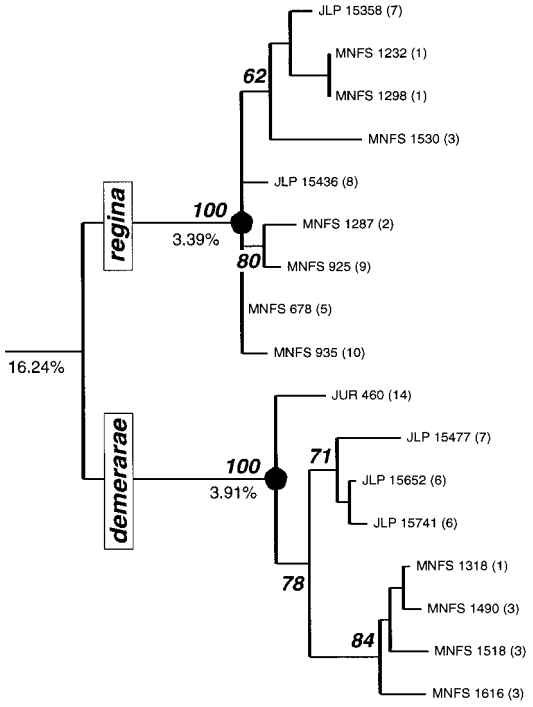

Fig. 50. Maximum parsimony tree of cytochrome-b haplotypes of *Micoureus demerarae* and *M. regina* from the Rio Juruá, based on 401 bp of sequence. The tree was rooted by comparison to homologous sequence from specimens of *Marmosa rubra* and *Monodelphis domestica* (data from Patton et al., 1996). Branch lengths are proportional to the number of character changes. Comparisons were specifically made between specimens collected at the same or nearby localities. Each unique haplotype is identified by locality designation and field number. Bold numbers at internal nodes are bootstrap values, based on 1000 iterations; percentages are average Kimura two-parameter distances. Tree length = 131 steps; CI = 0.740.

[1997] with area assignments by Anderson [1997]). Finally, populations from the middle elevations of the eastern Andean slopes in Perú (e.g., *rapposa* Thomas) and Bolivia (e.g., *mapiriensis* Tate) need critical evaluation in relation to those from lowland forests.

We examined 401 base pairs of cytochrome-b sequence for 23 individual woolly mouse opossums from the Rio Juruá. These comprise 17 separate haplotypes that form two deeply divergent clades that differ by more than 16% (fig. 50). Each of these clades is internally uniform with average divergences of less than 4%. We have placed these two clades in a broader set of geographic comparisons with specimens from Middle America, elsewhere throughout much of Amazonia, and the Mata Atlântica of coastal Brazil (fig. 51; table 12). For this larger data set, the 630 base pairs of sequence available identify four clades that differ by an average of 10 to 15% (fig. 52). Both taxa found along the Rio Juruá have broader distributions outside of that river basin, one linking to samples from northern Perú, and the other to a series of localities scattered throughout central, northeastern, and eastern Amazonia. The two additional clades are represented by a single individual of *M. alstoni* from Panamá and a series of specimens from the Mata Atlântica of coastal Brazil. The significance of the latter is discussed below under the account of *M. demerarae*.

Representatives of the two haplotype clades that occur within the Rio Juruá basin occupy generally separate habitats, although they are truly sympatric at some localities and broadly overlap in the middle and headwaters sections of the river. The two forms possess the morphological characteristics usually accorded to the western Amazonian *regina* and the eastern Amazonian *demerarae* (Tate, 1933; updated by Gardner, 1993). *Micoureus regina* occupies only the upper reaches of the Rio Juruá basin, while *M. demerarae* is found throughout the Rio Juruá basin.

Micoureus demerarae (Thomas, 1905)

TYPE LOCALITY: ''Comaccka, 80 miles up Demerara River,'' East-Demerara-West Coast Berbice, Guyana.

DESCRIPTION: A large-bodied murine opossum, this species is equivalent in size to others in the genus and cannot be distinguished in this respect from sympatric, or near-sympatric *M. regina* from the Rio Juruá (table 13). It has relatively long and distinctly ''woolly'' dorsal pelage, averaging 12 mm in length. One of the most distinctive features of this taxon is the extensively furred base of the tail (fig. 53). The fur extends onto the tail for an average length of 29 mm in specimens from the Rio Juruá (measurement tak-

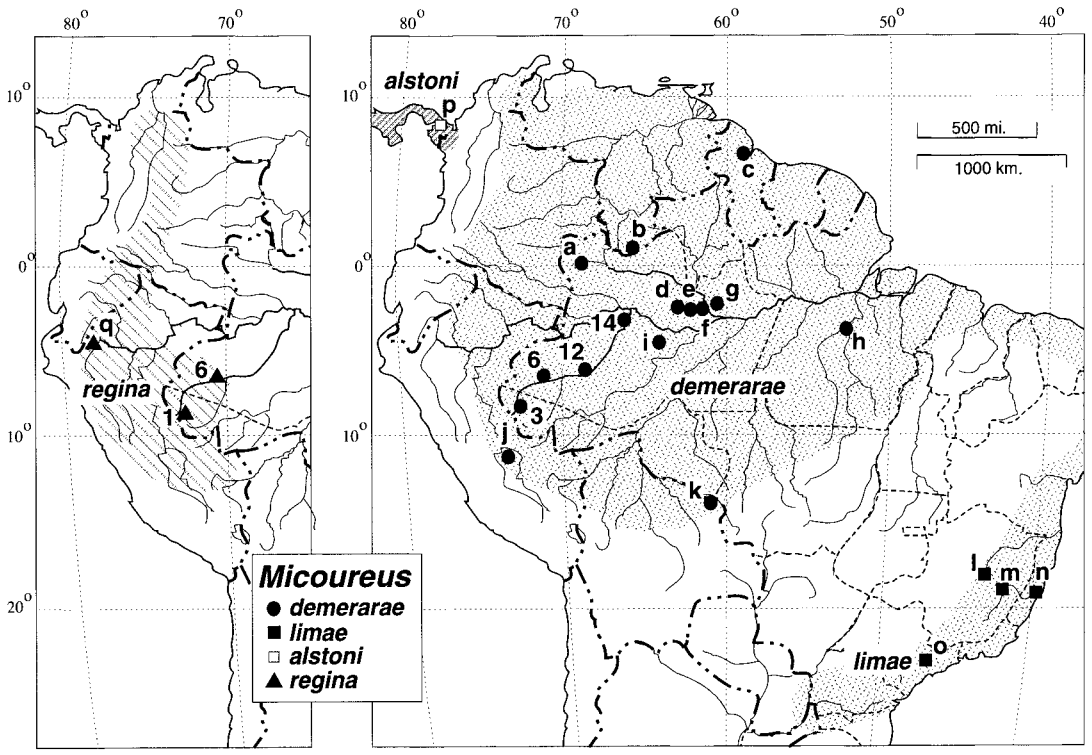

Fig. 51. Map of sampled localities of the woolly mouse opossums, genus *Micoureus*, for which cytochrome-b sequence data are available. Localities are identified as in the tree, fig. 52; specific localities and voucher specimen catalog numbers are given in table 12. The approximate range of each of the four species we recognize is indicated, largely based on the maps in Emmons and Feer (1997).

en from dried skins), but may be considerably longer in those from eastern Amazonia and especially the Mata Atlântica. The dorsal color is gray-brown with a pale yellowish or buff wash, the black eye-ring is distinct, and the cheeks are pale buff. Ventrally, uniformly buff hairs are confined to the throat and inguinal region in most specimens, with a broad lateral strip of gray-based, buffy tipped fur extending from the lateral margins of the dorsal fur onto the venter, from the upper thorax posteriorly across the entire abdomen (fig. 54). This gray-based fur coalesces along the midventral region in most specimens (35 of 39 adults); in the remainder there is a narrow (< 5 mm), purely buff stripe on the midline through the thoracic and abdominal regions. This buff coloration ranges from Light Buff to Warm Buff, or from Cartridge Buff to Cream Buff (Ridgway, 1912). Two specimens from locality **14** (Vira-Volta) near the mouth of the Rio Juruá have a distinctly pinkish cast to the midline ventral region that separates the lateral gray-based incursions; other specimens from this and nearby localities are more typical in color and color pattern. These two individuals share the same cranial dimensions and long-furred tail-base of other *M. demerarae*. The tail is uniformly colored gray-brown along its entire length in all specimens from the Rio Juruá; none have a terminal mottle of gray-brown and cream patches, as may be found in specimens elsewhere in the species range.

GEOGRAPHIC AND NONGEOGRAPHIC VARIATION: We performed a 2-way ANOVA to examine the effects of geographic variation among samples of adult *M. demerarae* along the river as well as sexual dimorphism within individual samples. Although the power of this analysis is limited because of the relatively small sample sizes for each locality, significant ($p < 0.05$) geographic variation was found for eight mensural variables

TABLE 12

Haplotypes, Voucher Numbers, and Localities for Taxa of Woolly Mouse Opossums, Genus *Micoureus*

Individual haplotypes listed from top to bottom in the tree, figure 52, with the catalog numbers of their respective voucher specimens, and localities (identified as in the map, fig. 51) for which 650-bp haplotypes of the mitochondrial DNA cytochrome-b gene are available.

Haplotype	Voucher no.	Locality
Micoureus demerarae		
1	JLP 16758	above mouth, right bank Rio Jaú, Amazonas, Brazil (locality f)
2	JLP 16769	above mouth, right bank Rio Jaú, Amazonas, Brazil (locality f)
3	JLP 16770	above mouth, right bank Rio Jaú, Amazonas, Brazil (locality f)
4	LC 132	Macaco, left bank Rio Jaú, Amazonas, Brazil (locality e)
5	MNFS 1998	Tambor, left bank Rio Jaú, Amazonas, Brazil (locality d)
6	INPA 2514	Comunidade Colina, right bank Rio Tiquié, Município São Gabriel da Cachoeira, Amazonas, Brazil (locality a)
7	INPA 2515	Comunidade Colina, right bank Rio Tiquié, Município São Gabriel da Cachoeira, Amazonas, Brazil (locality a)
8	JLP 16788	Lago Meduinim, left bank Rio Negro, Amazonas, Brazil (locality g)
9	JLP 16784	Lago Meduinim, left bank Rio Negro, Amazonas, Brazil (locality g)
10	USNM 560731	Cerro de la Neblina, camp VII, Amazonas, Venezuela (locality b)
11	ROM 98124	Quartermile Landing, Rupununi River, 5 km S Anna, Rupununi, Guyana (locality c)
12	MNFS 1490	Nova Vida, right bank Rio Juruá, Acre, Brazil (locality **3**)
13	JLP 15652	Seringal Condor, left bank Rio Juruá, Amazonas, Brazil (locality **6**)
14	MNFS 727	Barro Vermelho Condor, left bank Rio Juruá, Amazonas, Brazil (locality **12**)
15	JUR 460	Colocação Vira-Volta, left bank Rio Juruá, Amazonas, Brazil (locality **14**)
16	TTS 395	Flor de Oro, left bank Río Iténez, Parque Noël Kempff Mercado, Santa Cruz, Bolivia (locality k)
17	LHE 1447	2 km SW Tangoshiari, Río Pangoreni, Depto. Cusco, Perú, 1000 m, 11°46'S, 73°26.5'W (locality j)
18	LHE 1461	2 km SW Tangoshiari, Río Pangoreni, Depto. Cusco, Perú, 1000 m, 11°46'S, 73°26.5'W (locality j)
19	MRR 782	2 km SW Tangoshiari, Río Pangoreni, Depto. Cusco, Perú, 1000 m, 11°46'S, 73°26.5'W (locality j)
20	MNFS 185	alto Rio Urucu, Tefé, Amazonas, Brazil (locality i)
21	USNM 549287	52 km SSW Altamira, east bank Rio Xingu, Pará, Brazil (locality h)
Micoureus alstoni		
22	USNM 449565	Bocatorito, Isla San Cristobal, Bocas del Toro, Panamá (locality p)
Micoureus limae		
23	LC 61	Parque Estadual do Rio Preto, 15 km S São Gonçalo do Rio Preto, Minas Gerais, Brazil (locality l)
24	LC 86	Parque Estadual do Rio Doce, 13 km E Marliéria, Minas Gerais, Brazil (locality m)
25	YL 39	Fazenda Santa Terezinha, 33 km NE Linhares, Espírito Santo, Brazil (locality n)
26	MAM 47	Fazenda Intervales, Capão Bonito, São Paulo, Brazil (locality l)
Micoureus regina		
27	MNFS 1232	Igarapé Porongaba, right bank Rio Juruá, Acre, Brazil (locality **1**)
28	JLP 15435	Seringal Condor, left bank Rio Juruá, Amazonas, Brazil (locality **6**)
29	MVZ 154766	Huampami, Río Cenepa, Amazonas, Perú (locality q)

(TAL, HF, E, IOC, NL, C-M4, PL, and PW), and within-locality sexual dimorphism was found for two external characters (TAL and HF). However, when all individuals are pooled to increase sample size, significant sexual dimorphism is apparent in all four external measurements and eight of 15 cranial variables (CIL, MB, IOC, RL, C-M4, PL, BOL, and CD; $p < 0.05$, one-way ANOVA).

COMPARISONS: *Micoureus demerarae* is extremely similar to sympatric, or near-sympatric *M. regina* throughout the Rio Juruá ba-

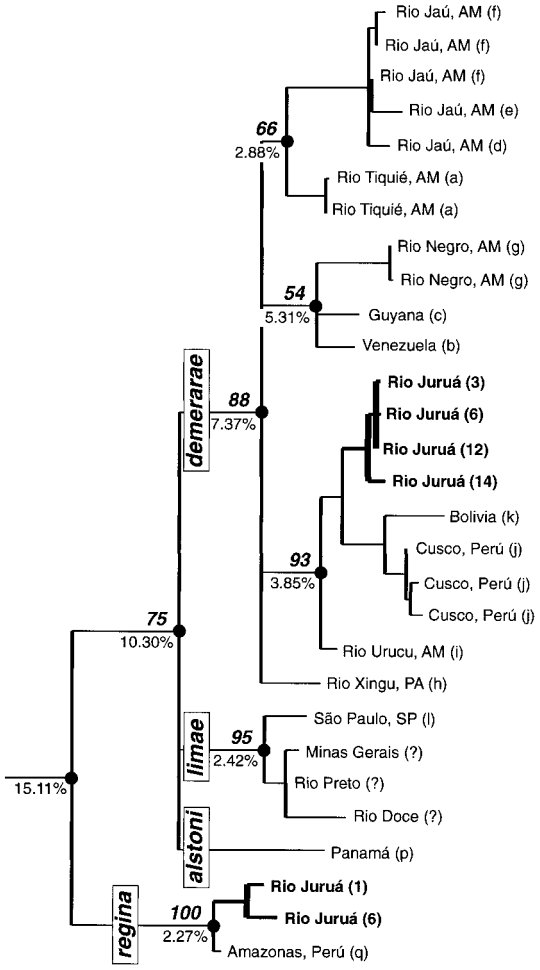

Fig. 52. Strict consensus tree of 36 equal-length maximum parsimony trees, based on 630 bp of the cytochrome-b gene and illustrating topological relationships among cytochrome-b haplotype clades of *Micoureus*. The tree is rooted by comparison to *Metachirus*, *Marmosa*, and *Monodelphis* (from Patton et al., 1996). Geographic provenance of haplotypes is indicated as in the map, fig. 51, and locality data are listed, from top to bottom, in table 12. Haplotypes for specimens from the Rio Juruá are identified by heavy lines and bold type. Bold numbers at internal nodes are bootstrap values, based on 1000 iterations; percentages are average Kimura two-parameter distances. Tree length = 450 steps; CI = 0.607; RI = 0.772.

sin. The two share the same overall size and general body proportions, but differ in color and color pattern, particularly of the venter, in the degree to which the base of the tail is furred, in external and cranial dimensions, and in some qualitative cranial features. In ventral color pattern, the pure color area is confined to the throat and upper thorax, with gray-based lateral fur coalescing in the midventral region in *M. demerarae* but widely separated in *M. regina* (fig. 54). *Micoureus demerarae* has a significantly longer ear and furred tail-base (fig. 53 and table 13), but averages fewer scale rows per centimeter along the tail (10 versus 13 in *regina*). While the two taxa are the same size in cranial length and depth, *M. demerarae* is consistently smaller in all other cranial dimensions, except BOL, even when the sexes are compared separately (table 13). The narrower interorbital breadth and palate of *M. demerarae* relative to *M. regina* are clearly evident in comparisons of representative skulls of the two species (fig. 55). These and other differences are also apparent in bivariate plots where overall size is represented by condyloincisive length (fig. 56). The slopes of the relationship between individual variables and CIL, a univariate size estimate, are not statistically different, although the Y-intercepts are, with that of *M. demerarae* significantly lower (ANCOVA, Fisher's Protected LSD, $p < 0.05$ in each comparison). The same patterns are present when the sexes are analyzed separately.

Principal components summaries of multivariate relationships indicate that PC-1 is a general size axis, with all cranial variables loading positive and highly (table 14). This axis accounts for 67.3% of the total variance; PC-2 accounts for 11.9%. The dispersion of individuals along PC-2 is influenced mostly by the width of the skull posterior to the supraoccipital processes (IOC-2) and molar toothrow length (M1-M4), which separate specimens with the generally narrower interorbits and shorter toothrows, characteristics of *M. demerarae*, from the larger *M. regina* (table 14 and fig. 57, top). PC-3 accounts for 6.5% of the variation in the data, but all variables load relatively evenly on this axis and it does not serve to separate the two species (fig. 57, middle). In a two-group discriminant

TABLE 13

External and Cranial Dimensions of Male and Female Woolly Mouse Opossums, Genus *Micoureus*, from the Rio Juruá

Measurements (mm) are given as mean ± standard error, with range and sample size. Individuals are pooled across all localities along the river. Significance levels are indicated based on one-way ANOVA (ns = $p > 0.05$; * $p < 0.05$; ** $p < 0.01$; *** $p < 0.001$).

	M. demerarae males				*M. regina* males		
Variable	Mean ± SE	Range	n	*p*	Mean ± SE	Range	n
TOL	439.6 ± 4.76	388–500	26	*	452.4 ± 3.71	403–492	22
TAL	258.8 ± 2.25	233–287	26	**	268.4 ± 2.24	248–294	22
HF	29.9 ± 0.30	27–34	27	ns	29.8 ± 0.32	26–32	22
E	27.7 ± 0.31	24–31	27	***	24.9 ± 0.29	22–27	22
CIL	44.40 ± 0.47	38.99–48.82	26	ns	45.42 ± 0.31	42.94–48.36	21
ZB	24.79 ± 0.28	21.64–27.92	27	**	26.19 ± 0.28	24.44–28.53	22
BB	15.36 ± 0.08	14.64–16.65	27	***	16.13 ± 0.11	15.25–17.27	22
IOC-1	7.87 ± 0.10	6.58–9.24	27	***	8.58 ± 0.11	7.77–9.73	22
IOC-2	6.91 ± 0.06	6.21–7.48	27	***	7.74 ± 0.11	6.96–8.63	22
RL	15.93 ± 0.17	14.07–17.47	27	***	16.86 ± 0.12	16.03–17.95	22
NL	19.59 ± 0.22	15.94–21.87	27	*	20.53 ± 0.23	18.89–22.93	22
RW	7.94 ± 0.11	6.95–9.57	27	**	8.44 ± 0.12	7.54–9.90	22
C–M4	17.86 ± 0.12	16.33–18.80	27	***	18.64 ± 0.11	17.75–19.32	21
M1–M4	9.00 ± 0.04	8.52–9.41	27	***	9.48 ± 0.63	8.85–10.06	21
PL	25.33 ± 0.22	22.44–27.13	27	**	26.08 ± 0.16	24.81–28.01	22
PW	13.68 ± 0.10	12.76–14.75	27	***	14.57 ± 0.08	13.76–15.51	22
MB	15.87 ± 0.12	14.62–17.76	27	***	16.92 ± 0.13	15.92–18.18	22
BOL	5.68 ± 0.08	4.79–6.57	26	ns	5.69 ± 0.08	5.16–6.34	21
CD	12.84 ± 0.07	12.10–13.47	26	ns	13.02 ± 0.10	12.01–13.76	21
Tail base	28.86 ± 0.57	24.21–32.17	14	***	15.19 ± 0.72	10.73–22.98	21

	M. demerarae females				*M. regina* females		
Variable	Mean ± SE	Range	n	*p*	Mean ± SE	Range	n
TOL	414.8 ± 6.67	378–463	13	*	432.1 ± 4.88	380–465	19
TAL	241.5 ± 3.64	227–272	13	**	255.5 ± 2.63	238–280	19
HF	27.7 ± 0.26	26–29	13	ns	28.5 ± 0.41	25–31	19
E	26.5 ± 0.39	25–30	13	***	24.6 ± 0.23	23–27	19
CIL	42.56 ± 0.56	39.70–46.14	13	ns	43.71 ± 0.38	39.13–46.42	20
ZB	23.90 ± 0.35	21.89–26.36	13	*	24.91 ± 0.25	22.61–26.58	20
BB	15.18 ± 0.14	14.38–16.38	13	**	15.73 ± 0.12	14.39–16.58	20
IOC-1	7.35 ± 0.10	6.84–7.92	13	***	8.11 ± 0.11	7.26–8.91	20
IOC-2	6.71 ± 0.09	6.23–7.16	13	***	7.58 ± 0.06	6.72–8.74	20
RL	15.29 ± 0.23	14.06–16.59	13	**	16.21 ± 0.19	14.32–17.53	20
NL	18.83 ± 0.16	17.48–20.19	13	**	19.49 ± 0.24	17.01–20.82	20
RW	7.70 ± 0.14	6.77–8.72	13	*	8.05 ± 0.09	7.21–8.62	20
C–M4	17.26 ± 0.15	16.56–18.04	13	***	18.24 ± 0.14	16.92–19.11	20
M1–M4	8.88 ± 0.05	8.52–9.17	13	***	9.38 ± 0.06	8.89–9.86	20
PL	24.29 ± 0.30	22.64–26.00	13	**	25.26 ± 0.22	23.04–26.46	20
PW	13.49 ± 0.14	12.69–14.23	13	***	14.25 ± 0.08	13.32–14.79	20
MB	15.27 ± 0.19	14.28–16.75	13	***	16.25 ± 0.13	15.04–17.12	20
BOL	5.29 ± 0.10	4.43–5.71	13	ns	5.43 ± 0.08	4.57–6.10	20
CD	12.46 ± 0.08	12.03–12.96	13	*	12.67 ± 0.06	12.05–13.06	20
Tail base	29.45 ± 1.40	24.22–40.51	10	***	13.63 ± 0.49	11.38–18.71	18

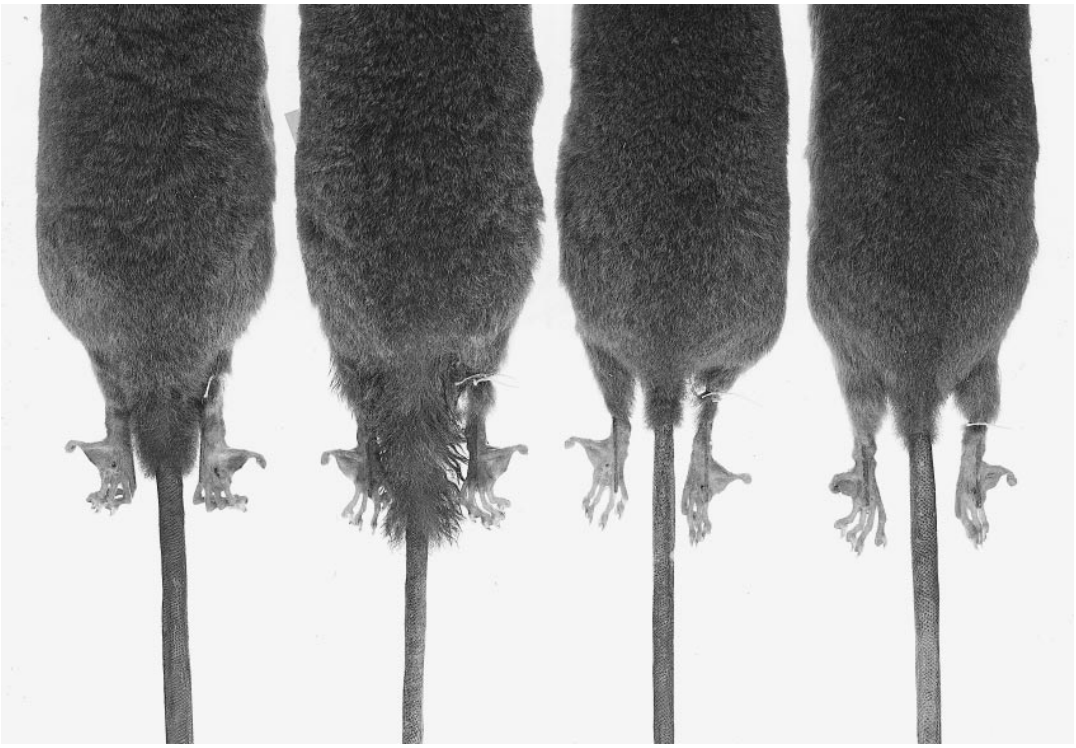

Fig. 53. Difference in the length of the furred base of the tail in species of *Micoureus* from the Rio Juruá. From left to right: *M. demerarae* (JLP 16051, Altamira [locality **9**]); *M. demerarae* (JLP 15652, Condor [locality **6**]); *M. regina* (MNFS 1287, opposite Igarapé Porongaba [locality **2**]); and *M. regina* (MNFS 935, opposite Altamira [locality **10**]).

analysis with samples allocated to each species identified a priori, the two taxa have completely nonoverlapping scores, with individual probabilities of group membership of 0.909, or higher (table 14; fig. 57, bottom).

DISTRIBUTION AND HABITAT: This species occurs throughout the Rio Juruá basin, as we took specimens in all four regional sampling areas. Most of these came from undisturbed terra firme forest or second-growth forest in upland, nonflooded areas. Only three of the 47 specimens collected in the Upper Central, Lower Central, or Mouth areas, where true várzea is present, were taken from seasonally flooded várzea forest. Both *M. demerarae* and *M. regina* were taken together at all four localities in the Headwaters region, including the quasi-várzea forest localities (opposite Porongaba, locality **2**, and Nova Vida, locality **3**). We also took both species in várzea at Boa Esperança (locality **9a**) in the Lower Central section of the river. Of the 55 total specimens obtained, 50 were taken in canopy traps placed at heights between 6 and 17 m, two were shot at heights above 2 m, and three were taken in terrestrial traps.

REPRODUCTION: We found parous or reproductive females (those with orange inguinal mammary areas, attached young, or lactating) in the months of February, March, April, September, October, and November. These months encompass both the rainy and dry seasons, suggesting that reproduction can occur throughout the year. All reproductive females were at least age class 5, with a completely erupted toothrow (following Gardner, 1982). A single female from Barro Vermelho (locality **12**) had 7 attached young. All males of age class 5 or older had testes at least 12 mm in length, with the average length 13.9 mm; all individuals of younger age had testes less than 9 mm.

KARYOTYPE: 2n = 14, FN = 20. The au-

Fig. 54. Color pattern of the venter of *Micoureus demerarae* (left, JLP 15741 [Condor, locality **6**]) and *M. regina* (right, MNFS 773 [Jainu, locality **11**]) illustrating differences in the degree of encroachment of the lateral gray-based hairs onto the midventral region in the thoracic and abdominal regions between the two species.

tosomal complement consists of four pairs of large biarmed and two pairs of medium uniarmed chromosomes; the X-chromosome is a small uniarmed element, and the Y an even smaller uniarmed chromosome. This karyotype is identical in gross chromosomal characteristics to that of *M. regina*, described below (fig. 47E). It has been described by Reig et al. (1977) and Palma and Yates (1996), under the name *M. cinerea*, and by Svartman (1998).

COMMENTS: As currently recognized, this species is distributed throughout Amazonia, from central Perú in the upper Río Urubamba drainage (Departamento de Cusco) east to the Guianan coast and eastern Estado do Pará, around the horn of northeastern Brazil, and south through gallery forests along the clear water tributaries of the Brazilian shield to the Mata Atlântica of coastal Brazil. The limited sequence data from the cytochrome-b gene show that this range is divisible into at least five reciprocally monophyletic regional lineages, with the Mata Atlântica representatives as nearly distinct from those of Amazonia as are *M. demerarae* and *M. regina*, and certainly as distinct as is the Central American *M. alstoni* (fig. 52). Amazonian and Mata Atlântica representatives differ by an average of 10.7% in sequence, and the four Amazonian clades differ by a maximum of 7.4% among themselves (see da Silva and Patton, 1998). While additional fieldwork is critically needed in geographically intermediate areas between the Mata Atlântica and Amazonia, the suggestion that these represent separate species is supported by the sequence data. If so, the name *demerarae* would be restricted to Amazonian forms. Alfred L. Gardner (personal commun.) believes that *limae* Thomas, 1920, with type locality of ''Ceará,'' Brazil, is the appropriate name to apply to the coastal Brazilian clade, although this needs to be confirmed by appropriate comparisons and analyses of variation within coastal Brazil. If *limae* proves to be associated with Amazonian *demerarae* instead, then *travassosi* (Miranda Ribeiro), with type locality in Estado do Rio de Janeiro would be the most likely name.

The four haplotype clades of *M. demerarae* within Amazonia (fig. 52) form regional units, with one in southwestern Amazonia (including our Rio Juruá samples), one north of the Rio Solimões and west of the Rio Negro, one in northeastern Amazonia (east of the Rio negro, Venezuela, and Guyana), and one in southeastern Amazonia (Estado do Pará). The southwestern Amazonian clade contains the haplotype from locality ''k'' in eastern Bolivia (fig. 51) that represents the taxon *M. constantiae* based on geographic position (Anderson, 1997). This suggests that *constantiae* might best be considered a junior synonym of *demerarae*, at least until a thorough revision of the genus is accomplished. Although there is strong geographic structure in identifying these four clades, there is also a reasonable level of se-

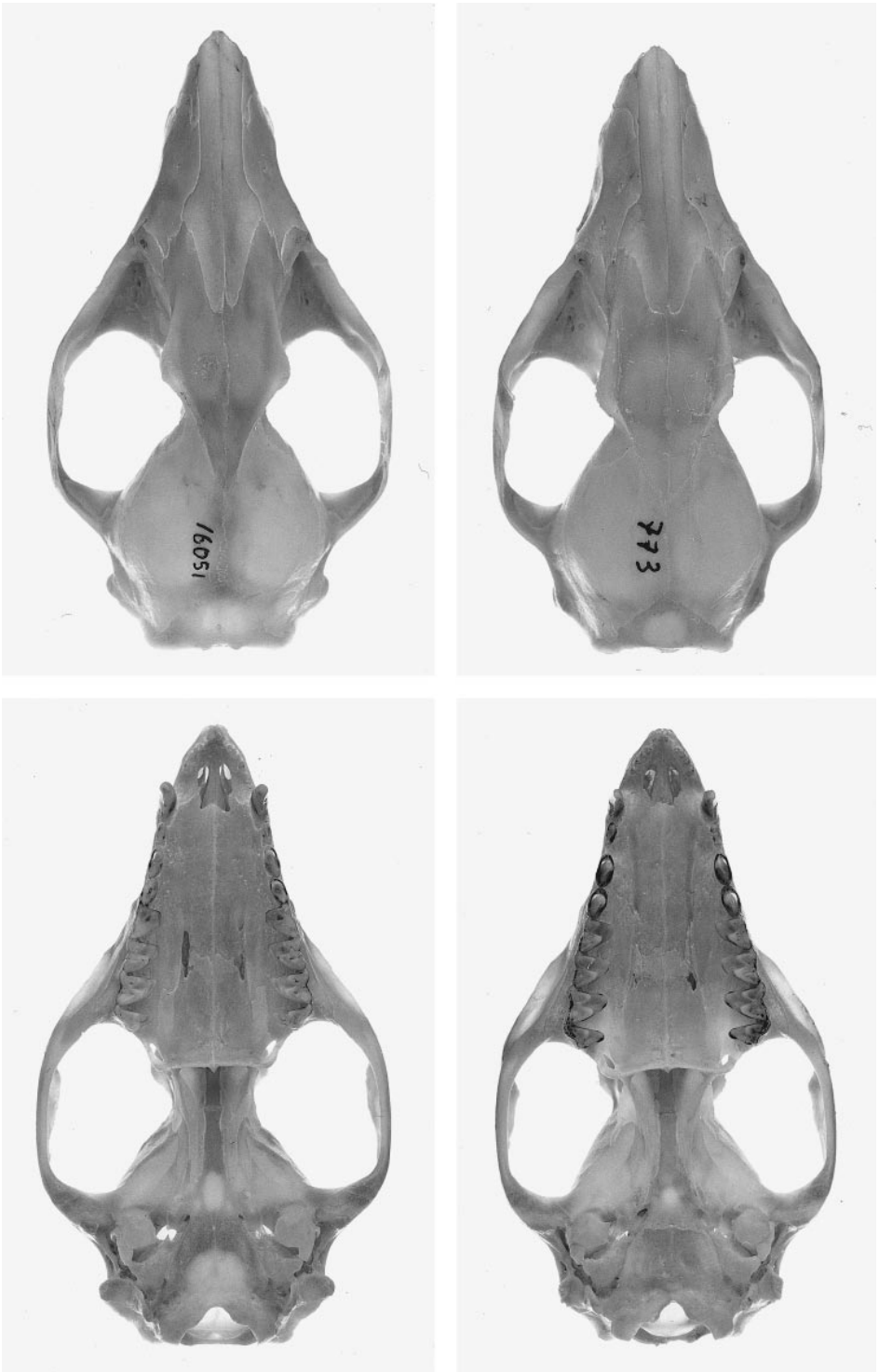

Fig. 55. Dorsal (top) and ventral (bottom) views of adult crania of *Micoureus* from the Rio Juruá. **Left**: *M. demerarae* (JLP 16051). **Right**: *M. regina* (MNFS 773). Magnification = ×2.

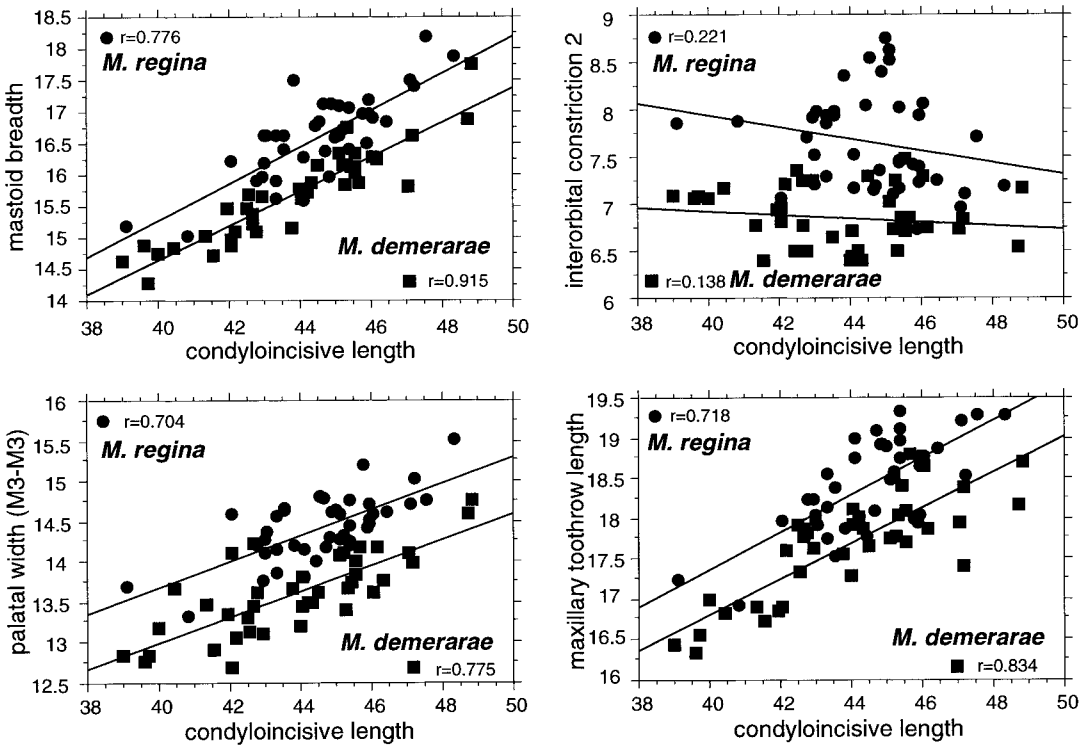

Fig. 56. Bivariate relationship of four cranial dimensions for *Micoureus demerarae* and *M. regina* and condyloincisive length, a univariate measure of overall size. Correlation coefficients for each set of relationships are given. The respective slopes for the two species in each relationship are not significantly different, but their Y-intercepts are (at $p < 0.01$ or 0.001).

quence divergence within each of those clades with several sampled localities, with haplotype differences ranging from a mean of 2.9% to 5.3% (fig. 52). Clearly, the woolly mouse opossums remain a rich source for much needed revisionary studies. Fortunately, relatively large samples are available in many museum collections, which will facilitate future studies.

SPECIMENS EXAMINED (n = 55): (**1**) 2m — MNFS 1365, 1672; (**2**) 1f — MNFS 1256; (**3**) 1m, 3f — MNFS 1490, 1513, 1616, JUR 209; (**4**) 1f — MNFS 1672; (**6**) 4m — JLP 15632, 15652, 15741; MNFS 727; (**7**) 5m, 3f — JLP 15357, 15368, 15423, 15477, MNFS 382, 397, 434, 475; (**9**) 4f — JLP 16050–16051, 16058, 16077; (**9a**) 2f — MNFS 904–905; (**12**) 2m, 2f — JLP 15833; MNFS 721, 727, 748; (**13**) 1m, 1f — JUR 267, 305; (**14**) 8m, 3f — JUR 411, 439, 452, 460, 469, 479, 507, 518, 535, 542, 565; (**15**) 1m — JUR 353; (**16**) 7m, 4f — JUR 412–413, 448–449, 451, 458, 484, 506, 517, 519–520.

Micoureus regina (Thomas, 1898)

TYPE LOCALITY: ''West Cundinamarca (Bogotá Region),'' Departamento de Cundinamarca, Colombia.

DESCRIPTION: Very similar to *M. demerarae* in overall body size, *M. regina* also has woolly dorsal fur and a black eye-ring. The dorsal pelage is slightly shorter than that of *M. demerarae*, averaging 10 mm along the middorsum. The overall color cast to the dorsal pelage is also richer, more orangish-gray-brown. The ventral color is similarly richer, with the cheeks, throat, thorax, abdomen, and inguinal regions ranging from Warm Buff to Antimony Yellow, or from Cream Buff to Chamois (Ridgway, 1912). In pattern, the purely buff-colored ventral region is contin-

TABLE 14
Principal Component Eigenvalues and Standardized Discriminant Functions for Log-Transformed Cranial Variables of *Micoureus demerarae* and *M. regina* from the Rio Juruá Basin

Variable	PC-1	PC-2	PC-3	DF-1
Log CIL	0.916	−0.304	0.133	0.803
Log ZB	0.926	−0.153	−0.235	−0.293
Log BB	0.769	0.236	−0.317	0.233
Log IOC-1	0.852	0.198	−0.185	−0.033
Log IOC-2	0.273	0.829	−0.286	−0.340
Log RL	0.924	−0.045	0.192	−0.730
Log NL	0.873	−0.219	0.278	0.429
Log RW	0.895	−0.123	−0.196	0.141
Log C–M4	0.845	0.245	0.426	−0.209
Log M1–M4	0.549	0.638	0.437	−0.433
Log PL	0.931	−0.142	0.245	0.142
Log PW	0.851	0.235	−0.120	−0.787
Log MB	0.934	0.087	−0.168	−0.582
Log BOL	0.741	−0.463	−0.078	0.227
Log CD	0.747	−0.236	−0.243	0.242
Eigenvalue	10.091	1.782	0.982	—
% contribution	67.3	11.9	6.5	—

uous from the chin to the genitals, typically widely separating the incursions of gray-based lateral fur (fig. 54). The latter is found only in the lower thoracic and abdominal regions, never in the upper thorax or throat, in contrast to the pattern of *M. demerarae*. The purely colored ventral stripe separates the lateral gray-based bands by a width of at least 15 mm, and more typically as much as 25–30 mm (measurements taken from skins). The skull is stout, as in *M. demerarae*, but with slightly wider interorbital region (particularly that behind the supraorbital processes). It is larger in most dimensions, on average, particularly when similar sized individuals are compared (see table 13 and fig. 56).

NONGEOGRAPHIC VARIATION: Our samples of *M. regina* come from a more limited region within the Rio Juruá than do those of *M. demerarae*. Over this area (Headwaters to Lower Central regions), geographic variation in mensural characters is nearly nonexistent, with only two cranial variables (CD and BB) exhibiting significant geographic differentiation (two-way ANOVA, $p < 0.05$ or 0.01, respectively). Similarly, sexual dimorphism within localities is limited to a single variable (PW; $p < 0.05$). However, when samples are pooled to increase size, sexual dimorphism characterizes most mensural variables in *M. regina*. Three of the four external measurements (TOL, TAL, and HF) and 13 of 15 cranial variables (CIL, ZB, BB, MB, OC, RL, NL, RW, C-M4, PL, PW, BOL, and CD) exhibit significant sexual dimorphism when all localities are pooled ($p < 0.05$ or 0.01, one-way ANOVA). Samples are not sufficient to examine the combined effects of age and sex.

COMPARISONS: Morphological comparisons with *M. demerarae* are given above under that species, and in figs. 53–57; external and cranial measurements are compared in table 13. Divergence in cytochrome-b sequences within the Rio Juruá basin is illustrated in fig. 50.

DISTRIBUTION AND HABITAT: We found *M. regina* at all but one of the 12 primary localities in the central and upper reaches of the Rio Juruá, but at no locality in the Mouth Region. It also has not been taken by us, or others, from localities further to the east or north in Estado do Amazonas, Brazil. Consequently, the records from Jainu (locality **11**) and Barro Vermelho (locality **12**) represent the easternmost ones for the species within Amazonia to our knowledge.

For the most part, *M. regina* was the only species of woolly mouse opossums we took in true várzea forest along the river margins. It was taken in all trap lines set within true várzea in the Upper and Lower Central regions of the Rio Juruá (localities **5** [Sacado], **8** [Nova Empresa], **9a** [Boa Esperança], **10** [opposite Altamira], and **11** [Jainu]), and also in the two quasi-várzea localities in the Headwaters (localities **2** and **3**). At the latter two it was sympatric with *M. demerarae*. We also took it in terra firme habitats at localities **6** (Condor), **7** (Penedo), and **12** (Barro Vermelho) with *M. demerarae*, and in near-equal numbers with that species at locality **7**. All specimens were caught in canopy traps placed from 5 to 10 m off the ground, or were shot off perches more than 2 m high.

REPRODUCTION: We obtained reproductive females in the months of February, September, October, and November. As with *M. demerarae*, these data suggest the possibility of breeding in both dry and wet seasons. Fe-

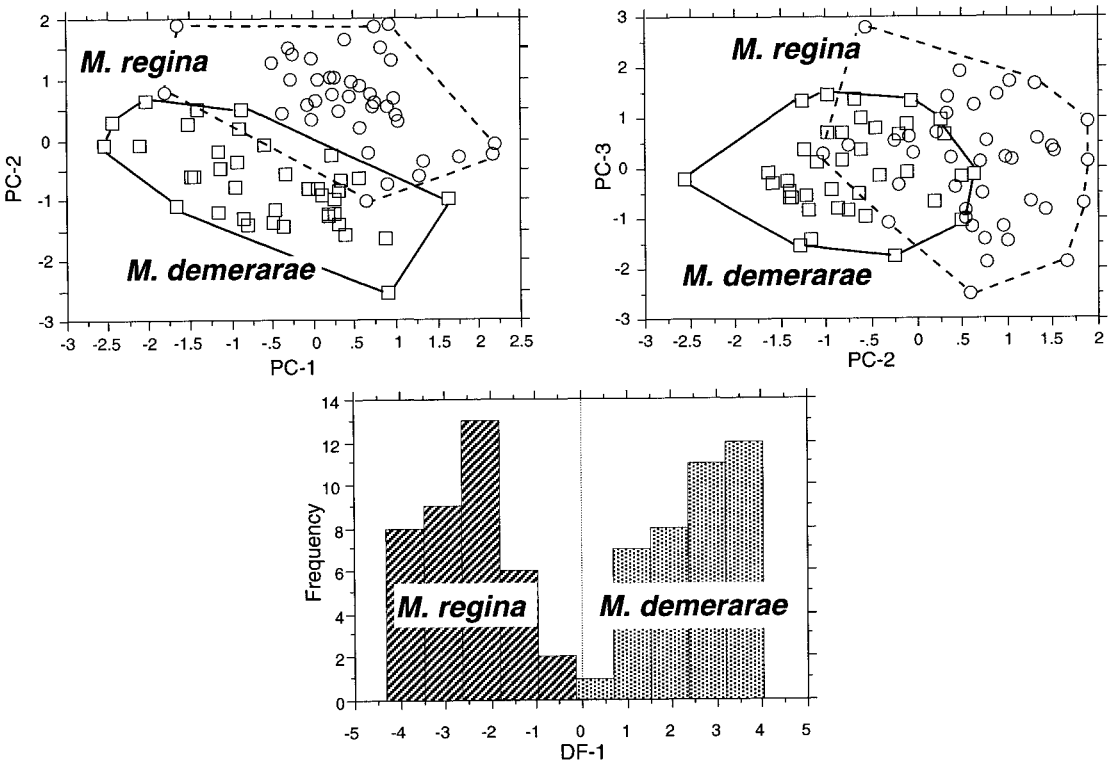

Fig. 57. Plots of the first (a general size axis) and second PC axes (**above, left**), of second versus third PC axes (**above, right**), and histogram of discriminant scores (**bottom**) for adult specimens of *Micoureus demerarae* and *M. regina* from the Rio Juruá. All localities for each species are pooled.

males with attached young were taken at localities **5** (Sacado), **8** (Nova Empresa), and **10** (opposite Altamira); the number of pups varied from 6 to 8. Males of age classes 5 and 6 had testes larger than 9 mm; those of younger ages had testes 8 mm or less.

KARYOTYPE: 2n = 14, FN = 20 (fig. 47E). The chromosomal complement of *M. regina* is identical in gross features to that described above for *M. demerarae*.

COMMENTS: This species appears to be relatively uniform over its range. At least with regard to variation in cytochrome-b sequences, there is no difference between individual haplotypes from the Rio Juruá basin and those from northern Perú (Río Cenepa, Departamento de Amazonas). The true range of this species is not known at present and, given the rather slight morphological differences between it and *M. demerarae*, sequence analysis of samples from other localities within western Amazonia may be necessary to define that range. The designation of the type locality as ''West Cundinamarca'' lacks geographic precision, but since the western half of the Departamento de Cundinamarca consists of the humid lowlands of the Río Magdalena valley, the true type locality is thus probably within the trans-Andean region as defined by Haffer (1975). On biogeographic grounds, therefore, it is likely that the name *regina* is inappropriately applied to the western Amazonian taxon we characterize here. Certainly, this Amazonian clade is quite distinct from all other sampled taxa of the genus, including *M. alstoni* from Panamá (fig. 52), the closest locality that we have sampled to the type locality of *regina*. If *M. regina* proves to be a species distinct from that in the western Amazonian lowlands, the earliest name applicable to the latter is *germana* Thomas, 1904.

SPECIMENS EXAMINED (n = 55): (**1**) 2m, 2f — MNFS 1161, 1232, 1298, 1417; (**2**) 3m,

1f — MNFS 1287, 1337, 1352, 1379; (**3**) 1m, 1f — MNFS 1530, 1673; (**4**) 1f — JUR 247; (**5**) 5m, 3f — MNFS 566–567, 608-611, 668, 678; (**6**) 1f — JLP 15703; (**7**) 4m, 3f — JLP 15358, 15496; MNFS 401, 426–428, 435; (**8**) 4m, 8f — JLP 15392, 15434–15437; MNFS 441-442, 486, 502–504, 509; (**9a**) 3m — JLP 16034–16035; JUR 198; (**10**) 4m, 2f — JLP 16031–16032; JUR 201; MNFS 902–903, 935; (**11**) 2m, 3f — MNFS 717, 755–756, 772–773; and (**12**) 2m — MNFS 728, 759.

MONODELPHIS BURNETT, 1830

Short-tailed mouse opossums

Short-tailed murine opossums are generally uncommon in the Amazon Basin, and only a few records of any species are available for the lowland forested regions of western Amazonia in Brazil, Bolivia, Perú, and Ecuador. Emmons and Feer (1997) remark on specimens of *M. emiliae* from localities east of the Rio Tapajós, near the mouth of the Rio Amazonas, and from Iquitos in northeastern Perú, some 2000 km upriver, with no records in between. Patterson (1992) recorded a specimen of this same species from the central Amazon near the mouth of the Rio Madeira, and Anderson (1997) lists one from extreme northern Bolivia, in the Departamento de Pando. The only other species of *Monodelphis* recorded from western Amazonia, including the Andean foothills, are *M. brevicaudata* and *M. adusta* in Perú and Bolivia (Anderson, 1997; Pacheco et al., 1993; Pacheco and Vivar, 1996; Patton et al., 1982; Woodman et al., 1991).

Monodelphis emiliae (Thomas, 1912)

TYPE LOCALITY: ''Boim, west bank Rio Tapajós, 24°9′S, 55°10′W,'' Estado do Pará, Brazil.

DESCRIPTION: This is a small-bodied, terrestrial species with a short tail (<50 mm in length, on average) and small feet without an opposable pollex. The body is a rich red-brown in general color with a grizzled gray neck and a rose-colored venter with overtones of purple. The distinct coloration and pattern is unique among species of this genus. Selected external and cranial measurements for six adult individuals is given in table 15.

TABLE 15
Selected External and Cranial Dimensions of Adult *Monodelphis emiliae*
Measurements (mm) are given as mean, with range and sample size.

Variable	Mean	Range	n
TOL	156.7	142–166	6
TAL	49.7	45–53	6
HF	18.5	17–21	6
E	13.7	13–15	6
CIL	29.3	27.0–30.9	6
ZB	17.0	15.4–18.2	6
BB	11.9	11.6–12.4	6
IOC-1	6.4	5.9–6.8	6
IOC-2	5.5	5.1–5.8	6
RL	12.1	10.9–13.3	6
NL	13.0	11.8–14.5	6
RW	5.6	5.2–6.1	6
C–M4	12.0	11.3–12.4	6
M1–M4	6.7	6.5–6.8	6
PL	15.7	14.8–16.5	6
PW	10.2	9.7–10.6	6
OCCB	6.8	6.6–7.0	6
BOL	3.7	3.6–4.0	6
CD	9.3	8.9–9.7	6

COMPARISONS: This species has previously been considered a subspecies of *Monodelphis brevicaudata* (Erxleben). Handley and Pine (1984) reviewed the available material and showed that *M. emiliae* and *M. brevicaudata* are, in fact, sympatric at two localities near the Rio Tapajós. These authors give details as to the differences between the two species.

DISTRIBUTION AND HABITAT: This species was previously known from only 13 specimens. Most of these are from localities along the Rio Amazonas: one from the Iquitos area of northeastern Perú and 11 from scattered localities in central and eastern Brazil, from Lago Tapayuna south of Manaus (Patterson, 1992) to Belém (Handley and Pine, 1984). Anderson (1997) records one specimen from Centro Dieciocho, Pando, Bolivia. To this list we add six specimens taken from four localities in the central and upper Rio Juruá, records which extend the range of the species some 900 km southwest of the Amazon river. The species was collected only on the ground in terra firme forest, typically in Sherman traps placed along fallen logs where the un-

derstory was moderately dense. Our impression is that animals were caught ''by accident,'' perhaps entering traps in search of insects attracted to our bait. Pitfall trapping with fencing (e.g., Voss and Emmons, 1996) would probably be a better method to obtain a more accurate picture of the abundance and distribution of this, and other, species of *Monodelphis*.

REPRODUCTION: One female with three attached young was collected in February, and parous females were taken in both February and September. All individuals with fully erupted molars of both sexes were either reproductively active or postreproductive; one female with M4 not in place was apparently nulliparous.

KARYOTYPE: 2n = 18, FN = 30, specimens karyotyped MNFS 524, 1195, 1412, JLP 15686. The autosomal complement is comprised of two pairs of large metacentric, five pairs of medium-sized to medium-small subtelocentrics, and one pair of medium-sized acrocentric elements. The X-chromosome is a small submetacentric and the Y is a small acrocentric chromosome. The karyotype appears identical to that published for several other species in the genus (Reig et al., 1977; Palma and Yates, 1996).

SPECIMENS EXAMINED (n = 6): (**1**) 3f — MNFS 1150, 1195, 1412; (**3**) 1m — MNFS 1426; (**6**) 1f — JLP 15686; (**7**) 1m — MNFS 524.

PHILANDER TIEDEMANN, 1808

Pouched four-eyed opossums

An extensive review of pouched four-eyed opossums of the genus *Philander* has been recently published by Hershkovitz (1997). This monograph compares *Philander* to other related genera, such as *Didelphis*; provides a specific and subspecific taxonomy, with synonymies; and summarizes available ecological and other life history characteristics. We differ from Hershkovitz in the delineation of species boundaries in the genus, and in the geographic ranges of particular subspecies (Patton and da Silva, 1997). These differences will be detailed in the accounts that follow.

Members of this genus are large-bodied (head and body length 250–350 mm; tail 250–330 mm; weight 240–600 grams), gray to black opossums with white to cream-colored spots above the eyes and a distinctly furred base to the tail. They are somewhat smaller and more gracile in appearance than *Didelphis*. The ears are either bicolored or black and appear naked. The tail is generally slightly longer than the length of the head and body, typically black over the proximal half up to two thirds of its length, and naked except for the extension of body hair over the proximal 5 to 6 cm. Color varies from gray above and creamy white below to black above and below; some otherwise gray forms have a blackish dorsal median stripe from the neck to over the rump. Considerable geographic variation in color and pattern exists within all species, but especially in *P. opossum*. Mature females have a well-developed pouch. The genus is superficially similar to the brown four-eyed opossum *Metachirus nudicaudatus*, which lacks a pouch in females, possesses elongated fore and hind legs with longer and narrower feet, and nearly lacks the furred base to the tail.

The skull is similar to that of *Didelphis* in general form and proportions, but is less robust and smaller in size in comparisons with same-age individuals. The nasals are somewhat less expanded laterally at the maxillofrontal junction, the rostrum is long and slender, the zygomatic arches flare broadly, the postorbital constriction is smoothly rounded and narrow, and the temporal ridges converge anterior to the frontoparietal suture to form a well-defined sagittal crest; in this respect the interorbital region is considerably distinct from the smoothly rounded region that lacks postorbital processes characteristic of *Metachirus* (see above).

Based on the combination of sympatry of morphologically recognizable forms and monophyletic clades of haplotypes of the cytochrome-b gene, Patton and da Silva (1997) recognized three species of pouched four-eyed opossums within Amazonia, with the ranges of *P. mcilhennyi* and *P. opossum* overlapping over much of eastern Perú and western Brazil south of the Rio Amazonas–Rio Solimões axis. Emmons and Feer (1997) mapped the ranges of these species, based on data supplied to them by us. Sympatry of these two species has been documented at

two localities in eastern Perú (Gardner and Patton, 1972; Hutterer et al., 1995), as well as along the Rio Juruá. The third species, *P. andersoni*, is known from northern Perú, largely north of the Rio Marañón, Ecuador, and southeastern Colombia, east to the Neblina region on the Brazil-Venezuela border and the Imerí region west of the Rio Negro and north of the Rio Solimões in central Brazil. It is possibly sympatric with *P. mcilhennyi* on the lower Rio Javarí in northeastern Perú (David Fleck, personal commun.), which would represent the first known area where these two species occur together. Our conclusion that *P. andersoni* and *P. mcilhennyi* are separate species differs from that of Hershkovitz (1997), based on his morphological examination of specimens from a limited number of localities. Patton and da Silva (1997) also suggested that the *P. opossum* within the Amazon Basin might represent more than one species, since cytochrome-b haplotypes from different geographic localities do not form a monophyletic assemblage relative to other species they recognize. They also argued that the Mata Atlântica taxon *P. frenata* should be recognized as a distinct species based on its deeply divergent mitochondrial genome.

We provide an updated summary of available molecular data for *Philander* sampled throughout much of its known range to illustrate the degree of divergence between regional morphological entities (figs. 58 and 59; table 16). Additional samples from the lower Rio Negro in central Brazil to those reported by Patton and da Silva (1997) only strengthen their conclusions regarding species boundaries. Samples from west of the lower Rio Negro along the Rio Jaú (localities g and h in the map, fig. 58, and tree, fig. 59) belong to the cytochrome-b clade we allocate to *P. andersoni*, and are sharply divergent from individuals directly opposite on the east side of the lower Rio Negro (sample j in figs. 58 and 59) that group with specimens we allocate to *P. opossum* from eastern and northeastern Amazonia

Philander opossum (Linnaeus, 1758)

TYPE LOCALITY: ''America,'' restricted to Surinam by J.A. Allen (1900: 195); further restricted to Paramaribo, Surinam, by Matschie (1916: 268).

DESCRIPTION: This species exhibits considerable geographic variation in coloration and pattern, and no review of this, or other aspects of character variation has yet been undertaken. Specimens from the Rio Juruá are uniformly gray with a creamy white venter, a distinct blackened median stripe on the midback, and a naked tail: the proximal two thirds is black with pale blotches and the terminal 20% or less is light. The fur is short, even along the midback, and coarse; the furred base of the tail is short, extending no more than 20% of the tail length. Selected external and cranial measurements are given in table 17. With the small sample available (7 male and 3 female adults, respectively), significant sexual dimorphism is evident only in cranial depth (CD; $p < 0.05$, one-way ANOVA).

COMPARISONS: This is a smaller animal than *P. mcilhennyi*, and distinctly different in coloration and pattern (see below). Cranially, *P. opossum* is significantly smaller in overall skull length (condyloincisive length), in measure of the toothrow and palatal length (C to M4 length, M1 to M4 length, and palatal length), and in palatal width (distance between metastyles of M3; see table 17). In external measurements, *P. opossum* is significantly smaller in total length, length of the tail, and height of the ear (see table 17).

DISTRIBUTION AND HABITAT: In the headwaters localities, *P. opossum* was truly sympatric (that is, found in adjacent trap stations) with *P. mcilhennyi* but apparently segregated from it by habitat downriver. Individuals taken in the Upper Central region (from Sacado and Nova Empresa, localities 5 and 8) were collected in várzea; all specimens but one taken in the Headwaters area were from the locally inundated margins of the river. This is in contrast to records of the black four-eyed opossum, *P. mcilhennyi*, from the same areas (see below). We caught all specimens in traps placed on the ground, although *Philander* individuals were seen to climb on fallen logs and windfalls.

REPRODUCTION: Females with pouch young were collected only during the months of February and March, within the rainy season. However, since only one individual (a male)

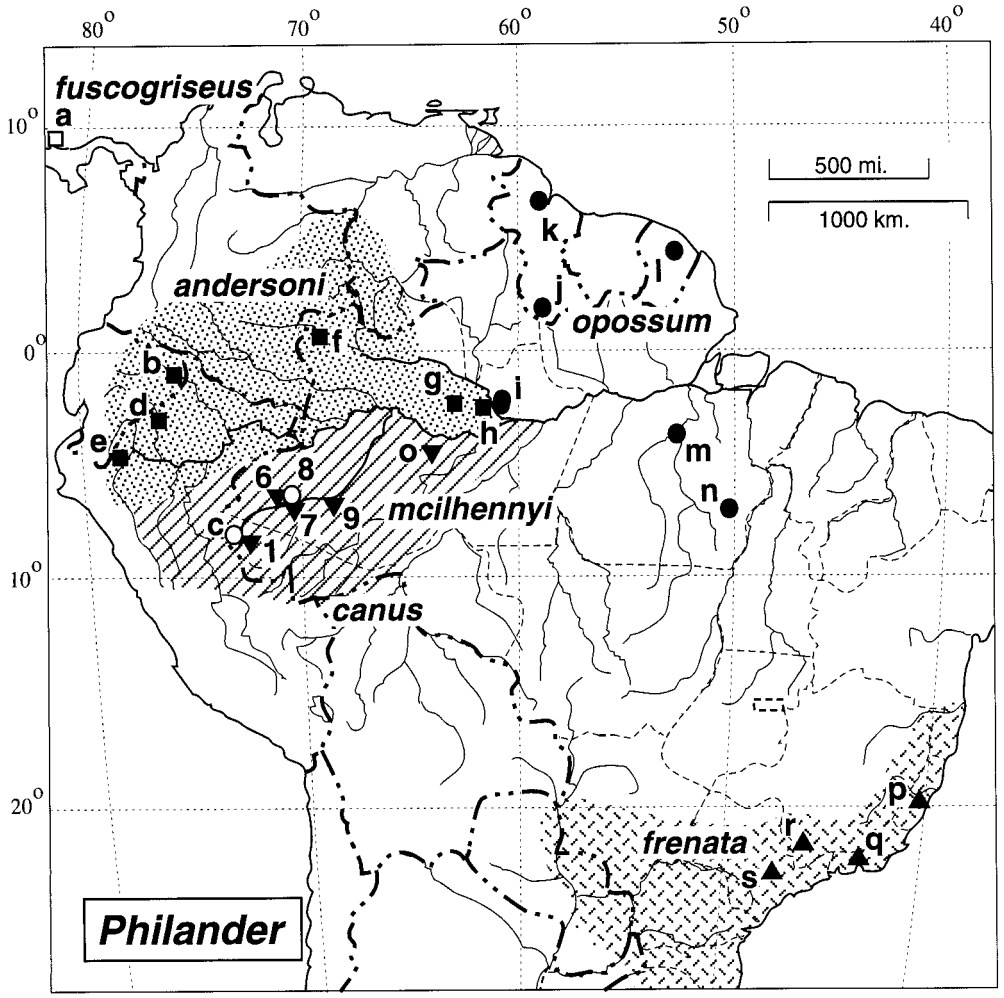

Fig. 58. Map of sample localities of species of pouched four-eyed opossums (*Philander*) from the lowland forests of Middle America, Amazonia, and the Atlantic Forest. Localities are numbered or lettered as in table 16, which provides provenance data and catalog numbers of voucher specimens. Approximate geographic limits to the ranges of the western Amazonian species *P. andersoni* and *P. mcilhennyi* are indicated. Sample localities are grouped by symbol into the cytochrome-b clades identified in fig. 59.

was taken during dry season months, little can be said about the seasonality of reproduction in this species. The modal number of young was 5 (range 4 to 5, n = 4). Literature reports on litter size vary from a mean of 3.4 (Eisenberg and Wilson, 1981) to 4.5 (Davis, 1947).

KARYOTYPE: 2n = 22, FN = 20 (fig. 40B). All chromosomes are uniarmed and form a graded series from large to small. This karyotype has been described and figured by Reig et al. (1977) and Palma and Yates (1996). Data are available for two specimens, MNFS 623 and MNFS 998.

COMMENTS: Hershkovitz (1997: fig. 5) allocates specimens from western Brazil (including the Rio Juruá, but for which he examined no specimens) to the nominate subspecies, while placing *canus* Osgood in synonymy with *quica* Temminck, a subspecies he maps to southeastern Brazil from Rio de Janeiro to Uruguay and northwest through

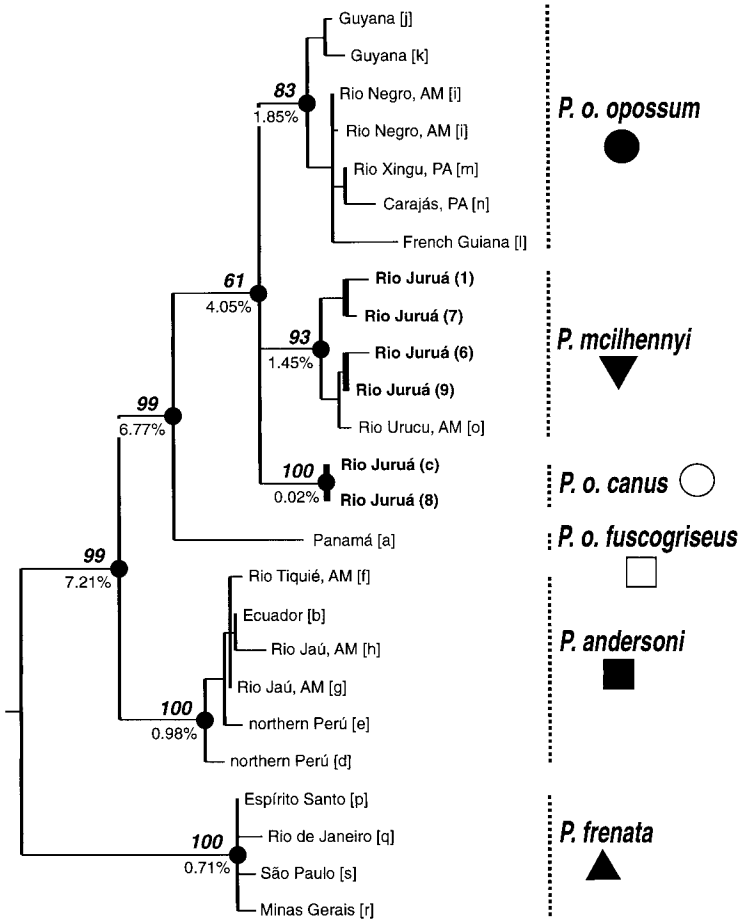

Fig. 59. Strict consensus tree of 24 equally minimum-length parsimony trees of 660 bp sequences of the mitochondrial cytochrome-b gene for haplotypes of *Philander*, rooted by comparison to sequences from *Micoureus* and *Marmosops*. Branch lengths are proportional to the number of character changes. Haplotypes for specimens from the Rio Juruá are identified by heavy lines and bold type; numbers refer to the specific locality as identified in the text and the map, fig. 1. Numbers at nodes are bootstrap values, based on 1000 replicates; percentages are average Kimura two-parameter distances. Individual haplotypes are keyed by number or letter to localities as mapped in fig. 58 and listed by voucher specimen numbers in table 16. Tree length = 309 steps; CI = 0.709; RI = 0.863.

the Paraná basin to eastern Bolivia and Perú. In part because of cytochrome-b sequence differences between our specimens from the Rio Juruá and those from Guyana, close to the type locality of *opossum* Linnaeus, we have suggested elsewhere that western and eastern Amazonian *P. opossum* are distinct and should be recognized as such (Patton and da Silva, 1997). We have also shown that samples from southeastern Brazil are quite different from Amazonian ones (fig. 59; Patton and da Silva, 1997), and have suggested that *quica* Temminck, 1824 with its type locality in Estado do Rio de Janeiro, should be considered a synonym of *frenata* Olfers, 1818 (type locality in Estado do Bahia, Brazil). Consequently, we apply the name *canus* to our samples from the Rio Juruá.

SPECIMENS EXAMINED (n = 14): (**1**) 1f — MNFS 1308; (**a**) 2m, 2f — MNFS 998, 1031, 1047, 1054; (**b**) 2m, 1f — MNFS 1039–1040, 1053; (**3**) 1m — MNFS 1579;

TABLE 16
Haplotypes, Voucher Numbers, and Localities for Taxa of Four-Eyed Opossums, Genus *Philander*
Individual haplotypes listed from top to bottom in the tree, figure 59, with the catalog numbers of their respective voucher specimens, and localities (identified as in the map, fig. 58) for which 660-bp haplotypes of the mitochondrial DNA cytochrome-b gene are available.

Haplotype	Voucher no.	Locality
Philander opossum opossum		
1	ROM 98045	30 km NE Surama, Rupununi, Guyana (locality j)
2	ROM 98910	Waikerebi, Northwest, Guyana (locality k)
3	JLP 16785	Ilha das Onças, left bank Rio Negro, Amazonas, Brazil (locality i)
4	LPC 164	Lago Meduiním, left bank Rio Negro, Amazonas, Brazil (locality i)
5	USNM 549297	52 km SSW Altamira, east bank Rio Xingu, Pará, Brazil (locality m)
6	CS 10	Floresta Nacional Tapirapé-Aquiri, Município de Marabá, Pará, Brazil, 5°48'05"S, 50°30'54"W (locality n)
7	T1819	La Trinité Mountains, French Guiana (locality l)
Philander mcilhennyi		
8	MNFS 1103	Igarapé Porongaba, right bank Rio Juruá, Acre, Brazil (locality **1**)
9	MNFS 383	Penedo, right bank Rio Juruá, Amazonas, Brazil (locality **7**)
10	JLP 15702	Seringal Condor, left bank Rio Juruá, Amazonas, Brazil (locality **6**)
11	JLP 16069	Altamira, right bank Rio Juruá, Amazonas, Brazil (locality **9**)
12	MNFS 146	alto Rio Urucu, Tefé, Amazonas, Brazil (locality o)
Philander opossum canus		
13	MNFS 1039	opposite Ocidente, left bank Rio Juruá, Acre, Brazil (locality c)
14	JLP 15395	Nova Empresa, left bank Rio Juruá, Amazonas, Brazil (locality **8**)
Philander opossum fuscogriseus		
15	USNM 464248	Old Point, Isla Bastimentos, Bocas del Toro, Panamá (locality a)
Philander andersoni		
16	INPA	Comunidade Colina, right bank Rio Tiquié, Município São Gabriel da Cachoeira, Amazonas, Brazil, 0°72'N, 60°04'W (locality f)
17	ROM 104030	Okone Gare, 38 km SE Pompeya Sur, Parque Nacional Yasuní, Napo, Ecuador (locality b)
18	MNFS 2088	above mouth, right bank Rio Jaú, Amazonas, Brazil (locality h)
19	YL 139	Macaco, left bank Rio Jaú, Amazonas, Brazil (locality g)
20	MVZ 153265	Huampami, Río Cenepa, Amazonas, Perú (locality e)
21	KU 144120	San Jacinto, Río Pastaza, Loreto, Perú (locality d)
Philander opossum frenata		
22	MAM 189	Estação Biologica Santa Lúcia, Santa Tereza, Espírito Santo, Brazil (locality p)
23	MN (Org1)	Garrafão, Est. Rio Terezópolis, Majé, Rio de Janeiro, Brazil (locality q)
24	MVZ 182066	Fazenda Intervales, Capão Bonito, São Paulo, Brazil (locality s)
25	MAM 208	Parque Estadual do Ibitipoca, 30 km N Lima Duarte, Minas Gerais, Brazil (locality r)

(**4**) 1m, 2f — MNFS 1453, 1465, 1528; (**5**) 1m — MNFS 623; (**8**) 1m — JLP 15395.

Philander mcilhennyi
Gardner and Patton, 1972

TYPE LOCALITY: "Balta, Río Curanja," Departamento de Ucayali (formerly in Departamento de Loreto), Perú.

DESCRIPTION: This is a larger animal than *P. opossum* in virtually all body and cranial measurements (table 17). Both the dorsum and venter are black; the middorsal hair is long and coarse; the haired portion at the base of the tail is long, averaging more than 25% of the tail length; the tail is black and lacks pale blotches, but approximately 47% of the terminal portion is generally paler. The lacrimals are expanded anteriorly, the poste-

TABLE 17
Selected External and Cranial Dimensions of Two Species of Pouched Four-Eyed Opossums, Genus *Philander*, from the Rio Juruá
Measurements (mm) are given as mean ± standard error, with range and sample size. Individuals are pooled across all localities along the river. Significance levels are indicated based on one-way ANOVA (ns = $p > 0.05$; * $p < 0.05$; ** $p < 0.01$).

	P. mcilhennyi				*P. opossum*		
Variable	Mean ± SE	Range	n	*p*	Mean ± SE	Range	n
TOL	628.8 ± 23.37	578–685	6	*	556.6 ± 12.29	478–606	10
TAL	328.0 ± 18.41	295–377	6	*	292.2 ± 5.42	271–318	10
HF	43.25 ± 1.11	41–46	6	ns	43.67 ± 0.62	42–47	10
E	40.25 ± 0.48	39–41	6	**	35.56 ± 0.67	31–38	10
CIL	78.51 ± 2.14	73.6–82.5	6	*	71.88 ± 1.22	65.6–76.6	10
ZB	38.54 ± 0.89	35.9–40.0	6	ns	37.57 ± 0.92	33.9–41.8	10
BB	20.86 ± 0.20	20.4–21.3	6	ns	20.29 ± 0.24	19.1–21.4	10
IOC-1	13.50 ± 0.30	12.7–14.1	6	ns	12.76 ± 0.25	11.7–14.3	10
IOC-2	8.88 ± 0.27	8.3–9.6	6	ns	8.83 ± 0.13	8.0–9.3	10
RL	30.44 ± 1.22	27.3–32.9	6	ns	28.03 ± 0.52	24.4–29.5	10
NL	40.02 ± 1.30	37.2–42.5	6	**	33.42 ± 0.55	30.2–35.4	10
RW	12.03 ± 0.32	11.3–12.8	6	ns	11.46 ± 0.34	10.2–13.1	10
C–M4	32.37 ± 1.04	30.1–34.4	6	*	30.08 ± 0.33	27.8–31.1	10
M1–M4	15.18 ± 0.60	13.8–16.5	6	*	13.77 ± 0.17	13.1–14.4	10
PL*	46.89 ± 1.05	44.9–48.7	6	*	43.60 ± 0.68	39.3–45.3	10
PW	22.08 ± 0.11	21.8–22.3	6	**	20.15 ± 0.34	18.6–21.7	10
MB	23.03 ± 0.37	22.1–23.8	6	ns	22.67 ± 0.44	20.7–24.3	10
BOL	8.59 ± 0.18	8.2–9.0	6	ns	8.28 ± 0.29	7.0–9.4	10
CD	18.51 ± 0.29	17.8–19.2	6	ns	18.15 ± 0.24	17.3–19.4	10

rior aspect of the expanded portion of the nasals is distinctly notched, and the labial margin of M3 deeply indented. These characters conform to those presented by Gardner and Patton (1972) in their diagnosis and description of *P. mcilhennyi*. As with *P. opossum*, our samples of adult *P. mcilhennyi* also exhibit little sexual dimorphism, with significant differences between the sexes for only three cranial variables (C-M4, M1-M4, and PW; $p < 0.05$ in each case by one-way ANOVA).

COMPARISONS: See section above for *P. opossum*. Comparisons of the color pattern of the face can be found in Hutterer et al. (1995).

DISTRIBUTION AND HABITAT: All specimens taken at midriver localities came from terrestrial traps in terra firme forest (n = 8); those from the headwaters localities were taken, again all on the ground, in both terra firme (n = 4) and inundated forest along the banks (n = 4). In the latter habitat, this species was truly sympatric with the gray four-eyed opossum, *P. opossum*.

REPRODUCTION: We recorded females with pouch young in the months of April and June at the type locality in eastern Perú (Gardner and Patton, 1972) and during July and August on the upper Rio Urucu in central Amazonas, Brazil (da Silva, unpubl. data). On the Rio Juruá, pouch young were found at Penedo in the midriver in August and September and in the headwaters during February and March. The combination of data from these three areas suggests that the species breeds throughout the year. We caught very young independent individuals (age classes 1 and 2 of Gardner, 1982) in September, November, February, and March. Litter size varied from 4 to 7 with a mode of 5 young (n = 8).

KARYOTYPE: 2n = 22, FN = 20 (fig. 40C). The chromosomal complement is identical in every respect in gross chromosome morphology to that of *P. opossum* (see Reig, et al., 1977). Specimens karyotyped include MNFS 1103, 1410, 1435, JLP 15355, 15677, 15702.

SPECIMENS EXAMINED (n = 22): (**1**) 1m, 2f

— MNFS 1103, 1196, 1271; (**2**) 1m, 5f — MNFS 1185–1186, 1255, 1286, 1299, 1410; (**3**) 2m — MNFS 1599, JUR 208; (**4**) 1m, 2f — MNFS 1435, 1437, 1496; (**6**) 2m — JLP 15677, 15702; (**7**) 2m, 1f — JLP 15355; MNFS 383, 402; (**9**) 1m, 2f — JLP 16057, 16069, 16074.

SUBFAMILY CALUROMYINAE Kirsch, 1977

CALUROMYS J. A. ALLEN, 1900

Woolly opossums

Caluromys lanatus (Olfers, 1818)

TYPE LOCALITY: ''Paraguay''; restricted to Caazapá, Caazapá (Cabrera, 1916).

DESCRIPTION: A medium-sized arboreal opossum (range in body mass of adults from 350 to 520 g), this species is beautifully colored with long, lax, and wavy hair with a thickly furred tail above for its proximal half and below for one fifth its length. The dorsal color is a marked red-brown mixed with gray, particularly on the upper arms and hips, otherwise brightest over the shoulders, forearms, and lower hindlegs. The head is grayish, but the face has a prominent dark stripe down the center from between the ears to the nose. There is a reddish brown eye-ring extending as a dark streak from the corner of the eye to the nose. The nonfurred distal part of the tail is whitish-yellow mottled with brown spots. The feet are reddish-brown. The venter is yellowish white with a grayish midsection. Selected external and cranial measurements for eight adult individuals are given in table 18. Our samples are inadequate to determine the degree, if any, of sexual dimorphism or interlocality differences among adult individuals.

TABLE 18
Selected External and Cranial Dimensions of Adult *Caluromys lanatus*
Measurements (mm) are given as mean, with range and sample size.

Variable	Mean	Range	n
TOL	700.9	675–722	8
TAL	422.4	400–446	8
HF	46.3	43–51	8
E	35.5	35–36	8
CIL	59.50	56.5–62.8	8
ZB	34.76	32.7–37.1	8
BB	20.58	19.4–22.3	8
IOC-1	11.02	9.8–13.1	8
IOC-2	8.38	7.6–9.2	8
RL	22.76	21.7–24.0	8
NL	25.79	22.2–27.1	8
RW	13.04	12.3–13.8	8
C–M4	20.57	18.2–22.2	8
M1–M4	9.75	9.2–10.1	8
PL	31.89	30.5–33.4	8
PW	17.67	17.1–18.2	8
MB	23.27	21.4–25.6	8
BOL	8.66	8.2–9.2	8
CD	18.88	16.6–21.1	8

DISTRIBUTION AND HABITAT: This species is known from throughout the western Amazon, east of the Andes in Colombia, western Venezuela, Ecuador, Perú, and Bolivia, eastern Paraguay, northeastern Argentina, and western Brazil to east of Manaus and south to Estado do Minas Gerais. Known localities of sympatry between *C. lanatus* and *C. philander* include the region of Manaus (Malcolm, 1991b; Voss and Emmons, 1996) as well as Guyana and eastern Bolivia (L. H. Emmons, personal commun.). The two also occur in close proximity in Estado do Minas Gerais, Brazil (L. P. Costa and Y. R. Leite, personal commun.). We collected all specimens in traps placed in trees at heights ranging from 5 to 15 m, with approximately equal numbers caught in terra firme and várzea forests.

REPRODUCTION: We obtained only two females with pouch young, one in November (Altamira, locality **9**) and one in June (Vira-Volta, locality **14**), but caught postlactating females in October, February, and March. These data, and the occurrence of very young individuals (age classes 1–2, calendar age about 4 months based on *Didelphis*, see Gardner, 1982) suggest that breeding takes place yearround, or nearly so, in *C. lanatus*. Litter sizes are the smallest recorded for didelphid marsupials (review in Harder, 1992), ranging only from one to two young (n = 3). The related species *C. philander* has an average litter of four in French Guiana (Charles-Dominique et al., 1981; Atramentowicz, 1986).

KARYOTYPE: 2n = 14, FN = 24 (fig. 47F). The autosomal complement consists of four pairs of large biarmed and two pairs of medium-sized subtelocentric autosomes; the X-

chromosome is a small biarmed element and the Y-chromosome is very small but appears distinctly biarmed. This karyotype differs from those reported for the three recognized species of *Caluromys* (Reig et al., 1977) only in the morphology of the Y-chromosome. These authors note that the Y-chromosome of both *C. derbianus* and *C. lanatus* is uniarmed and that of *C. philander* is biarmed. This, however, appears to be a misprint as the illustrated karyotype of *C. philander* shows a clearly uniarmed element, and both *C. derbianus* and *C. philander* are listed as having a uniarmed Y in an accompanying table. We karyotyped two individuals, MNFS 584 and MNFS 796. The karyotype of *C. lanatus* from Bolivia reported by Palma and Yates (1996) also has a biarmed Y-chromosome.

COMMENTS: While morphological variation among samples of *C. lanatus* has never been examined, the species is remarkably uniform geographically in cytochrome-b sequence haplotypes. We have 396 bp of data for four specimens from three localities spanning the entire length of the Rio Juruá (Porongaba [locality **1**], Altamira [**9**], and Vira-Volta [**14**]). These differ among themselves by a maximum of six substitutions (1.5%). One haplotype from Altamira is identical to that found in a single specimen from the upper Rio Urucu to the east in central Estado do Amazonas, Brazil, and none differ by more than four substitutions from a specimen from the Río Cenepa in northern Perú. The specimens from the upper Rio Urucu and Río Cenepa, two localities some 1600 km apart and spanning much of the known east-west distribution of the species, differ by only 1.5% in comparison of their entire cytochrome-b sequences (1200 bases; Patton et al., 1996b).

SPECIMENS EXAMINED (n = 20): (**1**) 1f — MNFS 1331; (**2**) 1m — MNFS 1237; (**a**) 1f — MNFS 1106; (**3**) 5f — MNFS 1518, 1537–1538, 1553, 1660; (**4**) 2m, 2f — MNFS 1628, 1670, JUR 215, 231; (**5**) 1f — MNFS 584; (**9**) 1f — JUR 191; (**10**) 1f — MNFS 944; (**12**) 1m — MNFS 796; (**13**) 1m — JUR 306; (**14**) 1m, 2f — JUR 478, 486, 559.

ORDER RODENTIA

SCIURIDAE HEMPRICH, 1820

There are three size classes of squirrels that occur together throughout most of Amazonia, with potentially three to five species sympatric, or nearly so, in the western part of the basin (Emmons and Feer, 1997). Included in this compilation are the large red squirrels of the *Sciurus igniventris-spadiceus* complex (subgenus *Urosciurus*, following Hoffmann et al., 1993), the intermediate sized and generally grayish- to reddish-yellow members of the *Sciurus aestuans* complex (subgenus *Guerlinguetus*, following Hoffmann et al., 1993), and dwarf and pygmy squirrels of the genera *Microsciurus* and *Sciurillus*. Patton (1984) examined geographic variation within *S. igniventris* and *S. spadiceus* and differences between the two species in Ecuador and Perú, but no other recent systematic analysis of these, or other, Amazonian tree squirrels has as yet been published. Lawrence (1988), in an evaluation of the holotype of *Sciurus duida* J. A. Allen, compared both *S. igniventris* and *S. spadiceus* based on characters given in Hershkovitz (1959) and Patton (1984). Dr. Mario de Vivo of the Museu de Zoologia of the Universidade de São Paulo is in the process of revising the large and intermediate squirrels usually placed in the genus *Sciurus*.

We made no extensive effort to obtain samples of squirrels during the Rio Juruá surveys, primarily because squirrels do not enter traps readily, even our canopy platform traps, and because our abilities to hunt locally were limited by the concomitant diurnal primate surveys being undertaken by Carlos Peres (see Peres, 1997). Specimens that were obtained are few in number and were mostly from sites other than the 16 primary survey points. Taxonomic and other information given below are based on specimens collected, with additional comments as to species presence based on observational records.

SCIURUS LINNAEUS, 1758

Tree squirrels

Sciurus igniventris Wagner, 1842

Northern Amazonian red squirrel

TYPE LOCALITY: Marabitanos, north of Rio Negro, Estado do Amazonas, Brazil.

DESCRIPTION: This is a large rufous squirrel with a long and bushy tail (Patton, 1984; see also summary in Lawrence, 1988: tables 1

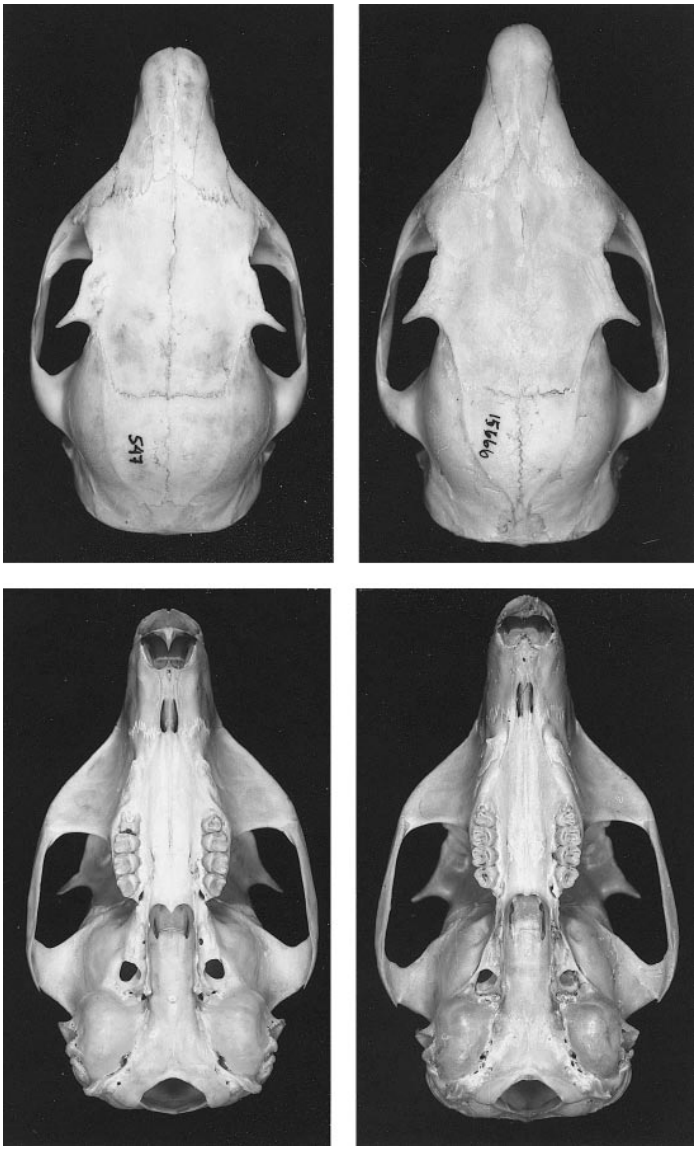

Fig. 60. Dorsal (top row) and ventral (bottom) views of the crania of large Amazonian *Sciurus*. **Left**: *S. igniventris* (JUR 547, locality **14**). **Right**: *S. spadiceus* (JLP 15666, locality f). Natural size.

and 2). The species is readily distinguished from the closely similar *S. spadiceus* by its conspicuous bright orange postauricular patches and uniformly rusty orange limbs and upper surfaces of both fore and hind feet that lack a mixture of black hairs. The single specimen collected from the Rio Juruá has a sparsely haired, pale orange, as opposed to white, venter, and its tail hairs have six alternating bands of black and orange color, with black at the base terminating in a deep-orange tip. The overall dorsal color is similar to that of *S. spadiceus*, but is darker orange, or rust, with fewer black hairs, resulting in a more uniform color. The skull is shorter, with larger orbits, shorter rostrum, and broader palate (fig. 60). In all respects, comparisons of measurements given in table 19 are of the same general magnitude, and direction of difference, as those recorded for samples of the

TABLE 19
Selected External and Cranial Dimensions of the Large Red Squirrels, Genus *Sciurus*, from the Rio Juruá
Measurements (mm) following Patton (1984); mean ± standard error, with range and sample size. Individuals are pooled across all localities along the river. Significance levels are indicated based on one-way ANOVA (ns = $p > 0.05$; * $p < 0.05$; ** $p < 0.01$; *** $p < 0.001$).

Variable	*S. spadiceus* Mean ± SE	Range	n	p	*S. igniventris* (n = 1)
TOL	540.7 ± 5.66	512–555	7	ns	547
TAL	266.4 ± 6.74	242–288	7	ns	305
HF	67.3 ± 0.89	65–70	7	*	62
E	32.4 ± 0.69	29–34	7	ns	36
GSL	66.23 ± 0.28	64.70–67.38	9	**	62.26
BAL	53.94 ± 0.31	52.64–55.73	9	**	49.76
MB	26.39 ± 0.11	26.01–27.00	9	ns	25.95
pIOC	20.03 ± 0.23	18.93–20.87	9	ns	20.33
IOC	21.32 ± 0.32	19.63–22.92	9	ns	19.66
ZB	38.79 ± 0.31	27.63–40.36	9	*	36.46
RL	28.35 ± 0.24	27.12–29.70	10	*	25.91
NL	21.57 ± 0.33	19.70–23.01	10	ns	19.77
RW	10.22 ± 0.08	9.89–10.58	10	*	10.92
D	20.75 ± 0.15	20.98–21.52	10	**	18.50
MTRL	10.26 ± 0.09	9.91–10.83	10	ns	10.12
PW	13.45 ± 0.09	13.07–13.88	10	**	14.53
MPFW	5.41 ± 0.06	5.18–5.77	9	ns	5.47
BOW	8.99 ± 0.38	8.48–9.39	9	***	6.71
BUL	10.54 ± 0.13	9.93–11.02	9	ns	11.23
CD	27.70 ± 0.22	26.64–28.54	9	ns	28.20
RAMH	24.73 ± 0.23	23.73–25.97	10	ns	24.61
RAML	41.49 ± 0.49	38.68–42.82	8	*	37.71
RAMHP4	14.41 ± 0.16	13.51–14.99	8	*	13.13

two species from throughout Ecuador and Perú (Patton, 1984).

DISTRIBUTION AND HABITAT: As mapped by Emmons and Feer (1997), this species extends across northern Amazonia, west of the Rio Branco and lower Rio Negro in north-central Brazil to the Andean foothills in southeastern Colombia, eastern Ecuador, and eastern and central Perú, extending as far south as the upper Río Ucayali drainage (Patton, 1984). It is apparently not known from central Amazonia south of the Solimões-Amazonas axis and east of the Rio Juruá. Our single specimen was taken on the left bank of the Rio Juruá near the river mouth (locality **14**). Large squirrels were observed, but not taken, in the central regions of the river on both banks, but all of these were identified in the field as *S. spadiceus*. Whether *S. igniventris* has a more extensive distribution within the Rio Juruá basin is unknown. Individuals of this species were observed only in undisturbed or second growth terra firme; none were seen or collected in várzea.

REPRODUCTION: Our single specimen is an adult female that lacked evidence of prior reproductive activity; it was collected in May 1992.

SPECIMENS EXAMINED (n = 1): (**14**) 1f—JUR 547.

Sciurus spadiceus Olfers, 1818

Southern Amazonian red squirrel

TYPE LOCALITY: "Brazil," restricted by Hershkovitz (1959) to Cuyabá (= Cuiabá), Estado do Mato Grosso.

DESCRIPTION: Similar in size and general color to *S. igniventris* (Patton, 1984; Lawrence, 1988; Emmons and Feer, 1997), *S. spadiceus* can be distinguished by its

somewhat more grizzled overall dorsal coloration, lack of orange post-auricular patches, and distinctly orange dorsal surfaces mixed with black on both fore and hind feet. The thighs are a uniform rust, somewhat darker in tone than those of *S. igniventris*. The venter of all Rio Juruá specimens is sparsely covered with white hairs. The tail is similar to that of *igniventris*, but the hairs have only four alternating bands of black and orange. Cranially, *S. spadiceus* is readily distinguished from *S. igniventris* by its somewhat larger size, distinctly longer and narrower rostrum, longer diastema, and narrower palate, among other dimensions (fig. 60, table 19, and Patton, 1984). The upper incisors also are distinctly more proodont in *S. spadiceus*, but more orthodont to opisthodont in *S. igniventris*.

DISTRIBUTION AND HABITAT: Emmons and Feer (1997) mapped the range of *S. spadiceus* to include the western Amazonia from southeastern Colombia south to northern Bolivia, east largely south of the Solimões-Amazonas axis, and west of the Rio Tapajós to the northern Pantanal. This range includes the entire Río Ucayali, Rio Juruá, Rio Madeira, and Rio Purus drainages. As with *S. igniventris*, we either collected or saw this species only in mature or disturbed terra firme forest, never in várzea.

REPRODUCTION: We caught scrotal males at Colocação Sabiá (locality f) in September and at Ocidente (locality b) in February. At the latter locality and time period, we also caught one lactating female with three placental scars, along with a subadult male and subadult female. As limited as these data are, it would appear that *S. spadiceus* breeds in both dry and wet seasons.

COMMENTS: Thomas (1926) described *Sciurus pyrrhonotus juralis*, with type locality of João Pessoa (= Eirunepé), Rio Juruá, and Vieira (1948) recorded additional specimens from Igarapé Grande, both situated on the Rio Juruá between our Upper and Lower Central regions (see comments and gazetteer in Patterson, 1992). Our specimens of *S. spadiceus* all come from localities upriver from Eirunepé (Upper Central or Headwaters regions, fig. 1), but we saw squirrels clearly belonging to the same taxon at Penedo (locality **7**), also above Eirunepé, and both Altamira (**9**) and Barro Vermelho (**12**) downriver from that town (Lower Central Region). Our specimens cannot be distinguished by any cranial dimension from those from the Río Ucayali or upper Río Purus in eastern Perú, which are clearly assignable to *spadiceus* (see Patton, 1984). Consequently, we agree with Hoffmann et al. (1993), who listed both *pyrrhonotus* and *juralis* as synonyms of *S. spadiceus*.

SPECIMENS EXAMINED (n = 12): (**b**) 5m, 4f - MNFS 989–992, 1007, 1041–1042, 1050, 1338; (**f**) 3m — JLP 15655, 15665–15666.

Sciurus ignitus (Gray, 1867)

Bolivian squirrel

TYPE LOCALITY: ''Bolivia,'' near Yungas, upper Río Beni, Departamento de Beni.

DESCRIPTION: This species is intermediate in size between the large red squirrels of the *S. igniventris-spadiceus* complex and the diminutive squirrels of the genus *Microsciurus*. The upper parts are a uniform olivaceous brown, finely grizzled by individual black hairs. There is a small buffy postauricular patch and an indistinct pale eye-ring. The tail is long and slender, of the same ground color as the dorsum, but the hairs are tipped with orange or deep yellow in contrast to that of *Microsciurus flaviventer*. All specimens from the Rio Juruá had buffy venters. The skull is small, with a distinctly short rostrum, proodont incisors, and rather domed cranium. There are four cheekteeth above and below. Table 20 presents external and cranial measurements for specimens from the Rio Juruá.

DISTRIBUTION: As mapped by Emmons and Feer (1997), this species ranges south of the Marañón-Solimões axis from northeastern Perú and adjacent Brazil south through eastern Perú throughout Amazonian Bolivia and western Brazil. They indicated a questionable distributional hiatus in the Rio Juruá basin. However, we collected specimens in the headwaters of the Rio Juruá on the right bank and Vieira (1948) recorded a specimen from João Pessoa (= Eirunepé), which is on the left bank in the central region of the river. Additional specimens from this locality and from Igarapé do Gordão (which is near Eirunepé on the left bank) are in the collection of the Royal Natural History Museum in

TABLE 20
Selected External and Cranial Dimensions for *Sciurus ignitus* and *Microsciurus flaviventer* from the Rio Juruá
Measurements (mm) following Patton (1984); mean ± standard error, with range and sample size. Individuals are pooled across all localities along the river.

	S. ignitus			*M. flaviventer*		
Variable	Mean ± SE	Range	n	Mean ± SE	Range	n
TOL	379.71 ± 5.90	348–398	7	274.33 ± 4.88	240–295	9
TAL	187.43 ± 6.26	152–203	7	132.78 ± 1.75	126–140	9
HF	49.75 ± 1.17	48–51	8	42.33 ± 0.37	41–45	9
E	23.75 ± 0.37	23–26	8	17.0	—	2
GSL	47.36 ± 0.41	46.19–49.56	7	37.04 ± 0.32	36.23–38.66	8
BAL	36.66 ± 0.49	34.70–38.53	7	28.18 ± 0.33	27.11–29.33	7
MB	20.83 ± 0.29	19.73–21.71	7	17.49 ± 0.18	16.99–18.74	9
plOC	16.20 ± 0.16	15.42–16.72	8	15.35 ± 0.12	14.94–16.06	8
IOC	14.79 ± 0.19	14.02–15.57	8	13.43 ± 0.17	12.74–14.09	8
ZB	27.93 ± 0.27	27.24–29.61	8	22.48 ± 0.20	21.66–23.44	8
RL	18.06 ± 0.18	17.33–18.71	8	14.22 ± 0.36	12.28–15.58	9
NL	12.76 ± 0.24	11.88–13.58	8	9.95 ± 0.14	9.36–10.47	9
RW	7.98 ± 0.08	7.51–8.20	8	6.13 ± 0.11	5.77–6.86	9
D	12.72 ± 0.20	12.02–13.52	8	8.85 ± 0.10	8.24–9.21	9
MTRL	7.49 ± 0.04	7.34–7.62	8	6.47 ± 0.07	6.16–6.75	9
PW	10.94 ± 0.16	10.24–11.35	8	8.81 ± 0.18	8.45–9.06	9
MPFW	4.63 ± 0.10	4.26–5.01	7	3.51 ± 0.06	3.31–3.73	8
BOW	6.68 ± 0.11	6.23–7.09	7	5.69 ± 0.08	5.28–5.92	8
BUL	8.80 ± 0.12	8.30–9.11	7	7.59 ± 0.15	6.94–8.48	9
CD	21.65 ± 0.23	21.07–22.84	7	17.80 ± 0.12	17.44–18.43	7

Sweden (Patterson, 1992). We took all specimens only in either undisturbed or second growth terra firme forest.

REPRODUCTION: All specimens were taken in February during the rainy season. The three females were either pregnant (one, with 2 embryos) or lactating (two, each with 2 placental scars), and all males had scrotal and enlarged testes.

COMMENTS: The intermediate-sized tree squirrels of Amazonia are often placed in the genus (or subgenus) *Guerlinguetus* Gray (e.g., Hoffmann et al., 1993). Species boundaries, no matter how conceptually defined, are poorly understood, as the distinction between the western Amazonian *S. ignitus* and eastern *S. aestuans* remains to be investigated. Patterson (1992) treats the single specimen he examined from João Pessoa as representative of *S. aestuans*, and allocates it to the subspecies *gilvigularis* Wagner, which is considered a distinct species by Emmons and Feer (1997) and Hoffmann et al. (1993).

SPECIMENS EXAMINED (n = 18): (**1**) 1f — MNFS 1362; (**3**) 1f — JUR 223; (**b**) 6m, 2f — MNFS 1009-1010, 1017-1018, 1021-1023, 1043. Specimens from Royal Natural History Museum, Stockholm (see Patterson, 1992): Igarapé do Gordão, 1f — RNHM 2314; João Pessoa [= Eirunepé], 6m, 1f — RNHM 2103–2106, 2248, 2250, 2382.

MICROSCIURUS J. A. ALLEN, 1895

Dwarf squirrels

Microsciurus flaviventer (Gray, 1867)

Amazon dwarf squirrel

TYPE LOCALITY: ''Brazil''; restricted to Pebas, Departamento de Loreto, Perú by Cabrera (1961), based on Thomas (1928).

DESCRIPTION: This is a very small squirrel, averaging nearly 275 mm in body length with a long, relatively slender but well-furred tail slightly less than half of the total length of the animal. It matches the dorsal and ventral colors of *S. ignitus* almost exactly, being a grizzled olivaceous brown above and yellowish-orange below. There is a very small yellowish postauricular patch; the ears are

short and do not protrude above the head. The tail hairs are frosted with pale yellow, as opposed to burnt orange as in *S. ignitus*. Table 20 lists external and cranial measurements for specimens from the Rio Juruá.

DISTRIBUTION AND HABITAT: The range of the Amazon dwarf squirrel extends throughout western Amazonia from southeastern Colombia to southern Perú east to near the confluence of the Rio Negro, Rio Purus, and Rio Solimões (Emmons and Feer, 1997; Patterson, 1992). As with the other squirrels, specimens of *M. flaviventer* were taken, or others seen, only in terra firme forest along the Rio Juruá.

REPRODUCTION: All four specimens obtained were adult males with scrotal testes, two each collected in October (dry season) and February (wet season).

SPECIMENS EXAMINED (n = 4): (**a**) 1m — MNFS 1029; (**b**) 1m — MNFS 1051; (**12**) 2m — JLP 15792, MNFS 684.

MURIDAE ILLIGER, 1815

SIGMODONTINAE WAGNER, 1843

Rats and mice of this family (subfamily Sigmodontinae) possess three cheekteeth and a myomorphic masseter muscle system coupled with a sciurognathus lower jaw. Those that occur within the Rio Juruá basin include a diverse set of arboreal and terrestrial taxa ranging in body size from quite small (20 grams) to very large (more than 250 grams). Some are habitat specialists, others have extremely broad ecological ranges. Two genera (*Holochilus* and *Nectomys*) are found primarily in inundated areas or along stream banks, as they readily enter water; two genera are either semiarboreal (*Oecomys*) or almost strictly arboreal (*Rhipidomys*); three are terrestrial and small-bodied, two with distinctly spinose fur (*Neacomys* and *Scolomys*) and the third with an extremely long tail (*Oligoryzomys*); and, finally, one is an ''average-sized'' terrestrial mouse (the ubiquitous *Oryzomys*). All but one of these genera are currently placed in the presumptively monophyletic tribe Oryzomyini (sensu Voss and Carleton, 1993); the remaining genus, *Rhipidomys*, is usually placed in the ''Thomasomyini,'' a collection of genera apparently united only by shared primitive features (Voss, 1993). As a group, this assemblage of genera is rather characteristic of most lowland faunas of Amazonia, particularly of the western regions of southern Colombia south to northern Bolivia and east into central Brazil.

Some of these genera and many species are difficult to distinguish, especially for individuals without access to adequately curated and identified museum collections. To assist proper identification, we describe and figure the skull of each genus and most species in the accounts below, and summarize their patterns of morphological and molecular variation throughout the Rio Juruá and elsewhere in Amazonia. We refer readers to the keys presented by Emmons and Feer (1997) and Anderson (1997) as well as to recently published revisions (Carleton and Musser, 1989; Musser et al., 1998; Voss and Carleton, 1993) for further help in identifying these genera.

TRIBE ORYZOMYINI VORONTSOV

Holochilus Brandt, 1835

Marsh rats

Holochilus sciureus Wagner 1842

TYPE LOCALITY: ''Eastern Brazil, Rio San [= São] Francisco,'' Estado de Minas Gerais (see Hershkovitz, 1955).

DESCRIPTION: This is a moderately large-bodied murid rodent with close, soft hair, slightly webbed hind feet, and a tail about equal to head and body length. The dorsal color is olivaceous or tawny brown, slightly darker on the midline and becoming paler on the sides. The lateral color grades evenly to that of the venter, with no sharp lateral line or demarcation between dorsal and ventral colors. The ventral color itself is gray washed with orange or buff. The fur is relatively short, rather silky to the touch, and glistening to the eye. The ears are short and round, hairy to the tips inside and out. The tail is never longer than head and body, sparsely haired so that the annular scales are readily apparent, and with only a very minimal pencil at the tip. The hind feet are wedge-shaped with a narrow heel but broad plantar surface, with webbing between the toes, and a fringe of down-turned stiff and

silvery hairs along both sides. The sole of the foot lacks prominent granular scales. Females from the Rio Juruá have four pair of mammae, consistent with populations from elsewhere in the states of Amazonas and Goiás in Brazil and Loreto in Perú (see Voss and Carleton, 1993).

The skull (fig. 61) is long and narrow, with strong, diverging zygomatic arches. A narrow, hourglass-shaped interorbital region with a raised edge extends over the temporal region as a distinct ridge. The zygomatic notches are deeply indented, forming an anteriorly projecting spine from the zygomatic plate when viewed from above. The rostrum is relatively short and broad. The palate is narrow and deeply grooved, with a long and oval incisive foramen that nearly extends to the anterior margins of the first molars, and the posterior palatal pits are deep. The parapterygoid fossae are deeply excised and the mesopterygoid fossa extends to the posterior edge of the last molar. A well-developed alisphenoid strut separates the buccinator-masticatory foramen from the foramen ovale acessorius. The otic capsules are globose and moderately inflated. The stapedial foramen is tiny to absent, and both a squamosal-alisphenoid groove and sphenofrontal foramen are lacking. These three characters are indicative of cephalic arterial pattern 3 of Voss (1988; see also Carleton and Musser, 1989). The cheekteeth are moderately high-crowned, with cusps and connecting lophs on a single occlusal plane; the principal cusps are arranged in an alternating pattern. Voss and Carleton (1993) provide a more complete description of *H. sciureus* and contrast its features with *H. brasiliensis*. Selected external and cranial measurements of 10 adult specimens of both sexes are given in table 21.

DISTRIBUTION AND HABITAT: As currently understood (Musser and Carleton, 1993), *H. sciureus* is broadly distributed in the Orinoco and Amazon river basins, through eastern and southern Venezuela, the Guianas, northern and central Brazil, and Amazonian Colombia, Ecuador, Perú, and Bolivia. Specimens of this species are known only from the middle sections of the Rio Juruá, up- and downriver from the town of Eirunepé. All specimens collected by us were taken in inundated grass patches along the river mar-

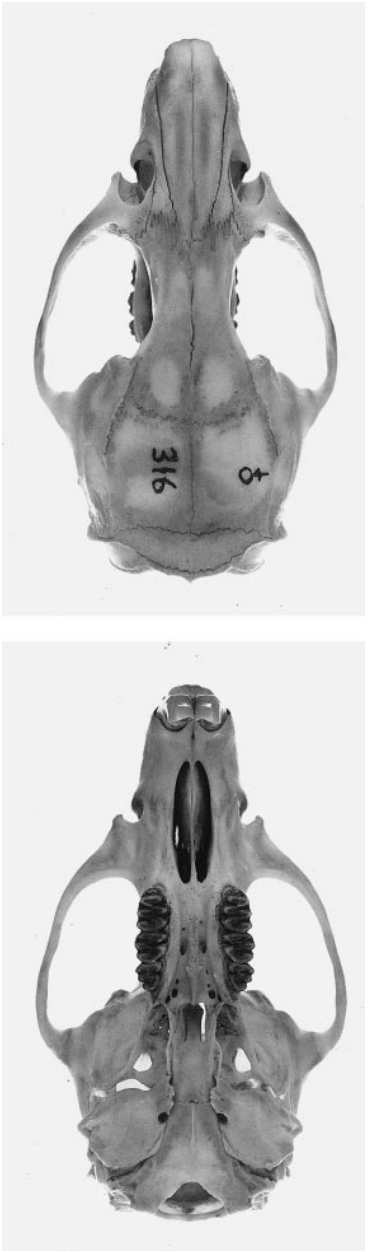

Fig. 61. Dorsal (top) and ventral (bottom) views of the cranium of *Holochilus sciureus* (MNFS 316, from Eirunepé, left bank Rio Juruá, Amazonas, Brazil [locality j]). Magnification = ×2.

TABLE 21
External and Cranial Dimensions for Adult Specimens of *Holochilus sciureus*
Measurements (mm) are given as mean, with range and sample size.

Variable	Mean	Range	n
TOL	342.5	307–380	10
TAL	155.2	126–174	10
HF	40.0	35–44	10
E	18.0	17–19	10
CIL	35.86	33.72–37.85	10
ZB	20.95	29.18–32.95	10
MB	14.38	13.67–15.20	10
IOC	4.89	4.44–5.23	10
RL	14.36	13.28–15.39	10
NL	15.01	3.62–16.15	10
RW-1	8.17	7.52–9.19	10
RW-2	6.90	6.58–7.37	10
OL	13.63	12.97–14.34	10
D	11.26	10.23–12.37	10
MTRL	7.44	6.72–7.97	10
IFL	7.97	7.51–8.55	10
PL	18.84	17.47–20.61	10
AW	7.40	7.07–8.14	10
MPFL	5.18	4.82–5.24	10
MPFW	2.20	1.94–2.54	10
OCB	8.20	7.85–8.54	10
BOL	5.49	5.02–6.32	10
ZPL	4.93	4.27–5.38	10
CD	14.44	13.41–16.28	10

gins or in small agricultural plots close to the river's edge.

REPRODUCTION: We caught specimens only in the months of August through November, at which time adult males had scrotal testes and adult females were either pregnant (one individual with 5 embryos) or lactating (one individual with 5 placental scars). Young animals were also taken at this time. A single lactating female was collected near Eirunepé by A. M. Olalla in August 1936.

KARYOTYPE: A single male (JLP 15924 from Altamira, locality **9**) had a diploid number of 56, with both autosomal and sex chromosome complements identical to those reported for a single specimen from central Perú (Gardner and Patton, 1976). There is considerable karyotypic variation within the genus, both between and within populations, throughout its range (Aguilera and Pérez-Zapata, 1989; Aguilera et al., 1993; Sangines and Aguilera, 1991; Nachman, 1992), with Amazonian populations allocated to *H. sciureus* characterized by a diploid number of 55 to 56.

COMMENTS: Boundaries of extant species within the genus *Holochilus* are undefined, pending a generic-level revision. Massoia (1981) presented evidence for the separation of *H. sciureus* from *H. brasiliensis*, a position provisionally followed by Voss and Carleton (1993) and by us here. Other authors (e.g., Reig, 1986; Aguilera and Pérez-Zapata, 1989; Aguilera et al., 1993) have suggested that *H. sciureus* itself is composite, with Reig noting that *amazonicus*, *guianae*, and *venezuelae* are probably valid species. As is true for so many South American mammals, the genus *Holochilus* requires critical revision.

SPECIMENS EXAMINED (n = 6): (**i**) 1m — MNFS 319; (**j**) 2f — JLP 15199, MNFS 316; (**7**) 1m, 1f — JLP 15470, 15479; (**9**) 1m — JLP 15924. Specimens from Royal Natural History Museum, Stockholm (see Patterson, 1992): Rio Eirú, Santo Antonio (2m, 1f — 2489, 2490, 2491); João Pessoa [= Eirunepé] (4f — 2376, 2388, 2462, 2476); Igarapé do Gordão (1m, 2f — 2300, 2311, 2408).

Neacomys Thomas, 1900

Spiny mice

Four species of spiny mice are currently recognized (Musser and Carleton, 1993). *Neacomys spinosus* (Thomas), from western Amazonia (eastern Colombia south to northern Bolivia [Anderson, 1997] and east into western Brazil), is the largest, with the other three species small-bodied and apparently replacing one another geographically: *Neacomys pictus* Goldman is recorded only from Panamá; *N. tenuipes* Thomas has been considered to range from western and central Colombia, northern Venezuela, and south through western Amazonia, where it has been recorded in sympatry with *N. spinosus* in eastern Ecuador (Lawrence, 1941) and southeastern Perú (Woodman et al., 1991); finally, *N. guianae* is distributed from the Guianan coast of Guyana, Surinam, and French Guiana south through eastern Brazil. However, as noted by Musser and Carleton (1993:708), a recent revisionary standard is lacking for taxa within the genus, and "traits

for species recognition and distributional limits [are] poorly delineated.'' Our collections from the Rio Juruá support this statement, as three distinct forms of *Neacomys* are present within this drainage. Two of these are small-bodied taxa that replace each other along the length of the river. The third is clearly referable to the larger *N. spinosus* and is sympatric with both small-bodied species. Moreover, sequence variation of the mtDNA cytochrome-b gene from localities scattered throughout Amazonia and central Colombia suggests a degree of taxonomic complexity to the genus previously unappreciated.

In the sections below, we outline the general pattern of geographic structure of spiny mice provided by our mtDNA sequence analyses. This structure defines, albeit in only a preliminary fashion, potential species boundaries within this complex genus. We then focus on the details of diversification of the genus within the Rio Juruá drainage before characterizing each of these species in terms of their morphology, genetics, distribution, and life history features.

Molecular Geographic Patterns within *Neacomys*

Sequence data are available from 53 mice representing the three species currently recognized as occurring within Amazonia (*guianae*, *spinosus*, and *tenuipes*) and from 20 separate localities (including those of sympatry, table 22). We have 801 base pairs of cytochrome-b sequence for most individuals. Only 672 are available from the four specimens from the Rio Jaú in north-central Brazil, and we obtained only 177 bp of sequence from a piece of skin for the single specimen of *tenuipes* from the Magdalena Valley of central Colombia (a skin-only specimen from the original type series, BM[NH] 99.10.3.34). Although this set of specimens, and localities, is far from adequate, it provides both reasonable geographic coverage (fig. 62) and a clear indication of the complexities present within the genus relative to species and their geographic limits. The consensus bootstrap tree of all unique haplotypes, based on 1000 iterations, defines the major clade structure for *Neacomys* throughout Amazonia (fig. 63). Kimura two-parameter distances among individual haplotypes within each of the clades defined by the bootstrap analysis, as well as those between all pairs of clades, are given in table 23. Although definitive conclusions are premature at this time, given the paucity of the data relative to the entire range of the genus, our general overview will provide a useful framework within which further studies of *Neacomys* can be placed. The salient features of this analysis are as follows:

(1) The large-bodied mouse, to which the name *spinosus* Thomas is universally applied, is strongly monophyletic, supported by a bootstrap value of 100 and with included haplotypes averaging only 2.09% in sequence divergence. This amount of differentiation is typical of intraspecific comparisons for the cytochrome-b gene in other South American murid rodents (Smith and Patton, 1991, 1993). Haplotypes of specimens of the Rio Juruá in western Brazil are monophyletic (bootstrap value of 93), as are those from eastern Ecuador (bootstrap of 98), while that from northern Perú is intermediate in the consensus tree. This grouping follows Lawrence's (1941) division of *N. spinosus* into two subspecies, *carceleni* Hershkovitz from Ecuador and Colombia and the nominate form from Perú, although it may also represent only the limited nature and geographic position of our samples. We also include within *N. spinosus* the named form *amoenus* Thomas, 1903, from Estado do Mato Grosso, Brazil, based on the direct comparison of our series of *N. spinosus* from the Rio Juruá with the holotype (BM[NH] 3.7.7.84) and type series of this taxon. These sets of specimens cannot be distinguished by discriminant analyses of cranial morphometric variables (J. L. Patton, unpubl. data).

(2) There are seven remaining clades, all of which comprise small-bodied individuals. Collectively, these amply illustrate the inadequacy of the current taxonomy in recognizing the true number of taxa within the genus. This group of clades includes a paratype of *N. tenuipes* from the Magdalena Valley in central Colombia as well as two distinct taxa within our samples from the Rio Juruá, exclusive of *N. spinosus*. One of these links with specimens from southeastern Perú; the other is known only from the central and

TABLE 22

Haplotypes, Voucher Numbers, and Localities for Taxa of Spiny Mice, Genus *Neacomys*

Individual haplotypes listed from top to bottom in the tree, figure 63, with the catalog numbers of their respective voucher specimens, and localities (identified as in the map, fig. 62) for which 801-bp haplotypes of the mitochondrial DNA cytochrome-b gene are available.

Haplotype	Voucher no.	Locality
Neacomys musseri (Clade 4)		
1	MVZ 171486	72 km NE Paucartambo, Cuzco, Perú
2	MVZ 171488	72 km NE Paucartambo, Cuzco, Perú
3	MNFS 1395	Igarapé Porongaba, right bank Rio Juruá, Acre, Brazil (locality **1**)
Neacomys sp. (Clade 3—northwestern Amazonia)		
4	MVZ 153530	Huampami, Rio Cenepa, Amazonas, Perú
5	MVZ 155014	Huampami, Rio Cenepa, Amazonas, Perú
6	ROM 105314	Parque Nacional Yasuní, Napo, Ecuador
7	ROM 104560	Parque Nacional Yasuní, Napo, Ecuador
8	ROM 105265	Parque Nacional Yasuní, Napo, Ecuador
9	ROM 105315	Parque Nacional Yasuní, Napo, Ecuador
Neacomys minutus (Clade 5—Rio Juruá)		
10	JLP 15365	Penedo, right bank Rio Juruá, Amazonas, Brazil (locality **7**)
11	MNFS 624	Sacado, right bank Rio Juruá, Amazonas, Brazil (locality **5**)
12	JLP 15846	Barro Vermelho, left bank Rio Juruá, Amazonas, Brazil (locality **12**)
13	JLP 16060	Altamira, right bank Rio Juruá, Amazonas, Brazil (locality **9**)
14	MNFS 1714	Vira-Volta, left bank Rio Juruá, Amazonas, Brazil (locality **14**)
15	MNFS 1734	Vira-Volta, left bank Rio Juruá, Amazonas, Brazil (locality **14**)
Neacomys spinosus		
16	ROM 104474	Parque Nacional Yasuní, Napo, Ecuador
17	ROM 105282	Parque Nacional Yasuní, Napo, Ecuador
18	USNM 574567	Tinguino, 130 km S Coca, Pastaza, Ecuador
19	MVZ 155015	Huampami, Rio Cenepa, Amazonas, Perú
20	MNFS 1262	Igarapé Porongaba, right bank Rio Juruá, Acre, Brazil (locality **1**)
21	MNFS 1565	Sobral, left bank Rio Juruá, Acre, Brazil (locality **4**)
22	JLP 15674	Condor, left bank Rio Juruá, Amazonas, Brazil (locality **6**)
23	JLP 15292	Penedo, right bank Rio Juruá, Amazonas, Brazil (locality **7**)
Neacomys sp. (Clade 7—southeastern Amazonia)		
24	MDC 593	52 km SSW Altamira, east bank Rio Xingu, Pará, Brazil
Neacomys sp. (Clade 6—north-central Amazonia)		
25	MNFS 2017	Tambor, left bank Rio Jaú, Amazonas, Brazil
26	MNFS 2023	Tambor, left bank Rio Jaú, Amazonas, Brazil
27	MNFS 2084	right bank above mouth, Rio Jaú, Amazonas, Brazil
28	MNFS 2104	right bank above mouth, Rio Jaú, Amazonas, Brazil
Neacomys guianae (Clade 2)		
29	ROM 101026	Baramita, Barima-Waini, Guyana
Neacomys tenuipes (Clade 1)		
30	BMNH 1899.10.3.34	El Patan, near Bogotá, Cundinamarca, Colombia

lower Rio Juruá. Also strongly distinct in sequence are specimens from northern Perú and eastern Ecuador, which presumably represent the same taxon recently compared to sympatric *N. spinosus* in northern Perú by Malygin and Rosmiarek (1996); those from the north-central Amazon in the region west of the Rio Negro and north of the Rio Soli-

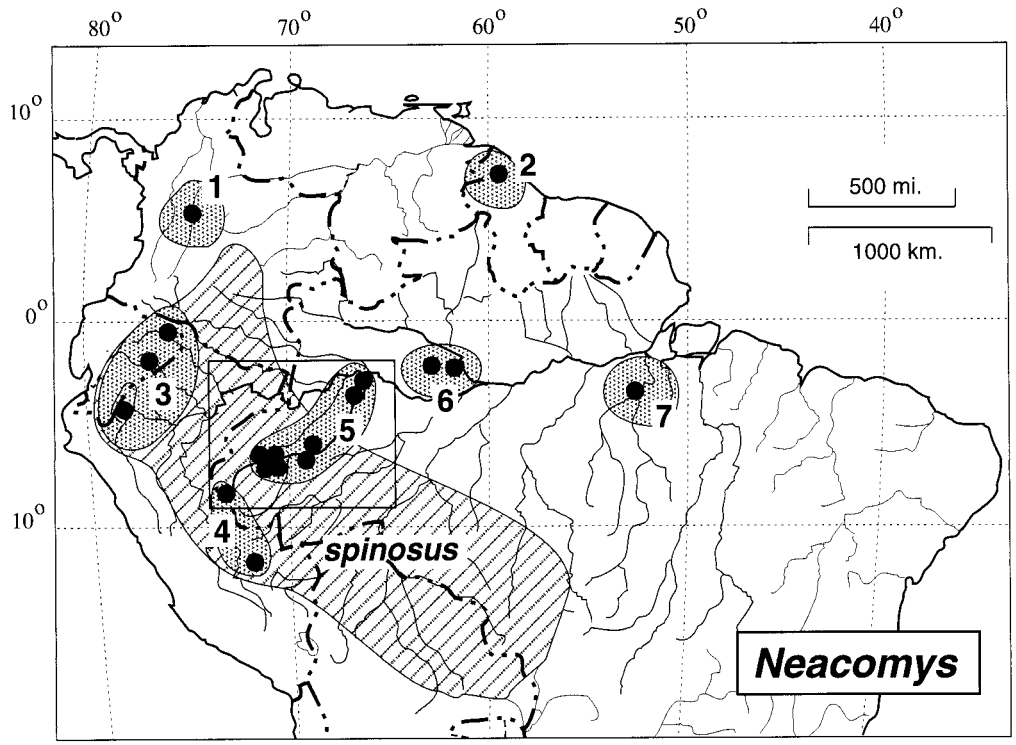

Fig. 62. Localities of *Neacomys* sampled for sequence variation in the cytochrome-b mitochondrial gene. Diagonal hatching indicates distribution of *N. spinosus*; each of the seven small-bodied haplotype clades identified in the consensus bootstrap maximum parsimony tree (fig. 63) are individually numbered and indicated by stippling. Localities are identified as in table 22. The box circumscribes the Rio Juruá basin of western Brazil, for which the included samples are analyzed and presented separately (fig. 64).

mões (the Rio Jaú); eastern Brazil south of the Rio Amazonas (the Rio Xingu); and the coastal lowlands of Guyana (fig. 63). Each of these is equally divergent from all others, with mean Kimura two-parameter values ranging between 11 and 17% (table 23). The high degree of differentiation between clades contrasts with within-clade divergences that are typically less than 2%, with the exception of the second small species from the Rio Juruá. We can assign names to some of these clades, but not to all.

Our specimen from Guyana is from Baramita, geographically close to the type locality of *guianae* (Demerara River, Guyana). We presume that this specimen represents *N. guianae*, but given the number of sympatric or near-sympatric species in western Amazonia, this may prove an incorrect presumption. Our specimen from the Rio Xingu might also be allocated to *guianae*, based on the current geographic limits of that species. However, the extreme degree of sequence divergence between these two specimens (17.4%) suggests that they represent different species. If so, no name is available for animals from eastern Amazonia south of the Rio Amazonas. Finally, although only limited data are available from the paratype of *tenuipes* examined, they do not suggest a special relationship between this taxon and any of the small-bodied geographic forms from western Amazonia (contrary to assignments in the literature, such as those of Lawrence [1941} and Woodman et al. [1991]). On geographic grounds alone, the lack of association between *tenuipes* and taxa from Amazonia is not unexpected. Few rodent species have distributions that encompass central and western Colombia and the Amazonian lowlands.

In summary, we would hypothesize that

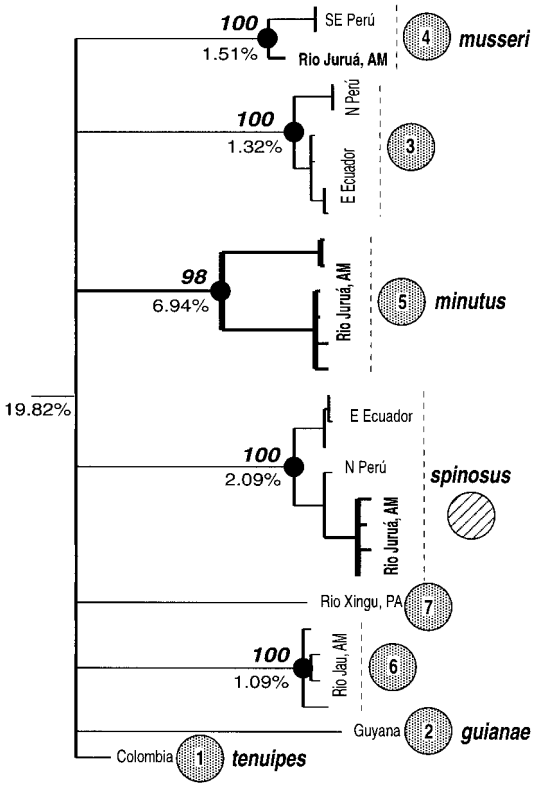

Fig. 63. Strict consensus maximum parsimony tree of haplotypes of spiny mice, genus *Neacomys*, based on 801 bp of cytochrome-b and rooted by comparison to species of *Oryzomys*. Branch lengths are proportional to the number of character changes. Each clade is identified as in the map (fig. 62). Haplotypes for specimens from the Rio Juruá are identified by heavy lines and bold type; numbers refer to the specific locality as identified in the text and the map, fig. 1. Numbers at nodes are bootstrap values, based on 1000 replicates; percentages are average Kimura two-parameter distances (see table 23). Tree length = 592 steps; CI = 0.514, RI = 0.790.

each clade of small-bodied forms identified in the molecular sequence analysis represents a separate species. Although we describe the two taxa from the Rio Juruá here, where our samples are adequate to ascertain diagnosable morphological features, we lack sufficient data to do so for the other small-bodied forms identified in figure 63. Future field collections and laboratory analyses are needed to resolve the true number of species contained within this series of clades, as well as others from elsewhere in Amazonia not included in our analyses. Clearly, however, our data suggest that species diversification within the spiny mouse genus *Neacomys* is substantially greater than is appreciated by its current taxonomy.

Neacomys of the Rio Juruá

Specimens of spiny mice from the Rio Juruá basin sort into three distinct groups by a combination of size, morphological features, and genetic characteristics. Two species are sympatric at two different localities (fig. 64) and all three form strongly supported monophyletic lineages on the basis of their cytochrome-b sequences (fig. 65 and table 23). The larger of these species is clearly assignable to *N. spinosus*. The two smaller taxa replace one another along the river, with one known only from a single locality (opposite Igarapé Porongaba, locality **2**) in the Headwaters Region and the other present at most localities in the Upper and Lower Central and Mouth regions (fig. 64). These two differ in a number of morphological features, including most external and cranial dimensions, in qualitative features of the skull, and in karyotype, as well as differing by an average of 13.2% in mtDNA sequence (table 23).

The name *N. tenuipes* (Thomas) has been applied to a smaller bodied species often sympatric with *N. spinosus* at localities in eastern Ecuador and in Perú (such as Boca Curaray [Lawrence, 1941], Panguana (Hutterer et al., 1995], and Cusco Amazónico [Woodman et al., 1991]). However, neither of the Rio Juruá small taxa has any mtDNA resemblance to a paratype of *N. tenuipes* from Colombia, nor do other small specimens from northern Perú or eastern Ecuador (fig. 63; table 23). It seems unlikely, therefore, that this name applies to any of the clades of small Amazonian taxa that we have uncovered to date.

All other available names for Amazonian *Neacomys* clearly apply to large-bodied forms, based on original descriptions and our examination of the respective holotypes (*amoenus* Thomas, 1903; *carcelini* Hershkovitz, 1940). Given, therefore, the lack of available names and the combined morpho-

TABLE 23
Kimura 2-Parameter Distances Among Eight 801-bp Cytochrome-b Haplotype Clades of Spiny Mice, *Neacomys*, from South America
Clades are identified as in figure 61. Data are given as mean ± standard error.
Numbers on the diagonal are values within clades.

Clade	*spinosus*	1 [*tenuipes*][a]	2 [*guianae*]	3	4 [*musseri*]	5 [*minutus*]	6	7
spinosus	2.088 ± 0.026							
1 [*tenuipes*]	12.432 ± 0.017	—						
2 [*guianae*]	15.265 ± 0.009	12.723	—					
3	15.528 ± 0.014	10.804 ± 0.009	15.388 ± 0.012	1.321 ± 0.018				
4 [*musseri*]	14.983 ± 0.018	11.231 ± 0.016	18.108 ± 0.021	12.059 ± 0.011	1.511 ± 0.013			
5 [*minutus*]	16.116 ± 0.014	13.092 ± 0.020	16.697 ± 0.005	13.051 ± 0.021	13.182 ± 0.014	6.941 ± 0.071		
6	17.019 ± 0.010	11.638 ± 0.011	15.064 ± 0.004	13.445 ± 0.010	14.803 ± 0.008	15.436 ± 0.013	1.090 ± 0.005	
7	14.165 ± 0.004	14.516	17.442	14.775 ± 0.007	15.205 ± 0.008	13.885 ± 0.010	15.329 ± 0.015	—

[a] Paratype (BMNH 99.10.3.34); only 177 bp of sequence available.

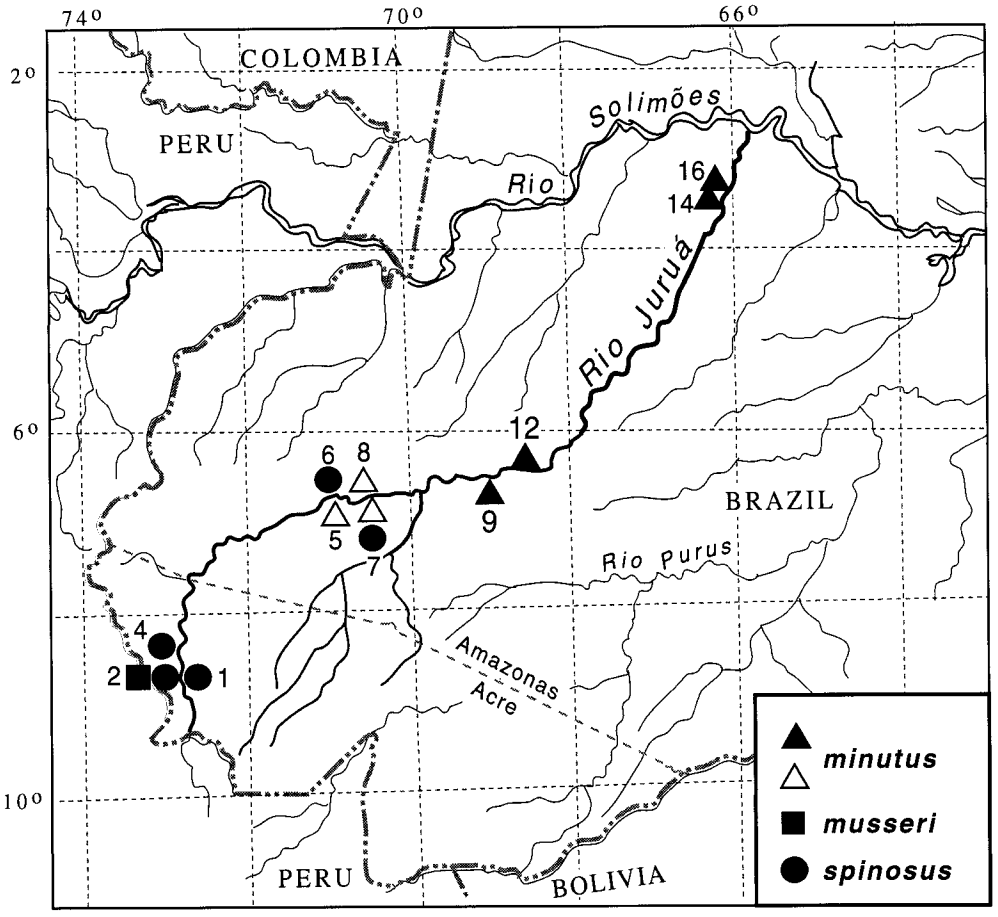

Fig. 64. Localities and distribution of samples of spiny mice, *Neacomys*, from the Rio Juruá, western Brazil. Solid circles = *N. spinosus*; solid square = *N. musseri*; triangles = *N. minutus* (open = upriver clade; solid = downriver clade).

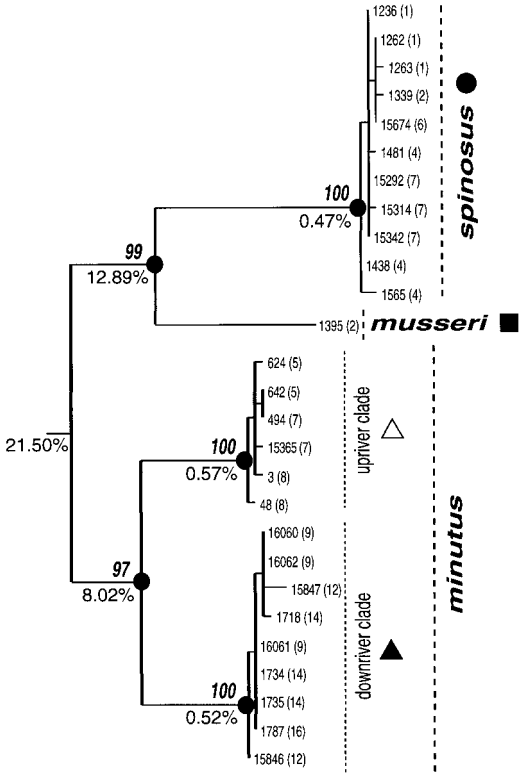

Fig. 65. Strict consensus maximum parsimony tree of spiny mice, genus *Neacomys*, from the Rio Juruá, based on 414 bp of cytochrome-b sequence and rooted by comparison to *Oligoryozmys microtis*. Branch lengths are proportional to the number of character changes. Numbers at nodes are bootstrap values, based on 1000 replicates; percentages are average Kimura two-parameter distances. Individual haplotypes are identified by field catalog and locality number (from the map, fig. 1). Tree length = 176 steps; consistency index = 0.795; retention index = 0.951.

logical, molecular, and karyotypic distinctness of these two diminutive taxa from the Rio Juruá, we describe each below. The first is known from the headwaters of the Rio Juruá and southeastern Perú. We describe this taxon as the following.

Neacomys musseri, new species

HOLOTYPE: MVZ 171486 (Museum of Vertebrate Zoology, University of California, Berkeley), adult male, collected 14 July 1985 by James L. Patton (original number 11890); skin with skull and mandibles, in good condition; and liver and kidney tissue, originally preserved in liquid nitrogen, maintained at −76°C in the frozen collection of the Museum of Vertebrate Zoology.

TYPE LOCALITY: 72 km NE Paucartambo (by road), at km 152, Departamento de Cusco, Perú, 1460m. Obtained in undisturbed upper tropical forest within the Manu Biosphere Reserve (figs. 66 and 67). The locality is just above San Pedro on the road from Paucartambo to Shintuya (in the Departamento de Madre de Dios) which courses down the steep valley of the Río Cosñipata in the watershed of the Río Alto Madre de Dios. Pacheco et al. (1993) provide a map of collecting localities, including this one, within the Manu Biosphere Reserve.

DIAGNOSIS: This is a small-bodied mouse (fig. 68) characterized by its small and delicate cranium (figs. 69, 70, and 71); short maxillary toothrow; apparently unique presence (among other species in the genus) of the derived cephalic arterial system (as in *Oligoryzomys*; see Carleton and Musser, 1989), in which the squamosal-alisphenoid groove and sphenofrontal foramen are absent (indicating that the supraorbital branch of the stapedial artery is missing), but large stapedial foramen persists (pattern 2, of Voss, 1988; see also Carleton and Musser, 1989); and first upper molar with a deep anteromedian flexus divides the procingulum into anterolabial and anterolingual conules (fig. 72).

PARATYPES: Twelve others, in addition to the holotype, from the type locality: MVZ 171481 (adult male), 171482 (adult male), 171483 (adult male), 171484 (adult female), 171485 (adult male), 171487 (adult male), 171488 (adult male), and 171489 (adult female); fluid: MVZ 172328 (adult male), 172329 (adult male), 172330 (adult female), 172331 (adult male), all collected in July, 1985. Additional referred specimen: MNFS 1395 (adult female, skin with skull), collected in February 1992 from opposite Igarapé Porongaba, left bank Rio Juruá, Acre, Brazil (to be cataloged in the Coleção de Mamíferos, INPA, Manaus, Brazil). Tissues (frozen and maintained at −76°C and/or in ethyl alcohol) are preserved from all specimens except those in fluid.

MEASUREMENTS OF HOLOTYPE: TOL, 153; TAL, 83; HF, 22; E, 13; CIL, 18.88; ZB,

Fig. 66. Habitat along the road from Paucartambo to Shintuya, in the Department de Cusco in southeastern Perú, at the type locality of *Neacomys musseri*. The species was taken in Victor rat traps and Sherman live traps baited with a mixture of peanut butter and rolled oats or sardines and rolled oats and placed in the thick vegetation along both sides of the road. Photograph by J. L. Patton, April 1984.

11.44; MB, 9.93; IOC, 4.51; RL, 7.33; NL, 7.80; RW-1, 4.03; RW-2, 3.30; OL, 7.22; D, 5.51; MTRL, 2.65; IFL, 2.99; PBL, 8.49; AW, 4.01; OCB, 5.24; BOL, 2.97; MPFL, 2.64; MPFW, 1.45; ZPL, 1.97; CD, 8.03.

ADDITIONAL MEASUREMENTS: See table 24.

DESCRIPTION AND COMPARISONS: *Neacomys musseri* is significantly larger in nearly all external and cranial dimensions than the second small-bodied species described below, but smaller than *N. spinosus* (table 24). The three species, however, have the same general proportions, as indicated by bivariate plots of external and cranial variables (fig. 73). The difference in size and great similarity in body proportions are highlighted by the significant differences in scores between the three species for PC-1 but generally not for subsequent PC axes (table 24). However, the three taxa are readily separable by a discriminant function analysis using log-transformed cranial variables (fig. 73, lower right; see table 25 for standardized character coefficients). Predicted group membership of individual specimens to their respective a priori groups is perfect, with individual posterior probabilities of 0.893 or higher. This species has generally the same spinose fur with color and tones as in other congeners, both large and small, from Amazonia. A delicate mouse, *N. musseri* has a slender tail that is weakly bicolored dark brown above, paler below, obviously scaled in appearance, and clothed in short hairs. Scale rows are narrower than in *N. spinosus*, but similar in size to those of the second small-bodied species from the Rio Juruá (averaging 16 per cm versus 13 in *spinosus*). The hind feet are narrow and elongate, with proportionately long digits, but similar in this respect to other species. All three species have six plantar tubercles of similar size and proportions. Cranially, *N.*

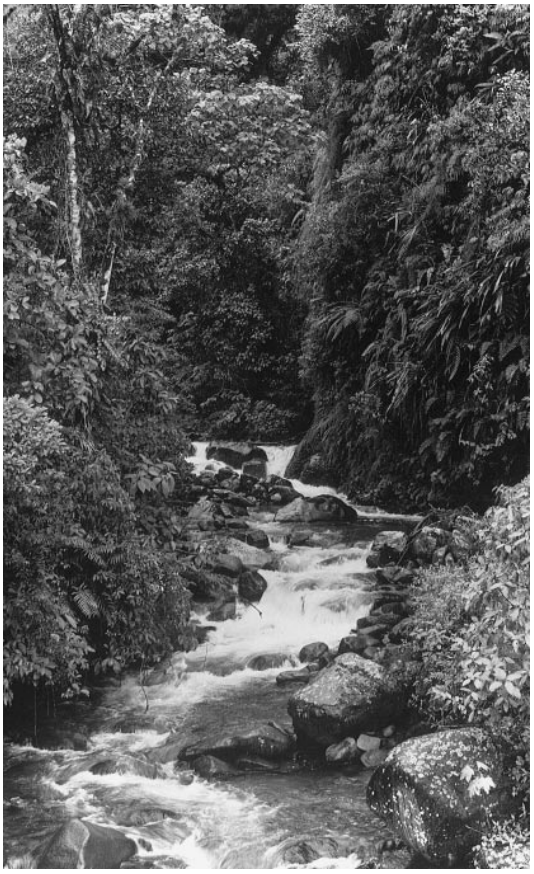

Fig. 67. Rio Cosñipata below the road in fig. 65, at the type locality of *Neacomys musseri*. Individuals were taken in the dense undergrowth back from the margins of the river. Photograph by J. L. Patton, April 1984.

musseri is unique among *Neacomys* from western Amazonia in its derived cephalic arterial system, lacking the supraorbital branch of the stapedial artery. Other species of *Neacomys* from western Amazonia (including *N. spinosus* and the second species described below, and the small-bodied forms from northern Perú and Ecuador or the Rio Jaú [clades 3 and 6 in figs. 62 and 63]) possess the squamosal-alisphenoid groove and sphenofrontal foramen indicative of the primitive cephalic arterial pattern. All species in the genus have rather delicate skulls, with rounded crania, diverging and well-developed supraorbital ridges that extend onto the temporal region, shallow zygomatic notches with relatively narrow but vertical zygomatic plates with rounded superior margins, weakly developed zygomatic arches, short and relatively broad rostra, opisthodont upper incisors, long palates with short incisive foramina, pronounced postpalatal pits, broad mesopterygoid fossae, and broad and moderately excavated parapterygoid fossae. The incisive foramen of *N. musseri* differs slightly, but consistently, in shape from those of other species, being widest at its midpoint and converging posteriorly, rather than diverging gradually to reach its widest dimension at its posterior margin, as in the second species described below (fig. 74). The posterior margin of the foramen nearly reaches the level of the first upper molars in *N. musseri*, but is widely separated from them in second species described below. The bullae are globular but small; the stapedial foramen is enlarged and obvious, indicative of a well-developed stapedial artery (as in *Oligoryzomys*; Carleton and Musser, 1989). Aside from the overall size of the molars (table 24) and the depth of the anteromedian flexus (-id), the occlusal patterns of the three species are closely similar (fig. 72). The molar teeth are pentalophodont, with high and narrow cusps in the unworn condition, with well-developed anterolophs (-ids), mesolophs (-ids), and posterolophs (-ids) on both first and second molars, and a small but moderately complicated third molar similar to that of *Microryzomys* (Carleton and Musser, 1989). The procingulum of the first upper and lower molars is divided into anterolabial and anterolingual conules (-ids) by a deeply excised anteromedian flexus (-id). In this respect, *N. musseri* differs strongly from *N. spinosus*, which appears to lack a demonstrable anteromedian flexus (-id). The anteromedian flexus (-id) of the other small-bodied species from the Rio Juruá basin (described below) is not as well developed as it is in *N. spinosus* (fig. 72).

DISTRIBUTION AND HABITAT: This species is known only from the type locality and from the headwaters of the Rio Juruá in western Brazil adjacent to the Peruvian border. The habitat at the type locality is upper tropical forest (''Bosque húmedo subtropical'' of the Holdridge [1967] system; Tosi, 1960; see figs. 66 and 67); that in the headwaters of the Rio Juruá is lowland rainforest, part of the

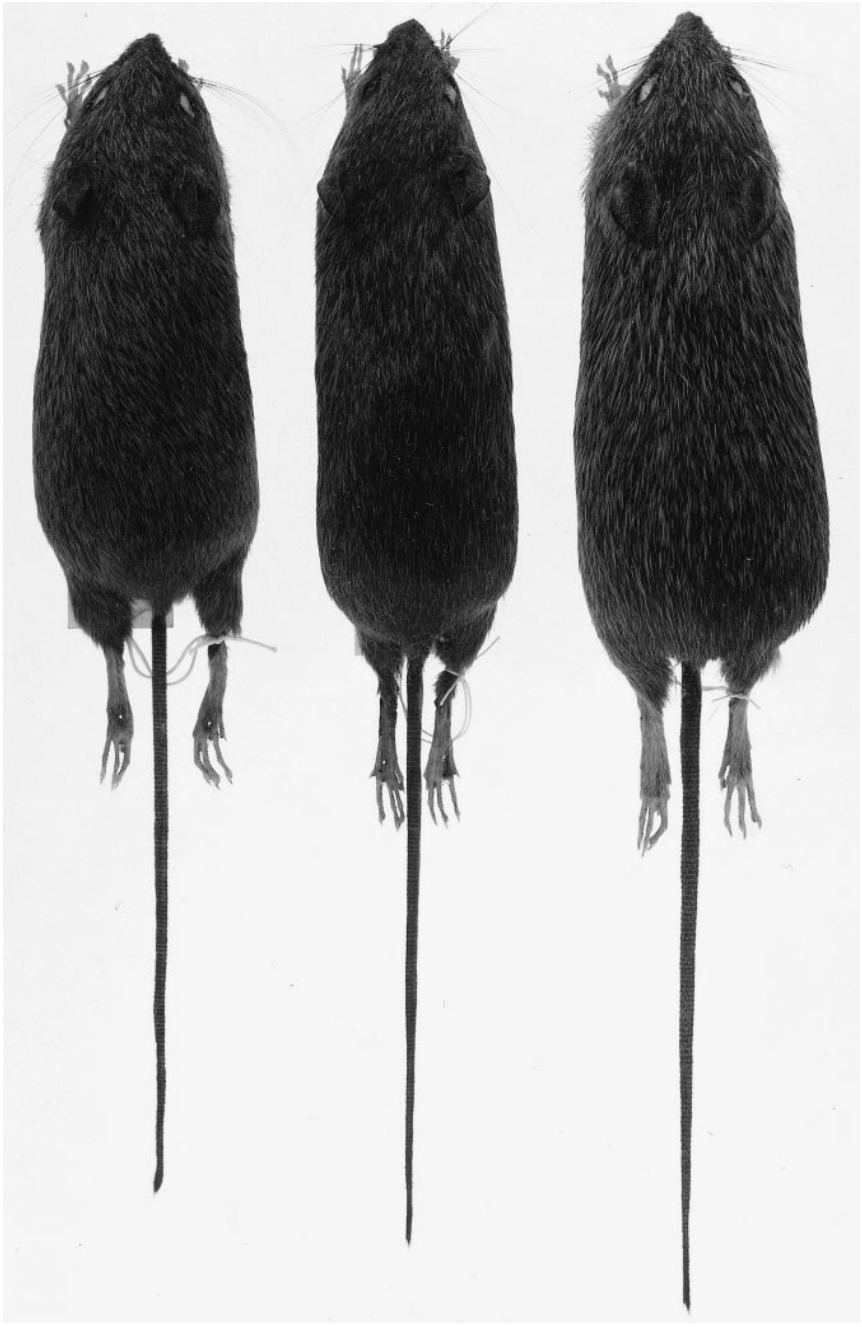

Fig. 68. Dorsal views of the stuffed study skins of three species of *Neacomys* from western Amazonia. From left to right: *Neacomys musseri* (holotype, MVZ 171486), *N. minutus* (holotype, INPA 2689), and *N. spinosus* (Rio Juruá, JLP 15314, locality **7**).

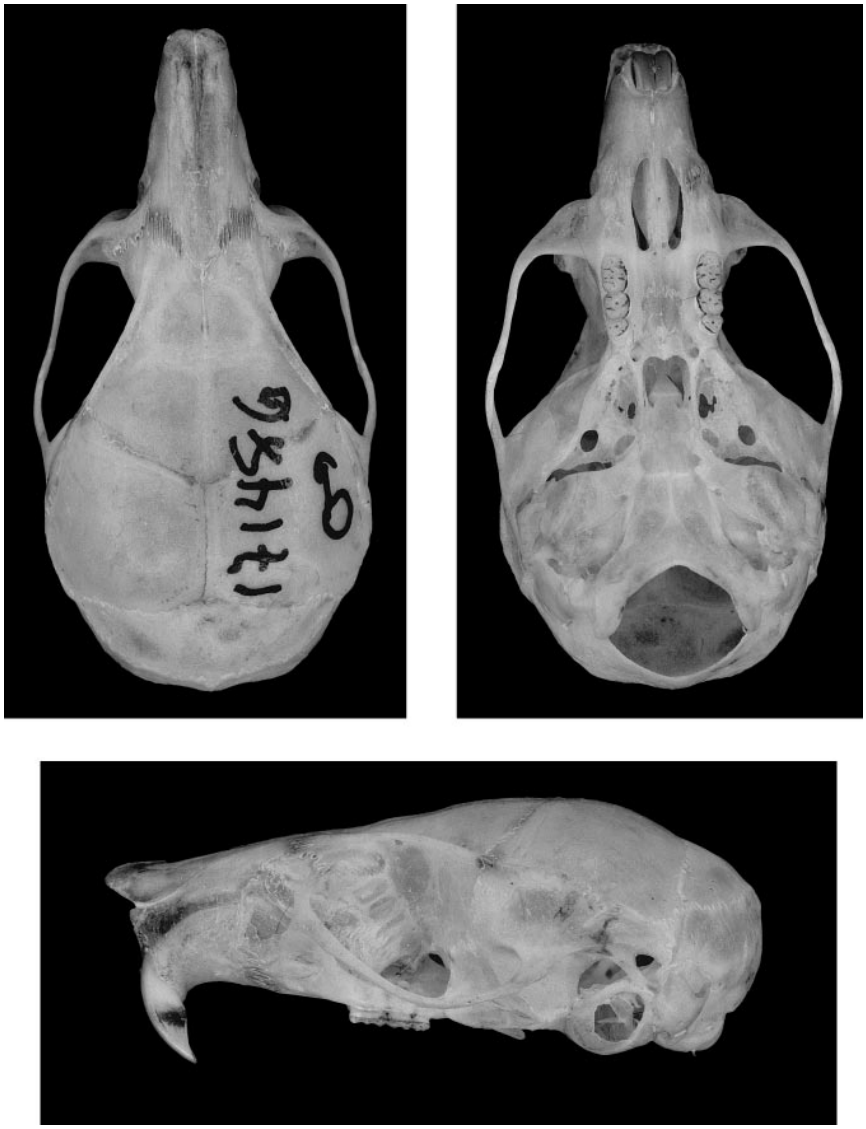

Fig. 69. Dorsal, ventral, and lateral views of the cranium of the holotype (MVZ 171486) of *Neacomys musseri*, an old adult. The skin and maxillary toothrows are illustrated in figures 67 and 70, respectively. Magnification = ×4.

phytogeographic domain termed ''Floresta Tropical Aberta'' (Projeto RadamBrasil, 1977). It is likely that specimens referred to *Neacomys tenuipes* from Cusco Amazónico, Departamento de Madre de Dios in southeastern Perú, by Woodman et al. (1991) represent this species, but we have not examined them. No small-bodied spiny mice that could represent this species have been recorded as yet from Bolivia (Anderson, 1997).

REPRODUCTION AND LIFE HISTORY: The series of specimens from the type locality in southeastern Perú was collected in July during the dry season. All individuals are adults, with most being old adults, judging from toothwear and pelage characteristics, but none were in reproductive condition. Each of the six males had small (4–5 mm), nonscrotal testes; both females were parous, one with obvious placental scars suggesting a prior

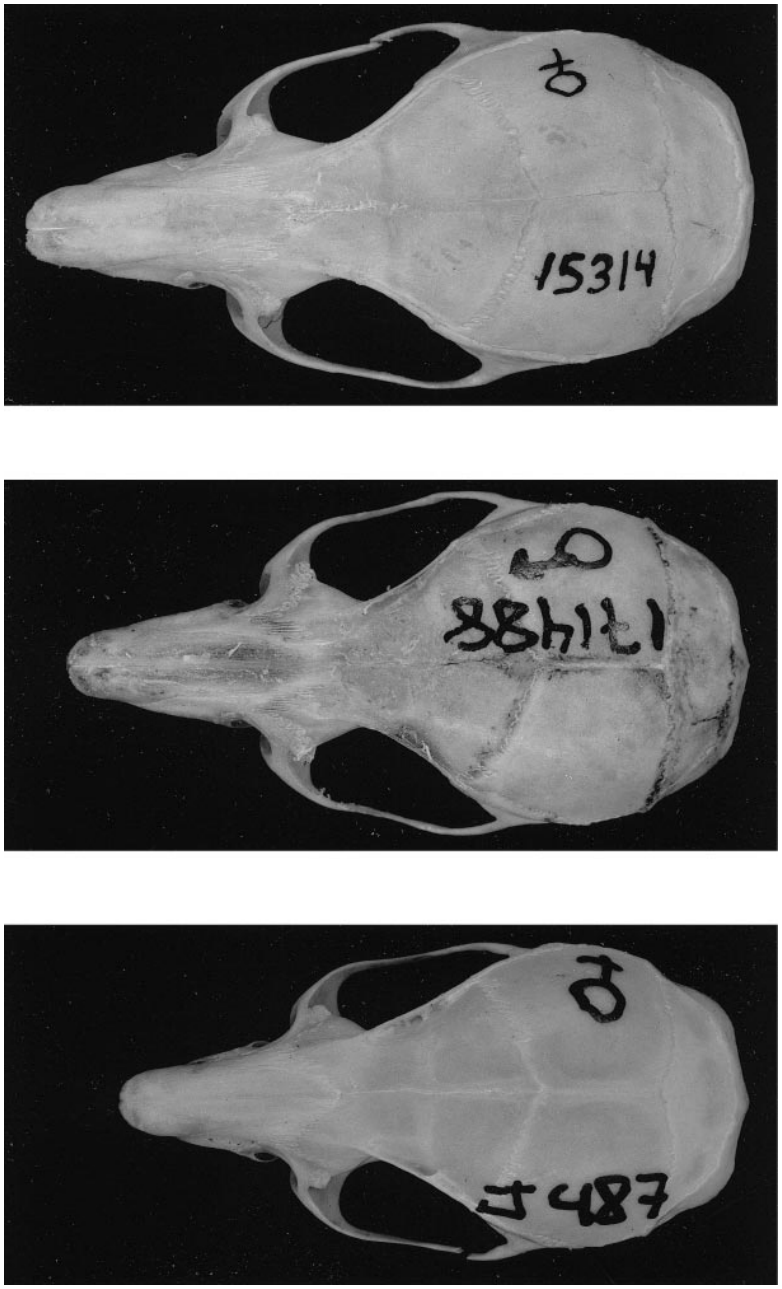

Fig. 70. Dorsal views of adult crania contrasting examples of three species of spiny mice, genus *Neacomys*. **Top**: *N. spinosus* (JLP 15314; Penedo [locality **7**], right bank Rio Juruá, Amazonas, Brazil). **Middle**: *N. musseri* (MVZ 171488, paratopotype). **Bottom**: *N. minutus* (nov. sp.; JUR 487; Colocação Vira-Volta [locality **14**], left bank Rio Juruá, Amazonas, Brazil). Magnification = ×4.

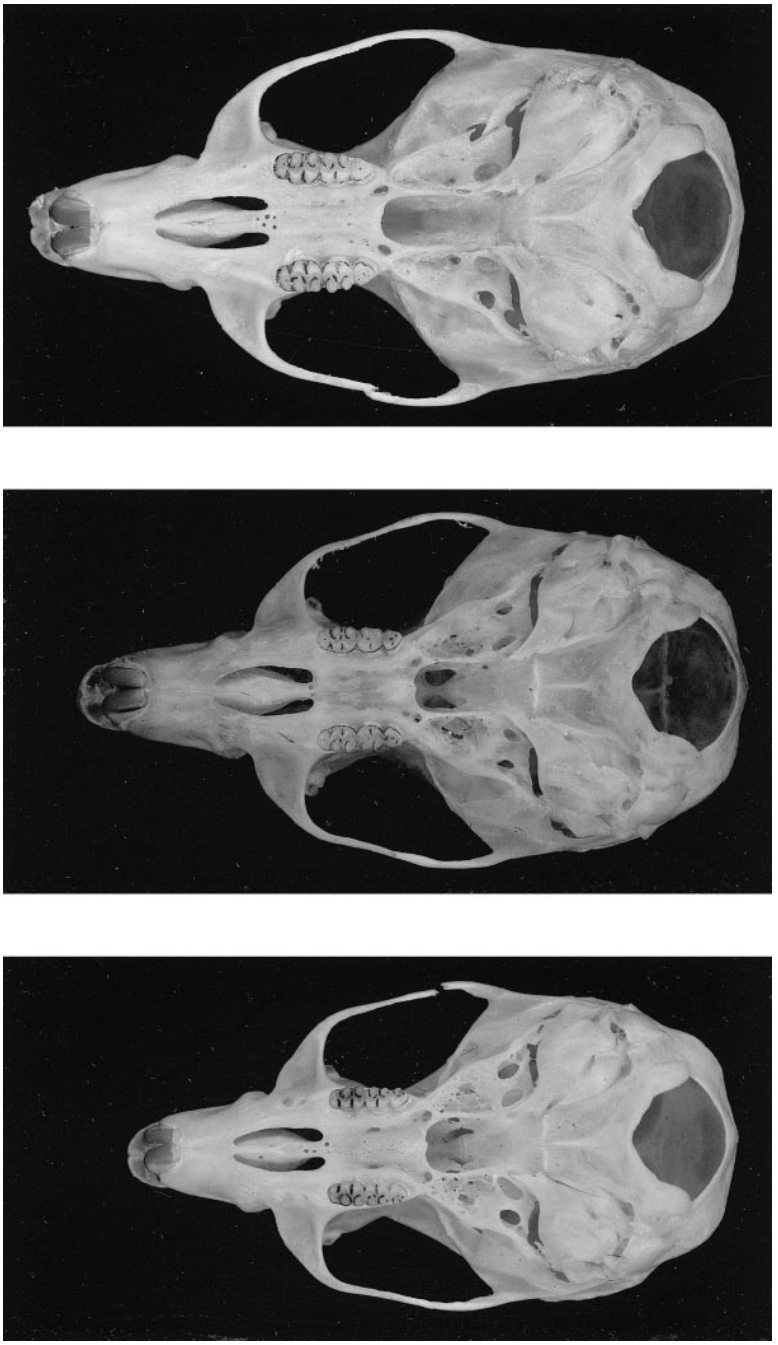

Fig. 71. Ventral views of the same crania shown in figure 69 on opposite page. **Top**: *N. spinosus*. **Middle**: *N. musseri*. **Bottom**: *N. minutus*.

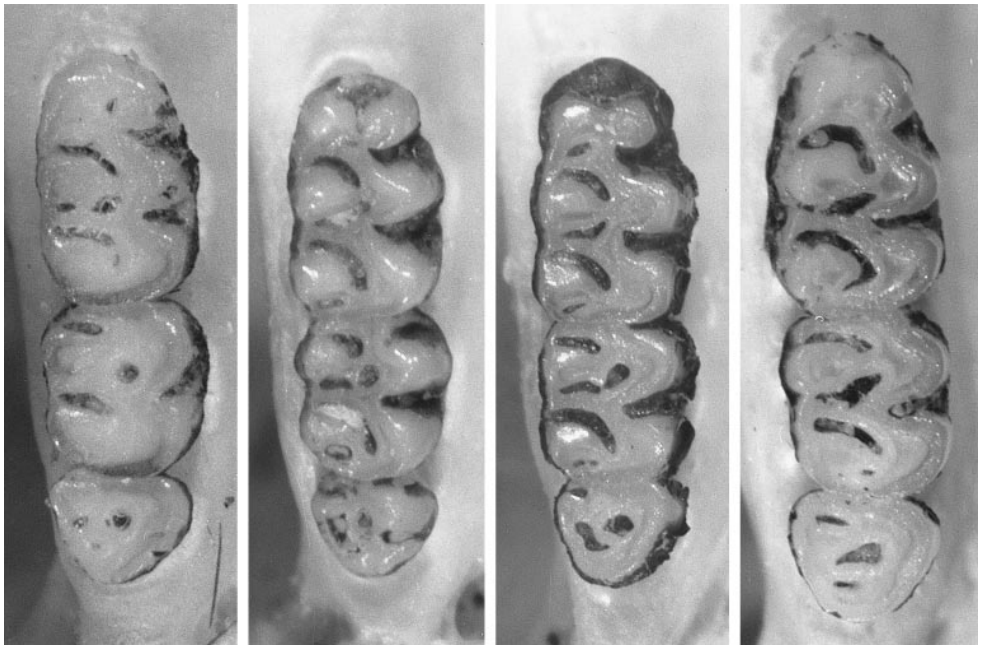

Fig. 72. Upper right toothrows of four specimens of *Neacomys* from eastern Perú and Rio Juruá basin of western Brazil. From left to right: *N. musseri* (holotype, MVZ 171486); *N. musseri* (MNFS 1395, locality **2**); *N. minutus* (JLP 16061, locality **9**); *N. spinosus* (JLP 15292, locality **7**).

breeding effort. The single specimen from the upper Rio Juruá in western Brazil is a subadult female captured in February, during the rainy season. This specimen has subadult, nonspinous pelage remaining on the rump, although it was pregnant with two near-term embryos, each 13 mm in crown-rump length.

ETYMOLOGY: Named in honor of Guy G. Musser for his long friendship and many outstanding contributions to our understanding of the systematics and evolutionary diversification of muroid rodents, including those of the Neotropical region.

KARYOTYPE: 2n = 34, FN = (64–68), with 15 pairs of biarmed chromosomes, grading in size from large to small, and two pairs of small uniarmed elements (fig. 75A). Since only a single female was examined, the sex chromosomes are unknown, but presumably the X-chromosome would represent one of the medium-sized biarmed elements characteristic of other known karyotypes in the genus (see below and Gardner and Patton, 1976). This complement contrasts sharply with the 2n = 64 and nearly uniarmed karyotype of *N. spinosus* (see Gardner and Patton, 1976, and fig. 75D) and differs substantially from that of the second small-bodied species from the Rio Juruá, described next.

Neacomys minutus, new species

HOLOTYPE: INPA 2689 (Instituto Nacional de Pesquisas da Amazônia, Manaus), adult female (lactating and pregnant, with three embryos), collected 17 November 1991 by James L. Patton (original number 16073); skin with skull and mandibles, in good condition; liver and kidney tissue preserved in 95% ethyl alcohol and maintained in the tissue collections of both INPA and the Museum of Vertebrate Zoology, University of California, Berkeley (MVZ).

TYPE LOCALITY: Altamira, left bank Rio Juruá, Amazonas, Brazil, 6°35′S, 68°54′W. Obtained in terra firme forest on our standardized trap line in a Sherman live trap, station number D-14.

DIAGNOSIS: This is a diminutive species with a long tail, dark orange dorsal coloration strongly but finely streaked with black (fig. 68), short ears (13 mm or less), small

TABLE 24

External and Cranial Dimensions of Three Species of Spiny Mice, *Neacomys*

Samples of *N. minutus* and *N. spinosus* are from the Rio Juruá; that of *N. musseri* is of the type series from southeastern Perú. Measurements (mm) are given as mean ± standard error, with range and sample size. Significance levels between pairs of taxa from one-way ANOVA (ns = $p > 0.05$; * $p < 0.05$; ** $p < 0.01$; *** $p < 0.001$).

	N. minutus				*N. musseri*				*N. spinosus*		
Variable	Mean ± SE	Range	n	*p*	Mean ± SE	Range	n	*p*	Mean ± SE	Range	n
TOL	147.7 ± 2.03	135–163	15	*	157.6 ± 1.40	153–163	8	***	182.0 ± 2.66	167–203	18
TAL	77.1 ± 1.25	70–84	15	*	83.4 ± 1.60	77–90	8	***	95.7 ± 1.48	83–107	18
HF	20.8 ± 0.21	19–22	16	***	22.2 ± 0.15	22–23	9	***	23.8 ± 0.20	22–25	18
E	12.3 ± 0.22	10–13	16	***	13.4 ± 0.24	13–15	9	***	14.6 ± 0.14	13–16	18
CIL	17.840 ± 0.111	16.84–18.74	20	***	18.939 ± 0.112	18.52–19.48	9	***	20.779 ± 0.156	19.24–22.42	25
ZB	10.706 ± 0.069	10.20–11.67	20	***	11.365 ± 0.101	10.95–11.78	8	***	12.219 ± 0.086	11.46–12.92	25
MB	8.954 ± 0.060	8.54–9.71	20	***	9.874 ± 0.101	9.27–10.22	9	***	11.007 ± 0.064	10.42–11.53	25
IOC	4.183 ± 0.038	3.92–4.50	20	ns	4.258 ± 0.056	4.03–4.51	9	*	4.412 ± 0.046	4.10–4.88	25
RL	6.932 ± 0.074	6.36–7.57	20	***	7.672 ± 0.086	7.26–7.98	9	ns	7.818 ± 0.078	7.02–8.55	25
NL	7.742 ± 0.081	7.16–8.46	20	***	8.418 ± 0.128	7.80–8.93	9	ns	8.542 ± 0.100	7.55–9.47	25
RW-1	3.973 ± 0.034	3.60–4.19	20	**	4.156 ± 0.033	4.03–4.33	9	***	4.433 ± 0.037	4.07–4.77	25
RW-2	3.063 ± 0.033	2.74–3.28	20	**	3.262 ± 0.042	3.06–3.47	9	***	3.622 ± 0.033	3.24–3.83	25
OL	6.944 ± 0.051	6.60–7.44	20	**	7.242 ± 0.053	7.01–7.46	9	***	7.820 ± 0.060	7.32–8.56	25
D	5.132 ± 0.040	4.80–5.44	20	***	5.532 ± 0.066	5.25–5.80	9	***	5.951 ± 0.058	5.42–6.47	25
MTRL	2.602 ± 0.019	2.42–2.75	20	***	2.739 ± 0.031	2.61–2.90	9	***	3.091 ± 0.018	2.91–3.26	25
IFL	2.907 ± 0.030	2.64–3.19	20	**	3.129 ± 0.047	2.84–3.31	9	***	3.478 ± 0.051	2.91–4.03	25
PL	8.047 ± 0.058	7.64–8.68	20	***	8.514 ± 0.066	8.13–8.80	9	**	9.262 ± 0.074	8.55–9.85	25
AW	4.024 ± 0.033	3.73–4.27	20	ns	4.091 ± 0.034	3.99–4.27	9	***	4.522 ± 0.031	4.18–4.87	25
OCB	5.028 ± 0.063	4.74–5.77	20	*	5.229 ± 0.047	5.10–5.48	8	***	5.686 ± 0.037	5.37–6.16	25
BOL	2.833 ± 0.040	2.42–3.29	20	ns	2.910 ± 0.033	2.78–3.010	8	***	3.330 ± 0.041	2.93–3.61	25
MPFL	2.641 ± 0.038	2.29–3.00	20	ns	2.509 ± 0.052	2.31–2.79	8	***	3.278 ± 0.038	2.93–3.59	25
MPFW	1.715 ± 0.025	1.47–1.95	20	*	1.575 ± 0.029	1.45–1.70	8	ns	1.681 ± 0.032	1.45–2.09	25
ZPL	1.842 ± 0.020	1.68–2.03	20	ns	1.886 ± 0.038	1.67–2.01	9	***	2.162 ± 0.031	1.90–2.58	25
CD	7.415 ± 0.034	7.09–7.74	20	ns	7.774 ± 0.067	7.49–8.11	9	***	8.189 ± 0.047	7.68–8.58	25
PC-1	−1.124 ± 0.080	−1.677–0.473	20	***	0.246 ± 0.093	−0.720–0.060	8	***	0.809 ± 0.094	−0.334–1.583	25
PC-2	0.860 ± 0.182	−1.195–1.990	20	***	−0.455 ± 0.310	−1.856–0.773	8	ns	0.208 ± 0.178	−1.260–1.707	25
PC-3	−0.008 ± 0.147	−1.541–1.424	20	ns	−0.514 ± 0.227	−1.838–0.171	8	ns	−0.035 ± 0.214	−1.535–2.540	25

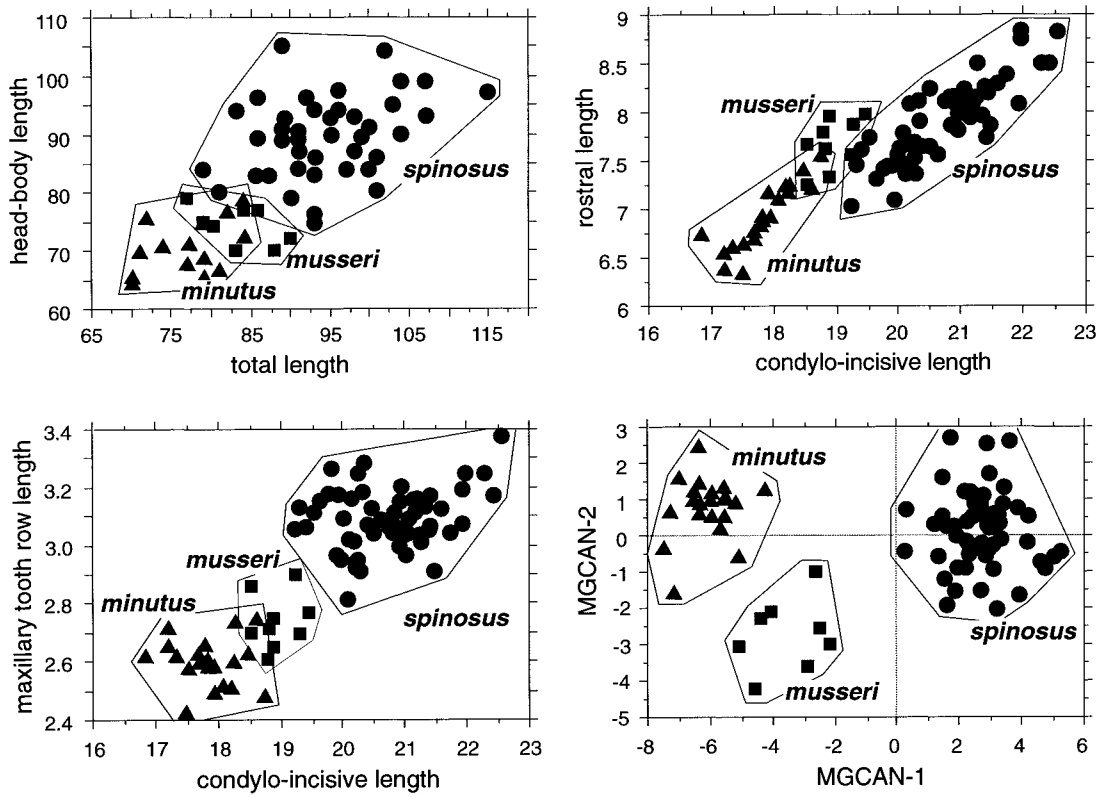

Fig. 73. Morphometric relationships among samples of *Neacomys* from Perú and western Brazil. **Upper Left**: bivariate relationship of head-body length versus total length. **Upper Right**: rostral length and condyloincisive length. **Lower Left**: maxillary toothrow length and condyloincisive length. **Lower Right**: first and second axes from a discriminant function analysis based on $\log_{10}$ cranial variables.

and delicate skull (figs. 70, 71, 76), short maxillary toothrow (< 2.75 mm), primitive carotid arterial system (pattern 1 of Voss, 1988; Carleton and Musser, 1989) with a squamoso-alisphenoid groove and sphenofrontal foramen, incisive foramen teardrop in shape (fig. 74), a weakly developed anteromedian flexus (-id) of both upper and lower first molars (fig. 72), and karyotype of 2n = 35–36, FN = 40 (fig. 75B-C).

REFERRED SPECIMENS: We obtained 31 additional specimens from seven localities within the Rio Juruá, including the type locality. These include Sacado (locality **5**)—MNFS 624 (adult female, skin with skull) and 642 (adult male, fluid); Penedo (locality **7**)—JLP 15356 (adult male, skull with body in fluid), JLP 15365 (adult male, skin with skull), MNFS 376 (adult male, skull with body in fluid), MNFS 409 (adult female, skin with skull), MNFS 410 (adult female, fluid), MNFS 493 (subadult male, complete skeleton), MNFS 494 (adult male, complete skeleton); Nova Empresa (locality **8**)—JUR 3 (adult female, skull only), JUR 48 (adult male, skull with body in fluid); Altamira (locality **9**)—JLP 16046 (adult male, fluid), JLP 16059 (adult female, fluid), JLP 16060 (adult female, skin and skull), JLP 16061 (adult male, skin with skull), JLP 16062 (subadult male, fluid), JLP 16063 (adult male, fluid), JLP 16064 (adult female, fluid), JLP 16065 (adult female, fluid), JLP 16078 (adult male, skin with skull), JLP 16079 (adult female, skin with skull); Barro Vermelho (locality **12**)—JLP 15846 (adult female, skin with skull), JLP 15847 (adult male, skin with skull); Vira-Volta (locality **14**)–JUR 487 (adult female, skin with skull), MNFS 1718 (adult male, skull with body in fluid), MNFS

TABLE 25
Standardized Discriminant Coefficients for Cranial Variables in Comparisons Among Three Species of *Neacomys* and Between the Two Cytochrome-b Clades of *N. minutus*

	3-species comparisons		*N. minutus* clades:
Variable	DF-1	DF-2	DF-1
Log CIL	0.52352	−0.50360	10.21152
Log ZB	−1.39365	−0.21488	−2.65715
Log MB	1.39136	−1.18183	−1.03434
Log IOC	0.52643	0.05332	−4.06877
Log RL	1.70547	−0.01005	−4.86278
Log NL	−0.11019	−0.69337	−2.66849
Log RW-1	0.40888	−0.13340	−5.38525
Log RW-2	−0.28743	0.07721	−0.83743
Log OL	0.00758	0.20532	
Log D	−1.48877	−0.38660	3.32103
Log MTRL	−1.11393	−0.14159	0.89284
Log IFL	−0.21653	−0.34726	3.08381
Log PL	0.32990	1.14130	
Log AW	−0.15649	−0.13125	4.63935
Log OCB	−0.56163	0.06027	2.19509
Log BOL	0.11197	0.66193	
Log MPFL	−0.46130	0.48894	
Log MPFW	0.07482	0.61801	−1.50614
Log ZPL	−0.51813	0.54955	0.25154
Log CD	0.23640	−0.39364	4.13025
Eigenvalue	44.108	3.2055	3.02953
% contribution	93.225	6.775	100.0

1734 (adult female, fluid), MNFS 1735 (adult female, skin with skull), MNFS 1742 (adult male, fluid), MNFS 1743 (adult female, skull with body in fluid), MNFS 1744 (adult male, skull with body in fluid), MNFS 1745 (adult male, fluid); and Ilhazinha (locality **16**)—MNFS 1787 (adult female, fluid).

MEASUREMENTS OF HOLOTYPE: TOL, 145; TAL, 74; HF, 20; E, 12; CIL, 17.49; ZB, 10.44; MB, 8.54; IOC, 4.11; RL, 6.36; NL, 7.27; RW-1, 3.93; RW-2, 3.12; OL, 6.67; D, 5.10; MTRL, 2.42; IFL, 2.90; PBL, 7.75; AW, 3.91; OCB, 4.92; BOL, 2.92; MPFL, 2.68; MPFW, 1.74; ZPL, 1.87; CD, 7.09.

ADDITIONAL MEASUREMENTS: See table 24.

DESCRIPTION AND COMPARISONS: This is the second small-bodied species in the Rio Juruá basin (skin, fig. 68; skull, figs. 70-71 ; table 24). Although these two are not sympatric (fig. 64), *N. minutus* is readily distinguished from *N. musseri* by a number of cranial characters and by karyotype, as well as by molecular sequences. It is smaller in virtually all external and cranial measurements, except with a slightly longer and much broader mesopterygoid fossa (table 24). It possesses the primitive carotid arterial system characteristic of other members of the genus, as opposed to the derived condition in *N. musseri*. The incisive foramen is distinctly teardrop in shape, rather than oval, with a narrower septum (fig. 74). The anteromedian flexus (-id) on both upper and lower first molars is weakly developed (fig. 72). And it has a 2n = 35–36, FN = 40 karyotype versus the 2n = 34, FN = 64–68 of *N. musseri*. *Neacomys minutus* does not differ appreciably, however, in cranial shape parameters, maintaining the same proportionality of length, width, and height as in *N. musseri*. This is evident in both bivariate plots of individual measurements as well as in the principal components analysis. Although the two species differ substantially in overall size (as evidenced by their respective scores on PC-1 axis; table 24), their significant difference on PC-2 is due solely to mesopterygoid fossa width, and they are statistically identical on all subsequent PC axes (table 24). *Neacomys minutus* is considerably smaller that *N. spinosus* in all external and cranial measurements, but shares with it the primitive carotid arterial pattern. The distinctly small hind feet, black instead of more brown ears, and darker dorsal pelage more finely streaked with black are characters useful for field separation of these two species, other than general body size.

DISTRIBUTION AND HABITAT: Known only from the central (Upper Central and Lower Central regions) and lower (Mouth Region) sections of the Rio Juruá, Estado do Amazonas, Brazil (fig. 62). Small-bodied taxa of generally similar morphology from adjacent areas in northern Perú and eastern Ecuador (clade 3, fig. 63), or on the opposite (northern) side of the Rio Solimões along the Rio Jaú in central Brazil (clade 6, fig. 63), belong to quite different mtDNA clades and are probably best considered to be separate species. We caught these mice in terra firme forest at localities **7**, **9**, **12**, **14**, and **16**, but in seasonally flooded várzea forest at localities **5** and **8**.

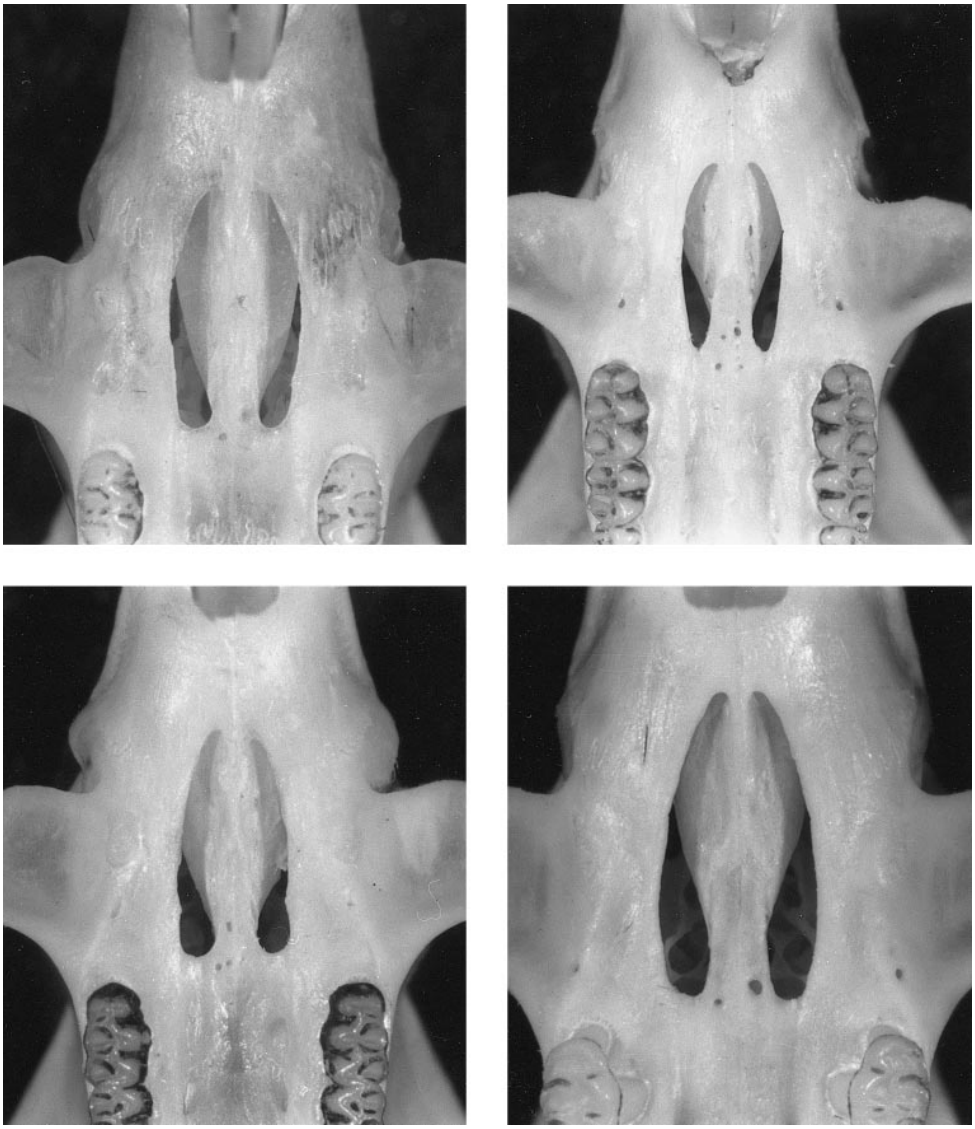

Fig. 74. Illustrations of the size and shape of the incisive foramina of four specimens of *Neacomys* from eastern Perú and Rio Juruá basin of western Brazil. **Upper Left**: *N. musseri* (holotype, MVZ 171486). **Upper Right**: *N. musseri* (MNFS 1395, locality **2**). **Lower Left**: *N. minutus* (JLP 16061, locality **9**). **Lower Right**: *N. spinosus* (MNFS 1236, locality **1**).

REPRODUCTION: We caught pregnant females in the months of August, September, October, November, May, and June. These span both the dry and wet seasons, and suggest that reproduction is yearround. Litter sizes were three in all cases. One female was both lactating and in the early stages of pregnancy, suggesting a postpartum estrus. Individuals of both sexes were in reproductive condition (pregnant females and males with scrotal testes and enlarged vesicular glands) while still partly in subadult pelage and with completely erupted but unworn molar teeth, suggesting that breeding commences at an early age.

ETYMOLOGY: Named for its distinctly small size and diminutive features.

KARYOTYPE: 2n = 35–36, FN = 40 (fig.

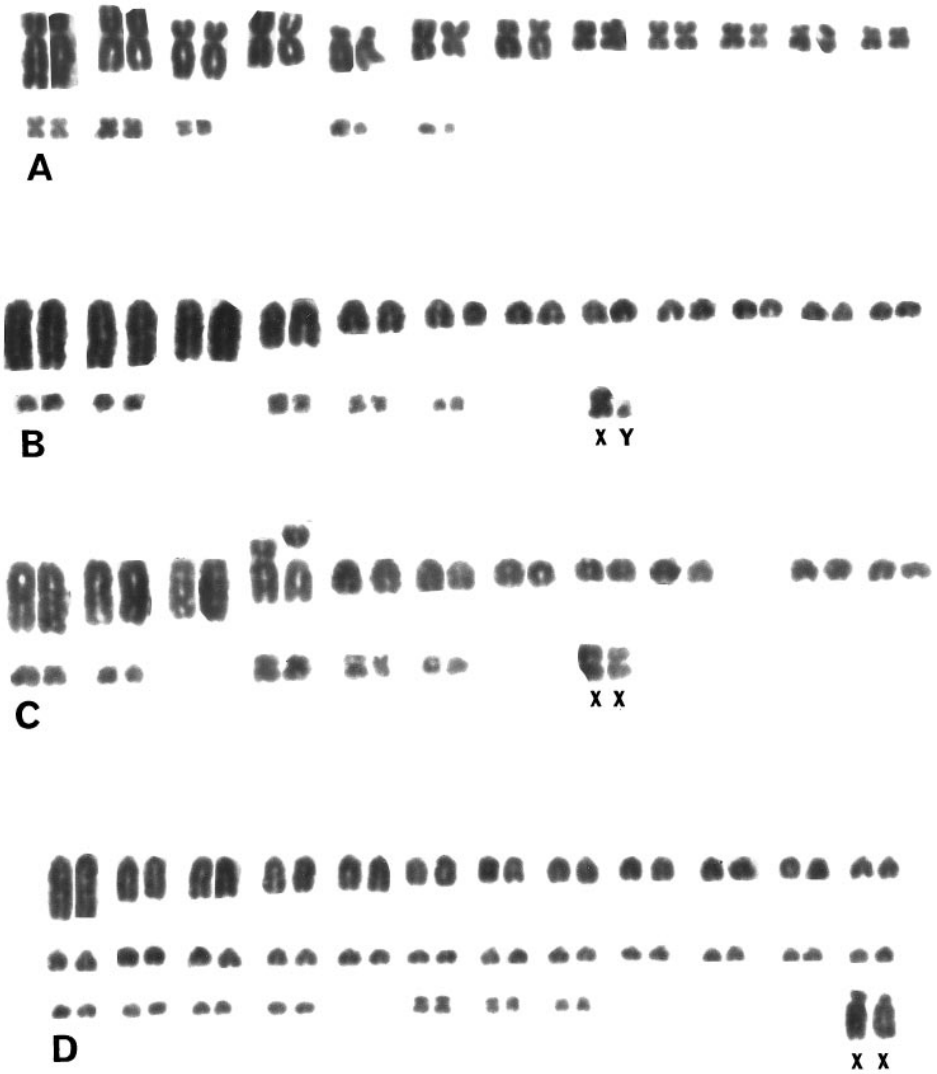

Fig. 75. Karyotypes of three species of *Neacomys* from the Rio Juruá, western Brazil. **A**, *N. musseri* (MNFS 1395, locality **2**), 2n=34. **B**, *N. minutus* (JLP 15847, locality **12**), 2n=36. **C**, *N. minutus* (MNFS 624, locality **5**), 2n=35. **D**, *N. spinosus* (MNFS 1481, locality **4**).

74B-C). The autosomes consists of 14 pairs of acrocentric elements, three distinctly large, one medium-sized, and the remainder grading in size from small to very small. The medium-sized element is apparently involved in a Robertsonian polymorphism, with heterozygous individuals found at both Sacado (locality **5**) and Altamira (locality **9**); all others (from Penedo [locality **7**], Barro Vermelho [locality **12**], and Vira-Volta [locality **14**]) were homozygous for the acrocentric condition. There are also three pairs of very small biarmed autosomal elements. The X-chromosome is a medium-small metacentric chromosome; the Y-chromosome is small and acrocentric.

COMMENTS: This species is morphologically similar to small-bodied *Neacomys* that we have examined from northern Perú and Ecuador (clade 6, fig. 63), although the two differ greatly in molecular sequence. The average Kimura two-parameter distance be-

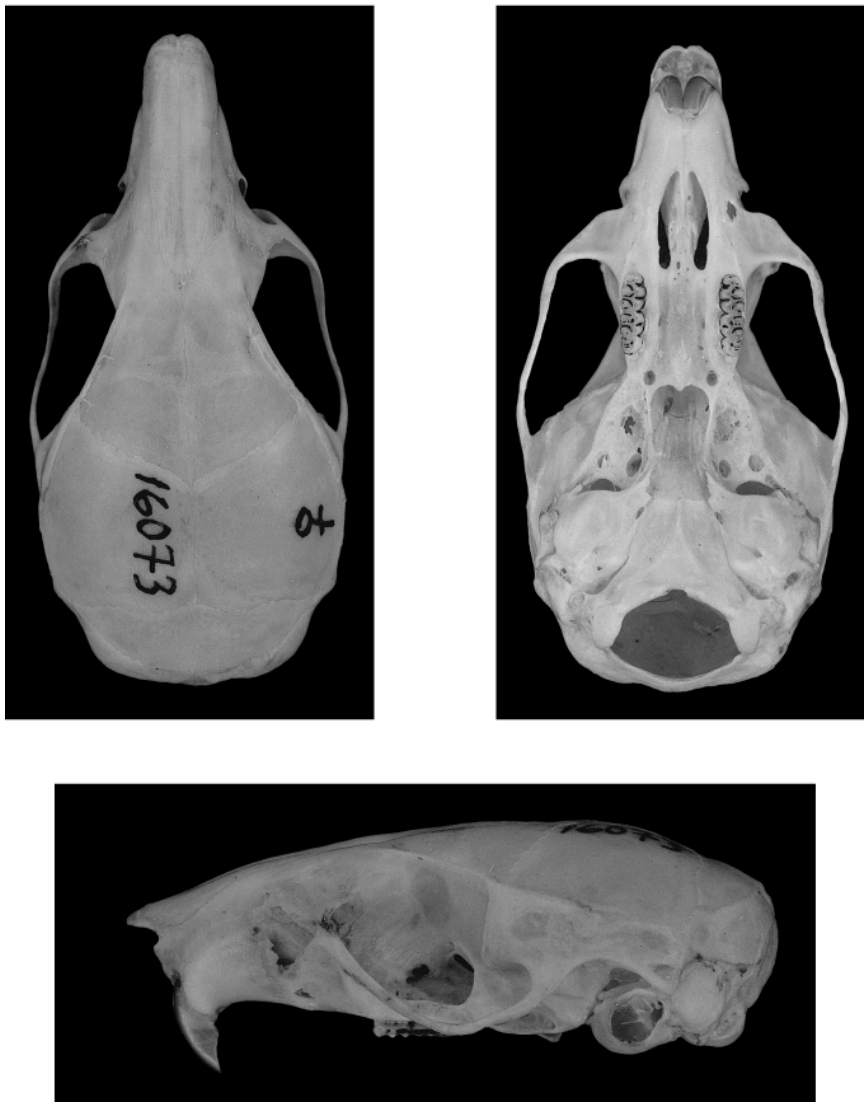

Fig. 76. Dorsal, ventral, and lateral views of the cranium of the holotype (INPA 2689) of *Neacomys minutus*, an adult. The skin and maxillary toothrows are illustrated in figures 68 and 71, respectively. Magnification = ×4.

tween these samples is 13.05% (table 23). Although it might be argued that this difference is due in part to the geographic distance between the samples, *N. spinosus* exhibits only 2% divergence among samples taken across the same large geographic region. Moreover, phylogenetic analyses provide no support for a sister-group relationship between the Rio Juruá and northwestern Amazonian forms, relative to any other identifiable clade (fig. 63).

This taxon also exhibits considerable geographic differentiation in cytochrome-b sequences within the Rio Juruá basin (fig. 64). Specimens from the Upper Central localities of Seringal Condor (**6**) and Penedo (**7**) differ, on average, from those from the Lower Central and Mouth regions (Altamira [**9**], Barro Vermelho [**12**], Vira-Volta [**14**], and Ilhazinha [**16**]) by 6.9% (table 23), with great similarity of haplotypes within each of these two geographic clusters (0.41%, or less). Com-

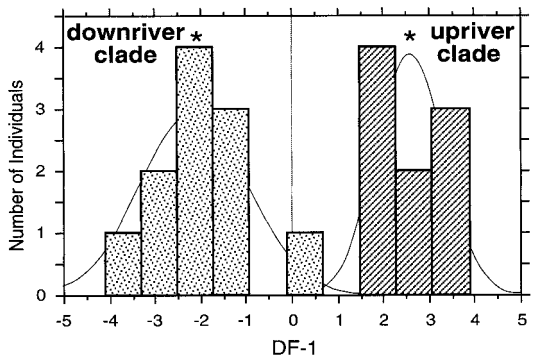

Fig. 77. Frequency distribution of discriminant scores for individuals of the upriver and downriver cytochrome-b clades of *Neacomys minutus*.

parisons between the limited samples of the two clades (9 adults for the upriver clade, 11 for the downriver clade) in morphometric characters revealed no significant differences for any single variable. Nevertheless, specimens belonging to the two clades are separable based on multivariate discriminant analysis, with the mean scores on the single discriminant axis significantly different ($F_{1,18} = 109.772$, $p < 0.001$). Table 25 lists the standardized discriminant coefficients for the 16 variables included in the analysis, and figure 76 provides a histogram of the scores for individuals of both clades on the single discriminant axis extracted. This analysis correctly classifies all 20 individuals to their respective cytochrome-b clades, despite what appears to be rather minimal separation on the single axis obtained in the analysis (fig. 77). For the moment, we assign no special taxonomic significance to this difference, although such may be supported by additional samples. Rather, we only highlight this difference, both to illustrate the parallel pattern of differentiation in molecular as well as morphological characters and to further emphasize the number of strongly defined and differentiated haplotype clades of small-bodied *Neacomys* that apparently replace one another across Amazonia.

Neacomys spinosus (Thomas, 1882)

TYPE LOCALITY: ''Huambo, 3700′,'' to the east of Chachapoyas and Chirimoto, on the banks of the Río Huambo, a tributary of the Huallaga (Thomas, 1882: 99), Departamento de Amazonas, Perú.

DESCRIPTION: This is the largest species in the genus, averaging over 180 mm in total length and 20.7 mm in condyloincisive length of the skull (table 24, figs. 69 and 70). From eastern Ecuador to southern Perú and east into western Brazil, *N. spinosus* is relatively uniform in body dimensions, but exhibits variation in the darkness of the dorsal pelage, ranging from a paler yellow-reddish brown mixed with black to a darker reddish-brown. An appreciation of this type of variation must await a more detailed and thorough analysis. Within our sample from the Rio Juruá, the skull is long with a relatively narrow braincase, but it differs only in general size, rather than in proportions, from other species in the genus (fig. 73, and above). The carotid circulation pattern is of the primitive type, retaining the well-developed squamosal-alisphenoid groove and sphenofrontal foramen indicative of the presence of the supraorbital branch of the stapedial artery (pattern 1; Voss, 1988; Carleton and Musser, 1989). The maxillary toothrow is longer than that of other species, averaging over 3 mm in length. The molar occlusal morphology is similar to that of other species (fig. 72), except that the procingulum of both upper and lower first molars is either entire, or only weakly divided into anterolabial and anterolingual conules by the anteromedian flexus (-id).

SELECTED MEASUREMENTS: See table 24.

DISTRIBUTION AND HABITAT: Specimens that can be clearly allocated to this species are known from southeastern Colombia south through eastern Ecuador and Perú into northern Bolivia, and east as far as the central Rio Juruá basin in Estado do Amazonas, Brazil (figs. 62 and 63; table 22). Along the Rio Juruá, we obtained specimens only in the Headwaters (localities **1**, **2**, and **4**) and Upper Central regions (localities **6** and **7**). In the former, both nonflooded terra firme and periodically flooded ''várzea'' forests were occupied, but the species is apparently limited to terra firme further downriver.

KARYOTYPE: 2n = 64, FN = 68 (fig. 75D). We have data from 13 individuals from four localities: Porongaba (locality **1**: MNFS 1236, 1262, 1263, 1322, 1404), opposite Po-

rongaba (locality **2**: MNFS 1339), Sobral (locality **4**: MNFS 1481, 1565), Condor (locality **6**: JLP 15674), and Penedo (locality **7**: JLP 15292, 15314, MNFS 348, 357). The autosomal complement is almost entirely acrocentric, with one distinctly large pair, four pairs of medium size, and 23 pairs that grade from small to very small. There are also three pairs of very small biarmed elements. The X-chromosome is a medium-large subtelocentric chromosome, and the Y-chromosome is a very small acrocentric element. This karyotype is identical to that described from specimens collected in Colombia and several localities throughout Perú (Gardner and Patton, 1976).

REPRODUCTION: Three of 12 females taken during August and September in the dry season were pregnant, with two or three embryos; others were either nulliparous young or postlactating without signs of current reproductive activity. Four of eight females taken in the months of February and March, during the rainy season, were pregnant (embryo count ranging from 2 to 4), two were postlactating, and two were young of the year.

COMMENTS: This species appears to be rather uniform in body size throughout its range in western Amazonia, and thus readily distinguishable by this feature alone from the various sympatric, small-bodied forms described above. The level of mtDNA sequence divergence across its sampled geographic range is also limited, with an average divergence of only 2.1% among specimens from eastern Ecuador, northern Perú, and the Rio Juruá basin. The maximum Kimura two-parameter distance between any two haplotypes is 3.7% (a specimen from Ecuador and one from the Rio Juruá). There is essentially no differentiation between localities within the Rio Juruá, with greater variation among haplotypes within some localities (e.g., Sobral, locality **4**) than among them (fig. 65). Names available that are probable synonyms of *N. spinosus* include *amoenus* Thomas (1903) and *carceleni* Hershkovitz (1940).

SPECIMENS EXAMINED (n = 33): (**1**) 5f — MNFS 1236, 1262–1263, 1322, 1404; (**2**) 1f — MNFS 1339; (**4**) 3f — MNFS 1438, 1481, 1565; (**6**) 1m — JLP 15674; (**7**) 10m, 13f — JLP 15292, 15314, 15341–15344, 15364, 15457, 15497, MNFS 348, 357–359, 374, 375, 377–379, 407, 424–425, 473, 523.

Nectomys Peters, 1861

Water rats

Chromosomal Diversity and Species Boundaries

Most accounts follow Hershkovitz (1944) and regard all Amazonian and Mata Atlântica populations of water rats to belong to a single species, *N. squamipes* (Brants, 1827) (e.g., Ernest, 1986). However, considerable chromosomal diversity is found throughout this broad area, and Musser and Carleton (1993:709) conclude that a ''fullscale generic revision is warranted.'' Individuals with diploid numbers of 38, 42, and 52 have been described from separate localities in western Amazonia alone (Gardner and Patton, 1976), although sympatry between any of these chromosomal morphs has not as yet been recorded. Barros et al. (1992) mapped the known range of each karyotype, and new data from several localities in Amazonian and coastal Brazil add substantial additional information (Bonvicino et al., 1996). Consequently, a more coherent picture of the geographical distribution of these morphs is beginning to emerge. By current information, four distinct diploid classes are known, each with a defined range within the total distribution of the genus *Nectomys* (fig. 78): (1) A 2n = 38 and 2n = 42 form is known from western Amazonia, with the former restricted to the middle reaches of the Río Apurimac in south-central Perú and the latter found more broadly, from eastern Ecuador (localities in both Sucumbíos and Zamora-Chinchipe provinces; A. L. Gardner, personal commun.), the Departamento de Amazonas in northern Perú (J. L. Patton, unpubl. data) and the Departamento de Ucayali in eastern Perú (Gardner and Patton, 1976), and as far east as the central Rio Juruá in western Brazil (data presented below). (2) A 2n = 52–54 karyotype is found elsewhere throughout greater Amazonia, from the central Río Ucayali basin of Perú (Gardner and Patton, 1976), north to western and southern Venezuela (Barros et al., 1992), then east to the states of Pará, Maranhão, Piauí, and Pernam-

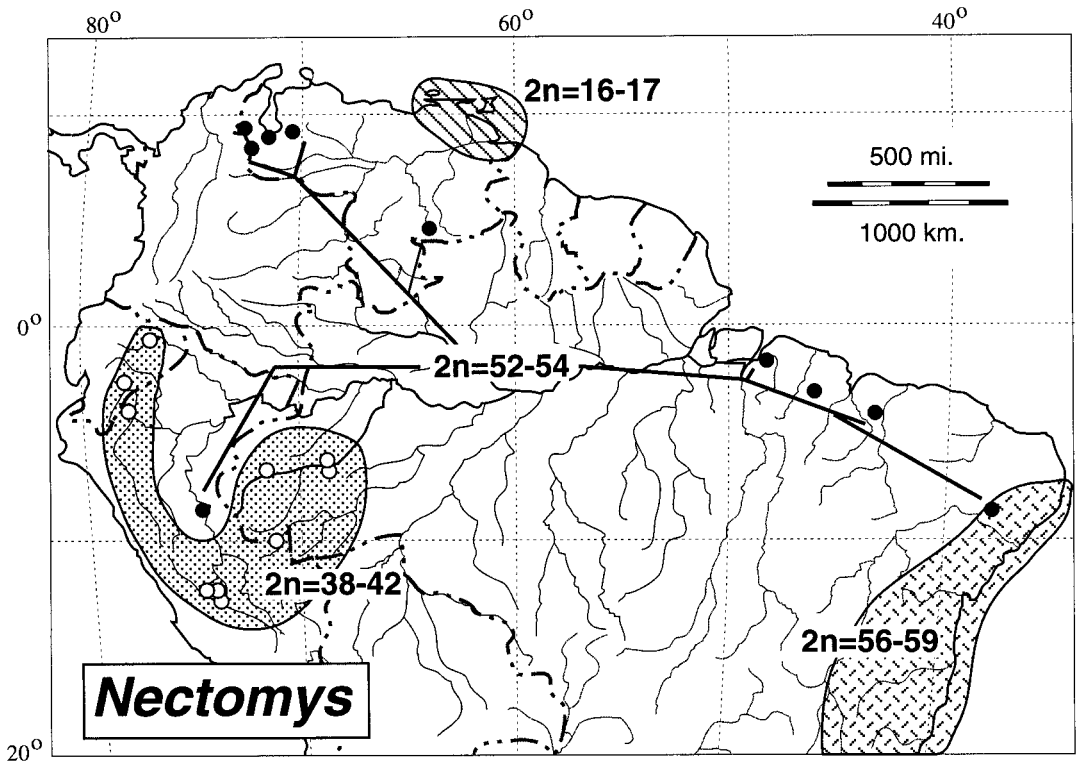

Fig. 78. Map of known localities for chromosomal morphs of water rats, genus *Nectomys*. See text for justification for the allocation of names to each of the four diploid number groups. Symbols denote localities for which karyotypic data are available. Data from Gardner and Patton (1976), Maia et al. (1984), Barros et al. (1991), Bonvicino et al. (1996), and this report.

buco and south to Mato Grosso do Sul in Amazonian, north-coastal, and south-western Brazil (Maia et al., 1984; Bonvicino et al., 1996). (3) A 2n = 56–59 karyotypic form occurs along the Atlantic seaboard of South America, from Provincia de Missiones in Argentina and from the states of Rio Grande do Sul north through São Paulo, Minas Gerais, Rio de Janeiro, Bahia, and Pernambuco in coastal Brazil (Maia et al., 1984; Barros et al., 1992; Bonvicino et al., 1996). Finally, (4) a 2n = 16–17 chromosomal form occurs in northern coastal Venezuela, the mouth of the Río Orinoco, and on Trinidad (Barros et al., 1992).

Numerical variation within each chromosomal class is either due to simple Robertsonian fusion/fission events (e.g., between 2n = 38 and 42, both with a fundamental number of 40) or to supernumerary chromosomes, and hence probably has no special systematic significance. On the other hand, the differences between chromosomal groups are either assumed to represent significant reproductive barriers or have been determined to be such. For example, Barros et al. (1992) argue that the number of structural differences between the 2n = 16–17 and 2n = 52–54 forms in Venezuela is so great as to preclude the possibility of fertile hybrids. Consequently, they raise the former to species status, as *N. palmipes* Allan and Chapman, which has its type locality on the island of Trinidad. Importantly, Bonvicino et al. (1996) document meiotic breakdown in laboratory-produced hybrids between the 2n = 56–59 and 2n = 52–54 forms, thus confirming the suggestions of Maia et al. (1984), based on chromosomal banding patterns, that these two are reproductively isolated. The type locality of *squamipes* has been restricted to São Sebastião, an island off the coast in the Estado do

São Paulo, Brazil (Hershkovtiz, 1944). As such, it remains to be determined if this name applies to the 2n = 56–59 karyomorphic form the mainland of coastal Brazil, or is a unique insular species. Whatever the case, however, the name *squamipes* cannot apply to either of the two karyotypic forms within Amazonia; which names do apply cannot be answered unambiguously at the present time.

Species of Amazonian *Nectomys*

Hershkovitz (1944) provided the most recent revision of the genus *Nectomys*, recognizing a single species, *N. squamipes*, with 15 subspecies, five of which he described in that paper. Simply based on geography, the names *aquaticus* Lund, 1841 (type locality near Lagoa Santa, Minas Gerais), and *olivaceus* Hershkovitz, 1944 (type locality near Teresópolis, Rio de Janeiro), would apply to *squamipes*, either as synonyms or as recognizable subspecies. Barros et al. (1992) argue that *garleppii* Thomas, 1899 (with its type locality in the Ocobamba Valley in the Departamento de Cusco, Perú) is the earliest name for the 2n = 38–42 form. However, the geographic extension of this karyomorph to northern Perú and eastern Ecuador (based on the unpublished data of J. L. Patton and A. L. Gardner cited above), suggests that *apicalis* Peters, 1861, with its type locality from Tena, in the Andean foothills of the Provincia de Napo-Pastaza, Ecuador, is the earliest available name. If the assignment of these two names to the 2n = 38–42 form is correct, then the earliest available name for the 2n = 52–54 form would be *mattensis* Thomas, 1903, as its type locality in the Serra da Chapada in Estado do Mato Grosso, Brazil, lies within the range of that form as identified by the available samples (see fig. 78).

The degree to which any of these assignments, with the probable exception of *squamipes* itself, can be made with confidence remains uncertain. Clearly, it would be advantageous to have karyotypic data from topotypic specimens and, at the very least, careful comparisons should be made between the vouchers of karyotyped specimens and the respective holotypes. Until this is done, however, there are tantalizing data provided by Hershkovitz in his 1944 revision regarding the grouping and assignment of available names to the two Amazonian karyotypic morphs. He emphasizes the shape (width/length) of the interparietal in comparisons, and there is reasonable separation of those Amazonian samples he allocated to subspecies into two classes (table 26). In general, lowland taxa, such as *mattensis*, *amazonicus*, and *mallenius* have a shallow but wide interparietal, with a width/length ratio approximately 0.30, while western, Andean-foothill forms (*apicalis* and *garleppii*) have deeper interparietals, with ratios ranging between 0.43 and 0.46. The ratio is significantly different ($F_{7,66} = 26.596$, $p < 0.001$) in all pairwise comparisons between these samples, but none is significant when comparisons are restricted to those within each group of taxa. Importantly, samples of known 2n = 38 and 42 chromosome individuals from eastern Ecuador and Amazonas and Ucayali departments, Perú, as well as those from the Rio Juruá, all have the deep and relatively narrow interparietal of *apicalis* and *garleppii* (table 26 and fig. 79), supporting the allocations of these names to that taxon. As a working hypothesis, therefore, we treat individuals from western Amazonia with a diploid number ranging from 38–42 as belonging to the species *N. apicalis*.

TABLE 26
Ratio of Interparietal Length to Width for Samples of Water Rats (*Nectomys*) from Amazonia
Values are given as mean ± standard error, with range and sample size.

Taxon/Locality	Mean ± SE	Range	n
apicalis[a]	0.467 ± 0.010	0.386–0.556	19
garleppii[a]	0.434 ± 0.012	0.366–0.500	11
Río Cenepa, Amazonas	0.505 ± 0.009	0.455–0.550	11
Balta, Ucayali	0.495 ± 0.017	0.464–0.522	3
Rio Juruá	0.484 ± 0.022	0.414–0.579	8
melanius[a,b]	0.347 ± 0.014	0.259–0.386	8
mattensis[a,c]	0.296	—	1
amazonicus[a]	0.305 ± 0.016	0.183–0.381	13

[a] Data for the subspecies listed are from Hershkovitz (1944); those for geographic areas are based on 2n = 42 karyotyped individuals in the collections of the Museum of Vertebrate Zoology as well as those from the Rio Juruá.

[b] Includes only those samples from northeastern Perú.

[c] Holotype.

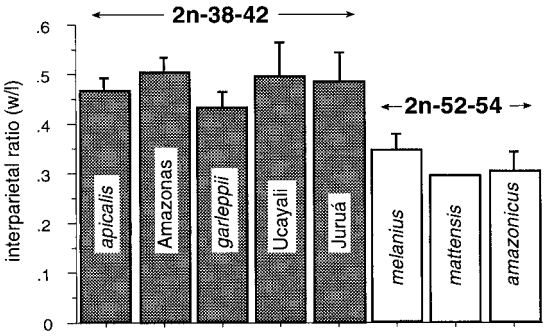

Fig. 79. Histograms of means, with standard errors, of the length to width ratio of the interparietal for samples allocated by Hershkovitz (1944) to five named forms of water rats, *Nectomys*, from Amazonia, as well as from three 2n = 38–42 geographic samples (Río Cenepa, Amazonas, Perú; Balta, Río Curanja, Ucayali, Perú; and Rio Juruá, Amazonas, Brazil). The presumptive association of each named form to diploid number class is indicated.

Nectomys apicalis Peters, 1861

TYPE LOCALITY: ''southwestern Ecuador, Guayaquil''; restricted by Hershkovitz (1944: 53) to Tena, Provincia de Napo, Ecuador, altitude 512 m.

DESCRIPTION: This is a large-bodied rat with soft, moderately long, and glossy dark brown upperparts finely mixed with yellow and black, with a tendency for a darker middorsal region, paling down the sides, without demarcation, to a gray venter washed with buff. The tail is longer than the head and body, robust, furred at the base but otherwise appears naked along its length. However, three short, stout hairs are associated with each scale. These hairs become slightly longer towards the tip, which ends with a very slight pencil. The hindfeet are wedge-shaped with a narrow heel and a broad palm at the base of the toes; the toes are partly webbed, and the sides possess a fringe of silver hairs. The sole of the foot is uniquely covered by roundish appearing scales. Females have four pairs of mammae.

The skull is large and robust, with a relatively short and broad rostrum, diverging zygomatic arches, an elongated cranium, and a broad interorbital region with strongly developed supraorbital ridges diverging posteriorly and extending on the temporal region as distinct ridges (fig. 80). The zygomatic notches are deep and the zygomatic plate has a prominent anterior extension, when viewed from above. The interparietal is shallow and broad, with an average length/width ratio of 0.484 (range 0.414–0.579) for those specimens from the Rio Juruá (table 26). There is no alisphenoid strut separating the buccinator-masticatory foramen from the foramen ovale acessorius. The stapedial foramen is tiny to absent, and there is no squamosal-alisphenoid groove, or sphenofrontal foramen (cephalic arterial pattern 3; Voss, 1988; Carleton and Musser, 1989). The bullae are small and uninflated, the mesopterygoid fossa is broad and without sphenopalatine vacuities in its roof, the parapterygoid fossae are long and narrow but relatively deeply excavated. The diastema is long, with a short and somewhat teardrop-shaped incisive foramen that ends well in front of the first molar; the palate is deeply grooved and ends with large, deep, and complex posterior pits. The teeth are pentalophodont with well-developed cusps and somewhat more high-crowned than relatives, such as *Oryzomys*. The third molar is particularly large and complex.

SELECTED MEASUREMENTS: Means and ranges for selected external and cranial measurements of adult individuals of both sexes are summarized in table 27.

DISTRIBUTION AND HABITAT: Within the Rio Juruá, specimens were taken only in the central portion of the river, at localities within the Upper and Lower Central Regions and at one minor locality between these regions (locality i). Given that the range of the genus comprises all of Amazonia (see Emmons and Feer, 1997), one can expect to find this species throughout the Juruá drainage. Specimens were obtained mostly along streams in undisturbed or second-growth forest, or in garden plots adjacent to such forest. At Altamira (locality **9**), we caught *Nectomys* in second-growth edge along a small stream while *Holochilus* was taken in the dense grasses that bordered the river. At Penedo (locality **7**), we found both genera in a relatively small patch of inundated dense grass inland from the river's edge (fig. 7).

REPRODUCTION: All specimens from the Rio Juruá were taken during the dry season

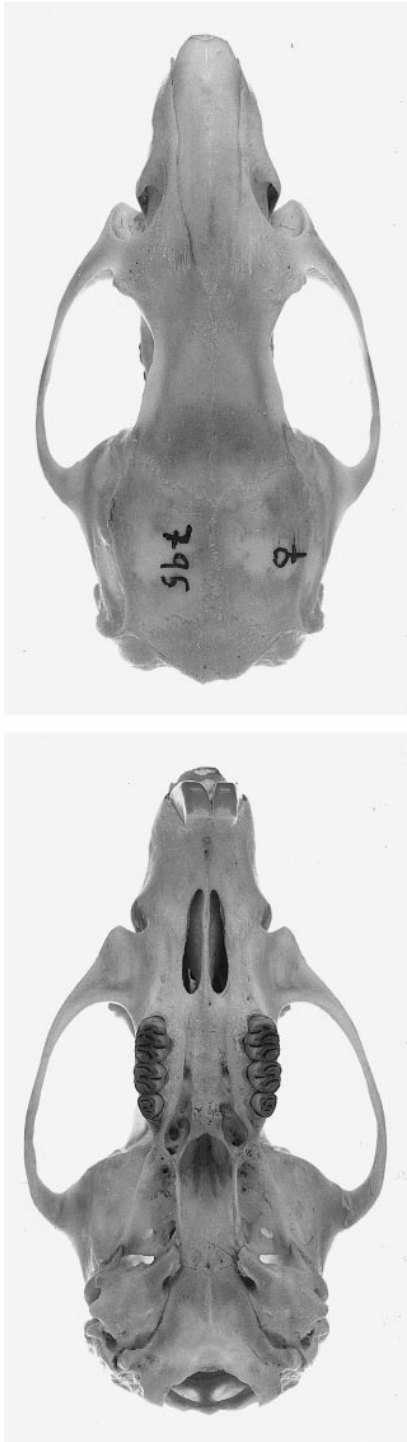

Fig. 80. Dorsal (top) and ventral (bottom) views of the cranium of *Nectomys apicalis* (MNFS 795, Barro Vermelho [locality **12**], left bank Rio Juruá, Amazonas, Brazil). Magnification = ×2.

TABLE 27
Selected External and Cranial Dimensions of *Nectomys apicalis* from the Rio Juruá Basin
Measurements (mm) are given as mean, with range and sample size.

Variable	Mean	Range	n
TOL	407.0	348–460	5
TAL	206.3	183–235	5
HF	50.0	46–55	5
E	21.8	21–23	5
CIL	41.04	36.63–43.48	5
ZB	23.22	21.55–24.03	5
MB	16.12	15.09–16.72	5
IOC	7.30	6.71–7.63	5
RL	16.68	15.04–17.77	5
NL	18.06	15.41–19.71	5
RW-1	9.26	8.25–9.82	5
RW-2	7.41	6.91–7.73	5
OL	14.57	13.55–15.57	5
D	12.04	10.19–12.98	5
MTRL	7.12	7.01–7.35	5
IFL	6.96	6.01–7.49	5
PL	19.92	18.00–21.03	5
AW	9.16	8.40–9.47	5
MPFL	7.01	6.30–7.71	5
MPFW	3.09	2.75–3.42	5
OCB	9.29	8.67–9.55	5
BOL	6.12	5.28–7.00	5
ZPL	4.93	4.76–5.47	5
CD	15.91	14.14–17.10	5

in the months of August through November. At this time, adult males were scrotal with enlarged testes and vesicular glands, adult females were either pregnant (one individual, with 3 embryos) or lactating (one individual, with 3 placental scars), or juveniles with unerupted or unworn third molars (four individuals).

KARYOTYPE: 2n = 42, FN = 40. We karyotyped four specimens, one from Condor (locality **6**; JLP 15565), one from Jainu (locality **11**; MNFS 793) and two from Barro Vermelho (locality **12**; JLP 15891 and MNFS 795). All had completely acrocentric autosomal complements with acrocentric sex-chromosomes. This is the same karyotype as recorded by Gardner and Patton (1976) from Balta, on the Río Curanja, Departamento de Ucayali, in eastern Perú. Bonvicino et al. (1996) examined one of our specimens (JLP 15565, Condor) and listed its

diploid number as 52; this specimen is clearly 2n = 42, however.

COMMENTS: *Nectomys* is superficially similar to *Holochilus*, in size, in general color and color pattern, and in wedge-shaped and slightly webbed hind feet. Fieldworkers conducting mark-and-release studies need to be cognizant that both taxa can be trapped together, and that their superficial resemblance can lead to misidentification. However, *Nectomys* can be readily distinguished in the hand by its shorter, less sleek and darker dorsal fur, and grayer venter; the proportionately longer and more readily apparent scaled tail; and especially the granular scales on the soles of the hind feet.

SPECIMENS EXAMINED (n = 11): (**6**) 1m — JLP 15565; (**f**) 1 unknown — MNFS 525; (**7**) 2f — JLP 15505, 15514; (i) 1m — DMN 3; (**9**) 1m, 1f — JLP 15966, MNFS 892; (**10**) 1f — MNFS 867; (**11**) 1m — MNFS 793; (**12**) 2f — JLP 15891, MNFS 795.

Oecomys Thomas, 1906

Arboreal rice rats

Members of this genus are small to medium-sized mice, scansorial in their habits and usually arboreal, commonly trapped in dense vine tangles within a few meters of the ground, and often in relatively disturbed forest. Considered a subgenus of *Oryzomys* in most early literature, *Oecomys* was revised by Hershkovitz (1960), who consolidated some 25 scientific names into only two species, the larger *O. concolor* and the smaller *O. bicolor*. The inadequacy of this arrangement has been recognized by many fieldworkers, who often can identify three or more distinct forms at a single locality (e.g., Patton et al., 1982; Woodman et al., 1991). The genus is under review by G. G. Musser, M. D. Carleton, and J. L. Patton. In their 1993 compilation of sigmodontine rodents, Musser and Carleton provisionally recognize 13 species, some of which they suggested were composites. Ten of these 13 have ranges that include greater Amazonia.

Oecomys shares a number of generalized characters with other oryzomyine rodents of Amazonia, but is readily separated from all other co-occurring genera. They lack the spinose fur of either *Neacomys* or *Scolomys*, and the webbed feet and large size of either *Holochilus* and *Nectomys*. Member species span the body size range represented by *Oligoryzomys* and *Oryzomys*, but can be distinguished easily from either by their short and broad feet with proportionately long toes, and from *Oryzomys* by a long tail that often terminates in a slight pencil. In foot and tail characteristics, *Oecomys* is closest to the climbing rats, *Rhipidomys*, and may be difficult to distinguish in the hand from small species of that genus. However, these two genera typically differ in the coloration of the dorsal surface of the hind feet, in the length of the tail pencil, and in number of mammae, as well as in those cranial characters that define the Tribe Oryzomyini relative to the ''Thomasomyini'' (see Voss, 1993; Voss and Carleton, 1993).

General external and cranial characters of *Oecomys* include: four pair of mammae in females; tail longer than head and body (averaging 112% to 135% for those species within the Rio Juruá); tail clothed in sparse, short hairs and usually terminating in a short pencil of hairs, 3–4 mm in length or less; short and broad hind feet with proportionately long toes; dorsal surface of hind foot without extensive dark patch as in *Rhipidomys*, but which still can be slightly darker relative to sides, particularly over metatarsals. General dorsal coloration ranges from orangish to reddish brown in all species in the Rio Juruá; ventral color ranges from pure white to gray-based fur tinged with either white or buff. The skull has a short and relatively broad rostrum; the zygomatic plate is relatively narrow, its anterior border straight and lacking a anterodorsal spine resulting in a shallow zygomatic notch when viewed from above; the upper incisors are slightly opisthodont; the interorbital region is broad with well-developed supraorbital ledges diverging strongly posteriorly and extending onto braincase as parietal ridges; the braincase relatively broad and short, distinctly more rounded in comparison to *Oryzomys*; all species within the Rio Juruá region have the primitive cephalic arterial pattern, with an enlarged stapedial foramen, squamosal-alisphenoid groove, and sphenofrontal foramen present; an alisphenoid strut is varyingly present in most species; hamular process of

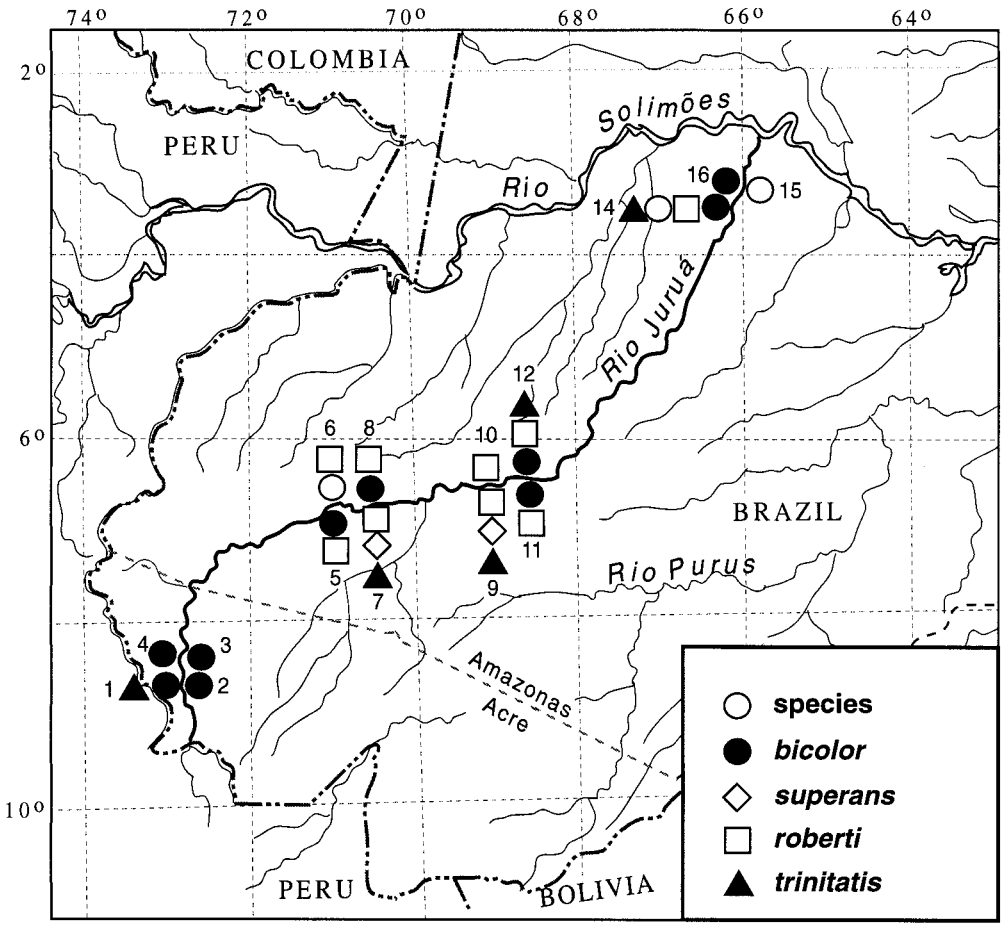

Fig. 81. Map of the occurrence of five species of arboreal rice rats, *Oecomys*, at each of the 16 principal localities sampled along the Rio Juruá.

squamosal short and broad, often with subsquamosal foramen totally occluded, or nearly so; the mesopterygoid fossa is rather broad with the anterior border either smoothly arched or squared; sphenopalatine vacuities are small to totally occluded so that the roof of the mesopterygoid fossa is solid; the parapterygoid fossae are typically rather deeply etched; and the cranium is vaulted in lateral view, not flat.

Oecomys of the Rio Juruá

Five species of *Oecomys* are clearly recognizable from the Rio Juruá and the names we employ were provided by G. G. Musser, who examined all of our specimens. Two or more species were found at 9 of the 16 major localities (fig. 81), with the small-bodied *O. bicolor* and the larger *O. roberti* most commonly together. However, three species were recorded at some sites (*O. bicolor*, *O. roberti*, and *O. trinitatis* at Barro Vermelho [locality **12**] and *O. roberti*, *O. superans*, and *O. trinitatis* at Penedo [locality **7**] and Altamira [locality **9**]), and four species were taken at Vira-Volta, locality **14** (*O. bicolor*, *O.* species, *O. roberti*, and *O. trinitatis*). As detailed below, each of these has a distinct morphology that makes them relatively easy to distinguish in the field, and each is well differentiated in molecular characters.

Three points are of significance in the bootstrap consensus maximum parsimony tree for haplotypes of cytochrome-b (based

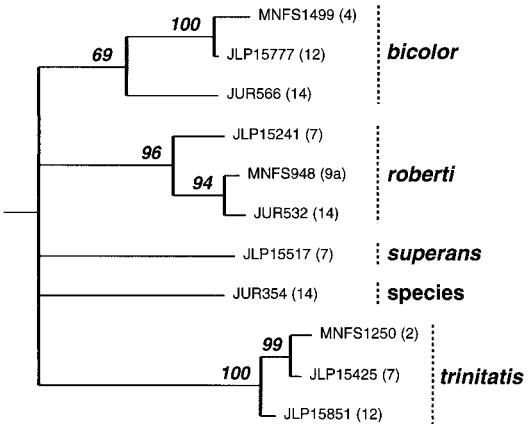

Fig. 82. Bootstrap consensus tree illustrating differentiation in an 801 bp fragment of the mtDNA cytochrome-b gene among species of *Oecomys* from the Rio Juruá. Bold numbers at internal nodes are bootstrap values, based on 1000 iterations; percentages are Kimura two-parameter distances. Field catalog numbers of specimens included in the analysis are indicated, as is the locality by number (see fig. 1). Branch lengths are drawn proportional to the number of character changes. The tree is rooted by sequence comparisons to species of *Oryzomys*. Tree length = 396 steps; CI = 0.642; RI = 0.593.

on 801 base pairs) for representatives of each of the five morphological species from the Rio Juruá illustrated in figure 82. First, the five species are nearly equidistant from one another, with interspecific comparisons ranging between 7.2% and 9.8% (Kimura two-parameter distances, table 28). Interestingly, these values are substantially less (50% or more) than those of other polytypic genera from the Rio Juruá (e.g., *Neacomys* and *Oryzomys*). If the rate of molecular evolution within each of these genera has been more or less equivalent, then diversification within *Oecomys* has been considerably more recent than in the other two. Second, as well differentiated as these species are, however, there are no clear patterns of phyletic relationships among them. All bootstrap values for hierarchical relationships among them are always less than 50%. Hence, the consensus bootstrap tree (fig. 82) has a basal polytomy with hierarchical relationships only between haplotypes of single species. A more expanded analysis, including more taxa and many more localities, will be presented as part of the forthcoming revisionary effort by Musser et al. Finally, there is substantial among-population differentiation for two species, *O. bicolor* and *O. roberti*, with average divergences of 5.43 to 4.1%, respectively, for reciprocally monophyletic geographic clades within each (table 28). These will be discussed at greater length in the individual accounts that follow.

There are two distinctly small-bodied species (*O. bicolor* and *O.* species) and three larger ones (*O. roberti*, *O. trinitatis*, and *O. superans*) (table 29). *Oecomys* species is significantly smaller in nearly all measurements than *O. bicolor* ($p < 0.01$ or 0.001 for 20 of 24 measurements; 2-tailed t-tests), and *O. bicolor* is, in turn, significantly smaller than the other three for all 24 variables ($p < 0.001$ in all comparisons). *Oecomys roberti* and *O. trinitatis* are both medium-large in size, and differ from each other only in the length of the incisive foramen ($p < 0.05$) with the samples available to us (fig. 83). Finally, *O. superans* is consistently larger than both *O. roberti* or *O. trinitatis* in all variables, significantly so in most. In general, *O. superans* has a proportionately longer and wider rostrum but shorter nasals than either *O. roberti* or *O. trinitatis*, but the overall proportional

TABLE 28
Kimura 2-Parameter Distances Among 801-bp Cytochrome-b Haplotypes of Species of *Oecomys*
Number of haplotypes examined and mean ± standard error; within-taxon measures are given on the diagonal.

Species	n	*bicolor*	species	*roberti*	*superans*	*trinitatis*
bicolor	3	5.430 ± 1.350	7.188 ± 0.217	7.266 ± 0.249	8.307 ± 0.221	9.777 ± 0.718
species	1		—	8.563 ± 0.295	8.970	9.383 ± 0.666
roberti	3			4.105 ± 0.712	7.471 ± 0.575	9.496 ± 0.267
superans	1				—	9.357 ± 0.601
trinitatus	3					1.263 ± 0.460

TABLE 29

Selected External and Cranial Dimensions for Five Species of *Oecomys* from the Rio Juruá

Measurements (mm) are given as mean ± standard error, with range and sample size. Individuals are pooled across all localities along the river.

	O. species			*O. bicolor*			*O. roberti*		
Variable	Mean ± SE	Range	n	Mean ± SE	Range	n	Mean ± SE	Range	n
TOL	181.00 ± 10.00	171–191	2	220.05 ± 2.92	196–240	20	286.67 ± 2.67	263–312	27
TAL	95.00 ± 4.00	91–99	2	116.30 ± 1.84	101–130	20	160.93 ± 1.69	142–177	27
HF	21.50 ± 1.50	20–23	2	22.67 ± 0.14	22–24	21	27.43 ± 0.21	26–31	28
E	13.50 ± 0.50	13–14	2	14.20 ± 0.19	12–15	20	16.14 ± 0.20	14–18	28
CIL	21.19 ± 0.89	20.30–22.07	2	25.05 ± 0.23	23.18–26.97	21	29.42 ± 0.20	27.58–31.57	29
ZB	11.95 ± 0.37	11.58–12.31	2	14.83 ± 0.14	13.53–16.07	22	17.53 ± 0.14	15.97–18.93	29
MB	10.25 ± 0.08	10.17–10.33	2	11.50 ± 0.07	10.85–12.06	22	12.70 ± 0.06	12.17–13.27	29
IOC	4.52 ± 0.04	4.48–4.56	2	4.93 ± 0.06	4.49–5.81	22	5.68 ± 0.05	5.29–6.54	29
RL	7.42 ± 0.60	6.82–8.01	2	9.09 ± 0.09	8.21–9.67	22	11.24 ± 0.11	10.21–12.36	29
NL	7.49 ± 0.75	6.74–8.24	2	9.33 ± 0.12	8.41–10.70	22	11.34 ± 0.13	10.55–13.37	29
RW-1	4.10 ± 0.27	3.83–4.37	2	5.18 ± 0.09	4.03–5.87	22	6.28 ± 0.06	5.83–6.90	29
RW-2	3.42 ± 0.24	3.18–3.65	2	4.16 ± 0.04	3.87–4.62	22	5.03 ± 0.05	4.67–5.80	29
OL	8.51 ± 0.35	8.16–8.86	2	9.71 ± 0.08	9.19–10.29	22	11.50 ± 0.07	10.85–12.26	29
D	5.82 ± 0.37	5.45–6.18	2	7.21 ± 0.08	6.57–8.01	22	8.63 ± 0.10	7.64–9.55	29
MTRL	3.58 ± 0.01	3.57–3.58	2	4.03 ± 0.02	3.83–4.17	22	4.99 ± 0.03	4.60–5.34	29
IFL	3.80 ± 0.46	3.34–4.25	2	4.70 ± 0.04	4.31–5.00	22	5.19 ± 0.06	4.71–5.99	29
PL	9.76 ± 0.61	9.15–10.37	2	11.42 ± 0.10	10.69–12.29	22	13.93 ± 0.12	12.75–15.25	29
AW	4.54 ± 0.01	4.54–4.55	2	5.11 ± 0.04	4.74–5.36	22	6.20 ± 0.04	5.85–6.54	29
OCB	5.54 ± 0.14	5.40–5.67	2	6.29 ± 0.04	5.94–6.70	21	7.03 ± 0.04	6.59–7.36	29
BOL	3.51 ± 0.16	3.35–3.67	2	4.14 ± 0.05	3.75–4.66	21	4.67 ± 0.05	4.15–5.33	29
MPFL	3.54 ± 0.11	3.43–3.65	2	4.27 ± 0.05	3.94–4.67	22	5.24 ± 0.05	4.72–5.87	29
MPFW	1.92 ± 0.09	1.83–2.01	2	2.07 ± 0.03	1.81–2.30	22	2.33 ± 0.04	1.97–2.73	29
ZPW	1.89 ± 0.18	1.71–2.06	2	2.20 ± 0.03	1.91–2.40	22	3.17 ± 0.04	2.67–3.65	29
CD	9.43 ± 0.17	9.26–9.59	2	10.49 ± 0.06	9.91–11.01	21	11.83 ± 0.07	11.16–12.92	29

	O. superans			*O. trinitatis*		
Variable	Mean ± SE	Range	n	Mean ± SE	Range	n
TOL	316.00 ± 7.00	309–323	2	293.50 ± 7.50	278–314	4
TAL	168.50 ± 5.50	163–174	2	161.75 ± 4.09	157–174	4
HF	32.00 ± 1.00	31–33	2	27.20 ± 0.63	26–29	4
E	—	—	—	16.50 ± 0.29	16–17	4
CIL	33.74	—	1	29.76 ± 0.60	28.53–30.99	4
ZB	18.41 ± 0.62	17.79–19.02	2	17.44 ± 0.25	17.05–18.12	4
MB	13.77	—	1	12.67 ± 0.11	12.37–12.89	4
IOC	6.13 ± 0.38	5.75–6.51	2	5.62 ± 0.01	5.60–5.65	4
RL	12.88 ± 0.08	12.80–12.96	2	11.29 ± 0.33	10.56–11.87	4
NL	12.27 ± 0.21	12.06–12.48	2	11.62 ± 0.33	11.18–12.60	4
RW-1	6.95 ± 0.40	6.55–7.35	2	6.34 ± 0.12	6.04–6.63	4
RW-2	5.87 ± 0.36	5.51–6.22	2	5.15 ± 0.02	5.10–5.20	4
OL	12.58	—	2	11.72 ± 0.28	11.15–12.37	4
D	9.31 ± 0.07	9.24–9.37	2	8.74 ± 0.33	7.95–9.45	4
MTRL	5.60 ± 0.19	5.41–5.78	2	5.05 ± 0.07	4.85–5.15	4
IFL	6.16 ± 0.05	6.11–6.20	2	5.50 ± 0.19	5.24–6.06	4
PL	15.58 ± 0.22	15.36–15.80	2	14.04 ± 0.34	13.17–14.72	4
AW	6.60 ± 0.27	6.33–6.86	2	6.17 ± 0.39	6.09–6.27	4
OCB	7.76	—	1	7.05 ± 0.09	6.90–7.30	4
BOL	5.58	—	—	4.64 ± 0.12	4.42–4.91	4
MPFL	5.60 ± 0.07	5.53–5.66	2	5.34 ± 0.13	5.11–5.69	4
MPFW	2.58 ± 0.16	2.42–2.73	2	2.34 ± 0.12	2.18–2.70	4
ZPW	3.58 ± 0.09	3.49–3.67	2	3.24 ± 0.12	2.94–3.50	4
CD	13.22	—	1	11.68 ± 0.36	11.25–12.74	4

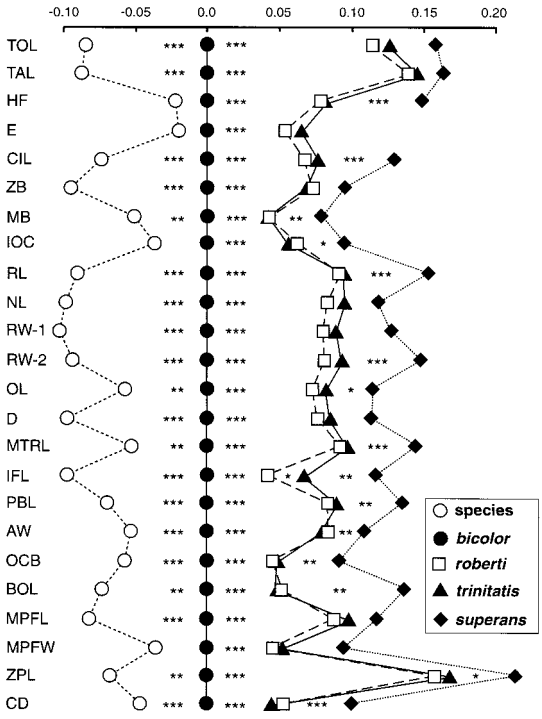

Fig. 83. Ratio diagram comparing the mean $\log_{10}$ values for each external and cranial dimension among five species of *Oecomys* from the Rio Juruá. Levels of significance in comparisons of the raw variables between pairs of taxa are indicated (* = $p < 0.05$; ** = $p < 0.01$; *** = $p < 0.001$).

pattern of character variation is very similar among the three larger species (fig. 83).

We performed two separate multiple-groups discriminant analyses in comparisons between these species, using log-transformed values for the cranial variables. One analysis included all five species; the other was restricted to the large-bodied taxa. Tables 30 and 31 provide the standardized discriminant coefficients for these analyses, and figure 84 illustrates the bivariate relationships between individual scores on the first two axes in comparisons between the different sets of species. In the analysis including all five species, the first axis explains over 92% of the total variation and serves to separate *O. bicolor*, and the three larger species, not surprising given the great disparity in size for all measurements (fig. 83). The second axis, while accounting for only 4.5% of the variance, separates *O. superans* from the others, with condyloincisive length and diastema contributing most strongly. The two species *O. roberti* and *O. trinitatis* remain totally overlapping in discriminant space along all axes. When analyses are restricted to the three larger species, however, *O. roberti* and *O. trinitatis* are somewhat more separable, but even here two of the four specimens of *O. trinitatis* are misclassified as *O. roberti*, with posterior probabilities of 0.528 and 0.696, respectively.

The less clear-cut discrimination between our samples of *O. roberti* and *O. trinitatis* is not surprising, since the two differ significantly in only one cranial variable, length of the incisive foramen. These two species differ in qualitative features, however, especially in both dorsal and ventral coloration and pelage quality, as noted in the individual accounts, below.

Oecomys bicolor (Tomes, 1860)

TYPE LOCALITY: ''Gualaquiza,'' Río Gualaquiza, 885 m, Provincia de Morona-Santiago, Ecuador.

DESCRIPTION: One of the two small-bodied species in the river basin, with average total length of 220 mm (table 29 and fig. 82) and a tail 112% of head and body length. The hind feet are short (22.7 mm) and broad, with tendency for a slightly darkened patch over the metatarsals. The tail is long and uniformly dark in color above and below, typically with 20 scale rows per cm, and clothed in short (about two scale rows long) hairs and terminating in a short, but distinct pencil. The dorsal pelage is short and rather bright, rufescent tawny in color; the ventral pelage is comprised of pure white hairs; a thin band of gray-based and white-tipped hairs may be present at the transitional boundary between the dorsal and ventral coloration, otherwise the dorsal and ventral coloration are sharply demarcated. The skull (fig. 85) is small (CIL averages 27.85 mm) with small toothrows (MTRL 4.03 mm), with very shallow zygomatic notches, more so than other species; well-developed and strongly diverging supraorbital ledges extending as ridges onto the parietals; upper incisors slightly opisthodont; bullae small and uninflated; incisive foramen

TABLE 30
Standardized Discriminant Coefficients for the First Three Discriminant Axes in Comparisons Among the Five Species of *Oecomys* from the Rio Juruá Basin

Variable	DF-1	DF-2	DF-3
Log CIL	−0.41348	−1.73319	−0.56595
Log ZB	0.31975	0.49868	−1.21751
Log MB	0.34034	−0.30774	−0.25099
Log IOC	−0.13147	−0.05459	0.56796
Log RL	−0.46098	−0.86408	0.31694
Log NL	0.40822	0.16205	−0.39775
Log RW-1	−0.28512	0.28512	−0.50089
Log RW-2	0.32657	−0.36673	−0.04352
Log OL	0.46908	0.07706	0.71721
Log D	0.75551	1.72730	−1.25508
Log MTRL	0.94428	0.02147	−0.37414
Log IFL	0.01662	−0.14620	−0.33222
Log PL	−0.98093	−0.21681	1.43582
Log AW	0.27562	0.46139	0.19930
Log OCB	0.24185	−0.38924	−0.21329
Log BOL	−0.54744	−0.50584	0.38763
Log MPFL	0.00361	0.83076	0.27536
Log MPFW	−0.53653	0.05457	0.05507
Log ZPL	0.83779	0.65044	0.25328
Log CD	0.10213	−0.18712	0.64385
Eigenvalue	52.0725	2.5348	1.3111
% contribution	92.762	4.515	2.336

TABLE 31
Standardized Discriminant Coefficients for the Two Discriminant Axes in Comparisons Among the Three Large Species of *Oecomys* from the Rio Juruá Basin (*O. roberti*, *O. superans*, and *O. trinitatis*)

Variable	DF-1	DF-2
Log CIL	−1.16474	−0.32271
Log ZB	0.07420	1.07916
Log MB	−0.71356	0.04015
Log IOC	−0.86156	1.48728
Log RL	−2.36009	3.27642
Log NL	0.15852	−0.75197
Log RW-1	0.54252	−1.95248
Log RW-2	−0.14544	−0.75484
Log OL	−0.86190	−0.17798
Log D	4.23711	−2.65771
Log MTRL	0.33483	−0.94391
Log IFL	−0.41853	−0.13582
Log PL	−0.69657	0.74835
Log AW	0.49717	−0.06523
Log OCB	−0.07100	−0.47436
Log BOL	−0.97152	0.93688
Log MPFL	0.91286	−0.61069
Log MPFW	0.43552	0.02222
Log ZPL	0.71316	−0.50401
Log CD	0.42347	0.40592
Eigenvalue	6.49089	0.96262
% contribution	87.085	12.015

short (4.7 mm) and teardrop in shape; posterior palatal pits small and undivided; parapterygoid fossae relatively deeply excavated; alisphenoid strut present in 19 of 22 individuals, at least on one side; hamular process of squamosal very short and broad, totally occluding subsquamosal foramen in most individuals; tegmen tympani not in contact, or only barely so, with squamosal. The combination of small size and pure white venter distinguishes *O. bicolor* from all other species within the Rio Juruá.

SELECTED MEASUREMENTS: See table 29.

NONGEOGRAPHIC VARIATION: The number of specimens of this species is limited, but when pooled across localities, there are substantial differences in nearly all individual measurements of the skin and skull relative to an individual's toothwear age class (table 32). In every case of significance, the relationship is strongly positive (Pearson product moment correlation coefficients at $p < 0.05$ range from 0.420–0.495; at $p < 0.01$, 0.560–0.627; and at $p < 0.001$, 0.648–0.753). No variables exhibit significant sexual dimorphism, however. Consequently, in studies of geographic variation in this species, although the sexes might be effectively pooled, care must be taken to account for age differences among samples. The apparent continual individual growth throughout life is a characteristic of many sigmodontine rodents, such as *Oligoryzomys* (Myers and Carleton, 1981), *Akodon* (Myers, 1989; Myers et al., 1990), and *Zygodontomys* (Voss, 1991), a phenomenon substantiated by laboratory growth studies on the latter genus (Voss et al., 1990).

GEOGRAPHIC VARIATION: Substantial differentiation among some localities in mtDNA cytochrome-b sequence exists for this species, with specimens from localities within the Mouth Region averaging over 5% different in relation to those from all upriver sites (fig. 86). Unfortunately, we lack sufficient materials to determine if a similar degree of differentiation exists between these geographic areas in morphological characters;

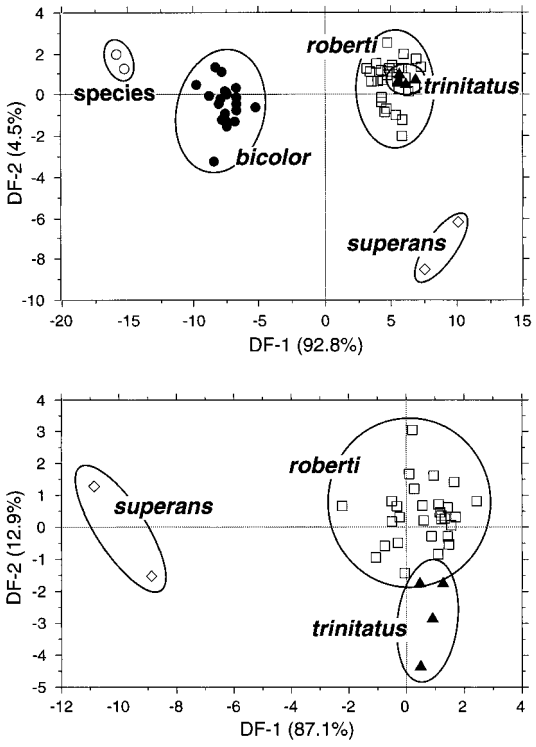

Fig. 84. Bivariate plots of discriminant scores for the first two axes in comparisons between (above) five species of *Oecomys* from the Rio Juruá and the three larger species (bottom), based on $\log_{10}$ cranial variables. The percent of the total variation explained by each axis is indicated in each plot.

only a single adult is available from the Mouth localities. In general color, size, or qualitative features of the skull, however, there are no notable differences between this specimen and those representing the upriver clade. Additional specimens should be sought to examine this question further.

DISTRIBUTION AND HABITAT: We found this species throughout the Rio Juruá, with specimens taken at localities within each of the four regional sample sites and on both sides of the river (fig. 81). The majority were taken in undisturbed várzea forest (36 of 43, or 84%); three were captured on the terra firme plots (two at Barro Vermelho [locality **12**] and one at Sobral [locality **4**]); and four were taken in second-growth forest at Igarapé Porongaba (locality **1**). Most individuals were obtained in canopy platform traps (32 of 43, or 74%); only four were taken in traps placed on the ground or on logs laying on the ground. The remainder (seven) were trapped or shot in low vine tangles approximately 2 m above ground.

REPRODUCTION: Pregnant females were taken from at least the months of August through February, a period spanning the dry season and the beginning of the rainy season. The modal litter size was 2 (mean 2.5, range 1–4; n = 11). Adult males with scrotal testes were taken in at sites from the months of September through March. The few data suggest that both sexes breed for a prolonged period of the year, perhaps continuously throughout. No females were taken, however, that were simultaneously pregnant and lactating.

KARYOTYPE: 2N = 80, FN = 140 (fig. 87). We karyotyped 17 specimens from seven separate localities, at least one in each of the four geographic sample regions as follows: locality **1** (n = 1), locality **2** (n = 5), locality **5** (n = 5), locality **8** (n = 3), locality **12** (n = 1), locality **13** (n = 1), and locality **14** (n = 1). All specimens exhibited the same karyotype with 19 pairs of medium to small metacentrics and submetacentric autosomes, 12 pairs of subtelocentric autosomes, and 8 pairs of acrocentric autosomes. The X-chromosome is a large metacentric, the largest in the complement; the Y-chromosome is a small chromosome that appears acrocentric. This karyotype differs slightly from that reported by Gardner and Patton (1976) for specimens of *O. bicolor* from eastern Perú (Balta, Río Curanja, Depto. Ucayali), which was reported with three additional pairs of uniarmed and three fewer biarmed autosomal elements. However, distinctions between the morphological categories can be quite difficult with such small chromosomes, and not too much emphasis should be placed on the presumptive differences between these two karyotypes. Certainly, there are no apparent differences between karyotypes belonging to individuals of the two geographic mtDNA clades illustrated in figure 86.

SPECIMENS EXAMINED (n = 43): (**1**) 1m, 3f — MNFS 1210, 1260–1261, 1320; (**2**) 2m, 4f — MNFS 1187, 1238, 1252, 1332–1333, 1396; (**b**) 1f — MNFS 1002; (**3**) 2m — MNFS 1514, 1679; (**4**) 1m — MNFS 1499;

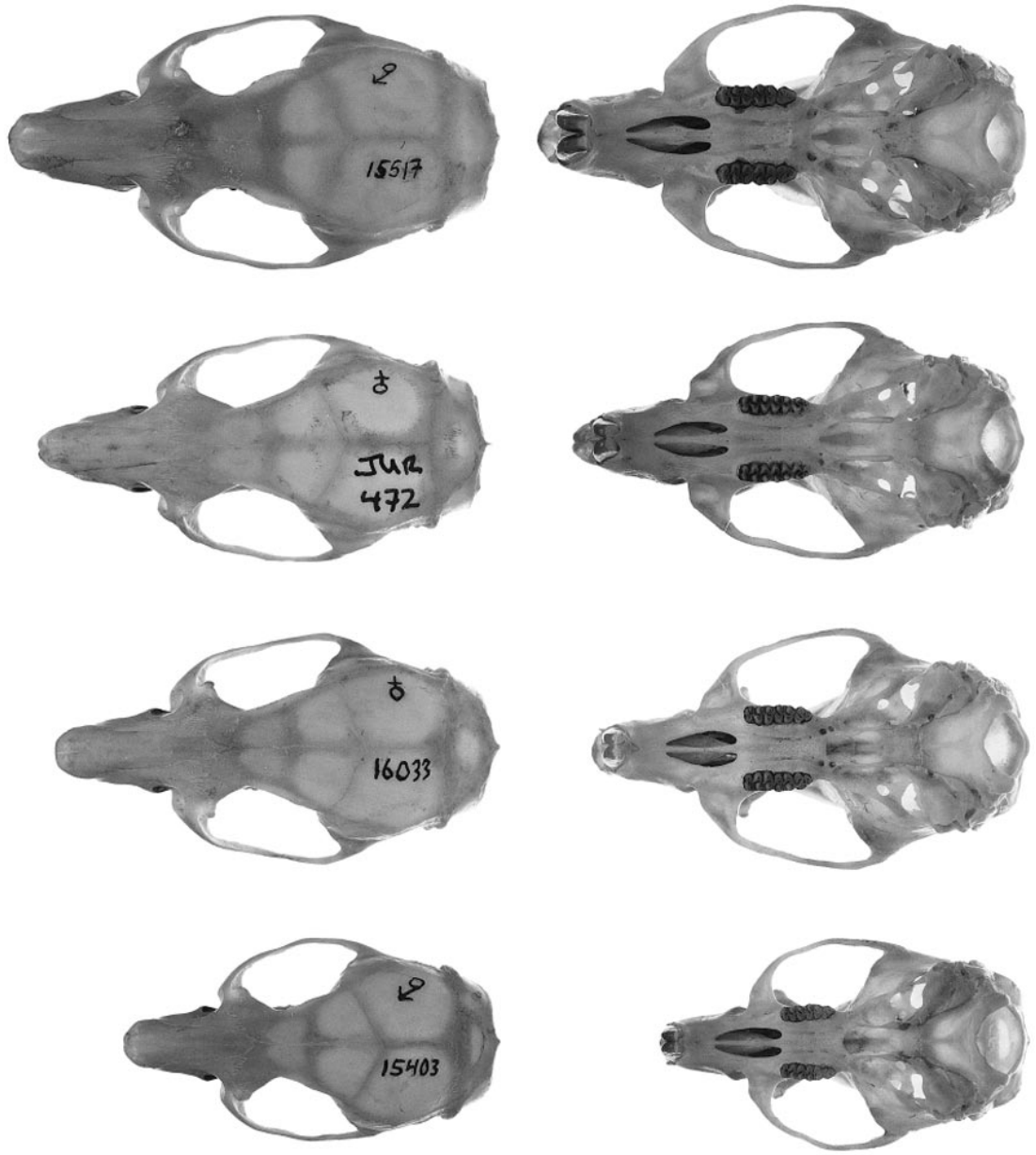

Fig. 85. Dorsal (left) and ventral (right) views of adult crania illustrating representatives of four species of arboreal rice rats, *Oecomys*. From bottom to top: *O. bicolor* (JLP 15403; Igarapé Nova Empresa [locality **8**], left bank Rio Juruá, Amazonas, Brazil), *O. roberti* (JLP 16033; Altamira [locality **9**], right bank Rio Juruá, Amazonas, Brazil); *O. trinitatis* (JUR 472, Colocação Vira-Volta [locality **14**], left bank Rio Juruá, Amazonas, Brazil); and *O. superans* (JLP 15517; Penedo [locality **7**], right bank Rio Juruá, Amazonas, Brazil). Magnification = ×2.

TABLE 32
External and Cranial Variables That Exhibit Statistically Significant Relationships with Individual "Age" (Toothwear Score) for Samples of *Oecomys bicolor* and *Oecomys roberti*[a]
Significance levels based on one-way ANOVA.

Species	$p < 0.05$	$p < 0.01$	$p < 0.001$	
O. bicolor	NL	TAL	TOL	D
	IFL	MB	CIL	RW-1
	MPFW	RW-2	ZB	PL
	ZPL	OL	IOC	BOL
		AW	RL	MPFL
O. roberti	MB	TOL	CIL	RW-2
	AW	BOL	ZB	OL
	ZPL	CD	RL	D
			NL	PL
			RW-1	

[a] All variables exhibit an increase in size with advancing "age," as the relationship between every variable and toothwear class shows a positive Pearson product moment correlation coefficient.

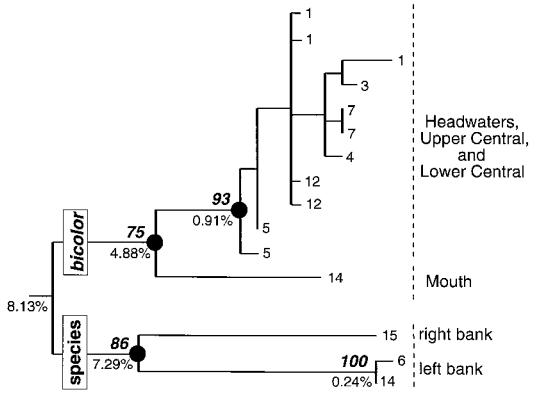

Fig. 86. Strict consensus of two equally minimal length maximum parsimony trees for 414 bp haplotypes of the mtDNA cytochrome-b gene of two species of the *Oecomys bicolor* group from the Rio Juruá. Catalog numbers for each haplotype (specimen) are listed from top to bottom following the order of terminal twigs: MNFS 1260, MNFS 1261, MNFS 1333, MNFS 1499, JLP 15414, JLP 15433, MNFS 1679, JLP 15777, MNFS 749, MNFS 652, MNFS 651, JUR 566, Jur 354, JUR 480, and JLP 15675. The locality number (from the map, fig. 1) of each haplotype is indicated at the end of each branch tip. Bold numbers at nodes are bootstrap values, based on 1000 iterations; percentages are mean Kimura two-parameter distances. The tree is rooted by comparison to sequences of other species of *Oecomys*. Branch lengths drawn proportional to the number of character changes. Tree length = 88 steps; CI = 0.784; RI = 0.802.

(**5**) 7m, 7f — JLP 15744, MNFS 581, 613, 625, 639–640, 651–653, 671–675; (**8**) 4m, 4f — JLP 15403, 15414, 15433, 15449, MNFS 466, 505, 507, 513; (**h**) 1m — JLP 15214; (**j**) 1f — MNFS 439; (**11**) 1f — MNFS 834; (**12**) 2f — JLP 15777, MNFS 749; (**13**) 1m — JUR 304; (**14**) 1f — 566.

Oecomys species

DESCRIPTION: We caught a second small-bodied species at three localities (Condor, locality **6**; Vira-Volta, locality **14**; and Vai-Quem-Quer, locality **15**). It was sympatric with *O. roberti* at the first of these, and with three other species, including *O. bicolor*, at the second, but was the only species found at the last locality (fig. 80). Only three individuals were trapped; one old adult and two young animals. This taxon is quite different from all others, including *O. bicolor* in molecular mtDNA sequence (figs. 82 and 86; table 28), and is also demonstrably distinct in morphology from *O. bicolor*, the only species with which it might be confused. G. G. Musser (personal commun.) provisionally considers it a member of the "*O. bicolor* group," largely by virtue of its small size.

In comparison to *O. bicolor*, this mouse is smaller in all external and cranial measurements, significantly so in most despite the very limited sample (table 29; fig. 83). Not surprisingly, therefore, it is completely separable from *O. bicolor* in multivariate space, based on a discriminant analysis (fig. 84, and above), with 100% of individuals of both species correctly assigned with posterior probabilities > 0.9999. It is darker dorsally, dull reddish brown as opposed to lighter, orangish brown. The venter is pure white as in *O. bicolor*, but there is a narrow band of gray-based hairs separating ventral and lateral coloration. The hind feet are slightly shorter than those of *O. bicolor*, and the dorsal surface is paler. The tail is uniformly dark brown both above and below and with a short pencil, as in *O. bicolor*. The dorsal fur is short and thick, but longer than that of *O. bicolor*. Cranially, this species has a somewhat more slender rostrum when paired with

Fig. 87. Karyotype of a female *Oecomys bicolor* (2n = 80, FN = 140) collected at Igarapé Porongaba (locality **1)**, Estado do Acre, Brazil (MNFS 1332).

similar aged *O. bicolor*, a narrower interorbital region, and distinctly shorter toothrows (mean MTRL = 3.58 vs 4.03; $p < 0.01$ by 2-tailed *t*-test). The incisive foramen is teardrop in shape rather than oval as in *O. bicolor*, widest posteriorly rather than at its midlength. The anterior border of the mesopterygoid fossa is flatter, less arched into the palate, and the parapterygoid fossae are deeper. The upper molar teeth are similar in occlusal details, except that distinct cuspules are evident at the entrance to both the proto- and hypoflexi in all three specimens. Although these cuspules are occasionally observed in the teeth of *O. bicolor*, they are never as distinctly well developed.

SELECTED MEASUREMENTS: See table 29.

MOLECULAR PHYLOGEOGRAPHY: Each of the three individuals came from separate localities. Interestingly, the two specimens from the left bank localities of Condor (locality **6**) and Vira-Volta (locality **14**), located some 660 km apart (table 1), are nearly identical in their respective cytochrome-b sequences. These two differ at only 6 sites of the 414 base pairs examined (Kimura two-parameter distance of 0.24%; fig. 85). The third specimen, however, is quite distinct, differing from the other two by an average Kimura two-parameter distance of 7.29% (fig. 86). It was trapped on the right bank at Vai-Quem-Quer (locality **15**), opposite Vira-Volta in the Mouth region of the river. These data suggest that two deeply divergent mitochondrial clades, perhaps signaling separate species status, are separated by the Rio Juruá, at least in its lower reaches. Additional collections of this mouse are badly needed from within the Rio Juruá Basin, as well as elsewhere, before its status can be adequately understood.

DISTRIBUTION AND HABITAT: This species was obtained only in terra firme forest in Sherman traps; one specimen was on the ground, the other two in canopy platforms positioned at 9.3 m and 12.5 m above the ground. We obtained so few specimens of this species that all data must be taken as preliminary, but it appears to occupy a distinctly different habitat than its similar sized relative, *O. bicolor*, which is found nearly exclusively in flooded várzea forest within the Rio Juruá basin.

REPRODUCTION: All three individuals collected were females, two subadults that were nulliparous and the third pregnant with three embryos when trapped in May during the wet season.

KARYOTYPE: 2n = 86; FN = 98 (fig. 88). We karyotype each of the three specimens of this species that we obtained. Despite deep differences in mtDNA sequences (see fig. 86), each of these appeared to have the same karyotype, although the specific determination of the number of arms for many of the very small autosomal elements is, admittedly, equivocal. The autosomal complement consists of seven pairs of small metacentrics and submetacentrics and 35 pairs of medium to small acrocentrics. Although no male specimens were examined, we identify the X-chromosome as a very large subtelocentric, an identification that is consistent with the X-chromosome of other species of *Oecomys* that we, and others, have karyotyped.

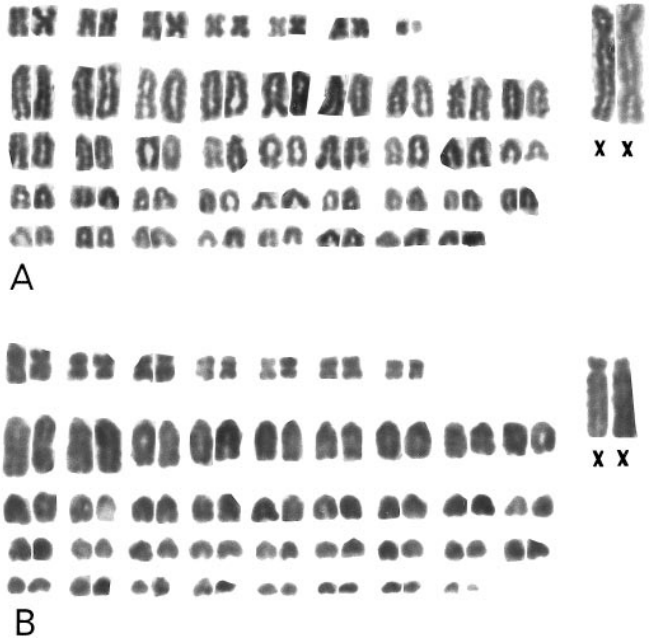

Fig. 88. Karyotypes of two female *Oecomys* species (2n = 86, FN = 98) representing each of the two major mitochondrial DNA clades identified in fig. 86: **A**: JUR 354, Vai-Quem-Quer (locality **15**), right bank Rio Juruá, Estado do Amazonas, Brazil ; **B**: JUR 480, Colocação Vira-Volta (locality **14**), left bank Rio Juruá, Estado do Amazonas, Brazil.

SPECIMENS EXAMINED (n = 3): (**6**) 1f — JLP 15675; (**14**) 1f — JUR 480; (**15**) 1f — JUR 354.

Oecomys roberti (Thomas, 1904)

TYPE LOCALITY: ''Santa Anna de Chapada, a village situated at an altitude of about 800 m; on the Serra de Chapada, some thirty miles N.E. Of Cuyabá [= Cuiabá],'' Chapada dos Guimarães, Estado do Mato Grosso, Brazil.

DESCRIPTION: This is the smallest of the three large-bodied species that occur within the Rio Juruá basin, averaging 287 mm in total length and with a tail 127% of head and body length (table 29). The tail is clothed in fine, short hairs (two scale rows in length), but appears naked when viewed by eye, and only a very slight pencil of fur extends beyond tip. It is paler below than above; dorsal color light brown. The hind feet are short and broad, orangish in color above. The dorsal pelage is bright reddish orange; the venter is white at the midline from chin to anus, but with broad lateral bands of white-tipped, gray-based fur. Dorsal and ventral coloration are sharply demarcated. This species has a relatively long skull (fig. 85; CIL, 29.4 mm) with relatively short and broad rostrum (11.2 × 6.3 mm, length to width); heavy supraorbital ledges diverge strongly and extend onto the parietals; upper incisors are opisthodont; bullae are small and uninflated; tegmen tympani is not in contact with the squamosal; hamular processes of squamosal are short and broad (although not as much as in *O. bicolor*), with subsquamosal foramen very small or completely closed; an alisphenoid strut is variably present (13 of 34 individuals, at least on one side); the incisive foramen is short and teardrop in shape; the molar toothrows are relatively short (MTRL 5.0 mm); posterior palatal pits are small but often divided, at least on one side; the mesopterygoid fossa is relatively narrow, and usually square at its anterior end; sphenopalatine vacuities are occasionally present as narrow slots along the presphenoid; and the parapterygoid fossae appear deeply excised.

SELECTED MEASUREMENTS: See table 29:

NONGEOGRAPHIC VARIATION: As with *O. bicolor*, this species also exhibits no sexual dimorphism in any external or cranial variable ($p > 0.05$ in all cases) although age contributes substantially to differences among individuals (table 32). Also, in a pattern similar to that found in *O. bicolor*, these variables increase with advancing toothwear age (Pearson product moment correlation coefficients for variables that exhibit significant age effects are all positive, ranging from 0.399–0.418 at $p < 0.05$; 0.502–0.591 at $p < 0.01$; and 0.580–0.742 at $p < 0.001$; table 32), reinforcing the conclusion that differences in age distributions should be considered when morphometric comparisons are to be made between localities for any species of *Oecomys*.

GEOGRAPHIC VARIATION: Strong structure in the mtDNA cytochrome-b gene sequences also occurs within *O. roberti*, although in this species linkage is between samples from the Lower Central and Mouth regions relative to those from the Headwaters and Upper Central ones (fig. 89). The average level of sequence divergence is not as great as it is in *O. bicolor* (4.1% versus 5.4%). Despite the degree of molecular differentiation, however, not one dimensional variable of either the skin or skull exhibited a significant difference in comparisons between pooled samples of each molecular clade. *Oecomys roberti* appears to be a markedly uniform morphological entity throughout its distribution within the Rio Juruá river basin.

DISTRIBUTION AND HABITAT: We took this species on both banks and in all geographic regions along the river, except for the Headwaters. However, it was found primarily in várzea forest on our standardized plots (44 of 50 specimens, or 88%), on the edge of *igapó* forest (2 of 50), or in highly disturbed second growth edges to seasonally flooded forest (4 of 50). The same number of individuals (n = 24) were taken on the ground and in the canopy, but this simple comparison is misleading since the terrestrial trap effort was nearly twice as great as that in the canopy (see table 2). We caught only two individuals in traps placed at approximately 1.5 m above the ground.

REPRODUCTION: All young individuals of both sexes (toothwear age class 2) were non-

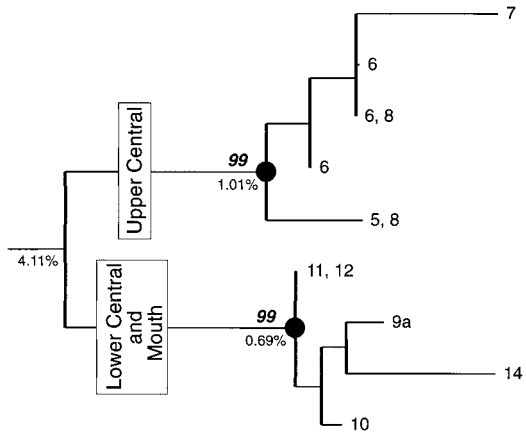

Fig. 89. Strict consensus of four equally minimal length maximum parsimony trees for 414 bp haplotypes of the mtDNA cytochrome-b gene of *Oecomys roberti* from the Rio Juruá. Catalog numbers for each haplotype (specimen) are listed from top to bottom following the order of terminal twigs: JLP 15241, MNFS 532, MNFS 537 and JLP 15402, MNFS 577, MNFS 578 and JLP 15404, MNFS 692 and 725, MNFS 948, JUR 532, and MNFS 955. The locality number (from the map, fig. 1) of each haplotype is indicated at the end of each branch tip. Bold numbers at nodes are bootstrap values, based on 1000 iterations; percentages are mean Kimura two-parameter distances. The tree is rooted by comparison to sequences of other species of *Oecomys*. Branch lengths drawn proportional to the number of character changes. Tree length = 41 steps; CI = 0.976; RI = 0.974.

reproductive (nulliparous females and nonscrotal males), and two of five age class 3 females were also nulliparous. Only a single pregnant female was taken, with two embryos, but two females exhibited recent placental scars that numbered either two or three. Time to reproductive maturity appears somewhat prolonged, in relation to other genera, such as *Oligoryzomys* and *Oryzomys*, as do pregnancy rates. The pregnant females and those with obvious scars were all taken early in the dry season, during late August or mid-September.

KARYOTYPE: 2n = 80, FN = 114 (fig. 90). To our knowledge, the karyotype of this species has not been reported to date. We have data for 20 specimens representing seven separate localities in the Upper and Lower Central and Mouth sample regions (locality

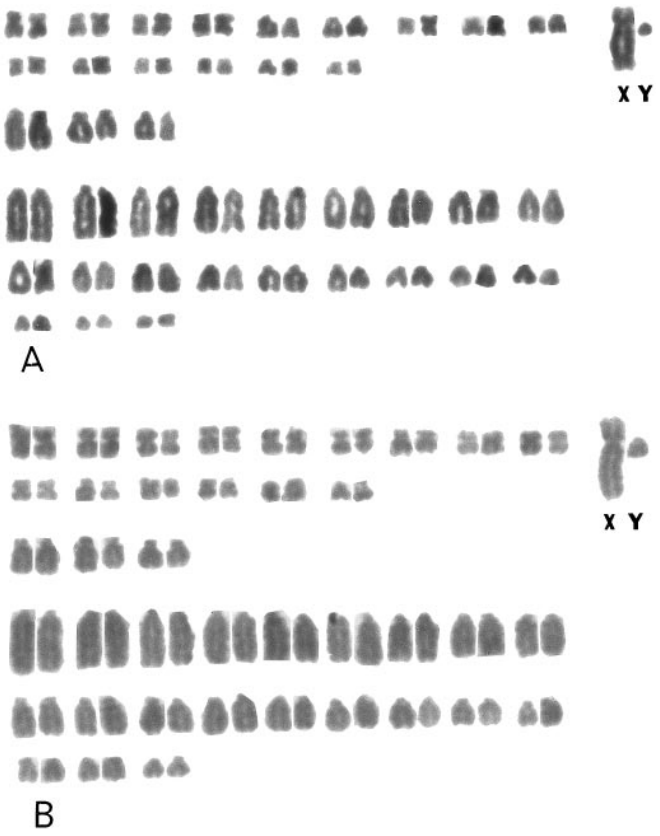

Fig. 90. Karyotypes from two male *Oeomys roberti* (2n = 80, FN = 114) representing the downriver mitochondrial DNA clade. **A**: MNFS 725, Barro Vermelho, left bank Rio Juruá, Estado do Amazonas, Brazil (locality **12**); **B**: JUR 532, Colocação Vira-volta, left bank Rio Juruá, Estado do Amazonas (locality **14**).

5, n = 4; locality **6**, n = 2; locality **8**, n = 4; locality **9a**, n = 1; locality **11**, n = 4; locality **12**, n = 3; and locality **14**, n = 2). The autosomal complement consists of 15 pairs of medium to small metacentric and submetacentric elements, three pairs of subtelocentric ones, and 21 pairs of acrocentric chromosomes. The X-chromosome is a very large submetacentric, the largest in the entire complement; the Ychromosome is a very small uniarmed element. This karyotype is the same in diploid number (2n = 80) and similar in fundamental number (FN = 114) to that described above for *O. bicolor* (FN = 140) and to that of *O. superans* from eastern Perú (FN = 108; Gardner and Patton, 1976; originally identified as *O. concolor*).

SPECIMENS EXAMINED (n = 50): (**5**) 11m, 3f — JLP 15743, MNFS 577–580, 589–591, 622, 638, 669–670, 676–677; (**6**) 1m, 1f — MNFS 532, 537; (**7**) 1m, 1 unknown — JLP 15241, 15413; (**8**) 8m, 7f — JLP 15402, 15404, 15432, 15448, 15466–15469, JUR 9, MNFS 430, 433, 508, 514 516; (h) 1f — MNFS 323; (j) 1f — JLP 15200; (**9a**) 1m, 1f — JLP 16033, MNFS 948; (**10**) 1f — MNFS 955; (**11**) 4m, 2f — MNFS 681, 692, 695, 702, 708, 769; (**12**) 4m — JLP 15916–15917, MNFS 725, 823; (**14**) 1m, 1f — JUR 532, 534.

Oecomys superans Thomas 1911

TYPE LOCALITY: ''Canelos, Rio Bobonaza, Orient of Ecuador. Alt. 2100′,'' Provincia de Pastaza, Ecuador.

DESCRIPTION: This is the largest among the five species of *Oecomys* present in the Rio

Juruá basin (TOL 316 mm; table 29 and fig. 83). It has a long tail, uniformly dark brown in color above and below; tail scales are visible to eye, with 16 scale rows per cm; caudal hairs are short (< 2 scale rows in length); and there is no apparent terminal pencil of hairs. The hind feet are distinctly broad and clothed in orangish hair above. The dorsal coloration is dark orangish brown, paling laterally with a weakly developed, but visible orange lateral line; ventral fur color is uniformly gray-based tipped with buff. The dorsal fur is thick and woolly in appearance. Distinct pale orange postauricular patches are present, uniquely so among the species encountered along the Rio Juruá. The skull (fig. 85) is large (CIL nearly 34 mm) and robust in appearance, with a short, broad rostrum, well-developed, distinctly diverging supraorbital ledges, and moderately shallow zygomatic notches. The upper incisors are more orthodont than in the other species. An alisphenoid strut is present in one, but not the other of the two available specimens; the tegmen tympani is in contact, but does not overlap, with the squamosal; the subsquamosal foramen is small, but open, in both specimens. The incisive foramen is short and slightly oval in shape, not distinctly teardrop in shape as in both *O. bicolor* and *O. roberti*; the maxillary toothrow is long (MTRL, 5.6 mm), more so than in other species in the Juruá basin; the posterior palatal pits are simple, but larger than in all other species; the mesopterygoid fossa is broad with a rounded anterior margin; the parapterygoid fossae are deeply excised; and the bullae are small and uninflated.

SELECTED MEASUREMENTS: See table 29.

DISTRIBUTION AND HABITAT: The capture of only two specimen within the Rio Juruá precludes any conclusions about the true distribution of *O. superans* within the basin. Both specimens came from right bank localities in the Upper and Lower Central Regions (fig. 81). Both were also taken on the ground in second growth and highly disturbed habitats, such as old garden plots (Altamira, locality **9**) and river-edge shrubs (Penedo, locality **7**). Our records from the Rio Juruá apparently extend the range of this species eastward from the ''Lower Andean slopes and foothills of E Colombia, Ecuador, and Peru'' (Musser and Carleton, 1993) into the lowlands of western Amazonia.

REPRODUCTION: The single female was pregnant, with two embryos; the single male was scrotal.

KARYOTYPE: 2n = 80; FN = 108. We have chromosome data for the one specimen from Penedo (locality **7**). The karyotype of this individual is identical to that described by Gardner and Patton (1976) for specimens from eastern Perú (Balta, Río Curanja, Departamento de Ucayali) originally allocated to *O. concolor*, following the nomenclature of Hershkovitz (1960). G. G. Musser (personal commun.), however, has correctly identified these specimens as *O. superans*. The chromosome complement is also extremely similar to that described above for *O. roberti*, but with 12 pairs of small metacentric and submetacentric and 24 pairs of acrocentric autosomes, a large submetacentric X-chromosome, and a small acrocentric Y-chromosome.

SPECIMENS EXAMINED (n = 2): (**7**) 1m — JLP 15517; (**9**) 1f — MNFS 846.

Oecomys trinitatis (Allen and Chapman, 1893)

TYPE LOCALITY: ''Princestown, Trinidad''; Princes Town, Trinidad and Tobago.

DESCRIPTION: This is the second largest species present in the Rio Juruá, but it cannot be distinguished in most mensural characters from *O. roberti* (fig. 83). The head-and-body length averages 132 mm, and the tail (162 mm) is much longer than the body (123%), either unicolored dark brown, or only slightly paler below, with scale rows visible to the eye (16 scale rows per cm), clothed with short hairs (< 2 scale rows long), and terminating in a slight pencil. The hind feet are short and broad, but not as broad as in *O. superans*; the toes are typically darker than the metatarsal area. The dorsal coloration is dull brown with a slight reddish perfusion; a bright orange lateral line separates the dorsal and ventral colors, especially in the shoulder and chin regions; and the ventral fur is gray-based with pale buff or white tips. The dorsal hairs appear distinctly thin, giving the pelage a sleeker appearance than in either *O. roberti* or *O. superans*, the latter which appears the

Fig. 91. Karyotype of a female *Oecomys trinitatus* (2n = 58, FN = 96) collected from Colocação Vira-Volta (locality **14**), left bank Rio Juruá, Estado do Amazonas, Brazil (JUR 472).

most woolly, but the hair is of the same overall length. The skull (fig. 85) is somewhat narrower than that of other large species; zygomatic notches are shallow; supraorbital ledges are broad and strongly diverging; upper incisors are strongly opisthodont; an alisphenoid strut is present in three of five specimens, at least on one side; the tegmen tympani is usually in contact with squamosal; the subsquamosal foramen is open as often as occluded; the hamular process of the squamosal is more elongate and narrower than in other species; the incisive foramen is short, broadest at its midpoint, and thus ovoid in shape; the toothrows are intermediate in length between those of *O. roberti* and *O. superans* (MTRL 5.05; fig. 83); the posterior palatal pits are moderate in size and often divided; the mesopterygoid fossa is relatively narrow with an arched anterior border; the parapterygoid fossae are relatively shallow; and the bullae are very small and distinctly uninflated. Our samples are limited, but *O. trinitatis* cannot be distinguished from *O. roberti* by any cranial measurement, except the length of the incisive foramen (figs. 82 and 83).

SELECTED MEASUREMENTS: See table 29.

DISTRIBUTION AND HABITAT: This is apparently an uncommon but widely distributed species within the Rio Juruá basin. We found it at one or more localities within each of the four sampling regions (fig. 81), and on both sides of the river. Three were trapped on terra firme standardized lines (Penedo, locality **7**; Barro Vermelho, locality **12**; and Vira-Volta, locality **14**); two were taken on the edge of flooded forest (Vira-volta, locality **14**), and three were taken on várzea standardized lines (opposite Igarapé Porongaba, locality **2**, and Barro Vermelho, locality **12**). We caught the species on the ground (n = 3) as often as on canopy platforms (n = 3) or in lower branches 1.5 m off the ground (n = 2).

REPRODUCTION: All adults of both sexes were reproductive; and one juvenile was taken (at Penedo, locality **7**, in August). One female was pregnant, with three embryos, and two others had fresh placental scars; these three were taken in both the late dry season (November) and late rainy season (May).

KARYOTYPE: 2n = 58, FN = 96 (fig. 91). We karyotyped four individuals, one each from localities **7** and **12** and two from locality **14**. This complement is quite different from those of the other species of *Oecomys* reported here, with a much lower diploid number and proportionately larger autosomes. There are 16 pairs of large to small metacentric and submetacentric autosomes, four pairs of large to medium subtelocentrics, and eight pairs of medium to small acrocentrics. The X-chromosome is a large submetacentric, again the largest of the entire complement, and the Y-chromosome is a small acrocentric element.

SPECIMENS EXAMINED (n = 8): (**2**) 1m — MNFS 1250; (**7**) 1m — JLP 15425; (**12**) 1m, 2f — JLP 15851, 15866–15867; (**14**) 1m, 2f — MNFS 1683, JUR 472, 497.

Oligoryzomys Bangs, 1900

Pygmy rice rats

The pygmy rice rats are a speciose but poorly known group that is widely distributed throughout the Neotropical Realm, from

southern México to Tierra del Fuego and to eastern Amazonia and the Mata Atlântica of coastal Brazil (Carleton and Musser, 1989; Emmons and Feer, 1997). Over this enormous range, member species may be common within habitats spanning lowland tropical forest to the high Andean *puna* grasslands or *páramo* above timberline. Often placed as a subgenus within *Oryzomys* by earlier workers, its generic status was solidified by Carleton and Musser (1989), who provide an emended diagnosis as well as a provisional list of species with generalized descriptions and geographic ranges. Their diagnosis includes, but is not limited to, the following traits: small body size; tail usually longer than head and body; six plantar tubercles, with hypothenar pad small and round; skull small but stout in appearance; rostrum relatively broad and stocky; interorbital region hourglass shaped with squared edges; braincase elongate, smooth, and flat, with foramen magnum directed posteriorly; zygomatic arches bowed laterally; jugal reduced or absent; zygomatic notches distinct; zygomatic plates broad, with the anterior edge reaching the nasolacrimal capsules; stapedial foramen large, posterior opening of alisphenoid canal large, squamosal-alisphenoid groove and sphenofrontal foramen absent (derived cephalic arterial supply; pattern 2 of Voss, 1988; Carleton and Musser, 1989); incisors opisthodont, asulcate; molars brachydont, cuspidate, with three roots in uppers and two in lowers; first molars ovate, anteromedian flexus (-id) shallow, anterolabial and anterolingual conules (-ids) small, anteroloph and mesoloph (-id) present; anterolabial cingulum well developed on lower third molar.

Oligoryzomys microtis (Allen, 1916)

TYPE LOCALITY: ''Lower Rio Solimoes (fifty miles above mouth),'' Estado do Amazonas, Brazil.

DESCRIPTION: This is a small-bodied, long-tailed, and short-haired mouse, yellowish brown above and grayish white below. The skull (fig. 92) is small, with a somewhat elongated braincase, broad but long rostrum, and hourglass-shaped interorbital region having squared edges.

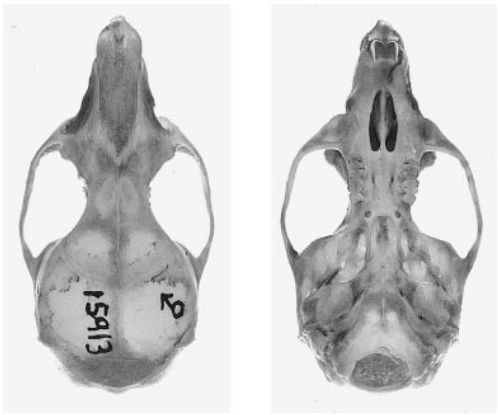

Fig. 92. Dorsal (left) and ventral (right) views of the skull of *Oligoryzomys microtis* (JLP 15913; Jainu [locality **11**], right bank Rio Juruá, Amazonas, Brazil). Magnification = ×2.

NONGEOGRAPHIC VARIATION: Table 33 provides descriptive statistics for four external and 20 cranial characters from all adult individuals pooled across their sampled localities. We examined the effects sex and age within localities on morphometric variation, as well as differences among localities, through an ANOVA nested by locality, sex, and age. These are also summarized in table 33 as variance components, or the percentage of total variation due to the successive nested effects. Sexual dimorphism is virtually nonexistent, accounting for an average of only 1.54% of the total pool of variation, with only tail length, hind foot length, and interorbital constriction exhibiting significance (at $p < 0.05$). Age accounts for a considerable amount of the variation, however, with an average of 22.0%. Most variables, particularly cranial, exhibit a significant age effect ($p < 0.01$ for all variables except TAL, HF, E, IOC, MTRL, OCB, and BOL). These variables generally increase in size with increasing age, a pattern of variation also found for *O. fornesi* (listed as a synonym of *O. microtis* by Musser and Carleton, 1993) and other species of *Oligoryzomys* from Paraguay by Myers and Carleton (1981). Comparisons between localities, therefore, should take differences in age distributions into account, as geographic patterns can be confounded by the age profiles of different samples.

GEOGRAPHIC VARIATION: Relatively large

TABLE 33
Descriptive Statistics and Variance Components for Four External and 20 Cranial Variables of *Oligoryzomys microtis* from the Rio Juruá
Measurements (mm) are given as mean ± standard error, with range and sample size.
Percentage contributions of the separate effects of locality, sex, and age are given, based on nested ANOVA (ns = $p > 0.05$; * $p < 0.05$; ** $p < 0.01$; *** $p < 0.001$).

				Variance component			
Variable	Mean ± SE	Range	n	Locality	Sex	Age	Error
TOL	191.40 ± 0.869	168–223	153	5.9*	0.0 ns	24.6**	69.4
TAL	103.03 ± 0.548	80–125	153	0.0 ns	10.5*	0.0 ns	89.5
HF	23.48 ± 0.094	21–26	156	4.6 ns	25.7***	3.8 ns	65.9
E	13.40 ± 0.055	11–15	156	4.5 ns	3.1 ns	1.0 ns	91.4
CIL	21.284 ± 0.076	19.13–23.71	157	12.6*	0.0 ns	43.2***	44.3
ZB	12.331 ± 0.045	11.05–13.74	157	10.7*	0.0 ns	38.8***	50.4
MB	10.879 ± 0.023	10.18–11.64	157	7.9*	0.0 ns	21.1**	70.9
IOC	3.776 ± 0.013	3.32–4.35	157	0.0 ns	7.8*	12.9*	71.3
RL	8.067 ± 0.037	6.99–9.30	157	8.1*	0.0 ns	41.5***	50.4
NL	9.057 ± 0.042	7.54–10.33	157	5.2 ns	0.0 ns	37.0***	57.8
RW-1	4.422 ± 0.023	3.76–5.42	157	9.8*	3.6 ns	27.2***	59.4
RW-2	3.524 ± 0.017	2.85–4.08	157	12.8**	0.0 ns	13.7**	73.5
OL	8.172 ± 0.028	7.35–9.08	157	17.1***	0.0 ns	28.0***	54.9
D	5.949 ± 0.030	5.15–7.00	157	12.4**	0.0 ns	45.9***	41.7
MTRL	3.199 ± 0.010	2.89–3.56	157	9.5*	0.0 ns	0.0 ns	90.5
IFL	4.029 ± 0.019	3.43–4.70	157	1.5 ns	0.0 ns	34.5***	64.0
PB	9.503 ± 0.037	8.4–10.78	157	11.3**	0.0 ns	28.4***	60.3
AW	4.304 ± 0.015	3.74–4.72	157	15.9**	0.0 ns	19.2**	64.9
OCB	5.488 ± 0.014	5.09–6.08	157	14.0**	0.9 ns	0.0 ns	85.1
BOL	3.417 ± 0.018	2.80–4.02	157	3.9 ns	0.4 ns	0.0 ns	95.7
MPFL	3.216 ± 0.020	2.54–3.84	157	16.6***	0.0 ns	24.5***	58.9
MPFW	1.619 ± 0.012	1.20–2.00	157	0.0 ns	0.0 ns	25.5***	74.5
ZPL	2.233 ± 0.013	1.89–2.79	157	16.7***	0.0 ns	23.8***	59.5
CD	8.289 ± 0.021	7.48–9.08	157	0.0 ns	5.0 ns	33.4***	61.6

samples are available from at least three localities within each of the Upper Central and Lower Central sampling regions of the Rio Juruá; we caught only four individuals in the Headwaters Region and none in the Mouth Region. We examined the extent of variation among localities, either as a general function of isolation by distance or as a function of which the side of the river from which samples came. All but four variables (MTRL, IFL, BOL, and MPFW) exhibit significant (one-way ANOVAs, $p < 0.01$) differences in comparisons between localities, even when comparisons are limited to those six samples of the Upper and Lower Middle regions. However, locality per se exhibits a relatively minor overall effect, averaging only 8.4% of the total variation, less than one half the age effect (table 33).

Because most dimensions increase with individual age, and since age distributions are different between localities ($\chi^2 = 57.137$, df = 16, $p < 0.0001$), we used a multiple groups principal components (MGPCA) approach (Thorpe, 1983) to avoid confusing within-group with among-group size. In this analysis, the first MGPCA axis is a general within-group allometric ''size'' vector, to which all individual variables are positively and significantly correlated ($p < 0.001$ in all comparisons). Overall size differences between locality samples, due in large measure to differences in their respective age distributions, were then ignored in a canonical discriminant analysis using individual scores for all MGPCA axes except MGPCA-1 (see Thorpe and Baez, 1987, and discussion in Patton and Smith, 1990). Exclusive of any overall size differences, there are no apparent differences between any pair of sampled lo-

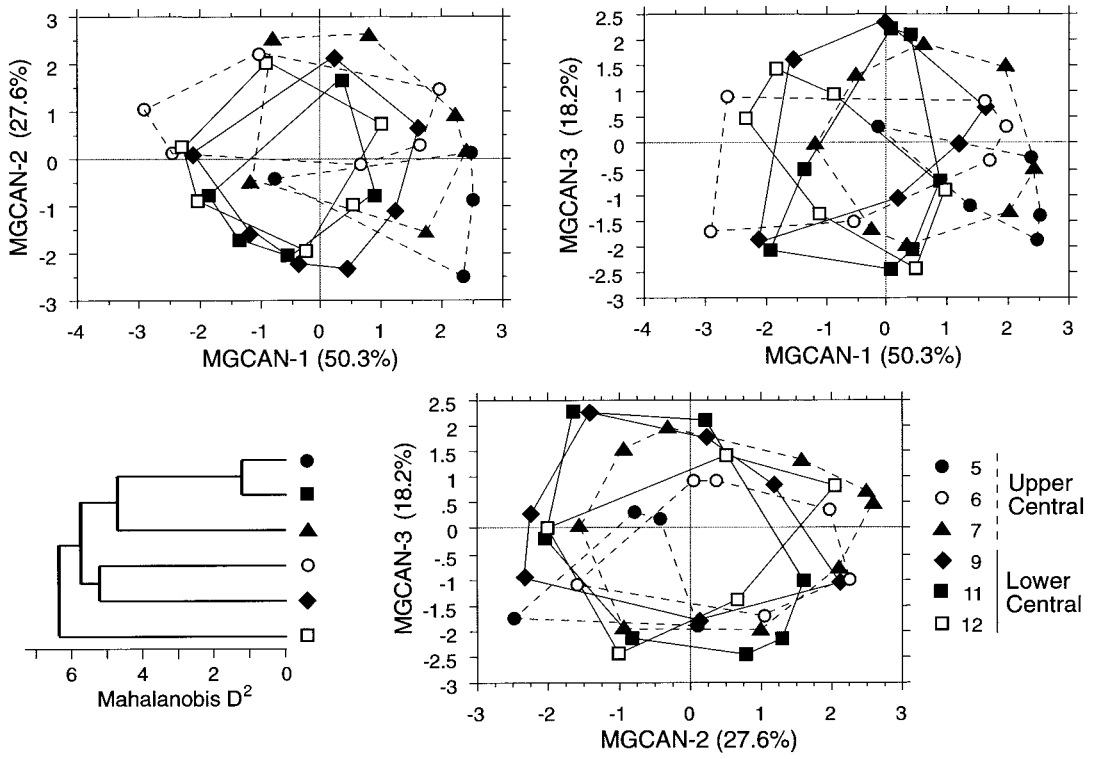

Fig. 93. Bivariate plots of individual scores on the first three axes derived from a canonical discriminant analysis of the cranial ''shape'' variables (excluding the first MGPC axis) for each of the six Upper Central (localities **5**, **6**, and **7**; broken lines) and Lower Central (localities **9**, **11**, and **12**; solid lines) sample sites of *Oligoryzomys microtis*. Right bank localities are identified by solid symbols; those from the left bank by open symbols. The proportion of the total variation explained by each MGCAN axis is given. The relationship between localities based on a matrix of squared Mahalanobis distances, clustered by the unweighted pair group method, is in the lower left.

calities in multivariate discriminant space. Figure 93 illustrates bivariate plots of the scores on the first three axes, which collectively account for 96.1% of the total variation. The analysis does not support multivariate separation of localities, either between Upper Central versus Lower Central regions or right bank versus left bank. Similarly, clustering of locality-average-squared Mahalanobis distances exhibits no pattern of among-locality geographic relationships (fig. 93, lower left). Finally, there is also no correlation between the matrices of Mahalanobis D^2 and geographic distances (Mantel's matrix $r = 0.173$; $t = 1.055$; $p = 0.854$), and thus no evidence for a general morphometric pattern of isolation by distance.

MOLECULAR PHYLOGEOGRAPHY: The morphological uniformity, at least along the approximately 200 km stretch of the middle Rio Juruá, is mirrored by lack of population differentiation, based on hierarchical analyses of haplotypes of the mtDNA cytochrome-b gene (Patton et al., 1996a). In these genetic traits, as with the morphological ones, most of the total pool of variation is that contained within populations (81.7% for the mtDNA haplotypes, roughly equivalent to the average error term of 66.1% for external and cranial variables, table 33). Again, we found no genetic differences between localities grouped either by geographic region or river bank. A weak isolation by distance relationship in among-population genetic traits exists in comparisons between localities from all sampled regions but not when analyses were re-

stricted to the Upper and Lower Central localities. Moreover, estimates of gene flow rates (Slatkin's [1993] M) between adjacent localities, either paired on the same or opposite sides, were all above 10.0. These values are sufficient to prevent local populations from diverging by the simple actions of genetic drift (reviewed by Mills and Allendorf, 1996).

DISTRIBUTION AND HABITAT: Although this species is distributed widely within the Rio Juruá basin, it has a very restricted and unique habitat range. All but one of the 321 specimens we captured were taken on the ground in seasonally available or disturbed habitats along the river margin during the dry season. A single individual was trapped on the terra firme standardized lines at Altamira (locality **9**), approximately 800 m inland from the grassy margins of the river (line C, fig. 28). The vast majority of specimens were taken in the dense grass (*capim*) that grows rapidly on the upper edges of sand bars, which become progressively exposed as the water recedes seasonally. The remainder were taken in other disturbed habitats close to the water's edge, such as old or active garden plots, pasture, or adjacent to human dwellings. There have been no populational studies of this species elsewhere within its range, but its occupation of what amounts to grass and disturbed shrub patches within otherwise primary lowland evergreen forest matches the habitat range of many other species in the genus (see, for example, summaries in Emmons and Feer, 1997, and Redford and Eisenberg, 1992).

As a result of the seasonal availability of its primary habitat, very few *O. microtis* were taken at localities in the Headwaters Region (localities **1** through **4**), and none were taken at those in the Mouth Region; both areas were sampled during the high water of the rainy season when this habitat is scarce. Thus, within the Mouth Region, it is not clear whether this species is truly absent, or simply at exceedingly low population numbers in refugial habitats that were not sampled.

Two aspects of importance relating to the seasonal rise and fall of the river must be considered when discussing the population biology and evolutionary potential of *O. microtis*. First, as a denizen of riverine edge habitats, particularly seasonally dense grasses (fig. 2), individuals are likely to be carried downriver during flood stages when grass mats are swept from their precarious footholds on exposed beaches. Such floating mats of grasses and other edge vegetation were commonly observed following rapid river rises (fig. 94). These could also explain the dendritic distribution along river courses of *O. microtis* throughout Amazonia. The second issue regarding the biology of this species involves the absolute seasonal availability of the preferred river-edge habitats. Where does it seek refuge during the high-water season, and, as a corollary, what kind of annual fluctuation in population numbers, age structure, and breeding strategy characterizes such a species? Both aspects suggest that rapid seasonal exploitation once riverine edge habitats become available can be a profitable adaptive ecological strategy.

REPRODUCTION AND LIFE HISTORY: We caught most specimens during the dry season, in the months of August through November. Although longitudinal studies were not possible, so individual growth patterns are unknown, the overall impression is that animals grow exceedingly rapidly, reach reproductive maturity quickly, and breed in successive reproductive bouts, all within the course of the single dry season. Virtually all females trapped (n = 86) were reproductively active, either pregnant, lactating, or parous with relatively fresh placental scars. We recorded reproductive activity by autopsy at the time of specimen preparation. For females, we noted whether individual females were (1) nulliparous and not in present reproductive condition (uteri nonvascularized, thin, and threadlike with no evidence of ripe follicles on the surface of the ovary, mammary nipples tiny), (2) undergoing their first estrous (ripe follicles visible, uterus swollen, mammary nipples tiny), (3) pregnant, (4) or postpartum (lactating and/or placental scars visible, nipples enlarged). For males, we recorded testis position (abdominal or scrotal) and size (length by width), greatest length of the vesicular glands, and visibility of seminiferous tubules in the cauda epididymides. Reproductively active males were those with scrotal testes over 9 mm in length, with ep-

Fig. 94. Floating mass of grass, originally growing on exposed sand bars during low water levels, being carried down river during flood stage. Photograph taken in the lower section of the Rio Juruá by M. N. F. da Silva, May 1992.

ididymal tubules visible to the naked eye, and with vesicular glands greater than 10 mm in total length. Nonreproductive individuals had abdominal and small testes (always < 6 mm), short and non-swollen seminal vesicles (< 5mm), and nonvisible epididymal tubules. We also recorded the relative age of each specimen, using the toothwear sequence proposed by Myers and Carleton (1981). Although we do not know the correspondence of these toothwear categories to chronological (calendar) age, M3 becomes fully erupted by day 30–35 post-partum in the piñon mouse, *Peromyscus truei* (Hoffmeister, 1951).

Individuals of both sexes apparently reach reproductive maturity early (fig. 95). For males, 50% of age class 1 individuals (those without fully erupted third molars; n = 8) were scrotal with visible epididymal tubules and enlarged seminal vesicles, whereas 82% (31 of 39) age class 2 and all of ages 3 or older were similarly reproductively active. As with males, most age class 1 females were reproductively active (9 of 15), seven of which were pregnant. A few nulliparous individuals persisted into higher age classes, but by age class 2, 81% (21 of 26) were either pregnant or post-partum. Indeed, the majority of all individuals in each age class were pregnant at the time of their capture. Litter sizes based on embryo counts ranged from 2 to 8, with a mode of 4 (n = 47). For both sexes, age class 1 individuals were all still in juvenile pelage, while those of age class 2 had either completed their adult molt, or were in the process of doing so. Although we have no notion of the relation between toothwear age classes and chronological ages, reproduction is obviously in full swing by age 2. Clearly, *O. microtis* exhibits the reproductive features of an *r*-selected life history, with fast growth, early reproductive maturity, and large litter sizes. These features are to be expected for a species that lives primarily in seasonally ephemeral habitats.

KARYOTYPE: 2n = 64, FN = 66. We karyotyped 59 individuals from 12 localities

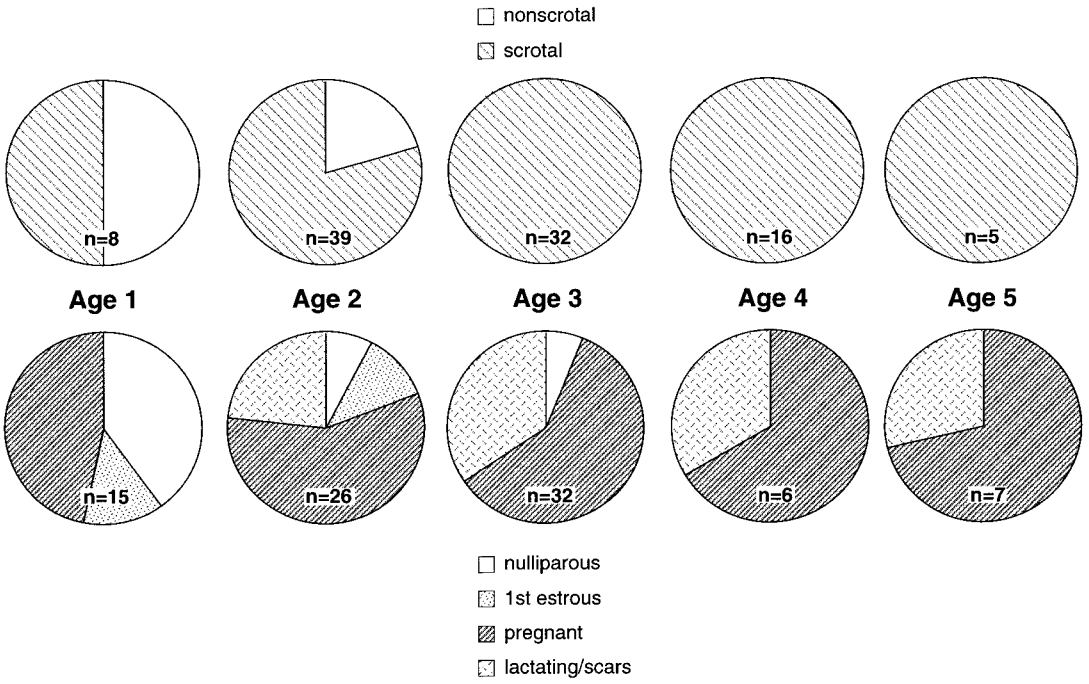

Fig. 95. Pie diagrams illustrating the proportion of nonreproductive and reproductive male (above) and female (below) *Oligoryzomys microtis* for each of the five toothwear age classes. Individuals are pooled from all localities, all but four of which are from the Upper Middle and Lower Middle regional localities and were collected during the months of August through November (see text for further details).

(Porongaba [locality **1**], n = 2; Sobral [locality **4**], n = 1; Condor [locality **6**], n = 11; opposite Condor [locality e], n = 1; Penedo [locality **7**], n = 6; União [locality g], n = 4; Caioá [locality h], n = 3; Miranda [locality I], n = 9; Eirunepé [locality j], n = 2; Altamira [locality **9**], n = 4; Jainu [locality **11**], n = 6; and Barro Vermelho [locality **12**], n = 10. The karyotype is described and figured by Gardner and Patton (1976), and an up-dated comparison of the chromosome complement of *O. microtis* to other species in the genus is provided by Silva and Yonenaga-Yassuda (1997).

SPECIMENS EXAMINED (n = 321): (**1**) 1m, 1f — MNFS 1321, 1360; (**4**) 1m, 2 unknown — MNFS 1425, 1576, 1619; (**6**) 28m, 14f — JLP 15520–15522, 15526–15528, 15537–15538, 15543–15546, 15550–15557, 15579–15588, 15606–15608, 15615–15616, 15629–15631, 15672, 15679, 15692–15693; (**e**) 7m, 5f — JLP 15714–15718, 15733–15739; (**7**) 31m, 29f — JLP 15233–15237, 15246, 15251–15252, 15406–15412, 15428–15430, 15438–15440, 15451–15454, 15471–15475, 15481–15494, 15502–15504, 15508–15513, 15515–15516, 15518, MNFS 328, 343, 491–492; (**g**) 1m, 3f — JLP 15226–15228, MNFS 327; (**h**) 8m, 3f — DMN 5–6, JLP 15216–152222, MNFS 324–325; (**i**) 11m, 5f — DMN 4, JLP 15205–15213, 15223–15225, MNFS 320–322, 326; (**j**) 5m, 3f — DMN 1–2, JLP 15201–15204, MNFS 317–318; (**k**) 1m, 3f — JLP 15190–15191, MNFS 313–314; (**9**) 51m, 38f — JLP 15925, 15929–15938, 15945, 15947–15965, 15969, 15973–15988, 16001–16012, 16022–16025, 16045, 16080, MNFS 835–845, 847–850, 888–891, 905–908; (**10**) 1m, 2f — JLP 15970, MNFS 950–951; (**11**) 11m, 12f — JLP 15760–15761, 15908–15914, MNFS 788–792, 798–806; (**12**) 26m, 18f — JLP 15774–15776, 15779–15791, 15795–15796, 15801–15808, 15815, 15831–15832, 15854, 15894–15900, 15914, 15918–15919, 15921, MNFS 811–816, 824–826, 829–832.

Oryzomys Baird, 1858

Rice rats

A review of the species of rice rats of the genus *Oryzomys* from the lowland tropical forests of South and Central America (including Amazonia, the Mata Atlântica of coastal Brazil, and the trans-Andean forests of the Pacific Coast of Ecuador and Colombia north into Central America) has been published recently by Musser et al. (1998). In this thorough and extremely important summary, these authors define, characterize, amply illustrate, and allocate all available names to 11 species, two of which they describe as new. Six of these species (*O. megacephalus*, *O. tatei*, *O. yunganus*, *O. macconnelli*, *O. nitidus*, and *O. emmonsae*) occur within Amazonia, and in various combinations of sympatry.

In the course of their studies, Musser et al. examined most specimens of *Oryzomys* in our collection from the Rio Juruá. They included these materials in both univariate and multivariate statistical summaries for each species, and they also examined patterns of morphological variation along the river among our samples that they allocated to *O. megacephalus*. We make no effort here to redo the more geographically extensive descriptions and analyses presented by these authors, as there is no point to duplicate the wealth of detail or exemplary illustrations. Rather, we provide sufficient information on character differences to permit the identification of each species found within the Rio Juruá. We also summarize in a more detailed way patterns of geographic differentiation of these species within the Rio Juruá, and provide details on population ecology and life history. Where data are available, we also place our samples in the broader context of Amazonia, summarizing comparisons between our samples from the Rio Juruá with those from elsewhere in Amazonia based on our molecular sequence data. Our results differ in a few key elements from the conclusions reached by Musser et al. (1998); we detail these differences under the appropriate sections below.

Phylogenetic relationships and species boundaries of rainforest *Oryzomys*

Musser et al. (1998) presented our preliminary molecular sequence data in describing geographic units of many of the species of the *Oryzomys* ''*capito*'' complex that they characterized. These data were totally concordant with the patterns of morphological variation they described. We now have expanded this database considerably, and here present a more substantial analysis of the relationships and species boundaries hypothesized by Musser et al. (1998). We present these analyses separately for each of the two morphological groupings of *Oryzomys*: (1) what we term the ''*megacephalus*'' group, those taxa with, among other features, a derived cephalic arterial system (*O. laticeps*, *O. megacephalus*, and *O. yunganus*), and (2) the ''*macconnelli*'' group, those with the primitive cephalic arterial condition (*O. emmonsae*, *O. macconnelli*, *O. nitidus*, and *O. russatus*).

The ''megacephalus'' Group: Sequences from the cytochrome-b gene are available for 37 individuals from 32 localities within Amazonia and the Mata Atlântica of coastal Brazil (fig. 96; table 34). The three species of this complex recognized by Musser at al. (1998) are readily separable on the basis of sequence differences, but four strongly divergent clades, with bootstrap values of 94 or higher, are apparent (fig. 97). Two of these correspond to the ''eastern'' and ''western'' clades they allocated to *Oryzomys megacephalus*, clades that are somewhat more divergent from each other (15.9%, on average) than either is from *O. laticeps* of the Mata Atlântica (12.9 and 13.4%, respectively). *Oryzomys yunganus*, which is sympatric with both ''eastern'' and ''western'' *O. megacephalus* at several localities (Musser et al., 1998), is the most divergent of the four clades, at an average of nearly 17%. Although our sampling of this species is limited, it exhibits only moderate sequence divergence averaging 5.5% among localities several thousands of kilometers distant (fig. 96). This is the maximal amount of sequence divergence found within any of the four sampled species (table 35).

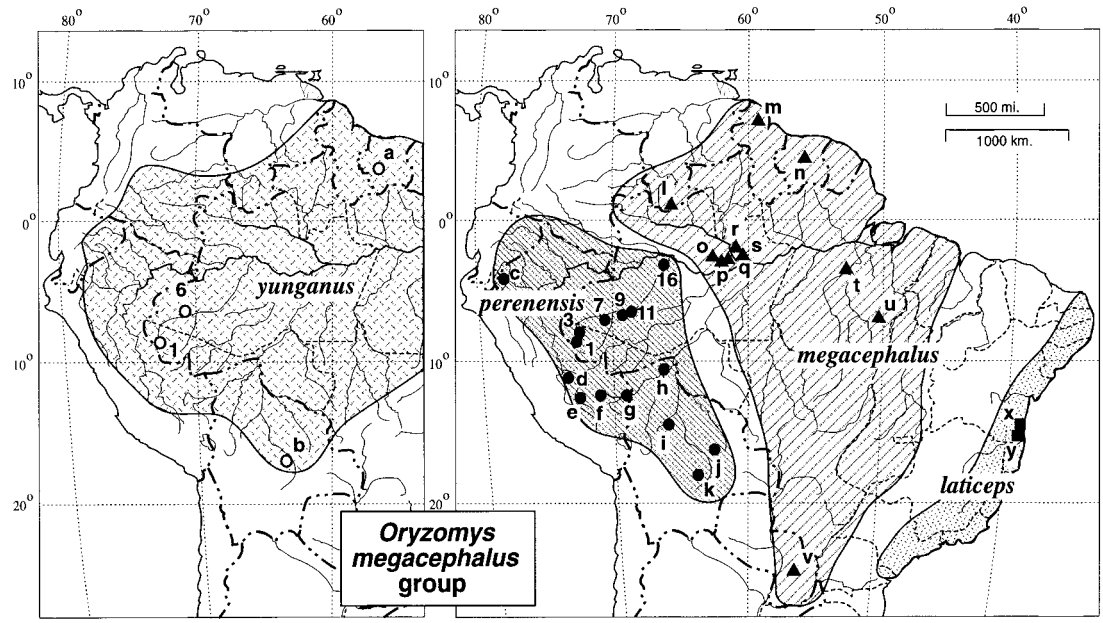

Fig. 96. Map of localities of members of the *Oryzomys megacephalus* group sampled for mtDNA cytochrome-b sequences: **left**: *O. yunganus* (open circles); **right**: *O. perenensis*, solid circles; *O. megacephalus*, solid triangles; *O. laticeps*, solid squares. Locality numbers correspond to the list of provenance and voucher specimen catalog numbers provided in table 34. Distributions are based on Musser et al. (1998).

Our enlarged data set presents the same topology of relationships illustrated by Musser et al. (1998; compare their fig. 6 with fig. 97). Most significantly, our broadened geographic sampling of both their ''western'' and ''eastern'' divisions of *O. megacephalus* continue to show that these groupings are both strongly divergent from one another with a very sharp region of transition in central Amazonia (fig. 96) and likely do not even form a monophyletic assemblage (fig. 97). Although Musser et al. (1998) could find only size differences among samples of *O. megacephalus* from western to eastern Amazonia, their two geographic units do differ in karyotype as well as in mtDNA sequences. All western samples that have been karyotyped (from localities 1–9, c, e, and f in fig. 96) are 2n = 52; those eastern samples (localities o, p, q, r, t, and v) are 2n = 54. The concordance of molecules, chromosomes, and body sizes suggests separate species status, despite the apparent lack of diagnosable morphological characteristics. Although a general size cline occurs among population samples across central Amazonia south of the Rio Solimões-Amazonas axis, a vast area for which no molecular or karyotypic data are available, we believe the summation of molecular, chromosomal, and size differences between the two clades identified in figure 97 and mapped in figure 96 justify species recognition. Consequently, contrary to Musser et al. (1998), we consider our samples from the Rio Juruá as well as those from throughout western Amazonia, to represent *O. perenensis* Allen, 1901. With its type locality in the Departamento de Junín in east-central Perú, this is apparently the earliest available name for the western Amazonian 2n = 52 taxon (Musser et al., 1998: 45).

THE ''MACCONNELLI'' GROUP: We have also augmented the molecular sampling of this group of species relative to the data summarized by Musser et al. (1998), although numerous critical geographic gaps remain (fig. 98, table 36). Results of this expanded data set are concordant with the morphological analyses presented by Musser et al. (1998), and thus support most hypotheses of

TABLE 34

Haplotypes, Map Localities, and Voucher Numbers for Taxa of the *Oryzomys megacephalus* Group

Individual haplotypes listed from top to bottom in the tree, figure 97, with the catalog numbers of their respective voucher specimens, and localities (identified as in the map, fig. 96) for which 801-bp haplotypes of the mitochondrial DNA cytochrome-b gene are available.

Haplotype	Voucher no.	Locality code	Locality name
Oryzomys yunganus			
1	MNFS 1101	1	Igarapé Porongaba, right bank Rio Juruá, Acre, Brazil (locality **1**)
2	JLP 15535	6	Seringal Condor, left bank Rio Juruá, Amazonas, Brazil (locality **6**)
3	CM 76936	a	Geyskes Creek, Tafelberg, Saramacca, Suriname
4	CM 76926	—	Agustus Creek, Arrowhead Basin, Saramacca, Suriname (not mapped separately from locality "a")
5	MSB 56001	b	4.5 km N, 1.5 km E Cerro Amboro, Río Pitasama, Santa Cruz, Bolivia
Oryzomys perenensis			
6	LHE 1474	d	2 km SW Tangoshiari, Río Pangoreni, Depto. Cusco, Perú, 1000 m, 11°46'S, 73°26.5'W
7	JLP 15758	11	Jainu, right bank Rio Juruá, Amazonas, Brazil
8	MVZ 154944	c	Huampami, Río Cenepa, Amazonas, Perú
9	MNFS 1100	1	Igarapé Porongaba, right bank Rio Juruá, Acre, Brazil
10	MVZ 166676	e	Kiteni, Río Urubamba, Cusco, Perú
11	MVZ 166674	f	Hda. Erika, Río Alto Madre de Dios, Madre de Dios, Perú
12	JLP 15311	7	Penedo, right bank Rio Juruá, Amazonas, Brazil
13	JLP 15968	9	Altamira, right bank Rio Juruá, Amazonas, Brazil
14	JUR 551	16	Ilhazinha, left bank Rio Juruá, Amazonas, Brazil
15	MNFS 1586	3	Nova Vida, right bank Rio Juruá, Acre, Brazil
16	MVZ 166026	g	Cusco Amazoníco, Río Madre de Dios, Madre de Dios, Perú
17	MSB 55998	i	1 km SW Estación Biologica del Beni, Totisal, Beni, Bolivia
18	MSB 56000	j	6 km W (by road) Ascensión, Santa Cruz, Bolivia
19	MSB 56004	k	San Rafael de Amboro, Santa Cruz, Bolivia
20	MSB 57160	h	Opposite Hamburgo, west bank Rio Beni, Pando, Bolivia
Oryzomys laticeps			
21	EDH 22	x	Fazenda Beijo Grande, 12 km S & 1.1 km E Itabuna, Bahia, Brazil
22	ML 101	y	Parque Zoobotânico da CEPLAC, 6 km E Itabuna, Bahia, Brazil
Oryzomys megacephalus			
23	ALG 14292	l	Neblina base camp, Río Mawarinuma, Amazonas, Venezuela
24	JLP 16787	r	Meduiním, left bank Rio Negro, Amazonas, Brazil
25	JLP 16791	r	Meduiním, left bank Rio Negro, Amazonas, Brazil
26	CCM 421	u	PDBFF, 82 km N Manaus, Amazonas, Brazil, 2°24'S, 59°52'W
27	MNFS 2015	o	Tambor, left bank Rio Jaú, Amazonas, Brazil
28	JLP 16781	q	right bank above mouth of Rio Jaú, Amazonas, Brazil
29	CM 76933	n	Geyskes Creek, Tafelberg, Saramacca, Surinam
30	LC 125	p	Macaco, left bank Rio Jaú, Amazonas, Brazil
31	JLP 16731	p	Macaco, left bank Rio Jaú, Amazonas, Brazil
32	ROM 97979	i	30 km NE Surama, Rupununi, Guyana
33	ROM 98090	i	30 km NE Surama, Rupununi, Guyana
34	CS23	u	Floresta Nacional Tapirapé-Aquiri, Município de Marabá, Pará, Brazil, 5°48'05"S, 50°30'54"W
35	LHE 510	t	52 km SWW Altamira, east bank Rio Xingu, Pará, Brazil
36	CS3	u	Floresta Nacional Tapirapé-Aquiri, Município de Marabá, Pará, Brazil, 5°48'05"S, 50°30'54"W
37	Myers et al. (1995)	v	13.3 km N Curuguaty (by rd.), Canendiyu, Paraguay

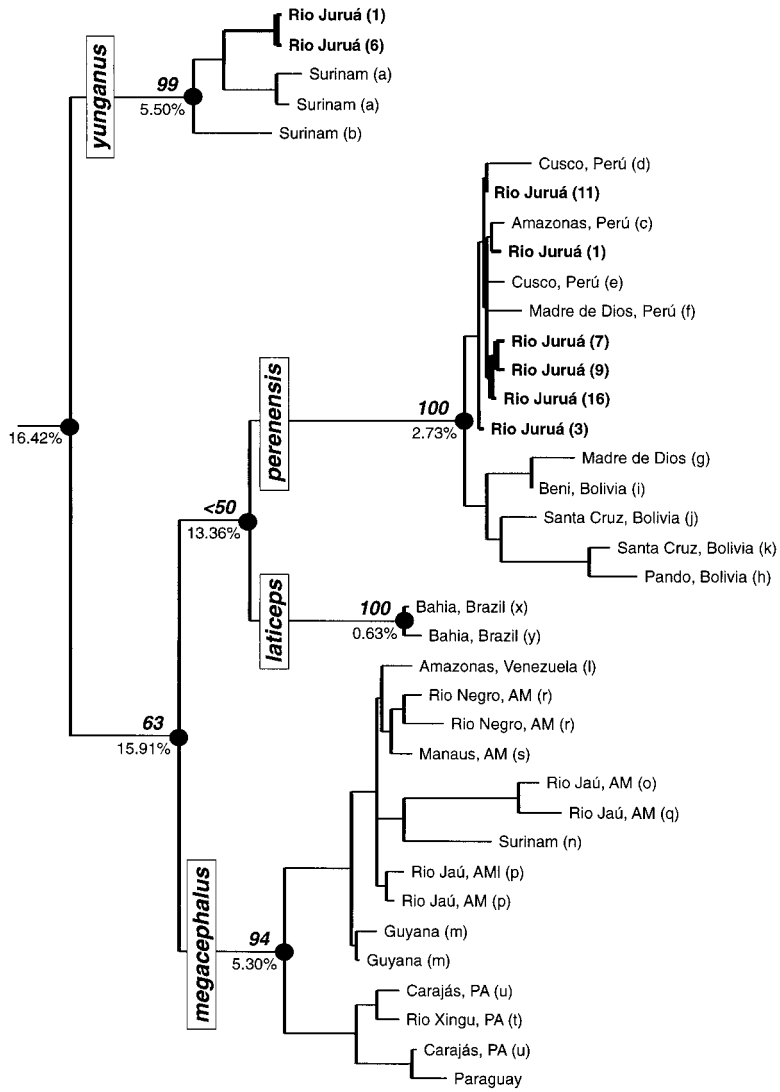

Fig. 97. Strict consensus tree of three equal minimum-length parsimony trees for haplotypes of the mitochondrial cytochrome-b gene (801 bp; only 401 bp are available for the individual from Paraguay [Myers et al., 1995]) for members of the *Oryzomys megacephalus* complex of species. Length = 627 steps, CI = 0.593, RI = 0.870. Sequences of members of the *Oryzomys macconnelli* species complex are used as the outgroup. Bold numbers at internal nodes are bootstrap values, based on 1000 replicates; percentages are mean Kimura two-parameter distances for all haplotypes below a given node. Haplotypes are identified by locality, as in the map, fig. 96, and provenance and voucher catalogue numbers are listed in table 34.

species boundaries they advanced. Two exceptions, however, are evident.

First, a larger number of reciprocally monophyletic and deeply divergent clades are identifiable than would be expected by the current species boundaries in the group. Specifically, samples of *O. macconnelli* form two strongly differentiated and geographically delimited clades, each with strong bootstrap support of 92 or 100%. These do join as a supportable monophyletic lineage, but only with a bootstrap value of 73% (fig. 99),

TABLE 35
Kimura 2-Parameter Distances Among Cytochrome-b Haplotypes for Species of the *Oryzomys megacephalus* Group
Number of haplotypes examined and mean ± standard error; within-species measures are given on the diagonal.

Taxon	n	*perenensis*	*megacephalus*	*laticeps*	*yunganus*
perenensis	15	2.728 ± 0.162	15.881 ± 0.219	13.360 ± 0.181	17.810 ± 0.155
megacephalus	15		5.301 ± 0.269	12.856 ± 0.336	17.201 ± 0.207
laticeps	2			0.628	16.562 ± 0.178
yunganus	5				5.495 ± 1.103

perhaps less than would be expected if they belonged to a single taxon. Our samples from north of the Rio Solimões comprise two groups (one from east and northeast of the Rio Negro, including north of Manaus in Brazil, Venezuela, and Surinam; the other from the Rio Jaú to the west of the Rio Negro) that differ by a substantial degree (5.7%, table 37) and that are karyotypically distinct. Specimens from Venezuela are 2n = 76, FN = 85 (Musser et al., 1998) whereas those from the Rio Jaú are 2n = 58, FN = 90 (M. N. F. da Silva, unpublished data). These northern samples, however, differ from a collection of samples of *O. macconnelli* from south of the Rio Solimões that stretch across southern Amazonia from central Perú through the Rio Juruá to as far east as the

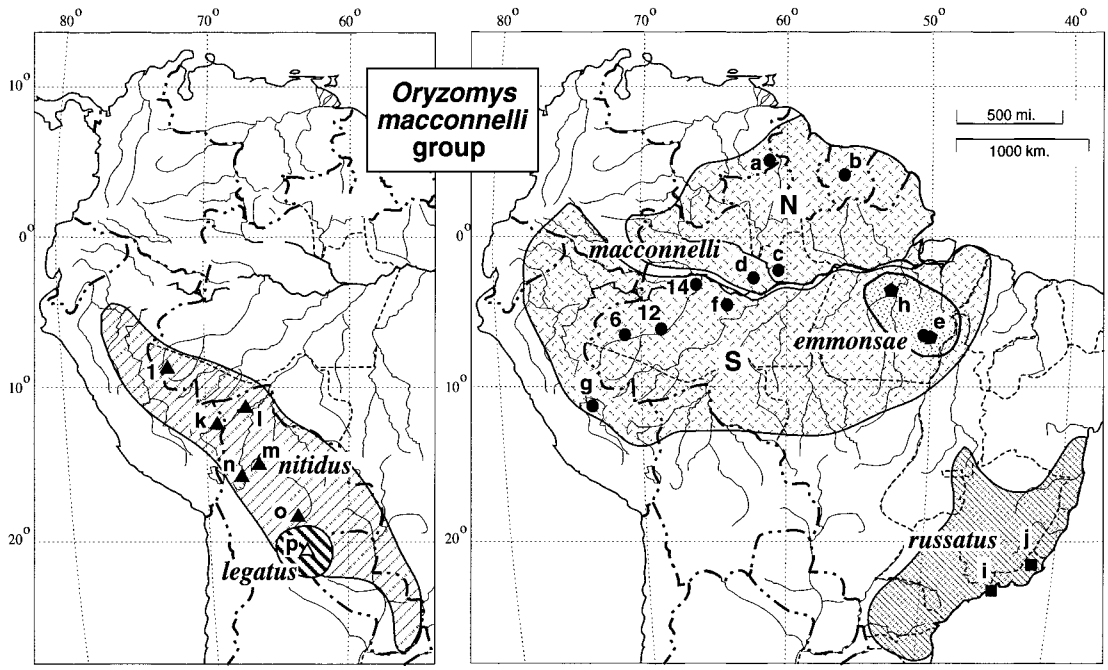

Fig. 98. Map of localities of members of the *Oryzomys macconnelli* group sampled for mtDNA cytochrome-b sequences: **left**: *O. nitidus* (solid triangles) and *O. legatus* (open triangle); **right**: *O. macconnelli* (solid circles), *O. emmonsae* (solid pentagons), and *O. russatus* (solid squares). Localities from the Rio Juruá are numbered; other localities are given letters. Both letters and numbers correspond to the list of provenance and voucher specimen catalog numbers provided in table 36. The transition in geographic units of *O. macconnelli* across the Rio Solimes is indicated by the hiatus in the cross-hatched distribution of the species. Distributions are based on Musser et al. (1998).

TABLE 36

Haplotypes, Map Localities, and Voucher Numbers for Taxa of the *Oryzomys macconnelli* Group

Individual haplotypes listed from top to bottom in the tree, figure 99, with the catalog numbers of their respective voucher specimens, and localities (identified as in the map, fig. 98) for which 801-bp haplotypes of the mitochondrial DNA cytochrome-b gene are available.

Haplotype	Voucher no.	Locality code	Locality name
Oryzomys macconnelli			
1	USNM 448585	a	San Ignacio de Yuruaní, Bolívar, Venezuela
2	INPA	c	PDBFF, 82 km N Manaus, Amazonas, Brazil, 2°24'S, 59°52'W
3	CM 64561	b	1.5 km W Rudi, Kappel Vliegveld, Brokopondo, Surinam
4	MNFS 2078	d	Macaco, left bank Rio Jaú, Amazonas, Brazil
5	JLP 16727	d	Macaco, left bank Rio Jaú, Amazonas, Brazil
6	CS 32	e	Floresta Nacional Tapirapé-Aquiri, Município de Marabá, Pará, Brazil, 5°48'05"S, 50°30'54"W
7	JUR 355	14	Colocação Vira Volta, left bank Rio Juruá, Amazonas, Brazil (locality **14**)
8	JUR 386	14	Colocação Vira Volta, left bank Rio Juruá, Amazonas, Brazil (locality **14**)
9	MNFS 85	d	Alto Rio Urucu, Amazonas, Brazil
10	MNFS 156	d	Alto Rio Urucu, Amazonas, Brazil
11	LLW 462	g	2 km SW Tangoshiari, Río Pangoreni, Depto. Cusco, Perú, 1000 m, 11°46'S, 73°26.5'W
12	LLW 447	g	2 km SW Tangoshiari, Río Pangoreni, Depto. Cusco, Perú, 1000 m, 11°46'S, 73°26.5'W
13	JLP 15563	6	Seringal Condor, left bank Rio Juruá, Amazonas, Brazil (locality **6**)
14	MNFS 747	12	Barro Vermelho, left bank Rio Juruá, Amazonas, Brazil (locality **12**)
Oryzomys russatus			
15	ML 48	i	Fazenda da Toca, Ilhabela, Ilha São Sebastião, São Paulo, Brazil
16	MN 31410	j	Mata da Rifa, Parque Estadual do Desengano, 1.7 km N & 5.1 km W Santa Maria Madalena, Rio de Janeiro, Brazil
Oryzomys emmonsae			
17	CS 37	e	Floresta Nacional Tapirapé-Aquiri, Município de Marabá, Pará, Brazil, 5°48'05"S, 50°30'54"W
18	LHE 536	g	52 km SSW Altamira, east bank Rio Xingu, Pará, Brazil
19	MZUSP 27150 (holotype)	g	52 km SSW Altamira, east bank Rio Xingu, Pará, Brazil
Oryzomys nitidus			
20	MNFS 1419	l	Igarapé Porongaba, right bank Rio Juruá, Acre, Brazil (locality **1**)
21	MVZ 166027	k	Cusco Amazónico, Río Madre de Dios, Madre de Dios, Perú
22	MSB 57116	l	Palmira, Pando, Bolivia
23	MSB 56057	m	45 km N Yacuma, Beni, Bolivia
24	MSB 63358	o	3 km SW Las Cruces, Santa Cruz, Bolivia
25	MSB 68452	n	La Reserva, La Paz, Bolivia
Oryzomys legatus			
26	MSB 67320	p	Tapecua, Tarija, Bolivia
27	MSB 67359	p	Tapecua, Tarija, Bolivia

Serra dos Carajás in Estado do Pará (fig. 98). The average sequence divergence between these geographic groupings of *O. macconnelli* is 11.1% (table 37), a value only slightly less than that between any other pair of species in the complex (range 12.4% to 15.7%, table 37), and more than twice the variation present within any single clade. The southern mitochondrial DNA clade also has a distinct karyotype, with 2n = 64, FN = 70

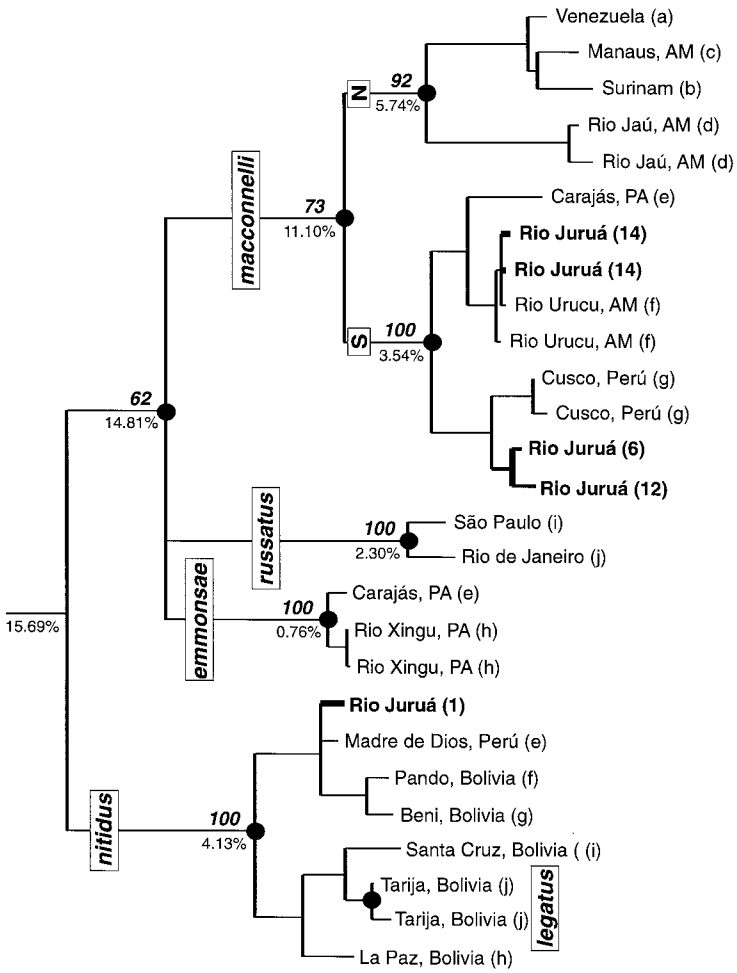

Fig. 99. Strict consensus of two equal minimum-length parsimony trees for haplotypes of the mitochondrial cytochrome-b gene (801 bp) for members of the *Oryzomys macconnelli* complex of species. Length = 550 steps, CI = 0.567, RI = 0.811. Sequences of members of the *Oryzomys megacephalus* species complex are used as the outgroup. Bold numbers at internal nodes are bootstrap values, based on 1000 replicates; percentages are mean Kimura two-parameter distances for all haplotypes below a given node. Haplotypes are identified by locality, as in the map, fig. 98, and provenance and voucher catalogue numbers are listed in table 36.

reported for specimens from the Rio Juruá (see below and Musser et al., 1998). Musser et al. (1998) document clinal size variation from west to east across the range of *O. macconnelli*, but they lacked samples from much of the geographically intermediate area between southern Venezuela and the south bank of the Rio Solimões necessary to determine whether the size cline is smoothly graded or stepped. As with *O. megacephalus* and *O. perenensis*, detailed sampling in the central Amazon on both sides of the Rio Solimões will provide the necessary documentation of whether *O. macconnelli*, as hypothesized by Musser et al. (1998), represents a single species, or is composite, as is suggested by the molecular and karyotypic data we summarize here.

The second area where the molecular sequence data suggest an alternative to the hypotheses advanced by Musser et al. (1998) is the species identification of specimens from

TABLE 37
Kimura 2-Parameter Distances Among Cytochrome-b Haplotypes of Members of the *Oryzomys macconnelli* Group
Number of haplotypes examined and mean ± standard error; within-taxon measures are given on the diagonal.

		macconnelli				
Taxon	n	N	S	*emmonsae*	*nitidus*	*russatus*
N	5	5.735 ± 0.926	11.103 ± 0.197	12.496 ± 0.169	14.627 ± 0.151	14.809 ± 0.182
S	9		3.542 ± 0.413	12.131 ± 0.203	14.677 ± 0.144	14.627 ± 0.204
emmonsae	3			0.756 ± 0.318	14.699 ± 0.211	12.399 ± 0.195
nitidus	8[a]				4.129 ± 0.308	15.689 ± 0.224
russatus	2					2.299

[a] Includes sequences from two specimens of *O. legatus* from Bolivia (MSB 67320 and 67359) which Musser et al. (1998) listed as *O. russatus*, based on their assessment that *legatus* is best associated with that taxon.

the Departamento de Tarija in southern Bolivia. Although this issue does not involve our perspectives of *Oryzomys* from the Rio Juruá, we provide the following comments both for completeness, and to suggest another future research direction. The voucher specimens for the two haplotypes from locality p in figure 98 and table 36 were examined by Musser et al. (1998), who considered them to represent the taxon *O. legatus* Thomas, which they further considered a synonym for *O. russatus* Wagner, otherwise distributed within the Mata Atlântica of southeastern Brazil. The sequence data, however, unequivocally link these two specimens within the clade of *O. nitidus* haplotypes, specifically those from specimens identified as that species by Musser et al. (1998) from localities in nearby Departamento de Santa Cruz (fig. 99). Consequently, the linkage of these specimens with *O. nitidus* in molecular characters suggests that the morphological similarly between *O. legatus* and *O. russatus* is convergent, and not indicative of common ancestry. Certainly, these data do not support the hypothesis that *legatus* is a synonym of *O. russatus*. Given the morphological distinctness of *legatus* relative to samples of *O. nitidus* from Bolivia (Musser et al., 1998), these taxa should be considered separate species, even if their mtDNA sequences are not reciprocally monophyletic. G. G. Musser (personal commun. to J.L.P., October 27, 1997) wrote that they "... almost kept *legatus* separate as a species but could not justify it morphologically."

As a final point, we note our specimens from the Serra dos Carajás (locality e in the map, fig. 98, and in table 36) are of both *O. macconnelli* and the recently described *O. emmonsae* (Musser et al., 1998), and thus represent the first instance of sympatry between these species.

Oryzomys species from the Rio Juruá

Four species of rice rats are present in the Rio Juruá basin: (1) *Oryzomys perenensis*, which occurs along the entire length of the Rio Juruá and is widespread throughout western Amazonia; (2) *Oryzomys yunganus*, morphologically similar to *O. perenensis* and also present throughout much of western and northern Amazonia, including the length of the Rio Juruá; (3) *Oryzomys macconnelli*, patchily distributed throughout much of Amazonia, as well as within the Rio Juruá basin; and (4) *Oryzomys nitidus*, which is limited largely to western Amazonia and the Paraná basin, and was only taken within the Headwaters Region of the Rio Juruá.

As noted above, these four are readily separable into two groups, each comprising two species, by several external and qualitative cranial features (table 38). The salient features of the skin are coloration and hair length, with both *O. perenensis* and *O. yunganus* typically dark brownish to reddish brown and with short dorsal fur. The range of color can be extensive within *O. perenensis*, both locally and geographically, but is much less so in *O. yunganus*. The pelage of *O. yunganus* also has a distinctive sheen that is hard to describe but evident to the expe-

TABLE 38
Distinguishing Features of Species of *Oryzomys* from the Rio Juruá[a]

Character	*perenensis*	*yunganus*	*macconnelli*	*nitidus*
Dorsal coloration	brownish tawny	brownish tawny	bright tawny	bright tawny
Ventral coloration	grayish white	grayish white	bright whitish	bright whitish
Juvenile dorsal color	brownish gray	brownish gray	reddish brown	reddish brown
Tail	monocolored	monocolored	bicolored	bicolored
Front and hind feet	white or pale tan	white or pale tan	solid white	solid white
Alisphenoid strut	present (>50%)	present (>50%)	absent (>98%)	absent (>98%)
Sphenofrontal foramen	absent	absent	present	present
Squamosal–alisphenoid groove	absent	absent	present	present
Second upper and lower molars	labial fossette (-id) only	labial and medial fossette (-id)	labial and medial fossette (-id)	labial and medial fossette (-id)

[a] Data largely from Musser et al. (1998).

rienced eye. In general, however, these two species are difficult to distinguish externally, so that identification may be quite problematical if one were only handling live animals in a longitudinal trapping program where vouchers are not prepared. *Oryzomys nitidus* has similar short, but yellowish or reddish brown dorsal fur, and immature individuals of this species have reddish, as opposed to grayish, fur. Finally, *O. macconnelli* is unique in its long and thickly luxuriant reddish brown pelage, making it one of the most readily recognizable murids in Amazonia. Both *O. macconnelli* and *O. nitidus* have the primitive cephalic arterial supply, characterized by the combination of enlarged stapedial foramen, squamosal-alisphenoid groove, and sphenofrontal foramen (pattern 1 of Voss, 1988; see Carleton and Musser, 1989). *Oryzomys perenensis* and *O. yunganus* lack the latter two features while maintaining an obvious stapedial foramen; they display a derived condition (pattern 2 of Voss, 1988; Carleton and Musser, 1989). In specimens with relatively unworn dentition, a medial fossette (-id) is present on the second molars of *O. yunganus*, *O. macconnelli*, and *O. nitidus*, but not in *O. perenensis*. Otherwise, *O. perenensis* and *O. yunganus* are quite similar morphologically, and careful examination of each specimen is required for secure identification. Additional characters, for example, which can be used to distinguish these two species include an increased degree in the development of palatal excrescences in *O. perenensis*, and shape of the incisive foraminal septum (Gardner and Patton, 1976; Musser et al., 1998), although the differences are subtle and comparisons must be carefully matched by age. Among other characters that are useful in distinguishing between *O. macconnelli* and *O. nitidus*, respectively, are shallow versus deep zygomatic notches, narrow versus wide zygomatic plates, teardrop-shaped and short rather than oval and long incisive foramina, and, therefore, long versus short palates. Exhaustive descriptions accompanied by informative illustrations of each of these taxa are presented by Musser et al. (1998), a work that should be examined carefully by anyone with an interest in any of these species.

External and cranial dimensions of our specimens of all four species from the Rio Juruá are given in table 39. All variables exhibit strong statistical significance when comparisons are made across all taxa simultaneously (one-way ANOVA, $p < 0.001$ for all variables except BOL and ZPL; table 40). Not surprisingly, however, individual variables exhibit combinations of significance and nonsignificance in pairwise comparisons, using Fisher's protected least significant difference, a multiple t-statistic, as a post hoc test of differences in one-way ANOVAs (table 40). The smallest species in virtually all measurements is *O. yunganus*, which is significantly smaller than *O. perenensis* in all dimensions except for IFL, AW, BOL, and ZPL. This is in contrast to other sites within western Amazonia where *O. yunganus* is typically larger (e.g., Quincemil, Perú [see

TABLE 39

Selected External and Cranial Dimensions for Four Species of *Oryzomys* from the Rio Juruá

Measurements (mm) are given as mean ± standard error, with range and sample size. Individuals are pooled across all localities along the river.

	O. perenensis			*O. yunganus*		
Variable	Mean ± SE	Range	n	Mean ± SE	Range	n
TOL	254.47 ± 1.11	197–303	245	227.83 ± 2.10	193–257	41
TAL	122.70 ± 0.67	82–151	245	104.39 ± 1.29	86–120	41
HF	31.88 ± 0.07	30–35	251	30.18 ± 0.18	28–32	41
E	20.37 ± 0.08	18–24	250	18.9 ± 0.19	16–22	41
CIL	29.85 ± 0.09	26.48–34.36	257	28.24 ± 0.19	25.75–30.42	45
ZB	16.61 ± 0.05	14.69–18.93	258	15.94 ± 0.09	14.46–16.99	46
MB	12.43 ± 0.03	11.28–13.70	258	12.04 ± 0.06	11.29–12.74	45
IOC	5.36 ± 0.01	4.69–6.32	258	5.14 ± 0.03	4.74–5.51	46
RL	12.48 ± 0.04	10.66–14.56	258	11.38 ± 0.09	10.19–12.79	46
NL	12.17 ± 0.05	9.92–14.30	258	11.52 ± 0.10	10.02–13.35	46
RW-1	6.44 ± 0.03	5.38–8.53	258	6.04 ± 0.07	5.30–7.00	46
RW-2	5.17 ± 0.02	4.26–6.31	258	4.80 ± 0.04	4.23–5.40	46
OL	11.16 ± 0.03	9.98–12.57	258	10.40 ± 0.07	9.28–11.33	46
D	8.83 ± 0.04	7.44–10.52	258	8.20 ± 0.07	7.22–9.12	46
MTRL	4.99 ± 0.01	4.58–5.51	258	4.80 ± 0.02	4.46–5.12	46
IFL	4.59 ± 0.02	3.62–5.66	258	4.59 ± 0.04	4.07–5.14	46
PL	14.45 ± 0.04	12.62–16.73	258	13.72 ± 0.10	12.54–14.86	46
AW	6.16 ± 0.02	5.43–7.29	258	6.23 ± 0.03	5.84–6.69	46
OCB	6.76 ± 0.02	6.15–7.68	257	6.65 ± 0.04	6.04–7.10	45
BOL	4.54 ± 0.02	3.76–5.42	257	4.50 ± 0.04	4.00–5.18	45
MPFL	4.97 ± 0.03	4.31–6.12	258	4.54 ± 0.04	4.03–5.07	45
MPFW	2.17 ± 0.01	1.68–2.56	258	2.40 ± 0.03	1.97–2.77	45
ZPW	3.59 ± 0.02	2.68–4.39	258	3.67 ± 0.04	3.19–4.38	45
CD	9.96 ± 0.02	9.05–10.84	258	9.64 ± 0.04	8.99–10.15	45

	O. macconnelli			*O. nitidus*		
Variable	Mean ± SE	Range	n	Mean ± SE	Range	n
TOL	290.79 ± 4.24	249–305	14	259.75 ± 9.81	204–293	4
TAL	149.50 ± 2.80	130–161	14	130.50 ± 9.35	105–150	4
HF	34.60 ± 0.39	33–38	15	34.00 ± 0.71	33–36	4
E	23.00 ± 0.32	21–25	15	21.50 ± 1.19	18–23	4
CIL	30.45 ± 0.31	27.56–32.07	17	30.07 ± 1.09	26.83–31.46	4
ZB	16.51 ± 0.18	14.88–17.48	17	16.64 ± 0.69	14.62–17.67	4
MB	12.70 ± 0.10	11.89–13.48	17	12.70 ± 0.31	11.85–13.17	4
IOC	5.50 ± 0.06	5.10–5.96	17	5.27 ± 0.10	5.01–5.49	4
RL	13.12 ± 0.13	11.85–13.73	17	13.02 ± 0.62	11.16–13.73	4
NL	13.25 ± 0.18	11.65–14.29	17	13.51 ± 0.80	11.24–14.88	4
RW-1	6.47 ± 0.10	5.85–7.16	17	6.38 ± 0.31	5.48–6.82	4
RW-2	5.18 ± 0.08	4.54–5.72	17	5.14 ± 0.26	4.40–5.60	4
OL	10.99 ± 0.11	9.89–11.71	17	11.41 ± 0.43	10.29–12.19	4
D	9.04 ± 0.13	7.72–9.71	17	8.73 ± 0.36	7.66–9.13	4
MTRL	5.09 ± 0.03	4.86–5.42	17	4.84 ± 0.12	4.61–5.09	4
IFL	5.14 ± 0.08	4.66–5.79	17	5.65 ± 0.20	5.27–5.99	4
PL	14.80 ± 0.15	13.59–15.90	17	13.91 ± 0.46	12.56–14.62	4
AW	6.44 ± 0.06	5.99–6.87	17	6.28 ± 0.13	5.92–6.51	4
OCB	6.98 ± 0.08	6.23–7.45	17	6.66 ± 0.17	6.32–7.14	4
BOL	4.58 ± 0.07	4.02–5.08	17	4.46 ± 0.25	3.77–4.91	4
MPFL	5.04 ± 0.09	4.05–5.69	17	5.29 ± 0.18	4.81–5.58	4
MPFW	2.39 ± 0.04	2.13–2.80	17	2.12 ± 0.09	1.87–2.24	4
ZPW	3.46 ± 0.04	3.12–3.81	17	3.72 ± 0.27	2.95–4.19	4
CD	9.98 ± 0.09	9.50–10.96	17	10.19 ± 0.24	9.52–10.54	4

TABLE 40
Character Significance Between Four Species of *Oryzomys* from the Rio Juruá
Overall significance is based on factorial ANOVA, with pairwise comparisons between size-ranked (from left to right) species based on a post-hoc Fisher's protected least squares difference, a multiple *t*-statistic (ns = $p > 0.05$; * $p < 0.05$; ** $p < 0.01$; *** $p < 0.001$).

Variable	df	*F*	*p*	Size ranking and significance[a]					
TOL	3, 300	52.667	***	y	***	p	***	n	***	m
TAL	3, 300	73.286	***	y	***	p	ns	n	***	m
HF	3, 307	49.933	***	y	***	p	***	n	ns	m
E	3, 306	40.138	***	y	***	p	ns	n	*	m
CIL	3, 319	18.349	***	y	***	p	ns	n	ns	m
ZB	3, 321	8.966	***	y	ns	m	*	p	**	n
MB	3, 321	15.753	***	y	***	p	***	m	ns	n
IOC	3, 321	15.783	***	y	ns	n	ns	p	*	m
RL	3, 321	39.338	***	y	***	p	ns	n	ns	m
NL	3, 321	23.738	***	y	***	p	***	m	ns	n
RW-1	3, 321	8.815	***	y	***	p	ns	n	ns	m
RW-2	3, 321	19.016	***	y	*	n	ns	p	ns	m
OL	3, 321	31.230	***	y	***	m	ns	p	ns	n
D	3, 321	17.842	***	y	ns	n	ns	p	ns	m
MTRL	3, 321	20.278	***	y	ns	n	ns	p	*	m
IFL	3, 321	26.463	***	y	ns	p	***	m	**	n
PL	3, 321	17.310	***	y	ns	n	ns	p	*	m
AW	3, 321	6.090	***	p	ns	y	ns	n	ns	m
OCB	3, 321	6.832	***	y	ns	n	ns	p	***	m
BOL	3, 321	0.443	ns	n	ns	y	ns	p	ns	m
MPFL	3, 320	17.433	***	y	***	p	ns	m	ns	n
MPFW	3, 320	32.831	***	n	ns	p	***	m	ns	y
ZPL	3, 321	2.479	ns	m	ns	p	ns	y	ns	n
CD	3, 321	13.156	***	y	***	p	ns	m	ns	n

[a] Size increases from left to right. y = *O. yunganus*; p = *O. perenensis*; m = *O. macconnelli*; n = *O. nitidus*.

Musser et al., 1998]). *Oryzomys macconnelli* is the largest species, in 15 of 24 variables, and *O. nitidus* is usually next largest. Thus, the combination of size dimensions coupled with coloration, fur quality, cephalic arterial pattern, and details of the second molars serve to differentiate all four species (table 38).

Multivariate relationships among the four species were ascertained by discriminant analysis, using $\log_{10}$ transformations of the 20 cranial variables. Standardized coefficients for each variable for the three possible discriminant axes are given in table 41. The first axis cleanly separates *O. yunganus* from *O. perenensis* (fig. 100), with taxa combining relatively short skulls with longer rostra, or the reverse, based on those characters with the highest loadings. The second axis primarily separates *O. macconnelli* and *O. nitidus*, as a pair, from the first two, while these two species become completely separated on the third axis (fig. 100). Posterior probability scores generated from the discriminant analysis allocated individual specimens nearly perfectly to their appropriate species. Three of 258 specimens of *O. perenensis* were misclassified as *O. yunganus* and two of 46 *O. yunganus* were misclassified as *O. perenensis*. All specimens of both *O. macconnelli* and *O. nitidus* were correctly classified.

In the species accounts below, we present analyses of patterns of morphometric variation relative to age and sexual dimorphism, and examine interpopulation differentiation along the Rio Juruá for both *O. perenensis* and *O. yunganus*. Inadequate sample sizes precluded these analyses for the other two species. We also summarize habitat and other ecological data and discuss patterns of reproduction.

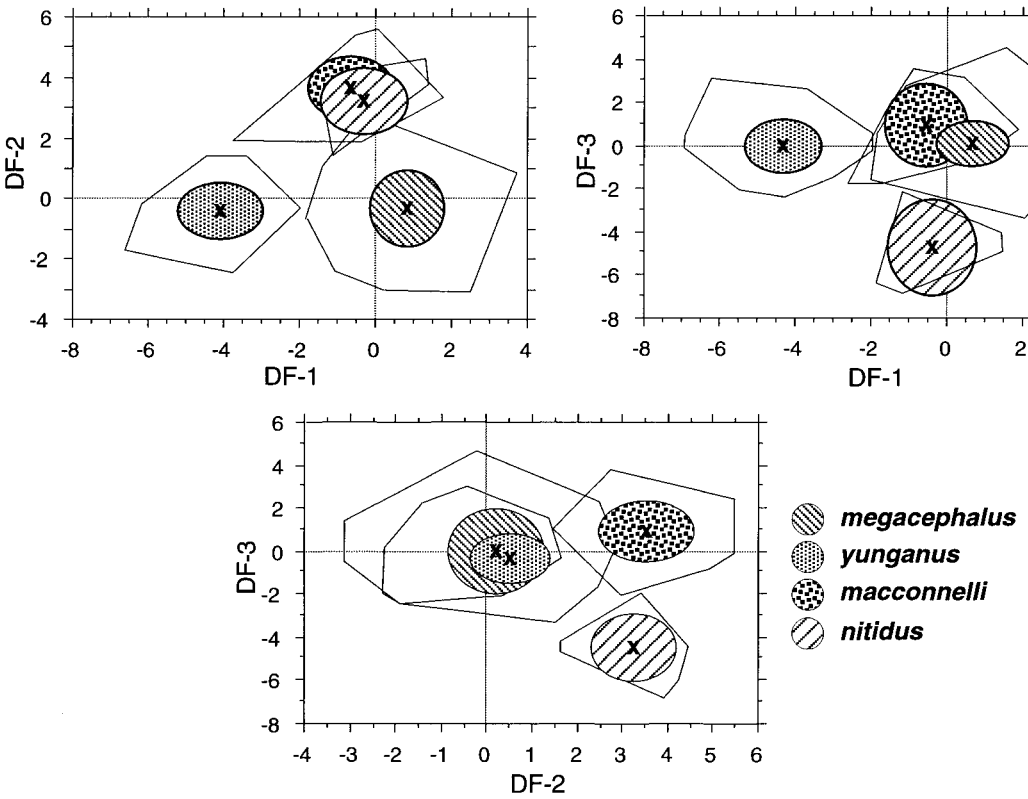

Fig. 100. Bivariate plots of the three discriminant axes in comparisons between the four species of *Oryzomys* that occur along the Rio Juruá. The open polygons surround the placement of all individuals of each species; the ellipses represent the 95% confidence limits of the mean scores for each species on the respective axes being contrasted.

Oryzomys perenensis (Allen, 1901)

TYPE LOCALITY: ''Perené, Department of Junin, Peru; altitude 800 m''; given by Musser et al. (1998: 51) as ''Valle Perené, Colonia del Perené; a coffee plantation at junction of ríos Paucartambo and Chanchamayo' [Stephens and Traylor, 1983: 161], 10°51′S/75°13′W, 1000 m.''

DESCRIPTION: See discussion, above, tables 38 and 40, and figure 101. Musser et al. (1998: 18–42) provide thorough analyses of qualitative and quantitative morphological variation along with excellent illustrations of crania and teeth of this, and other species of the *O.* ''*megacephalus*'' complex.

MORPHOMETRIC VARIATION: The proportion of variation in mensural dimensions of the skin and cranium of adults (age classes 3 and above) due to sex, age, or geographic locality was examined by an ANOVA nested by locality, sex, and age (table 42). Sexual dimorphism is virtually non-existent, accounting for an average of less than 1% of the total pool of variation. In a similar fashion, variation due to locality is also minimal, with an average of only 2.6% due to differences among localities along the 1000 km length of the Rio Juruá. However, a substantial degree of the total variation (31.4%) is related to an individual's age, regardless of sex or locality. Indeed, all variables exhibited a significant relationship with age ($p < 0.001$), except IOC and MTRL (fig. 102). While pooling sexes is justifiable because of the lack of demonstrable sexual dimorphism, ordinarily some adjustment for the large age effect might be required in comparisons between localities (see, for example, Myers et al., 1990, for such an ''adjustment'' in geographic analyses of Andean mice of the ge-

TABLE 41
Standardized Discriminant Coefficients in Comparisons Among Four Species of *Oryzomys* from the Rio Juruá
Analyses are based on $\log_{10}$-transformed cranial variables only.

Variable	DF-1	DF-2	DF-3
Log CIL	−1.16097	0.67179	−0.40062
Log ZB	0.21994	−0.87319	−0.03073
Log MB	0.09118	0.32535	−0.20331
Log IOC	0.07436	0.13261	0.14281
Log RL	1.08398	0.57515	−0.14227
Log NL	−0.53550	0.85364	−0.11233
Log RW-1	−0.28208	−0.32385	−0.37139
Log RW-2	0.58299	0.06472	0.18223
Log OL	0.90921	−0.20314	−0.69163
Log D	1.03580	−0.62718	0.52176
Log MTRL	0.53291	−0.05901	0.29090
Log IFL	−0.37462	0.46528	−0.55464
Log PL	−0.38005	−0.19950	1.43522
Log AW	−0.49142	0.53555	0.20512
Log OCB	0.07172	0.02447	0.23689
Log BOL	−0.21418	−.033282	0.23535
Log MPFL	0.19947	−0.10335	0.02861
Log MPFW	−0.49693	0.22145	0.31883
Log ZPL	−0.60366	−0.59528	−0.52735
Log CD	0.10682	−0.04173	−0.24442
Eigenvalue	2.80949	0.864001	0.294215
% contribution	70.809	21.776	7.415

nus *Akodon*). However, as there were no differences among those samples of reasonable sizes ($n > 20$) in their respective age distributions ($\chi^2 = 13.417$, df = 13, $p = 0.3395$), we pooled all individuals regardless of their ages and sex. Interlocality comparisons based on simple pooled or on age-corrected data did not differ in their results.

Musser et al. (1998) examined the pattern of variation among our samples from the Rio Juruá, and for a set of cranial variables similar to those we measured. Based on a standard principal components analysis (PCA), they found no pattern of differentiation, and particularly none associated with samples from opposite banks of the river. That is, there was no measurable ''riverine'' effect. We used the multiple groups principal components analysis (Thorpe, 1983; Thorpe and Baez, 1987) to ask the same question. This method has the advantage over ordinary PCA in that it does not confuse the within- and among-group variation when several groups are used; rather, MGPCA gives pooled within-group components, with the first axis derived from the variance-covariance matrix usually an index of overall size. The results of the multiple groups PCA (fig. 103) are identical to those of Musser et al. (1998). There is no statistical difference in pairwise comparisons between opposite-bank samples, nor is there any difference between samples for the four geographic regions ($p > 0.05$ in all comparisons of individual scores for any of the MGPCA axes). Furthermore, only 42.4% of individual specimens are correctly allocated to their appropriate locality, based on posterior probabilities stemming from a discriminant analysis. Not surprisingly, therefore, there is also no relationship between matrices of morphometric Mahalanobis distances and the geographic distances among localities (Mantel's matrix $r = 0.0905$; $t = 1.220$; $p = 0.888$).

MOLECULAR PHYLOGEOGRAPHY: The lack of demonstrable geographic differentiation in morphometric variables among samples of *O. perenensis* collected along the nearly 1000 km length of the Rio Juruá is completely concordant with the pattern of mtDNA cytochrome-b haplotype variation these same samples exhibit (Patton et al., 1996a). For the latter, hierarchical analyses showed that the majority (89.2%) of the molecular variance was apportioned among individuals within populations, and that only a small fraction could be either attributed to differences among localities within one of the regional samples (6.6%) or even between the regions themselves (4.2%). There was also no evidence of isolation by distance, as there was no significant relationship between logM and logDistance (Mantel's matrix $r = 0.094$, $t = 0.802$, $p > 0.788$; Patton et al., 1996a). Either populations of this species throughout the Rio Juruá have recently entered and expanded within the river basin, and thus have not yet achieved genetic equilibrium, or local populations are, and have been, linked by considerable gene flow (see discussion in Patton et al., 1996a). The second possibility seems likely, since estimates of the gene flow parameter, M (Slatkin, 1993), were uniformly high, averaging 17.34 across all among-population comparisons. To put this value into perspective, it only takes a single successful

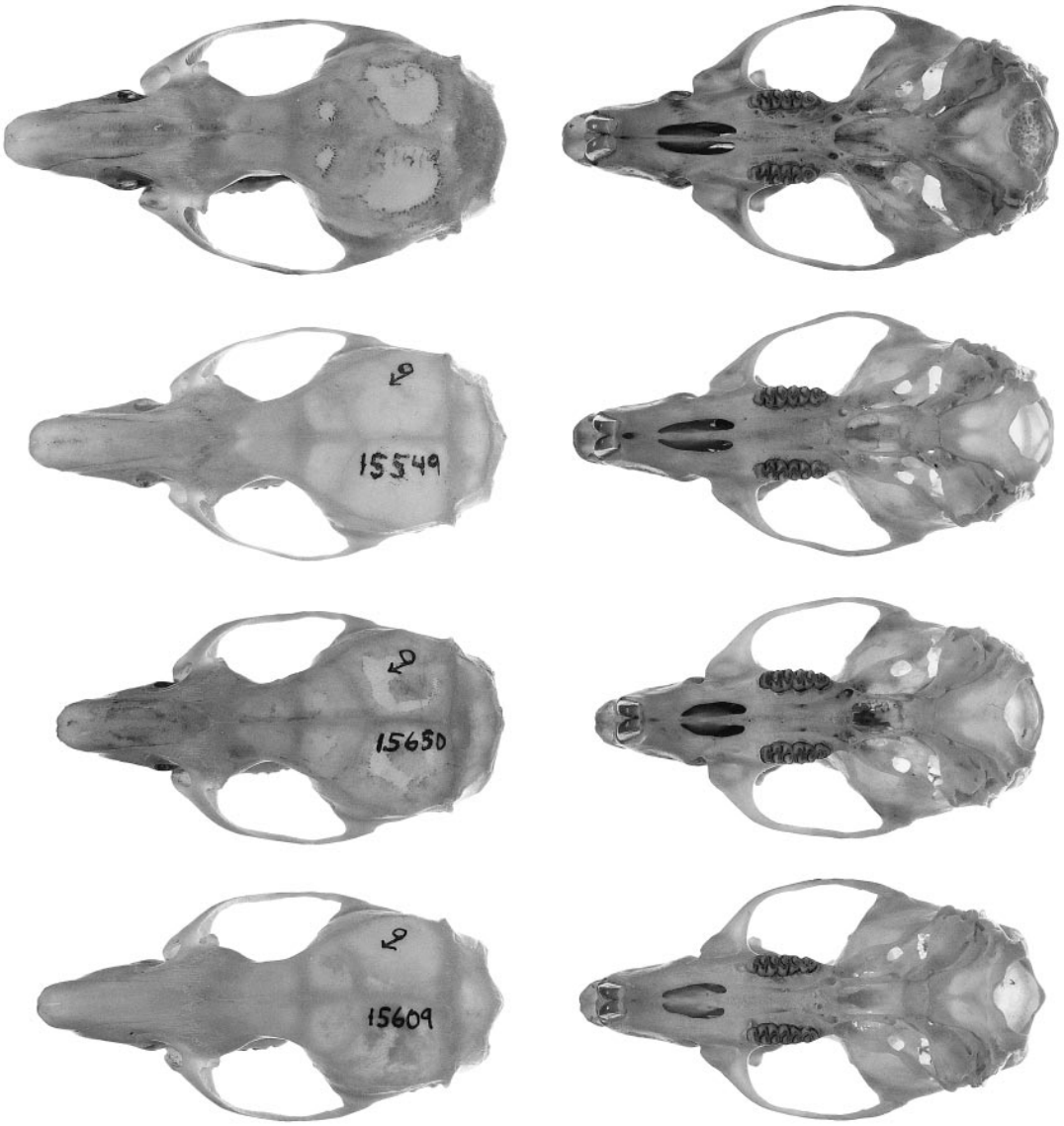

Fig. 101. Dorsal (left) and ventral (right) views of the crania of four species of rice rats, *Oryzomys*, from the Rio Juruá. From bottom to top: *O. perenensis* (JLP 15609; Seringal Condor [locality **6**], left bank Rio Juruá, Amazonas, Brazil); *O. yunganus* (JLP 15650; Seringal Condor [locality **6**], left bank Rio Juruá, Amazonas, Brazil); *O. macconnelli* (JLP 15549; Seringal Condor [locality **6**], left bank Rio Juruá, Amazonas, Brazil); and *O. nitidus* (MNFS 1419; Igarapé Porongaba [locality **1**], right bank Rio Juruá, Acre, Brazil).

migrant per generation (M of 1.0) to prevent two populations from diverging by drift alone (see review by Mills and Allendorf, 1996). Both the large number of haplotypes found (47 within a total sample of 158 individuals) and the large number of unique, but low-frequency haplotypes recovered from each population and geographic region, suggest that the genetically effective population of this species has been historically large and remains so today. These conclusions are in harmony with what few data are

TABLE 42
Proportion of Variance in Mensural Variables of Adult Specimens (Age Classes 3–5) of *Oryzomys perenensis* due to Sex, Age, or Locality
Based on a nested analysis of variance (see text)
(ns = $p > 0.05$; * $p < 0.05$; ** $p < 0.01$; *** $p < 0.001$).

	% explained variance			
Variable	Sex	Age	Locality	Error
TOL	0.00 ns	40.97**	1.26 ns	57.77
TAL	0.00 ns	34.10**	6.49 ns	59.41
HF	9.82 ns	3.97 ns	0.00 ns	86.31
E	0.00 ns	17.51 ns	11.53*	70.96
CIL	0.00 ns	56.78***	4.59 ns	38.63
ZB	0.00 ns	57.78***	1.39 ns	40.93
MB	0.00 ns	0.00 ns	2.16 ns	97.84
IOC	0.00 ns	0.00 ns	0.54 ns	99.46
RL	0.00 ns	44.10***	5.26 ns	50.64
NL	0.00 ns	39.25**	1.92 ns	58.83
RW-1	0.00 ns	53.40***	0.00 ns	46.60
RW-2	0.00 ns	46.82***	5.72 ns	47.45
OL	0.00 ns	41.23**	4.30 ns	54.47
D	0.00 ns	56.20***	1.73 ns	42.07
MTRL	0.00 ns	5.19 ns	0.00 ns	94.81
IFL	6.61 ns	8.84 ns	0.00 ns	84.55
PL	0.00 ns	56.64***	0.32 ns	43.04
AW	0.00 ns	35.10**	0.85 ns	64.05
OCB	0.88 ns	18.06 ns	0.81 ns	80.25
BOL	0.00 ns	35.40**	0.00 ns	64.60
MPFL	0.00 ns	39.30**	2.99 ns	57.71
MPFW	0.00 ns	16.94 ns	4.82 ns	78.23
ZPL	0.00 ns	34.50**	6.24 ns	59.26
CD	2.48 ns	11.41 ns	0.15 ns	85.96
Mean	0.825	31.395	2.638	65.142

available on reproductive potential and habitat range, as summarized next.

DISTRIBUTION AND HABITAT: Individuals of *O. perenensis* were found in virtually every terrestrial habitat present along the river, even occasionally in the dense grass growing on exposed sand bars during low water seasons. However, this species was twice as common in várzea forest than terra firme, or other habitats (table 43). Its numbers in relatively open, disturbed habitats, such as those along the river margins, were exceeded only by *Oligoryzomys microtis*. It was also uniformly the most common terrestrial rodent in both our terra firme and várzea standardized plots, being exceeded in numbers at particular sites only by one or more species of spiny rats, *Proechimys*. The species was captured only in traps placed on the ground, never in those placed a meter or two in the lower vegetation, nor in the canopy platform traps on the standardized lines. The high densities and broad habitat tolerances of *O. perenensis* along the Rio Juruá is typical of our, and others, experiences with this species elsewhere within western Amazonia (e.g., the Río Cenepa, Departamento de Amazonas, and Balta, Departamento de Ucayali, Perú [J. L. Patton, personal observations], and Cuzco Amazónico, Departamento de Madre de Dios, Perú [Woodman et al., 1995]).

REPRODUCTION: We caught reproductively active individuals of both sexes at each site, and during every survey month from August through June. At each locality and regardless of month, nearly every adult male had scrotal testes and enlarged vesicular glands (>16 mm in length, maximum 24 mm) indicative of breeding activity. This suggests that males are competent throughout the year. More than 75% (79/105) of the total sample of adult females (those of age class 3 or older) were pregnant, and pregnant females comprised more than 50% of all adults at each site. The modal litter size, based on fetal counts, was 4; range 2–5. Pregnancy rates were lowest during the months of August through September in the Upper Central Region (13 of 23 adult females, 56.5%), but much higher in all other sampling periods and areas (Lower Central Region, October and November, 19 of 24, 79.2%; Headwaters Region, February and March, 33 of 40, 82.5%; Mouth Region, May and June, 14 of 18, 77.8%). All remaining nonpregnant adult females were either lactating or parous, with evident placental scars indicating relatively recent pregnancies. As with males, therefore, females probably breed yearround. Finally, juveniles of both sexes in sparse, gray pelage, were captured at all sampling periods throughout the year, although not at every site, again supporting rather continuous reproductive activity spanning both dry and rainy seasons. A similar pattern of reproductive activity was observed for *O. megacephalus* in French Guiana (Henry, 1994).

Both males and females begin breeding at early ages, at least based on the association of reproductive state and toothwear age classes. Males apparently do not reach reproduc-

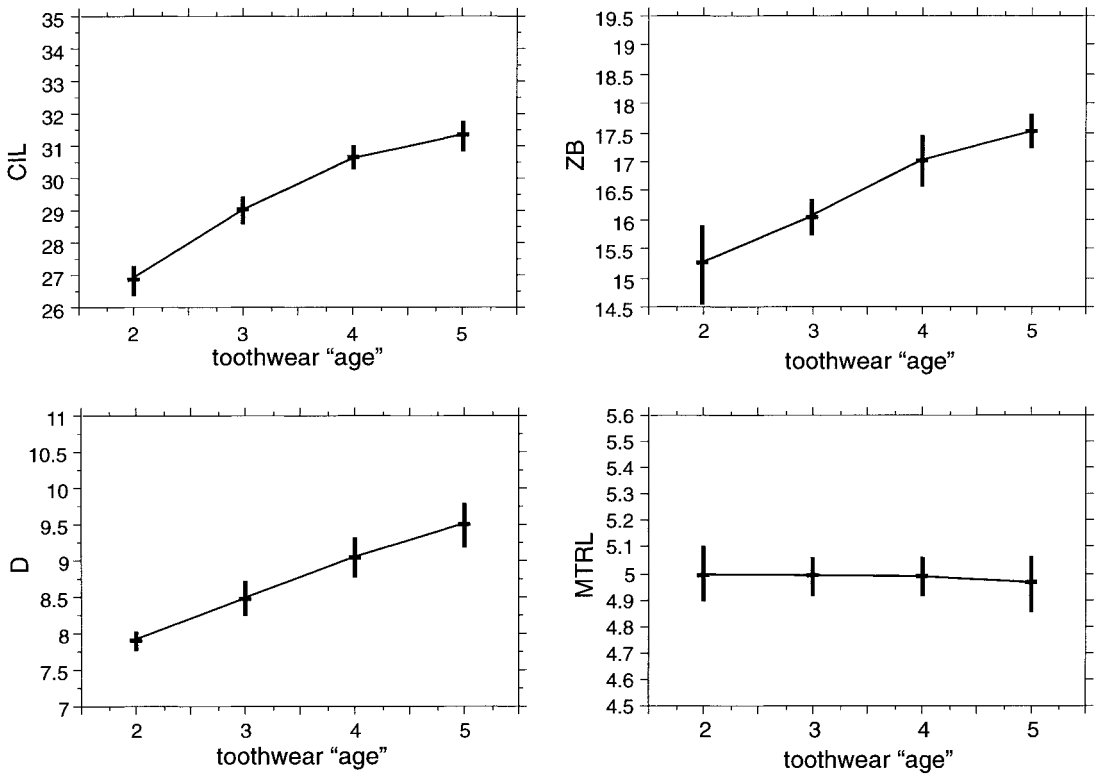

Fig. 102. Size versus age (toothwear class) for four cranial dimensions from pooled samples of *Oryzomys perenensis* from the Rio Juruá. Solid curve for each plot shows average value of the measurement for each class; vertical lines are 95% confidence limits.

tive competency until age class 2, and even a small fraction of older individuals were apparently not breeding (fig. 104). Females, however, entered what appeared to be their first estrous even before their third molars were fully in place (age class 1), and more than 25% of age class 2 individuals were pregnant (fig. 104). If growth in rice rats is at all similar to that of deer mice (e.g., *Peromyscus truei*; Hoffmeister, 1951), breeding commences within one month after birth in both sexes.

Males were invariably more commonly trapped than females in all months (and therefore at all individual sites), although the proportion of females in each sample was higher when the pregnancy rates were highest. Perhaps males are more exploratory, or have larger home ranges than females, and females with young in the nest make fewer nightly movements than do those that are pregnant.

KARYOTYPE: 2n = 52, FN = 62. The autosomal complement consists of 25 acrocentric chromosomes grading in size from large to small and six pairs of small metacentric or submetacentric elements. The X-chromosome is a medium large acrocentric chromosome, the Y is small and acrocentric. This karyotype was described and figured by Gardner and Patton (1976) based on specimens from localities in eastern Perú, and individuals with the same karyotype have been reported from central Perú and eastern Ecuador (Musser et al., 1998: table 13). Seventy-six individuals were karyotyped, from the following localities: Porongaba (locality **1**), n = 18; Nova Vida (locality **3**), n = 6; Sobral (locality **4**), n = 3; Sacado (locality **5**), n = 4; Condor (locality **6**), n = 4; Penedo (locality **7**), n = 3; Boa Esperança (locality **9a**), n = 1; Jainu (locality **11**), n = 3; Barro Vermelho (locality **12**), n = 6; Vira-Volta (locality **14**), n = 22; Vai-Quem-Quer (lo-

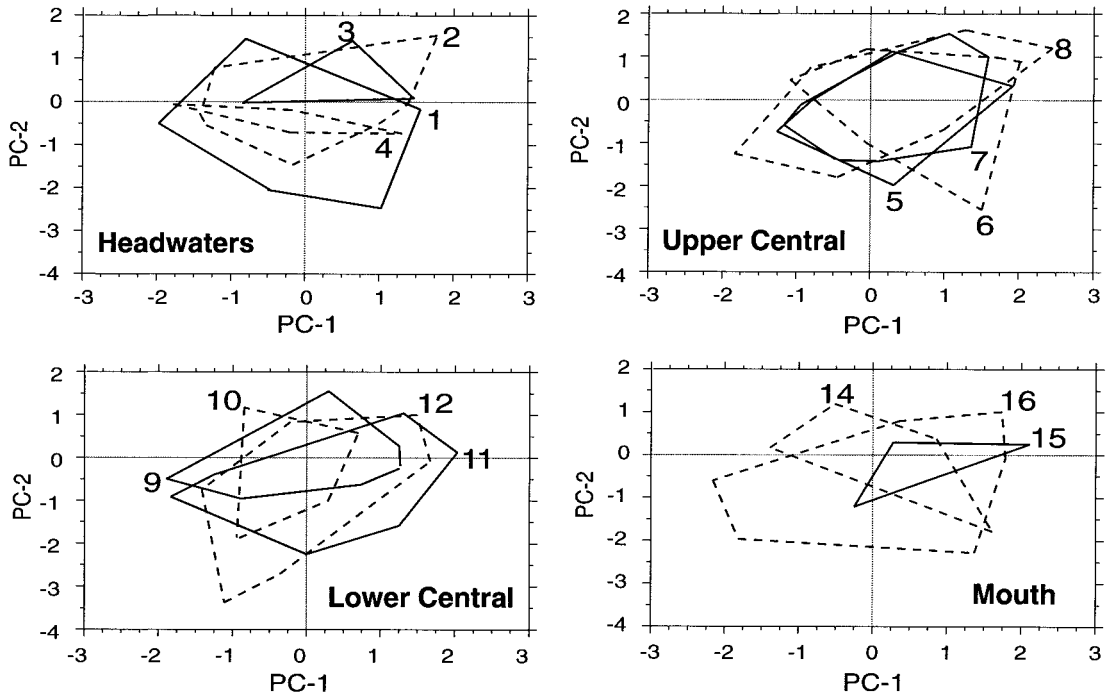

Fig. 103. Bivariate plots of the first and second multiple groups principal components axes for *Oryzomys perenensis* from the Rio Juruá. Panels separate samples from each of the four geographic sample regions (see fig. 1); polygons enclose all individual points for a given sample, which is identified by locality number.

TABLE 43
Captures of *Oryzomys perenensis* and *Oryzomys yunganus* Relative to Habitat Type and Geographic Region[a]

Region	Terra firme	Várzea	Other[b]
	O. perenensis		
Headwaters	38	83	13
Upper Central	34	97	24
Lower Central	10	86	3
Total	82	266	40
	O. yunganus		
Headwaters	11	21	4
Upper Central	47	18	9
Lower Central	3	10	0
Total	61	49	13

[a] Excludes the Mouth Region, which was sampled during the high water season so that várzea forest was not available.
[b] Includes all disturbed habitats, natural or man-induced.

cality **15**), n = 3; and Ilhazinha (locality **16**), n = 3.

SPECIMENS EXAMINED (n = 466): (**1**) 21m, 17f — MNFS 1100, 1115–1116, 1120, 1143–1146, 1148–1149, 1168–1170, 1173, 1204–1207, 1224–1227, 1229, 1259, 1264, 1268, 1296–1297, 1309, 1329–1330, 1381–1382, 1400, 1418, 1421–1423; (**2**) 23m, 24f — MNFS 1180, 1239, 1241–1244, 1246, 1248–1249, 1251, 1276–1282, 1304–1307, 1334–1335, 1340–1346, 1348, 1367–1375, 1388, 1390–1391, 1405–1408; (**3**) 13m, 16f, 1 unknown — JUR 213, 228, 237, MNFS 1554, 1558–1560, 1582–1587, 1597, 1609, 1612–1614, 1622, 1629, 1631–1632, 1641, 1648–1649, 1651, 1675–1678; (**4**) 9m, 10f — JUR 216, 218–219, 233, 246, MNFS 1436, 1454, 1462, 1464, 1466, 1480, 1492, 1497–1498, 1534, 1566, 1574–1575, 1669; (**5**) 27m, 19f, 4 unknown — JUR 132, 135, 144–156, 158–169, 171, 173–175, MNFS 582, 586–588, 621, 629–635, 643–646, 655–657; (**6**) 15m, 10f — JLP 15529, 15536,

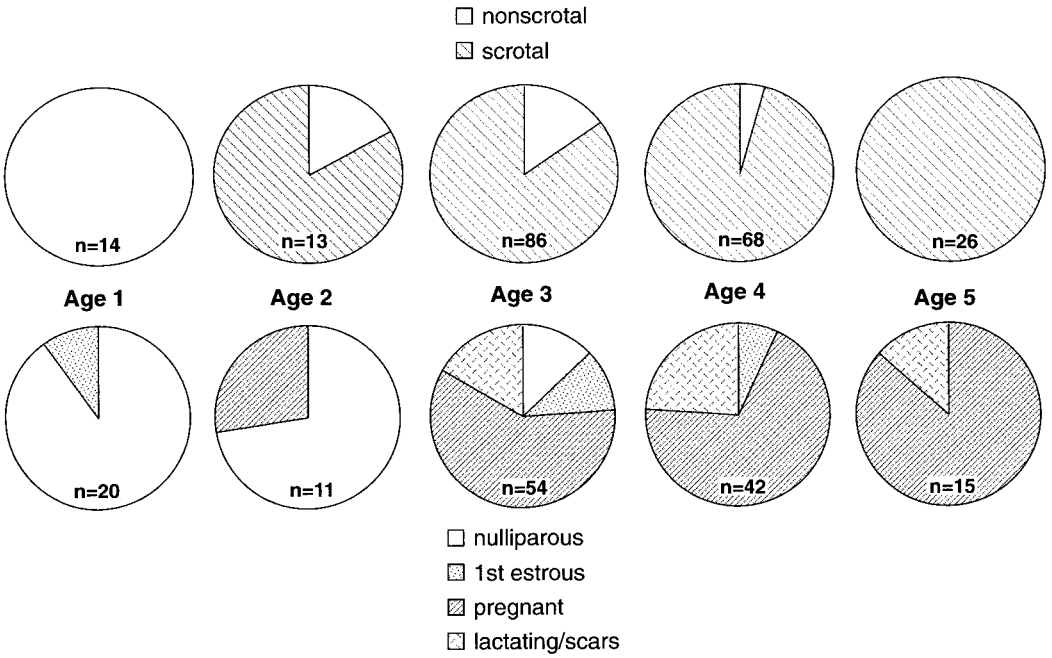

Fig. 104. Pie diagrams of the proportion of reproductive states for toothwear age classes of male (above) and female (below) *Oryzomys perenensis* pooled across all localities from the Rio Juruá. See text for explanation of character states for both sexes.

15564, 15604, 15609, 15646–15647, 15663, 15667, 15687–15689, 15694–15697, 15706–15707, 15719, 15723, 15726–15729, 15740; (**e**) 1f — JLP 15713; (**7**) 34m, 11f, 4 unknown — JLP 15229–15232, 15238–15240, 15243, 15248–15249, 15256, 15259, 15263, 15272, 15274, 15291, 15302, 15304, 15311, 15322, 15330–15332, 15362, 15427, 15441–15442, 15455–15456, 15480, 15499, 15507, MNFS 329–330, 385, 389, 404–405, 420–423, 488–490, 498, 510, 518, 520–521; (**8**) 18m, 11f, 2 unknown — JLP 15415–15422, 15447, JUR 1, 4, 6, 10–11, 14, 33–34, 36, 38–40, 42–43, 47, 72, 76–79, 114, MNFS 440; (**9**) 4m, 5f — JLP 15967–15968, 15989, 16026–16029, 16067, 16081; (**9a**) 6m, 3f — JUR 190, MNFS 922, 924, 930, 937–938, 960–962; (**10**) 4m, 3f — JLP 16030, MNFS 896–897, 917, 952–954; (**11**) 13m, 11f — JLP 15752, 15758, 15822–15825, MNFS 693–694, 696, 698–699, 705–707, 712–713, 716, 751, 765–768, 786–787; (**12**) 40m, 15f — JLP 15748, 15762–15763, 15768–15773, 15782–15783, 15790, 15813, 15828, 15839–15845, 15865, 15871–15872, 15875–15877, 15881–15884, 15892–15893, 15901, MNFS 682, 685–686, 736–738, 750, 761, 774–779, 807–808, 818, 821–822, 827–828; (**13**) 1f — JUR 263; (**14**) 31m, 16f — JUR 418–427, 441–444, 446–447, 454–456, 465, 473, 475, 481–482, 490–493, 514–516, 522–523, 525, 531, 536, 552, 554, 556, 558, 561–562, 568–570; MNFS 1685, 1791; (**15**) 2m, 2f — JUR 288, 295, 300, 394; (**16**) 10m, 10f — JUR 510–513, 527–530, 537–539, 551, 553, 563–564, MNFS 1785–1786, 1794.

Oryzomys yunganus Thomas 1902

TYPE LOCALITY: ''Charuplaya, 1350 m,'' Río Securé, Departamento de Cochabamba, Bolivia, 16°36′S, 66°37′W (see Musser et al., 1998: 52).

DESCRIPTION: This is the second species of *Oryzomys* found within the Rio Juruá basin with the derived cephalic arterial pattern. As noted above and as detailed by Musser et al. (1998), *O. yunganus* is extremely similar in both external and cranial features to *O. perenensis*, but can be distinguished from that species by a combination of pelage and cranial qualitative features (table 38). However,

as also emphasized by these authors, careful examination of voucher specimens will likely be required to distinguish *O. yunganus* and *O. perenensis*. Certainly, identification of these in the field during live-trapping studies cannot be readily accomplished, and will require considerable experience with both taxa. See tables 38 and 40 and figures 99 and 100.

SELECTED MEASUREMENTS: Means, standard errors, and ranges of selected external and cranial dimensions are given in table 39.

GEOGRAPHIC VARIATION: Samples of *O. yunganus* are limited in size, but available for most localities and, thus, all geographic regions along the length of the Rio Juruá. The pattern of nongeographic variation due to age and sex is of the same nature as described above for *O. perenensis*, with virtually no contribution of sex to the overall variation (average of 1.2% across the four external and 20 cranial variables; table 44). Not surprisingly, age exhibits a much greater proportion to the total pool of variation, averaging 35.7% across all variables for adult individuals. Also as was characteristic for *O. perenensis*, there is virtually no among-locality differentiation detectable, with only 3.1% of the variation referable to this component. As a consequence, it is not possible to distinguish among any of the samples of *O. yunganus*, whether comparisons are made along or across the river. Again, this species is morphologically uniform throughout the Rio Juruá basin, an observation fully concordant with our limited molecular haplotype data.

TABLE 44
Proportion of Variance in Mensural Variables of Adult Specimens (Age Classes 3–5) of *Oryzomys yunganus* due to Sex, Age, or Locality
Based on a nested analysis of variance (see text) (ns = $p > 0.05$; * $p < 0.05$; ** $p < 0.01$; *** $p < 0.001$).

	% explained variance			
Variable	Sex	Age	Locality	Error
TOL	0.00 ns	47.37*	0.99 ns	51.64
TAL	0.00 ns	30.38 ns	6.63 ns	62.99
HF	0.00 ns	10.74 ns	11.07 ns	78.19
E	0.00 ns	4.72 ns	19.29 ns	75.99
CIL	0.00 ns	60.80*	0.00 ns	30.20
ZB	0.00 ns	56.50*	0.00 ns	43.50
MB	0.00 ns	39.03 ns	0.00 ns	60.97
IOC	21.85 ns	12.93 ns	0.00 ns	65.22
RL	0.00 ns	55.61*	0.00 ns	44.39
NL	0.00 ns	52.04*	6.39 ns	41.57
RW-1	0.00 ns	55.74*	0.00 ns	44.26
RW-2	0.00 ns	22.42 ns	0.00 ns	77.58
OL	0.00 ns	52.22*	0.00 ns	47.78
D	0.00 ns	63.07*	0.00 ns	36.93
MTRL	2.82 ns	0.00 ns	3.04 ns	94.14
IFL	0.00 ns	33.68 ns	10.76 ns	55.56
PL	0.00 ns	53.30*	0.00 ns	46.70
AW	0.00 ns	23.07 ns	13.67 ns	63.26
OCB	0.00 ns	30.29 ns	0.98 ns	68.73
BOL	0.00 ns	58.51*	0.00 ns	41.49
MPFL	0.00 ns	37.15 ns	0.75 ns	62.10
MPFW	5.03 ns	15.50 ns	0.00 ns	79.47
ZPL	0.00 ns	24.68 ns	1.77 ns	73.56
CD	0.00 ns	17.58 ns	0.00 ns	82.42
Mean	1.238	35.722	3.139	59.901

MOLECULAR PHYLOGEOGRAPHY: While our sampling for molecular variation is not nearly as extensive as it was for *O. perenensis* (above, and Patton et al., 1996a), we have examined 25 individuals from 12 localities. Eleven separate haplotypes were recovered from sequences of the initial 414 bp of the cytochrome-b gene. An unrooted network of these is shown in figure 84. A few haplotypes are reasonably divergent from all others, differing by six or seven steps from adjacent ones in the network, but most differ only by one or two steps. The average number of steps between adjacent haplotypes is 3.2, which is, however, nearly three times that observed for haplotype variation in *O. perenensis* (Patton et al., 1996a, as *O. capito*). Nevertheless, this still represents an average divergence of less than 1%. Viewed geographically, there is some apparent structure along the river, but none related to samples from opposite banks. With the exception of a single haplotype from locality **2** and another from locality **12**, there is an exact correspondence between position of haplotypes in the network and the geographic placement of the localities from which they were sampled (fig. 105). One haplotype is broadly shared between the Headwaters localities of Nova Vida (locality **3**) and Sobral (locality **4**) as well as all of those from the Upper Central Region (Condor, Penedo, and Nova Empresa [localities **6**, **7**, and **8**, respectively]). The remainder of those haplotypes from Headwaters sites are closely related to this broadly

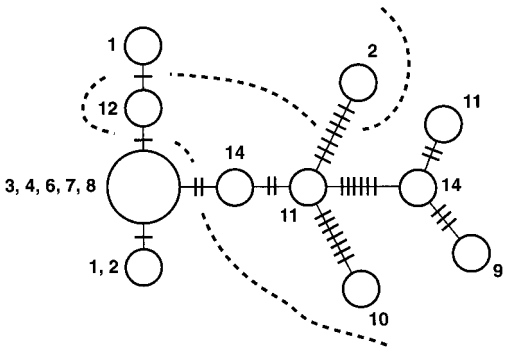

Fig. 105. Unrooted network of 11 haplotypes of a 414 bp fragment of the mtDNA cytochrome-b gene obtained from 25 individuals of *Oryzomys yunganus*. The number of mutational steps between adjacent haplotypes is indicated by the bars. Numbers indicate the localities from which each haplotype was recovered (from the map, fig. 1). The dashed line separates haplotypes from the Headwaters and Upper Central regions (to the left) from those of the Lower Central and Mouth regions.

distributed one, with the single exception from the left bank opposite Igarapé Porongaba (locality **2**), noted above. This group shares a much greater degree of similarity among themselves than do the cluster of haplotypes from either Lower Central or Mouth sites. It is also noteworthy that only two of the four haplotypes found in upriver sites are apparently limited to single localities, while each of the seven downriver haplotypes are confined to a given site. Samples equivalent to those of *O. perenensis* would be required for proper hierarchical comparisons between these two species, but the limited data suggest that *O. yunganus* contains more divergent haplotypes that exhibit greater geographic structure along the river. The greater reliance on terra firme habitats, the lower reproductive potential, and the smaller population sizes estimated from trapping data for *O. yunganus* (see below) could contribute to the types of differences in molecular population characteristics we have observed between this species and *O. perenensis*.

DISTRIBUTION AND HABITAT: This species is not as abundant as *O. perenensis* at any given locality, nor within the entire Rio Juruá basin. It was captured, however, at one or more sites within each of the four regional areas sampled, from the headwaters to the mouth of the river. It was also present in all habitats, except the river-edge grasses and *Cecropia*. On balance, it was more common in terra firme forest than in várzea, the opposite of the pattern of habitat usage exhibited by *O. perenensis* (table 43). The difference in the relative abundances of these two species in different habitats is highly significant ($\chi^2 = 39.533$, $p < 0.001$), although there is also heterogeneity in habitat occurrence across the sample sites for each species.

REPRODUCTION: We trapped reproductively active males (those with scrotal testes and enlarged vesicular glands) at all sites where the species was present and at all seasons over the year of our sampling. Pregnant, lactating, or postlactating females were also obtained at all sites; therefore, at least some females breed in all seasons over the year. The modal litter size was 2 (range 1–4, n = 14), however, with the mean litter size significantly lower than that for *O. perenensis* ($t = 3.191$, df = 13, $p = 0.0071$). Moreover, while more than 50% of all reproductively active females of *O. perenensis* were pregnant at any single sampling period, pregnancy rates were much lower for *O. yunganus*. The proportion of reproductively active (pregnant, lactating, or postlactating) females in each toothwear age class was also significantly different between the two species ($\chi^2 = 31.769$, df = 4, $p < 0.001$), with *O. yunganus* apparently delaying breeding to an older age, on average. This is not true for males, however, where both species exhibit the same proportions of breeding and nonbreeding individuals in each age class ($\chi^2 = 2.536$, df = 4, $p = 0.469$). Consequently, the differences in modal litter size, apparent pregnancy rates, and longer time to reproductive maturity in females may explain, at least in part, the differences in relative abundances of these two species of *Oryzomys* within the Rio Juruá basin. This may also be a general pattern, as *O. perenensis* has been uniformly much more commonly taken at localities where both species are sympatric (Musser et al., 1998).

KARYOTYPE: Chromosomal preparations were made from 20 individuals, four from localities in the Headwaters Region, nine from the Upper Central Region, one from the

Lower Central Region, and six from the Mouth Region. The diploid number is uniformly 58, the fundamental number 62. The autosomal complement comprises 25 pairs of large to small acrocentric and three pairs of small metacentric elements. The X-chromosome is a medium large acrocentric and the Y-chromosome is a small acrocentric chromosome. This karyotype is the same as that reported for specimens from eastern Perú by Gardner and Patton (1976).

SPECIMENS EXAMINED (n = 138): (**1**) 9m, 4f — MNFS 1093, 1101, 1171–1172, 1194, 1228, 1265–1267, 1295, 1323, 1380, 1401; (**2**) 4m, 4f — MNFS 1181, 1240, 1245, 1247, 1275, 1303, 1347, 1389; (b) 1m — MNFS 1004; (**3**) 6m, 7f — JUR 212, 214, 227, MNFS 1555–1556, 1588, 1608, 1610–1611, 1630, 1650, 1652, 1657; (**4**) 1m, 1f — MNFS 1444, 1455; (**6**) 7m, 3f — JLP 15523, 15535, 15571, 15605, 15650, 15720–15721, MNFS 527–528, 553; (**7**) 32m, 16f, 1 unknown — JLP 15242, 15250, 15257, 15262–15263, 15265–15266, 15275, 15281–15283, 15288–15290, 15301, 15303, 15312, 15319, 15321, 15323–15329, 15361, 15443, 15476, 15495, 15500, 15519, MNFS 335, 341, 349, 367–368, 373, 384, 386–388, 390–392, 412, 419, 511, 519; (**8**) 8m, 9f — JUR 2, 5, 7–8, 12–13, 35, 37, 41, 45–46, 73–75, 110; (**9**) 1m, 2f — JLP 16013, 16021, 16068; (**9a**) 2m, 1f — MNFS 921, 923, 929; (**10**) 2m — MNFS 868, 918; (**11**) 2f — JLP 15759, MNFS 697; (**12**) 3f — JLP 15784, 15829–15830; (**14**) 5m, 7f — JUR 440, 445, 463–464, 474, 483, 489, 494, 509, 524, 543, 557.

Oryzomys macconnelli Thomas, 1910

TYPE LOCALITY: ''River Supinaam, a tributary of the lower Essequibo, Demerara, British Guiana,'' Supenaam River, District Demerara, Guyana, 06°59′N, 58°31′W (Musser et al., 1998: 178).

DESCRIPTION: See above, figures 95 and 96, and tables 38 and 40.

SELECTED MEASUREMENTS: See table 39.

MOLECULAR PHYLOGEOGRAPHY: The number of specimens is too few to permit any valid morphometric comparison between localities along the river. However, we do have at least 414 base pairs of cytochrome-b sequence from seven different individuals, three from Condor (locality **6**), two from Barro Vermelho (locality **12**), and two from Vai-Quem-Quer (locality **15**). Sequences from individuals taken from the same locality are identical, so all variation recorded is distributed among populations. Haplotypes from Condor and Barro Vermelho differ by 1.71%, but these two differ by an average of 4.11% relative to that from the mouth of the river, which in turn is nearly identical to haplotypes from the upper Rio Urucu to the east of the Rio Juruá (see map, fig. 98 and tree, fig. 99). Considerable structure thus occurs over a relatively short distance for this species within the Rio Juruá basin, and further geographic sampling of this species in western Amazonia would be profitable.

DISTRIBUTION AND HABITAT: This species is widely distributed within Amazonia (Musser et al., 1998), but nowhere is it apparently common. Within the Rio Juruá, we obtained specimens only at three localities: Condor (locality **6**) in the Upper Central Region, Barro Vermelho (locality **12**) in the Lower Central Region, and Vai-Quem-Quer (locality **15**) in the Mouth Region. In all cases, the species was only taken in undisturbed terra firme forest, where it was sympatric with both *O. perenensis* and *O. yunganus*. Indeed, its presence seemed to be a good indicator of relatively pristine forest, which has been our experience with this species at other sites in Amazonia, including the Río Cenepa in the Departamento de Amazonas, Perú (Patton et al., 1982), Balta, on the Río Curanja, Departamento de Ucayali, Perú (Gardner and Patton, 1976; Voss and Emmons, 1996), the upper Rio Urucu (M. N. F. da Silva, J. R. Malcolm, and C. A. Peres, unpublished), and the Rio Jaú (M. N. F. da Silva and J. L. Patton, unpublished), both in central Estado do Amazonas, Brazil. At the reserves of the INPA/WWF/Smithsonian-sponsored Biological Dynamics of Forest Fragments Project north of Manaus (PDBFF), *O. macconnelli* was only one of two small mammal species negatively affected by forest fragmentation (Malcolm, 1991b; the other was *Caluromys philander*). All specimens were taken in terrestrial traps.

REPRODUCTION: All individuals of both sexes collected were adults of toothwear age class 3 or older. Pregnant or lactating females

were taken at a both Condor (locality **6**) and Vai-Quem-Quer (locality **15**), and hence in both dry and rainy seasons (September and May, respectively); embryo counts ranged from 2 to 4, with a mode of 3.

KARYOTYPE: 2n = 64, FN = 70. The karyotype from JUR 386 (Vai-Quem-Quer, locality **15**) is figured in Musser et al. (1998: fig. 106). Additional preparations are available from five specimens from Condor (JLP 15548, 15549, 15563, MNFS 529, 530) and two others from Vai-Quem-Quer (JUR 355 and 393). The autosomal complement consists of 27 pairs of acrocentrics grading evenly from large to small and four pairs of small biarmed elements. The sex chromosomes include a large subtelocentric X and a small acrocentric Y.

SPECIMENS EXAMINED (n = 24): (**6**) 12m, 7f — JLP 15548–15549, 15563, 15572, 15600, 15619, 15645, 15648, 15662, 15670–15671, 15685, MNFS 529–530, 536, 548–550, 563; (**12**) 2m — JLP 15859, MNFS 747; (**15**) 1m, 2f — JUR 355, 386, 393.

Oryzomys nitidus (Thomas, 1884)

TYPE LOCALITY: Valley of Río Tulumayo, 10 km south of San Ramón, Amable María, 2000 ft, Departamento de Junín, Perú (as located by Gardner and Patton, 1976).

DESCRIPTION: See above, figures 95 and 96, and tables 38 and 40.

SELECTED MEASUREMENTS: See table 39.

DISTRIBUTION AND HABITAT: This species is widely distributed through the western margins of Amazonia, from Perú south through Bolivia, western and south-central Brazil, eastern Paraguay, and northeastern Argentina (Musser et al., 1998). As noted by these authors, *O. nitidus* is apparently absent from the ''vast core of the Amazon Basin'' (p. 187). In our survey of the Rio Juruá, we obtained specimens of this species only in terra firme forest and at only one locality, Igarapé Porongaba (locality **1**) in the Headwaters Region. The six specimens collected were all taken in Sherman traps set on the ground. At this locality, *O. nitidus* was sympatric with both *O. perenensis* and *O. yunganus*.

REPRODUCTION: We captured specimens only during the month of February. Three adult males had scrotal testes and enlarged vesicular glands (16 to 17 mm long) indicative of reproductive activity. Of the two adult females, one was pregnant with 5 embryos and the second was parous but neither pregnant nor lactating. A single nonreproductive young female (age class 1) was in sparse, reddish juvenile pelage.

KARYOTYPE: 2n = 80, FN = 86. The chromosomal complements from two males (MNFS 1147 and 1419) and two females (MNFS 1223 and 1420) are identical to each other and the same as those reported by Gardner and Patton (1976) for samples from several localities in eastern Perú. The autosomes consist of 35 pairs of acrocentrics, one distinctly large and the remainder graded from large to small, and four pairs of small metacentrics; the sex chromosomes are a large subtelocentric X and a small acrocentric Y.

SPECIMENS EXAMINED (n = 6): (**1**) 3 m, 3 f — MNFS 1147, 1208, 1223, 1310, 1419–1420.

Scolomys Anthony, 1924

Gray spiny mice

Scolomys juruaense Patton and da Silva 1995

TYPE LOCALITY: ''Seringal Condor, left bank Rio Juruá, Amazonas, Brazil 70°51′W 6°45′S.''

DESCRIPTION: This genus consists of small-bodied, spiny mice with a tail shorter than head and body length, short and fleshy feet, short and rounded ears, and dark reddish-black to brownish-black dorsal coloration and gray venter. It can be confused only with members of the genus *Neacomys*, which also have spiny dorsal fur. A complete set of comparisons between the two genera is given in Patton and da Silva (1995). The readily recognizable and salient differences between *Scolomys* and *Neacomys* include, respectively, the following characters: (1) gray, as opposed to generally pure white venters; (2) three, as opposed to four pairs of mammae; (3) skull (fig. 106) short with blunt rostrum flanked by very shallow zygomatic notches, as opposed to more narrow and elongate rostrum with deeper notches; (4) supraorbital margins rounded with moderately developed

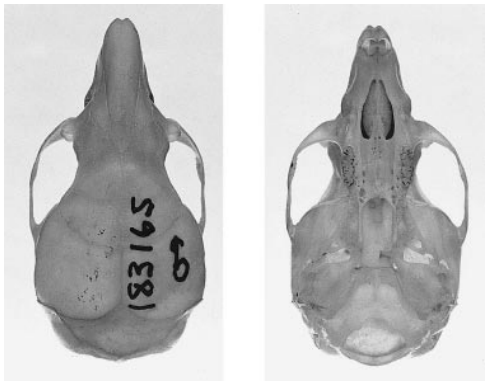

Fig. 106. Dorsal (left) and ventral (right) views of the cranium of *Scolomys juruaense* (MVZ 183165; Penedo [locality **7**], right bank Rio Juruá, Amazonas, Brazil).

overhanging ledges, rather than raised ridges; (5) interorbital region broad, greater than width of rostrum, as opposed to equal to or less than rostral width; (6) derived carotid circulation pattern comprised only of internal carotid artery, with greatly reduced to absent stapedial foramen, no squamoso-alisphenoid groove or sphenofrontal foramen, as opposed to either primitive carotid pattern or derived, but with well-developed stapedial foramen indicative of a stapedial artery; (7) sphenopalatine vacuities greatly reduced, as opposed to broadly open; (8) upper incisors proodont to orthodont, as opposed to opisthodont; and (9) molar teeth with weakly developed cusps that obliterate quickly with wear, as opposed to well-developed and long-lasting cusps.

Scolomys juruaense, the species we have recently described from the Rio Juruá basin, is readily distinguished from the type species of the genus, *S. melanops*, which is now known from extreme northern Perú and eastern Ecuador, by its combination of (1) longer and more slender rostrum, (2) orthodont rather than proodont upper incisors, (3) somewhat larger cranial dimensions, (4) narrow and parallel zygomatic arches, (5) occluded subsquamosal fenestra; and (6) gracile mandible with longer, more curved, and narrower coronoid process. This species is very similar in cranial shape to the third known member of the genus, *S. ucayalensis* Pacheco from northern Perú, but differs in larger cranial dimensions, reddish-brown as opposed to dark gray dorsal coloration, ''stepped'' rather than evenly tapered lateral margins of the incisive foramina, and square rather than distinctly rounded anterior margin of the mesopterygoid fossa.

TABLE 45
Selected External and Cranial Dimensions of *Scolomys juruaense* from the Rio Juruá Basin
Measurements (mm) are given as mean, with range and sample size.

Variable	Mean	Range	n
TOL	152.4	142–163	11
TAL	69.0	62–76[a]	11
HF	20.6	19–22	16
E	15.6	15–17	16
CIL	20.43	18.60–21.97	16
ZB	12.13	11.18–13.30	16
MB	10.29	9.70–10.73	16
IOC	5.59	4.55–6.13	16
RL	7.86	6.93–8.48	15
NL	8.31	7.83–9.34	15
RW-1	4.81	4.36–5.40	16
RW-2	3.64	2.79–4.05	16
OL	7.38	6.67–7.89	16
D	6.23	5.73–6.75	16
MTRL	2.66	2.31–2.88	16
IFL	3.94	3.17–4.32	16
PL	9.14	8.28–9.87	16
AW	4.62	4.29–4.96	16
MPFL	3.61	3.35–3.92	16
MPFW	1.97	1.78–2.20	16
OCB	6.01	5.64–6.46	16
BOL	3.23	2.83–3.60	16
ZPL	1.71	1.54–1.93	16
CD	8.89	8.18–9.49	16

[a] Range erroneously given as 26 to 76 in Patton and da Silva (1995:326).

SELECTED MEASUREMENTS: Means and ranges (from Patton and da Silva, 1995) are given in table 45.

DISTRIBUTION AND HABITAT: Known only from four localities in the central and upper reaches of the Rio Juruá, Amazonas and Acre states, western Brazilian Amazon. Although we caught all of our specimens in undisturbed terra firme forest on the ground, these sites were often in areas of local, natural disturbances, such as tree falls.

REPRODUCTION: Pregnant females or those with a perforate vagina were obtained from August through March, suggesting that

breeding occurs in both wet and dry seasons and perhaps throughout the year. Embryo counts ranged from one to three.

COMMENTS: While superficially similar in external morphology to spiny mice of the genus *Neacomys*, these two genera differ so trenchantly in other features that they cannot be considered close relatives (Patton and da Silva, 1995). This view is supported by the preliminary molecular sequence data provided by Patton and da Silva (1995) for seven genera of oryzomyine rodents, including *Scolomys*. In this analysis, *Scolomys* was quite divergent from all other genera in the tribe, and no particular relationship could be supported given the 801 base pairs of sequence then available. The genus is apparently unique among the Oryzomyini in having only three, as opposed four, or more, pairs of mammae (see Voss and Carleton, 1993, for a discussion of the morphological characters of oryzomyine rodents).

SPECIMENS EXAMINED (n = 23): (**4**) 1m, 4f — INPA 2485–2486, MPEG 24023–24024, MVZ 183172; (**6**) 3m, 2f — MPEG 23824 (holotype), 24019–24020, MVZ 183167–183168; (**7**) 3m, 2f — INPA 2487–2488, MPEG 24022, MVZ 183165–183166; (**12**) 6m, 2f — INPA 2489–2492, MPEG 24021, MVZ 183169–183171.

TRIBE THOMASOMYINI VORONTSOV, 1959

Rhipidomys Tschudi, 1845

Climbing rats

Relatively few specimens of *Rhipidomys* have been collected from Amazonia. The genus appears to be either difficult to trap or generally uncommon, although exceptionally high numbers have been collected at some localities (e.g., the PDBFF reserves north of Manaus; Malcolm, 1991b). The scattered number of localities, and the general lack of adequate series even from those sites where specimens are known, has stifled interest in the systematics of this group. Christopher Tribe's (1996) recent revision represents a quantum leap beyond our existing understanding of the systematics of *Rhipidomys*, but clearly there remains much to do, and to learn, as he himself concludes (Tribe, 1996: 254–257). Hopefully Tribe's work will energize further interest in this enigmatic group of sigmodontine rodents.

Rhipidomys is a broadly ranging genus, and species exhibit considerable differentiation in body size and both external and craniodental characters. However, this large group of species can be distinguished from other sympatric murids, and specifically those of the Rio Juruá basin, by a tail that is much longer than head and body, and typically terminated by a relatively long tuft of hairs; short and very broad feet with proportionately long toes and with pale sides but darker dorsal patch over the metatarsals; and six mammae in females. Cranially (fig. 107), these taxa are readily recognizable by a combination of very shallow zygomatic notches; a narrow zygomatic plate with a vertical anterior edge and no anterior projecting spine; moderate supraorbital ledges that extend divergently onto the sides of the cranium as parietal ridges; a short and broad palate with the incisive foramina extending to the level of the anterior root of first molar, the mesopterygoid fossa extending to the posterior margin of the third molar, and no large posterolateral palatal pits; no or only minute sphenopalatine vacuities; a robust alisphenoid strut; small bullae with the tegmen tympani overlapping the posterior suspensory process of the squamosal; nonsulcate upper incisors; and molars cuspidate, brachydont, and pentalophodont with cusps (-ids) opposite rather than alternate. The cephalic arterial pattern may either be derived (pattern 3, of Voss, 1988; Carleton and Musser, 1989), with a minute stapedial foramen, no squamosal-alisphenoid groove, and no sphenofrontal foramen, or primitive (pattern 1).

Tribe (1996) records only a single species of *Rhipidomys* from lowland localities of western Amazonia. This is *R. leucodactylus*, one of the largest members of the genus. He characterizes, and maps, other similar-sized species from extreme western Amazonia, but each of these is distributed along the lower Andean slopes at elevations above 700 m. Included in this group are three taxa with the derived carotid arterial system, including: *R. modicus*, from north through central Perú (Amazonas to Junín departments); an undescribed species known only from a single locality in the Departamento de La Paz, Boliv-

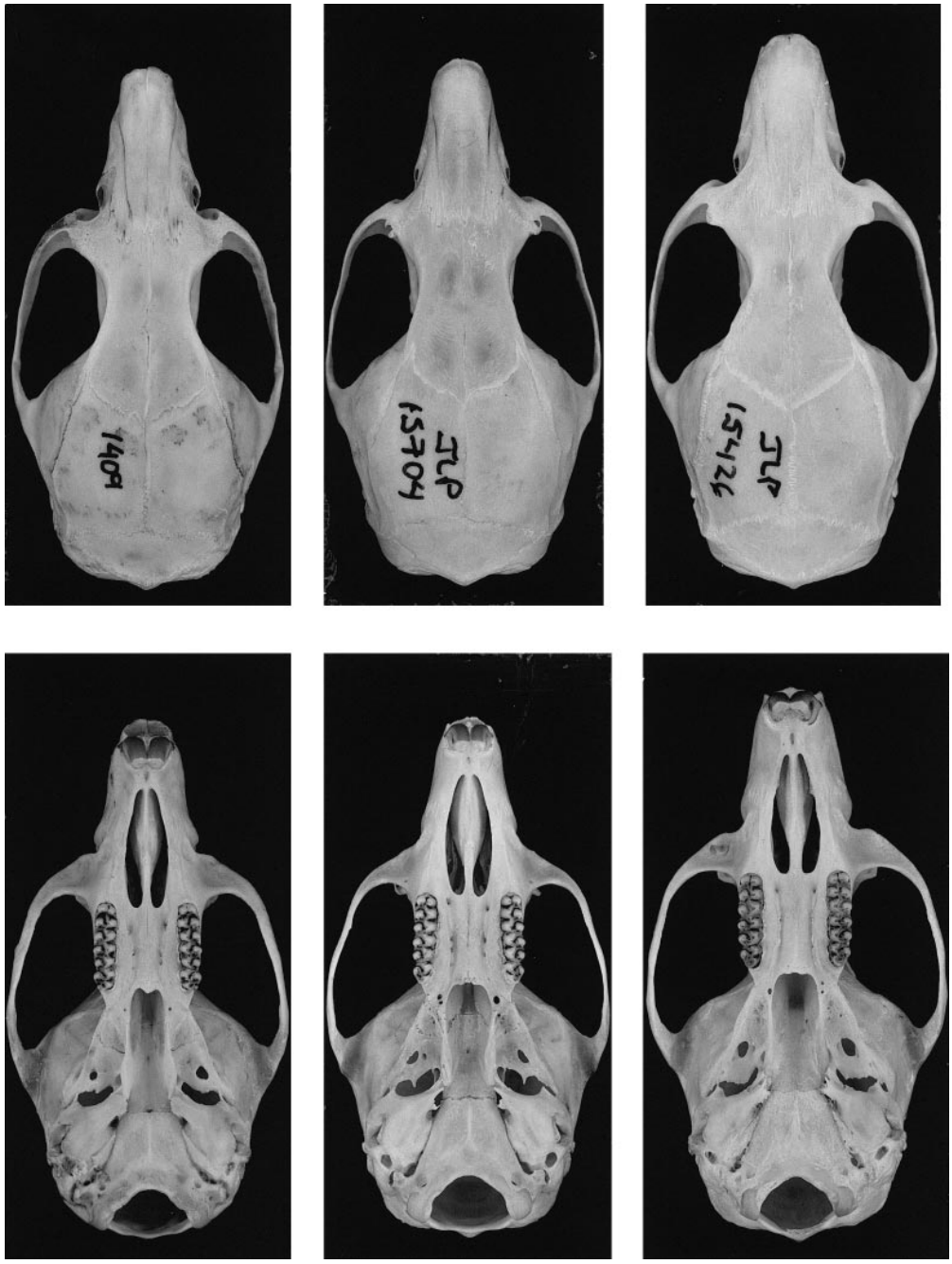

Fig. 107. Dorsal and ventral views of crania of *Rhipidomys* from the Rio Juruá, contrasting examples of *R. gardneri* (**left**, a subadult; MNFS 1409; opposite Igarapé Porongaba [locality **2**], left bank Rio Juruá) and *R. leucodactylus* (**middle**, JLP 15704, a subadult, Seringal Condor [locality **6**], left bank Rio Juruá; **right**, JLP 15426, an adult, Penedo [locality **7**], right bank Rio Juruá). Magnification = ×2.

ia; and *R. austrinus*, distributed through the *yungas* from northern Bolivia (Departamento de La Paz) to northwestern Argentina (Departamento de Jujuy). Also present in southern Perú is *R. ochrogaster*, a species restricted to the Río Inambarí in northern Departamento de Puno that is characterized by the primitive cephalic arterial pattern. Woodman et al. (1991) suggested that two species of *Rhipidomys* occur at the lowland Amazonian site of Cuzco Amazónico, on the Río Madre de Dios (Departamento de Madre de Dios) in southeastern Perú, describing one as large and the other smaller. Tribe (1996), who apparently examined the relevant specimens, allocates all to *R. leucodactylus*, and Voss and Emmons (1996), in their compilation of the fauna from this site, also list only a single species.

We obtained only nine specimens of *Rhipidomys* in the more than 45,000 trap-nights of effort along the Rio Juruá, including over 19,000 trap-nights on canopy platforms (table 2), and one of these was captured by hand from a tree hole. All are large-bodied, with head-and-body lengths of 150 mm or greater. However, two forms are distinguishable among these specimens based on a number of morphological characters as well as karyotype. A single specimen of one type was collected within the Headwaters Region in Estado do Acre; the other form was found throughout the remaining length of the river in Estado do Amazonas. Tribe (1996) examined all of the specimens we obtained from the Upper and Lower Central sections of the Rio Juruá, and allocated these to *R. leucodactylus*. He also assigned our single specimen from the Headwaters Region (for which he gave the locality as ''Acre: Rio Juruá, above Cruzeiro do Sul'' [p. 289]) to this species, based on chromosomal information that one of us (J. L. Patton) supplied to him rather than from personal examination of the specimen. Unfortunately, as we document below, the information was misleading, and emendation of Tribe's conclusions regarding our specimens is necessary.

In his discussion of *R. leucodactylus*, Tribe (1996: 204–205) states that ''Considerable geographic variation is present in this species. Karyotypic or molecular data may in the future demonstrate that it is composite,

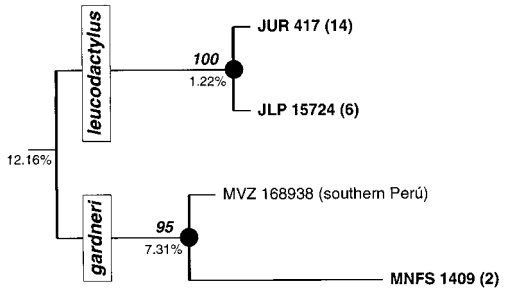

Fig. 108. The single most-parsimonious tree, based on an exhaustive search, for haplotypes of the mitochondrial cytochrome-b gene (500 bp) for specimens of climbing rats, *Rhipidomys*, from southwestern Amazonia. Length = 183 steps, CI = 0.885, RI = 0.741. The sequence for MVZ 168938 (Cusco Amazónico, Madre de Dios, Perú) is from Smith and Patton (1993). Tree is rooted by comparison to sequences of *Thomasomys aureus* (also from Smith and Patton, 1993). Bold numbers at internal nodes are bootstrap values, based on 1000 replicates; percentages are average Kimura two-parameter distances. Haplotypes are identified by field number and locality.

but on the basis of currently available material it cannot be split unquestionably into separate taxa even at the subspecies level. The most divergent populations occur in the Peruvian region of Inka (i.e., the former departments of Cuzco and Madre de Dios) and the Ucayali valley, where pelage is often shorter without gray bases to ventral hairs, tails are less hairy with shorter pencils, and hind feet have a narrower dark patch; skulls are generally rather smaller, with less pronounced supraorbital ridges, narrow mesopterygoid fossae and smaller molars.'' This combination of features characterizes the single specimen we have from the headwaters of the Rio Juruá, and differentiates it from those downriver. The two also differ in karyotype (see below) and in sequence data from the cytochrome-b gene. Figure 108 illustrates the relationship between cytochrome-b haplotypes, based on 500 bp, for four specimens of *Rhipidomys*. These include two specimens from the central and mouth regions of the Rio Juruá that share close similarity (Kimura two-parameter distance of 1.22%) and the single specimen from the Headwaters Region, which is more than 12% different. This specimen groups with one

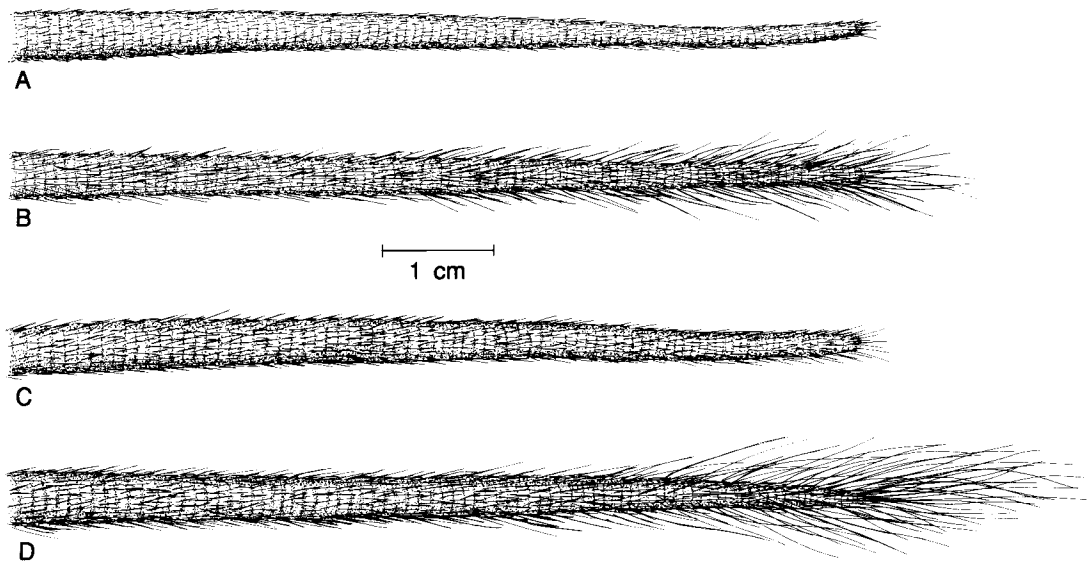

Fig. 109. Development of the tail tuft in young individuals (age class 3) of: **A**, *R. gardneri* (MNFS 1409, locality **2**) and **B**, *R. leucodactylus* (JLP 15724, locality **6**), both from the Rio Juruá; and in adult individuals (age class 4) of **C**, *R. gardneri* from Cuzco Amazónico, Rio Madre de Dios, Madre de Dios, Perú (MVZ 168960) and **D**, *R. leucodactylus* from the Rio Juruá (JLP 15426, locality **7**).

from Cusco Amazónico in southeastern Perú that shares similar morphological features, although the two are still quite different in sequence (7.31%).

We allocate the larger series of our specimens to the species *R. leucodactylus*, primarily on the revised diagnosis provided by Tribe (1996: 203), who describes the tail as "... long, abundantly furred distally, with long pencil" and the hind feet with a "... dark patch covering most of foot and extending onto digits." The second species, apparently without an available name (Tribe, 1996), we describe here.

Rhipidomys gardneri, new species

HOLOTYPE: MVZ 168938 (Museum of Vertebrate Zoology, University of California, Berkeley), adult male, collected June 7, 1984, by Richard M. Warner (original number 711); skin with skull and mandibles, in good condition; and liver and kidney tissue, originally preserved in liquid nitrogen, maintained at −76° C in the frozen collection of the Museum of Vertebrate Zoology.

TYPE LOCALITY: Reserva Cusco Amazónico, left (= north) bank of the Río Madre de Dios, 14 km east of Puerto Maldonado, Departamento de Madre de Dios, Perú, elevation about 200 m (12°33′S, 69°03′W). A detailed site description, including climate, vegetation, soils, history, and maps can be found in Duellman and Koechlin (1991). Lists of mammals present are given in Woodman et al. (1991, 1995) and Voss and Emmons (1996).

DIAGNOSIS: A large-bodied species with short fur without gray bases to the ventral hairs; a long but sparsely haired tail with a short terminal pencil of hairs (< 6 mm; fig. 109); hind feet with a narrow dark dorsal patch limited to the metatarsals; cranium with only moderately developed supraorbital ridges; deep zygomatic notch when viewed from above (figs. 107 and 110); distinctly narrow mesopterygoid fossa with a scalloped anterior border (fig. 111); short toothrow (< 6 mm, on average); and karyotype with 2n = 44, FN = 50 (fig. 112).

PARATYPES: MVZ 168999, an adult male, and MVZ 168960, an adult female, both from the type locality, and MNFS 1409, from the left bank of the Rio Juruá opposite Igarapé Porongaba, Acre, Brazil. All three specimens are skins with skull and mandible, in good condition, and with tissues preserved

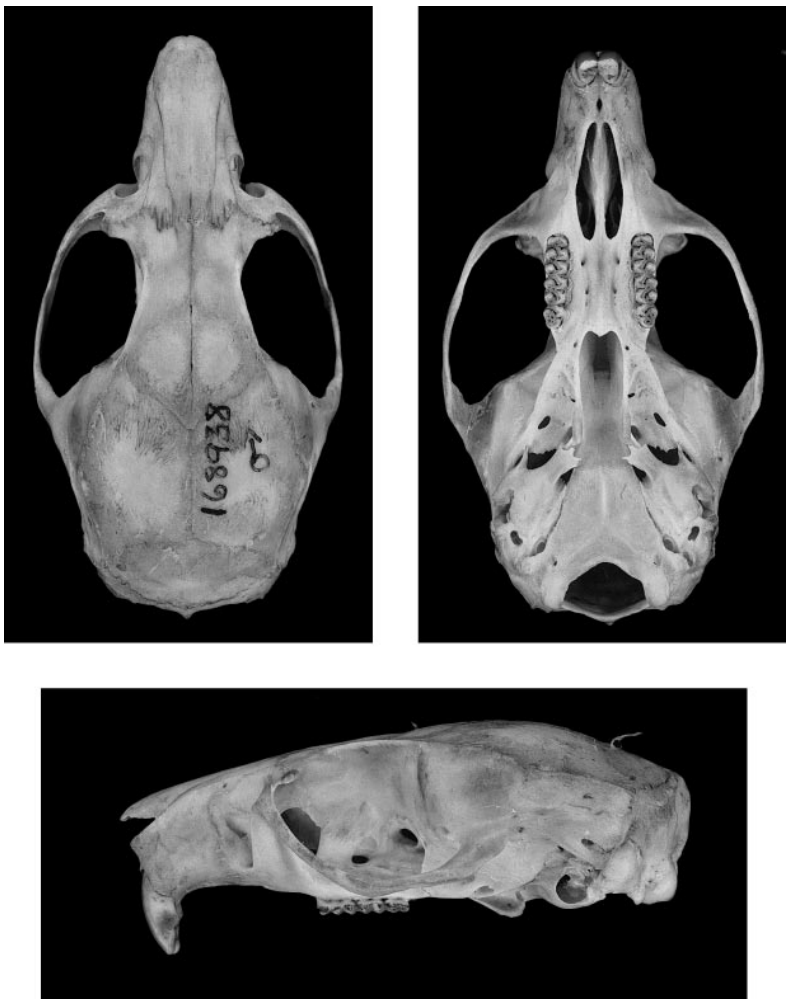

Fig. 110. Dorsal, ventral, and lateral views of the cranium of the holotype (MVZ 168938) of *Rhipidomys gardneri*. Magnification = ×4.

either frozen at −76° C or in 95% ethyl alcohol.

MEASUREMENTS OF HOLOTYPE: TOL, 365; TAL, 215; HF, 33; E, 24; CIL, 36.16; ZB, 21.31; MB, 14.97; IOC, 6.40; RL, 13.41; NL, 13.12; RW-1, 7.55; RW-2, 5.94; OL, 13.49; D, 10.10; MTRL, 6.30; IFL, 7.74; PBL, 16.19; AW, 7.21; OCB, 8.45; BOL, 6.25 MPFL, 7.57; MPFW, 2.85; ZPL, 3.47; CD, 13.66.

ADDITIONAL MEASUREMENTS: See table 46.

DESCRIPTION AND COMPARISONS: This also is a large-bodied species, but slightly smaller than *R. leucodactylus* in nearly every measurement (table 46). The single specimen obtained from the Rio Juruá is still in juvenile pelage, although all three molars are in place and exhibit some wear (e.g., age class 3). As a result, this specimen is difficult to compare to specimens of *R. leucodactylus* from the Rio Juruá in external characters. In the four specimens examined, including both this young individual and three adults from southeastern Perú, the darkened surface of the hind feet is narrower and does not extend onto the toes (i.e., the toes are pale from base to tip), and the venter is paler, with gray-based hairs limited to the midline of the throat and chest; the chin and inside of both fore and hind legs are white. The tail is long,

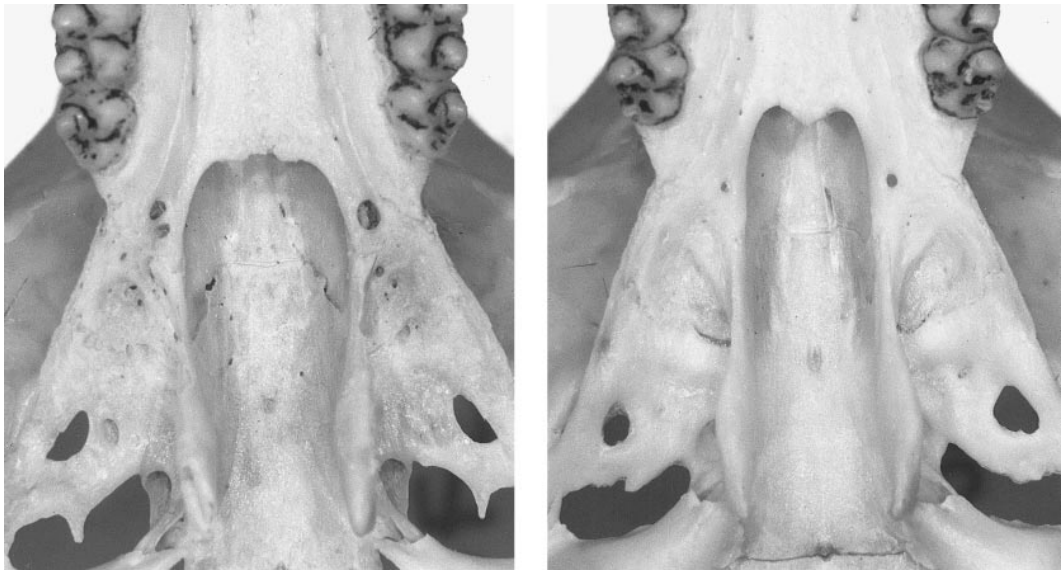

Fig. 111. Comparisons of the mesopterygoid fossa of specimens of *R. leucodactylus* (**left** -JLP 15704, locality **7**) and *R. gardneri,* (**right** -MNFS 1409, locality **2**).

but with only a short pencil of hairs extending beyond the tip (6 mm; fig. 109). The tail is also less hairy with individual hairs barely extending over two scales. As a result, the scales are clearly visible, although small, averaging 16 rows per cm. In direct comparison to specimens of *R. leucodactylus* of similar toothwear (e.g., JLP 15704), the skull has deeper zygomatic notches (figs. 107 and 110) and a narrower and longer mesopterygoid fossa that possesses a scalloped anterior border with a distinct, posteriorly projecting median spine (fig. 111).

COMMENTS: Tribe (1996) regarded the holotype and paratype of *R. gardneri* from southeastern Perú as *R. leucodactylus* yet

Fig. 112. Chromosome complements of: **A,** *R. leucodactylus* (JLP 15683, male, locality **6**) and **B,** *R. gardneri* (MNFS 1409, female, locality **2**).

TABLE 46
External and Cranial Dimensions of Two Age Classes of *Rhipidomys leucodactylus* and of *R. gardneri*
Measurements (mm) are given as mean ± standard error, with range and sample size.

Variable	*R. leucodactylus* age class 3			*R. leucodactylus* age class 4			*R. gardneri*
	Mean ± SE	Range	n	Mean ± SE	Range	n	(MNFS 1409)
TOL	349.0 ± 11.9	329–380	3	389.3 ± 7.9	379–405	3	326
TAL	194.3 ± 5.8	184–204	3	213.3 ± 5.4	203–221	3	177
HF	35.7 ± 0.9	34–37	3	35.0 ± 0.6	34–36	3	32
E	19.7 ± 0.3	19–20	3	20.3 ± 0.3	20–21	3	20
CIL	34.94 ± 0.67	33.7–38.9	4	37.58 ± 0.67	35.8–38.9	4	33.59
ZB	19.48 ± 0.43	18.8–20.6	4	21.35 ± 0.16	21.1–21.7	4	19.57
MB	14.26 ± 0.31	13.5–14.9	4	15.20 ± 0.09	15.0–15.4	4	14.18
IOC	5.95 ± 0.15	5.6–6.3	4	6.29 ± 0.18	5.8–6.6	4	5.83
RL	12.94 ± 0.37	12.3–14.2	4	14.32 ± 0.35	13.3–14.9	4	12.85
NL	12.99 ± 0.62	12.0–14.6	4	14.00 ± 0.15	13.6–14.2	4	12.15
RW-1	7.15 ± 0.18	6.8–7.7	4	8.26 ± 0.0.24	7.7–8.8	4	7.44
RW-2	5.57 ± 0.12	5.3–5.8	4	6.27 ± 0.16	6.0–6.6	4	5.55
OL	13.03 ± 0.30	12.4–13.8	4	13.69 ± 0.23	13.3–14.3	4	12.65
D	10.28 ± 0.25	10.0–11.0	4	11.30 ± 0.27	10.5–11.8	4	9.5
MTRL	6.18 ± 0.04	6.1–6.2	4	6.34 ± 0.14	5.9–6.6	4	5.98
IFL	8.23 ± 0.19	7.9–8.7	4	8.70 ± 0.21	8.3–9.3	4	8.19
PL	16.24 ± 0.30	15.6–16.8	4	17.17 ± 0.13	16.8–17.4	4	15.08
AW	7.25 ± 0.11	7.0–7.4	4	7.65 ± 0.06	7.5–7.8	4	7.37
OCB	8.36 ± 0.22	8.0–8.8	4	8.68 ± 0.17	8.3–9.0	4	8.47
BOL	5.73 ± 0.22	5.3–6.3	4	6.24 ± 0.11	6.0–6.4	4	5.18
MPFL	7.63 ± 0.17	7.4–8.1	4	8.46 ± 0.38	7.4–9.1	4	7.80
MPFW	3.04 ± 0.17	2.6–3.3	4	3.20 ± 0.18	2.7–3.5	4	2.31
ZPL	2.93 ± 0.12	2.7–3.3	4	3.18 ± 0.11	3.0–3.5	4	3.07
CD	13.71 ± 0.42	13.2–14.9	4	14.08 ± 0.14	13.7–14.3	4	12.96

noted their distinction from other specimens he diagnosed separately as that species. While we have not seen specimens reported by Woodman et al. (1991, 1995; also listed in Voss and Emmons, 1996) from the type locality, we assume these to represent *R. gardneri*.

DISTRIBUTION AND HABITAT: The single specimen we caught came from a canopy platform trap on the left bank of the Rio Juruá opposite Igarapé Porongaba (locality **2**) in Estado do Acre. The habitat here is várzea forest that is flooded only occasionally rather than annually. Specimens at the type locality were taken in traps placed in trees in undisturbed lowland evergreen forest that did not flood during the wet season (see Woodman et al., 1995). This species is distributed from the headwaters of the Rio Juruá at least to the lowlands of southeastern Perú, and, following Tribe (1996), probably into the Ucayali valley.

ETYMOLOGY: Named in honor of Alfred L. Gardner, who introduced one of us (J. L. P.) both to mammalogy (in 1963) and to Amazonia (in 1968), for his many seminal contributions to the systematics and distribution of South American mammals.

REPRODUCTION: The single individual from the Rio Juruá was a nulliparous female, in juvenile pelage with the minimal toothwear for assignment to age class 3. The three adults from the type locality are adults; the holotype had abdominal testes (12 mm × 7 mm, length to width) and small vesicular glands (7 mm long) suggesting that it was nonreproductive.

KARYOTYPE: This species has a diploid number of 44 and a fundamental number of 50 (fig. 112B). As only a female was examined, the sex chromosomes are unknown. However, the autosomal complement is likely to have 17 pairs of large to small acrocentric, three pairs of small metacentric, and one pair of large subtelocentric autosomes, and the X-chromosome is considered to be a

medium-sized subtelocentric, one with a very small short arm. This is the chromosome complement listed by Tribe (1996: 111, 113), which Patton erroneously told him by letter characterized all specimens that we karyotyped.

Rhipidomys leucodactylus Tschudi, 1845

TYPE LOCALITY: ''im Oststriche'', the region east of the Andean Cordillera in central Perú; restricted to Montaña de Vitoc in the Chanchamayo Valley, Departamento de Junín, Perú, by Tribe (1996).

DESCRIPTION: This is a large-bodied species, with head-and-body length exceeding 175 mm, on average (table 46). The tail is especially long, averaging 122% of head-and-body length, and terminates in an elongated and distinctive tuft of hair averaging 27 mm (range 20–36 mm; fig. 109). Even two subadult individuals (age class 2) have a distinct pencil, with lengths of 16 and 17 mm, respectively, more than twice the length of the tail tuft of *R. gardneri*. The tail is also well haired along its entire length, with individual hairs extending over more than three scale rows. Although partially hidden from view by hairs, the tail scales appear rather coarse, and average 11 rows per cm. The dorsal pelage varies from grayish to orangish brown in color; it is thick and somewhat woolly in texture. The ventral pelage is gray-based throughout in all specimens, with either off-white or pale buffy tips; three specimens have a buffy suffusion on the upper thorax. The hind foot is large, distinctly broadened, with a dark patch covering most of the dorsal surface of the foot and extending onto the digits; only the terminal ungual tufts are white in most specimens. The skull (fig. 107) is large, averaging 36 mm in condyloincisive length, with shallow zygomatic notches, a broad and relatively short rostrum, a long maxillary toothrow averaging 6.3 mm, and a relatively short but conspicuously broad mesopterygoid fossa, the anterior border of which is typically smoothly arched and without a median projection (fig. 111).

DISTRIBUTION AND HABITAT: We caught all but one of our specimens in mature terra firme forest in canopy platform traps; the other individual was obtained by hand from a tree hole. We recorded the species at five localities, three on the right bank and two on the left, from the Upper Central, Lower Central, and Mouth sections of the river (see ''Specimens Examined,'' below).

REPRODUCTION: Both female specimens were nulliparous, with thin and threadike uteri lacking any vascularization, and ovaries lacked obvious mature follicles. Interestingly, one female was a relatively young individual (age class 3) but still molting from subadult to adult pelage across the shoulder region; the other was an older adult (age class 4). As limited as these data are, they do suggest that breeding is delayed in this species relative to other sympatric sigmodontines. This may account, at least in part, for the relative rarity of these rats.

KARYOTYPE: We have chromosomal data from seven of the eight specimens collected. All are uniform in possessing a diploid number of 44 with fundamental number of 46. The karyotype (fig. 112A) consists of 19 pairs of acrocentric autosomes grading in size from large to small, and with the first pair distinctly larger than the next, and two pairs of small metacentric autosomes. The X-chromosome is a medium-small acrocentric with a slightly visible short second arm; the Y-chromosome is a small acrocentric. This complement is similar to a specimen reported to be of this species from the Rio Jamarí in the Estado do Rondônia, Brazil, which differs only by having three pairs of small metacentric and one fewer pair of acrocentric autosomes, and consequently a fundamental number of 48 instead of 46 (Zanchin et al., 1992).

SPECIMENS EXAMINED (n = 8): (**6**) 2m, 1f — JLP 15683, 15704, 15724; (**7**) 1f — JLP 15426; (**9**) 1m — JLP 15923; (**14**) 2m — JUR 417, 438; (**15**) 1f — JUR 384.

ECHIMYIDAE GRAY, 1825

The terrestrial spiny rats and tree rats of the family Echimyidae are second only to the Muridae as the most diverse family of rodents within lowland Amazonian forests. Some taxa, especially the terrestrial spiny rat genus *Proechimys*, are also among the most abundant in any local mammalian commu-

nity. On the other hand, virtually all arboreal genera are poorly represented in museum collections, due either to inadequate sampling of the canopy or to true rarity.

We encountered five genera of echimyids in the Rio Juruá basin: eight species of *Proechimys* (see da Silva, 1995, 1998); two species of the spiny tree rat, *Mesomys*; two species of bamboo rats, *Dactylomys*; and one species each of the red-nosed tree rat, *Makalata*, and brush-tailed rat, *Isothrix*. *Proechimys* were exceedingly numerous at all sites, generally the most common of all mammals trapped. Nearly 40% of our specimens were of this genus. We heard the distinctive nocturnal calls of *Dactylomys* at most sites, and all along the river during travel periods, but few specimens were acquired, and none in our traps. *Mesomys* were among the more common members of the canopy community, as ascertained by our platform trapping program. *Isothrix* was considerably less common, yet encountered routinely at most sites, both captured in our canopy traps or observed at the entrances of tree-hole nests. Finally, *Makalata* was uncommon throughout the river, as individuals were only rarely captured by any means and it was never seen at night while hunting, unlike the other arboreal taxa.

Generic limits and relationships among echimyids are poorly resolved for the most part. Lara et al. (1996) argue that the extant generic lineages diverged nearly simultaneously from a common ancestor in the Miocene. Thus, the rapidity of this early radiation, coupled with combinations of uniquely derived traits and broadly shared primitive ones, has resulted in considerable confusion in the diagnosis of genera and in the allocation of species to them. The traditional separation of extant genera into three subfamilies (summarized in Woods, 1993)—the Dactylomyinae (*Dactylomys*, *Kannabateomys*, and *Ollalamys*), Echimyinae (*Echimys*, *Isothrix*, *Makalata*, and *Nelomys*), and Eumysopinae (*Hoplomys*, *Mesomys*, *Proechimys*, and *Trinomys*)—is not supported by molecular analyses of either proteins or mtDNA sequences (Patton and Reig, 1989; Lara et al., 1996).

The difficulties in defining and diagnosing genera are exacerbated severalfold when one considers the problems of circumscribing species in nearly all of these groups. For example, the terrestrial spiny rats of the genus *Proechimys* are among the most notorious of Neotropical taxa for posing difficulties in the recognition of species boundaries. The confusion surrounding species recognition in this genus was aptly stated by Oldfield Thomas (1928: 262) some 70 years ago in his often quoted statement: ''The bewildering instability of characters . . . makes it at present impossible to sort them according to locality into separate species, subspecies, or local races.'' Nevertheless, great strides have been made in recent years in understanding the patterns of morphological character variation in this difficult genus (Patton and Gardner, 1972; Gardner and Emmons, 1984; Patton, 1987; Aguilera and Corti, 1994; da Silva, 1995, 1998). The number of actual species of *Proechimys*, including those sympatric at single sites, remains underappreciated for the most part, and we know little or nothing about even the most simple ecological relationships among them (but see Emmons, 1982; Malcolm, 1992). As documented by da Silva (1995, 1998), at least eight species of *Proechimys* are present along the Rio Juruá. This is double the number we expected based on the prior work by one of us in adjacent Perú (Patton and Gardner, 1972; Patton, 1987). As we also document below, and as already alluded to in earlier publications on this fauna (da Silva and Patton, 1993, 1998; Patton et al., 1994, 1996a), additional species of *Proechimys* and other echimyid genera can be recognized elsewhere in Amazonia based on the Rio Juruá materials. One of these, a *Mesomys*, appears to be unknown to science, and we describe it here. For the others, we assign existing names in the appropriate generic accounts, below.

The genera of echimyids present in the Rio Juruá, indeed throughout much of Amazonia, are each recognizable by a combination of external (spinose or nonspinose fur, brushy or naked tail) and craniodental (shape of the interorbital region; development of supraorbital ledges; laminate or nonlaminate cheekteeth; parallel or diverging maxillary toothrows) features. In the accounts below, we describe and figure each taxon that we found within the Rio Juruá basin.

DACTYLOMYINAE TATE, 1935

Dactylomys I. Geoffroy Saint-Hilaire, 1838

Bamboo rats

The bamboo rats are among the largest arboreal rodents in Amazonia, equivalent in size to the tree squirrels *Sciurus igniventris* and *S. spadiceus* but considerably smaller than porcupines of the genus *Coendou*. They are also remarkable for their loud vocalizations that can be heard for considerable distances. Despite their conspicuousness, however, they are very poorly known in all aspects of their biology and evolutionary relationships. They are folivores that do not readily enter traps, either because the baits used are not attractive or for other reasons, and their weak eye-shine and methodical movements make them difficult to see at night. Indeed, individuals are more readily detected by their distinctive vocalization or by the strong, musky odor that permeates their living areas rather than seen (Emmons, 1981; Emmons and Feer, 1997). The common name stems from their characteristic association with patches of bamboo, apparently a major food item, but they also occur in riverine vegetation, especially canebrakes, and in upland forest on the rich soils of western Amazonia (Emmons, 1981).

The genus is readily recognizable by both external and cranial characteristics. It is the largest echimyid within Amazonia, with body lengths in excess of 280 mm; the tail is furred at the base but otherwise naked and distinctly scaly, and exceeds the head and body length; the ears are small; the dorsal coloration is grizzled yellow-olivaceous streaked with black, with thighs and sides varyingly yellow to rusty orange, and with either a pale beige or blackish stripe that extends from between the eyes to the nape of the neck; the muzzle is distinctly square in lateral profile; and the forefeet have four long digits (the middle ones separated by a gap) with nails, not claws. The skull (fig. 113) is large and robust, flat in lateral profile, with a short rostrum, broadly overhanging supraorbital ledges with triangular postorbital processes, deep and massive zygomatic arches with dorsal postorbital processes comprised equally of squamosal and jugal, and enlarged cheekteeth comprised of complete, or nearly complete transverse laminae (fig. 114).

Three species of bamboo rats were listed by Woods (1993): *D. dactylinus* (Desmarest), occurring throughout most of lowland Amazonia; *D. boliviensis* Anthony, apparently restricted to lowland Bolivia and southeastern Perú; and *D. peruanus* Allen, known only from the cloud forests of southeastern Peru above 1000 m. Da Silva and Patton (1993) suggested that two species are present in lowland Amazonia, while Emmons and Feer (1997) listed only the single species *D. dactylinus*. These latter authors noted, however, that both external color pattern and vocal call structure (number and timing of pulses) varies geographically, and acknowledged that more than one species might be present.

Da Silva and Patton (1993) based their conclusion that two species of bamboo rats occurred in western Amazonia on mtDNA sequences from the few specimens obtained from the Rio Juruá and elsewhere, supplemented by notes on vocalizations. The limited geographic sampling of that study has been supplemented only minimally by more recent sampling in central Brazil and central Perú (fig. 115, top; table 47). Sequences separate into two well-differentiated groups, one restricted to the headwaters of the Rio Juruá and adjacent Perú and the other found throughout central and eastern Amazonia of Brazil and northern Bolivia (fig. 115, bottom). These differ by an average of 8.74% sequence divergence, and the two haplotypes obtained from the Rio Juruá (one from the Headwaters region [locality a, the other from the Mouth region [locality **14**]) differ by 9.53%. The seven haplotypes from the broad area across central and eastern Amazonia differ among themselves by only 2.88%, on average.

We follow da Silva and Patton (1993) in recognizing two species in western Amazonia in general, and along the Rio Juruá specifically. However, we are unsure of the proper application of the available names to either species. Da Silva and Patton used the name *D. boliviensis* Anthony to refer to the mitochondrial clade in the Rio Juruá headwaters, and *D. dactylinus* (Desmarest) to that in central Amazonia. The type locality of *boliviensis* is in the Departamento de Cocha-

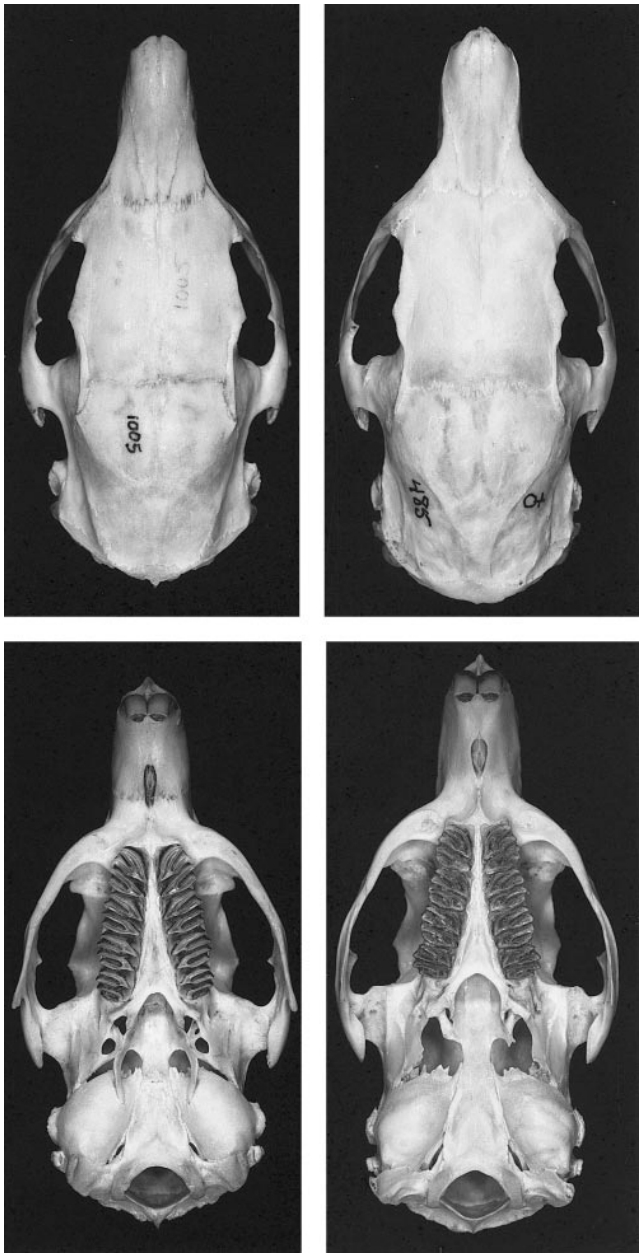

Fig. 113. Dorsal (top) and ventral (bottom) views of the cranium of Amazonian Bamboo rats, *Dactylomys*. **Left**: *D. boliviensis* (MNFS 1005, locality **a**). **Right**: *D. dactylinus* (JUR 485, locality **14**). Natural size.

bamba, Bolivia, but the Bolivian specimens of bamboo rats for which mtDNA data are available (from the Departamento de Pando) belong to the central Amazonian clade we allocate to *D. dactylinus* (fig. 115). We have not examined the specimens from the Departamento de Pando for which we have mtDNA data, but, based on comparisons with the holotype of *D. boliviensis* (AMNH 38709), we apply this name to our specimens

Fig. 114. Occlusal surface of the left maxillary toothrows of (**Left**) *Dactylomys boliviensis* (MNFS 1005, locality **a**) and (**Right**) *D. dactylinus* (JUR 485, locality **14**).

from the Headwaters clade. The holotype of *D. boliviensis* has the same overall color pattern (including color of middorsal hairs and dark head stripe) and cranial features described below for these specimens. The type locality of *D. dactylinus* is unknown, although Thomas (1911) restricted it to the upper Amazon, and proposed the name *canescens* for individuals from central Amazonia with the rusty underfur characteristic of the specimens we allocate to *dactylinus*. However, Lönnberg (1921) correctly noted that the holotype of *dactylinus* in the Paris Museum has rusty underfur, and thus probably came from somewhere downriver from Iquitos in northwestern Perú. The genus is under current review by Louise H. Emmons. Clearly there is much remaining to understand about species boundaries as well as the most basic aspects of the natural history of these animals.

Dactylomys boliviensis Anthony, 1920

TYPE LOCALITY: ''Mission San Antonio, Rio Chmore [sic, Chimoré], Prov. Cochabamba, Bolivia; altitude 1300 feet.''

DESCRIPTION: This is a large rat, with more muted dorsal color tones and a proportionately longer tail than *D. dactylinus* (table 48). The mystacial vibrissae are short, extending only to one half the length of the superciliary vibrissae, in contrast to the much longer mystacial vibrissae of *D. dactylinus* (fig. 116. The face is distinctly gray above and below the eyes with an olivaceous black stripe bordered by pale tipped hairs extending on the midline from the nose posteriorly between the ears to the nape, darkening progressively to blackish brown from above the eyes to the neck (fig. 116). The dorsal body color is grizzled grayish-olivaceous streaked with black, becoming paler on the sides, and gradually merging with the sparsely furred, pure white venter. There is only a slight hint of orange on the inside of the thighs. Individual hairs of the middorsum are of two types: somewhat heavier and longer hairs that are tricolored, with an elongated basal black band, a narrow subterminal pale yellow one, and a black tip; and shorter, thinner, and more common totally black hairs. As a result, if one parts the hair the undercolor is black to the skin. This color pattern contrasts sharply with specimens of *D. dactylinus*, as noted in the account of that species below. The tail has a well-furred base that extends for about 65 mm; it is heavily scaled and naked in appearance from furred base to tip, but the scales appear finer, averaging six annuli per cm near the tail base and 7.5 per cm near the tip, and less distinctly pentagonal than those of *D. dactylinus*. Each caudal scale-hair is distinctly dark brown or black over the basal half, becoming completely colorless along the terminal half to third of the tail. The median hair extends 1.5 to 2 scale rows. The tail is also distinctly bicolored, especially over the anterior two thirds of its length, but with the broad and dark dorsal stripe becoming gradually paler towards the tip.

The skull is large, with a short rostrum and broad, well-developed supraorbital ledges that form sub-triangular supraorbital processes (fig. 113). The few specimens of *D. bo-*

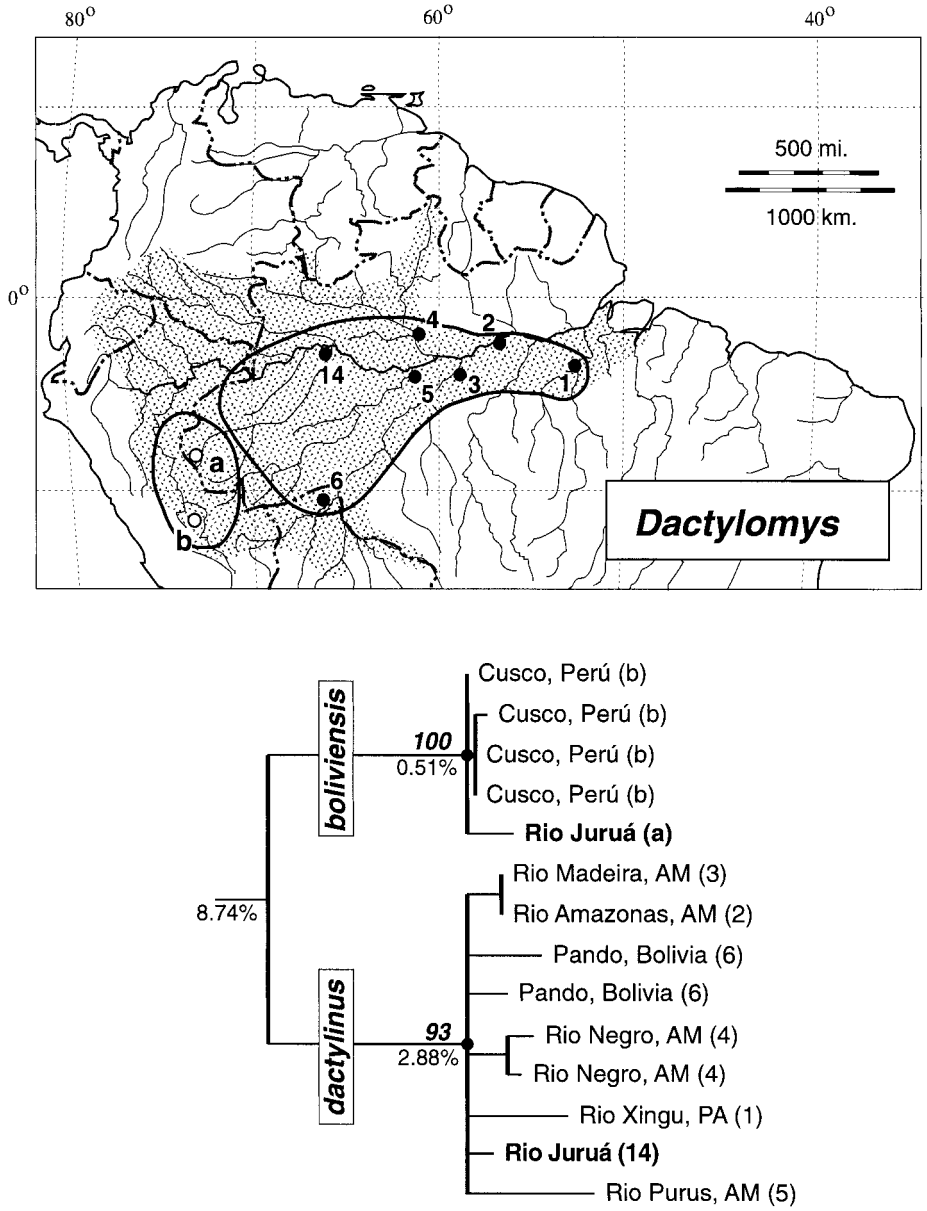

Fig. 115. (**Above**) Map of the approximate distribution of *Dactylomys* within Amazonia (from Emmons and Feer, 1997); localities for which mtDNA cytochrome-b sequence data are available are plotted and identified by number or letter as in the tree, below. Solid circles identify localities belonging to a central and eastern Amazonian clade, which we refer to *D. dactylinus*; open circles represent the two localities of *D. boliviensis* for which we have sequence data. (**Below**) Bootstrap consensus parsimonious tree generated from an exhaustive search, based on 798 bp of the cytochrome-b gene; length = 376 steps; CI = 0.747; RI = 0.751; rooted by comparison to sequences from the tree rats *Makalata* and *Mesomys*. Haplotypes representing the two clades occurring within the Rio Juruá are highlighted. Bold numbers at internal nodes are bootstrap values, based on 1000 iterations; percentages are average Kimura two-parameter distances. Provenance and voucher numbers for individuals examined are given in table 47.

TABLE 47
Haplotypes, Voucher Numbers, and Localities for Taxa of Bamboo Rats, Genus *Dactylomys*
Individual haplotypes listed from top to bottom in the tree, figure 115 (below), with the catalog numbers of their respective voucher specimens, and localities (identified as in the map, fig. 115, above) for which 798-bp haplotypes of the mitochondrial DNA cytochrome-b gene are available.

Haplotype	Voucher no.	Locality
Dactylomys boliviensis		
1	LHE 1444	2 km SW Tangoshiari, Río Pangoreni, Depto. Cusco, Perú, 1000 m, 11°46'S, 73°26.5'W (locality b)
2	LHE 1444A	2 km SW Tangoshiari, Río Pangoreni, Depto. Cusco, Perú, 1000 m, 11°46'S, 73°26.5'W (locality b)
3	LHE 1445	2 km SW Tangoshiari, Río Pangoreni, Depto. Cusco, Perú, 1000 m, 11°46'S, 73°26.5'W (locality b)
4	LHE 1480	2 km SW Tangoshiari, Río Pangoreni, Depto. Cusco, Perú, 1000 m, 11°46'S, 73°26.5'W (locality b)
5	MNFS 988	Fazenda Santa Fé (=Flora), left bank Rio Juruá, Acre, Brazil (locality a)
Dactylomys dactylinus		
6	AMNH 91865	Borba, Rio Madeira, Amazonas, Brazil (locality **3**)
7	AMNH 93952	Villa Bella Imperatriz (=Parintins), Amazonas, Brazil (locality **2**)
8	LHE 878	Centro, ca 18 km NNW San Juan de Nuevo Mundo, Abuna, Pando, Bolivia (locality **6**)
9	USNM 579620	Centro, ca 18 km NNW San Juan de Nuevo Mundo, Abuna, Pando, Bolivia (locality **6**)
10	MNFS 2119	Ilha das Onças, left bank Rio Negro, Amazonas, Brazil (locality **4**)
11	MNFS 2123	Ilha das Onças, left bank Rio Negro, Amazonas, Brazil (locality **4**)
12	LHE 607	52 km SSW Altamira, east bank Rio Xingu, Pará, Brazil (locality **1**)
13	JUR 485	Colocação Vira-Volta, left bank Rio Juruá, Amazonas, Brazil (locality **14**)
14	INPA 2477	right bank Rio Purus, Município de Beruri, Amazonas, Brazil (locality **5**)

liviensis we examined differ from all individuals in a larger series of *D. dactylinus* by having anteriorly directed paroccipital processes that follow the curvature of the auditory bulla, and having a postorbital process of the zygomatic arch comprised primarily of the jugal. The upper toothrows diverge strongly posteriorly, with left and right PM4 nearly meeting at the midline. The individual teeth exhibit coronal hypsodonty, have well-developed roots, and a planar occlusal surface. Each consists of four transverse lophs, with both an anterior and posterior pair separated by a deep median flexus but joined lingually and thus form a distinctive Y shape; the two pairs of lophs are separated by a transverse flexus that extends completely across the tooth (fig. 114, left). Both the individual lophs and lingual confluence appear narrower, and with sharper corners, in *D. boliviensis* than in *D. dactylinus*, although this is partly due to differences in absolute wear between the specimens available to us for comparison (fig. 114).

SELECTED MEASUREMENTS: We list external and cranial measurements of one individual in table 48.

DISTRIBUTION AND HABITAT: Individuals were observed, collected, or detected by their odor only in the dense and extensive bamboo thickets at Igarapé Porongaba (locality **1**) or at the community of Flora (locality a) in the headwaters of the Rio Juruá. These, and all other individuals heard along the river above Cruzeiro do Sul in Estado do Acre exhibited the same vocal structure with a staccato series of short pulses, ranging from about 15 to 45 and averaging around 20 (based on counts made by ear, not by recordings).

REPRODUCTION: All specimens were collected in the month of February; neither sex exhibited any indication of reproductive activity although the vagina of the single female was perforate.

COMMENTS: As noted by da Silva and Patton (1993), the call structure of the vocalizations of this animal differs markedly from that of *D. dactylinus* heard in middle and lower reaches of the Rio Juruá. The latter expressed no more than five to 10 individual

TABLE 48
Selected Dimensions (mm) of Two Adult Specimens of Bamboo Rats, *Dactylomys*, from the Rio Juruá, Western Amazonia

Variable	*D. boliviensis* (MNFS 988)	*D. dactylinus* (JUR 485)
TOL	706	704
TAL	435	389
HF	62	62
E	19	20
CIL	63.36	68.25
ZB	34.55	36.76
MB	26.74	27.73
IOC	18.10	19.47
RL	26.71	27.80
NL	22.88	21.92
RW-1	11.40	11.38
RW-2	10.30	10.97
RD	13.16	13.31
OL	18.01	19.05
D	15.56	16.05
MTRL	19.66	20.02
IFL	5.12	4.36
PL	19.02	19.24
AW	13.97	13.72
BUL	13.23	13.77
OCB	11.81	12.57
MPFL	13.71	—
MFPW	7.45	—
CD	23.27	24.19

pulses in a given vocalization, with an average of about seven. Call structure varies extensively throughout Amazonia (Emmons, 1981; Emmons and Feer, 1997), but is organized geographically into high or low pulse numbers that likely correspond to the two species we recognize here (P. Santos, J. Podos, and M. N. F. da Silva, unpubl. data). The two species likely encounter one another somewhere along the upper Rio Juruá between our Upper Central sampling sites and Cruzeiro do Sul (fig. 1). We did not travel this section of the river, and thus have no notes on the nature of vocalizations through this area.

SPECIMENS EXAMINED (n = 3): (**a**) 2m, 1f (MNFS 988, 1005, 1105).

Dactylomys dactylinus (Desmarest, 1817)

TYPE LOCALITY: No locality given in original description, but presumed to be eastern Perú; restricted to ''Upper Amazon area'' (Thomas, 1912: 88). However, this restriction is likely to be in error, as most specimens from Amazonia in the Muséum d'Histoire Naturelle in Paris, where Desmarest's type is housed, are probably from central Brazil, the lower Amazon, or French Guiana (R. S. Voss, personal commun.).

DESCRIPTION: This taxon is similar to *D. boliviensis*, described above, but clearly differs in several features. Among our specimens, this taxon is absolutely larger in most cranial dimensions, but has a shorter tail relative to head and body length (table 48). The face is pale tan above and below the eyes, nose, and over the rostrum, gradually darkening to chestnut between the ears and posteriorly onto the neck (fig. 116). This stripe is never blackish-brown, as in *D. boliviensis*, and it contrasts sharply with the grizzled yellowish dorsum, which is streaked with black hairs. The dorsal hairs are chestnut at their bases, with a subterminal black band and yellow or pale yellow tips. The sides become progressively more fulvous, with the thighs distinctly burnt orange. There is a white band encircling the ankle. The middorsal hairs are also of two types, but these contrast sharply in color pattern compared to *D. boliviensis*. The heavier and longer hairs are bicolored, black basally with a short pale yellow tip; the more abundant thinner hairs are reddish basally with short dark tips. As a result, the parted hair appears distinctly dull reddish to the skin, with a mixture of black streaks. As in *D. boliviensis*, the venter is sparsely covered with completely white hairs. The base of the tail is fully haired for about 60 mm, then appearing naked to the tip. The scales are large, prominent, more pentagonal and coarser in appearance than in *D. boliviensis*, and average about five annuli per cm near the base or six per cm at the tip. The scale hairs appear correspondingly shorter, extending less than 1.5 scale rows. All scale hairs are completely colorless along the entire length of the tail distal to its furred base.

The general cranial conformation is the same as described above for *D. boliviensis*, as are the rooted but hypsodont and strongly diverging cheek toothrows (fig. 113). As noted, however, the transverse lophs of *D. dac-*

Fig. 116. Dorsal view of the head and neck of *Dactylomys boliviensis* (**top:** MNFS 1005, locality **a**) and *D. dactylinus* (**bottom:** JUR 485, locality **14**).

tylinus appear broader and rounded (fig. 114, right), although caution must be taken to compare individuals of equivalent toothwear. While the skull of *D. dactylinus* is larger in almost all dimensions, our comparisons are limited to just two specimens, each with different levels of toothwear and, thus, presumptive age. Further details of cranial morphology must await comparisons of adequate series of specimens. However, all specimens of *D. dactylinus* we have examined (those from the Rio Juruá, the Rio Jaú, and from along the Rio Solimões from northeastern Perú to below Manaus have more vertically oriented paroccipital processes that do not follow the contour of the auditory bulla.

SELECTED MEASUREMENTS: See table 48.

DISTRIBUTION AND HABITAT: We collected our two specimens in bamboo and cane thickets on the margins of várzea and terra firme forest.

REPRODUCTION: The single female was pregnant with two fetuses, each measuring 97 mm from crown to rump. The male had enlarged testes and was presumably reproductively active. Both were caught in June, during the high-water season.

COMMENTS: All individual *D. dactylinus* heard throughout the lower and middle sections of the Rio Juruá produced vocalizations with a range from 5 to 10 pulses, with a mean of 7 (see da Silva and Patton, 1993; P. Santos, J. Podos, and M. N. F. da Silva, unpubl. data). This call structure contrasts sharply with that described above for *D. boliviensis*. Emmons and Feer (1997: 244) suggest that the head patch of museum specimens may bleach severely with age, thus accounting for the range in color from ''almost white to brown or tan and black sometimes with a rusty stripe.'' However, the differences in head stripe we describe here for *D. dactylinus* as opposed to *D. boliviensis* were evident in freshly collected specimens from these, and other, localities, and the blackish-brown patch of our specimens of *D. boliviensis* has not bleached in the nearly six years since they were collected, including specimens that were preserved in formalin and have been maintained in 70% ethanol.

SPECIMENS EXAMINED (n = 2): (**14**) 1m, 1f (JUR 485, MNFS 1736).

ECHIMYINAE GRAY, 1825

Isothrix Wagner, 1845

Bushy-tailed tree rats

The Amazonian taxa of brush-tailed tree rats of the genus *Isothrix* were reviewed by Patton and Emmons (1985). They recognized two species, which replace one another geographically from west to east within the basin. *Isothrix bistriata* is widely distributed in western Amazonia, from southeastern Colombia south along the base of the Andes to northern and eastern Bolivia, thence east on both sides of the Rio Solimões to at least the Rio Madeira and Rio Negro (fig. 117). Throughout this area, the species is most commonly encountered in seasonally flooded forest, either várzea or *igapó*. On the east banks of the Rio Negro and Rio Madeira, *I. bistriata* is replaced by *I. pagurus* Wagner, the second species recognized by Patton and Emmons (1985), which apparently prefers terra firme forest (e.g., Malcolm, 1990). A third species of brush-tailed rat has recently been described from French Guiana, *I. sinnamariensis* (Vié et al., 1997). This species is similar to *I. pagurus*, its geographically closest relative, in both morphological and mtDNA sequences, but differs extensively in chromosome complement.

Isothrix is unusual among echimyid rodents of Amazonia because it has soft fur that lacks any stiffened hairs or spines characteristic of other genera, and its tail is well-haired, bushy along its entire length instead of naked or with a long terminal pencil. By virtue of the bushy tail, the Aguaruna Jívaro of northern Perú grouped *Isothrix* with the tree squirrels rather than with its biological relatives (Patton et al., 1982). The skull has a short, broad rostrum and somewhat flat lateral profile, broad interorbital region with parallel, overhanging supraorbital ledges extending posteriorly as ridges onto the parietals (fig. 118). The maxillary cheek-toothrows are parallel, slightly bowed posteriorly, and separated by a narrow palate with the mesopterygoid fossa penetrating to the level of M2. The teeth (fig. 119A) are nearly laminate, each with three labial flexi extending two thirds across the tooth surface and meeting a short median flexus in the unworn condition. All flexi are notably broad, being wid-

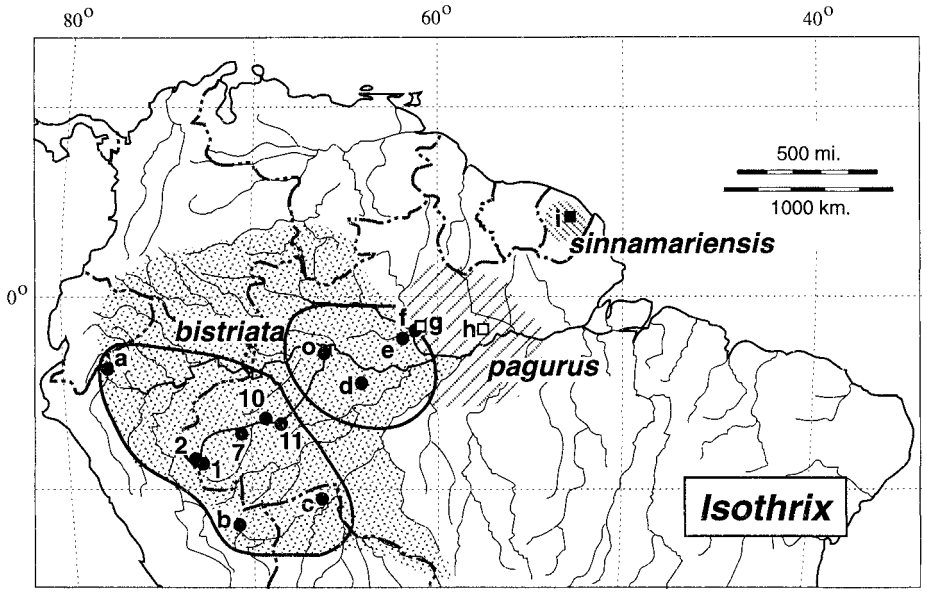

Fig. 117. Map of the distribution of *Isothrix* in greater Amazonia (from Emmons and Feer, 1997, supplemented by Vié et al., 1997). Localities from which individual specimens have been examined for sequence of the mtDNA cytochrome-b gene are indicated, and these are grouped geographically as the reciprocally monophyletic clades identified in the tree, fig. 120.

er than the lophs they separate. The median flexus is particularly wide and confluent with the first lateral flexus in early stages of wear on all four teeth. The first and third lateral flexi close with minimal wear, becoming islands surrounded by oval lophs. The combination of flat frontal region with strongly developed but parallel supraorbital ledges, short, broad rostrum, and distinctive cheek-teeth readily differentiate the skull of *I. bistriata* from any other sympatric, or nearly sympatric echimyid taxa.

A limited view of molecular phylogeographic variation in *Isothrix* was provided by da Silva and Patton (1993), who identified two clades within *I. bistriata* that were nearly equidistant between each other and *I. pagurus*. Vié et al. (1997) provided sequence data for *I. sinnamariensis* from French Guiana, and compared it with both *I. bistriata* and *I. pagurus*. We have added slightly to this database recently, and summarize all available mtDNA cytochrome-b data in fig. 120, a strict consensus tree based on 798 base pairs of sequence for 20 haplotypes from the three known species. Available geographic localities are mapped in fig. 117, as are regional monophyletic clades based on the topology presented in fig. 120. Provenance and voucher specimen catalog numbers are given in table 49. Average Kimura two-parameter distances among regional clades and species are provided in table 50.

Consistent with earlier findings (da Silva and Patton, 1993), *I. bistriata* comprises two geographically differentiated forms, both of which are found within the Rio Juruá basin but replace one another geographically. One of these, an upriver clade, matches specimens from northern and southern Perú and northern Bolivia. The other, a downriver clade, also is known from both sides of the lower Rio Negro north of Manaus and on the opposite side of the Rio Solimões (figs. 117 and 120). Also consistent with our previous results, these two clades do not form a sister-pair relationship according to available data. Rather, they differ by 12.2% from each other, and together average only 12.4% different from the species pair of *I. pagurus* and *I. sinnamariensis* (table 50). Substantial additional variation exists between haplotypes within each of the two clades of *I. bistriata* with up to 7% divergence between some lo-

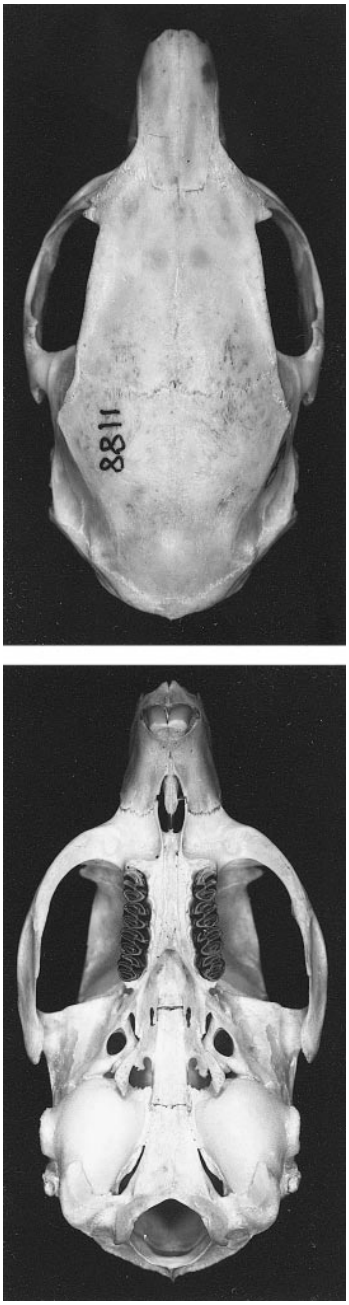

Fig. 118. Dorsal (**top**) and ventral (**bottom**) views of the skull of an adult *Isothrix bistriata* (MNFS 1188, locality **2**). Natural size.

calities in the upriver clade and nearly this level within the downriver clade (da Silva and Patton, 1993: fig. 120). Additional geographic sampling and analyses are required to determine if the mtDNA clades of *I. bistriata* represent separate species, as implied by their deep divergence and lack of sister relationship. Meanwhile, we continue to treat both clades as members of a single polytypic species.

Isothrix bistriata Wagner, 1845

TYPE LOCALITY: Rio Guaporé, Estado do Mato Grosso, Brazil.

DESCRIPTION: This is the largest of the three known species in the genus. External, craniodental, and genetic characteristics by which *I. bistriata* differs from *I. pagurus*, and the closely similar *I. sinnamariensis*, are detailed in Patton and Emmons (1985) and Vié et al. (1997). As this is the only species of *Isothrix* known to occur west of the rios Negro-Madeira axis, it differs from other cooccurring echimyids in the Rio Juruá and elsewhere in western Amazonia by the same set of characters detailed above for the genus. The most obvious external features of *I. bistriata* are its grizzled yellow-brown to olive dorsal coloration mixed with black hairs, its well-defined black or dark brown supraorbital stripes extending over the forehead to the nape and bordering a median pale creamy patch on the crown, its pale yellow to buff venter, and its bushy tail typically rust or golden-colored over the basal third to half with the terminal portion black. The skull is illustrated in figure 118.

SELECTED MEASUREMENTS: We present the mean, range, and standard error of the four external and 22 cranial variables in table 51. We separate these data for each of the two mitochondrial DNA clades identified in figures 117 and 120.

GEOGRAPHIC VARIATION: The number of specimens available to us is insufficient to examine either geographic or nongeographic patterns of morphometric characters within the Rio Juruá basin. However, because of the extensive degree of sequence divergence between individuals from the central and headwaters region, and from those at river's mouth (12.2%, table 50), we compare them

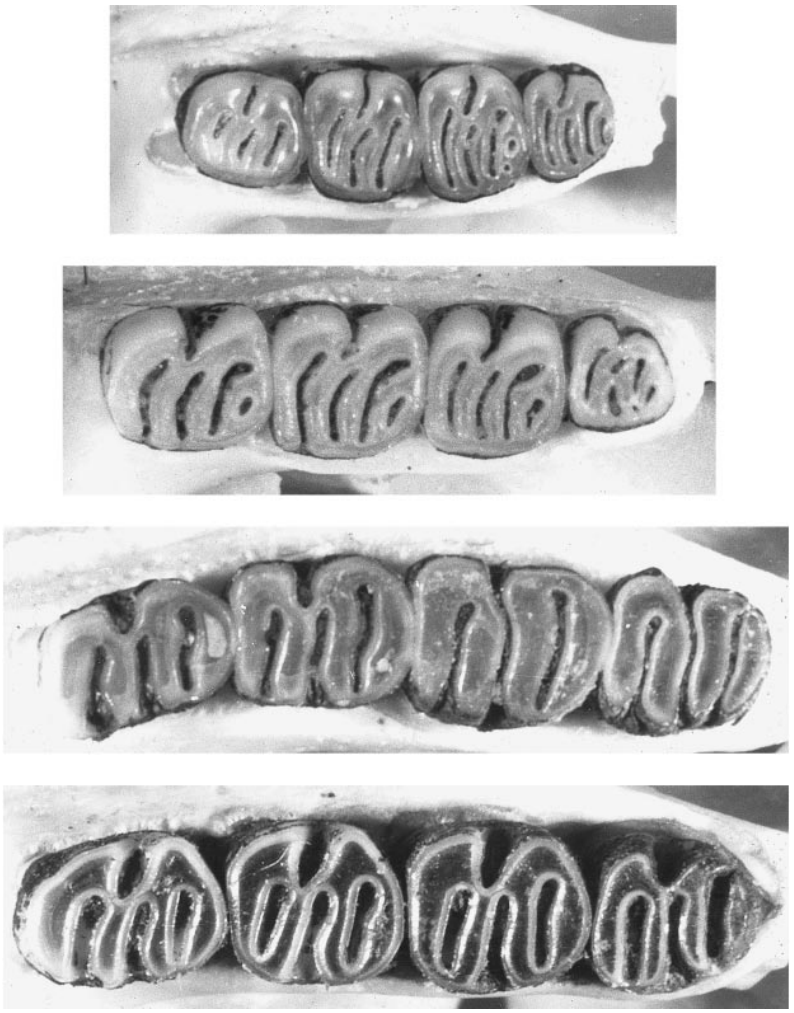

Fig. 119. Occlusal surface of the right maxillary toothrows of five genera of rodents of the family Echimyidae: **A**, *Isothrix bistriata* (MNFS 471, locality 7); **B**, *Makalata macrura* (JLP 15394, locality **8**); **C**, *Proechimys steerei* (JLP 15245, locality 7); and **D**, *Mesomys hispidus* (JUR 502, locality **14**).

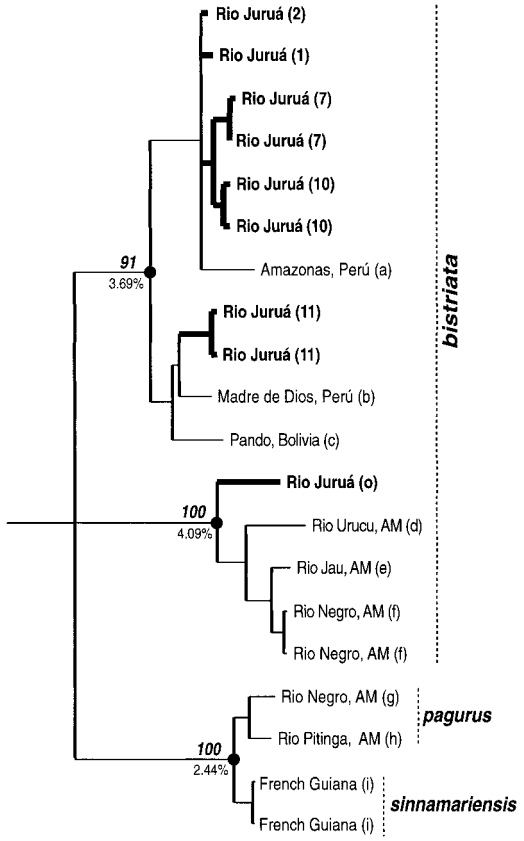

Fig. 120. Strict consensus of three minimum-length parsimony trees for haplotypes of the mitochondrial cytochrome-b gene (798 bp) for the genus *Isothrix*. Length = 512 steps, CI = 0.684, RI = 0.803. Sequences of *Proechimys* and *Mesomys* were used as outgroups to root the tree. Bold numbers at internal nodes are bootstrap values, based on 1000 replicates; percentages are mean Kimura two-parameter distances. Haplotypes are identified by locality, as in the map, fig. 117, and provenance and voucher catalogue numbers are listed in table 49.

morphometrically using discriminant function analysis. We include samples of *I. bistriata* from southern Venezuela and northern and eastern Perú because Patton and Emmons (1985) demonstrated that samples from Venezuela, for example, were nonoverlapping in discriminant space relative to those from Perú and Bolivia. Here, therefore, we wished to determine not only the degree to which the two mtDNA clades from the Rio Juruá are distinct, but also to examine their morphometric relationship to specimens from elsewhere in the species' range.

The downriver sample is larger in most measurements compared to individuals of the upriver mtDNA clade (table 51), significantly so in 13 of the 20 cranial variables despite its small size (n = 3) (one-way ANOVA, $p < 0.05$ — RD, OL, BUL, CD; $p < 0.01$ — CIL, ZB, RL, RW-2; $p < 0.001$ — MB, IOC, RW-1, and D). The two are not significantly different in any external dimension, although the downriver clade still tends to be larger. Bivariate plots of the four geographic samples on the first three discriminant axes are illustrated in figure 117, with the standardized discriminant functions given in table 52. The two Juruá clades do not differ significantly (one-way ANOVA, Fisher's PLSD mean difference = −0.566, $p > 0.359$) in their placement on the first axis, but do on the second and third (one-way ANOVA, Fisher's PLSD mean difference = 3.334 and 32.059, respectively, $p < 0.001$ in both cases). The sample from northern and eastern Perú is indistinguishable from that of the upriver Juruá clade on all three axes (one-way ANOVA, Fisher's PLSD mean difference = 0.512, 0.900, and −0.555 respectively, $p > 0.05$). This parallels the mtDNA data in which haplotypes from northern Perú fall well within that clade (figs. 117 and 120). Interestingly, the sample from the mouth of the Rio Juruá is not intermediate in discriminant space between the upriver and Peruvian group of samples and that from southern Venezuela, as might be expected by its somewhat intermediate geographic position. Rather, the downriver clade and specimens from Venezuela are the most divergent in mensural characters among the set of geographic samples examined, differing significantly along all three axes (one-way ANOVA, Fisher's PLSD mean difference = 4.413, −2.130, and −2.860 respectively, $p < 0.001$). On the other hand, the upriver and Peruvian samples differ from those from Venezuela only on the first axis (one-way ANOVA, Fisher's PLSD mean difference = 3.848 and −3.328, respectively, $p < 0.001$), and not on the other two.

Despite the limited sample sizes, there appear to be at least three lineages of *I. bistriata* within Amazonia. The first of these

TABLE 49

Haplotypes, Voucher Numbers, and Localities for Taxa of Brushy Tree Rats, Genus *Isothrix*

Individual haplotypes listed from top to bottom in the tree, figure 120, with the catalog numbers of their respective voucher specimens, and localities (identified as in the map, fig. 117) for which 798-bp haplotypes of the mitochondrial DNA cytochrome-b gene are available.

Haplotype	Voucher no.	Locality
Isothrix bistriata—Western clade		
1	MNFS 1273	opposite Igarapé Porongaba, left bank Rio Juruá, Acre, Brazil (locality **2**)
2	MNFS 1411	Igarapé Porongaba, right bank Rio Juruá, Acre, Brazil (locality **1**)
3	MNFS 471	Penedo, right bank Rio Juruá, Amazonas, Brazil (locality **7**)
4	MNFS 500	Penedo, right bank Rio Juruá, Amazonas, Brazil (locality **7**)
5	MNFS 893	opposite Altamira, left bank Rio Juruá, Amazonas, Brazil (locality **10**)
6	MNFS 901	opposite Altamira, left bank Rio Juruá, Amazonas, Brazil (locality **10**)
7	MVZ 157974	La Poza, Río Santiago, Amazonas, Perú (locality a)
8	MNFS 797	Jainu, right bank Rio Juruá, Amazonas, Brazil (locality **11**)
9	MNFS 833	Jainu, right bank Rio Juruá, Amazonas, Brazil (locality **11**)
10	VPT 735	Pakitza, Río Manu, Madre de Dios, Perú (locality b)
11	LHE 881	18 km NNW San Juan de Nuevo Mundo, Pando, Bolivia (locality c)
Isothrix bistriata—Central clade		
12	JUR 545	Tres Unidos, left bank Rio Juruá, Amazonas, Brazil (locality o)
13	MNFS 97	Alto Rio Urucu, Amazonas, Brazil (locality d)
14	JLP 16749	right bank Rio Jaú near mouth, Amazona, Brazil (locality e)
15	MNFS 2111	Ilha das Onças, left bank Rio Negro, Amazonas, Brazil (locality f)
16	MNFS 2122	Ilha das Onças, left bank Rio Negro, Amazonas, Brazil (locality f)
Isothrix pagurus		
17	MNFS 2126	Lago Meduiním, left bank Rio Negro, Amazonas, Brazil (locality g)
18	INPA 2463	UHE Pitinga, Rio Pitinga, Amazonas, Brazil (locality h)
Isothrix sinnamariensis		
19	MNHN 1995.1321 (holotype)	right bank, Sinnamary River, 21 km upstream Petit Saut Dam, French Guiana (locality i)
20	MNHN 1995.1322	right bank, Sinnamary River, 22 km upstream Petit Saut Dam, French Guiana (locality i)

TABLE 50

Kimura 2-Parameter Distances Among Cytochrome-b Haplotypes of Clades and Species of Brush-tailed Rats, *Isothrix*

Number of haplotypes examined and mean ± standard error. Within-taxon measures are given on the diagonal.

		bistriata			
Taxon	n	Western	Central	*pagurus*	*sinnamariensis*
Western	11	3.692 ± 1.936	12.168 ± 1.545	12.459 ± 0.439	12.301 ± 0.320
Central	5		4.093 ± 2.347	12.436 ± 0.483	11.950 ± 0.478
pagurus	2			1.910	2.436 ± 0.187
sinnamariensis	2				0.250

TABLE 51
Selected External and Cranial Dimensions, and Average Discriminant Scores, for the Two mtDNA Clades of *Isothrix* from the Rio Juruá
Measurements (mm) are given as mean ± standard error, with range and sample size. Individuals are pooled across all localities along the river.

	Upriver clade			Downriver clade		
Variable	Mean ± SE	Range	n	Mean ± SE	Range	n
TOL	491.7 ± 6.44	447–533	18	499.5 ± 25.5	474–525	2
TAL	242.9 ± 3.93	215–271	18	226.5 ± 44.5	182–271	2
HF	47.9 ± 0.55	43–52	24	49.3 ± 3.28	43–54	3
E	18.4 ± 0.46	15–24	18	18.7 ± 0.88	17–20	3
CIL	50.57 ± 0.39	46.03–53.40	24	53.74 ± 1.47	50.94–55.93	3
ZB	28.83 ± 0.26	26.33–31.28	24	31.43 ± 0.99	29.45–32.43	3
MB	23.04 ± 0.17	21.61–24.93	24	24.80 ± 0.45	23.92–25.23	3
IOC	13.72 ± 0.17	12.49–15.16	24	15.48 ± 0.77	13.96–16.48	3
RL	18.79 ± 0.18	16.76–20.34	24	20.78 ± 1.08	18.64–22.09	3
NL	16.40 ± 0.21	14.74–18.12	24	17.18 ± 0.70	15.89–18.28	3
RW-1	9.81 ± 0.11	8.93–10.70	24	11.05 ± 0.65	9.94–12.22	3
RW-2	8.23 ± 0.10	7.35–9.33	24	9.33 ± 0.58	8.23–10.14	3
RD	11.83 ± 0.14	10.20–12.92	24	12.77 ± 0.39	12.04–13.34	3
OL	15.41 ± 0.14	13.61–16.64	24	16.23 ± 0.23	15.81–16.62	3
D	12.23 ± 0.15	11.10–13.44	24	13.87 ± 0.54	12.83–14.52	3
MTRL	11.05 ± 0.10	10.40–12.08	24	10.93 ± 0.27	10.41–11.22	3
IFL	5.91 ± 0.12	3.71–6.33	24	5.80 ± 0.23	5.49–6.25	3
PL	19.90 ± 0.21	17.44–21.21	24	20.93 ± 0.79	19.42–22.09	3
AW	3.82 ± 0.09	3.11–4.58	24	4.05 ± 0.17	3.71–4.23	3
OCB	10.14 ± 0.08	8.96–11.00	24	10.11 ± 0.48	9.24–10.91	3
BUL	12.39 ± 0.13	11.31–14.14	24	13.23 ± 0.32	12.63–13.61	3
MPFL	14.52 ± 0.17	13.32–16.24	24	15.47 ± 0.49	14.54–16.11	3
MPFW	5.14 ± 0.09	4.26–6.08	24	5.39 ± 0.42	4.55–5.83	3
CD	16.88 ± 0.14	15.92–18.64	24	17.87 ± 0.88	16.74–19.63	3
DF-1	1.058 ± 0.191	−0.468–3.007	23	1.624 ± 0.565	0.562–2.488	3
DF-2	1.370 ± 0.224	−1.239–3.214	23	−1.964 ± 0.840	−3.411 to −0.504	3
DF-3	−0.156 ± 0.21	−2.227–1.378	23	−2.867 ± 1.287	−5.093 to −0.634	3

occurs throughout western Amazonia, ranging from northern Perú south to Bolivia and east as far as the middle Rio Juruá in western Brazil. This form exhibits limited geographic variation in mtDNA sequences (table 50) and (with available specimens) minimal morphometric variation as well. On distributional grounds, it is likely that specimens from Estado do Mato Grosso, Brazil, where the type locality of *bistriata* Wagner is located, belong to this form, and thus Wagner's name would apply to it. If this proves not to be the case, the earliest name available for the western Amazonian taxon would be *villosa* Deville, 1852 (see Patton and Emmons, 1985). The second lineage would contain samples of the second mtDNA clade, namely those from the mouth of the Rio Juruá, the upper Rio Urucu southeast of Tefé, and from both sides of the lower Rio Negro northwest of Manaus (Rio Jaú and Ilha das Onças, table 49). This form is likewise distinct in mtDNA sequence (fig. 120, table 50) and apparently morphometrically as well, although larger samples are needed for verification. The earliest available name for this taxon is most likely *negrensis* Thomas, 1920, since the type locality of Acajutuba, on the lower Rio Negro above Manaus, is within this range. Finally, the third taxon is that from the upper Río Orinoco region in east-central Colombia and the Casiquiare region of southern Venezuela. Although mtDNA sequences are lacking, this form remains nearly nonoverlapping in cranial morphometric pattern relative to the other two, especially on the first discrim-

TABLE 52
Standardized Discriminant Coefficients in Comparisons Among Four Geographic Samples of *Isothrix bistriata* from Amazonia
Analyses are based on $\log_{10}$-transformed cranial variables only.

Variable	DF-1	DF-2	DF-3
CIL	−0.43172	−0.48512	0.19526
ZB	−0.55261	−0.22370	0.09889
MB	−0.12434	−0.67433	−0.23503
IOC	−0.03371	−0.62788	0.59394
RL	1.41798	0.33640	−0.77077
NL	−1.53707	0.49324	0.01037
RW-1	−0.17103	−0.47401	−0.19455
RW-2	0.46028	0.34036	−0.25428
RD	0.70516	0.20847	0.17112
OL	0.10594	−0.26730	0.38636
D	−0.13233	−0.38955	−1.31027
MTRL	0.35616	0.20219	−0.03792
IFL	−0.01290	0.00640	0.24282
PL	0.24262	0.26926	0.74389
AW	0.54536	0.21103	−0.13514
BUL	−0.32931	−0.30680	0.36701
OCB	0.12623	0.18311	0.10114
BOL	0.30724	0.56188	0.10711
MPFW	−0.12320	0.35146	0.11890
CD	0.32240	0.72226	−0.50679
Eigenvalue	2.34232	0.96475	0.40581
% contribution	63.086	25.984	10.930

inant axis (fig. 121). As documented by Patton and Emmons (1985), the name *orinoci* Thomas, 1899, with its type locality at Maipures on the upper Río Orinoco in Intendencia Vichada, Colombia, most likely applies to this form. Additional specimens are required for both molecular and morphological analysis before it is possible to determine if each of these three groups warrants separate status at the species level.

DISTRIBUTION AND HABITAT: *Isothrix bistriata* is a denizen of seasonally inundated forest, either igapó or várzea. All specimens (n = 32) were obtained either in canopy platform traps placed within these forest types (or along their edge, such as on line "P" at Vai-Quem-Quer, locality **15**; see fig. 23), were shot in trees, or were taken from tree holes. In the latter case, we tied Tomahawk traps over the mouth of a tree hole and beat on the trunk forcing the animal into the trap. We commonly saw individuals with their heads protruding from tree holes during daylight hours. In such cases, those trees were climbed and Tomahawk live traps nailed over the nest entrance, usually with successful capture during the night.

REPRODUCTION: We caught this species in all months we trapped, and from localities within each of the four geographic regions along the river (fig. 1). None of the females were pregnant, although all adults (those with all cheekteeth erupted and exhibiting some wear) were parous and had enlarged nipples. One female taken at Penedo (locality **7**) in late August was lactating, and another taken at Lago Três Unidos (locality o) was captured together in the same trap with a small (49 g) young individual, presumably her offspring. Placental scars were noted in several individuals but were never more than two, suggesting a small litter size. All fully adult males had developed midventral chest glands, approximately 25 mm in length. The testes in these individuals were large, averaging 24 × 12 mm (length × width), but were always abdominal in position rather than descended into the obvious scrotum. These same individuals also had enlarged vesicular glands and enlarged seminiferous tubules in the cauda epididymides, suggesting reproductive competency. Pairs of adult individuals, presumably a male and female, were observed on three occasions, one time each at Sacado (locality **5**), Nova Empresa (locality **8**), and opposite Altamira (locality **10**).

KARYOTYPE: The karyotype of *I. bistriata* was described by Leal-Mesquita (1991), who illustrated both non-differentially stained and C-band complements for a female specimen from the hydroelectric dam at Samuel, Estado do Rondônia, near Porto Velho on the Rio Madeira. Chromosomal data from 16 specimens from the Rio Juruá (10 males and 6 females) do not differ. The diploid number is 60, the fundamental number 116. The autosomal complement consists of one pair of large subtelocentric elements and 28 pairs of metacentrics and submetacentrics grading in size from large to small. The X-chromosome is a large acrocentric and the Y a very small metacentric. In contrast, the diploid and fun-

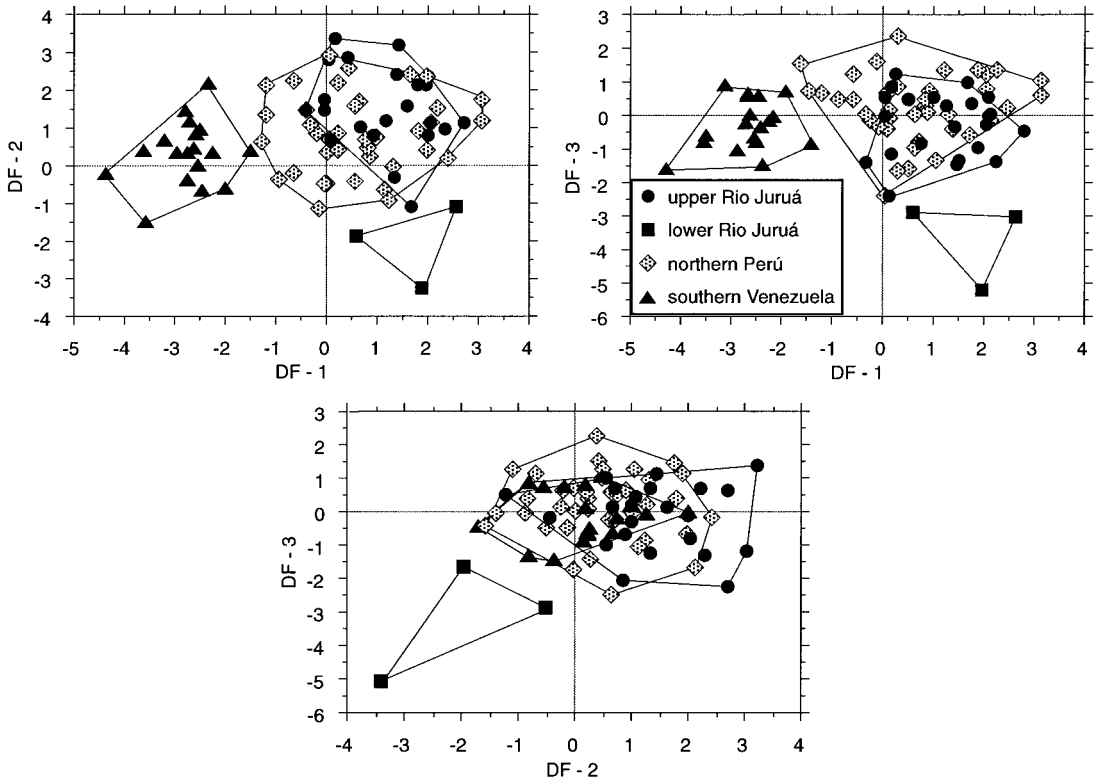

Fig. 121. Bivariate plots of three discrimant function axes based on log-transformed cranial variables for four geographic samples of *Isothrix bistriata*: the upriver Rio Juruá mtDNA clade (solid circles), the downriver Rio Juruá mtDNA clade (solid squares), pooled samples from northern and eastern Perú (stippled diamonds), and pooled samples from southern Venezuela (solid triangles). Provenance data for the latter two samples can be found in Patton and Emmons (1985).

damental numbers of *I. pagurus* are 22 and 38, respectively (Patton and Emmons, 1985); those of *I. sinnamariensis* are 28 and 42 (Vié et al., 1997).

SPECIMENS EXAMINED (n = 41): (**1**) 1f — MNFS 1411; (**2**) 1m, 1f — MNFS 1188, 1273; (**3**) 1m — JUR 240; (**5**) 2m, 1f, 1 unknown — JLP 15568, 15625–15627; (**7**) 1m, 1f — MNFS 471, 500; (**8**) 1m, 1f — MNFS 431, 506; (**10**) 6m, 5f — JUR 199–200, MNFS 893, 900–901, 914, 920, 934, 941–942, 957; (**11**) 3m, 1f — MNFS 797, 809–810, 833; (**14**) 1m — MNFS 1725; (**o**) 3f — JUR 544–546; (**15**) 1f — JUR 296. Specimens from Royal Natural History Museum, Stockholm (see Patterson, 1992): João Pessoa [= Eirunepé] (5m, 3f — 2118, 2138, 2140, 2161, 2183, 2217, 2235, 2475); Lago Grande (1m — 2488).

Makalata Husson, 1978

Red-nosed tree rats

Makalata is readily distinguished from all other echimyids from the Rio Juruá by the combination of bristly fur with a mixture of stiffened hairs and flattened but flexible spines, reddish-orange nose, and short (less than head-and-body length), naked, and scaly tail lacking a terminal tuft of hairs. Cranially (fig. 122), *Makalata* is similar to *Isothrix*. Both genera have short, deep rostra and broad interorbital regions with overhanging supraorbital ledges that extend onto the parietals as distinct, but short ridges. The interorbital region of *Makalata*, however, diverges posteriorly, rather than being parallel as in *Isothrix*, and the rostrum is decidedly longer and narrower. The maxillary tooth-

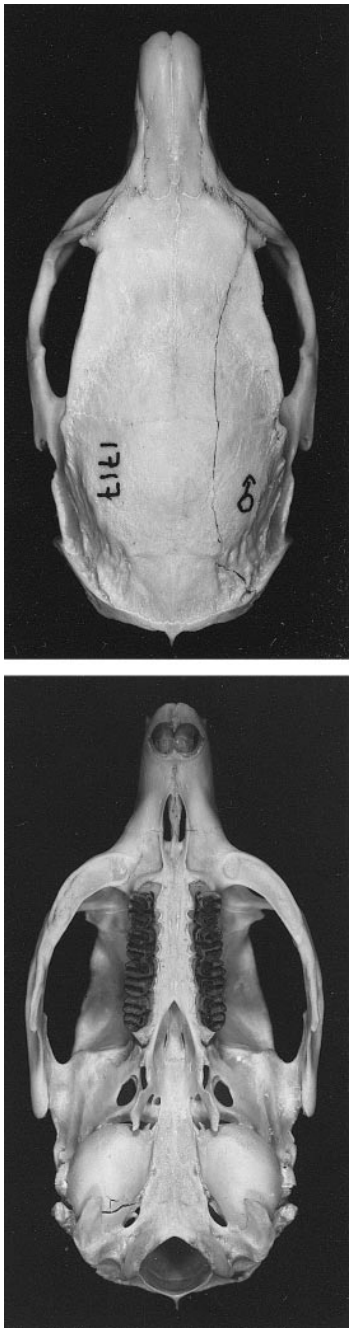

Fig. 122. Dorsal (top) and ventral (bottom) views of the cranium of *Makalata macrura* from the Rio Juruá (MNFS 1717, locality **14**). Natural size.

rows are parallel and separated by a narrow palate. The toothrows are longer than in *Isothrix*, making the teeth appear more massive since the overall skull length is similar. The palate is also longer, accommodating the longer toothrows, with the mesopterygoid fossa extending only to M3. The cheekteeth (fig. 119B) are similar to those of *Isothrix*, with each tooth having three deep flexi on the labial side isolating four lophs, and a short medial flexus. In the unworn condition, these lophs form pairs of U-shaped anterior and posterior units joined on their medial side. Each pair in all four cheekteeth may become connected labially with progressive wear. Both lateral and medial flexi are narrow, more so than the lophs, a condition opposite to that seen in *Isothrix*. The second lateral and medial flexi are joined and completely separate the anterior and posterior pair of U-shaped lophs in both M2 and M3. This condition differentiates the cheekteeth of *Makalata* from those of either *Mesomys* or *Proechimys*. Their relatively small size and parallel, as opposed to divergent, toothrows readily distinguish the teeth of *Makalata* from those of *Dactylomys*.

The genus was erected by Husson in 1978 to include the single species *M. armata* (I. Geoffroy St.-Hilaire) (= *didelphoides* Desmarest; see Emmons, 1993), which had previously been included within the genus *Echimys* by most earlier workers (e.g., Ellerman, 1940; Cabrera, 1961). The generic status of many of the species commonly listed within *Echimys* are under review by Louise H. Emmons, as is the complete species membership within *Makalata*. However, preliminary assessments indicate that the genus contains more than one species. Emmons (1993) limits the range of *M. didelphoides* to the Guiana region, including that part of Amazonian Brazil north of the Amazon and east of the Rio Negro and south of the Amazon from at least the Rio Xingu eastward. She suggested that specimens from the central Amazon belong to a second species, *M. macrura* (Wagner). Finally, Emmons and Feer (1997) list *grandis*, *occasius*, and *rhipidurus* as valid species of *Makalata*, rather than of *Echimys*, in addition to *didelphoides*. Our preliminary mitochondrial DNA sequence data (da Silva and Patton, 1993) also suggested that *Mak-*

alata is composite, with at least two and possibly more entities replacing one another from west to east across Amazonia. We summarize the available molecular data below, again to emphasize the need for further geographic sampling and to help identify areas where critical samples would be especially beneficial.

We have examined individuals from only 11 geographic localities (20 individuals), but these are distributed across Amazonia from northern Perú to the Rio Xingu in eastern Brazil and south to eastern Bolivia (fig. 123, table 53). There is, however, extensive divergence among cytochrome-b haplotypes (798 bp), with two major geographic clades recognizable that differ by more than 16% (Kimura two-parameter distance). The first of these is from the Rio Xingu in Estado do Pará, Brazil, which, within itself, includes two quite divergent lineages that differ by an average of 10%. The Rio Xingu clade groups with strong bootstrap support (97%) to haplotypes from the Río Iténez in eastern Bolivia, but at an average divergence of 11.5%. The second major geographic clade is widespread, ranging from northern Perú east to at least the right bank of the lower Rio Negro north of Manaus and south to include samples from the Rio Juruá and the Rio Purus near its mouth. The groupings depicted in the tree (fig. 123) are generally concordant with the geographic distinction between morphs recognized by Patterson (1992) that differ in pelage characteristics, and recognized as separate species by Emmons (1993). These are the western *M. macrura* (Wagner), characterized by a gray-brown venter, and the eastern and southern *M. didelphoides*, with a pale cream or buff venter. We follow Emmons' guidance here, and allocate our specimens from the Rio Juruá to *M. macrura* However, we note that substantial geographic structure exists within both presumptive species. Within *M. macrura*, for example, three well-differentiated geographic units are evident that differ by an average of 6.0% and that exhibit a maximum pair-wise divergence of 9.7%. One of these includes specimens from northern Perú and the central portion of the Rio Juruá, a second constitutes the single individual from the mouth of the Rio Juruá (locality **14**), a third comprises specimens from the Rio Purus and the Arquipélago de Anavilhanas in the lower Rio Negro, and a fourth represents individuals from three adjacent localities on the Rio Jaú west of the Rio Negro. Similarly, as mentioned above, specimens from the Rio Xingu divide into two sharply defined groups, one from the right bank and the second from a near-by but well-isolated island, and both differ substantially from the Bolivian specimens despite strong support for their phyletic linkage. Rats currently allocated to the genus *Makalata* offer a rich subject for systematic analysis, research that is currently being pursued by Louise H. Emmons.

Makalata macrura (Wagner, 1842)

TYPE LOCALITY: Borba, Rio Madeira, Amazonas, Brazil (Emmons, 1993).

DESCRIPTION: As for the genus, above, with a generally dark overall coloration and gray-brown venter.

SELECTED MEASUREMENTS:: We give the mean, standard errors, and range of external and cranial measurements in table 54.

DISTRIBUTION AND HABITAT: Specimens are available from only four localities along the central and lower regions of the Rio Juruá: Nova Empresa (locality **8**), near Miranda (locality i), opposite Altamira (locality **10**), and Colocação Vira-Volta (locality **14**). Three of the five specimens collected were obtained in canopy platform traps, one was shot in a tree at night, and the fifth was found swimming in the river during the day, perhaps having been dropped by a raptor. Those trapped or shot were taken in seasonally inundated forest (várzea or *igapó*), which is consistent both with the suggestion of Emmons and Feer (1997) and our observations elsewhere within the central Amazon. It is unclear whether our trapping program simply failed to ascertain the true abundance of this species, or whether, in fact, *M. macrura* is rare throughout the Rio Juruá. Emmons and Feer (1997) suggested that the species is locally common. This species has the especially large caecum and long colon suggestive of a folivorous diet, and thus they may not have been attracted by the baits we used.

REPRODUCTION: The single adult female, taken in September, was pregnant, with one

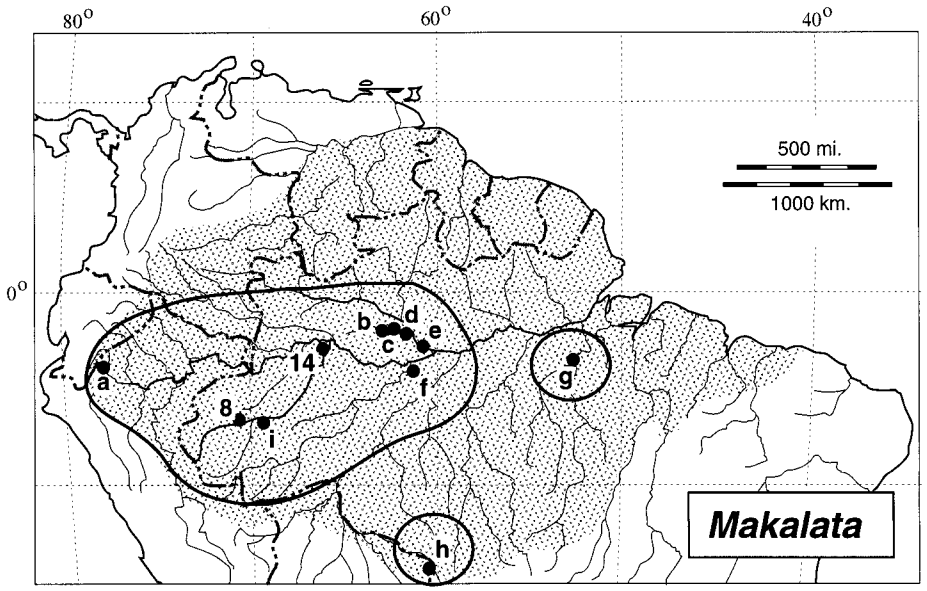

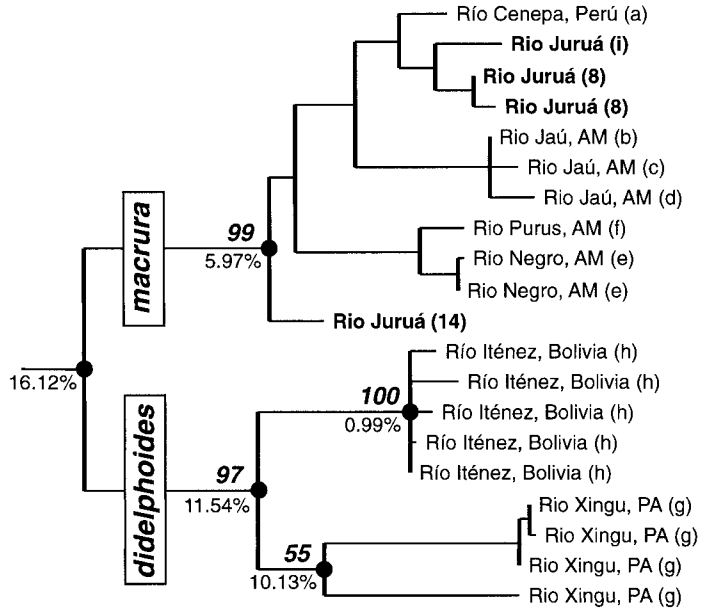

Fig. 123. (**Above**) Map of the approximate combined ranges of *Makalata didelphoides* in eastern and southern Amazonia and *M. macrura* from western Amazonia (redrawn from Emmons and Feer, 1997). Geographic localities from which specimens have been examined for 798 bp of the mitochondrial cytochrome-b gene are indicated by solid circles; localities are identified as in table 53, which provides provenance and voucher catalogue numbers. (**Below**) The strict consensus of six equally minimal length parsimony trees for cytochrome-b haplotypes, based on a branch-and-bound analysis: length = 542 steps, CI = 0.673, RI = 0.820. Sequences of *Proechimys* and *Mesomys* were used as outgroups to root the tree. Numbers at internal nodes are bootstrap values, based on 1000 replicates; percentages are average Kimura two-parameter distances.

TABLE 53

Haplotypes, Voucher Numbers, and Localities for Taxa of Red-nosed Tree Rats, Genus *Makalata*

Individual haplotypes listed from top to bottom in the tree, figure 123 (below), with the catalog numbers of their respective voucher specimens, and localities (identified as in the map, fig. 123, above) for which 798-bp haplotypes of the mitochondrial DNA cytochrome-b gene are available.

Haplotype	Voucher no.	Locality
Makalata macrura		
1	MVZ 153636	Huampami, Río Cenepa, Amazonas, Perú (locality a)
2	JLP 15214	Miranda, right bank Rio Juruá, Amazonas, Brazil (locality i)
3	JLP 15394	Nova Empresa, left bank Rio Juruá, Amazonas, Brazil (locality **8**)
4	MNFS 465	Nova Empresa, left bank Rio Juruá, Amazonas, Brazil (locality **8**)
5	MNFS 2048	Tambor, left bank Rio Jaú, Amazonas, Brazil (locality b)
6	YL 123	Macaco, left bank Rio Jaú, Amazonas, Brazil (locality c)
7	MNFS 2094	left bank, above mouth Rio Jaú, Amazonas, Brazil (locality d)
8	INPA 2474	right bank Rio Purus, Município de Beruri, Amazonas, Brazil (locality f)
9	CM 39	Arquipélago Anavilhanas, Rio Negro, Amazonas, Brazil (locality e)
10	CM 40	Arquipélago Anavilhanas, Rio Negro, Amazonas, Brazil (locality e)
11	MNFS 1717	Colocação Vira-Volta, left bank Rio Juruá, Amazonas, Brazil (locality **14**)
Makalata didelphoides		
12	TTS 380	Flor de Oro, left bank Río Iténez, Parque Noël Kempff Mercado, Santa Cruz, Bolivia (locality h)
13	TTS 383	Flor de Oro, left bank Río Iténez, Parque Noël Kempff Mercado, Santa Cruz, Bolivia (locality h)
14	JLS 170	Flor de Oro, left bank Río Iténez, Parque Noël Kempff Mercado, Santa Cruz, Bolivia (locality h)
15	LHE 1323	Flor de Oro, left bank Río Iténez, Parque Noël Kempff Mercado, Santa Cruz, Bolivia (locality h)
16	ECH 4	Flor de Oro, left bank Río Iténez, Parque Noël Kempff Mercado, Santa Cruz, Bolivia (locality h)
17	LHE 554	52 km SSW Altamira, east bank Rio Xingu, Pará, Brazil (locality g)
18	LHE 600	52 km SSW Altamira, east bank Rio Xingu, Pará, Brazil (locality g)
19	LHE 632	52 km SSW Altamira, east bank Rio Xingu, Pará, Brazil (locality g)
20	LHE 595	52 km SSW Altamira, east bank Rio Xingu, Pará, Brazil (locality g)

fetus. A second female was young with M3 still unerupted; it was nulliparous. All three males were adult with enlarged testes; they were taken in the months of September, November, and May.

COMMENTS: The number of specimens from the Rio Juruá is inadequate for any analysis of geographic variation in morphology, but the material available does not suggest any substantive differentiation among populations along the river. However, the single specimen taken from the Mouth region of the river differed by 5.9% in cytochrome-b sequence (399 bp) from those specimens from the central part of the river basin (see da Silva and Patton, 1993).

SPECIMENS EXAMINED (n = 8): (**8**) 1m, 1f — JLP 15394, MNFS 465; (**i**) 1f — JLP 15214; (**10**) 1m — MNFS 894; (**14**) 1m — MNFS 1717. Specimens from Royal Natural History Museum, Stockholm (see Patterson, 1992): João Pessoa [= Eirunepé] (1m, 2f - 2117, 2163, 2333).

SUBFAMILY EUMYSOPINAE RUSCONI, 1935

Mesomys Wagner, 1845

Spiny tree rats

Spiny tree rats of the genus *Mesomys* are common components of the arboreal fauna of Amazonia, yet are only rarely collected unless effort is made to place traps in vine tangles or trees, or to hunt at night. Individuals will, on occasion, come to the ground and be taken in terrestrial traps baited with standard foods (mixtures of seeds, raisins, peanut butter, etc.), and they are often com-

TABLE 54
Selected External and Cranial Dimensions of *Makalata macrura* from the Rio Juruá Basin
Measurements (mm) are given as mean, with range and sample size.

Variable	Mean	Range	n
TOL	433.7	427–444	4
TAL	204.0	194–211	4
HF	42.8	41–46	4
E	16.3	15–17	4
CIL	49.84	47.99–52.01	4
ZB	27.48	26.96–27.92	4
MB	22.89	21.84–23.67	4
IOC	14.08	13.57–14.64	4
RL	20.56	19.69–21.34	4
NL	17.43	16.73–18.62	4
RW-1	7.93	7.59–8.63	4
RD	11.64	11.42–11.94	4
D	12.49	11.89–13.31	4
MTRL	12.02	11.53–12.95	4
IFL	4.16	3.83–4.45	4
PL	22.02	21.59–22.59	4
AW	8.22	7.91–8.89	4
MPFL	11.18	9.81–12.11	4
MPFW	4.11	4.00–4.22	4
BUL	11.58	11.38–11.77	4
CD	21.21	20.21-21.93	4

mon in tree falls or disturbed areas, as around villages where they can be found on rafters in houses. This is a relatively small-bodied animal, with the short and broad feet, large plantar pads, and sharply decurved claws indicative of arboreal habits. Among the echimyid climbing rats, *Mesomys* (and its close relative *Lonchothrix*; see Lara et al., 1996) is unique in its combination of dorsal pelage comprised of broad and stiff spines, a sparsely haired tail that terminates in a distinct brush, or pencil, and small, rounded cheekteeth with flexi wearing to isolated oval fossettae or pits rather than tending to form transverse lamellae. *Mesomys* shares these tooth characters with the terrestrial spiny rats (*Proechimys*, *Hoplomys*, and *Trinomys*) and its subfamilial placement has been uncertain as a result (see Patton and Reig, 1989, for discussion, and fig. 119C and D for comparisons).

Mesomys occurs throughout Amazonia, from the eastern flank of the Andes in Colombia south to Bolivia and eastward to the Guianas and the mouth of the Rio Amazonas in eastern Brazil (Emmons, 1994; Emmons and Feer, 1997). Woods (1993) lists five species, two of which (*didelphoides* Desmarest and *obscurus* Wagner) have now been allocated to the genus *Makalata* (Emmons, 1993). Of the other three, *M. hispidus* is considered to be widespread throughout Amazonia, *M. leniceps* is known only from the Andean foothills in northern Perú, and *M. stimulax* ranges in eastern Brazil south of the Rio Amazonas (Emmons and Feer, 1997). Although the genus is in clear need of revisionary attention, the molecular data we have accumulated offer substantial help in apportioning the demonstrable geographic variation of this taxon into reasonable phylogenetic units.

Da Silva and Patton (1993) and Patton et al. (1994) provided an initial review of the degree of differentiation in the genus based on variation in the mitochondrial cytochrome-b gene. These papers documented well-defined regional geographic clades that shared deep divergences, suggestive of separate species status. In particular, they documented sympatry between spiny tree rats at two localities where cytochrome-b sequences differed by more than 13%, more so than the divergence between eastern Amazonian *M. stimulax* and any other sample from central Brazil to Perú and Bolivia. We expand on these accounts, and assign the broadly distributed haplotype clade we define below to the species *M. hispidus*. As a consequence, we argue that the highly divergent and sympatric, but very localized clade is an unknown species, and we describe it here as a new species. Our rationale for these actions is given in the accounts below.

First, however, we describe the regional patterns of molecular divergence, based on all available geographic samples of spiny tree rats. We then describe the new taxon, after which we examine patterns of differentiation within the dominant Amazonian taxon, *M. hispidus*, within the Rio Juruá basin.

Species Units of Spiny Tree Rats, Genus *Mesomys*

We have examined samples of *Mesomys* from 26 localities from throughout Amazonia

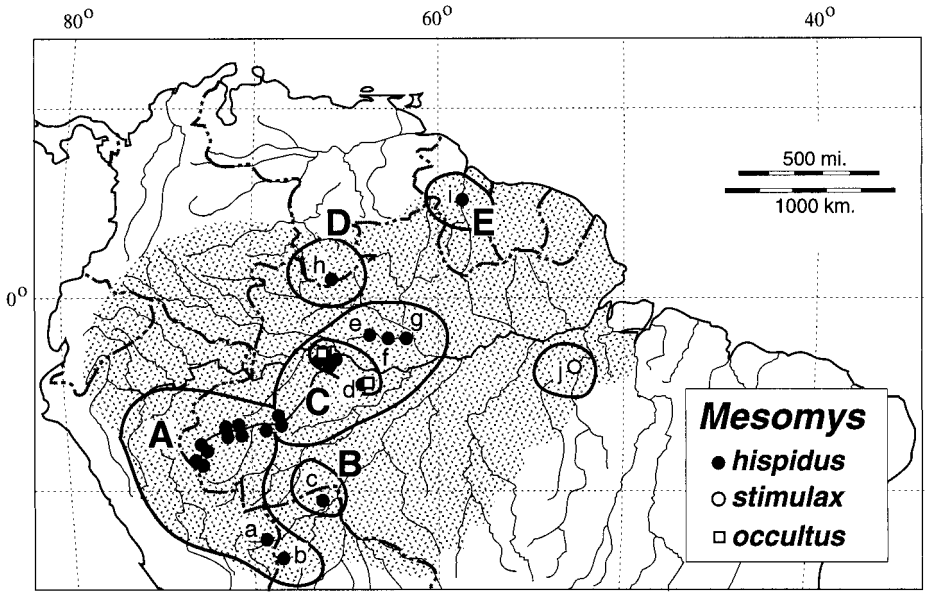

Fig. 124. Map of the distribution of *Mesomys* in greater Amazonia (from Emmons and Feer, 1997). Localities from which individual specimens have been examined for sequence of the mtDNA cytochrome-b gene are indicated; those from localities outside of the Rio Juruá are lettered, and all localities are listed in table 55. Solid circles indicate localities of *M. hispidus*, the open circle that of *M. stimulax*, and the open box identifies the two localities from which the new species described herein was found. Localities are grouped geographically according to the reciprocally monophyletic clades identified in the tree, fig. 127.

(fig. 124, table 55). These samples cover much of western Amazonia, with 15 localities along the Rio Juruá itself, although much additional work remains. The data are sufficient, however, to define five equally divergent, geographically regional clades for the species *M. hispidus*, which is demonstrably different in sequence from *M. stimulax* and particularly from the new species we describe beyond (fig. 125). The important points with regard to the phylogenetic analysis include the following:

(1) Our single sample of *M. stimulax* from the Rio Xingu differs from all samples assigned to *M. hispidus* by an average Kimura two-parameter distance of 8.1%, nearly twice the level of divergence found among the five clades of the latter. The level of difference cannot be attributed solely to geographic distance, since our sample of *M. stimulax* is no further distant from the main sampling of *M. hispidus* than is the sample of the latter from Guyana, for example (see fig. 124). The level of differentiation, and its phyletic position well outside the cluster of *M. hispidus* haplotypes, supports the suggestion of Emmons and Feer (1997) that *stimulax* is a valid species.

(2) With the available samples, *M. hispidus* is divisible into five essentially equally divergent clades broadly positioned within northern and western Amazonia. These differ from one another by an average of 4.63% (fig. 125). Samples from northern Perú to northwestern Bolivia and eastward to the middle reaches of the Rio Juruá form one clade (labeled A in the map, fig. 124, and tree, fig. 125), which overlaps in distribution at one locality on the Rio Juruá (Barro Vermelho, locality **12**; see Patton et al., 1994, and below) with another large geographic unit, labeled clade C. This latter clade is distributed throughout central Amazonia, from the middle part of the Rio Juruá eastward to the upper Rio Urucu and then north of the Rio Solimões to the Rio Jaú west of the Rio Negro. The three remaining clades are represented by single localities, one each in

TABLE 55

Haplotypes, Voucher Numbers, and Localities for Taxa of Spiny Tree Rats, Genus *Mesomys*

Individual haplotypes listed from top to bottom in the tree, figure 125, with the catalog numbers of their respective voucher specimens, and localities (identified as in the map, fig. 124) for which 798-bp haplotypes of the mitochondrial DNA cytochrome-b gene are available.

Haplotype	Voucher no.	Locality
Mesomys hispidus—Clade A		
1	LHE 748	Moira Camp, Río Madidi, Prov. Iturraldi, La Paz, Bolivia (locality b)
2	VPT 727	Reserva Cusco Amazónico, Río Madre de Dios, Madre de Dios, Perú (locality a)
3	MNFS 1231	Igarapé Porongaba, right bank Rio Juruá, Acre, Brazil (locality **1**)
4	MNFS 1519	Nova Vida, right bank Rio Juruá, Acre, Brazil (locality **3**)
5	MNFS 1230	Igarapé Porongaba, right bank Rio Juruá, Acre, Brazil (locality **1**)
6	MNFS 1573	Sobral, left bank Rio Juruá, Acre, Brazil (locality **4**)
7	MNFS 1363	Igarapé Porongaba, right bank Rio Juruá, Acre, Brazil (locality **1**)
8	MNFS 1257	opposite Igarapé Porongaba, left bank Rio Juruá, Acre, Brazil (locality **2**)
9	MNFS 1353	opposite Igarapé Porongaba, left bank Rio Juruá, Acre, Brazil (locality **2**)
10	MNFS 568	Sacado, right bank Rio Juruá, Amazonas, Brazil (locality **5**)
11	MNFS 436	Penedo, right bank Rio Juruá, Amazonas, Brazil (locality **7**)
12	JLP 15725	Seringal Condor, left bank Rio Juruá, Amazonas, Brazil (locality **6**)
13	MNFS 564	Seringal Condor, left bank Rio Juruá, Amazonas, Brazil (locality **6**)
14	MNFS 432	Nova Empresa, left bank Rio Juruá, Amazonas, Brazil (locality **8**)
15	JLP 15852	Barro Vermelho, left bank Rio Juruá, Amazonas, Brazil (locality **12**)
16	MNFS 745	Barro Vermelho, left bank Rio Juruá, Amazonas, Brazil (locality **12**)
Mesomys hispidus—Clade B		
17	USNM 579619	Centro, ca. 18 km NNW San Juan de Nuevo Mundo, Prov. Abuna, Pando, Bolivia (locality c)
Mesomys hispidus—Clade C		
18	MNFS 909	Altamira, right bank Rio Juruá, Amazonas, Brazil (locality **9**)
19	MNFS 754	Jainu, right bank Rio Juruá, Amazonas, Brazil (locality **11**)
20	MNFS 729	Barro Vermelho, left bank Rio Juruá, Amazonas, Brazil (locality **12**)
21	JUR 453	Colocação Vira-Volta, left bank Rio Juruá, Amazonas, Brazil (locality **14**)
22	JUR 459	Ilhazinha, left bank Rio Juruá, Amazonas, Brazil (locality **16**)
23	MNFS 149	alto Rio Urucu, Tefé, Amazonas, Brazil (locality d)
24	MNFS 157	alto Rio Urucu, Tefé, Amazonas, Brazil (locality d)
25	MNFS 188	alto Rio Urucu, Tefé, Amazonas, Brazil (locality d)
26	MNFS 200	alto Rio Urucu, Tefé, Amazonas, Brazil (locality d)
27	MNFS 2087	right bank above mouth Rio Jaú, Amazonas, Brazil (locality g)
28	JLP 16735	Macaco, left bank Rio Jaú, Amazonas, Brazil (locality f)
29	MNFS 2016	Tambor, left bank Rio Jaú, Amazonas, Brazil (locality e)
30	MNFS 2055	Tambor, left bank Rio Jaú, Amazonas, Brazil (locality e)
31	MNFS 2028	Tambor, left bank Rio Jaú, Amazonas, Brazil (locality e)
Mesomys hispidus—Clade D		
32	MBUCV-ALG 14162	Río Mawarinuma, Neblina base camp, Amazonas, Venezuela (locality h)
Mesomys hispidus—Clade E		
33	LHE 968	Maipaima Creek, W. Kanuku Mtns., Guyana (locality i)
Mesomys stimulax		
34	LHE 572	52 km SSW Altamira, east bank Rio Xingu, Pará, Brazil (locality j)
35	MDC 550	52 km SSW Altamira, east bank Rio Xingu, Pará, Brazil (locality j)
Mesomys occultus		
36	JUR 501 (holotype)	Vira-Volta, left bank Rio Juruá, Amazonas, Brazil (locality **14**)
37	MNFS 201	alto Rio Urucu, Tefé, Amazonas, Brazil (locality d)

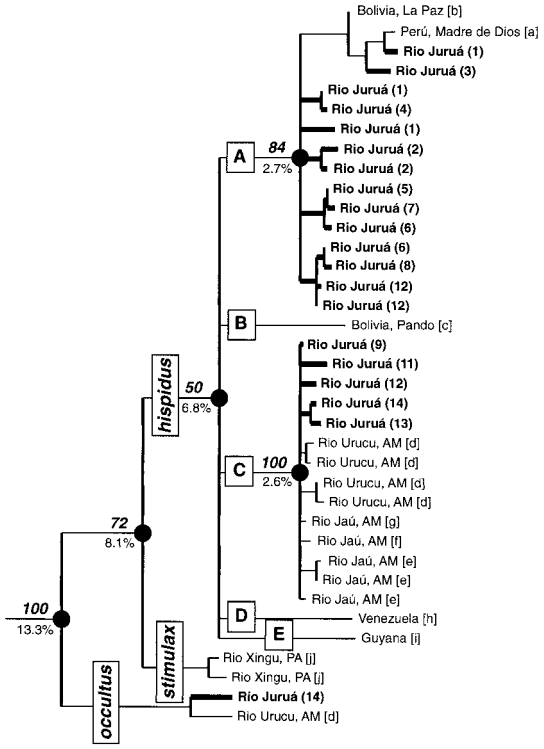

Fig. 125. Bootstrap consensus minimum-length parsimony tree for haplotypes of the mitochondrial cytochrome-b gene (798 bp) for spiny tree rats, genus *Mesomys*. Length = 644 steps, CI = 0.554, RI = 0.733. Sequences of *Proechimys* and *Isothrix* were used as outgroups to root the tree. Bold numbers at internal nodes are bootstrap values, based on 1000 replicates; percentages are average Kimura two-parameter distances. Haplotypes are identified by locality, as in the map, fig. 124, and provenance and voucher catalog numbers are listed in table 55.

northern Bolivia (clade B), southern Venezuela (clade D), and northern Guyana (clade E). The five clades form an unresolved polytomy, although the two widely distributed ones (clades A and C) are each strongly supported, with bootstrap values of 94% or higher and internal levels of divergence among included haplotypes about 2.5%. We discuss clade structure within the Rio Juruá in the account of this species, below.

(3) A limited number of specimens were obtained at two localities in the geographic region of clade C of *M. hispidus* that differ substantially in molecular sequence (an average of 13.3%) from all other specimens we have examined from those and all other localities (fig. 125). Specimens with these divergent haplotypes are sympatric with *M. hispidus* at these two localities (Colocação Vira-Volta [locality **14**] in the Mouth Region of the Rio Juruá and the upper Rio Urucu to the east). As a consequence of demonstrable sympatry and deep molecular divergence, as well as diagnosable morphological features described below, we describe this taxon as:

Mesomys occultus, new species

HOLOTYPE: INPA 2690, adult female collected by J. R. Malcolm on June 4, 1992, (original number JUR 501); body, naturally missing tail at the base, preserved in formalin and maintained in 70% ethanol with skull removed; skull and mandibles in good condition; liver sample maintained in 95% ethanol; and chromosome cell suspension maintained frozen.

TYPE LOCALITY: Colocação Vira-Volta, left bank Rio Juruá on Igarapé Arabidi, affluent of Paraná Breu, Amazonas, Brazil (3°17′S , 66°14′W); locality **14** in the map, figure 1.

DIAGNOSIS: A spinose and moderate-sized arboreal rat. Middle band of aristiform spines of the neck and shoulder region orange. Tail especially hirsute but with narrow and largely colorless hairs associated with individual scales, and terminating in a distinct crest and elongated tuft of hairs extending 30 mm or more beyond the tip (fig. 126). Skull (fig. 127) with a short, broad, and distinctly diamond-shaped incisive foramen with a short premaxillary septum, one third, or less, the length of the opening; weak grooves on anterior palate extend posteriorly from border of incisive foramen; median palatal ridge only weakly developed or absent; orthodont upper incisors; and narrow, attenuated, and angled paroccipital processes. Four flexi on PM4, M1, and M2, with the fourth small and lost with wear in older individuals; usually only three flexi on M3 or, if four, medial flexi coalesced (fig. 128). Karyotype with diploid number of 42, fundamental number of 54 (fig. 129).

REFERRED SPECIMENS: Known from four specimens in addition to the holotype, as follows: three topotypes, JUR 502 (adult fe-

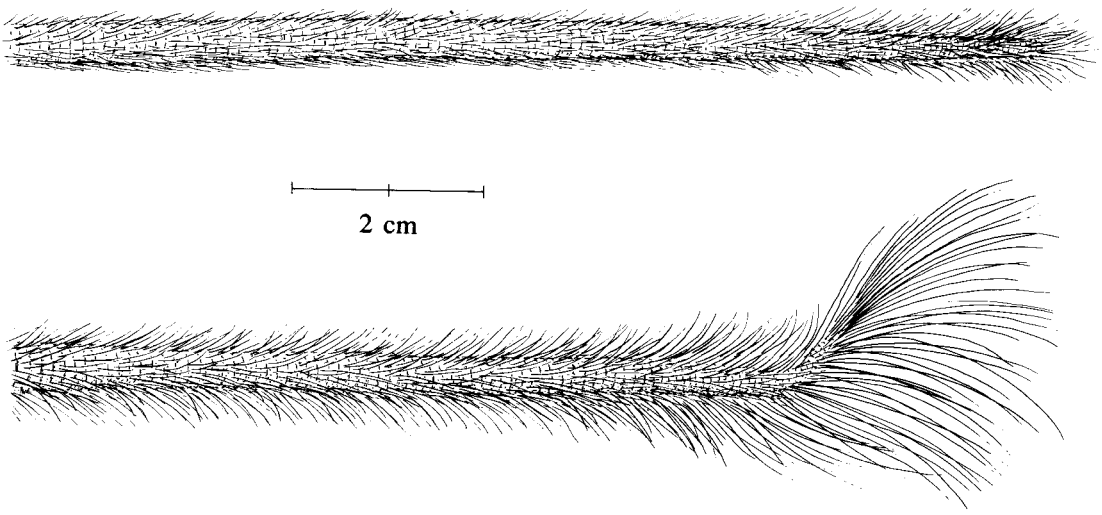

Fig. 126. Lateral views of the terminal portion of the tails of *Mesomys hispidus* (**top:** MNFS 569, locality **5**) and *M. occultus* (**bottom:** MNFS 201, upper Rio Urucu), illustrating differences in degree to which the tail is hairy as well as the length of terminal tuft.

male, fluid preserved body with skull removed, chromosome cell suspension, and tissues in 95% ethanol); JUR 567 (subadult male, fluid preserved body with skull removed, chromosome cell suspension, and tissues in 95% ethanol); and MNFS 1701 (subadult male, fluid preserved body with skull removed, chromosome cell suspension, and tissues in 95% ethanol); and MNFS 201 from the upper Rio Urucu, Pref. Tefé, Amazonas, Brazil (adult female, fluid preserved body with skull removed and tissues in 95% ethanol).

MEASUREMENTS OF HOLOTYPE: See table 56.

ADDITIONAL MEASUREMENTS: See table 56.

DESCRIPTION AND COMPARISONS: A small rat, equivalent in size to *M. hispidus*, to which it is similar in color, color pattern, and degree of aristiform spine development. Externally, these two are so similar that they were not recognized as distinct until the genetic data were examined. Subsequent comparisons of the series available to us, however, revealed the subtle, but consistent differences in external, cranial, and tooth characters enumerated above in the diagnosis. In contrast to *M. occultus*, *M. hispidus* lacks an orange midband in the aristiform spines of the neck and shoulder region. It has black, petiolate tail hairs as opposed to the colorless, thin hairs of *M. occultus*. *Mesomys hispidus* has a longer and narrower incisive foramen with either slightly bowed or parallel sides and a longer premaxillary septum (fig. 130), along with two deep groves on the anterior palate that extend to the level of M1 and flank a well-developed median ridge. The paroccipital processes of *M. occultus* are flatter and broader, oriented more in the dorso-ventral plane. All cheekteeth have four flexi, with all flexi independent and the last small but always discernible into advanced age (fig. 128). Finally, while the length of the terminal tail tuft is highly variable in *M. hispidus*, it is significantly shorter than that of *M. occultus*. Only one of the five known specimens of *M. occultus* has a complete tail, but the length of its tail tuft nonoverlaps with and is significantly longer than that of *M. hispidus* whether it is compared to the entire series of the latter or only those from the same locality (33.31 mm versus 5.04 to 21.28, critical difference = 8.521 and $p < 0.001$ by Fisher's PLSD, or 6.54 to 17.50, critical difference = 11.787 and $p = 0.0046$, respectively). The tail of *M. occultus* is also more hirsute and has a terminal dorsal crest, in addition to the pencil, in contrast to that of *M. hispidus* (fig. 127). The two species also differ substantially in karyotype, as that

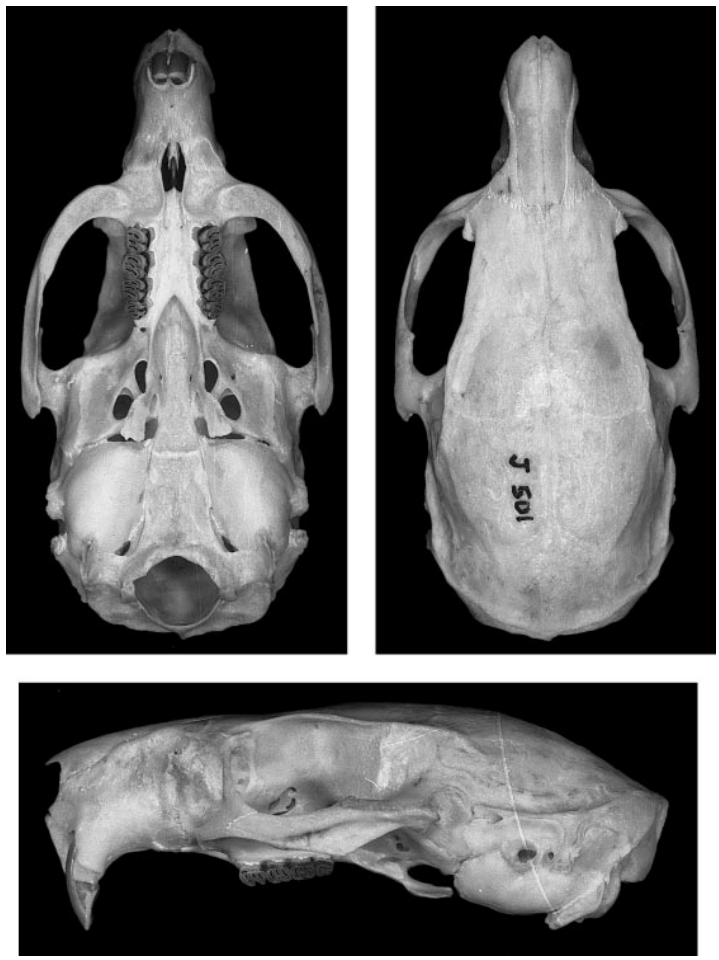

Fig. 127. Dorsal, ventral, and lateral views of the skull of the holotype of *Mesomys occultus* (INPA 2690, locality **14**). Magnification = ×2.

of *M. hispidus* is 2n = 60, FN = 116 (see below and fig. 129A and B).

We compared the two species morphometrically by a discriminant analysis, using $\log_{10}$-transformed cranial variables and treated all specimens of *M. hispidus* as a single group. They exhibit completely nonoverlapping distributions along the single discriminant axis recovered (fig. 131). Each specimen was correctly classified to its respective taxon, with posterior probabilities of 0.96 or higher. Although no single variable differs significantly between the two species (two-tailed *t*-tests; *p* always > 0.07), overall cranial length measures contrast with the more restricted rostral, palate, and mesopterygoid fossa lengths in influencing most of the multivariate separation (table 57).

COMMENTS: Through the kindness of Louise H. Emmons, we compared the crania of our specimens of *M. occultus* to photographs she had taken of the holotypes of *ferrugineus* Günther, *spicatus* Thomas, *leniceps* Thomas, and *stimulax* Thomas, all in the British Museum (Natural History). Although both *ferrugineus* and *spicatus* are also characterized by ''tassels about an inch long on the end of their tails'' (Thomas, 1924: 535), neither possesses the cranial characters, especially the distinctive incisive foramina, of *M. occultus*. Both *ferrugineus* and *spicatus* are usually listed as synonyms of *M. hispidus*

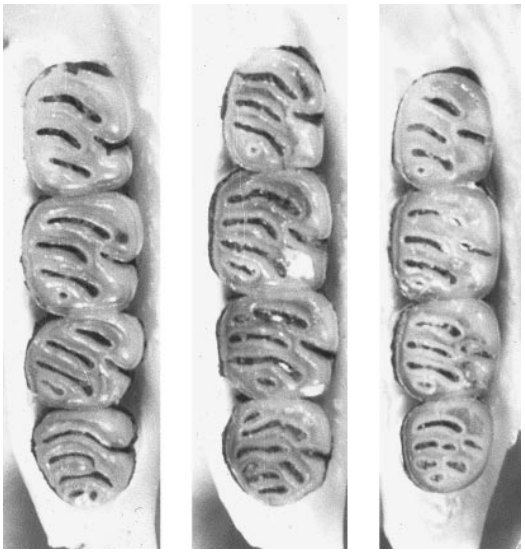

Fig. 128. Occlusal surfaces of the right upper toothrows of sympatric **A**, *M. occultus* (JUR 502) and **B-C**, *M. hispidus* (JUR 533 and JUR 453), all from locality **14**.

(e.g., Woods, 1993). It is possible that the new species described here is the same as *ecaudatus* Wagner, with type locality at Borba on the lower Rio Madeira in central Amazonia, and another taxon considered a synonym of *M. hispidus*. Unfortunately, as the name implies, the type and only referred specimen of *ecaudatus* lacks a tail, and the skull, if extant, has not been examined or figured.

DISTRIBUTION AND HABITAT: This species is known only from two localities in central Amazonian Brazil, both south of the Rio Solimões in Estado do Amazonas: the type locality at Colocacao Vira-Volta (locality 14), left bank of Rio Jurua, and the upper Rio Urucu, Prefeitura Tefe (see map, fig. 124). We obtained all specimens in traps placed in trees in terra firme forest, one at 1.5 m above the ground, the others in canopy platforms positioned between 9.6 and 15.4 m.

ETYMOLOGY: From the Latin word meaning ''unknown'' or ''hidden,''in reference to being hidden within *M. hispidus*, its sympatric and morphologically similar congener.

KARYOTYPE (fig. 129A): Chromosome data are available from four individuals, including the holotype, all from Vira-Volta (locality **14**) at the mouth of the Rio Juruá. 2N = 42, FN = 54. The autosomal complement consists of 7 pairs of large and medium-large biarmed elements, the smallest of which has distinct, near-terminal secondary constric-

Fig. 129. Karyotypes of sympatric **A**, *M. occultus* (2n = 42, FN = 54; JUR 567 male) and **B**, *M. hispidus* (2n = 60, FN = 116; JUR 540, male).

tions, and 13 pairs of acrocentric chromosomes varying in size from medium to small. The X-chromosome is a large submetacentric and the Y is a small subtelocentric. This karyotype contrasts sharply with the 2n = 60, FN = 116 complement of *M. hispidus* and *M. stimulax* (fig. 129B, described below). The differences between the two karyotypes are substantial, and must have involved a large number of complex rearrangements.

REPRODUCTION AND LIFE HISTORY: Of the two adult females collected in early June, one was pregnant with a single embryo, and the second had an open vagina and an enlarged uterus. Both males were nonreproductive.

Mesomys hispidus (Desmarest, 1817)

TYPE LOCALITY: "Amérique Méridionale," restricted to Borba, right bank Rio Madeira, Amazonas, Brazil by Tate (1939).

DESCRIPTION: This is a moderate-sized, heavily spinose, and broad- and short-footed arboreal rat with a long, moderately hirsute tail with a terminal, but short, tuft of hairs. Samples of *M. hispidus* are extremely similar to *M. occultus* in all gross aspects, including size, color, and color pattern; as noted above, it cannot be distinguished from that species by any of the univariate measurements of the skin or skull. Views of the skull are presented in figure 130, of the upper cheekteeth in figure 128, and of the tail tip in figure 126. See description of *M. occultus* for a comparison.

SELECTED MEASUREMENTS: Means, standard errors, and ranges of selected external and cranial measurements are given in table 58 where we treat the two molecular clades evident within the Rio Juruá Basin separately.

NONGEOGRAPHIC VARIATION: Sample sizes were adequate to determine whether significant variation due to either sexual dimorphism or age, at least among specimens otherwise considered to be adult, characterizes *M. hispidus*. One-way ANOVAs detected no dimorphism in any variable, external or cranial (sample size for adult males, 26; for adult females, 44; $p > 0.05$ in all comparisons). However, and perhaps not surprisingly, we detected significant differentiation among adult age classes for most variables. Age was categorized by toothwear, following the scheme developed by Patton and Rogers (1983) for *Proechimys*. Adults are those in toothwear category 7 or above. Only hind foot length and ear height, among the external variables, and maxillary toothrow and occipital condyle breadth, among cranial characters, exhibited no significant variation as a function of age. A few variables were marginally significant ($p < 0.05$), but most showed a highly significant increase in size with an increase in age category ($p < 0.001$; CIL, ZB, MB, IOC, RL, NL, RW-1, RW-2, RD, OL, D, IFL, PL, and BUL). As a result, future detailed analyses of geographic variation in this species should consider the potential differences in age profiles of samples compared.

MOLECULAR PHYLOGEOGRAPHY: Our sam-

TABLE 56
Selected External and Cranial Dimensions of the Holotype and Combined Sample of *Mesomys occultus* from the Rio Juruá and Rio Urucu
Measurements (mm) are given as mean ± standard error, with range and sample size.

Variable	Holotype	Combined sample		
		Mean	Range	n
TOL	—	350	—	1
TAL	—	183	—	1
HF	34	34.33 ± 1.45	32–37	3
E	14	13.67 ± 0.33	13–14	3
CIL	40.00	38.17 ± 1.27	35.74–40.04	3
ZB	23.3	22.55 ± 0.51	21.57–23.37	3
MB	19.07	18.97 ± 0.16	18.09–19.74	3
IOC	10.78	10.55 ± 0.54	10.24–10.78	3
RL	14.95	14.09 ± 0.71	13.09–14.95	3
NL	14.00	12.72 ± 0.12	11.54–14.00	3
RW-1	7.82	7.58 ± 0.18	7.41–7.82	3
RW-2	6.20	5.87 ± 0.30	5.57–6.20	3
RD	8.90	8.46 ± 0.27	7.89–8.90	3
OL	12.64	12.24 ± 0.42	11.72–12.64	3
D	10.50	9.76 ± 0.18	9.06–10.50	3
MTRL	6.86	7.20 ± 0.18	6.86–7.49	3
IFL	3.71	4.07 ± 0.27	3.71–4.26	3
PL	15.35	14.84 ± 0.05	14.42–15.35	3
AW	7.35	7.43 ± 0.24	7.35–7.52	3
BUL	9.82	9.41 ± 0.18	8.99–9.82	3
OCB	8.64	8.44 ± 0.48	8.09–8.64	3
MPFL	10.80	10.18 ± 0.60	8.97–10.80	3
MPFW	3.30	3.30 ± 0.08	3.16–3.44	3
CD	14.27	14.27 ± 0.18	13.97–14.58	3

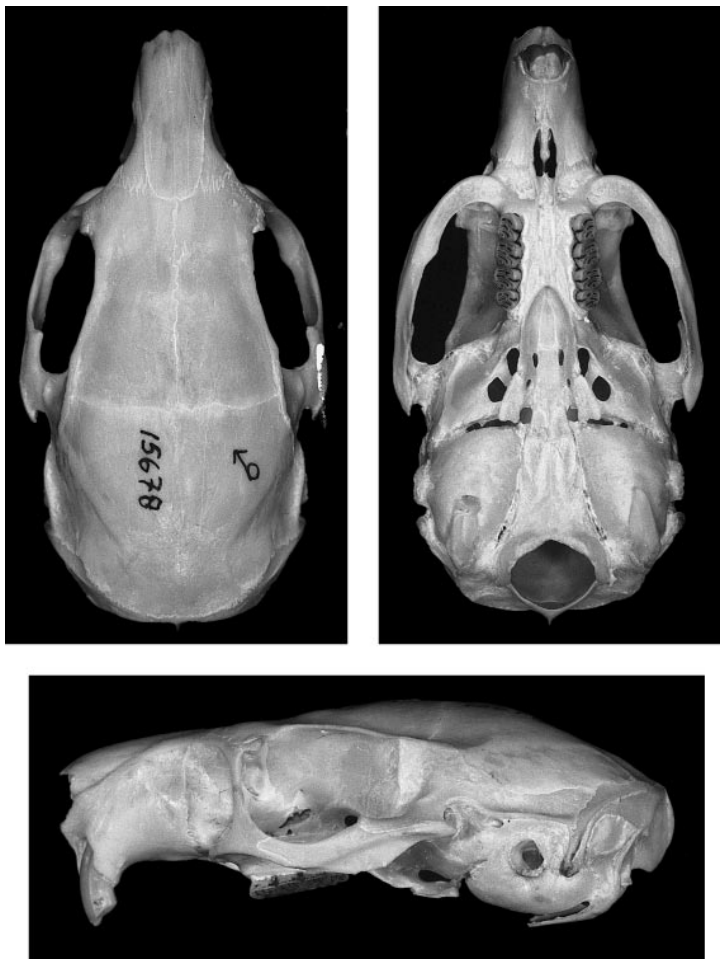

Fig. 130. Dorsal, ventral, and lateral views of the skull of *Mesomys hispidus* (JLP 15678, locality **6**). Magnification = ×2.

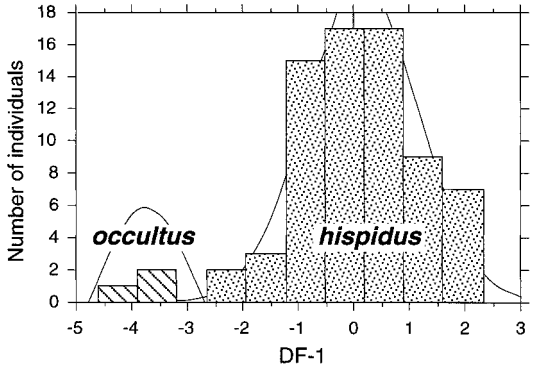

Fig. 131. Distribution of discriminant scores on the single axis obtained in a comparison of cranial measurements of *Mesomys occultus* and *M. hispidus*.

ples of *M. hispidus* have already figured in two publications examining patterns of cytochrome-b sequence variation within the Rio Juruá basin (Patton et al., 1994, 1996a). In the first of these, we used coalescence methodologies to examine the effects of the river itself on patterns of haplotype diversity. Although two divergent clades were identified, these did not correspond to right versus left sides of the river, but rather segregated sites into those distributed upriver versus downriver. Haplotypes belonging to each of the two clades were found together at one locality in the Lower Central Region (Barro Vermelho, locality **12**); otherwise, the two clades displayed allopatric distributions

TABLE 57
Standardized Discriminant Coefficients in Comparisons Between *Mesomys occultus* and *Mesomys hispidus* from the Rio Juruá
Analyses based on $\log_{10}$-transformed cranial variables only.

Variable	Standardized coefficient
Log CIL	3.29994
Log ZB	0.22806
Log MB	0.10082
Log IOC	0.54184
Log RL	−1.53543
Log NL	−0.49494
Log RW-1	−0.11662
Log RW-2	−0.56918
Log RD	0.05819
Log OL	−0.32479
Log D	−0.15084
Log MTRL	−0.03358
Log IFL	−0.06031
Log PL	−1.16127
Log AW	−0.15296
Log BUL	0.15365
Log OCB	−0.02157
Log MPFL	−1.04900
Log MPFW	0.35743
Log CD	−0.25710

along the river. These are clades A and C identified in both the map and tree (figs. 124 and 125), and they differ by an average of 6.8%. A second study (Patton et al., 1996a) used an analysis of molecular variance approach (Excoffier et al., 1992) to examine the degree to which haplotypes are apportioned within as opposed to between the four sample regions along the river, and to determine the extent to which populations sampled linearly along the river exhibited isolation-by-distance patterns of differentiation. This analysis showed that most of the total pool of variation was distributed across sample sites, rather than being contained within any one of them, indicative of low apparent gene flow between sample regions, either in the recent past or presently. These observations were consistent with the documentation of strong isolation-by-distance differentiation along the river, suggesting that current populations are at equilibrium with respect to gene flow and local differentiation, either due to drift or to linearly arranged selection gradients.

To determine whether morphometric variation was partitioned in a similar fashion to the cytochrome-b sequences (fig. 125), we divided the series of specimens available from the Rio Juruá into their respective haplotype clades and compared these by univariate and multivariate means. The only character that differs between samples of the two clades is MTRL, and that is only minimally different (one-way ANOVA, $F_{1,64} = 6.418$, $p = 0.0138$). However, as with the comparison between the two species, both clades are largely separable along the single axis generated by a discriminant function analysis (fig. 132). Mean scores are significantly different ($F_{1,68} = 84.772$, $p < 0.001$), although the distributions overlap. Predicted clade membership was good, with 30 of 36 individuals of the upriver clade correctly allocated, with posterior probabilities greater than 73%, and 27 of 34 individuals of the downriver clade were likewise correctly placed, mostly with posterior probabilities higher than 68%. Misclassified individuals in both groups were not from any particular locality, or geographic region, but rather were scattered throughout the sampled areas. Separation of the two groups on the single discriminant axis was primarily influenced by rostral length contrasting with the combination of condyloincisive length and zygomatic breadth (table 59). Our samples of *M. hispidus* along the Rio Juruá thus exhibit parallel patterns of geographic differentiation at both molecular and morphometric levels.

DISTRIBUTION AND HABITAT: We encountered spiny tree rats at every major locality along the Rio Juruá, except one (opposite Altamira, locality **10**), and obtained reasonable series at several. Of the 88 individuals taken on the standardized lines, 85 (96.7%) were taken in the canopy platform traps; the remaining three were taken in traps placed on the ground. We took 11 additional individuals either in traps placed at about 1.5 m in height, or were shot in vine tangles within 3 m of the ground. We found this species more common in terra firme forest (49) than in várzea (31), with 19 taken at the edge of terra firme and flooded várzea in the Mouth Region. In general, however, *M. hispidus* is

TABLE 58
Selected External and Cranial Dimensions of *Mesomys hispidus* from the Rio Juruá Basin
Measurements (mm) are given as mean ± standard error, with range and sample size.
Specimens are divided into the two mitochondrial DNA clades.

	Upriver clade			Downriver clade		
Variable	Mean ± SE	Range	n	Mean ± SE	Range	n
TOL	355.1 ± 3.64	313–385	25	365.0 ± 5.05	320–404	22
TAL	180.5 ± 2.01	150–197	25	185.3 ± 3.06	150–205	22
HF	32.7 ± 0.25	30–37	36	32.4 ± 0.31	29–37	33
E	13.2 ± 0.16	11–15	36	13.4 ± 0.21	11–17	33
CIL	38.71 ± 0.29	35.40–42.43	37	38.45 ± 0.35	33.30–43.30	34
ZB	22.87 ± 0.14	21.15–24.65	37	22.98 ± 0.16	22.97–25.02	34
MB	19.35 ± 0.12	17.90–20.89	37	19.14 ± 0.14	17.53–21.05	34
IOC	10.93 ± 0.11	9.85–12.51	37	10.70 ± 0.11	9.30–11.98	34
RL	14.02 ± 0.14	12.33–15.58	37	13.65 ± 0.15	11.70–15.71	34
NL	12.25 ± 0.12	11.07–14.11	37	11.98 ± 0.15	10.30–14.32	34
RW-1	7.52 ± 0.05	6.65–8.83	37	7.41 ± 0.07	6.41–8.67	34
RW-2	5.81 ± 0.06	5.14–6.64	37	5.64 ± 0.07	4.83–6.54	34
RD	8.43 ± 0.09	7.45–9.82	37	8.46 ± 0.09	7.47–9.63	34
OL	12.25 ± 0.09	11.37–13.43	37	12.27 ± 0.10	11.10–13.71	34
D	9.46 ± 0.12	8.13–10.93	37	9.38 ± 0.13	7.78–10.81	34
MTRL	7.29 ± 0.04	6.83–7.83	37	7.14 ± 0.05	6.62–7.70	34
IFL	3.38 ± 0.07	2.98–3.85	37	3.49 ± 0.07	3.06–3.77	34
PL	14.57 ± 0.14	13.25–16.46	37	14.36 ± 0.17	12.38–16.35	34
AW	7.43 ± 0.09	6.48–8.67	37	7.22 ± 0.05	6.61–7.87	34
OCB	8.54 ± 0.06	7.96–9.39	37	8.52 ± 0.05	7.96–9.50	34
BUL	9.63 ± 0.07	9.04–10.59	37	9.70 ± 0.09	8.64–10.63	34
MPFL	9.82 ± 0.11	8.31–11.03	37	9.84 ± 0.11	8.85–11.55	34
MPFW	3.48 ± 0.05	2.88–4.24	37	3.55 ± 0.04	3.01–3.99	34
CD	14.22 ± 0.07	13.30–15.21	37	14.33 ± 0.11	13.00–15.82	34
DF-1	1.039 ± 0.172	−0.729–3.199	36	−1.165 ± 0.165	−3.059–0.532	34

widely distributed in a variety of forest types, including naturally and human-disturbed habitats where some arboreal components remain (e.g., tree-fall gaps).

REPRODUCTION: We caught pregnant females, males with enlarged testes and seminal vesicles, and young animals in all four trapping periods, showing that reproduction continues throughout the year. Litter sizes ranged from 1 to 3, with most individuals (19 of 24) having but a single young. There is no obvious scrotum in males, but all adults (toothwear age classes 8 and above; following Patton and Rogers, 1983) had enlarged testes averaging 20 × 9 mm (length × width) and swollen vesicular glandes (> 18 mm in length), while individuals of younger ages had testes sizes of 10 × 5 mm, or less, and vesicular glands less than 10 mm in length. We noted no differences in reproductive condition between samples collected simultaneously in terra firme and várzea forests.

KARYOTYPE: 2N = 60, FN = 116 (fig. 129B). We found no chromosomal differences among any of the 81 individuals analyzed, which included specimens belonging to the two different mtDNA clades. Leal-Mesquita (1991) reported the same karyotype from a single specimen from the Samuel dam site below Porto Velho on the Rio Madeira, Estado do Rondônia, and we also have the same karyotype from specimens from the upper Rio Urucu and the Rio Jaú north of the Rio Solimões. In addition, Louise H. Emmons has kindly shown us karyotypes of specimens of *M. hispidus* from southeastern Perú (Tambopata, Departamento de Madre de Dios) and *M. stimulax* from eastern Brazil (Rio Xingu, Estado do Pará), all of which have the same karyotype. The autosomal

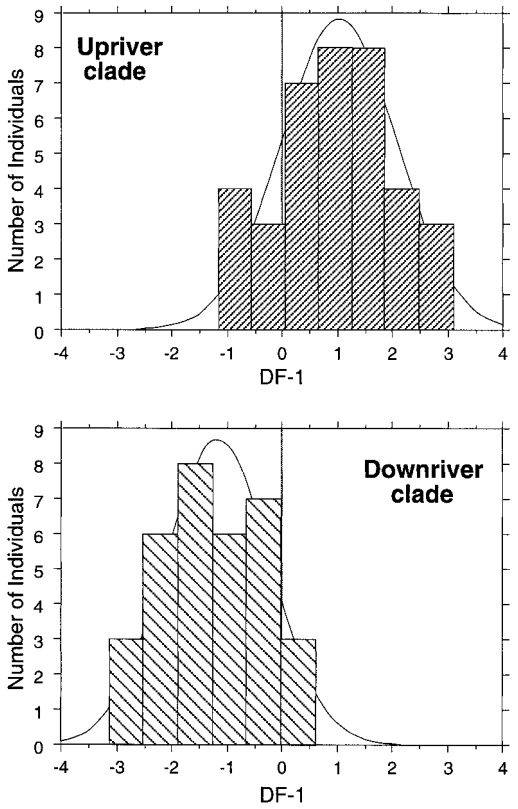

Fig. 132. Distribution of discriminant scores on the single axis obtained in a comparison of cranial measurements for the upriver and downriver cytochrome-b clades of *Mesomys hispidus*.

TABLE 59
Standardized Discriminant Coefficients in Comparisons Between Cytochrome-b Clades of *Mesomys hispidus* from the Rio Juruá Basin
Analyses are based on $\log_{10}$-transformed cranial variables only.

Variable	Standardized coefficient
Log CIL	−1.67479
Log ZB	−1.18014
Log MB	0.66669
Log IOC	0.00428
Log RL	2.00129
Log NL	0.15464
Log RW-1	−0.17874
Log RW-2	0.85273
Log RD	−0.61131
Log OL	0.33272
Log D	−0.20882
Log MTRL	0.39299
Log IFL	−0.03040
Log PL	0.83621
Log AW	0.42284
Log BUL	−0.60973
Log OCB	−0.03967
Log MPFL	0.27545
Log MPFW	−0.33840
Log CD	−0.05654

complement in all of these consists of 29 pairs of biarmed elements decreasing in size from large to small, with the first element distinctly larger than all other. The sex chromosomes are similar to those of *M. occultus*, with a large submetacentric X and a small subtelocentric Y. Leal-Mesquite (1991) provides data on C- and G-bands, noting that the former are typically large on all autosomes but with pericentromeric positions. Aniskin (1993) reports the same karyotype for specimens from northern Perú that he identified as *Lonchothrix emiliae*. This taxon, however, is known only from eastern Amazonia along the lower Rio Tapajoz, and we suggest that Aniskin's specimens are really *Mesomys hispidus*.

SPECIMENS EXAMINED (n = 99): (**1**) 3m, 2f — MNFS 1230–1231, 1294, 1363, 1416; (**2**) 4f — MNFS 1257, 1258, 1353, 1354; (**3**) 4m, 5f — MNFS 1519, 1531, 1539, 1596, 1615, 1636, 1658, JUR 221, 249; (**4**) 1f — MNFS 1573; (**5**) 3m, 5f — MNFS 568–569, 583, 592–593, 612, 637, 654; (**6**) 3m, 4f — JLP 15624, 15651, 15678, 15701, 15708, 15725, MNFS 564; (**7**) 2m, 6f — JLP 15366–15367, 15424, 15465, 15501, MNFS 411, 436, 470; (**8**) 5m, 4f — JLP 15385, 15393, 15431, 15444–15445, MNFS 432, 464, 485, 517; (**9**) 3m, 5f — JLP 16047–16049, 16066, JUR 194, MNFS 909–911; (**11**) 1f — MNFS 754; (**12**) 2m, 2f — JLP 15852–15853, MNFS 729, 745; (**13**) 1m, 3f — JUR 291, 325, 337, 369; (**14**) 9m, 6f — JUR 416, 453, 457, 461–462, 471, 488, 498–499, 503, 533, 540–541, MNFS 1739, 1784; (**15**) 5m, 7f — JUR 268–269, 284–285, 321–322, 332–335, 370, 398; (**16**) 1m, 3f — JUR 414, 415, 459, 500.

Proechimys Allen, 1899

Terrestrial spiny rats

The spiny rats of the genus *Proechimys* are often the most abundant nonvolant mammals

of the lowland Neotropical forests, and perhaps the most easily recognizable genus as well. In contrast to other echimyids of Amazonia, all species of this diverse genus are terrestrial, with elongated heads and long rostra, large and erect ears, and narrow and long hind feet. The tail is always shorter than head-and-body length, the dorsal pelage comprises a mixture of soft hairs (= setiforms; Moojen, 1948) and expanded, varyingly stiffened spines (= aristiforms); the dorsal and lateral color is generally a reddish brown and the venter white, although tinged reddish or grayish, especially in the throat, thoracic region, and inner thighs in some species. The narrow and elongate hind feet have slender toes and small plantar tubercles. The ears are distinctly larger than those of all similar-sized arboreal genera, absolutely so in all comparisons. These animals can be heard scurrying through the leaf litter and readily seen at night, by virtue of their bright red eye shine, freezing when caught in a spotlight, or bounding off with a distinctive loping gait.

The quality of our knowledge of the systematics of *Proechimys* stands in stark contrast to their ubiquitous presence in all forest types, disturbed and pristine. Three to five species might be present at single localities, may be actually syntopic, and may even occupy the same burrows at different times (e.g., Emmons, 1982; Malcolm, 1992). Although it is sometimes relatively easy to distinguish species when sympatric, identifying living animals to species takes a skilled eye, and defining species boundaries over larger segments of geography has often proven extremely difficult. Only a few studies have succeeded in documenting and adequately describing sympatric entities (e.g., Patton and Gardner, 1972), and only Gardner and Emmons (1984) and Patton (1987) have made much progress in defining geographic character trends within definable taxa over any but the shortest distances, at least for those taxa within Amazonia. As noted by most earlier workers, the diagnosis of species and thus the delineation of their geographic boundaries have been greatly hampered by an extreme level of character variability, both within and among population samples (e.g., Thomas, 1928; Moojen, 1948; Hershkovitz, 1948). Even karyotypes, which have proven useful in differentiating sympatric taxa (Patton and Gardner, 1972; da Silva, 1995, 1998) may be highly variable geographically (Reig et al., 1980; Gardner and Emmons, 1984). Patton and Rogers (1983) showed that individuals essentially grow continuously throughout life, so that mensural variables increase substantially with advancing age. As a consequence, one must be exceedingly careful in morphometric comparisons between taxa and not be confused by age-related variation.

Patton (1987) evaluated several qualitative craniodental and bacular characters for their utility in defining taxa of *Proechimys*, and allocated the 59 available names to one of nine species groups, five of which occur within Amazonia. For each of these, he provided hypotheses of species units and remarked on their probable geographic limits. This work was, of course, available to us both during the field phases of the Juruá research and subsequently while we worked to identify the large series of spiny rats we obtained. Our collections comprise nearly 1200 specimens, obtained at all 16 primary sites. Despite our previous experience with the genus throughout eastern Perú and in central Brazil, we had great difficulty in allocating many specimens to the taxa diagnosed by Patton (1987), both in the field and during initial examination of prepared specimens. The chromosomal preparations and molecular sequences of the mtDNA cytochrome-b gene that we examined subsequent to returning to the laboratory gave us reason to understand our difficulties in the field. We encountered eight species along the Rio Juruá. In the sections immediately below, we provide the molecular evidence for these eight lineages, describe general morphological characters of each, and provide multivariate morphometric comparisons. Finally, in the accounts for each species, we further characterize their external and craniodental morphology, describe their karyotypes, provide available molecular data to place each into a broader geographic context within Amazonia, and summarize life history characteristics. Although it is clear that both chromosomal and molecular data greatly aid in the discrimination of local species, we emphasize mor-

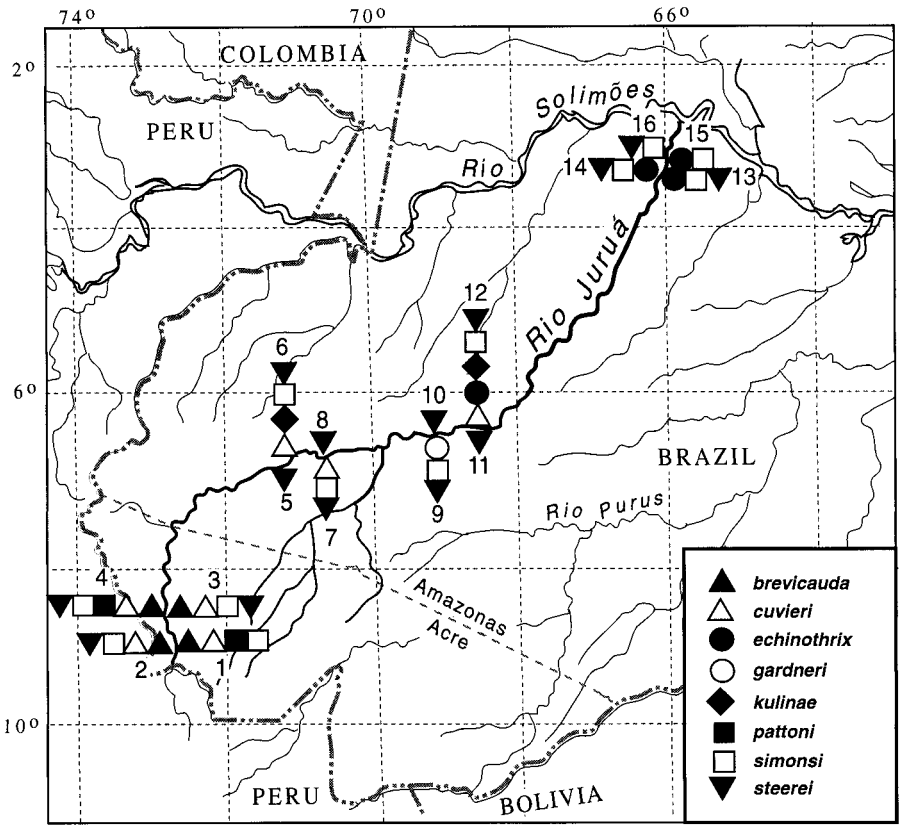

Fig. 133. Distribution of eight species of *Proechimys* at the 16 primary sample sites along the Rio Juruá, western Brazil.

phological features that will aid workers identify these animals in the field.

Molecular Phylogenetics and Species Limits of Spiny Rats of the Rio Juruá Basin

At the initiation of our survey of the Rio Juruá we were reasonably comfortable with our ability to distinguish species of *Proechimys* in the field, and with the probability that five taxa would be found within the river basin. These species included *P. brevicauda*, *P. cuvieri*, *P. simonsi*, *P. steerei*, and a species undescribed at the time but that we've known about since 1972 (see Patton and Gardner, 1972; Patton, 1987) and that has recently been described by da Silva (1998) as *P. pattoni*. We based this prospective species list on our prior experiences in nearby localities in eastern Perú (Balta, on the Río Curanja, Departamento de Ucayali; see Voss and Emmons, 1996) and central Brazil (the upper Rio Urucu, southeast of Tefé, Estado do Amazonas). It quickly became apparent, however, that either the characters outlined by Patton (1987) to diagnose these species had grossly underestimated the true nature of morphological variation exhibited by them, or that there were more taxa present along the river than could be accounted for by the five taxa identified above. The second alternative proved to be the case, with eight species among our materials from the Rio Juruá now recognized, four of which were undescribed at the time we made our collections (da Silva, 1998). In recognizing these species, we generally follow a species concept based both on demonstrable monophyly of mitochondrial DNA clades and diagnosability by a combination of morphological and chromosomal characteristics. In many cases,

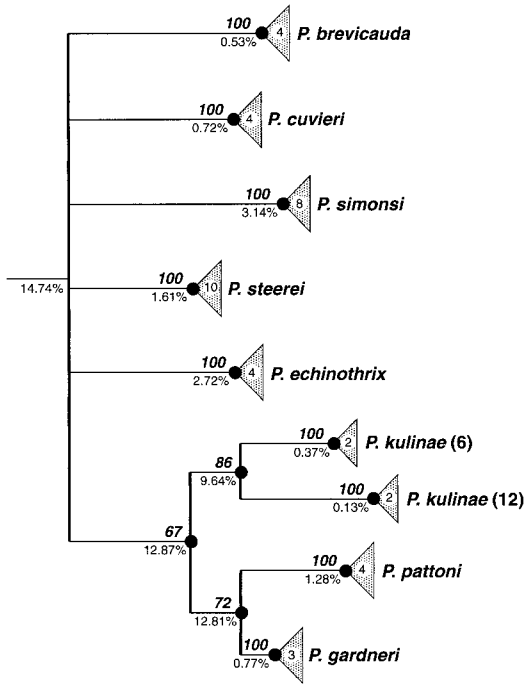

Fig. 134. Bootstrap 50% majority-rule consensus minimum-length parsimony tree for cytochrome-b haplotypes (798 bp) for the eight species of *Proechimys* from the Rio Juruá. The tree is based on a weighted analysis that discounted third-position transitions (see text for explanation). The terminal triangles encompass the individual haplotypes of each species included in the analysis, the number of which is indicated within each triangle. The tree is rooted by comparison to *Isothrix*, *Makalata*, and *Mesomys*. Length = 351 steps, CI = 0.721, RI = 0.779. Bold numbers at internal nodes are bootstrap values, based on 1000 replicates; percentages are average Kimura two-parameter distances.

this view is supported by sympatry of the taxa in question without evidence for reticulation by hybridization, so that the taxa we recognize also conform to the biological species concept commonly used by many mammalogists. As many as four species were found in terra firme forest at single sites (Igarapé Porongaba [locality **1**], Sobral [locality **4**], and Barro Vermelho [locality **12**]) and five species may be found at localities with both terra firme and várzea forests (Sobral and Barro Vermelho) (fig. 133). At least three species occur at most localities, although true várzea forest contains only a single species (*P. steerei*).

As will be emphasized in the detailed descriptions below, each of these eight species is diagnosable by morphological, chromosomal, and molecular characteristics, and each strongly diverges from all others by their respective cytochrome-b sequences. da Silva (1998) provided a preliminary assessment of phylogenetic relationships among these and other Amazonian species based on the initial 798 bp of cytochrome-b sequence. In figure 134 we offer molecular evidence for the distinctness of the eight species we recognize within the Rio Juruá basin. In both our data and those presented by da Silva (1998), geographic samples allocated to most species exhibit close sequence similarity, with Kimura two-parameter distances averaging less than 3%, and usually less than 1%. The one exception to this pattern is *P. kulinae*, which comprises two very divergent haplotype clades that differ by 9.6%, nearly as much as that between *P. brevicauda* and *P. cuvieri* (fig. 134). Other than this exception, however, differences between the species we recognize are uniformly large, always above 10% and often above 15%, and haplotypes we have identified for each are always strongly linked in phylogenetic analyses, with bootstrap values consistently at 100%.

Our wish in presenting the data in figure 134 is solely to show that eight separate clades of spiny rats are readily identifiable within the Rio Juruá. Nevertheless, the length of cytochrome-b sequence examined provides little phylogenetic resolution among any of these species, with the minor exception of the three small-bodied taxa described recently by da Silva (1998). Not surprisingly, the terminal nodes (individual haplotypes) of each taxon are highly supported, with bootstrap values of 100% in all cases except that of *P. kulinae*. However, only *P. pattoni* and *P. gardneri* group as species with relatively strong support (72%), with this pair grouping with *P. kulinae* at a lower bootstrap value of 67. No other taxon exhibits close relationship to any other. This is true even when the data are weighted to accommodate for site saturation (fig. 134; see also Lara et al., 1996).

TABLE 60
Selected Characters of All Eight Species of *Proechimys* from the Rio Juruá
All measurements provided include adult individuals only (age classes 8–10; Patton and Rogers, 1983).

Character	*P. echinothrix*	*P. kulinae*	*P. gardneri*	*P. pattoni*
EXTERNAL				
Body size	medium to large, total length range from 327 to 440 mm	small; total length not exceeding 328 mm	small; total length not exceeding 353 mm	small; total length not exceeding 328 mm
Aristiform hair	extremely heavy, very broad and long with blunt tip, much stiffer to the touch than any other species	wider and longer than in *P. gardneri* and *P. pattoni*, with blunt tip at the mid-back, stiff to the touch	narrow and short, stiff to the touch	narrower and shorter then *P. gardneri*, stiff to the touch
Dorsal and ventral coloration of the body	dorsum reddish-brown streaked with black; no lateral stripe; venter, chin, and under surfaces of forelimbs and hind limbs pure white	dorsum uniform reddish-brown streaked with black; no lateral stripe; venter, chin, and undersurfaces of forelimbs and hind limbs pure white; area around the upper lips dark, generally lacking patches of white hair	dorsum reddish-brown streaked with black; no lateral stripe; venter and chin, pure white	dorsum reddish-brown streaked with black; no lateral stripe; venter, chin, sides of the upper lips and undersurfaces of forelimbs and hind limbs pure white; white spot generally present at base of vibrissae
Ear size	large (19–28 mm)	small (17–23 mm)	small (18–24 mm)	small (18–23 mm)
Tail size and color	long (max. length 195 mm; on average 73% of body length); bicolored, sharply defined white venter and dark dorsum; hair almost completely covering scales	short, (max. length 140 mm; on average 68% of body length); bicolored, with white venter and dark dorsum	short (max. length 146 mm; on average 72% of body length); hairier and bicolored with sharper contrast than in *P. pattoni*	short (max. length 141 mm; on average 70% of body length); dark brown above, pale brown to white below
Hind-foot and ankle	medium to large hind-foot (41–54 mm); nearly unicolored pure white on dorsum without dark ring at tarsal joint	small and narrow hind-foot (38–44 mm); mostly white on dorsum; tarsal joint either covered by dark and rusty hair or with white hair confluent with inner surface of the hind limbs	small and narrow hind-foot (32–45 mm); mostly white on dorsum; tarsal joint either covered by dark and rusty hair or with white hair confluent with inner surface of the hind limbs	small and narrow hind-foot (37–43 mm); mostly white on dorsum but also golden or brownish, with a dark band around the ankle
CRANIAL				
Skull	large (50–61 mm)	small (42–51 mm)	small (42–55 mm)	small and delicate (43–50 mm)
Maxillary toothrow	long (7.6–9.2 mm); relatively large teeth; pm4 usually with 3 folds (66%) or 4 folds (33%)	short (6.3–8.6 mm); small teeth; pm4 with 3 and 4 folds in about the same number of specimens	short (6.9–8.2 mm); small teeth; pm4 has 4 folds in most specimens	very short (6.7–7.5 mm); tiny teeth; pm4 has 3 folds in most specimens

TABLE 60
(Continued)

Character	*P. echinothrix*	*P. kulinae*	*P. gardneri*	*P. pattoni*
Incisive foramen	ovate to lyrate, posterolateral margins mostly flat; premaxillary long and narrow; maxillary attenuate to expanded anteriorly, very weak or no contact with premaxillary	squarish to slightly ovate or moderately lyrate, weakly developed posterolateral margins; premaxillary short; maxillary attenuate to expanded anteriorly, usually in contact with premaxillary	ovate to slightly lyrate, posterolateral margins flat to slightly flanged; premaxillary rather broad, in contact with maxillary	ovate to slightly squarish, weakly developed to almost flat posterolateral margins; maxillary and premaxillary either not touching or connected by very attenuate keel
Mesopterygoid fossa	extends either to anterior or to posterior one-half of M3	extends to anterior one-half of M3	extends to anterior one-half of M3 to near middle of M2	extends to near middle of M2
Postorbital process of the zygomatic arch	weakly developed, rounded	well developed, spinose	weakly developed and rounded, or absent	moderately developed, more spinose than in *P. gardneri* (see da Silva, 1988), always present
Canal on the floor of the infraorbital foramen	moderate to strongly developed	weakly developed	weakly developed	weakly developed
BACULUM	broad and short, with expanded base	elongate and relatively narrow, moderately developed apical wings	similar to *P. pattoni*, except that apical extensions are shorter	distal end with long and divergent apical extensions
KARYOTYPE	2n = 32 and FN = 60	2n = 34 and FN = 52	2n = 40 and FN = 56	2n = 40 and FN = 56

Character	*P. brevicauda*	*P. cuvieri*	*P. simonsi*	*P. steerei*
EXTERNAL				
Body size	medium to large, total length range from 306 to 403 mm	medium to large, total length range from 312 to 437 mm	large, total length range from 220 to 480 mm	large, total length range from 215 to 493 mm
Aristiform hair	long and narrow, tip rather blunt, not very stiff to the touch	wider and longer than all other species except *P. echinothrix*; blunt tip, stiff to the touch	long and narrow, whip-like tip, not very stiff to the touch	long, narrow, and very delicate, whip-like tip, soft to the touch
Dorsal and ventral coloration of the body	dorsum uniformly dark reddish-brown streaked with black; fulvous lateral stripe may extend onto the venter, the chin, the throat, and the abdominal region	dorsum appears brightly colored with a strong reddish overall tint and streaked with black; no lateral stripe; venter almost pure white	dorsum brownish and streaked with black; no lateral stripe; venter, chin, sides of the upper lips, undersurfaces of forelimbs, and hind limbs pure white	dorsum reddish streaked with black; no lateral stripe; venter pure white with thicker, more velvety fur than other species

TABLE 60
(Continued)

Character	*P. brevicauda*	*P. cuvieri*	*P. simonsi*	*P. steerei*
Ear size	large (18–24 mm)	large (19–25 mm)	very large (20–28 mm)	large (19–25 mm)
Tail size and color	medium (max. length 163 mm; on average 64% of body length); dorsum darker than venter, but also unicolored brown; sparsely covered by hair; scales visible	medium to long (max. length 180 mm; on average 67% of body length); distinctly bicolored (venter creamy to ligth brown, dorsum dark brown); sparsely covered by hair; scales visible	very long (max. length 231 mm; on average 82% of body length); distinct dark dorsal stripe and white ventrum; sparsely covered by hair; scales visible	long (max. length 207 mm; on average 70% of body length); dark brown in the dorsum and white to cream in the venter; well covered by hair; scales visible
Hind-foot and ankle	medium hind-foot (42–53 mm); cream to dark brown dorsum usually lacking dark ring at tarsal joint	medium to large hind-foot (44–54 mm); brownish dorsum usually with fulvous ring at tarsal joint	medium to large hind-foot (36–57 mm); generally self-colored white dorsum without dark ring at tarsal joint; occasionaly have brownish hair around the ankle and in the foot	large hind-foot (43–63 mm); dorsum generally have a pale to dark brown outer band and a whitish inner band from the tarsal joint to the end of the toes
CRANIAL				
Skull	large (48–-60 mm)	large (48–62 mm)	large (44–64 mm)	very large (51–69 mm)
Maxillary toothrow	long (7.7–9.2 mm); large teeth; typically 3 folds in all cheek-teeth, but sometimes 2–5 folds	long (7.7–10 mm); large teeth; typically 3 folds in all cheek-teeth, except for pm4 which has 4 folds	medium to long (7.1–8.7 mm); moderately large teeth; 3 folds in PM4 and M1, 3 or 4 folds in M2 and M3	long (7.7–10.2 mm); large teeth; typically 3 folds in dPM4, M1 and M3; 4 folds in M2 and pm4, and 3 folds in m1, m2, and m3
Incisive foramen	lyrate; posterolateral margins strongly constricted forming grooves that extend into anterior palate; premaxillary portion long, maxillary portion keeled and both generally in contact; vomer visible	lyrate; posterolateral margins weakly flanged forming weak grooves onto palate; premaxillary portion long, maxillary portion with slight or no keel, and both usually in contact; vomer visible	ovoid; never constricted posteriorly; posterolateral margins flat, rarely with weak flange and without groove onto palate; short, rounded premaxillary portion, attenuate maxillary portion, both never in contact	lyrate; posterolateral margins slightly to well flanged, forming grooves that extend into the palate; premaxillary portion short, maxillary portion keeled and both are generally in contact; typically vomer not visible
Mesopterygoid fossa	extends into posterior palate as far as posterior margins of M3	penetrates palate moderately, typically extending either to posterior margins or to posterior half of M3	penetrates deeply into the palate, minimally reaching anterior half of M3 or extending to middle of M2	generally extends into anterior one-half of M3, but never beyond posterior margins of M3
Postorbital process of the zygomatic arch	usually present but not well developed; equal contribution of squamosal and jugal	absent or not well developed; mostly squamosal	usually present but not well developed; similar number of specimens with mostly squamosal or squamosal/jugal contribution	usually present but not well developed; most specimens with equal contribution of squamosal and jugal

TABLE 60
(Continued)

Character	*P. brevicauda*	*P. cuvieri*	*P. simonsi*	*P. steerei*
Canal on the floor of the infraorbital foramen	barely visible, floor of the foramen usually smooth	slightly developed with weak lateral flanges	canal almost always present, yet development of lateral flanges moderate; but sometimes medial floor smooth with no groove	not well developed; groove may be present or absent; lateral flanges weakly developed if groove present
BACULUM	elongated and broad, with well-developed apical wings	short and massive, with broad shaft and expanded base	very long and narrow, with a rounded and slightly broadened base	long and narrow specially relative to *P. cuvieri*, but wider compared to *P. simonsi*
KARYOTYPE	2n = 28 and FN = 48–50	2n = 28 and FN = 46–48	2n = 32 and FN = 58	2n = 24 and FN = 40–42

Characters and the Identification of Species of *Proechimys* of the Rio Juruá Basin

We characterize each of the eight species from the Rio Juruá basin in the individual accounts below. In so doing, we provide greater detail than that provided for other mammals in this volume, emphasizing external characteristics which we hope will aid the identification of live animals in the field. The craniodental characters outlined by Moojen (1948), Patton and Gardner (1972), and especially those figured extensively by Patton (1987) provide features upon which museum series can be segregated. Body size, stiffness of the dorsal aristiform hairs, dorsal color pattern and especially ventral coloration, color and color pattern of the hind feet, number and relative size of plantar tubercles, and length and hairiness of the tail can all be used to identify specimens of adults in the field. The assignment of young individuals still in juvenile pelage, however, can be very difficult without examination of the skull or knowledge of the karyotype. Special care must be taken in species assignments of these specimens. Finally, we emphasize that adult males of most, if not all species, can often be distinguished by characteristics of the phallus, including the baculum which is usually visible through the thin dorsal skin of that organ. The phallus of live animals can be easily everted for examination in hand. The soft structures of the phallus have been given scant attention in the taxonomic and morphological literature (but see Patton and Gardner, 1972, and da Silva, 1998), although all eight species from the Rio Juruá can be distinguished by phallic structures.

Table 60 compares each of the eight species from the Rio Juruá by selected external, craniodental, phallic/bacular, and karyotypic features. As emphasized by Patton (1987), the best suite of qualitative craniodental characters for species identification are those of the incisive foramina, anterior palate, mesopterygoid fossa, floor of the infraorbital foramen, parietal ridging, and number of flexi in the cheekteeth. There is, admittedly, considerable individual variation in these and the other characters listed in table 60 for any given taxon, and we have tried to indicate the degree of such variation in our descriptions of each species below. Finally, we caution that the species we recognize, and the characters we use to distinguish them, apply to specimens from the Rio Juruá and, certainly, adjacent areas in western Amazonia. Given our experiences with these taxa, and in other geographic areas, it is likely that additional species of *Proechimys* will be uncovered in regional faunas. Also, given the degree of sequence divergence and strong regional monophyly in our limited samples, it is also likely that even well-characterized and reasonably well-known species of spiny rats will be found to be composites of indepen-

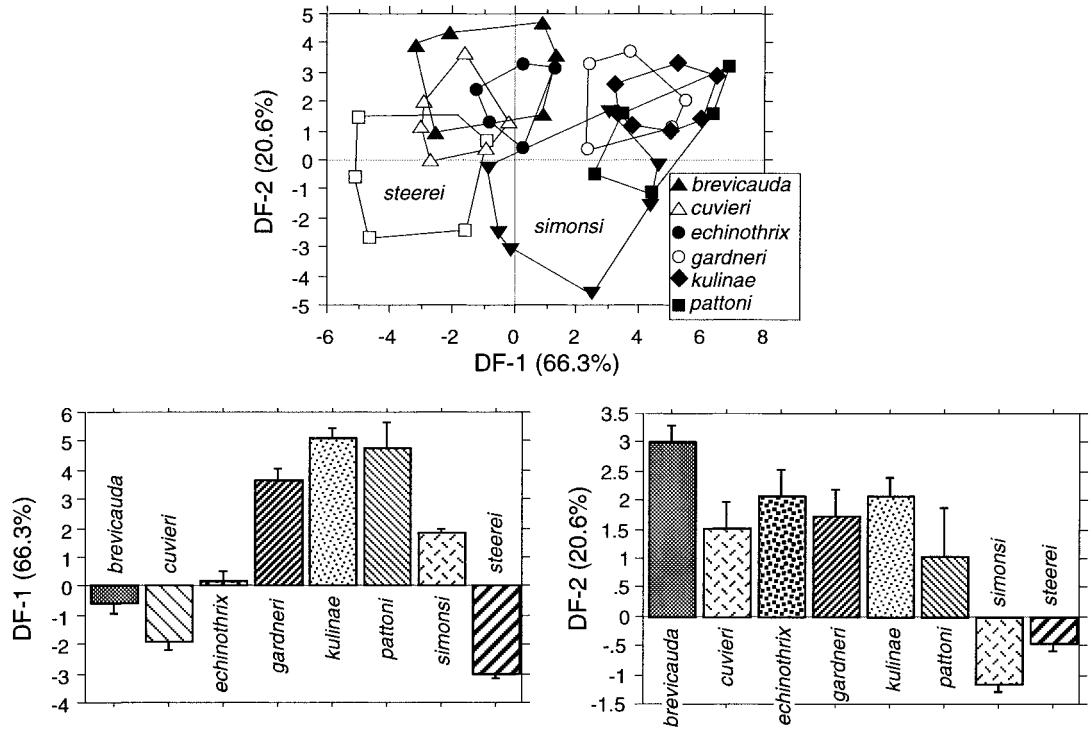

Fig. 135. (**Top**) Bivariate plots of the first two discriminant axes comparing morphometric relationships among the eight species of *Proechimys* obtained from the Rio Juruá. (**Bottom, left**) Histograms, with 95% confidence limits, of individual scores on the first discriminant axis. (**Bottom, right**) Histograms, with 95% confidence limits, of individual scores on the second discriminant axis.

dently evolving lineages that may demand subsequent taxonomic recognition.

We examined the morphometric distinctness of each of the eight species we recognize by a series of discriminant function analyses, using $\log_{10}$ transformations of 21 cranial measurements for adult specimens (age classes 8, 9, and 10 combined). Four separate groups are evident in plots of the first two discriminant axes, which combine to explain 86.9% of the total variation present (fig. 135, top). *Proechimys simonsi* and *P. steerei* are individually separable from each other on the first axis and from the other six species on the second axis. The other six species divide into two triads of species (*P. brevicauda*, *P. cuvieri*, and *P. echinothrix* versus *P. gardneri*, *P. kulinae*, and *P. pattoni*, respectively) that are separable from each other on the first axis and from *P. simonsi* and *P. steerei* on the second. The uniqueness of each of the four groups is evident in histograms of mean discriminant scores for the first two axes (fig. 135, bottom). Misclassification of specimens to species based on a posteriori probabilities of group membership is relatively minimal (always less than 5%), except for those species in each of the two triads. The length of the rostrum contrasts with cranial depth at M1, diastema length, and length of the maxillary toothrow as those variables contributing most strongly to separation on the first axis; mesopterygoid fossa width contrasts with nasal length on the second axis (table 61).

Separate discriminant analyses were performed for each of the two triads of species to further examine their morphometric relationships. The triad consisting of *P. brevicauda*, *P. cuvieri*, and *P. echinothrix* are each completely separable in the bivariate plot of the first and second discriminant axes (fig. 136, top), with greater than 95.8% correct assignments of individuals based on their a

TABLE 61
Standardized Discriminant Coefficients for the First Three Discriminant Axes in Comparisons Among the Eight Species of *Proechimys* from the Rio Juruá Basin

Variable	DF-1	DF-2	DF-3
Log CIL	0.17886	0.17276	0.64986
Log ZB	−0.11414	−0.35997	0.47297
Log MB	−0.06903	0.36322	−0.01191
Log IOC	−0.24031	0.13278	0.48365
Log RL	0.54747	−0.48730	−0.13232
Log NL	0.19045	−0.76689	0.96800
Log RW-1	0.16286	0.00162	−0.58242
Log RD	0.59040	0.74256	−0.89432
Log OL	−0.45217	−0.64883	−0.15093
Log D	−0.61300	−0.02844	−0.52883
Log MTRL	−0.52648	−0.14891	−0.23494
Log IFL	−0.38813	0.31727	0.09968
Log PL	0.28484	0.24946	0.19656
Log PPL	0.13787	0.05609	−0.16693
Log BUL	0.20356	0.12533	0.03971
Log MAXB	0.33336	−0.16687	−0.44559
Log OCW	−0.31155	−0.28683	−0.25478
Log MPFW	0.11553	0.42354	−0.51414
Log CD	0.01917	0.07802	−0.40684
Log CDM	−0.79784	−0.56659	0.42528
Eigenvalue	6.54906	2.03193	0.60663
% contribution	66.332	20.580	6.144

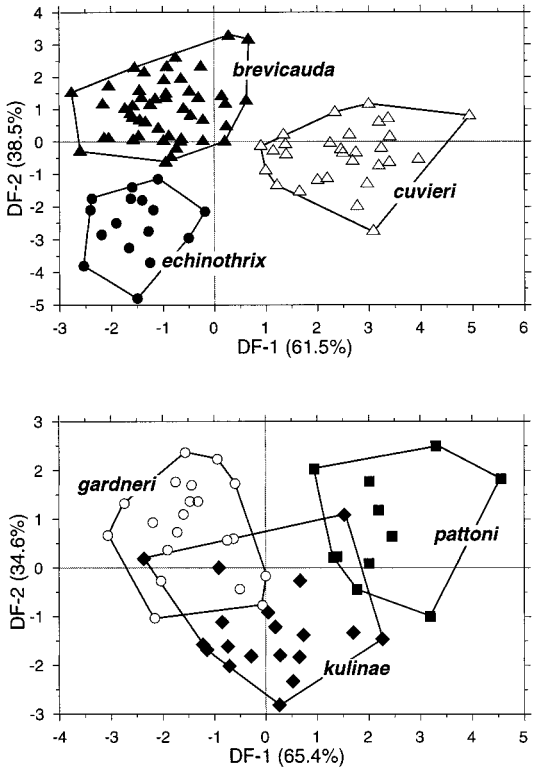

Fig. 136. Bivariate plots of the first two discriminant axes in separate analyses of two triads of species of *Proechimys* from the Rio Juruá: (**top**) *P. brevicauda*, *P. cuvieri*, and *P. echinothrix*; (**bottom**) *P. gardneri*, *P. kulinae*, and *P. pattoni*.

posteriori probabilities. For the second triad, *P. kulinae* overlaps somewhat with both *P. gardneri* and *P. pattoni*, which themselves separate completely on DF-1 (fig. 136, bottom). All individuals of *P. pattoni* are correctly allocated while only 84% of either *P. gardneri* or *P. kulinae* group correctly. These are obviously morphologically closely similar species, as noted by da Silva (1998) in her description of these taxa. *Proechimys cuvieri* differs from both *P. brevicauda* and *P. echinothrix* primarily by rostral length, postpalatal length, and width of the mesopterygoid fossa, while condyloincisive length contrasts with rostral length in separating the latter two on the second axis (table 62). For the triad of small-bodied species, mastoid breadth, diastemal length, and width of the mesopterygoid fossa combine to separate species on the first axis, and rostral depth contrasts with maxillary toothrow length as primary variables on the second (table 62; the number of variables included in this analysis was necessarily reduced because of the small sample size of *P. pattoni*).

Habitat Distribution of *Proechimys* within the Rio Juruá Basin

As many as five species of *Proechimys* can be found at single localities within the Rio Juruá basin (fig. 133). Four of these were typically present in terra firme habitats, although the assemblage of species is different across the sampled regions of the river. In contrast, only one species was found in the seasonally flooded várzea at all localities. Table 63 compares the number of captures of each species by habitat (the standardized terra firme and várzea lines, with all other habitats pooled) for each of the four regional sampling areas. *Proechimys steerei* is the várzea specialist, especially evident in the

TABLE 62
Standardized Discriminant Coefficients for the First Three Discriminant Axes in Comparisons Among Two Groups of Species of *Proechimys* from the Rio Juruá Basin

	P. brevicauda, *P. cuvieri*, and *P. echinothrix*		*P. gardneri*, *P. kulinae*, and *P. pattoni*	
Variable	DF-1	DF-2	DF-1	DF-2
Log CIL	−0.00376	1.25438	0.69781	−0.27788
Log ZB	0.57412	−0.66850	0.34565	0.57411
Log MB	0.64090	−0.06871	−0.75806	−0.01122
Log IOC	0.41131	−0.72921	−0.41751	0.22461
Log RL	−0.91215	−1.14274	0.72185	0.47975
Log NL	0.59085	0.24038	—	—
Log RW-1	−0.48542	0.69004	0.29459	−0.08413
Log RD	−0.15135	0.18510	−0.59752	−0.70145
Log OL	0.34396	−0.79874	—	—
Log D	0.75163	−0.33342	−1.25243	−0.44490
Log MTRL	0.28052	0.13617	−0.68358	0.69226
Log IFL	0.10072	0.30353	—	—
Log PL	−0.51197	−0.67888	−0.08992	0.24368
Log PPL	−1.06919	−0.35597	0.62770	−0.01625
Log BUL	−0.03791	0.48010	—	—
Log MAXB	0.12974	−0.40011	0.40627	−0.04178
Log OCB	0.41754	0.18692	—	—
Log MPFW	−0.99928	0.09042	−0.82972	0.01891
Log CD	0.11061	0.92668	−0.00937	0.34892
Log CDM	0.17113	0.60181	—	—
Eigenvalue	2.60664	1.63260	2.00992	1.06298
% contribution	61.488	38.512	65.408	34.592

central and lower reaches of the river where seasonal flooding occurs every year. Only one specimen of another species was captured in this habitat (*P. simonsi*, at locality **9** in the Lower Central Region), and only five specimens of *P. steerei* (of a total of 461 for which data are available) were taken on all of the eight terra firme standardized trap plots combined. Even in the Headwaters Region, where the várzea is both narrow in extent and only floods in exceptional years, no *P. steerei* were trapped on our standardized lines in mature terra firme forest, although individuals were obtained in mixtures of disturbed habitats on the elevated terra firme landscape. This difference in habitat between *P. steerei* and the other seven species is highly significant by contingency table analysis for each of the four sampling regions: Headwaters — $\chi^2 = 60.278$, df = 2, $p < 0.0001$; Upper Central — $\chi^2 = 182.081$, df = 2, $p < 0.0001$; Lower Central — $\chi^2 = 1878.988$, df = 2, $p < 0.0001$; and Mouth — $\chi^2 = 130.579$, df = 1, $p < 0.001$ (only two habitats [terra firme and ''other''] were compared in the Mouth Region since true várzea could not trapped during the high water season). As we will discuss below, this sharp dichotomy in habitat preference between *P. steerei* and the other species of *Proechimys* within the Rio Juruá basin is also reflected in differences in life history characteristics of these species.

In contrast to *P. steerei*, all other seven species were always found on our terra firme plots, even though each was also trapped in other terra firme habitats that ranged from second growth forests to garden plots. There are, however, differences in habitat distribution among those species co-occurring in the terra firme. For example, in the Headwaters Region *P. pattoni* is nearly restricted to undisturbed terra firme forests whereas the three other co-occurring species (*P. brevicauda*, *P. cuvieri*, and *P. simonsi*) are each found commonly in disturbed second growth forests, active and abandoned cultivated plots, and various edge habitats. Interesting-

TABLE 63
Captures of *Proechimys* Species Relative to Habitat Type and Geographic Region

Taxon	Terra Firme	Várzea	Other[a]
Headwaters Region			
P. brevicauda	32	22	47
P. cuvieri	7	5	4
P. pattoni	24	0	5
P. simonsi	75	22	30
P. steerei	0	31	29
Upper Central Region			
P. cuvieri	19	0	15
P. kulinae	23	0	6
P. simonsi	106	0	7
P. steerei	4	226	8
Lower Central Region			
P. cuvieri	2	0	3
P. echinothrix	7	0	0
P. gardneri	17	0	4
P. kulinae	3	0	0
P. simonsi	67	1	10
P. steerei	1	95	2
Mouth Region			
P. echinothrix	31	0[b]	12
P. simonsi	62	0	16
P. steerei	0	0	65

[a] Includes all disturbed habitats, natural or man-induced (e.g., second growth forest, active or abandoned gardens) and transitional habitats (e.g., terra firme-várzea edge).

[b] No várzea was trapped in the Mouth Region, which was sampled only during the high water season.

ly, *P. brevicauda* and *P. cuvieri* exhibit nonsignificant habitat distributions ($\chi^2 = 3.855$, df = 1, $p = 0.1455$), and were found in quite different relative abundances at those Headwaters localities where they are sympatric. Since *P. cuvieri* maintained the same habitat distribution at other sites downriver ($\chi^2 = 5.926$, df = 2, $p = 0.0517$), and *P. brevicauda* was only taken in the Headwaters, perhaps these morphologically similar species compete with one another, thus affecting each others distributional limits and relative abundances.

Clearly much remains to be learned about habitat requirements of these species, as well as their ecological roles as seed predators and dispersal agents within the habitats in which they occur (e.g., Forget, 1991; Adler, 1995).

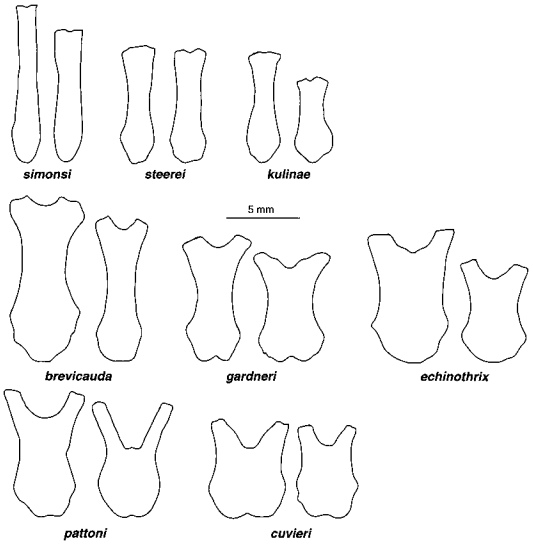

Fig. 137. Outlines of representative bacula of each of the eight species of *Proechimys* that occur within the Rio Juruá basin.

Proechimys brevicauda Gunther, 1877

TYPE LOCALITY: "Chamicuros, Huallaga River," Departamento de Amazonas, Perú.

DESCRIPTION: *Proechimys brevicauda* is medium-sized with relatively short ears, hind feet, and tail, although by its size alone, it cannot be distinguished from other sympatric species, especially *P. cuvieri* (table 60). The length of the tail is approximately twothirds that of the body; the dorsum of the tail is a darker brown than the venter, and may be almost entirely unicolored brown or grade from cream to light brown towards the tip in some specimens; hair on the tail is sparse and the scales are conspicuous to the eye (approximately 10 annuli per cm). The color of the dorsal surface of the hind foot varies from cream to dark brown, and in most specimens the paler color of the inner surface of the hind limbs extends across the tarsal joint. The aristiform hairs are medium in length and narrow, with a whiplike tip (see da Silva, 1998: fig. 3). One of the most distinctive features of this species is the characteristically fulvous lateral stripe and the rufous wash which extends ventrally over the chin, throat, and abdominal region, covering the entire venter in the most extreme examples. The

TABLE 64
Selected External and Cranial Dimensions for Adult Individuals of Eight Species of *Proechimys* from the Rio Juruá
Measurements (mm) are given as mean ± standard error, with range and sample size. Individuals are pooled across all localities along the river.

	P. brevicauda			*P. cuvieri*		
Variable	Mean ± SE	Range	n	Mean ± SE	Range	n
TOL	347.95 ± 3.66	306–403	38	359.88 ± 5.59	312–432	32
TAL	137.11 ± 1.86	110–163	38	144.52 ± 2.57	117–180	33
HF	45.63 ± 0.32	42–53	54	48.64 ± 0.36	44–54	44
E	21.00 ± 0.17	18–24	54	22.09 ± 0.31	19–25	33
CIL	43.84 ± 0.33	39.10–48.83	53	39.65 ± 0.44	39.65–49.84	42
ZB	25.14 ± 0.17	22.41–28.37	51	26.19 ± 0.21	23.48–30.22	44
MB	20.28 ± 0.13	18.00–22.83	53	20.71 ± 0.16	18.82–22.62	44
IOC	11.29 ± 0.10	9.74–12.94	53	12.10 ± 0.11	10.72–13.45	44
RL	20.78 ± 0.20	17.76–23.86	53	21.37 ± 0.29	18.45–24.48	40
NL	19.33 ± 0.20	16.73–22.23	53	20.17 ± 0.29	16.45–23.60	40
RW-1	8.28 ± 0.06	7.24–9.50	54	8.30 ± 0.08	7.02–9.20	45
RD	10.38 ± 0.10	8.90–11.77	54	10.47 ± 0.10	9.43–11.91	45
OL	13.81 ± 010	12.53–15.38	53	14.20 ± 0.11	12.74–15.42	44
D	11.09 ± 0.13	9.58–13.54	53	11.40 ± 0.15	9.88–14.04	45
MTRL	8.43 ± 0.05	7.69–9.18	53	8.55 ± 0.06	7.67–9.96	45
IFL	5.42 ± 0.10	3.80–7.11	54	5.69 ± 0.09	4.39–7.02	45
PL	18.81 ± 0.19	15.97–21.56	52	18.90 ± 0.19	16.40–21.98	45
PPL	21.99 ± 0.15	19.80–24.64	53	22.29 ± 0.21	19.53–24.67	42
BUL	10.56 ± 0.06	9.44–11.84	53	10.64 ± 0.10	9.56–12.15	43
MAXB	8.38 ± 0.07	7.14–9.29	51	8.55 ± 0.07	7.59–10.08	45
OCB	9.33 ± 0.06	8.49–10.65	53	10.06 ± 0.07	8.71–10.85	43
MPFW	5.14 ± 0.06	4.13–6.20	52	4.77 ± 0.06	4.16–5.49	36
CD	18.28 ± 0.11	16.55–19.91	53	18.37 ± 0.11	16.74–19.75	41
CDM	14.32 ± 0.12	12.88–16.66	53	14.60 ± 0.13	13.29–16.20	43

	P. echinothrix			*P. gardneri*		
Variable	Mean ± SE	Range	n	Mean ± SE	Range	n
TOL	382.30 ± 6.97	317–440	20	310.13 ± 5.23	242–353	24
TAL	165.55 ± 5.81	106–209	20	127.38 ± 2.91	88–152	24
HF	48.33 ± 0.54	41–54	27	40.61 ± 0.48	32–45	31
E	24.15 ± 0.37	19–28	26	20.75 ± 0.31	18–24	28
CIL	44.27 ± 0.42	39.84–49.04	24	38.78 ± 0.50	34.54–46.11	28
ZB	25.22 ± 0.23	22.46–27.12	24	22.54 ± 0.17	20.80–24.52	27
MB	20.02 ± 0.14	18.76–21.31	24	18.40 ± 0.17	16.94–19.91	28
IOC	11.73 ± 0.16	10.27–13.18	26	10.29 ± 0.09	9.11–11.37	29
RL	21.96 ± 0.32	17.64–25.29	25	18.74 ± 0.24	16.59–22.17	30
NL	20.21 ± 0.35	15.55–23.36	25	17.51 ± 0.25	15.35–20.50	29
RW-1	7.81 ± 0.11	7.13–9.39	26	7.17 ± 0.07	6.35–8.03	31
RD	10.29 ± 0.12	9.20–11.65	27	8.92 ± 0.09	7.94–9.83	30
OL	14.03 ± 0.12	13.00–15.16	24	12.34 ± 0.11	11.32–13.43	29
D	11.61 ± 0.17	9.21–13.90	26	9.75 ± 0.12	8.60–11.39	31
MTRL	8.26 ± 0.08	7.57–9.23	27	7.50 ± 0.05	6.86–8.21	31
IFL	5.29 ± 0.10	3.97–6.14	26	4.10 ± 0.09	3.35–5.03	31
PL	18.79 ± 0.26	14.87–20.93	26	15.83 ± 0.19	13.51–18.35	31
PPL	22.22 ± 0.19	20.29–24.64	25	19.37 ± 0.20	16.99–21.94	29
BUL	10.23 ± 0.09	9.32–11.03	26	9.91 ± 0.08	9.01–10.60	30
MAXB	8.30 ± 0.10	7.57–9.62	26	7.33 ± 0.08	6.53–8.24	31
OCB	9.32 ± 0.07	8.71–9.85	24	8.59 ± 0.07	8.03–9.41	28
MPFW	5.43 ± 0.07	4.85–6.05	23	4.26 ± 0.07	3.74–5.27	29
CD	17.86 ± 0.15	16.59–19.40	24	15.97 ± 0.11	15.02–17.07	29
CDM	14.12 ± 0.15	12.64–15.24	24	12.32 ± 0.10	11.31–13.10	29

TABLE 64
(Continued)

Variable	*P. kulinae*			*P. pattoni*		
	Mean ± SE	Range	n	Mean ± SE	Range	n
TOL	289.67 ± 5.57	252–328	15	305.60 ± 5.37	278–328	10
TAL	119.63 ± 2.92	95–140	16	125.30 ± 3.53	106–141	10
HF	41.22 ± 0.30	38–44	23	41.09 ± 0.55	37–43	11
E	20.29 ± 0.35	17–23	21	20.82 ± 0.26	20–22	11
CIL	37.29 ± 0.47	33.91–40.80	20	37.59 ± 0.35	36.11–39.53	11
ZB	21.83 ± 0.18	20.45–23.06	21	22.30 ± 0.16	21.52–22.99	11
MB	17.81 ± 0.12	16.55–18.60	22	17.77 ± 0.15	16.93–18.55	11
IOC	9.79 ± 0.10	8.88–10.57	22	9.75 ± 0.18	8.88–10.90	11
RL	17.86 ± 0.22	15.72–20.05	23	18.12 ± 0.22	16.86–18.93	11
NL	16.60 ± 0.21	14.94–18.76	23	15.40 ± 0.31	15.40–18.37	11
RW-1	6.94 ± 0.06	6.40–7.34	23	7.07 ± 0.12	6.41–7.92	11
RD	8.75 ± 0.12	7.73–9.90	23	8.52 ± 0.19	7.91–9.92	11
OL	11.83 ± 0.12	11.00–13.08	22	12.03 ± 0.13	11.24–12.79	11
D	9.48 ± 0.15	8.42–10.98	23	8.86 ± 0.21	7.31–9.68	11
MTRL	7.00 ± 0.05	6.57–7.48	23	7.29 ± 0.06	6.92–7.54	11
IFL	4.06 ± 0.07	3.09–4.59	23	3.93 ± 0.14	3.00–4.56	11
PL	14.96 ± 0.19	13.33–16.71	23	14.84 ± 0.22	13.97–16.18	11
PPL	18.92 ± 0.24	17.30–21.51	21	19.21 ± 0.24	18.08–20.44	11
BUL	9.81 ± 0.06	9.28–10.24	23	9.78 ± 0.14	9.20–10.92	11
MAXB	6.96 ± 0.06	6.37–7.53	23	7.08 ± 0.13	6.33–7.98	11
OCB	8.21 ± 0.05	7.81–8.69	23	8.03 ± 0.13	7.34–9.02	11
MPFW	4.01 ± 0.06	3.57–4.62	22	3.86 ± 0.19	14.50–16.61	11
CD	15.55 ± 0.09	14.74–16.23	21	15.80 ± 0.11	15.02–17.07	11
CDM	11.83 ± 0.12	11.08–12.76	22	12.11 ± 0.10	11.45–12.46	11

Variable	*P. simonsi*			*P. steerei*		
	Mean ± SE	Range	n	Mean ± SE	Range	n
TOL	382.47 ± 3.13	303–480	131	408.50 ± 3.10	357–493	94
TAL	174.28 ± 1.70	118–231	131	167.23 ± 1.54	120–207	94
HF	48.87 ± 0.21	45–56	163	54.01 ± 0.28	49–63	132
E	24.40 ± 0.14	21–28	161	23.61 ± 0.13	20–26	129
CIL	43.03 ± 0.21	37.15–50.03	166	48.37 ± 0.27	40.97–55.41	130
ZB	24.99 ± 0.10	22.18–28.32	166	27.31 ± 0.13	24.24–30.89	130
MB	19.76 ± 0.08	17.79–22.95	165	21.63 ± 0.10	18.56–24.24	132
IOC	11.21 ± 0.06	9.55–14.03	167	12.58 ± 0.08	10.89–15.80	133
RL	21.36 ± 0.15	17.97–26.21	156	24.03 ± 0.17	19.19–28.25	131
NL	20.21 ± 0.15	17.53–25.16	156	23.01 ± 0.18	18.62–27.71	131
RW-1	8.23 ± 0.05	7.02–10.31	167	8.73 ± 0.06	7.35–10.51	133
RD	10.20 ± 0.07	8.60–12.08	165	11.16 ± 0.07	9.16–13.25	133
OL	13.59 ± 0.06	12.24–16.14	167	15.37 ± 0.07	13.40–17.20	132
D	11.02 ± 0.07	8.78–12.96	167	12.69 ± 0.09	10.42–15.34	132
MTRL	7.94 ± 0.03	7.06–8.72	167	8.75 ± 0.03	7.69–10.25	133
IFL	4.44 ± 0.04	3.15–5.94	167	5.62 ± 0.05	4.29–6.82	132
PL	17.14 ± 0.10	14.57–20.87	167	20.67 ± 0.14	16.96–24.26	132
PPL	21.56 ± 0.09	18.34–25.11	166	23.80 ± 0.14	20.67–28.50	132
BUL	10.29 ± 0.04	9.19–11.81	166	10.72 ± 0.05	9.36–12.60	132
MAXB	8.10 ± 0.05	4.79–9.78	167	8.63 ± 0.05	7.28–10.58	132
OCB	9.45 ± 0.03	8.66–10.84	164	10.13 ± 0.04	8.79–11.34	130
MPFW	4.57 ± 0.03	3.57–5.61	164	4.83 ± 0.04	3.96–5.91	131
CD	17.75 ± 0.08	16.03–20.61	166	19.46 ± 0.10	17.04–22.97	130
CDM	14.01 ± 0.08	12.93–16.62	167	15.87 ± 0.09	13.55–18.11	133

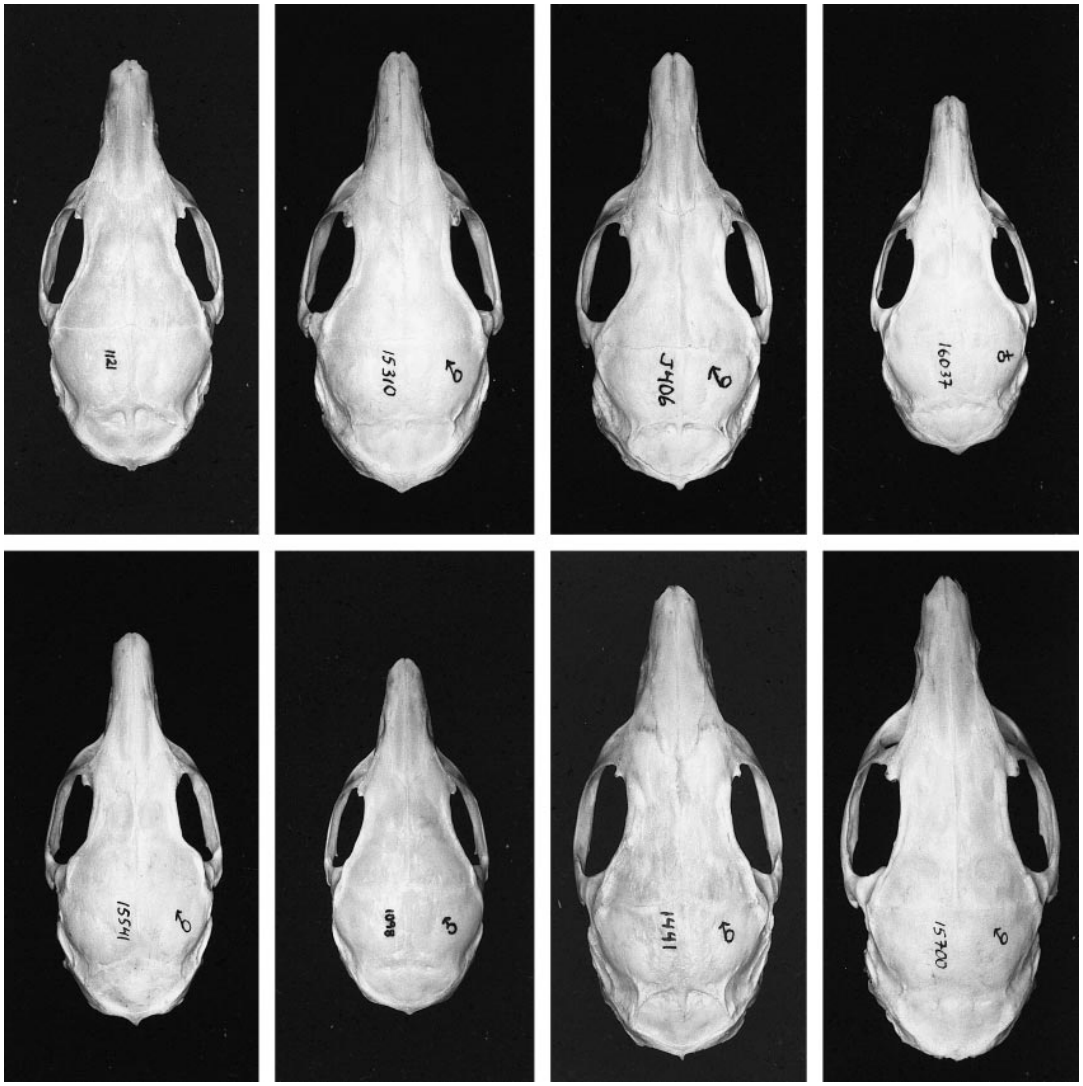

Fig. 138. Dorsal views of the skulls of the eight species of *Proechimys* that occur within the Rio Juruá basin. (**Top**) from left to right: *P. brevicauda* (MNFS 1121, locality **1**), *P. cuvieri* (JLP 15310, locality **7**), *P. echinothrix* (MVZ 187182, locality **14**), *P. gardneri* (MVZ 187209, locality **9**). (**Bottom**) from left to right: *P. kulinae* (MPEG 25502, locality **6**), *P. pattoni* (MVZ 187194, locality **1**), *P. simonsi* (MNFS 1441, locality **4**), *P. steerei* (JLP 15700, locality **6**). Natural size.

dorsal color is uniformly dark reddish-brown streaked with black.

The baculum is elongated and broad, with well-developed apical wings (fig. 137) (for characterization and list of references in which the baculum of this species has been previously presented, see Patton, 1987).

The skull is relatively large (figs. 138 and 139) with a long and narrow rostrum (table 64) and well-developed supraorbital ridges, but with barely perceptible temporal ridges. The incisive foramen of *P. brevicauda* is as described and figured by Patton (1987: 323 and fig. 13) for members of the *longicaudatus*- group. It is lyrate in shape, slightly to strongly constricted posteriorly, with flanged posterolateral margins (in 52 out of 53 specimens) that form a groove extending onto the

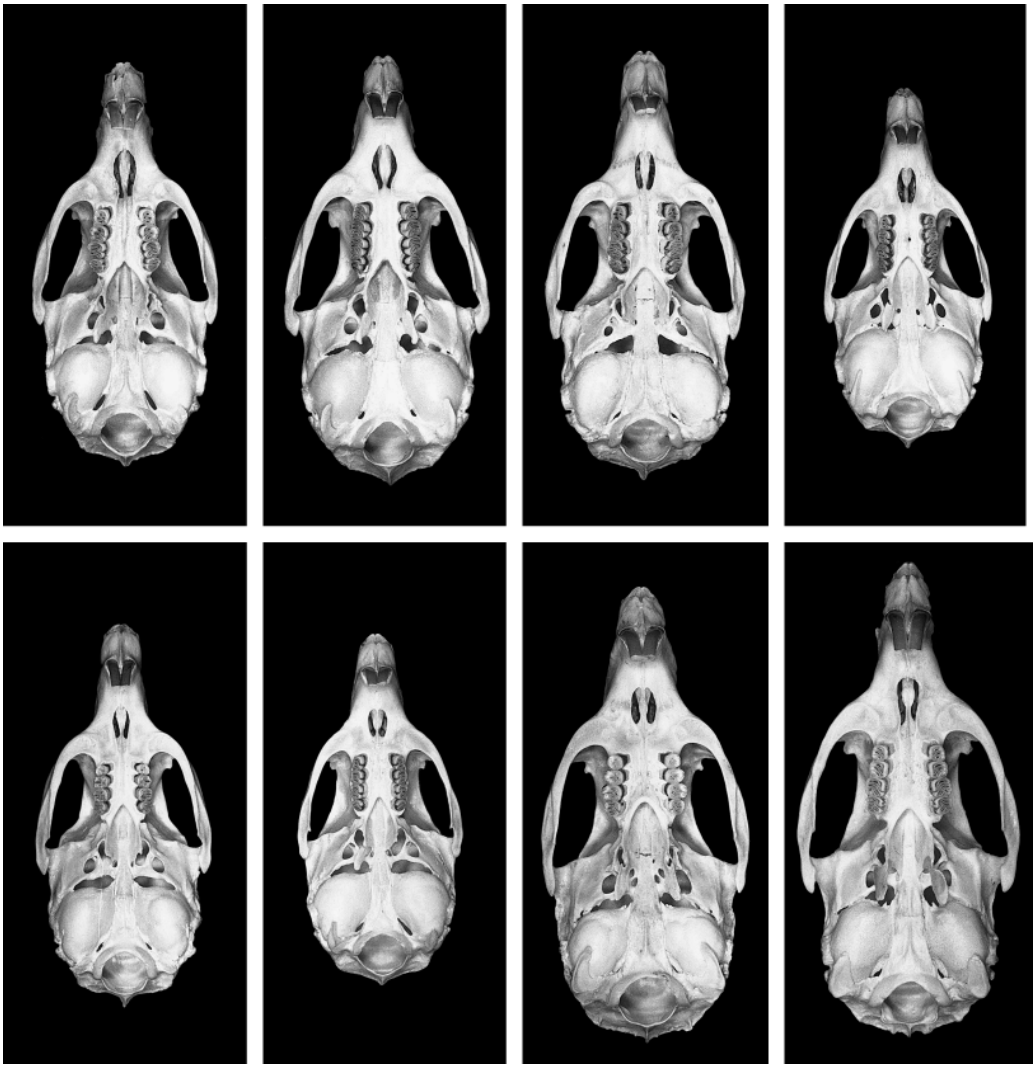

Fig. 139. Ventral views of the skulls of the eight species of *Proechimys* that occur within the Rio Juruá basin. (**Top**) from left to right: *P. brevicauda* (MNFS 1121, locality **1**), *P. cuvieri* (JLP 15310, locality **7**), *P. echinothrix* (MVZ 187182, locality **14**), *P. gardneri* (MVZ 187209, locality **9**). (**Bottom**) from left to right: *P. kulinae* (MPEG 25502, locality **6**), *P. pattoni* (MVZ 187194, locality **1**), *P. simonsi* (MNFS 1441, locality **4**), *P. steerei* (JLP 15700, locality **6**). Natural size.

anterior palate (fig. 140). The premaxillary portion of the septum is long, the maxillary portion is keeled in most specimens (46 out of 53) and both are in contact in all individuals examined; the vomer is visible in all but one individual. The groove on the floor of the infraorbital foramen that accommodates the infraorbital nerve is barely visible and the floor of the foramen is rather smooth (51 out of 53 specimens). The mesopterygoid fossa is broad and shallow (fig. 141), matching closely specimens from central Perú, southern Perú, and northern Bolivia described by Patton (1987: 330 and table 4). It penetrates into the posterior palate to the posterior margins of M3 in 12 specimens, to the posterior half of M3 in 33, and the anterior half in 7 individuals. Most specimens have three folds in all upper and lower teeth (n = 50 and 46 upper and lower toothrows, respectively).

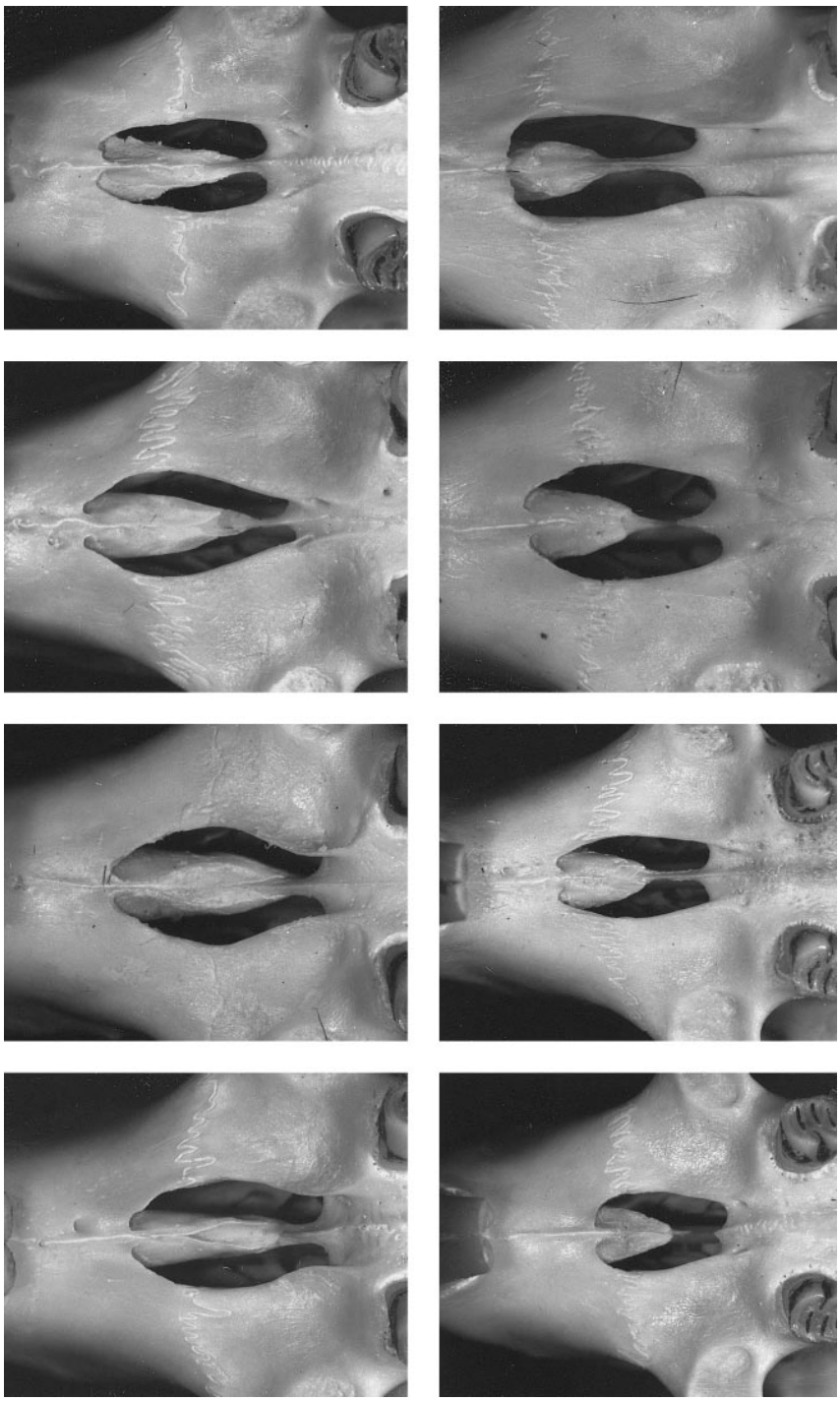

Fig. 140. Shape and structure of the incisive foramina of the eight species of *Proechimys* that occur within the Rio Juruá basin. (**Top**) from left to right: *P. brevicauda* (MNFS 1325, locality **1**); *P. cuvieri* (JLP 15310, locality **7**); *P. echinothrix* (JUR 377, locality **15**); *P. gardneri* (MVZ 187203, locality **9**). (**Bottom**) from left to right: *P. pattoni* (MVZ 187197, locality **4**); *P. kulinae* (MVZ 187186, locality **6**); *P. simonsi* (JLP 15539, locality **6**); and *P. steerei* (MNFS 595, locality **5**).

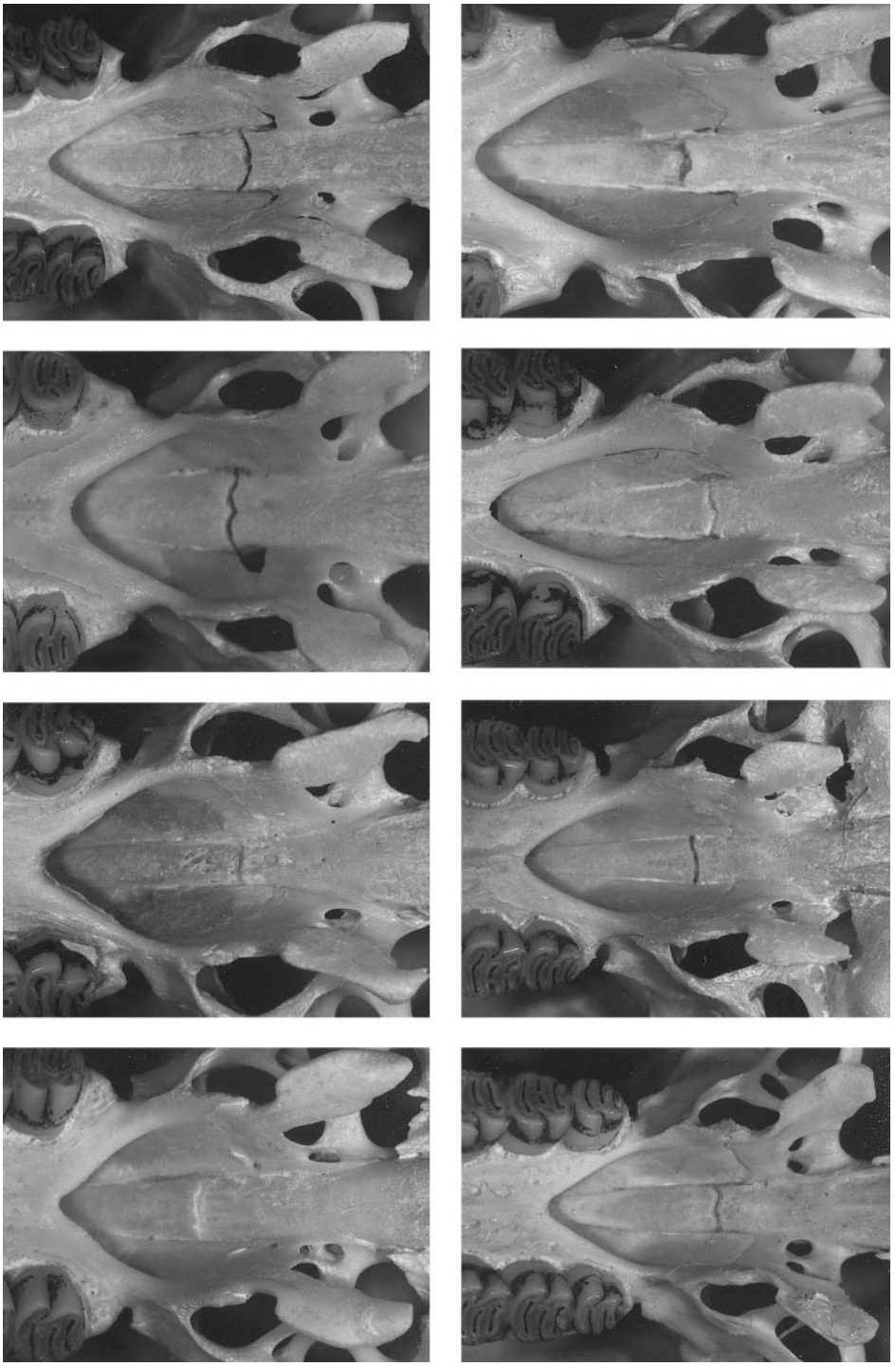

Fig. 141. Shape and depth of the mesopterygoid fossa in the eight species of *Proechimys* that occur within the Rio Juruá basin. (**Top**) from left to right: *P. brevicauda* (MNFS 1325, locality **1**); *P. cuvieri* (JLP 15310, locality **7**); *P. echinothrix* (JUR 377, locality **15**); *P. gardneri* (MVZ 187206, locality **9**). (**Bottom**) from left to right: *P. pattoni* (MVZ 187195, locality **1**); *P. kulinae* (MVZ 187186, locality **6**); *P. simonsi* (JLP 15296, locality **7**); and *P. steerei* (MNFS 595, locality **5**).

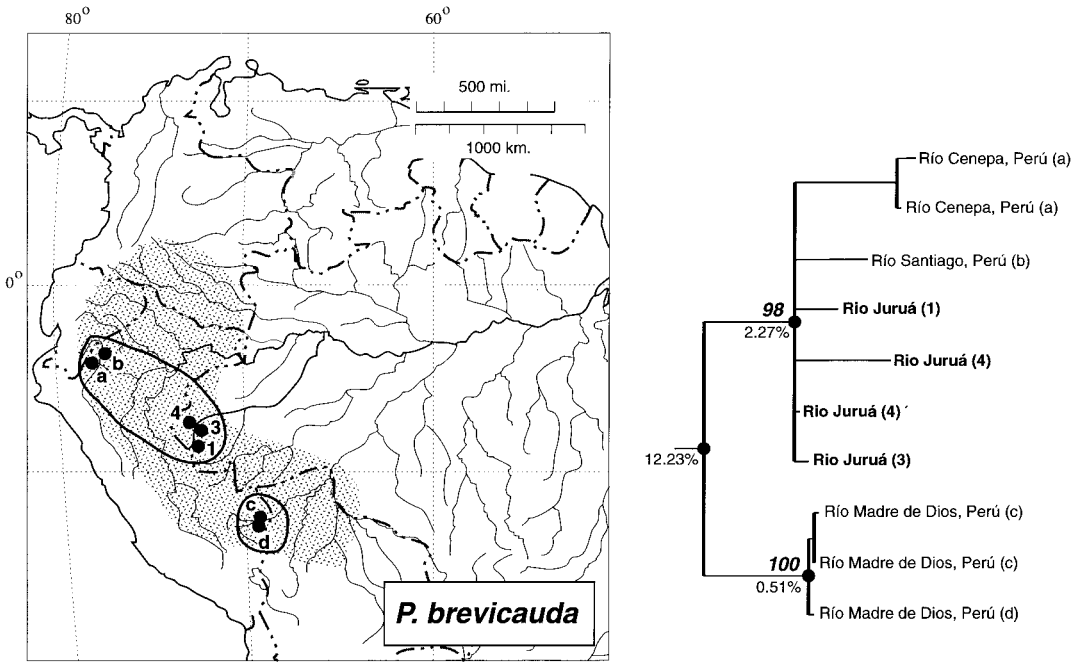

Fig. 142. (**Left**) Map of the distribution of *Proechimys brevicauda* (modified from Patton, 1987) illustrating localities for which 798 bp of cytochrome-b sequence are available, lettered or numbered as in the tree (right). Localities belonging to each of the two mtDNA clades are encompassed by ellipses. (**Right**) Strict consensus maximum parsimony tree of eight equally minimal length trees for 10 individual haplotypes from the seven localities in the map (left). Length = 265 steps; CI = 0.872; RI = 0.757. Sequences of *Proechimys simonsi* and *Mesomys* were used to root the tree. Bold numbers at internal nodes are bootstrap values, based on 1000 replicates; percentages are average Kimura two-parameter distances. Voucher catalog numbers and localities for each haplotype are given in table 65.

However, a small number of individuals (11) have four folds in pm4 and two folds in m3, a characteristic of samples from southern Perú and adjacent Bolivia (Patton, 1987: table 5). Finally, a few individuals (8) have four or five folds in a given tooth.

SELECTED MEASUREMENTS: Representative external and cranial measurements are summarized in table 64.

COMPARISONS: Externally, *P. brevicauda* can be readily distinguished from all other sympatric species within the Rio Juruá basin by its dark overall body color, short, dark tail, and dark dorsal surfaces of the hind feet. It is also the only species along the Rio Juruá with a fulvous lateral stripe and venter, features clearly evident even in younger-aged individuals (also see table 60). It also differs from all other species in bacular shape (fig. 137), which can be seen in live animals in the field by eversion of the phallus. In cranial characters, *P. brevicauda* is unique in its combination of lyrate and distally flanged incisive foramen with a complete and keeled septum (fig. 140), strongly grooved palate with a median ridge, wide and shallow mesopterygoid fossa (fig. 141), generally smooth floor of the infraorbital foramen, and relatively simple cheekteeth with three folds in each, above and below. Only *P. cuvieri* can be confused with *P. brevicauda*, as it is similar in size and has dark dorsal coloration and a lyrate incisive foramen (fig. 140). However, *P. cuvieri* has a white, as opposed to rufous venter, white rather than dark hind feet, a short and broad baculum with distinct apical extensions (fig. 137), and a somewhat narrower and more deeply penetrating mesopterygoid fossa (fig. 141).

MOLECULAR PHYLOGEOGRAPHY: We have sequence data from the cytochrome-b gene for 10 individuals from seven localities in

TABLE 65
Haplotypes, Voucher Numbers, and Localities for *Proechimys brevicauda*
Individual haplotypes listed from top to bottom in the tree, figure 142 (right), with the catalog numbers of their respective voucher specimens, and localities (identified as in the map, fig. 142, left) for which 798-bp haplotypes of the mitochondrial DNA cytochrome-b gene are available.

Haplotype	Voucher no.	Locality
1	MVZ 155047	Huampami, Río Cenepa, Amazonas, Perú, 4.47°S, 78.17°W (locality a)
2	MVZ 155125	Huampami, Río Cenepa, Amazonas, Perú, 4.47°S, 78.17°W (locality a)
3	MVZ 157878	La Poza, Río Santiago, Amazonas, Perú, 4.02°S, 77.77°W (locality b)
4	MNFS 1129	Igarapé Porongaba, right bank Rio Juruá, Acre, Brazil (locality **1**)
5	MNFS 1443	Sobral, left bank Rio Juruá, Acre, Brazil (locality **4**)
6	MNFS 1458	Sobral, left bank Rio Juruá, Acre, Brazil (locality **4**)
7	MNFS 1541	Nova Vida, right bank Rio Juruá, Acre, Brazil (locality **3**)
8	MVZ 168951	Cusco Amazónico, Río Madre de Dios, Madre de Dios, Perú (locality c)
9	MVZ 168958	Cusco Amazónico, Río Madre de Dios, Madre de Dios, Perú (locality c)
10	MVZ 157855	Lago Sandoval, Río Madre de Dios, Madre de Dios, Perú (locality d)

northern and southern Perú as well as the Headwaters Region of the Rio Juruá (fig. 142, left; table 65). Two clearly delineated clades differ by an average of 12% (fig. 142, right). All specimens from the Rio Juruá cluster closely (average divergence of 2.3%) with individuals from the Río Cenepa and Río Santiago from Departamento de Amazonas in northern Perú, while those specimens from southern Perú along the Río Madre de Dios (Departamento de Madre de Dios) form the second clade. As noted below, our Rio Juruá samples share the rufous venter with specimens from the upper Rio Marañón region of northern Perú, not the pure white venters of specimens from southern Perú.

We also examined relationships among 18 individuals from all Headwaters Region localities, based on 450 bp of cytochrome-b sequence. In this analysis, we were interested in any evidence for haplotype segregation relative to the side of the river from which samples were taken. We do not present these results, but simply note that no pattern of haplotype segregation was found (i.e., there was no tendency for haplotypes to cluster either by individual locality or by river margin). The average Kimura two-parameter distance among all separate haplotypes recovered from the 18 individuals was only 1.116% (0.106 standard error).

MORPHOMETRIC VARIATION: Our samples of this species are limited both in number and geographically, to the Headwaters Region of the Rio Juruá in Estado do Acre. The total number of adults (n = 53) precluded an examination of nested patterns of variation in mensural variables with regard to locality, sex, and age. However, in one-way ANOVA's, we found no significant locality or sex effects for any external or cranial variable ($p > 0.05$ in all cases). Consequently, the extent of either geographic differentiation or sexual dimorphism within *P. brevicauda* over this limited region is trivial.

DISTRIBUTION AND HABITAT: *Proechimys brevicauda* has been recorded at localities from northern Perú south to northern Bolivia (Patton, 1987: map, fig. 3; Anderson, 1997). Our data provide the first records of this species for western Brazil, based on specimens examined by us in museums in the United States and England.

We trapped individuals in approximately equal numbers on both sides of the Rio Juruá (60 and 52, on the right and left banks, respectively), but only in the Headwaters Region. The majority (78%) were obtained in terra firme forest, including naturally disturbed forest with either high densities of bamboo or in second growth, while 22% came from forest that floods only occasionally, not seasonally (table 64). We collected a few specimens with shotguns (9%), but most were trapped either in Sherman (33%) or Tomahawk live traps (58%). Young and subadults were captured in about the same numbers in both kinds of traps, but 91% of adults were caught in Tomahawk traps.

TABLE 66
Summary of Karyotypic Data for Samples of *Proechimys brevicauda* (sensu Patton, 1987)

		Autosomes[a]						Sex chromosomes			
		M & SM		ST		A					
Locality	2n	Lg	Med/sm	Lg	Med	Med	Sm	X	Y	FN	Reference
Río Cenepa and Río Santiago, Amazonas, Perú	30	1	7	2	1	—	4	A	A	48	Gardner and Emmons, 1984
Rio Juruá, Acre, Brazil	28	1	8	2	—	—	2	A	A	48	da Silva, 1995; this report
Río Curanja, Ucayali, Perú	28	1	8	2	1	—	1	A	A	50	Patton and Gardner, 1972
Río Tambopata, Madre de Dios, Perú	28	1	7	2	1	—	2	A	A	48	Gardner and Emmons, 1984

[a] M = metacentric; SM = submetacentric; ST = subtelocentric; A = acrocentric (nomenclature follows Patton, 1967).

REPRODUCTION: We obtained all specimens of *P. brevicauda* during the rainy season in the months of February and March, during our survey in the Headwaters Region. Hence, we have no information regarding reproductive seasonality. All reproductively active males were of toothwear age classes 7 or higher; most (15 of 17) belonged to ages 9 or 10. However, while all individuals of younger age classes were nonreproductive, so were two individuals of age 8. Of the total number of females collected, 39.1% were pregnant (27 of 69). While pregnancies were recorded in animals as young as age 5, most (18) were from females in classes 9 or 10. Seven other females were parous, as evidenced by a vascularized uterus and placental scars, with two of these lactating. No pregnant individuals were also lactating. The modal litter size was 2, (range 1–4). These results agree with data for *P. brevicauda* from northern Perú (Patton and Rogers, 1983) where females began breeding by age class 5 and males by age 7. Young (age classes 1 to 5) and subadult (ages 6 and 7) individuals were found at each of the four standard sites in the Headwaters Region (localities **1** through **4**), suggesting that breeding minimally commenced by the end of the previous dry season two to three months earlier. However, since we have no samples of this species from sites visited at other seasons, we do not know whether reproduction is seasonal or largely aseasonal.

KARYOTYPE: Available data on karyotypic diversity for *P. brevicauda* (sensu Patton, 1987) are summarized in table 66, which only includes data for localities from which we personally examined specimens. Data are available for nearly the entire range of *P. brevicauda*, from northern to southern Perú and western Brazil. Diploid number varies from 28 to 30, with differences among samples in the number of morphological classes of autosomes present. We karyotyped 88 specimens combined from all sampled localities within the Headwaters Region of the Rio Juruá. The karyotype of all individuals was consistently 2N = 28 and FN = 48, with a single pair of large metacentrics, eight pairs of medium-sized to small metacentrics and submetacentrics, two pairs of large subtelocentrics, and two pairs of medium-sized to small acrocentrics; the X chromosome is a medium-sized acrocentric and the Y is a minute one (fig. 143). This karyotype appears identical to that published by Aniskin et al. (1990, 1991) for animals from Pucallpa, Departamento de Ucayali, Perú, which surely represent *P. brevicauda* although we have not examined the relevant specimens. All differences in the numbers of each type of autosome listed in table 66 involve chromosomes whose small size sometimes makes their correct morphological classification difficult (see Gardner and Emmons, 1984).

COMMENTS: *Proechimys brevicauda* was

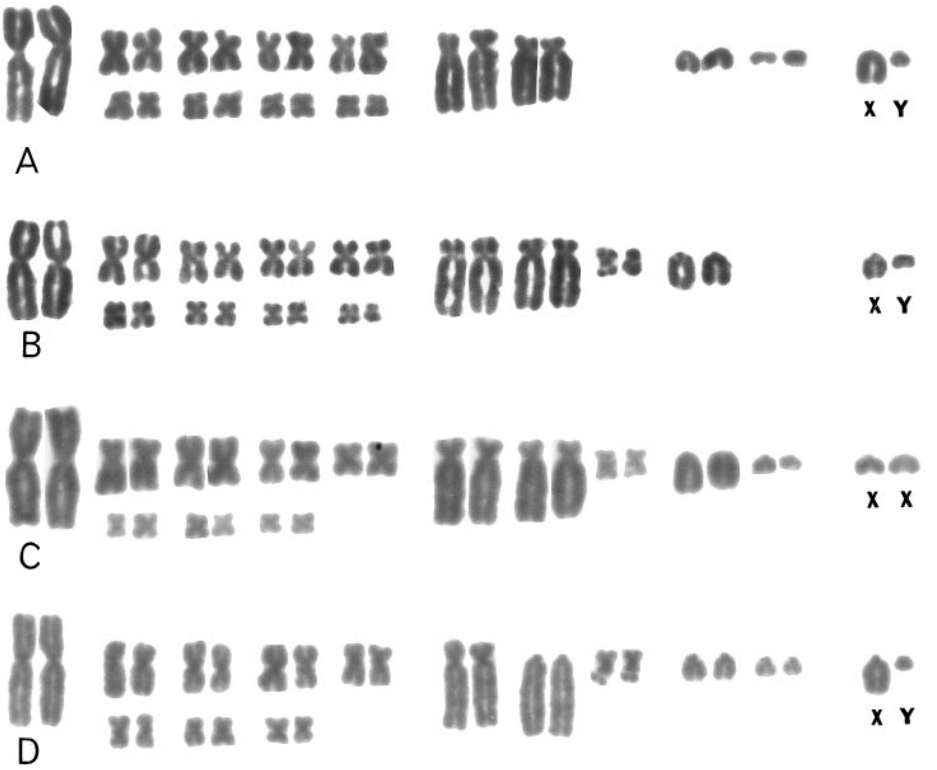

Fig. 143. Karyotypes of four specimens of *Proechimys*: **A**, a male *Proechimys brevicauda*; MNFS 1079; 2n = 28, NF = 48; Igarapé Porongaba (locality **1**), right bank Rio Juruá, Acre, Brazil. **B**, a male *Proechimys cuvieri*; JUR 238; 2n = 28, FN = 50; right bank Nova Vida (locality **3**), Rio Juruá, Acre, Brazil. **C**, a female *Proechimys cuvieri*; LHE 538; 2n = 28, FN = 48; 52 km S of Altamira, Rio Xingu, Pará, Brazil. **D**, a male *Proechimys cuvieri*; LPC 165; 2n = 28, FN = 46; Macaco, left bank Rio Jaú, Amazonas, Brazil.

one of two species listed by Patton (1987) in his *longicaudatus*- group. He suggested that *P. brevicauda* and *P. longicaudatus* were geographic replacements of one another, documented by "... sharp character transition, particularly in pelage color and color pattern but also in bacular measurements..." (Patton, 1987: 338) between the upper Río Iténez and Río Mamoré of southern Beni and Santa Cruz departments, Bolivia. Gardner and Emmons (1984) also suggested that Ecuadoran specimens referable to *gularis* Thomas, 1911 were specifically distinct from northern Peruvian *P. brevicauda* based on karyotypic differences (2n = 30, FN = 48, without large subtelocentric autosomes, versus 2n = 30, FN = 48, with two pairs of large subtelocentric autosomes). They also suggested that the central and southern Peruvian populations might represent a valid subspecies of *P. brevicauda*, to which the name *elassopus* Osgood, 1944 would apply, based on both karyotypic (2n = 28, FN = 50) and color differences. Our specimens from the Rio Juruá have the rufous venter characteristic of typical *brevicauda* from northern Perú, rather than the white venter of *elassopus*, and they group with specimens from northern Perú in cytochrome-b sequences (fig. 142). Karyotypically, the Rio Juruá samples are the same as those from the Rio Ucayali in central Perú (table 66), and differ slightly from those from southern Perú. The deep molecular sequence divergence between the northern Peruvian and Rio Juruá clade relative to that from southern Perú (fig. 142) supports a specific separation of *brevicauda* and *elassopus*. As noted by Patton (1987: 338), "... a thor-

ough analysis of geographic variation within this group is certainly warranted.''

SPECIMENS EXAMINED (n = 112): (**1**) 13 m, 27 f — MNFS 1069, 1074, 1079, 1083, 1094–1095, 1097, 1110, 1121–1122, 1127–1130, 1132, 1137, 1139, 1152–1155, 1158–1159, 1189, 1202–1203, 1211, 1215, 1218–1219, 1221–1222, 1312–1313, 1325, 1328, 1397–1398, 1413, 1415; (**2**) 3 m, 6 f — MNFS 1175, 1177, 1253, 1285, 1300–1302, 1392–1393; (**a**) 4 m, 2 f — MNFS 1013–1014, 1030, 1055, 1058–1059; (**b**) 2 m — MNFS 999, 1044; (**c**) 2 f — MNFS 1034, 1052; (**3**) 7 m, 11 f — JUR 204, 224; MNFS 1520, 1541, 1546, 1549–1550, 1581, 1595, 1602–1604, 1606–1607, 1634–1635, 1654, 1681; (**4**) 14 m, 21 f — JUR 242, 248; MNFS 1429, 1443, 1448, 1450, 1458, 1460–1461, 1467, 1472, 1482, 1487, 1500, 1502, 1504, 1508–1510, 1522, 1524, 1552, 1562, 1567–1568, 1572, 1618, 1626–1627, 1642, 1645–1646, 1665–1667.

Proechimys cuvieri Petter, 1978

TYPE LOCALITY: ''Saül (S 21), Guyane française,'' French Guiana.

DESCRIPTION: Proechimys *cuvieri* is similar to *P. brevicauda* with its medium-sized body and relatively short ears, hind feet, and tail (tables 60 and 64). The tail is approximately two thirds the length of the body; in most specimens it is distinctly bicolored, with the ventral coloration varying from creamy to pale brown. In no specimen does the tail appear uniformly dark, as is often the case in *P. brevicauda*. The tail hairs are prominent but scales remain visible to the eye; these range from 9–12 per centimeter. Overall, this species has a relatively dark-colored body, tail, and feet. As in other species, the color of the midline of the dorsum appears darker than the sides of the body, especially over the rump. In contrast especially to *P. brevicauda*, *P. cuvieri* is brightly colored with a strong reddish overall hue. The aristiform hairs are stiff to the touch, larger and wider than those of all other species except *P. echinothrix*, but with a whiplike tip (da Silva, 1998: fig. 3). The dorsal surface of the hind foot is brownish, and in most specimens the pale color of the inner surface of the hind limbs extends across the tarsal joint as a fulvous stripe. No lateral line is present and the reddish color of the sides contrasts sharply with the almost pure white venter. In addition to its medium-sized body and moderately stiff aristiforms, a helpful character for identifying *P. cuvieri* males in the field is the very short and massive baculum, which has a broad shaft, expanded base, and apical extensions (fig. 137).

The skull is relatively large, with a long, narrow rostrum (figs. 138 and 139; table 64) and well-developed supraorbital ridges, but with weakly developed temporal ridges (Patton, 1987: fig. 21d). The overall shape of the incisive foramen is lyrate, but only moderately constricted posteriorly in contrast to *P. brevicauda* (see Patton, 1987: figs. 13 and 14). The posterolateral margins of the foramen are flanged (fig. 140) in all individuals (n = 25), but the flanges are not as developed as in *P. brevicauda*, forming only weak grooves that extend into the palate (in 33 of 35 specimens). The premaxillary portion of the septum is long and almost always (31 of 35) in contact with the maxillary portion, which may be equally either slightly keeled or smooth; the vomer is slightly to well exposed ventrally in most specimens (n = 25), but in some (n = 9) it is completely enclosed within the premaxillary sheath. The groove on the floor of the infraorbital foramen is slightly developed in the majority of specimens (26 of 35), but the degree of development of the lateral flanges is weak; in two of the remaining individuals, the floor is smooth without any groove, and in seven it has a groove present with moderately developed lateral flanges. The mesopterygoid fossa penetrates the posterior palate to a moderate degree (fig. 141), extending to the posterior margins of M3 in 16 specimens, but in approximately equal number of individuals it reaches into the posterior half of M3 (17 specimens) or to its anterior half (2 specimens). The counterfold pattern is typically three folds in all four upper and lower teeth, except for pm4 which has four folds in most specimens examined (24 of 34). A smaller number of individuals (n = 7) has either two, four, five, two to three, three to four or four to five folds in a given tooth.

SELECTED MEASUREMENTS: Selected exter-

nal and cranial measurements are summarized in table 64.

COMPARISONS: In overall morphology, *P. cuvieri* is most similar to *P. brevicauda*. Both are characterized by a medium-sized body, ears, and hind feet and relatively short tail (table 60). In comparisons of series of both species, *P. cuvieri* is brighter and more reddish dorsally than *P. brevicauda,* which tends to be duller and more brownish; it also has a white venter that lacks the rufous patches typical of *P. brevicauda*. In the latter species, the coloration of the ventral surface of the tail tends to be darker towards the tip, but appears uniformly paler than the dorsal surface in the specimens of *P. cuvieri* we studied. The aristiform hairs of *P. cuvieri* are stiffer to the touch, being much larger and wider than those of *P. brevicauda* , but less so than in *P. echinothrix* (da Silva, 1998). As in other species of spiny rats, except *P. brevicauda*, *P. cuvieri* has no lateral stripe and the reddish color of the sides contrasts sharply with the mostly pure white ventral coloration. The baculum of *P. cuvieri* is most similar in general shape to that of *P. echinothrix* and *P. pattoni* (fig. 136), although the three differ in size (see Patton, 1987).

MOLECULAR PHYLOGEOGRAPHY: We have cytochrome-b sequence data for individuals from 11 localities throughout the extensive geographic range of *P. cuvieri* (fig. 144, above; table 67). We examined relationships among the 16 haplotypes for which 798 bp were available from these 10 localities by maximum parsimony. There are two major clades, with an average divergence of 9.8%, one of which is divided into three equally divergent groups (fig. 144, below). The first clade groups all specimens from the Rio Juruá, from the Headwaters through the Lower Central sections of the river. We did not find apparent subgrouping by either regional area or river bank; haplotypes from the four available localities differ by an average of less than 1%. The second major clade includes a group of widely scattered localities in eastern Amazonia, from the Guianan region of eastern Venezuela and French Guiana to the Carajás region of Estado do Pará south of the Rio Amazonas and the left (= east) bank of the Rio Negro near the city of Manaus in central Amazonia. Haplotypes from these five localities differ from each other by an average of 3%. Also included in the second clade are single localities in the upper Rio Negro of northwestern Brazil and the Río Santiago of the Departamento de Amazonas in northern Perú. Collectively, these three groups differ by an average of 7.3%. Clearly, *P. cuvieri* is comprised of a series of quite divergent clades that replace one another across Amazonia, but additional sampling is needed to determine whether any of these correspond to separate species. Morphologically, this taxon is relatively uniform with little evidence of geographically distinguishable populations.

MORPHOMETRIC VARIATION: Our samples of adults are limited in number, although the species was trapped at localities in the Headwaters and both Upper and Lower Central regions (fig. 133). Across this region, however, only one cranial dimension exhibits any interlocality differentiation (OCB; one-way ANOVA, $F_{5,32} = 4.954$, $p = 0.0018$); all other cranial and all external dimensions display uniform variation across their sampled range within the Rio Juruá. Sexual dimorphism is also nonexistent ($p > 0.05$ for all variables in one-way ANOVAs).

DISTRIBUTION AND HABITAT: *Proechimys cuvieri* is known from scattered localities throughout Amazonia from the coastal Guianan region west along the Amazon River from near its mouth to northern Perú (Patton, 1987: fig. 4). Our specimens from the Rio Juruá extend this distribution about 400 km to the south. All individuals were collected in the Headwaters, Upper, and Lower Central regions, but not in the Mouth Region. It is likely that the species is present in the latter region, since specimens of *P. cuvieri* have been taken localities along the length of the Rio Solimões–Rio Amazonas from near Iquitos to Belém. The majority of specimens were trapped in terra firme forests (28 of 57), but the species was also collected in locally inundated forest (5 individuals) or secondary upland forest and abandoned gardens (22 individuals; table 63). We captured animals in Tomahawk and Sherman traps in all habitats as well as by hunting and with the use of snap traps (Victor rat traps and a similar all-metal trap made and sold in Manaus for domestic use). Although the total

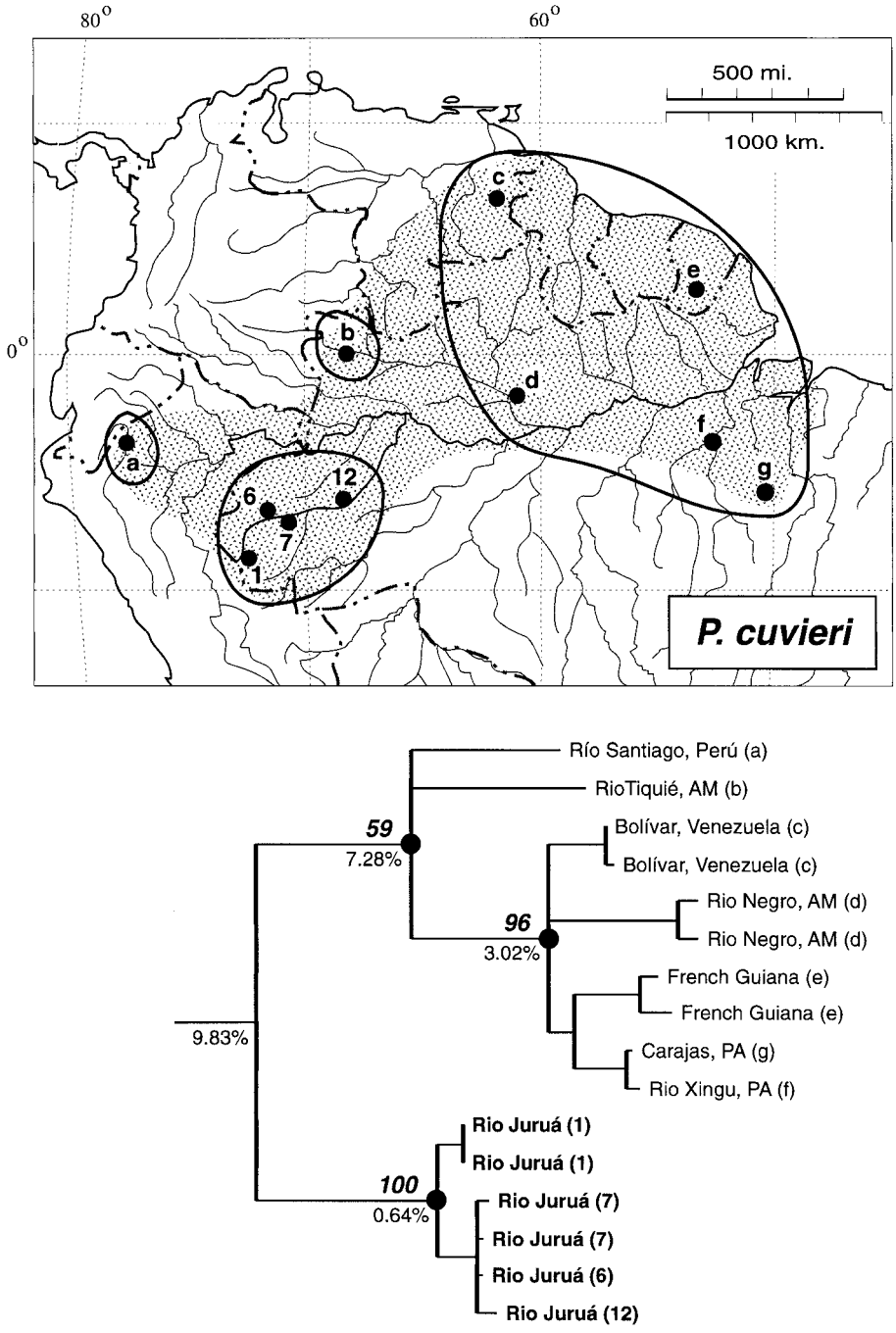

Fig. 144. (**Above**) Map of the distribution of *Proechimys cuvieri* (modified from Patton, 1987). Localities from which individual specimens have been examined for sequence of the mtDNA cytochrome-b gene are indicated; those from localities outside of the Rio Juruá are lettered. Regionally monophyletic clades, identified in the tree below, are circumscribed by solid lines. (**Below**) Bootstrap consensus minimum-length parsimony tree for haplotypes of the mitochondrial cytochrome-b gene (798 bp); length = 351 steps, CI = 0.721, RI = 0.779. Sequences of other species of *Proechimys* and of *Mesomys* were used as outgroups to root the tree. Bold numbers at internal nodes are bootstrap values, based on 1000 replicates; percentages are average Kimura two-parameter distances. Voucher catalog numbers and localities for each haplotype are given in table 67.

TABLE 67
Haplotypes, Voucher Numbers, and Localities for *Proechimys cuvieri*
Individual haplotypes listed from top to bottom in the tree, figure 144 (below), with the catalog numbers of their respective voucher specimens, and localities (identified as in the map, fig. 144, above) for which 798-bp haplotypes of the mitochondrial DNA cytochrome-b gene are available.

Haplotype	Voucher no.	Locality
1	MVZ 157874	La Poza, Río Santiago, Amazonas, Perú, 4.02°S, 77.77°W (locality a)
2	INPA 2529	Comunidade Colina, right bank Rio Tiquié, Município São Gabriel da Cachoeira, Amazonas, Brazil, 0°72'N, 60°04'W (locality b)
3	MVZ 160091	69 km (by road) SE Río Cuyuní, Bolívar, Venezuela (locality c)
4	MVZ 160092	69 km (by road) SE Río Cuyuní, Bolívar, Venezuela (locality c)
5	JLP 16783	Lago Meduinim, left bank Rio Negro, Amazonas, Brazil, 1°46'58"S, 60°23'14"W (locality d)
6	JLP 16804	Lago Meduinim, left bank Rio Negro, Amazonas, Brazil, 1°46'58"S, 60°23'14"W (locality d)
7	T-1833	La Trinité Mountains, French Guiana, 4°37'N, 53°22'W (locality e)
8	T-1834	La Trinité Mountains, French Guiana, 4°37'N, 53°22'W (locality e)
9	USNM 549559	52 km SSW Altamira, east bank Rio Xingu, Pará, Brazil (locality f)
10	CS 22	Floresta Nacional Tapirapé-Aquiri, Município de Marabá, Pará, Brazil, 5°48'05"S, 50°30'54"W (locality g)
11	MNFS 1077	Igarapá Porongaba, right bank Rio Juruá, Acre, Brazil (locality **1**)
12	MNFS 1080	Igarapá Porongaba, right bank Rio Juruá, Acre, Brazil (locality **1**)
13	JLP 15308	Penedo, right bank Rio Juruá, Amazonas, Brazil (locality **7**)
14	JLP 15310	Penedo, right bank Rio Juruá, Amazonas, Brazil (locality **7**)
15	MNFS 510	Seringal Condor, left bank Rio Juruá, Amazonas, Brazil (locality **6**)
16	JLP 15903	Barro Vermelho, left bank Rio Juruá, Amazonas, Brazil (locality **12**)

number of each kind of trap varied greatly, the most of our sample (66%) were caught in Tomahawk traps with only 20% in Sherman traps; 4% were shot, 10% were caught with snap traps. Of the animals captured in Sherman and Tomahawk traps, young and subadults were caught in nearly equal numbers in both kinds of traps, but 89% of adults were caught in the larger Tomahawk traps.

REPRODUCTION: We caught specimens of *P. cuvieri* during the interval from August through March, a period that includes most of the dry season and the early rainy season. We classified 13 of the 17 male specimens for which autopsy data are available as reproductively active; all belonged to age classes 9 or 10. The four reproductively inactive individuals were of age classes 3, 5, 7, and 9. We caught pregnant females (n = 4) only in the months of February and March; one lactating individual was collected in August. Finally, we found young animals (ages 1 to 5) in all sample regions. These data are too limited to determine whether breeding is largely confined to the wet season or extends through the dry period as well. Eight of nine pregnant and parous females were old adults (ages 9 or 10); one pregnant female was of age 7. Litters consisted of two in all cases.

KARYOTYPE: We karyotyped 35 specimens of *P. cuvieri* from six different localities (locality **1** [n = 5], locality **3** [n = 3], locality **4** [n = 3], locality **6** [n = 8], locality **7** [n = 13], and locality **12** [n = 3]). All specimens were 2n = 28, FN = 48 (fig. 143B). The autosomes include a pair of large metacentrics, eight pairs of medium-sized to small metacentrics and submetacentrics, two pairs of large and one pair of small subtelocentrics (of which the small pair possess terminal satellites on the long arms), and a single pair of medium-sized acrocentrics. The X chromosome is a small acrocentric and the Y is a minute one. There is some karyotypic variation in *P. cuvieri* over its sampled range (table 68), and we illustrate karyotypes from specimens from the Rio Jaú (Estado do Amazonas, Brazil) and the Rio Xingu (Estado do Pará, Brazil) in figure 143 along with one from the Rio Juruá to show the known extent of variation present. Diploid number remains constant at 2n = 28, but FN varies between

TABLE 68
Summary of Karyotypic Data from Samples of the *Proechimys cuvieri*-Group (sensu Patton, 1987)

		Autosomes[a]						Sex chromosomes			
		M & SM		ST		A					
Locality	2n	Lg	Med/sm	Lg	Med	Med	Sm	X	Y	FN	Reference
French Guiana	28	1	8	1	1	1	1	A	A	48	Reig et al., 1979
Bolívar, Venezuela	28	1	8	1	—	1	2	A	A	46	M. A. Barros, pers. comm.
Rio Xingu, Pará, Brazil	28	1	8	2	—	—	2	A	A	48	this report
Manaus, Amazonas, Brazil	28	1	8	2	—	1	2	A	A	46	Louise H. Emmons, pers. comm.
Rio Jaú, Amazonas, Brazil	28	1	8	1	—	1	2	A	A	46	this report
Rio Juruá, Brazil	28	1	8	2	1	1	—	A	A	48	da Silva, 1995; this report

[a] M = metacentric; SM = submetacentric; ST = subtelocentric; A = acrocentric (nomenclature follows Patton, 1967).

46 and 50, due to differences in the number of subtelocentric and acrocentric autosomes. The karyotype of *P. cuvieri* is similar, if not identical in nondifferentially stained preparations, to some samples of *P. brevicauda* (compare figs. 143A and 143D and tables 66 and 68).

COMMENTS: Patton (1987) placed two taxa within his *cuvieri*- group based on similarities in bacular structure, although he recognized that these were not closely related. One of these corresponds to *P. cuvieri* and the other has been recently described as *P. pattoni* (da Silva, 1998). Our cytochrome-b analyses corroborate the distinctiveness of both taxa and, as they do not form a monophyletic clade (fig. 134), suggesting that their bacular similarity is convergent rather than indicative of close relationship. Although *P. pattoni* should not be considered a member of the *cuvieri*- group, *P. cuvieri* itself is likely to prove a composite. While there is general cranial similarity in *P. cuvieri* throughout its range as mapped by Patton (1987: fig. 4), our geographic samples of this species exhibit divergent regional units with levels of sequence divergence equivalent to those we found between other species of the genus. Clearly, a more refined examination of detailed geographic sampling is needed to assess the possibility that each of these clades may represent a distinct species.

SPECIMENS EXAMINED (n = 55): (**1**) 2 m, 7 f — MNFS 1080, 1085, 1070, 1075–1077, 1192–1193, 1385; (**2**) 1 m — MNFS 1283; (**3**) 1 m, 3 f — MNFS 1580, JUR 207, 236, 238; (**4**) 2 f — MNFS 1486, 1644; (**6**) 5 m, 4 f — JLP 15603, 15636, 15638, 15642, 15664, MNFS 531, 534–535, 551; (**7**) 14 m, 10 f, 1 unknown — JLP 15258, 15260, 15267, 15271, 15278, 15284–15285, 15308, 15310, 15369, 15405, 15460–15463, 15478, MNFS 331–332, 346, 353, 363, 365, 408, 499, 512; (**12**) 2 m, 3 f — JLP 15886, 15903, 15890, 15922, JUR 187.

Proechimys echinothrix da Silva, 1998

TYPE LOCALITY: "Brazil, Amazonas: Colocação Vira-Volta, left bank Rio Juruá on Igarapé Arabidi, affluent of Paraná Breu, 3°17′S, 66°14′W."

DESCRIPTION: This is one of the most easily distinguishable and among the largest spiny rats occurring in western Brazil. In general morphology, these animals are relatively robust, have long ears, a moderately long tail, and large hind feet (tables 60 and 64). Overall, the color of the body is uniformly reddish-brown, coarsely streaked on the back and sides with varying amounts of black; the interspersed heavy, dark brown guard-hairs make the middorsum appear somewhat darker, but this grades evenly into the brighter

and paler sides of the body. The aristiform hairs are long and much broader than those of any other species of spiny rats on the Rio Juruá (da Silva, 1998: table 4), with distinctly strong and blunt tips that are very conspicuous to the eye and touch, especially in the middorsal region. The color of the venter, chin, and inner surfaces of forelimbs and hind limbs is pure white. The tail is indistinctly bicolored, dark above and white ventrally. It is well haired, with the scales nearly completely obscured from view. The hind feet are long and narrow, nearly unicolored white in most specimens and lack a dark band on the ankle joint. The juvenile pelage varies from uniformly grayish brown (age class 1) to pale brown mixed with Sanford Brown (age class 6). The plantar surface of the hind feet has six tubercules; the lateral metatarsal tubercule is weakly to moderately developed, but is always visible and shorter than the medial metatarsal tubercule.

The baculum is massive and relatively short; its shaft is broad with a thick and expanded base and the distal end has a pair of divergent apical extensions that are separated by a shallow median depression (fig. 137; table 3 in da Silva, 1998). Da Silva (1998) figures and describes the soft anatomy of the male phallus.

The skull is moderately large, with a long and narrow rostrum (figs. 138 and 139) and a well-developed supraorbital ledge extending over the orbits but discontinuous across the parietals. The zygoma usually lack a postorbital process or, if present, it is low and rounded with equal contributions by the jugal and squamosal. A well-developed groove with a lateral flange is present on the floor of the infraorbital foramen. The incisive foramen is ovate to lyrate in general shape, with posterolateral margins mostly flat, or only weakly flanged with very shallow grooves extending onto the anterior palate, which lacks a median ridge (fig. 140). The premaxillary portion of the septum is long and narrow, extending between one half and two thirds of the length of the opening; the maxillary portion is typically attenuate and has weak to no contact with the premaxillary portion; and the vomer is visible in most specimens. The mesopterygoid fossa is moderate in depth but broad (fig. 141), with an angle of indentation into the posterior margin of the palate averaging about 70° and extending to the anterior half of M3. The median number of folds in all upper cheekteeth is three, although M3 occasionally only has two folds.

SELECTED MEASUREMENTS:: Selected external and cranial measurements are given in table 64.

COMPARISONS: This is one of the most readily identifiable species of *Proechimys* in western Amazonia. It can be distinguished from all other sympatric species by the following combination of characters: medium to large-sized body covered by very heavy aristiform hairs, especially along the dorsum; long and very broad aristiforms with a distinctly sharp tip lacking any whiplike extension as seen in *P. simonsi* and *P. steerei*; ears large; tail hairy and distinctly clear white below, almost brushy in comparison to other species; tail approximately two thirds of the length of the body, relatively and absolutely shorter than the tail of *P. simonsi*; hind foot nearly unicolored white; cranial features include weakly developed posterior portion of the temporal ridges; uniformly three folds on all upper teeth; oval to lyre-shaped incisive foramen with an expanded and long contribution of the premaxillary portion (in contrast to *P. simonsi*, but similar to *P. brevicauda*) but with both attenuate flanges and a maxillary portion of septum that lacks a keel (in contrast to *P. brevicauda*); vomer visible, although only barely so. The broad and short baculum of *P. echinothrix* distinguishes this species from all others, except *P. cuvieri* and *P. pattoni*, both of which are distinctive in other morphological features.

MOLECULAR PHYLOGEOGRAPHY: We have examined cytochrome-b sequences from individuals collected at each of the three localities from the Upper and Lower Central and Mouth regions of the Rio Juruá, as well as from the upper Rio Urucu south of the Rio Solimões, and from the Rio Jaú and Rio Tiquié, all to the north of the Solimões and west of the Rio Negro (fig. 145, above; table 69). Two clearly defined and deeply divergent clades are evident, one north of the Rio Solimões and the other to the south (fig. 145, below). These differ by an average of 10.8%. All specimens from north of the Rio Soli-

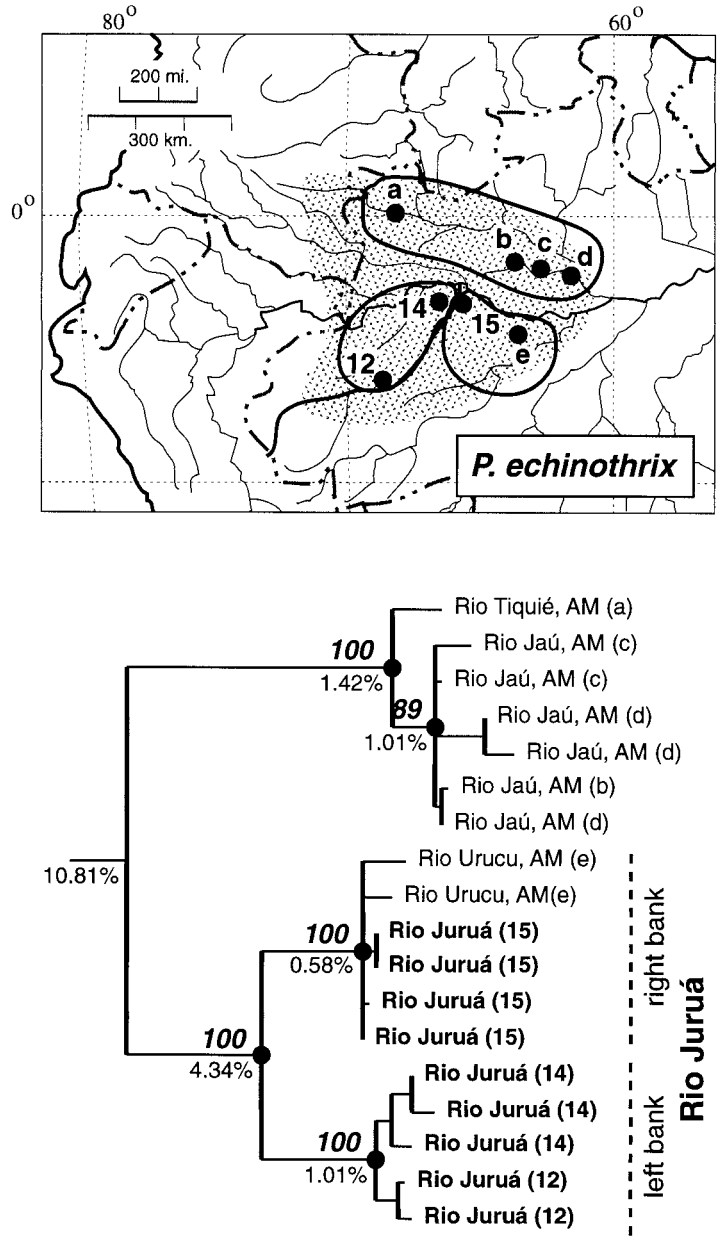

Fig. 145. (**Above**) Map of the distribution of *Proechimys echinothrix* (modified from da Silva, 1998) illustrating localities for which 801 bp of cytochrome-b sequence are available, lettered or numbered as in the tree (bottom). Localities belonging to each of the three mtDNA clades are encompassed by ellipses. (**Below**) Single most parsimonious tree generated by the branch-and-bound procedure for 18 individual haplotypes from the eight localities in the map (top). Length = 341 steps; CI = 0.757; RI = 0.872. Sequences of other species of *Proechimys* and of *Mesomys* were used to root the tree. Bold numbers at internal nodes are bootstrap values, based on 1000 replicates; percentages are average Kimura two-parameter distances. Voucher catalog numbers and localities for each haplotype are given in table 69.

TABLE 69
Haplotypes, Voucher Numbers, and Localities for *Proechimys echinothrix*
Individual haplotypes listed from top to bottom in the tree, figure 145 (below), with the catalog numbers of their respective voucher specimens, and localities (identified as in the map, fig. 145, above) for which 801-bp haplotypes of the mitochondrial DNA cytochrome-b gene are available.

Haplotype	Voucher no.	Locality
1	INPA 2526	Comunidade Colina, right bank Rio Tiquié, Município São Gabriel da Cachoeira, Amazonas, Brazil, 0°72'N, 60°04'W (locality a)
2	JLP 16730	Macaco, left bank Rio Jaú, Amazonas, Brazil, 2°05'29"S, 62°08'22"W (locality c)
3	JLP 16736	Macaco, left bank Rio Jaú, Amazonas, Brazil, 2°05'29"S, 62°08'22"W (locality c)
4	JLP 16746	right bank Rio Jaú above mouth, Amazonas, Brazil, 1°57'54"S, 61°29'14"W (locality d)
5	JLP 16747	right bank Rio Jaú above mouth, Amazonas, Brazil, 1°57'54"S, 61°29'14"W (locality d)
6	MNFS 1986	Tambor, left bank Rio Jaú, Amazonas, Brazil, 2°13'S, 62°26'W (locality b)
7	MNFS 1987	Tambor, left bank Rio Jaú, Amazonas, Brazil, 2°13'S, 62°26'W (locality b)
8	MNFS 133	alto Rio Urucu, Amazonas, Brazil, 6°14'S, 58°15'W (locality e)
9	MNFS 191	alto Rio Urucu, Amazonas, Brazil, 6°14'S, 58°15'W (locality e)
10	JUR 298	Vai-Quem-Quer, right bank Rio Juruá, Amazonas, Brazil (locality **15**)
11	MVZ 187181	Vai-Quem-Quer, right bank Rio Juruá, Amazonas, Brazil (locality **15**)
12	JUR 357	Vai-Quem-Quer, right bank Rio Juruá, Amazonas, Brazil (locality **15**)
13	MVZ 187180	Vai-Quem-Quer, right bank Rio Juruá, Amazonas, Brazil (locality **15**)
14	MVZ 187183	Colocação Vira-Volta, left bank Rio Juruá, Amazonas, Brazil (locality **14**)
15	MNFS 1724	Colocação Vira-Volta, left bank Rio Juruá, Amazonas, Brazil (locality **14**)
16	MNFS 1723	Colocação Vira-Volta, left bank Rio Juruá, Amazonas, Brazil (locality **14**)
17	INPA 2551	Barro Vermelho, left bank Rio Juruá, Amazonas, Brazil (locality **12**)
18	MPEG 25500	Barro Vermelho, left bank Rio Juruá, Amazonas, Brazil (locality **12**)

mões, from the upper Rio Negro as well as the Rio Jaú, form a tight cluster of haplotypes that differ, on average, by only 1.4%. Specimens from the Rio Juruá and upper Rio Urucu, however, differentiate into two clades with the moderate divergence of 4.3% between them. One of these clades includes localities from the left bank of the Rio Juruá (Barro Vermelho [locality **12**] and Colocação Vira-Volta [locality **14**]); the other pairs the sole locality from the right bank of the Rio Juruá (Vai-Quem-Quer [locality **15**]) with that from the upper Rio Urucu, which is further to the east. Thus, the Rio Juruá appears to separate this species into definable monophyletic haplotype clades.

MORPHOMETRIC VARIATION: Our samples are of limited size, but geographic divergence is evident in three morphometric variables in comparisons between individuals from opposite sides of the Rio Juruá. Ear length ($F_{1,25} = 4.471$, $p = 0.0391$), mastoid breadth ($F_{1,24} = 12.129$, $p = 0.0019$), and occipital condyle breadth ($F_{1,23} = 6.552$, $p = 0.0178$) are all significantly different by one-way ANOVAs. Thus, there is minimal morphological differentiation to match that observed in mtDNA haplotypes.

DISTRIBUTION AND HABITAT: In her description of *P. echinothrix,* da Silva (1998) allocated only specimens from the Rio Juruá and upper Rio Urucu to this species, both sets of localities south of the Rio Solimões in west-central Amazonian Brazil. However, she noted that *echinothrix*-like animals had been collected throughout the Parque Nacional Jaú northwest of the mouth of the Rio Negro in the central Amazon and that one of us (J. L. Patton) had examined specimens from the Río Vaupés (= Uaupés) in Amazonian Colombia in the collection of the Instituto de Ciencias Naturales, Universidad Nacional de Colombia, in Bogotá that he believed to represent this same taxon. Finally, we have recently obtained specimens of this same taxon from Comunidade Colina, on the right bank of the Rio Tiquié, a tributary of the Rio Uaupés. Thus, the range of this species, or a complex of closely related taxa, covers a large part of western Amazonian Brazil and

adjacent Colombia on both sides of the Rio Solimões, and is likely to be found in northeastern Perú as well (fig. 145, top). It's distinctive external morphology should make this one of the more easily identifiable species of *Proechimys* in regional faunas of this area.

We collected specimens in the Rio Juruá only in the Lower Central (locality **12**) and Mouth regions (localities **14** and **15**), but on both banks of the river (figs. 133 and 145). Of the 50 specimens collected, 43 are from the terra firme forests of the Mouth Region, often at the edge of flooded várzea; the remaining seven specimens are from terra firme forest at Barro Vermelho (locality **12**). We captured animals in Tomahawk (63%) and Sherman (29%) traps on the standardized lines; we also obtained specimens by hunting (2%) and in Victor snap traps (6%) set along other trails within terra firme forest. Young and subadult individuals were caught in both Sherman and Tomahawk traps in about equal numbers (46% and 53% respectively); all but one adult individual were caught in Tomahawk traps.

REPRODUCTION: We caught *P. echinothrix* only in the months of October and May. Our sample comprises an approximately equal number of males and females, as well as young and adult individuals. Eight of the 24 males were reproductively active, all of which were of age classes 9 and 10. In contrast, reproductively inactive individuals belonged to age classes 1 and 3 (1 specimen each), 5 (3 specimens), and 6 (4 specimens). We caught pregnant females in October (n = 2) and May (n = 9), in both dry and wet seasons. One pregnant individual was also lactating, suggesting postpartum estrous. Most pregnancies were in females of age class 9 or 10, although two individuals of age 6 were pregnant. Signs of estrous were first observed in individuals of age 5. The modal litter size was 2, the range 1–3.

KARYOTYPE: We prepared chromosomes from 31 individuals, including four from Barro Vermelho (locality **12**) and all specimens from both Vira-Volta (locality **14**) and Vai-Quem-Quer (locality **15**). The karyotype is illustrated in da Silva (1998). It has a 2n = 32 and FN = 60, with the autosomes comprising two pairs of very large metacentrics, eight pairs of medium-sized to small metacentrics and submetacentrics, one pair of large and four pairs of small to medium-sized subtelocentrics. The X-chromosome is a small acrocentric and the Y-chromosome is a smaller acrocentric. The karyotype of *P. echinothrix* is similar to that of *P. simonsi*, which also has 2n = 32, but differs by having one extra pair of small subtelocentrics and lacking the large pair of acrocentric chromosomes (see Patton and Gardner, 1972).

SPECIMENS EXAMINED (n = 50): (**12**) 3 m, 4 f — INPA 2551–2552; JLP 15816; JUR 188; MPEG 25500; MVZ 187167–187168; (**13**) 1 f — MNFS 1792; (**14**) 8 m, 5 f — INPA 2550; MNFS 1694, 1698–1699, 1704, 1714–1716, 1719, 1723–1724; MVZ 187169, 187183; (**15**) 13 m, 16 f — JUR 273, 287, 290, 298, 301, 319, 324, 336, 342–343, 356–358, 360, 377; MPEG 25501; MVZ 187170–187182.

Proechimys gardneri da Silva, 1998

TYPE LOCALITY: ''Brazil: Amazonas; Altamira, right bank Rio Juruá; 68°54′W, 6°35′S.''

DESCRIPTION: *Proechimys gardneri* is one of three small-bodied spiny rats within the Rio Juruá basin, with short ears, small hind feet, and proportionately long tail (tables 60 and 64). The tail is bicolored, dark brown above and cream to white below; the scales are relatively small, but not completely hidden by the hair. The overall color of the body is between Sanford's Brown and Auburn (Ridgway, 1912), coarsely streaked with varying amounts of black both on the dorsum and sides; as with other species of spiny rats, the dorsum looks darker, especially on the rump, due to the presence of the heavy, dark brown aristiform hairs. The venter and chin are pure white; in 12 out of 26 specimens the sides of the upper lips, sometimes confluent with a spot at base of vibrissae, are also white; the pure white of the inner surface of the hind limbs extends across the ankle along the hind foot in 7 of the 13 Rio Juruá specimens (the dark tarsal bank is incomplete) e color of the hind foot is yellowish-white rather than the pure white of the venter and inner thighs. In some specimens

the first and second digits of the hind foot, in combination or not with the distal portion of the digits, are brownish (for more information about the external morphology of this species, especially of young individuals from the Rio Juruá and elsewhere, see da Silva, 1998).

The baculum is massive and relatively long, especially in relation to the average body size, with short, broad, and distolaterally directed apical extensions separated by a shallow medium depression (fig. 137). The midshaft is relatively broad, the base is thick and expanded.

The skull is small and delicate, with a relatively long and narrow rostrum (figs. 138 and 139), and a beaded supraorbital ledge above the orbits that extends posteriorly as a weakly developed ridge on the anterior parietals. The postorbital process of the zygoma is obsolete (see da Silva, 1998: fig. 11). The floor of the infraorbital foramen is smooth, lacking a ventral canal. The incisive foramen is ovate to slightly lyrate in shape, with posterolateral margins flat or weakly flanged, at best outlining only a shallow groove in the anterior palate (fig. 140). The maxillary portion of the septum is dorsoventrally compressed posteriorly and narrow anteriorly, visible over almost half the length of the foraminal opening, and fully connected to the premaxillary portion, which is broad and usually about half the length of the foramen. The vomer is not visible on the ventral margin of the septum. The palate is smooth, without a median ridge. The mesopterygoid fossa is long and narrow (fig. 141), with an acute angle of indentation into the posterior margin of the palate averaging 61°, and penetrates deeply, often to the middle of M2. The cheekteeth are remarkably small, averaging only 7.5 mm in length. All upper teeth typically have three folds, although only two folds may be found on M3 in some individuals.

SELECTED MEASUREMENTS:: External and cranial measurements are given in table 64.

COMPARISONS: This species can be confused only with the two other small-bodied taxa along the Rio Juruá, *P. kulinae* and *P. pattoni* (figs. 135 and 136). Morphologically, *P. pattoni* and *P. gardneri* are very difficult to distinguish in that both have a short toothrow length, similar general pattern of the incisive foramen (although with much individual variation), ventral color of tail less brilliantly white than, for example, *P. simonsi*, but tail still bicolored in most specimens and more so in *P. gardneri* than in *P. pattoni*; and relatively narrow, small white hind foot with a dark ring around the ankle. Subtle differences between them, however, are present. For example, *P. pattoni* is slightly smaller than *P. gardneri*; the aristiform hairs of *P.pattoni* are narrower but stiffer to the touch; the postorbital process of the zygomatic arch of *P. pattoni* is slightly but consistently more spinose; the maxillary and premaxillary portions of the incisive foramen are either not touching or are connected by a very attenuate keel in 6 of 11 specimens of *P. pattoni* (on the remaining specimens, the maxillary portion was expanding in a spatulate shape in the area of contact between it and the premaxillary bone), whereas in *P. gardneri* the maxillary and premaxillary portions are in contact in all but one of the 32 specimens examined. In *P. pattoni*, the color of the dorsum and ventral surface of the tail does not contrast as sharply as in *P. gardneri*; in fact the ventral side of the tail tends toward brown in several specimens and has relatively larger scales, and less hair than in specimens of *P. gardneri*. In addition to these external differences, the shape of the baculum (fig. 137) and the external morphology of the glans is clearly distinct between these two species (see da Silva, 1998). Comparisons to *P. kulinae* are given below in the account of that species.

MOLECULAR PHYLOGEOGRAPHY: The limited data on this taxon suggests some geographic substructure for the available cytochrome-b haplotypes. Specimens from the central Rio Juruá (Altamira [locality **9**]) differ only by 2%, on average, from individuals obtained at two localities in northern Bolivia some 300 km to the south (fig. 146; table 70); those from the upper Rio Urucu, 500 km to the northeast, differ by only a slightly greater amount, at 2.2%.

DISTRIBUTION AND HABITAT: This species is known from only two localities in western Brazil and one in northern Bolivia (fig. 146, top). The distribution is perhaps delimited by the Rio Juruá on the west and the Rio Ma-

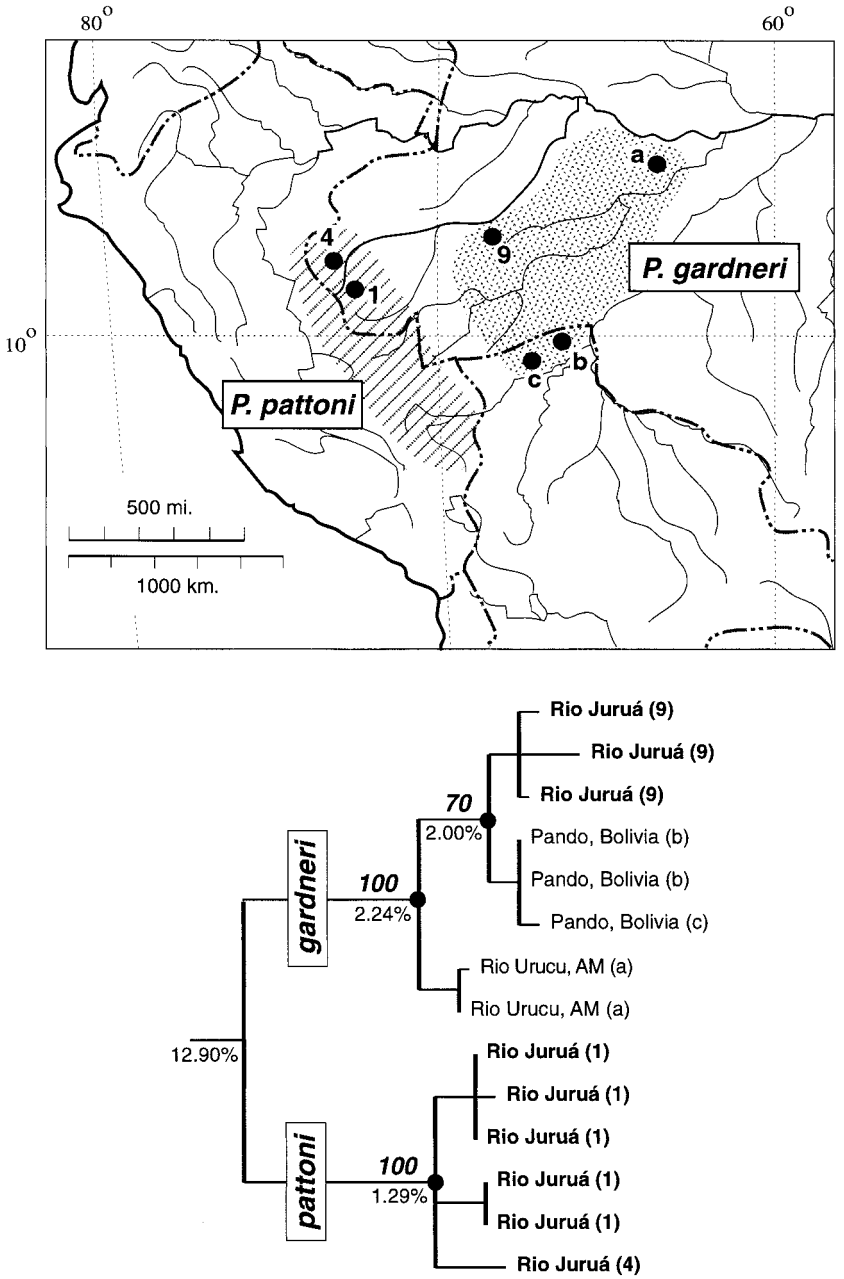

Fig. 146. (**Above**) Map of the distribution of *Proechimys gardneri* and *P. pattoni* (modified from da Silva, 1998). Localities from which individual specimens have been examined for sequence of the mtDNA cytochrome-b gene are indicated; those from localities outside of the Rio Juruá are lettered. (**Below**) Single most-parsimonious tree, based on a branch-and-bound analysis, of haplotypes of the mitochondrial cytochrome-b gene (798 bp); length = 246 steps, CI = 0.752, RI = 0.847. Sequences of other species of *Proechimys* and of *Mesomys* were used as outgroups to root the tree. Bold numbers at internal nodes are bootstrap values, based on 1000 replicates; percentages are average Kimura two-parameter distances. Voucher catalog numbers and localities for each haplotype are given in table 70.

TABLE 70
Haplotypes, Voucher Numbers, and Localities for *Proechimys gardneri* and *P. pattoni*
Individual haplotypes listed from top to bottom in the tree, figure 146 (below), with the catalog numbers of their respective voucher specimens, and localities (identified as in the map, fig. 146, above) for which 798-bp haplotypes of the mitochondrial DNA cytochrome-b gene are available.

Haplotype	Voucher no.	Locality
P. gardneri		
1	MVZ 187209	Altamira, right bank Rio Juruá, Amazonas, Brazil (locality **9**)
2	JLP 16039	Altamira, right bank Rio Juruá, Amazonas, Brazil (locality **9**)
3	MVZ 187206	Altamira, right bank Rio Juruá, Amazonas, Brazil (locality **9**)
4	LHE 891	Río Negro, Pando, Bolivia, 9°52'S, 65°42'W (locality b)
5	LHE 890	Río Negro, Pando, Bolivia, 9°52'S, 65°42'W (locality b)
6	LHE 834	ca. 18 km NNW San Juan de Nuevo Mundo, Pando, Bolivia, 10°46'S, 66°44'W (locality c)
7	MNFS 88	alto Rio Urucu, Amazonas, Brazil, 6°14'S, 58°15'W (locality a)
8	MNFS 121	alto Rio Urucu, Amazonas, Brazil, 6°14'S, 58°15'W (locality a)
P. pattoni		
9	MVZ 187194	Igarapá Porongaba, right bank Rio Juruá, Acre, Brazil (locality **1**)
10	MPEG 25509	Igarapá Porongaba, right bank Rio Juruá, Acre, Brazil (locality **1**)
11	MVZ 187199	Igarapá Porongaba, right bank Rio Juruá, Acre, Brazil (locality **1**)
12	MPEG 25510	Igarapá Porongaba, right bank Rio Juruá, Acre, Brazil (locality **1**)
13	MVZ 187195	Igarapá Porongaba, right bank Rio Juruá, Acre, Brazil (locality **1**)
14	MVZ 187197	Sobral, left bank Rio Juruá, Acre, Brazil (locality **4**)

deira to the east. Specimens from the Rio Juruá are all from the terra firme forest at Altamira (locality **9**) (table 63), with most (17 of 21) coming from the standardized trap plot. The majority (43%) of our sample was caught in Sherman traps, 38% came from Tomahawk traps, 14% were shot, and 5% was caught with Victor snap traps. Of the animals captured in both types of live traps, young and subadults (n = 8) were taken in Sherman traps while most adults (8 out of 9) were captured in Tomahawk traps. The higher proportion of adult animals in the larger Tomahawk traps may be associated with the behavior of these animals since the relatively small adult size (maximum weight about 270 g) should not show bias against use of the smaller Sherman traps.

REPRODUCTION: We obtained all specimens of *P. gardneri* near the beginning of the rainy season in the month of November. All females and all but one male were adults (age class 8 to 10); the single nonadult male was a young animal of age 2. All adult males (7) were reproductively active and 8 of the 13 females were pregnant, all of which were adults (age classes 8 to 10). The modal litter size was 2, range 1–3. Data are inadequate to judge seasonality of reproduction, but the one young individual and the large number of pregnancies clearly indicates that this species breeds at least during the dry season.

KARYOTYPE: We have karyotype data from 14 individuals from the type locality at Altamira, and from 6 individuals from the upper Rio Urucu. The diploid number is 40, the fundamental number 56, and the karyotype itself is figured in da Silva (1998). The autosomal complement includes seven pairs of medium-sized to small metacentrics and submetacentrics with one pair minute, two pairs of moderately small subtelocentrics, the smallest of which bear secondary constrictions on the long arms, and three pairs of medium-sized and seven pairs of small acrocentrics. The X-chromosome is a moderately small acrocentric and the Y is a small acrocentric. This complement is identical to that of *P. pattoni* (see Patton and Gardner, 1972; da Silva, 1998), a feature that is concordant with the apparent sister relationship between these two species based on mtDNA sequence data (see above and fig. 134).

SPECIMENS EXAMINED (n = 21): (**9**) 8 m, 13 f (INPA 2565–2569; JLP 16039; JUR

192; MNFS 853–854; MPEG 25512–25516; MVZ 187203–187209).

Proechimys kulinae da Silva, 1998

TYPE LOCALITY: ''Brazil: Amazonas; Seringal Condor, left bank Rio Juruá, 70°51′W, 6°45′S.''

DESCRIPTION: *Proechimys kulinae*, *P. gardneri*,and *P. pattoni* are the smallest spiny rats occurring in the Rio Juruá basin. In general morphology these specimens of *P. kulinae* are relatively slight in build, have small ears, and moderately short tail and hind feet (tables 60 and 64). Overall, the color of the body is uniform reddish brown, coarsely streaked with varying amounts of black on both the dorsum and sides. The dorsal pelage is interspersed with thick, dark brown aristiform hairs that form a darker medial band contrasting with the sides of the body. The venter, chin, and undersurfaces of fore and hind limbs are pure white; the upper lips are dark, generally lacking patches of white hair; the tarsal joint is either ringed by dark and rusty-colored hair, or the tarsal ring is interrupted by white hair confluent with that of the undersurface of the hind limbs and feet; the hind foot, including the digits, is white, with some golden tones in most individuals. The tail appears almost naked, distinctively bicolored with dark brown dorsum and white venter. In juveniles, the color of the pelage varies from dark grayish brown (age class 2) to pale brownish mixed with rusty-colored hair (age class 5). Five plantar tubercles are present in the majority of specimens (12 of 16), with the lateral metatarsal tubercule missing. The baculum is elongate and relatively narrow, with stout and short apical extensions; the proximal and distal ends are about equal in width (fig. 137).

The skull is relatively small, with a short, narrow rostrum (figs. 138 and 139) and a well-developed supraorbital ledge extending onto the anterior portion of the parietals. The postorbital process of the zygoma is well developed and formed mostly by the squamosal. The floor of the infraorbital foramen is generally smooth, without a demonstrable groove for the maxillary nerve. The incisive foramen is mostly square to oval in shape (fig. 139), with nearly flat posterolateral margins; the anterior palate is smooth, lacking grooves extending posteriorly from the incisive foramen, and lacking a median ridge; the premaxillary portion of the septum is short, extending for less than half the length of the foramen; the maxillary portion is variable, attenuate to expanded anteriorly, and usually in contact with the premaxillary portion; the vomer is either completely enclosed or only barely visible. The mesopterygoid fossa is narrow (fig. 141), with an angle of indentation into the posterior palate averaging 57°; it is moderately deep, usually extending to the anterior half of M3. All upper cheekteeth have three folds except M3, which usually has three but may have only two.

SELECTED MEASUREMENTS: Means and ranges of selected external and cranial measurements are given in table 64.

COMPARISONS: Overall, *P. kulinae* is most similar to the other small species, *P. pattoni* and *gardneri* (figs. 135 and 136). Interestingly, these three apparently replace one another along the Rio Juruá, as no combination of these species occurs sympatrically at our various sample sites—*P. pattoni* is known only from the Headwaters Region, *P. gardneri* from the right bank in the Lower Central Region, and *P. kulinae* is known only from left bank localities in the Upper and Lower Central regions; fig. 133). *Proechimys kulinae* does co-occur with *P. cuvieri*, *P. simonsi*, and *P. steerei*, all three of which are much larger in body size with absolutely larger hind feet, ears, and tail (fig. 133; table 64). The baculum of *P. kulinae* is most similar in shape to those of *P. simonsi* and *P. steerei* (fig. 137), especially so relative to *P. simonsi*, although shorter and with somewhat more expanded apical wings. Along with *P. pattoni*, this is the smallest species of *Proechimys* currently known from Amazonia, with a total length less than 330 mm. It has wider and longer aristiform hairs than either *P. gardneri* or *P. pattoni* (da Silva, 1998: table 4 and fig. 3); usually has only five, instead of the six plantar tubercles characteristic of the other two small species; and a stronger, more spinose postorbital process of the zygoma. *Proechimys kulinae* differs from all known species, including both *P. gardneri*

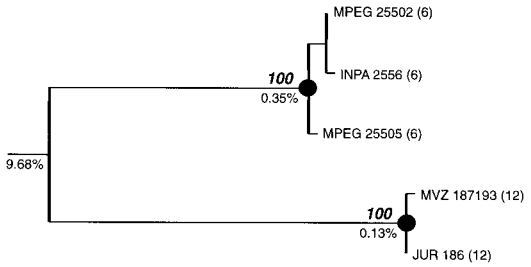

Fig. 147. Single most-parsimonious tree, based on an exhaustive search, of haplotypes of the mitochondrial cytochrome-b gene of *Proechimys kulinae* from the Rio Juruá (801 bp); length = 137 steps, CI = 0.993, RI = 0.989. Sequences of other species of *Proechimys* and of *Mesomys* were used as outgroups to root the tree. Bold numbers at internal nodes are bootstrap values, based on 1000 replicates; percentages are average Kimura two-parameter distances. Voucher catalog numbers and localities (by number) are identified for each haplotype.

and *P. pattoni*, in its 2n = 34, FN = 52 karyotype.

MOLECULAR PHYLOGEOGRAPHY: Sequence data are available from only the two locations along the central portion of the Rio Juruá. Haplotypes from individuals from the same population are closely similar, varying by no more that 0.1 to 0.4%, but individuals from the two known localities are quite divergent, differences averaging nearly 10% (fig. 147). This is a striking degree of divergence, particularly for localities only 238 km apart and on the same side of the river (table 1 and fig. 133). Additional data from other populations will be needed to assess the significance of this level of divergence. The species presumably is more widely distributed as, based on morphological characters, da Silva (1998) assigned individuals from northeastern Perú, south of the Amazon, to this species. Unfortunately, we lack tissue samples from these individuals so that their degree of molecular divergence remains unknown.

DISTRIBUTION AND HABITAT: This species is known from only two localities in the Upper and Lower Central regions (Condor [locality **6**] and Barro Vermelho [locality **12**]) on the left bank of the Rio Juruá in the Estado do Amazonas, Brazil, and two localities in the Departamento de Loreto, Perú (da Silva, 1998). All specimens collected along the Rio Juruá are from primary or second-growth terra firme forest (table 63). In our sample of 33 individuals, the majority (52%) were caught in Tomahawk live traps, 27% in Shermans, and 21% were caught in snap traps. Of those captured in both types of live traps, twice as many young and subadults (4 out of 6) were caught in Shermans, and three times the number of adults were captured in Tomahawk traps (15 out of 20).

REPRODUCTION: We obtained all specimens of *P. kulinae* towards the end of the dry season in the months of September and October. Eight of the 14 male specimens we classified as reproductively active, the other six as inactive. All reproductively active males were full adults of age classes 9 or 10 whereas the inactive ones ranged in age from 3 to 9. Five of the 18 females were pregnant, and all were adults (age classes 8 to 10). Evidence of estrous activity (swollen and vascularized uteri) was observed in one age class 7 female, and all parous females were old adults. The modal litter size was 1, and the range 1–2

KARYOTYPE: We karyotyped 20 of the 33 individuals trapped, two from Barro Vermelho and 18 from Seringal Condor. The karyotype of *P. kulinae* (illustrated in da Silva, 1998) has a 2n = 34 and FN = 52. The autosomes comprise a pair of very large metacentrics, six pairs of medium-sized to small metacentrics and submetacentrics, one pair of large and one pair of medium-sized subtelocentrics (the latter has a secondary constriction on the longer arms), one pair of large and five pairs of small to minute acrocentrics. The X-chromosome is a moderately small metacentric and the Y-chromosome is a minute submetacentric. This is the first *Proechimys* from Amazonia reported with 34 chromosomes. This same karyotype is reported for specimens of *Proechimys* sp. from northern Perú by Aniskin (1993). These likely represent *P. kulinae*, as da Silva (1998) allocated specimens from nearby localities to this species.

Specimens Examined: (n = 33): (**6**) 13 m, 16 f, 1 unknown — INPA 2553–2557; JLP 15534, 15612, 15660; MPEG 25502–25506; MVZ 187184–187190, 187192; JUR 178–

182, 185; MNFS 546, 552, 554; (**12**) 1 m, 2 f — INPA 2558; JUR 186; MVZ 187193.

Proechimys pattoni da Silva, 1998

TYPE LOCALITY: ''Brazil: Acre; Igarapé Porongaba, right bank Rio Juruá, 72°47′W, 8°40′S.''

DESCRIPTION: *Proechimys pattoni* is the third of the small spiny rats presently known from the Rio Juruá. Individuals are slender, have relatively short ears and tail, and small hind feet (tables 60 and 64). The skull is small, relatively narrow with a pointed snout; the maxillary toothrow is very short (less than 7.5 mm) and the individual teeth appear especially tiny. The dark brown dorsal surface of the tail grades evenly, rather than contrasting sharply, with the paler brown to cream color of the ventral surface; the scales on the tail are relatively small (approximately 10 to 12 annuli per cm), but visibly conspicuous. Overall, the color of the body varies between Sanford's Brown and Auburn (Ridgway, 1912), but is coarsely streaked with varying amounts of black both on the dorsum and sides; the interspersed thick dark brown aristiform hairs of the dorsum give it a somewhat darker aspect, but the contrast between the color of the dorsum and sides is not sharp. The color of the venter and chin is pure white as are the sides of the upper lips; a white spot is present at the base of vibrissae in most specimens. The white color of the inner surface of the hind limbs is interrupted by a dark ring around the tarsal joint. The juvenile pelage is uniformly grayish brown (age class 3); one specimen of age class 6 and one of age class 7 have adult, aristiform hair throughout the midback, and soft juvenile hair streaked with black and fulvous tips on the sides, shoulders, and rump. The dorsal surfaces of the hind feet are entirely white in most specimens, although in some the entire hind foot seems more golden than pure white or is slightly brownish on the sides, including the third and fourth digits, or across the entire middorsum. There are six tubercles on the plantar surface of the hind feet in most specimens (11 of 14), with a very long medial metatarsal tubercule (mmt) extending from about one to two thirds the distance between the calcaneus and the first predigital tubercule.

The baculum is massive in proportion to body size. It has a broad shaft, a thick and expanded base, and a long pair of divergent apical extensions separated by a wide and deep median depression (see fig. 137, and illustrations in Patton and Gardner, 1972, and da Silva, 1998).

The skull is small and rather delicate for a *Proechimys* (figs. 138 and 139), with overhanging supraorbital ledges but with only weakly developed beading extending onto the temporal region. A low but distinct postorbital process of the zygoma is present, usually formed solely by the squamosal. The floor of the infraorbital foramen is smooth, lacking a groove or lateral flange. The incisive foramen is ovate to slightly squarish, with flat posterolateral margins, an attenuate or dorsoventrally compressed maxillary portion of the septum, and a broad and short premaxillary portion, which usually is not in contact with the maxillary portion (fig. 140). The foramen of a specimen from eastern Perú was described and figured by Patton (1987: fig. 14d). The palate is smooth, without a median ridge. The mesopterygoid fossa is long and narrow (fig. 141), angle of indentation on posterior margin acute (50°–60°), and may penetrate as far as the middle of M2. There are typically three folds on each of the upper cheekteeth, although occasional specimens have only two folds on PM4 and/or M3. Additional characters of the skull and phallus are described by da Silva (1998).

SELECTED MEASUREMENTS: Means and ranges of selected external and cranial measurements are given in table 64.

COMPARISONS: Table 60 compares characters of *P. pattoni* with those of other species from the Rio Juruá. This species can be recognized by its small body size and relatively short tail, whitish feet, and very short toothrow; but these are all characters shared with both *P. gardneri* and *P. kulinae*. Indeed, as noted above under the accounts for these other two species and as emphasized in the multivariate analyses (figs. 135 and 136), all three are quite difficult to distinguish, except by the male phallus and baculum (fig. 137; see also da Silva, 1998: fig. 5), subtle differ-

ences in cranial characters, and karyotype (*P. kulinae* from both *P. pattoni* and *P. gardneri*). The individual cheekteeth appear distinctly smaller in *pattoni* than in the other two, although *P. kulinae* has the shortest toothrow (table 64) and significant differences in this character occur in comparisons between any pair of these three species (one-way ANOVA comparing all three, $F_{2,61} = 19.068$, $p < 0.0001$; Fisher's PLSD *p*-values in pairwise comparisons, < 0.0001 [*gardneri* vs *kulinae*], 0.0192 [*gardneri* vs *pattoni*], and 0.0234 [*kulinae* vs *pattoni*]). The dark band around the ankle, the typical lack of contact between premaxillary and maxillary portions of the septum of the incisive foramen, the low and rounded but distinct postorbital process on the zygomatic arch, and the narrower and more deeply penetrating mesopterygoid fossa are a few external and cranial characters that help to distinguish *P. pattoni* from the other two species (table 60).

MOLECULAR PHYLOGEOGRAPHY: Cytochrome-b sequence data are available for only two localities in the Headwaters Region of the Rio Juruá (Igarapé Porongaba [locality **1**] and Sobral [locality **4**]; fig. 146, table 70). There is, however, as much variation among the five individuals from Porongaba as there is between any of these and the single specimen from Sobral. Given the close proximity of the two localities, even though they are on opposite sides of this river, the lack of demonstrable differentiation between localities should not be surprising. The average difference between all six individuals sequenced is only 1.3%.

DISTRIBUTION AND HABITAT: *Proechimys pattoni* is currently known from only five localities in western Amazonia: two in the Headwaters Region of the Rio Juruá (Porongaba, locality **1**, and Sobral, locality **4**) in Estado do Acre, Brazil, and three in eastern and southeastern Perú in the departments of Ucayali, Madre de Dios, and Puno (see da Silva, 1998, and figs. 132 and 145). All specimens from the Rio Juruá (n = 29) were collected in terra firme forest, five of these in disturbed areas dominated by bamboo. We captured *P. pattoni* using live traps placed on the ground close to fallen logs, at the base of trees, underneath dense ground cover, or in open forest understory; 59% of the specimens were captured with Sherman and the remaining with Tomahawk traps. All but one young along with all subadult individuals (n = 6) were caught in Sherman traps, with most adults obtained (7 out of 11) in Tomahawk traps.

REPRODUCTION: We caught all specimens of *P. pattoni* during the rainy season in the months of February and early March. Since this species does not occur in downriver sites, no information is available regarding seasonality of reproduction on the Rio Juruá. Of the 10 male specimens collected, we classified five as reproductively active, all of which were adults of age classes 8 to 10. One individual of age classes 9 was reproductively inactive. Four of the 19 females were pregnant; their ages ranged from toothwear class 6 to 10. No female was lactating. The modal litter size is 2, with the range 1–2.

KARYOTYPE: 2N = 40; FN = 56. This species has the same karyotype as *P. gardneri* (see above and da Silva, 1998). The karyotype of *P. pattoni* was also illustrated and described by Patton and Gardner (1972) under the name *P. guyannensis*.

COMMENTS: Specimens of *P. pattoni* from Balta were referred by Patton and Gardner (1972) to *P. guyannensis*, whereas Patton (1987) placed them provisionally in his *P. cuvieri* species group. As discussed above, this species and *P. gardneri* are extremely similar morphologically and are unusual among species in the genus in sharing identical karyotypes. However, da Silva (1998) recognized them as separate species because each forms a well supported and highly differentiated haplotype clade (figs. 134 and 146) and each is morphologically diagnosable, although their character differences are rather subtle. Each also has a relatively wide, but nonoverlapping geographic range (fig. 146). Future studies to determine areas of contact between the two species in western Amazonia will be the ultimate test to the degree of evolutionary independence of these two very similar yet distinct lineages.

SPECIMENS EXAMINED (n = 29): (**1**) 10 m, 18 f — INPA 2559–2562, 2564; MNFS 1087–1088, 1096, 1111, 1131, 1167, 1290–1291, 1311, 1358; MPEG 25507–25511; MVZ 187194–187196, 187198–187202; (**4**) 1 f — MVZ 187197.

Proechimys simonsi Thomas, 1900

TYPE LOCALITY: ''Perené River, Junin Province, Peru. Altitude 800 m''; Departamento de Junín, Perú.

DESCRIPTION: A thorough description of this species was provided by Patton and Gardner (1972) under the name *P. hendeei*. Patton (1987) included *P. simonsi* as the sole member of his *simonsi*- group, based on details of the baculum and qualitative features of the cranium, with *hendeei* listed as a synonym. This is one of the largest species of spiny rats to occur on the Rio Juruá, equaled or exceeded in size only by individuals of *P. echinothrix* and *P. steerei* (table 64). It is characterized by an elongated body, long and narrow face, long ears, proportionately and absolutely long tail, and large hind feet (tables 60 and 64). The tail is bicolored, with a distinct dark dorsal stripe and white ventrum; it is covered by sparse, fine hair, although the scales remain conspicuous to the eye (9–13 annuli per cm). As in most species of *Proechimys*, the middorsal color is somewhat darker than the sides of the body, with the rump the darkest portion of the body, coarsely streaked with black hairs and interspersed dark brown aristiforms. The aristiform hairs are long and thin with a distinctly whiplike tip (da Silva, 1998: fig. 3). The venter, chin, sides of the upper lips, undersurfaces of forelimbs, and hind limbs are pure white. The white of the inner leg extends across the tarsal joint onto the foot in most specimens, but in some, dark hair forms a ring around the ankle, interrupting the white stripe. The hair of the dorsal surface of the hind foot is usually white. Occasional specimens, however, have the tarsals, the entire first and the second digits, or just the distal end of the digits, in combination or not, covered with brownish hair.

The baculum of *P. simonsi* from the Rio Juruá is identical to that described and figured by Didier (1962), Patton and Gardner (1972), and Patton (1987); it is long and narrow, with a rounded and slightly broadened base (fig. 137).

Our specimens of *P. simonsi* do not differ in any detail from the craniodental descriptions given by Patton (1987) for this species, based on materials that he examined from Colombia, Ecuador, Perú, and Bolivia. The skull is large, the rostrum is distinctly long and narrow (figs. 138 and 139 and table 64), and supraorbital ridges are well developed, but do not extend across the parietals. The incisive foramen is ovoid in shape, sometimes slightly elongated but never strongly constricted posteriorly; its posterolateral margins are mostly flat, rarely with a weakly developed flange, but even then lacking grooves extending onto the anterior palate (fig. 140). The premaxillary portion of the septum is short, rounded, and usually no more than half the length of the foramen; the maxillary portion is attenuate and usually not in contact with the premaxillary portion. The floor of the infraorbital foramen is usually grooved, with moderately developed lateral flanges. The anterior border of the mesopterygoid fossa is acutely angled (30°–35°) and penetrates deeply into the palate, reaching the anterior half of M3 or the middle of M2 (fig. 141). The counter fold pattern of both upper and lower teeth from the Rio Juruá is the same for other samples of this species (Patton, 1987), with three folds in PM4 and M1 and three to four folds in M2 and M3 as the general condition. Overall, the character trends observed in the Rio Juruá specimens are in complete agreement with those described by Patton (1987) in specimens from other localities outside the Rio Juruá Basin but throughout the range of *P. simonsi*.

SELECTED MEASUREMENTS: See table 64.

COMPARISONS: This is one of the two largest spiny rats found in the terra firme forests of the Rio Juruá, the other being *P. echinothrix* (table 64). Externally, it can be distinguished from all other species by a combination of its large body size, absolutely and proportionately long tail, large ears and feet, and relatively soft aristiforms (table 60). The tail is sharply bicolored and sparsely covered by hair; the undersurface of the body and the dorsal surface of the foot is mostly pure white, and the baculum is long and narrow. Cranially, *P. simonsi* is easily separable from all other spiny rats by a long and distinctly narrow skull and rostrum, ovoid incisive foramen with largely incomplete septum, and smooth anterior palate, as well as by the very narrow and deeply penetrating mesopterygoid fossa.

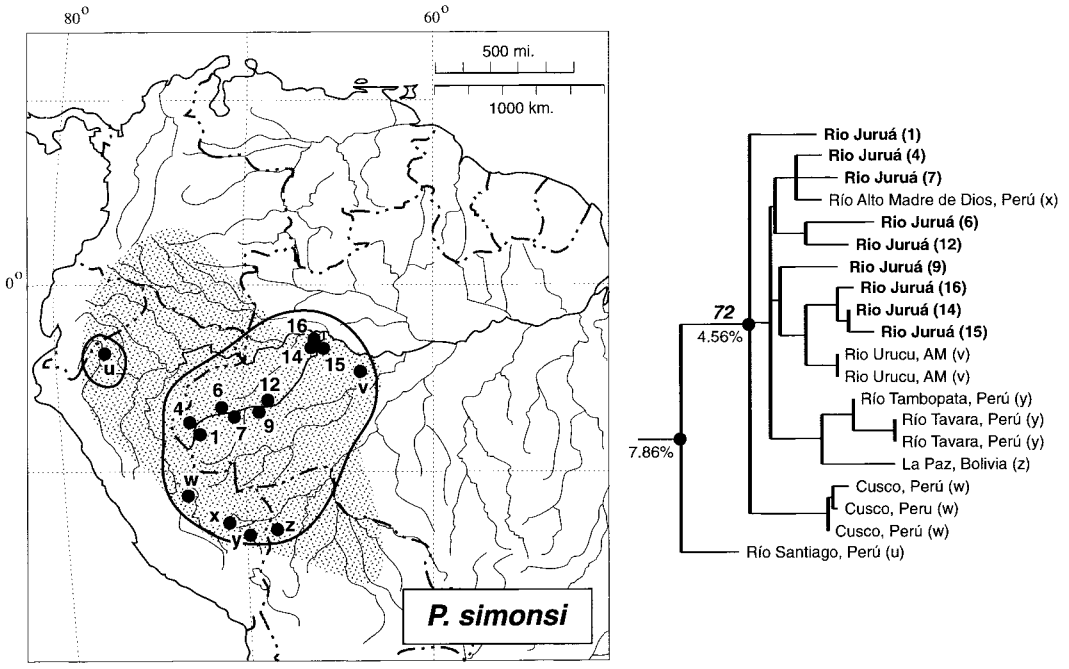

Fig. 148. (**Left**) Map of the distribution of *Proechimys simonsi* (modified from Patton, 1987) illustrating localities for which 801 bp of cytochrome-b sequence are available, lettered or numbered as in the tree (right). Localities belonging to each of the two mtDNA clades are encompassed by ellipses. (**Right**) Strict-consensus maximum parsimony tree of five equally minimum-length trees for 20 individual haplotypes from 15 localities in Perú, Bolivia, and Brazil, as identified in the map (left). Length = 498 steps; CI = 0.677; RI = 0.588. Sequences of other species of *Proechimys* and of *Mesomys* were used to root the tree. Bold numbers at internal nodes are bootstrap values, based on 1000 replicates; percentages are average Kimura two-parameter distances. Voucher catalog numbers and localities for each haplotype are given in table 71.

MOLECULAR PHYLOGEOGRAPHY: We have extensive sequence data for the cytochrome-b gene for this species from a substantial portion of its range, including the entire Rio Juruá drainage area and the upper Rio Urucu in western Brazil, as well as for localities in northern and southeastern Perú and northern Bolivia (fig. 148, left; table 71). The cladogram (fig. 148, right) is based on 801 base pairs for 20 haplotypes taken from localities throughout the species' range. Sequence divergence is moderate over most of this range, although the sample from the Río Santiago in the Departamento de Amazonas in northern Perú diverges by nearly 8% from all those to the east and south. The latter samples differ by an average of nearly 5% among themselves.

Within the Rio Juruá, we have examined haplotype variation in a 399 base pair fragment of the cytochrome-b gene for 150 individuals from the 11 terra firme forest localities. A total of 47 different haplotypes were recovered, with an average divergence of 3.6%. These data are being analyzed separately by Marjorie Matocq, in conjunction with M. N. F. da Silva and J. L. Patton, with regard to the pattern of haplotype apportionment among localities along the river. A synopsis is presented in the section beyond on riverine diversification patterns.

MORPHOMETRIC VARIATION: We summarize variation in mensural characters for adult individuals according to locality, sex, and age by a nested ANOVA in table 72. For the four external and 21 cranial variables, there is virtually no geographic component, as locality explains an average of only 4.4% of the total variation. Both sexual dimorphism and age (toothwear scores of 8, 9, and 10) are some-

TABLE 71
Haplotypes, Voucher Numbers, and Localities for *Proechimys simonsi*
Individual haplotypes listed from top to bottom in the tree, figure 148 (right), with the catalog numbers of their respective voucher specimens, and localities (identified as in the map, fig. 148, left) for which 801-bp haplotypes of the mitochondrial DNA cytochrome-b gene are available.

Haplotype	Voucher no.	Locality
1	MNFS 1099	Igarapá Porongaba, right bank Rio Juruá, Acre, Brazil (locality **1**)
2	MNFS 1485	Sobral, left bank Rio Juruá, Acre, Brazil (locality **4**)
3	JLP 15295	Penedo, right bank Rio Juruá, Amazonas, Brazil (locality **7**)
4	MVZ 166083	Aguas Calientes, left bank Río Alto Madre de Dios below Shintuya, Madre de Dios, Perú (locality x)
5	JLP 15660	Seringal Condor, left bank Rio Juruá, Amazonas, Brazil (locality **6**)
6	JLP 15874	Barro Vermelho, left bank Rio Juruá, Amazonas, Brazil (locality **12**)
7	MNFS 88	Altamira, right bank Rio Juruá, Amazonas, Brazil (locality **9**)
8	MNFS 1751	Ilhazinha, left bank Rio Juruá, Amazonas, Brazil (locality **16**)
9	MNFS 1761	Colocação Vira-Volta, left bank Rio Juruá, Amazonas, Brazil (locality **14**)
10	JUR 270	Vai-Quem-Quer, right bank Rio Juruá, Amazonas, Brazil (locality **15**)
11	MNFS 190	alto Rio Urucu, Amazonas, Brazil, 6°14'S, 58°15'W (locality v)
12	MNFS 192	alto Rio Urucu, Amazonas, Brazil, 6°14'S, 58°15'W (locality v)
13	LHE 820	Río Tavara, Fila Boca Guacamayo, Madre de Dios, Perú, 13°30.2'S, 69°41.0'W (locality y)
14	LHE 814	Ccolpa de Guacamayo, Río Tambopata, Madre de Dios, Perú, 13°08.5'S, 69°36.4'W (locality y; not mapped separately from LHE 820)
15	LHE 813	Ccolpa de Guacamayo, Río Tambopata, Madre de Dios, Perú, 13°08.5'S, 69°36.4'W (locality y; not mapped separately from LHE 820)
16	LHE 742	Río Madidi, La Paz, Bolivia, 13°35'S, 68°46'W (locality z)
17	LHE 1468	2 km SW Tangoshiari, Cusco, Perú, 11°46'47"S, 73°20'26.5"W (locality w)
18	LHE 1435	2 km SW Tangoshiari, Cusco, Perú, 11°46'47"S, 73°20'26.5"W (locality w)
19	LHE 1431	2 km SW Tangoshiari, Cusco, Perú, 11°46'47"S, 73°20'26.5"W (locality w)
20	MVZ 157914	La Poza, Río Santiago, Amazonas, Perú, 4.02°S, 77.77°W (locality u)

what more important, contributing 16.7% and 14.1%, respectively. However, when analyses were restricted to the two largest samples (Condor [locality **6**], n = 39 adults, and Penedo [locality **7**], 43 adults), and a nested ANOVA used to determine the relative contributions of sex and age on total variation, no variable exhibited significant sexual dimorphism, but 16 of the 25 characters showed a significant age effect. While sexual dimorphism within localities appears to be limited or nonexistent, cranial age score contributes importantly to within-locality variation. This result is consistent with the observation that growth is essentially indeterminant in other species of *Proechimys*, and related genera, as size continues to increase even among adult toothwear age classes (Patton and Rogers, 1983; dos Reis et al., 1990; Lara et al., 1992).

The rather small amount of variation attributable to locality comparisons is mirrored by the uniform pattern of haplotype variation in cytochrome-b sequences within the Rio Juruá basin and, in general, in qualitative morphological features throughout the species range (Gardner and Emmons, 1984; Patton, 1987). There is negligible differentiation among populations assignable to this species, other than weak character clines, making *P. simonsi* perhaps the "most consistently recognizable group of spiny rats" (Patton, 1987: 337). However, slight but significant geographic differentiation is apparent within *P. simonsi* along the Rio Juruá, based on multivariate analyses. In a principal components analysis, samples pooled into the four regional sample areas overlap broadly in multivariate space (fig. 149, top), yet average individual scores for each region differ significantly along both the first and second axes ($F_{3,203}$= 13.932, $p < 0.001$; $F_{3,203}$ = 3.177, $p < 0.025$, respectively). Table 73 provides the factor coefficients for the first two axes, which combine to explain 73.9% of the total variance. The first PC axis is a multivariate

TABLE 72
Descriptive Statistics and Variance Components for Four External and 21 Cranial Variables of *Proechimys simonsi* from the Rio Juruá
Measurements (mm) are given as mean ± standard error, with range and sample size.
Percentage contributions of the separate effects of locality, sex, and age are given, based on nested ANOVA (ns = $p > 0.05$; * $p < 0.05$; ** $p < 0.01$; *** $p < 0.001$).

Variable	Mean ± SE	Range	n	Variance component			
				Locality	Sex	Age	Error
TOL	379.18 ± 2.64	287–480	178	3.0 ns	23.2***	17.1***	56.7
TAL	172.76 ± 1.40	121–231	179	1.9 ns	16.1***	11.0*	71.0
HF	48.00 ± 0.20	40–57	220	5.3 ns	9.1 ns	4.2 ns	81.4
E	24.23 ± 0.10	21–28	218	10.9 ns	3.6 ns	4.6 ns	85.0
CIL	42.82. ± 0.19	36.47–50.11	222	4.9*	23.4***	20.4***	51.3
ZB	24.87 ± 0.09	21.21–28.32	221	3.2 ns	23.8***	21.3***	51.8
MB	19.67 ± 0.07	16.82–23.04	222	3.8 ns	23.8***	20.6***	51.9
IOC	11.05 ± 0.05	8.91–13.23	223	3.3 ns	6.7 ns	5.0 ns	85.0
RL	21.24 ± 0.13	17.13–26.21	212	4.9 ns	23.6***	21.1***	50.3
NL	20.02 ± 0.13	15.81–25.16	212	5.2 ns	21.5***	20.1***	53.2
RW	8.17 ± 0.04	6.51–10.06	223	1.9 ns	19.2***	17.3***	61.5
RD	10.12 ± 0.06	7.82–12.08	222	5.1 ns	22.5***	19.4***	61.5
OL	13.78 ± 0.05	11.61–16.14	223	6.1 ns	18.3***	15.9***	59.7
D	10.95 ± 0.06	8.93–13.60	223	4.8 ns	20.0***	17.1***	58.1
MTRL	7.91 ± 0.02	7.06–8.65	223	8.7*	4.9 ns	7.7 ns	78.7
IFL	4.43 ± 0.03	3.17–5.94	223	2.2 ns	13.0***	10.9**	73.9
PL	17.03 ± 0.09	13.79–20.87	223	5.4*	20.4***	16.7***	57.5
PPL	21.49 ± 0.08	18.12–25.11	222	3.6 ns	15.6***	10.9**	69.8
BUL	10.28 ± 0.03	8.98–11.43	222	4.7 ns	7.0*	6.9 ns	81.4
MAXB	8.07 ± 0.04	6.77–9.78	223	1.6 ns	22.6***	19.4***	56.5
OCB	9.41 ± 0.03	8.42–10.78	219	2.9 ns	8.4*	5.8 ns	82.9
MPFW	4.50 ± 0.03	3.51–5.61	219	4.4 ns	15.2***	11.9***	68.6
CD	17.66 ± 0.07	15.27–20.61	221	3.2 ns	21.7***	17.9***	57.1
CMD	13.90 ± 0.07	11.55–16.62	223	3.5 ns	23.4***	19.4***	53.7

representation of overall size, as indicated by the high and positive factor coefficients (table 73) and the strongly positive correlations of individual scores with their respective mensural variables (data not shown). The correlation coefficient for the relationship between PC-1 scores and individual values for condyloincisive length, a univariate index of overall size, is 0.973, for example. Overall size, however, does decrease clinally from localities in the Headwaters Region to those in the Lower Central Region, with samples in the Mouth Region reversing the trend by being the largest of all (fig. 150).

Although regional samples exhibit some pattern to the character variation along the Rio Juruá, the river itself does not appear to represent a barrier between opposite-bank populations. A nested ANOVA with region as the main effect and river bank as a secondary one yielded no significant effect due to either river bank ($F_{1,199} = 0.544$, $p = 0.461$, for PC-1) or to the interaction between region and river bank ($F_{3,199} = 1.344$, $p = 0.261$). The lack of differentiation due to river bank is readily apparent in a bivariate plot of principal component scores for the first two axes, with left and right bank samples pooled and plotted separately (fig. 149, bottom). However, if samples are pooled by river bank and subjected to a discriminant function analysis, which maximizes between-group variance while minimizing that within groups, slight segregation of opposite-bank populations is apparent. A one-way ANOVA of individual scores on the first discriminant axis yields a significant river bank effect ($F_{1,205} = 54.057$, $p < 0.001$), and histograms of these scores (fig. 151, left) illustrate the slight differences among the samples. Only

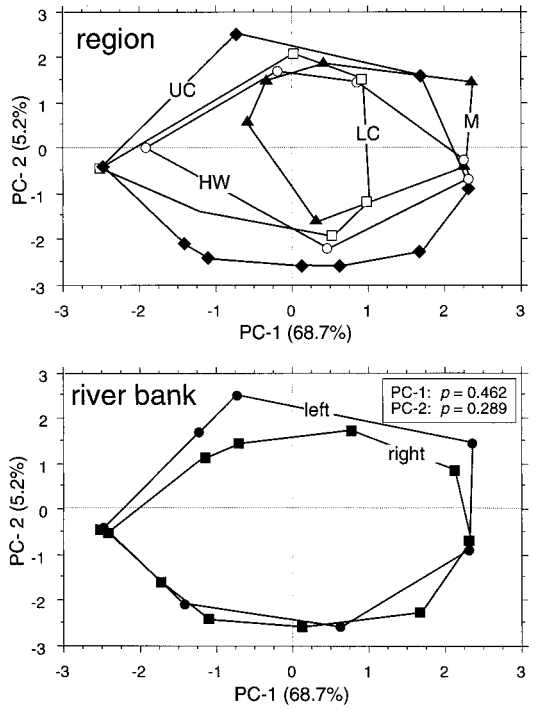

Fig. 149. Bivariate plots of the first and second principal components axes illustrating the morphometric relationships between samples of *Proechimys simonsi* by geographic regions along the Rio Juruá (above) and between river bank samples (below).

TABLE 73
Principal Components Analysis of Adult (Age Class 8–10) *Proechimys simonsi* from the Rio Juruá, Brazil

Variable	PC-1	PC-2
Log CIL	0.973	−0.059
Log ZB	0.923	−0.059
Log MB	0.891	0.007
Log IOC	0.805	0.008
Log RL	0.949	−0.106
Log NL	0.937	−0.078
Log RW	0.824	−0.082
Log RD	0.949	−0.106
Log OL	0.905	−0.051
Log D	0.934	−0.146
Log MTRL	0.311	0.851
Log IFL	0.522	−0.145
Log PL	0.919	0.023
Log PPL	0.884	0.074
Log BUL	0.659	0.213
Log MAXB	0.847	−0.005
Log OCB	0.534	0.436
Log MPFW	0.644	−0.060
Log CD	0.924	−0.033
Log CMD	0.952	−0.090
Eigenvalue	14.432	1.099
% contribution	68.73	5.22

64.7% and 76.2% of the 207 individual specimens included in the analysis are allocated to their correct side of the river by a posteriori probabilities of group membership. Table 74 provides the standardized character coefficients from the discriminant analysis.

We also examined the relationship between the morphometric and genetic distances among our samples of *P. simonsi*, as well as the relationship between each of these variables and geographic distance. We used the Mahalanobis D^2 matrix generated from a discriminant function analysis that specified localities as the a priori groups as a measure of morphometric distance, and a matrix of genetic similarities (Slatkin's [1993] M-statistic) generated from the population cytochrome-b haplotypes by the AMOVA program of Excoffier et al. (1992). These were compared to the $\log_{10}$ of the straight-line geographic distances among localities given in table 1. Morphometric distances increase significantly with an increase in geographic distance among locality pairs (fig. 152; Mantel's matrix correlation coefficient $r = 0.551$, $p =$

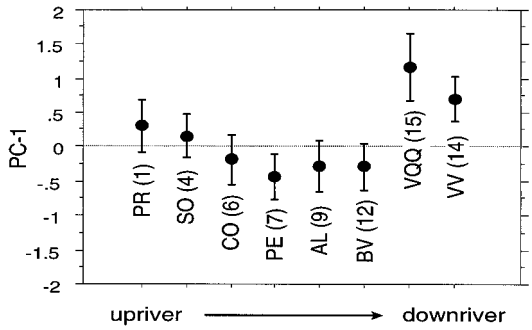

Fig. 150. Geographic trend in overall size, as indexed by mean scores on the first principal components axis for samples of *Proechimys simonsi* along the Rio Juruá. Samples are positioned from left to right from the headwaters downriver to mouth localities. Solid circles represent population means; bars on either side represent 95% confidence limits.

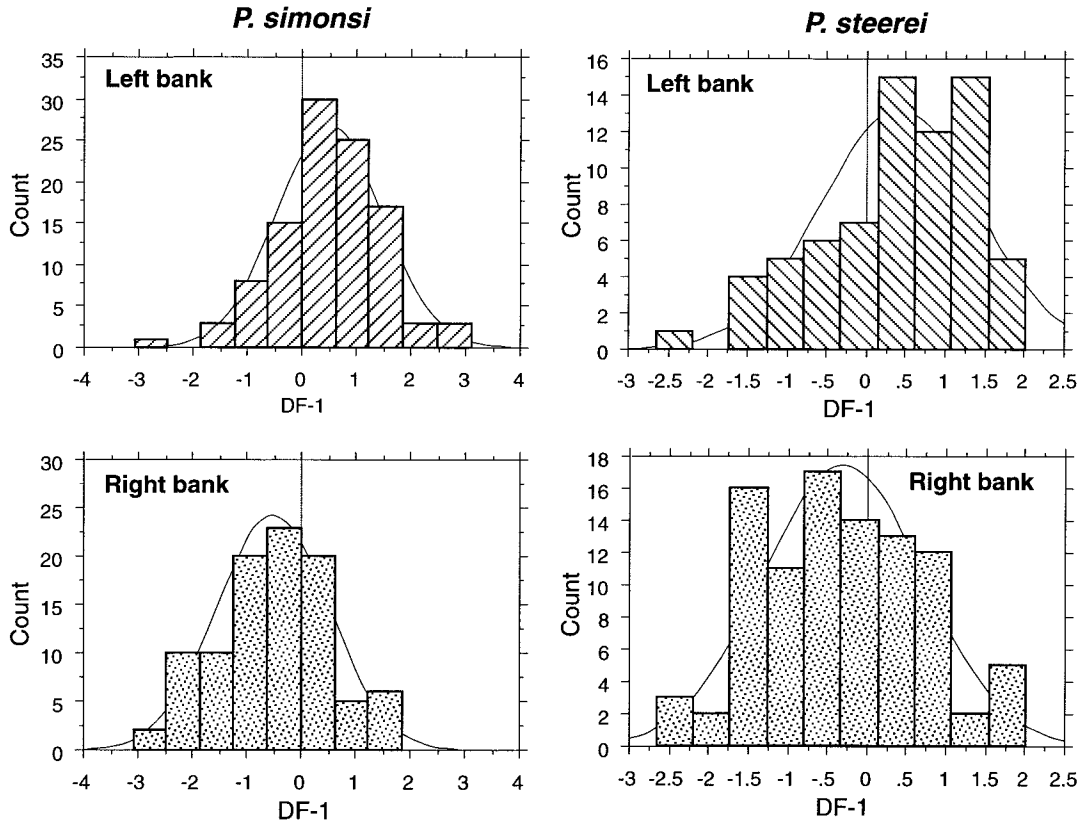

Fig. 151. (**Left**) Histograms of individual scores in a discriminant function analysis for *Proechimys simonsi* with river bank identified as a priori groupings. Slight differentiation is apparent in the distributions for left bank and right bank population samples. (**Right**) Histograms of individual scores in a discriminant function analysis for *Proechimys steerei* with river bank identified as *a priori* groupings. Slight differentiation is apparent in the distributions for left bank and right bank population samples.

0.0014), and genetic similarity decreases equally significantly with geography (fig. 152; $r = -0.518$, $p = 0.0021$). Not surprisingly, morphometric distance and genetic similarity are intercorrelated ($r = -0.521$, $p = 0.012$). Populations of *P. simonsi* along the Rio Juruá thus exhibit a clinal, isolation-by-distance pattern in both morphometric and genetic traits.

DISTRIBUTION AND HABITAT: *Proechimys simonsi* occurs throughout the western Amazon Basin from southern Colombia to northern Bolivia (fig. 148, and Patton, 1987; Anderson, 1997). The specimens we record here, as well as those obtained by us on the upper Rio Urucu southeast of Tefé in Estado do Amazonas represent the first records for the species from Brazil known to us. We found *P. simonsi* to be common along the length of the Rio Juruá, and well represented in the fauna of all four regional areas (table 63). The great majority of individuals was collected in terra firme forest (78.3%; 310 out of 396), 23 (5.8%) in várzea forest, and 63 (15.9%) in a variety of terra firme habitats, such as secondary or disturbed forest, gardens, or terra firme–várzea edge. Interestingly, all but one of the individuals trapped in the várzea are from the Headwaters region, where the flooding regime of the várzea forest is sporadic across years, not annual. Most specimens (79%) were caught in Tomahawk traps, with only 22% in Sherman traps; 6% were shot and 3% were caught in snap traps or by hand. Of the animals captured in live traps, 39% of young and sub-

TABLE 74
Standardized Discriminant Coefficients in Comparisons Between Right and Left Bank Population Samples of *P. simonsi* and *P. steerei*
Analyses based on $\log_{10}$-transformed cranial variables only.

Variable	*P. simonsi* standardized coefficient	*P. steerei* standardized coefficient
Log CIL	0.03614	−0.13471
Log ZB	0.35017	−0.05664
Log MB	−0.46625	−0.29066
Log IOC	−0.00785	−0.37182
Log RL	0.47359	−1.02831
Log NL	−0.41006	−0.45874
Log RW	0.32330	−0.34455
Log RD	−0.33967	−0.57382
Log OL	1.20299	0.80080
Log D	0.76482	0.50488
Log MTRL	−0.11834	0.39595
Log IFL	−1.28964	−0.10631
Log PL	−0.05194	0.65754
Log PPL	0.06575	0.66497
Log BUL	−0.31931	−0.63431
Log MAXB	0.12245	0.55415
Log OCB	0.23789	0.03461
Log MPFW	−0.21962	−0.45972
Log CD	−1.66695	−0.75103
Log CMD	1.29922	1.50675
Eigenvalue	0.26369	0.12678
% contribution	100%	100%

adults were caught in Sherman traps and 61% in Tamahawk traps; 90% of the adults were collected in Tomahawk traps and only 10% in the smaller Sherman traps.

REPRODUCTION: We obtained specimens of *P. simonsi* along the entire river and at all seasons of the year. Of the 117 males with complete autopsy data, 66 were reproductively active by our criteria. These ranged in age class from 6 to 10, although the majority (79%) were relatively old adults (age classes 9 and 10). All young individuals (ages 1–5) and most subadults (ages 6 or 7) were reproductively inactive, although this category also included some age class 9 animals. Detailed reproductive data are available for 154 individual females (table 75); of those, 65% were either pregnant or postpartum whereas 35% had apparently not yet reproduced. Pregnant, lactating, or postpartum females were obtained at all sites, suggesting that at

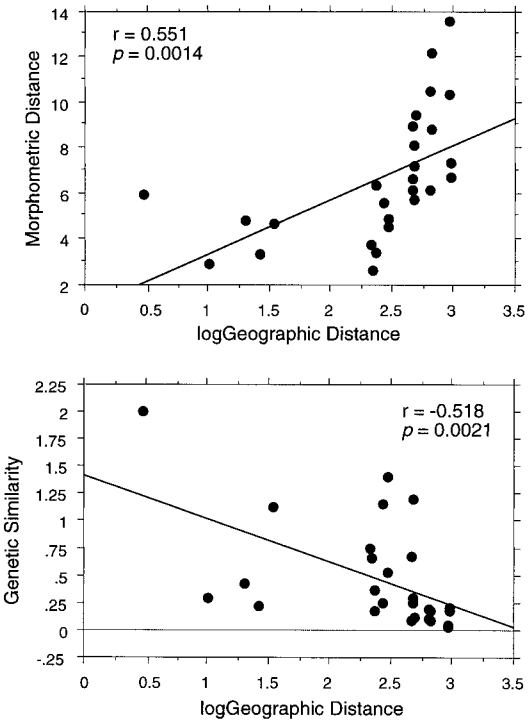

Fig. 152. Bivariate relationship between morphometric distance (Mahalanobis D^2; above) and genetic similarity (Slatkin's [1993] M-statistic; below) and the log of the straight-line geographic distance between sample localities of *Proechimys simonsi* along the Rio Juruá. Mantel's matrix correlation coefficients and their significance are indicated for each.

TABLE 75
Comparative Reproductive Characteristics for Female *Proechimys steerei* and *P. simonsi* from the Rio Juruá
Age is determined by the toothwear criteria of Patton and Rogers (1983): young = age classes 1–5, subadult = age classes 6–7, adult = age classes 8–10.

Reproductive characteristic	*P. steerei* (n = 179)	*P. simonsi* (n = 154)
Age class of first signs of breeding	4	6
Age class of pregnant females	5–10	6–10
Modal litter size (range)	3 (1–7)	2 (1–3)
Percent parous young and subadults	17%	3%
Percent nulliparous adults	2%	30%
Percent females with postpartum estrous	18%	6%

TABLE 76
Summary of Karyotypic Data for Samples of *Proechimys simonsi*

		Autosomes[a]						Sex chromosomes			
		M & SM		ST		A					
Locality	2n	Lg	Med/sm	Lg	Med	Med	Sm	X	Y	FN	Reference
Limoncocha, Napo, Ecuador	32	2	8	1	3	1	—	A	A	58	Gardner and Emmons, 1984
Río Perené, Junín, Perú	32	2	8	1	3	1	—	A	A	58	Gardner and Emmons, 1984
Río Curanja, Ucayali, Perú	32	2	8	1	3	1	—	A	A	58	Patton and Gardner, 1972
Río Tambopata, Madre de Dios, Perú	32	2	8	1	3	1	—	A	A	58	Gardner and Emmons, 1984
Rio Urucu, Amazonas, Brazil	32	2	8	1	3	1	—	A	A	58	this report
Rio Juruá, Amazonas, Brazil	32	2	8	1	3	1	—	A	A	58	this report

[a] M = metacentric; SM = submetacentric; ST = subtelocentric; A = acrocentric (nomenclature follows Patton, 1967).

least some females breed in all seasons over the year. Of the parous individuals, almost all (90 of 93) are adults (age classes 8–10, with only four of age class 8), and only three are subadults (age class 6). Sixty-seven females were pregnant. The majority of these (91%) were full adults of ages 9 or 10, although pregnancies were observed at ages as young as 6. Four of the 67 pregnant females were also lactating, suggesting that a postpartum estrous is possible, if uncommon, in this species. The modal litter size was 2, with a range from 1–3. Individuals recorded as nulliparous were present in all age categories except 10; subadults and adults comprise almost half of those (23 of 50), with the proportion of nulliparous adults (age class 8 and 9) around 30%. Both males and females appear to reproduce only after they are fully grown, and a relatively large proportion of adults in a population does not reproduce at a given time.

KARYOTYPE: 2n = 32; FN = 58. The autosomes consist of two pairs of large submetacentrics, eight pairs of medium-sized to small metacentrics and submetacentrics, one pair of large and three pairs of medium-sized to small subtelocentrics (one of which has a secondary constriction on the long arm), and a single pair of medium-sized acrocentrics. The X chromosome is a medium-sized acrocentric and the Y is a minute one. This karyotype was previously described and figured by Patton and Gardner (1972), and is apparently invariant throughout the species range. Table 76 provides a summary of karyotype data for specimens which we have personally examined. In addition to these specimens, the same karyotypes have been published for specimens presumptively of this species from southern Colombia (Reig and Useche, 1976). We have not examined these specimens.

COMMENTS: Patton (1987) remarked that the *P. simonsi* group showed relatively low levels of morphological character variation throughout its geographic range, and available data suggested karyotypic uniformity as well. Our samples from the Rio Juruá and upper Rio Urucu extend the geographic distribution of this species approximately 1000 km to the east, as mapped by Patton (1987), and are fully consistent with this view of uniform character variation. As noted above, the cytochrome-b sequence data also generally support the interpretation of uniformity throughout the majority of the species' range. However, the single sample from northern Perú is rather divergent, and additional samples from the northern portion of the range of this species are needed to determine the

extent to which *P. simonsi* is structured into regional, reciprocally monophyletic lineages.

SPECIMENS EXAMINED (n = 416): (**1**) 21m, 31f — MNFS 1071–1073, 1078, 1081–1082, 1084, 1086, 1089–1092, 1099, 1108, 1112, 1114, 1124–1126, 1133–1136, 1140–1142, 1156–1157, 1162–1164, 1197, 1199, 1209, 1212–1214, 1216–1217, 1288–1289, 1314–1317, 1324, 1357, 1359, 1364, 1383, 1386–1387, 1414; (**2**) 6m, 4f, 1 unknown — MNFS 1176, 1178–1179, 1284, 1336, 1349–1351, 1376–1378; (**b**) 2m — MNFS 1000–1001; (**3**) 6m, 11f — JUR 205, 222, 229–230, 239, MNFS 1542, 1544, 1551, 1593–1594, 1600–1601, 1605, 1653, 1656–1657, 1680; (**4**) 16m, 29f — JUR 217, 232, 234–235, 243, 250, MNFS 1427, 1431–1434, 1440–1442, 1449, 1451, 1456–1457, 1468–1471, 1473, 1483–1485, 1488–1489, 1501, 1503, 1505, 1511, 1523, 1525, 1536, 1561, 1563–1564, 1570–1571, 1647, 1661, 1663–1664, 1668; (**6**) 28m, 25f, 1 unknown — JLP 15530–15531, 15533, 15539–15540, 15547, 15560, 15573, 15576, 15578, 15589–15595, 15610–15611, 15613, 15617–15618, 15621–15622, 15639–15641, 15643–15644, 15649, 15656–15659, 15668–15669, 15681, 15684, 15702, JUR 177, 184, MNFS 538–540, 542–544, 547, 555–559, 561; (**7**) 40m, 18f — JLP 15261, 15264, 15270, 15276–15277, 15279–15280, 15286–15287, 15293–15300, 15307, 15309, 15315–15318, 15320, 15333–15339, 15347–15352, 15363, 15370–15374, 15464, 15506, MNFS 339–340, 344–345, 347, 350–352, 355, 362, 364, 406, 476; (**9**) 18m, 23f — JLP 15928, 15991–15998, 16015–16018, 16038, 16041, 16055, 16082–16083, 16086–16090, JUR 195, MNFS 852, 855–856, 858, 860–864, 878–880, 884, 886–887, 912–913; (**12**) 13m, 24f — JLP 15747, 15764, 15778, 15785–15787, 15797, 15809–15812, 15817–15820, 15834, 15855, 15873–15874, 15887–15888, 15904–15905, 15907, JUR 189, MNFS 723–724, 726, 732, 741, 743–744, 762–764, 819–820; (**13**) 1f — JUR 346; (**14**) 14m, 43f — JUR 428–429, 431–432, 434, MNFS 1684, 1687–1693, 1695–1697, 1702, 1705–1713, 1720–1722, 1726–1733, 1740–1741, 1746–1748, 1758–1762, 1773–1776, 1778, 1781–1782, 1788–1790; (**15**) 23m, 16f — JUR 270–272, 286, 289, 294, 299, 302–303, 318, 320, 323, 344, 359, 362, 365–368, 371–373, 376, 379–380, 382–383, 387–389, 391–392, 400, 402, 405, 407–410; (**16**) 2f — MNFS 1751, 1754.

Proechimys steerei Goldman, 1911

TYPE LOCALITY: ''Rio Purus, a southern tributary of the Amazon, in northwestern Brazil''; recorded as Hyutanahan, upper Rio Purus, Provincia Lábrea, Estado do Amazonas, Brazil by Moojen (1948: 338).

DESCRIPTION: *Proechimys steerei* is the largest species of spiny rats found in the Rio Juruá, with individuals from true várzea sites during the flooding season maximally weighing nearly 1 kg. The ears and hind feet are large, and the tail is proportionately short, approximately two thirds that of the body (tables 60 and 64). The color of the tail is dark brown above and white to cream ventrally; it is clothed by hair but the scales remain conspicuous to the eye. The color of the dorsal surface of the hind foot is characteristic of this species: a pale to dark brown outer band and whitish inner band along the length of the foot, from the tarsal joint to the end of the toes, in most individuals. Another distinctive feature is the narrow, short, and rather lax aristiform hairs on the dorsum (da Silva, 1998: fig. 3), that contribute to a characteristically softer fur than is found in any other spiny rat, not only along the Rio Juruá but in all of western Amazonia. As is true of most species of *Proechimys*, there is no lateral stripe and the reddish color of the sides of the body contrasts sharply with the pure white venter. The texture of the ventral fur in *P. steerei* also seems thicker and distinctly more velvety to both the eye and touch than in other species.

The baculum of our specimens of *P. steerei* is similar to that described by Patton (1987) for his *goeldii*- group; it is moderately long and narrow, especially when compared to bacula of *P. brevicauda* and *P. cuvieri*, although it is shorter and wider than that of *P. simonsi* (fig. 137).

The skull is large, with a long and narrow rostrum (figs. 138 and 139) and well-developed supraorbital ledge (Patton, 1987: fig. 21b). The incisive foramen is lyrate to oval in outline, with slightly to well-flanged posterolateral margins in the great majority of

individuals (130 out of 134 specimens) that form grooves extending onto the palate (fig. 140). The premaxillary portion of the septum is short, less than half the length of the opening, the maxillary portion is distinctly narrow, and both are in contact in most specimens (104 out of 135); the vomer is usually not visible (101 out of 133 specimens). A groove is present on the floor of the infraorbital foramen, but development of the lateral flange is weak (of 134 specimens, 79 had a shallow groove but without lateral flanges and only four had a groove present with moderately developed lateral flanges; all 51 remaining specimens had a smooth floor without any groove). The mesopterygoid fossa is relatively broad, but penetrates the palate to a level between the posterior and anterior margins of M3 (fig. 141). Most specimens show three folds in PM4, M1, and M3 (118, 97, and 93 out of 134 specimens, respectively; the remaining individuals have four folds in those teeth) and four folds in M2 (91 out of 134 specimens, with 3 folds in all others). Overall, these characters observed for specimens from the Rio Juruá compare with those described by Patton (1987) for specimens of his *goeldii*- group from other localities outside the Rio Juruá Basin.

SELECTED MEASUREMENTS: Means and ranges of selected external and cranial measurements are given in table 64.

COMPARISONS: *Proechimys steerei* is perhaps the most easily recognized species of spiny rat in the Rio Juruá basin, being distinguished from all other *Proechimys* by the combination of very large body size, relatively short and bicolored tail, laterally bicolored dorsal surface of the hind foot, and the distinctly soft adult pelage covering the entire body, especially along the dorsum where the aristiforms are not stiff to the touch. The relatively short and narrow baculum is indicative of a short and thin phallus in the male, a structure that also easily separates this species from all other sympatric spiny rats throughout western Amazonia. Cranially, *P. steerei* can be distinguished from other sympatric species by the combination of its large size, typically four folds on M2, structure of the incisive foramina, and broad but relatively deep mesopterygoid fossa. Illustrations of these features are given in figures 139 and 140 as well as Patton (1987).

MOLECULAR PHYLOGEOGRAPHY: We have sampled 25 localities that span a substantial portion of the mapped range of the *goeldii*-group of species, as diagnosed and mapped by Patton (1987: fig. 2). Included are samples of *P. steerei* from 14 of the primary localities within the Rio Juruá basin (fig. 153; table 77). Up to five individuals were sequenced per population. Three major haplotype clades are recognizable, one of which is further divisible into two groups (fig. 154). Haplotypes from specimens allocated to *P. goeldii* from two localities in Estado do Pará are so well differentiated from all others (13.2% relative to other members of the group) that it is basal to all other species of Amazonian *Proechimys* in analyses containing all taxa and geographic representatives (da Silva, 1998: fig. 13). The other two clades separate samples from largely south of the Rio Solimões, but including those from the Rio Jaú west and south of the Rio Negro, from those in northern Perú, southern Venezuela, and Brazil east of the Rio Negro (fig. 153). These differ by an average of 10.9%. Although samples from the northern clade are sparse, sequence divergence is low, averaging only 2.6% across the 2000 kilometers between northern Perú and central Brazil north of Manaus. The southern clade, however, does exhibit substantial geographic variation, with the samples from north of the Rio Solimões along the Rio Jaú differing from those to the south by an average of 6.6%. A more extensive analysis of haplotype variation among localities within the Rio Juruá is in preparation for publication elsewhere (M. D. Matocq, J. L. Patton, and M. N. F. da Silva). A synopsis of these data is given below in the section on riverine barriers. However, from the tree in fig. 154 it is apparent that a reasonable degree of haplotype diversity is present along the river, as 801 bp haplotypes from 11 different localities differ by an average of more than 5%. Importantly, those haplotypes from the Headwaters form a monophyletic assemblage distinct from those from the other three sample regions.

We consider the three clades identified in the mtDNA tree (fig. 154) to represent sep-

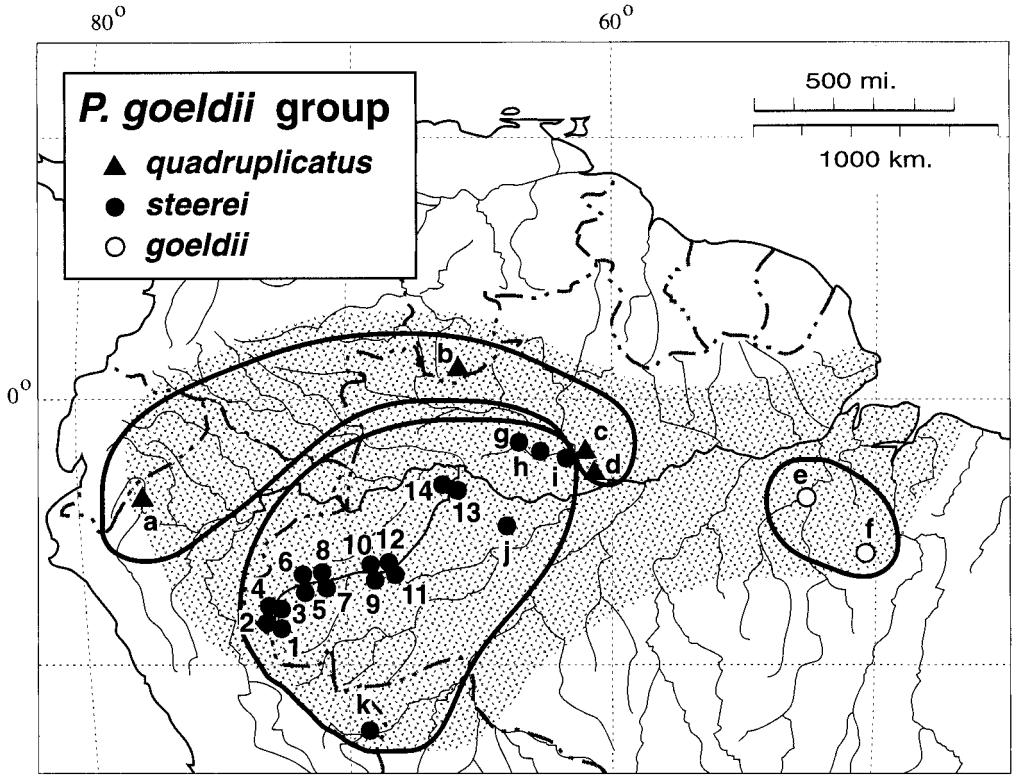

Fig. 153. Map of the distribution of three species of the *Proechimys goeldii* group (modified from Patton, 1987) illustrating localities for which 801 bp of cytochrome-b sequence are available, lettered or numbered as in the tree (fig. 154). Localities from which individual specimens have been examined are identified by number (Rio Juruá) or letter, and are listed in table 77. Solid triangles = *P. quadruplicatus*; solid circles = *P. steerei*; and open circles = *P. goeldii*.

arate species. Based both on comparisons of specimens of each of these clades to holotypes of the various named forms that Patton (1987) allocated to his *goeldii*- group, the eastern mtDNA clade represents *P. goeldii* Thomas, 1905, although the oldest name for the southern clade is *P. steerei* Goldman, 1911. The northern clade is *P. quadruplicatus* Hershkovitz, 1948, a name published in the same year but somewhat earlier than its junior synonym, *P. amphichoricus* Moojen, 1948. Thorough analyses of morphological character variation for this group have yet to be performed, but the data summarized by Patton (1987) suggest that each clade is diagnosable by morphological traits as well as cytochrome-b sequences. For example, most individuals of *P. quadruplicatus* (more than 60%) possess four folds on all four upper cheekteeth, while this character state is much less frequent in *P. steerei*, and few individuals of *P. goeldii* have four folds on any teeth (Patton, 1987: table 5).

MORPHOMETRIC VARIATION: As with *P. simonsi*, above, we summarize the variation in mensural characters for adults (toothwear classes 8, 9, and 10) of *P. steerei* that is due to locality, sex, and age effects by a nested ANOVA (table 78). No character exhibits significant interlocality differences, and the average contribution of this factor to character variation is only 5.6%. However, considerable differences due to both sexual dimorphism and age variation are apparent. More than two thirds of the variables exhibit significant variant components for sex and age, with an average of 23.3% of the total pool of variation due to sex and 20.6% due to age. Hence, the degree of sexual dimorphism and the extent to which dimensions

TABLE 77

Haplotypes, Voucher Numbers, and Localities for Taxa of the *Proechimys goeldii*-Group

Individual haplotypes listed from top to bottom in the tree, figure 154, with the catalog numbers of their respective voucher specimens, and localities (identified as in the map, fig. 153) for which 801-bp haplotypes of the mitochondrial DNA cytochrome-b gene are available.

Haplotype	Voucher no.	Locality
P. quadruplicatus		
1	ALG 14039	San Carlos de Río Negro, ca. 4 km N Isla Sarama, Amazonas, Venezuela (locality b)
2	MVZ 157871	La Poza, Río Santiago, Amazonas, Perú (locality a)
3	MVZ 157875	La Poza, Río Santiago, Amazonas, Perú (locality a)
4	JLP 16794	Lago Meduinim, left bank Rio Negro, Amazonas, Brazil (locality c)
5	CCM 35	Arquipélago Anavilhanas, Rio Negro, Amazonas, Brazil (locality d)
6	CCM 36	Arquipélago Anavilhanas, Rio Negro, Amazonas, Brazil (locality d)
P. steerei		
7	MVZ 166036	Cusco Amazónico, Río Madre de Dios, Madre de Dios, Perú (locality k)
8	MNFS 1447	Sobral, left bank Rio Juruá, Acre, Brazil (locality **4**)
9	MNFS 1547	Nova Vida, right bank Rio Juruá, Acre, Brazil (locality **3**)
10	JUR 254	opposite Igarapé Porongaba, left bank Rio Juruá, Acre, Brazil (locality **2**)
11	MNFS 114	alto Rio Urucu, Amazonas, Brazil, 58°15'W, 6°14'S (locality j)
12	MNFS 134	alto Rio Urucu, Amazonas, Brazil, 58°15'W, 6°14'S (locality j)
13	JLP 15269	Penedo, right bank Rio Juruá, Amazonas, Brazil (locality **7**)
14	JLP 15396	Nova Empresa, left bank Rio Juruá, Amazonas, Brazil (locality **8**)
15	JLP 15692	Seringal Condor, left bank Rio Juruá, Amazonas, Brazil (locality **6**)
16	MNFS 689	Jainu, right bank Rio Juruá, Amazonas, Brazil (locality **11**)
17	JLP 15789	Barro Vermelho, left bank Rio Juruá, Amazonas, Brazil (locality **12**)
18	MNFS 688	Jainu, right bank Rio Juruá, Amazonas, Brazil (locality **11**)
19	MNFS 871	Altamira, right bank Rio Juruá, Amazonas, Brazil (locality **9**)
20	JLP 15705	Seringal Condor, left bank Rio Juruá, Amazonas, Brazil (locality **6**)
21	MNFS 1749	Colocação Vira-Volta, left bank Rio Juruá, Amazonas, Brazil (locality **14**)
22	JUR 257	Ilha Paxiuba, right bank Rio Juruá, Amazonas, Brazil (locality **13**)
23	MNFS 1777	Colocação Vira-Volta, left bank Rio Juruá, Amazonas, Brazil (locality **14**)
24	JLP 16737	Macaco, left bank Rio Jaú, Amazonas, Brazil (locality h)
25	JLP 16766	Macaco, left bank Rio Jaú, Amazonas, Brazil (locality h)
26	MNFS 2085	left bank Rio Jaú above mouth, Amazonas, Brazil (locality i)
27	JLP 16738	Macaco, left bank Rio Jaú, Amazonas, Brazil (locality h)
28	MNFS 994	Tambor, left bank Rio Jaú, Amazonas, Brazil (locality g)
P. goeldii		
29	USNM 549572	52 km SSW Altamira, east bank Rio Xingu, Pará, Brazil (locality e)
30	CS 48	Floresta Nacional Tapirapé-Aquiri, Município de Marabá, Pará, Brazil (locality f)

continue to increase in older toothwear classes even in fully adult individuals is somewhat greater in this species than it is in *P. simonsi*, although the differences in patterns between the two species is not great (compare tables 72 and 78). When an analysis nested by sex and age is applied to our largest sample from Nova Empresa (locality **8**, n = 41), seven cranial variables exhibit significant sexual dimorphism ($p < 0.05$: CIL, MB, RL, MPFW; $p < 0.01$: NL, D, and PL) and six show significant age differences ($p < 0.05$: MB, RL, NL, MPFW; $p < 0.01$: D, PL). Again, within-locality variance is partitioned somewhat differently than it is in *P. simonsi*, particularly in the degree of character sexual dimorphism.

The small amount of morphometric variation attributable to interlocality differences contrasts somewhat with the mtDNA haplotype data, which indicates both a reasonable amount of sequence differentiation among haplotypes (over 5%) and some geographic structuring into two reciprocally monophyletic clades along the river. In order to examine geographic trends in morphology

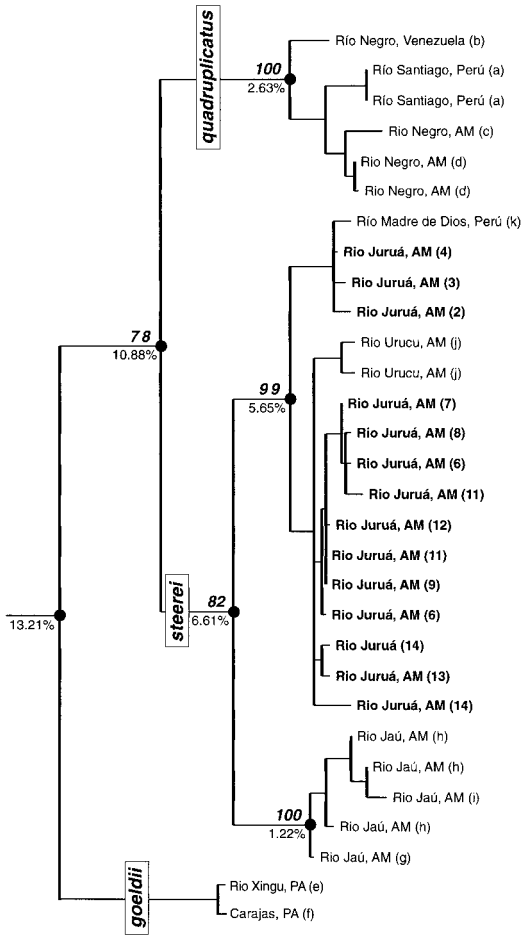

Fig. 154. Strict consensus maximum parsimony tree of 27 equally minimal length trees for 30 individual haplotypes of species of the *Proechimys goeldii*-group from 23 localities in Perú, Venezuela, and Brazil, as identified in the map (fig. 153). Length = 509 steps; CI = 0.672; RI = 0.814. Sequences of other species of *Proechimys* and of *Mesomys* were used to root the tree. Bold numbers at internal nodes are bootstrap values, based on 1000 replicates; percentages are average Kimura two-parameter distance. Provenance data and catalog numbers for each specimen can be found in table 77, listed in order from top to bottom in the tree.

more thoroughly, we used both principal components and discriminant function analyses, and compared samples from the four sample regions as well as those from the left and right banks of the river. Despite negligible interlocality variation in univariate dimensions, limited regional effects are apparent. In a principal components analysis, samples from each of the four geographic regional sample areas overlap extensively in multivariate space in combinations of the first three axes, which combine to explain 76.1% of the total pool of variation (fig. 155, top). Nevertheless, there are significant differences between the regions in mean PC scores on each axis (PC-1: $F_{3,161} = 7.086$, $p = 0.0002$; PC-2: $F_{3,161} = 9.111$, $p = 0.0001$; PC-3: $F_{3,161} = 15.410$, $p = 0.0001$, respectively). The first PC axis represents a general size axis, as indicated by high and positive factor coefficients (table 79) and by positive correlations of individual scores with their respective mensural variables. The correlation between PC-1 scores and individual values for logCIL, for example, is 0.976 ($p < 0.001$).

The trend in overall size in *P. steerei* along the Rio Juruá from its headwaters to its mouth is more complex then in *P. simonsi*, with parallel increases in size from the Headwaters Region to the Upper Central Region, and from the Lower Central Region to the Mouth Region (fig. 156). The differences between samples from the Upper and Lower Central regions are significant, as are those between the Lower Central and Mouth (Duncan's multiple range critical differences = 0.479 and 0.495, respectively, both $p < 0.05$). This complex pattern parallels interlocality variation in karyotype, as discussed below.

As was the case for *P. simonsi*, although regional samples of *P. steerei* exhibit a pattern of size increase along the length of the Rio Juruá, there is no differentiation between opposite-bank samples when characters are examined either in a univariate fashion or by multivariate principal components analysis. For example, there is broad overlap in the bivariate plot of PC-1 and PC-2 scores for samples pooled by right and left bank localities (fig. 155, bottom), and one-way ANOVAs for PC scores were nonsignificant for each of the three axes of table 78: for PC-1, $F_{1,163} = 1.943$, $p = 0.1652$; for PC-2, $F_{1,163} = 0.133$, $p = 0.7161$; and for PC-3, $F_{1,163} = 0.648$, $p = 0.4221$. However, also as was true for *P. simonsi*, if samples are pooled by river bank and subjected to a discriminant function

TABLE 78
Descriptive Statistics and Variance Components for Four External and 21 Cranial Variables of *Proechimys steerei* from the Rio Juruá
Measurements (mm) are given as mean ± standard error, with range and sample size.
Percentage contributions of the separate effects of locality, sex, and age are given, based on nested ANOVA (ns = $p > 0.05$; * $p < 0.05$; ** $p < 0.01$; *** $p < 0.001$).

Variable	Mean ± SE	Range	n	Variance component			
				Locality	Sex	Age	Error
TOL	404.30 ± 2.74	328–493	125	3.1 ns	28.8***	24.4***	43.8
TAL	166.58 ± 1.17	130–207	127	6.1 ns	21.5**	18.4*	54.0
HF	53.03 ± 0.29	43–63	180	7.4 ns	14.0 ns	11.9 ns	68.1
E	22.75 ± 0.10	19–25	175	10.3 ns	13.2 ns	12.5 ns	64.0
CIL	4810 ± 0.24	37.54–55.41	176	1.7 ns	32.6***	27.7***	38.0
ZB	27.21 ± 0.11	23.23–30.89	178	5.7 ns	26.7***	24.0**	44.3
MB	21.51 ± 0.09	18.11–24.17	178	2.9 ns	29.4***	27.5***	40.2
IOC	12.46 ± 0.06	10.09–14.70	181	7.2 ns	16.1 ns	13.5 ns	51.7
RL	23.79 ± 0.15	17.94–28.25	178	1.5 ns	32.1***	27.3***	39.1
NL	22.82 ± 0.16	17.32–27.71	177	2.2 ns	29.9***	25.3***	42.6
RW	8.63 ± 0.05	7.12–10.51	181	6.7 ns	17.3 ns	15.1 ns	60.9
RD	11.08 ± 0.06	8.90–13.25	181	3.6 ns	26.3***	22.5**	47.6
OL	15.31 ± 0.07	12.51–17.20	181	4.8 ns	26.9***	24.0**	44.3
D	12.61 ± 0.08	9.47–15.34	181	2.1 ns	33.2***	28.8***	36.0
MTRL	8.73 ± 0.03	7.01–9.98	182	12.6 ns	9.5 ns	7.9 ns	70.1
IFL	5.66 ± 0.04	3.77–6.93	180	12.3 ns	12.3 ns	14.0 ns	61.5
PL	20.56 ± 0.13	14.63–24.26	180	3.7 ns	30.7***	26.9***	38.6
PPL	23.64 ± 0.11	19.40–27.29	178	2.7 ns	22.5*	17.7 ns	57.1
BUL	10.76 ± 0.04	9.35–12.60	180	7.8 ns	27.9***	27.9***	36.4
MAXB	8.60 ± 0.04	7.13–10.58	180	4.3 ns	22.9**	22.1**	50.8
OCB	10.12 ± 0.03	8.79–11.34	176	7.2 ns	13.1 ns	11.1 ns	68.6
MPFW	4.84 ± 0.03	3.96–5.91	178	7.0 ns	18.6*	17.7*	56.7
CD	19.32 ± 0.08	16.29–22.72	177	4.3 ns	27.1***	23.5**	45.1
CMD	15.76 ± 0.08	12.70–18.11	181	5.2 ns	29.9***	27.3***	37.7

analysis (table 74), which maximizes between-group variance while minimizing that within groups, some segregation of opposite-bank populations is apparent. A one-way ANOVA of individual scores on the first discriminant axis yields a significant river bank effect ($F_{1,163} = 20.660$, $p < 0.0001$), and histograms of these scores (fig. 151, right) illustrate the slight differences among the samples.

We also examined the relationship between the morphometric and genetic distances among our samples of *P. steerei*, as well as that between each of these variables and geographic distance. We used the Mahalanobis D^2 matrix generated from the discriminant function analysis that specified localities as the a priori groups as a measure of morphometric distance, and a matrix of genetic similarities (Slatkin's [1993] M-statistic) generated from the population cytochrome-b haplotypes by the AMOVA program of Excoffier et al. (1992). These were compared to the $\log_{10}$ of the straight-line geographic distances among localities given in table 1. Morphometric distances increase significantly with an increase in geographic distance among locality pairs (fig. 157; Mantel's matrix correlation coefficient $r = 0.460$, $p = 0.0015$), and genetic similarity decreases sharply with geography (fig. 157; $r = -0.804$, $p < 0.0001$). Not surprisingly, therefore, there is a significant, if weak, correlation between genetic similarity and morphometric distance ($r = -0.275$, $p = 0.0192$). Populations of *P. steerei* along the Rio Juruá, as is true of *P. simonsi*, exhibit a clinal, isolation-by-distance pattern in both morphometric and genetic traits.

REPRODUCTION: We obtained specimens of

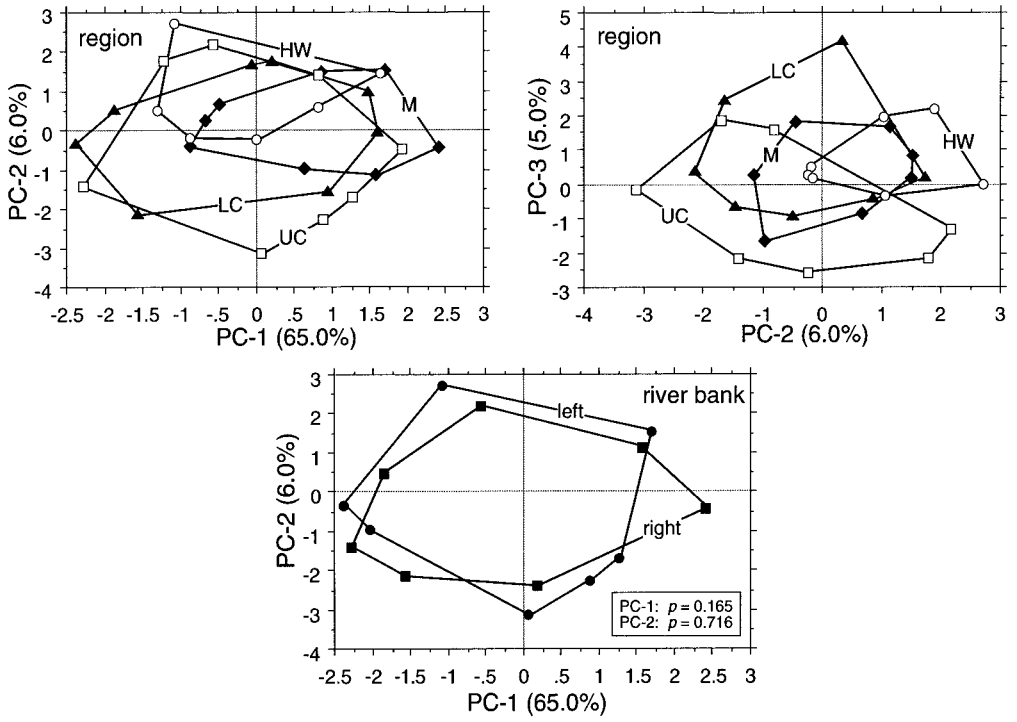

Fig. 155. Bivariate plots of the first and second principal components axes (**top, left**) and second and third principal components axes (**top, right**) illustrating the morphometric relationships between samples of *Proechimys steerei* by geographic regions along the Rio Juruá. (**Bottom**) Plot of the first and second principal components axes in comparisons between samples of *P. steerei* on opposite river banks of the Rio Juruá.

P. steerei along the entire river and at all seasons during the year of our sampling. Of the 183 males we autopsied, 88 were reproductively active. These ranged in age from toothwear class 3 to 10, although 82% (68 of 83) were adults (age classes 8 to 10) and 17% (14 of 83) were subadults (age classes 6 and 7). Reproductively inactive males include both young and adult individuals (age classes 1 to 9), with 68% (59 or 87) individuals of age classes 3, 5, and 6, and 9% (8 of 87) full adults (age classes 8 and 9). We have reproductive data for 179 females (table 75). Off these, 65% showed signs of current or previous pregnancy whereas 35% apparently had not yet reproduced. We caught pregnant, lactating, or postpartum females at all sites indicating that at least some females are breeding in all seasons of the year. Of the parous females, 83% (87 of 105) were adults, 16% subadults, and 1% young individuals. Seventy-five females were pregnant. The age class of these individuals ranged from 6 to 10; 87% (65 of 75) were fully adult (age classes 8 to 10) and the remaining subadults. Seventeen percent (14 of 84) were both pregnant and lactating. Modal litter size is 3; range, 1–7. The great majority of nulliparous females are young (47 of 58) or subadults (10 of 58). Relative to other species of spiny rats, particularly *P. simonsi*, which is also distributed along the entire river and for which we also have large samples, *P. steerei* exhibits reproductive characteristics tending towards a more *r*-selected life history, with somewhat earlier reproductive maturity, larger litter sizes, larger percentage of young animals breeding, a larger percentage of postpartum estrous females, and a smaller proportion of nonbreeding adults (table 75). These features might be expected for a species that lives primarily in strongly seasonal habitats, such as the várzea forests of the Rio Juruá.

TABLE 79
Principal Components Analysis of Adult (Age Class 8–10) *Proechimys steerei* from the Rio Juruá, Brazil

Variable	PC-1	PC-2	PC-3
Log CIL	0.973	0.033	−0.068
Log ZB	0.907	−0.039	−0.020
Log MB	0.895	−0.091	−0.062
Log IOC	0.748	−0.236	0.080
Log RL	0.942	0.013	−0.081
Log NL	0.928	0.015	−0.120
Log RW	0.755	−0.142	−0.029
Log RD	0.920	−0.063	−0.031
Log OL	0.872	−0.032	−0.105
Log D	0.932	0.066	−0.135
Log MTRL	0.236	0.092	0.919
Log IFL	0.285	0.748	0.022
Log PL	0.937	0.069	−0.018
Log PPL	0.914	−0.019	0.023
Log BUL	0.719	0.070	0.032
Log MAXB	0.756	0.067	0.289
Log OCB	0.231	−0.673	0.189
Log MPFW	0.570	0.348	0.025
Log CD	0.938	−0.078	−0.015
Log CMD	0.946	0.052	−0.078
Eigenvalue	13.649	1.268	1.055
% contribution	65.04	6.03	5.02

DISTRIBUTION AND HABITAT: Although distributional limits of *P. steerei* remain poorly understood, we have identified this species from localities from central Perú south of the Río Marañón to northern Bolivia and east through western Brazil in Acre and Amazonas states as far as the west bank of the Rio Negro, north of the Rio Solimões (fig. 152; da Silva and Patton, 1998: fig. 1). We found the species throughout the Rio Juruá, although most specimens (74.6%) were collected in the extensive várzea forests of the Upper and Lower Central regions. The lower numbers of specimens collected at localities in the Mouth Region (only 15.5% of the total sample) likely reflect our sampling of that area during the rainy season when the habitat of *P. steerei* was reduced by flooding, probably resulting in a seasonal decrease in population density. However, the relatively low percentage of animals found in the Headwaters Region (9.9%) might be due to other

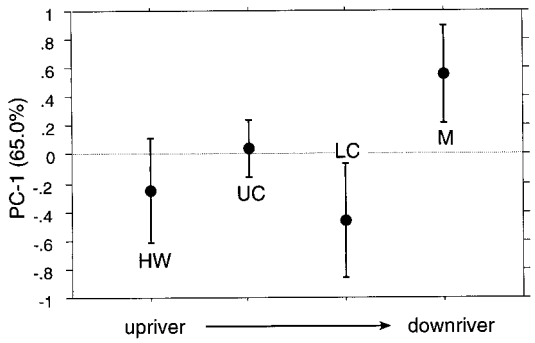

Fig. 156. Geographic trend in overall size, as indexed by mean scores on the first principal components axis for samples of *Proechimys steerei* along the Rio Juruá. Samples are positioned from left to right from the headwaters downriver to mouth localities. Solid circles represent population means; bars on either side represent 95% confidence limits.

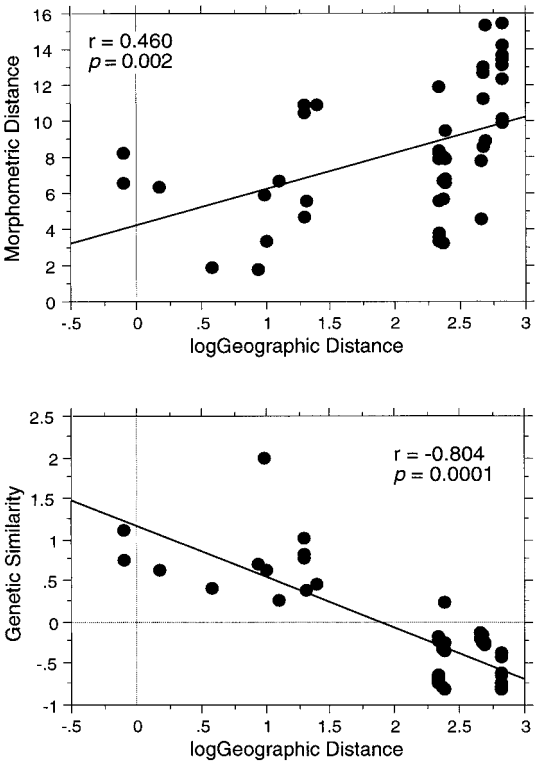

Fig. 157. Bivariate relationship between morphometric distance (Mahalanobis D^2; above) and genetic similarity (Slatkin's [1993] M-statistic; below) and the log of the straight-line geographic distance between sample localities of *Proechimys steerei* along the Rio Juruá. Mantel's matrix correlation coefficients and their significance are indicated for each.

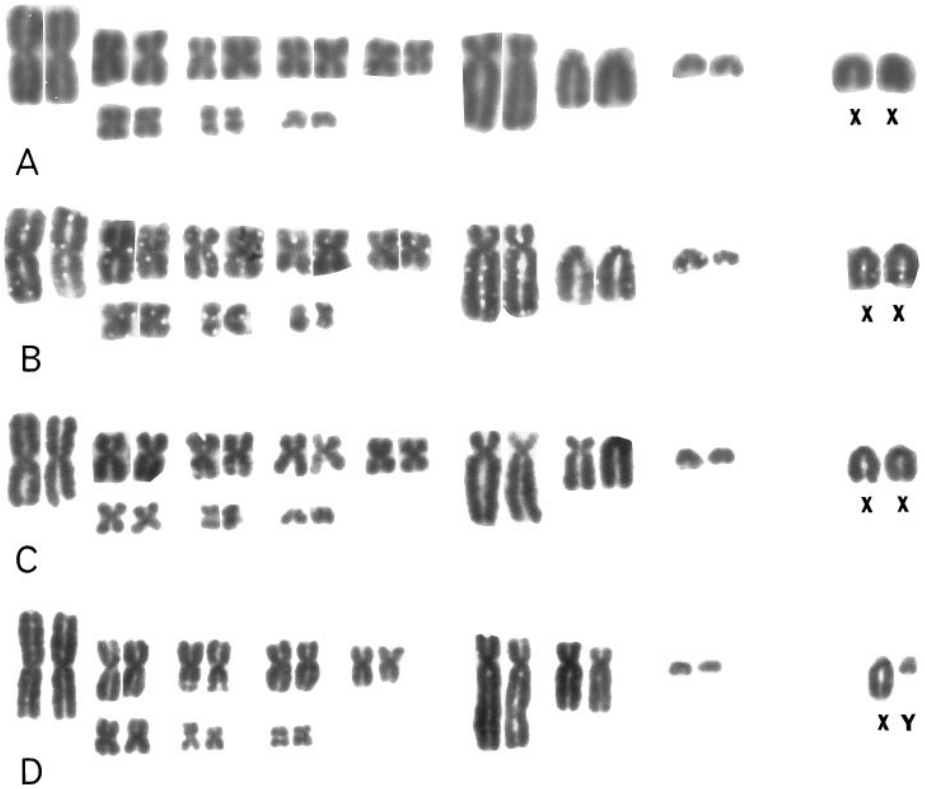

Fig. 158. Karyotypes of four specimens of *Proechimys steerei*: **A**, Female; 2n = 24, FN = 40; MNFS 2096; Macaco, left bank Rio Jaú, Amazonas, Brazil. **B**, Female; 2n = 24, FN = 40; JUR 307; Vai-Quem-Quer (locality **15**), right bank Rio Juruá, Amazonas, Brazil. **C**, Female; 2n = 24, FN = 41; Sacado (locality **5**), right bank Rio Juruá, Amazonas, Brazil. And, **D**, Male; 2n = 24, FN = 42; MNFS 1545; Nova Vida (locality **3**), right bank Rio Juruá, Acre, Brazil.

habitat features, or to competitive interactions with other species, since strict segregation by habitat is not evident in this region (table 63) and true, seasonally flooded várzea is not present.

While most common in seasonally flooded várzea, *P. steerei* was also found occasionally in secondary and disturbed terra firme forests, active and abandoned gardens, and margins of flooded grasslands (table 63). Elsewhere in Amazonia, we have taken this species in igapó (seasonally flooded black water) forests and along small creeks and river edge habitats within terra firme forest. The totality of our observations strongly suggest that *P. steerei* prefers flooded forests and riparian habitats within the lowland Amazon.

We captured the species in the Tomahawk and Sherman traps in our standardized lines; in addition we also took specimens by hunting and with Victor and metal snap traps. Although the total number of each kind of traps varied, in our sample of specimens (n = 313) the majority (72%) was caught in Tomahawk traps and only 16% in Sherman traps, 4% were shot, 6% were caught with Victor snap traps, and 2% with the metal snap traps. Of the animals captured in live traps, most young and subadults (129 out of 178) were caught in Tomahawk traps and the remaining 49 individuals in Sherman traps; the same is true for adults with 129 (out of 135) caught in Tomahawk traps, and only six in the Sherman traps. Considering the large size (maximum weight 800 g) of individual *P. steerei*, these results are not surprising.

KARYOTYPE: 2n = 24; FN = 40–42. We prepared karyotypes from 148 individuals, at

TABLE 80
Summary of Karyotypic Data for Samples of the *Proechimys goeldii*-Group (sensu Patton, 1987)

Locality	2n	Autosomes[a] M & SM Lg	Autosomes[a] M & SM Med/sm	Autosomes[a] ST Lg	Autosomes[a] ST Med	Autosomes[a] A Med	Autosomes[a] A Sm	Sex chromosomes X	Sex chromosomes Y	FN	Reference
					P. goeldii						
Rio Xingu, Pará, Brazil	24	1	8	1	—	—	1	A	A	44	this report (fig. 159A)
					P. quadruplicatus						
Limoncocha, Napo, Ecuador	28	1	7	1	—	—	4	A	A	44	Gardner and Emmons, 1984
Río Santiago, Amazonas, Perú	28	1	6	1	—	—	5	A	A	42	this report (fig. 159B)
La Esmeralda, Amazonas, Venezuela	26	1	7	1	—	—	3	A	A	42	Reig and Useche, 1976
Rio Negro, Amazonas, Brazil	28	1	6	1	—	—	4	A	A	42	this report (fig. 159C)
					P. steerei						
Rio Jaú, Amazonas, Brazil	24	1	7	1	—	1	1	A	A	40	this report (fig. 158A)
Rio Juruá, Amazonas, Brazil	24	1	7	1	1	—	1	A	A	42	da Silva, 1995;
	24	1	7	1	0.5	0.5	1	A	A	41	this report
	24	1	7	1	—	1	1	A	A	40	(fig. 158A–D)
Yarinacocha, Ucayali, Perú	24	1	7	1	1	—	1	A	A	42	Patton and Gardner, 1972
Río Curanja, Ucayali, Perú	24	1	7	1	1	—	1	A	A	42	Patton and Gardner, 1972
Pakitza, Río Manu, Madre de Dios, Perú	24	1	7	1	1	—	1	A	A	42	Gardner and Emmons, 1984

[a] M = metacentric; SM = submetacentric; ST = subtelocentric; A = acrocentric (nomenclature follows Patton, 1967).

least one from each locality from which *P. steerei* was collected. All specimens had an autosomal complement consisting of two pairs of large and seven pairs of medium to small meta and submetacentrics, one pair of large subtelocentrics, and one pair of small acrocentrics. Specimens from the Headwaters Region had a second, smaller pair of subtelocentrics (fig. 158D); those from the Mouth Region typically had this pair as a medium-sized acrocentric (fig. 158B). Finally, specimens from localities in the Upper and Lower Central Regions had one or the other of these two homozygous conditions, or were heterozygous (fig. 158C). The X-chromosome was a small acrocentric and the Y-chromosome an even smaller one in all individuals, regardless of autosomal complement. We caught heterozygous individuals at localities **9**, **10**, and **14**. At localities **9** and **14**, the parental homozygotes with medium-sized acrocentrics were more abundant (9 of 11 and 8 of 10 karyotyped individuals in each locality, respectively); the two remaining individuals from each locality were of both types, the parental homozygote with medium-sized subtelocentric and the heterozygote. At locality **10**, three of six karyotyped individuals were homozygotes with medium-sized acrocentrics, and three were heterozygotes. The downriver karyotype with the single pair of medium-sized acrocentrics also characterizes samples from the Rio Jaú, to the north of the Rio Solimões and west of the Rio Negro (fig. 158A). The upriver karyotype with the two pairs of subtel-

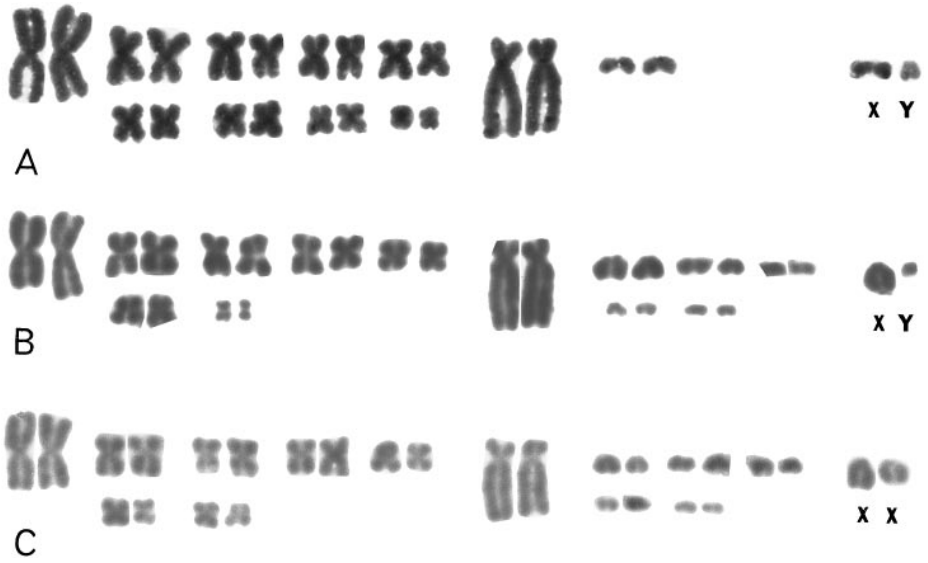

Fig. 159. Karyotypes of three specimens of *Proechimys*: **A**, a male *Proechimys goeldii*; USNM 549573; 2n=24, FN=42; 52 km S Altamira, Rio Xingu, Pará, Brazil. **B**, A male *Proechimys quadruplicatus*; MVZ 157860; 2n=28, FN=42; La Poza, Río Santiago, Amazonas, Perú. And, **C**, A female *Proechimys quadruplicatus*; JLP 16794; 2n=28, FN=42; Lago Meduiním, left bank Rio Negro, Amazonas, Brazil.

ocentrics is also found in samples from central, eastern, and southern Perú (table 80). Despite the slight variation in the karyotype of *P. steerei*, it is readily distinguishable from that of *P. goeldii* (2n = 24, FN = 42) from the Rio Xingu in Estado do Pará to the east, or to those of *P. quadruplicatus* (2n = 26–28, FN = 42–44) in northwestern and north-central Estado do Amazonia (table 75; fig. 159).

COMMENTS: Patton (1987) included *P. steerei* within his *goeldii*- group, which he noted varied more over its geographic range than any other species group that he examined, and suggested the existence of an eastern (*P. goeldii*) and a western (*P. steerei*) species. The cytochrome-b analyses (fig. 154), however, subdivide western populations even further and, along with karyotypic data, suggest at least three species within the *goeldii*- group. The senior names that would apply to each clade are: (1) *P. quadruplicatus* Hershkovitz, 1948 (with *amphichoricus* Moojen, 1948 a junior synonym), which occurs from Perú north of the Rio Marañón through eastern Ecuador to southeastern Colombia and east across southern Venezuela and adjacent Brazil north and east of the Rio Negro to at least the vicinity of Manaus. Available geographic samples of this taxon are 2n = 26 (Venezuela [Reig and Useche, 1976]) or 2n = 28 (Perú and Ecuador [Gardner and Emmons, 1984] and Brazil [this report]; see table 80 and fig. 159B–C). We referred to this clade as *P. amphichoricus* in earlier papers (e.g., da Silva and Patton, 1998). (2) *P. steerei* (with *pachita* Thomas, 1923, and *rattinus* Thomas, 1926, clearly junior synonyms, and probably *kermiti* Allen, 1915, *hilda* Thomas, 1924, and *liminalis* Moojen, 1948, as well) with 2n = 24, FN = 40 or 42 karyotype (table 80 and figs. 158). The range of this species is delimited above and in figure 153. And, (3) *P. goeldii* (with *hyleae* Moojen, 1948, *nesiotes* Moojen, 1948, and *leioprimna* Moojen, 1948 synonyms), from Estado do Pará in the eastern Amazon Basin of Brazil. Our samples of this taxon from the lower Rio Xingu and the Serra Carajás are inadequate to do more than simply document the extensive degree of sequence divergence between *P. goeldii* and either *P. quadruplicatus* or *P. steerei* (average from 13.2 to 14.4%). These samples also

have a different karyotype, with 2n = 24 and FN = 42 (fig. 159A; table 80). Additional sampling throughout the range of the *goeldii*-group is needed to further refine the geographic boundaries of the three species we identify here, as well as to determine if other taxa deserve recognition.

SPECIMENS EXAMINED (n = 453): (**2**) 1f — MNFS 1254; (**a**) 7m, 4f — MNFS 995–997, 1032, 1046, 1056–057, 1060–1063; (**c**) 1f — MNFS 1037; (**3**) 4m, 9f — JUR 206, MNFS 1521, 1543, 1545, 1547–1548, 1589–1592, 1633, 1655, 1682; (**4**) 8m, 13f — JUR 241, 245, MNFS 1430, 1445–1447, 1459, 1462, 1474–1477, 1506–1507, 1569, 1617, 1623–1625, 1643, 1662; (**d**) 1m — JLP 15628; (**5**) 39m, 31f, 1 unknown — JUR 118–129, 133–134, 136–143, 170, 172, MNFS 570–576, 585, 594–607, 614–620, 626–628, 641, 647–650, 658–667; (**6**) 12m, 7f — JLP 15558, 15614, 15690–15692, 15698–15700, 15705, 15709–15712, 15722, 15730–15732, JUR 176, MNFS 526; (**7**) 10m, 8f — JLP 15244–15245, 15254–15255, 15268–15269, 15458–15459, MNFS 333–334, 337–338, 342, 346, 354, 472, 496–497; (**8**) 68m, 61f — JLP 15375–15382, 15386–115391, 15396–15401, JUR 15–32, 44, 49, 50–71, 80–109, 111–113, 115–116, MNFS 443–463, 467–469, 477–483, 501; (**9**) 3m, 2f — JLP 15926–15927, 16019, 16053, MNFS 851; (**9a**) 5m, 5f — DMN 16–17, MNFS 926–928, 939, 949, 958–959, 963; (**10**) 15m, 9f — DMN, 12–13, MNFS 869–877, 895, 898–899, 915–916, 919, 932–933, 940, 945–947, 956; (**11**) 12m, 17f — JLP 15749–15750, 15753–15757, MNFS 679–680, 688–691, 700–701, 704, 709–711, 714–715, 720, 752–753, 770–771, 784–785, 794; (**12**) 17m, 13f — JLP 15789, 15799–15800, 15835–15838, 15856–15858, 15860–15864, 15878–15880, 15889, 15915, MNFS 687, 730–731, 733–735, 780, 781, 782, 783; (**13**) 19m, 27f — JUR 252–262, 264–266, 274–282, 293, 307–314, 326–330, 338–341, 345, 347, 349–351; (**14**) 1f — MNFS 1777; (**o**) 3m, 2f — MNFS 1737–1738, 1770–1772; (**16**) 12m, 6f — JUR 477, 504, MNFS 1749–1750, 1752–1753, 1755–1756, 1763–1769, 1783, 1792–1793.

PATTERNS OF COMMUNITY STRUCTURE AND SPECIES DIVERSITY

The environmental and biogeographic factors determining differences in community structure and diversity within Amazonia remain poorly understood. Nevertheless, comparative studies of community diversity have generally revealed substantial contributions of regional processes, geography, and unique historical events to patterns of the species richness (Ricklefs and Schluter, 1993). Emmons (1984), in a survey of seven nonvolant mammal communities, concluded that soil fertility and undergrowth density were primary ecological factors responsible for local species richness, whereas the quantity or annual pattern of rainfall was relatively less important. Her limited number of sites also indicated a general decrease in species diversity from western to eastern Amazonia. Peres (1997) showed that the species richness of primate communities was related to forest type, with higher richness, but lowered densities and overall biomass, in upland, nonflooded terra firme forests than in the seasonally flooded várzea. He attributed this observation to differences in soil fertility, resource productivity, and natural disturbance regimes. Peres also suggested that species richness itself was primarily a function of habitat diversity, whereas densities and biomass were influenced more by the nutrient-rich alluvial soils of young floodplains compared to the heavily weathered terra firme soils. Similarly, Kay et al. (1997) related primate species richness to plant productivity, which is highest in western Amazonia and declines to the east.

In this section we examine patterns of species richness on two geographic scales, based on our samples of nonvolant mammals from the Rio Juruá basin. The first, alpha diversity, examines species composition at the individual sites along the river. In the second, gamma diversity, we place these data into a broader geographic context, comparing our Rio Juruá sites with others sampled throughout Amazonia and adjacent lowland forested

regions. Our analyses for the Rio Juruá area are based on inventories from the 16 primary localities. Depending on the analysis, data are either restricted to the standardized sample plots or include all captures from each of these localities, grouping those from the standardized plots with captures from other habitats. We also limit our analyses to the three groups of mammals for which our sampling program was specifically designed: marsupials and both murid and echimyid rodents. A thorough analysis of primate community patterns from our samples along the Rio Juruá can be found in Peres (1993, 1997). Specimens of xenarthrans, carnivores, ungulates, and all rodents except murids and echimyids were obtained only serendipitously. As a consequence, although these taxa are listed in appendix C, they are not covered in the generalized accounts above and are excluded from our discussion of community composition here.

Our 16 primary sampling sites were chosen specifically to permit simultaneous comparison of terra firme and várzea forests at single points, although sampling along the length of the river necessarily spanned different seasonal phenologies. These differences in temporal sampling likely affect local densities and, to the extent that richness is influenced by abundance (i.e., the probability of capture), they may affect the species obtained. We have no way to determine whether this potential problem exists with our data, nor to assess its magnitude if present. Nevertheless, we limit our analyses only to species richness within and among habitats and localities, and make comparisons of relative abundances only to sites sampled nearly simultaneously (i.e., those within any one of the four sample regions identified in fig. 1).

COMMUNITY COMPOSITION: RIO JURUÁ

We obtained a total of 81 species of nonvolant mammals for all sample sites along the Rio Juruá combined (appendix C). This list includes mainly those taxa for which specimens were secured, except for primates for which Carlos Peres censused largely by observations made along standardized trail transects (Peres, 1993, 1997). Thirteen species of marsupials were taken throughout the basin, with species of at least three or four other genera probably there but missing from our samples (*Caluromysiops*, *Chironectes*, *Gracilinanus*, and *Glironia*). We caught eighteen species of sigmodontine rodents. It is possible that one or more other species might be present, such as the newly discovered *Amphinectomys* from nearby northeastern Perú (Malygin et al., 1994). However, we believe our list for the Rio Juruá is essentially complete, based on comparisons with other faunas in western Amazonia (summaries in Voss and Emmons, 1996). Finally, the 14 species of echimyid rodents collected likely reflect all that occur within the basin, although it is possible that the range of one or more other species of tree rat genus *Makalata* extend eastward from Perú into the Rio Juruá (based on the maps in Emmons and Feer, 1997).

Oryzomys perenensis is the only species we collected at all 16 primary localities from the headwaters to the mouth (appendix A and C). Others, which are restricted in habitat to either terra firme or várzea forests, were found at each of the sites where those habitats were sampled (e.g., *Proechimys simonsi* in terra firme and *P. steerei* in várzea). Still others, such as *Didelphis marsupialis*, *Oryzomys yunganus*, and *Mesomys hispidus*, were nearly ubiquitous, missing only from a few localities (appendix A and C). Apart from these taxa, there remain likely biases in the species lists for most or all of our sites, even though that species accumulation curves for both the terrestrial and canopy trapping generally reached a plateau with our sample effort (fig. 37, and discussion above). Certain taxa were undoubtedly overlooked at any particular locality because of inadequate sampling. While we acknowledge these caveats, patterns of community structure, and variation in that structure along the course of the Rio Juruá, are apparent.

The most obvious pattern of species richness among our sampled localities along the Rio Juruá is one of numerical constancy. The number of species at any given pair of cross-river sites is essentially the same along the total length of the river (appendix C), although the composition of species changes and a pattern of among-site community

structure is apparent (see below). Any differences in total species numbers between adjacent sites, or those farther apart, probably reflect inadequate sampling and/or the effects of sampling during different seasons. For example, the total number of marsupials and murid and echimyid rodents at any single sample site varies only from 23 to 28 species, with highs of 25, 28, 26, and 25 at cross-river paired sites in each of the four sampled regions (appendix C). The pattern of similarity in species numbers in communities along the river is also apparent when each individual taxonomic group is considered separately. As a consequence, there is no evident gradient in species numbers per locality along the approximately 1000 km length of the Rio Juruá. These numbers are also generally consistent with species richness estimates for western Amazonian sites in adjacent Perú (see Voss and Emmons, 1996, and below).

Despite the similarity in overall species richness, the 16 communities exhibit considerable structure with regard to which species were present in each. These localities form four distinct groups, each comprised of four localities, when a matrix of Jaccard's similarity coefficients is clustered (fig. 160). The mean Jaccard's similarity coefficient within each of these groups is, on average, nearly twice that of the mean between any pair (0.577 [range, 0.38–0.72] vs 0.318 [range 0.13–0.51]). The four groupings reflect a mixture of both geographic and habitat associations. All four localities in both the Headwaters and Mouth regions form unified clusters unto themselves, respectively, whereas the eight localities of the Upper and Lower Central regions segregate strongly by habitat, those of the terra firme versus the várzea. The Headwaters Region contains six species not found elsewhere (*Neacomys musseri*, *Oryzomys nitidus*, *Rhipidomys gardneri*, *Dactylomys boliviensis*, *Proechimys brevicauda*, and *Proechimys pattoni*). In contrast, only a single species is apparently unique to the Mouth Region (*Mesomys occultus*). Five species were found only in the combined Upper and Lower Central Region, namely *Holochilus sciureus*, *Nectomys apicalis*, *Oecomys superans*, *Proechimys gardneri*, and *Proechimys kulinae*. With the exception of the two species of *Proechimys*, the others in this list have broader ranges within western Amazonia and likely occur in one or both of the other two sample regions. Moreover, the Upper and Lower Central regions do not group together relative to those of the Headwaters and Mouth. Rather, terra firme localities, which are identifiable by 18 species not present in the várzea of the Upper and Lower Central regions (table 81), group with the Headwaters localities, while the várzea localities are the most divergent of all four clusters (fig. 159). These localities contain seven species not found in the terra firme (table 81, and discussion below).

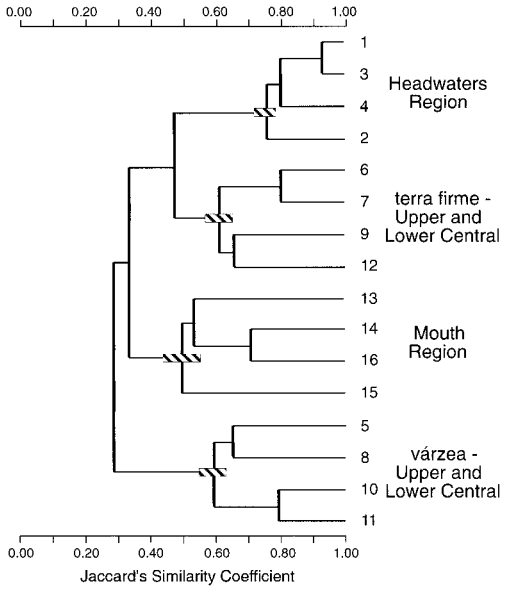

Fig. 160. Phenogram of Jaccard's similarity coefficients in comparisons of species composition between all documented species of marsupials, murid rodents, and echimyid rodents from each of the 16 primary sample sites along the Rio Juruá. Terminal branches are identified by locality number (see map, fig. 1); hatched boxes at basal nodes represent 95% confidence limits. Mantel's matrix correlation coefficient for the association between the similarity matrix and the cophenetic correlation matrix is 0.873, $p < 0.001$.

Table 82 summarizes the total number of species for each habitat type in the Headwaters, Upper Central, and Lower Central sample regions, as well as the number of species essentially restricted to either terrestrial or arboreal horizons within terra firme and várzea forests. Note that the numbers in each

TABLE 81
Habitat Distribution of Marsupials and Murid and Echimyid Rodents in the Upper and Lower Central Regions, Rio Juruá

Terra firme only	Várzea only	Both
	Marsupialia	
Marmosa murina	*Marmosops neblina*	*Caluromys lanatus*
Marmosops impavidus	*Philander opossum*	*Didelphis marsupialis*
Marmosops noctivagus		*Micoureus demerarae*
Marmosops parvidens		*Micoureus regina*
Metachirus nudicaudatus		
Monodelphis emiliae		
Philander mcilhennyi		
	Muridae	
Neacomys spinosus	*Oecomys bicolor*	*Neacomys minutus*
Oecomys species	*Oecomys roberti*	*Nectomys apicalis*
Oecomys trinitatus		*Oryzomys perenensis*
Oryzomys macconnelli		*Oryzomys yunganus*
Scolomys juruaense		
Rhipidomys leucodactylus		
	Echimyidae	
Proechimys cuvieri	*Isothrix bistriata*	*Mesomys hispidus*
Proechimys echinothrix	*Makalata didelphoides*	
Proechimys gardneri	*Proechimys steerei*	
Proechimys kulinae		
Proechimys simonsi		

category for the two habitat types in the Headwaters are equivalent, an observation that underscores the difference in the extent of the várzea along the upper reaches of the river, where flooding occurs only periodically rather than yearly (see above, and Peres, 1993, 1997). Our sampling of the Mouth sites during the height of the flood season precluded an effective evaluation of várzea versus terra firme forests, and thus this set of samples is not included in the comparisons. However, in both Central regions, the faunas are uniform with respect to numbers and actual species occurrences as these partition into terra firme versus várzea, and then by vertical stratum in both. Várzea forests contain only 65% of the species diversity of the terra firme (an average of 14 versus 21.5 species). The number of arboreal species in both forest types is nearly equivalent, so the difference resides primarily in terrestrial taxa, with terra firme forests containing twice the number of species (15.5 vs 7, on average across our sites). These observations are similar to those for primates of the Rio Juruá (Peres, 1997).

In part because of the segregation of localities in the central sections of the river into

TABLE 82
Numbers of Species per Habitat in Three Regional Areas of the Rio Juruá[a]

	Terra firme			Várzea		
Region	Total	Terrestrial	Canopy	Total	Terrestrial	Canopy
Headwaters	20	16	4	22	15	7
Upper Central	22	16	6	13	7	6
Lower Central	21	15	5	15	7	7

[a] Data compiled only for standardized plots at each locality within the three geographic regions.

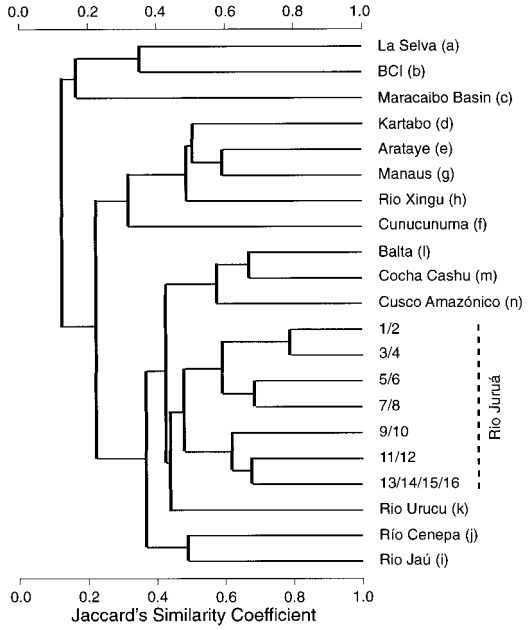

Fig. 161. Phenogram of Jaccard's similarity coefficients in comparisons of species composition between all documented species of marsupials, murid rodents, and echimyid rodents from each of 21 lowland Neotropical forest sample sites (see text). Terminal branches are identified by locality, as in the map (fig. 162). Mantel's matrix correlation coefficient for the association between the similarity matrix and the cophenetic correlation matrix is 0.946, $p < 0.001$.

habitat as opposed to geographic units, there is no significant global pattern of community composition and geographic position along the Rio Juruá (Mantel's matrix correlation $r = -0.5538$, $p > 0.05$, in the comparison of Jaccard's similarity and straightline distance matrices). However, calculations of Jaccard's similarity indices within forest types for all possible pairs of standardized samples do provide more detailed insights into both riverine and distance patterns in community structure throughout the river basin. In a separate set of analyses that we will present elsewhere, we classified each pair of samples as being from the same river bank or not, and used two-way ANCOVA with geographic distance as a covariate to examine variation due to forest type (terra firme or várzea) and river bank. Because the riverine barrier effect was expected to be strongest when nearby sites were contrasted, we included all possible interaction terms in the model (including all interactions between the covariate and the main effects). Analyses were run separately for terrestrial and canopy samples. We found no evidence of a riverine barrier effect in either the terrestrial or canopy samples (main effects $F_{1,1} = 1.19$, $p = 0.28$ and $F_{1,1} = 0.10$, $p = 0.76$, respectively; all riverine barrier interaction terms were $p > 0.28$). However, significant differences in terrestrial similarity were indicated between the two forest types (forest type main effect $F_{1,1} = 6.54$, $p = 0.01$), as were differences in the community similarity/geographic distance relationship (forest type/distance interaction $F_{1.1} = 5.22$, $p = 0.03$). Terrestrial similarity between nearby upland sites was high, but decreased markedly with increasing distance between the sites. In contrast, terrestrial similarity between nearby sites was lower in the floodplain, and did not appear to decrease with distance. Canopy pairs showed the same trends, but the corresponding tests were not close to significant (forest type main effect $F_{1,1} = 0.31$, $p = 0.58$; forest type-by-distance interaction $F_{1,1} = 0.58$, $p = 0.45$). The significant overall decrease in community similarity with increasing distance between samples was significant for the terrestrial samples (main effect $F_{1,1} = 0.513$, $p = 0.03$), but not for the canopy ones (main effect $F_{1,1} = 0.32$, $p = 0.57$).

Thus, regional (gamma) diversity patterns within the Rio Juruá basin appear to vary with forest type and forest stratum, supporting suggestions that models of speciation in the Amazon Basin must be complex and multifactorial (Bush, 1994; Patton and da Silva, 1998). Concerning the first difference in regional diversity patterns noted above, namely greater site-to-site turnover in species composition in upland versus floodplain forests, Terborgh et al. (1990) also noted that the avian fauna of mature várzea appeared to be relatively homogeneous compared to terra firme forest. One possibility for this pattern is that speciation has been less frequent in the floodplain, perhaps due to longer-term connectivity among local populations and/or fewer vicariant events. If true, this in turn would support the possibility of restricted distributions of upland forests during xeric

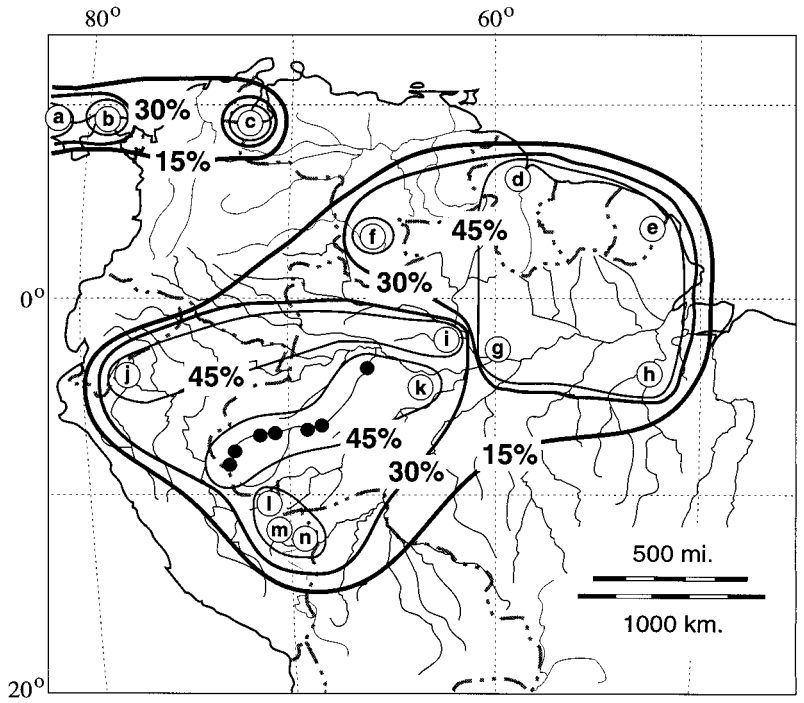

Fig. 162. Sample sites in lowland neotropical forests for which reasonably complete species inventories are available for marsupials, murid rodents, and echimyid rodents (data largely from Voss and Emmons, 1996; see text). Regional groupings of localities, based on the phenogram of Jaccard's similarity coefficients in fig. 161, are drawn to indicate geographic relationships in community composition. Localities outside of the Rio Juruá are identified by letters corresponding to the names given in the phenogram, fig. 161.

periods in the past (Haffer, 1993b; Joseph et al., 1995) as well as a possible role for the greater topographic diversity in upland landscapes. Alternatively, catastrophic flooding events (e.g., Blair, 1939; Campbell, 1984) may have periodically destroyed differentiation in the floodplain through local extinction events. Interestingly, analysis of mtDNA variation suggests relatively recent invasions of the Rio Juruá basin by some taxa (such as *Oryzomys perenensis*; see Patton et al., 1996a, and below). Either hypothesis, suppressed speciation or higher extinction rates in várzea forest, seems to argue against the importance of refuge-like vicariance events in the floodplain (Salo et al., 1986). The contrast in biogeographic patterns between the two habitats also argues against the practice of using patterns in one habitat to study processes in the other (e.g., Terborgh et al., 1990). The second difference noted above, namely higher species turnover in the terrestrial versus arboreal fauna, may reflect differences in the biology of the two groups of small mammals. Arboreal species are faced with complex locomotory requirements, which may result in relatively more ''*K*-selected'' life-history parameters. Also, variation in resource availability can be expected to be greater for terrestrial organisms than arboreal ones (Peres, 1999), because most rainforest primary productivity takes place in the canopy. These differences may in turn influence population persistence and, ultimately, rates of speciation in the two groups.

COMMUNITY COMPOSITION: GREATER AMAZONIA

We examined the relationship between communities of nonvolant mammals along the Rio Juruá relative to 14 other sites within the lowland Neotropical forests for which equivalent species inventories are available.

We used the species lists provided by Voss and Emmons (1996), which have been updated to current taxonomy and to which we can make legitimate comparisons because we use the same taxonomic perspective. We also include data from other sites which we have worked in Perú and Brazil (Río Cenepa, Amazonas, Perú [updated from Patton et al., 1982]; alto Rio Urucu, Amazonas, Brazil [M. N. F. da Silva and J. R. Malcolm, unpubl. data]; and Rio Jaú, Parque Nacional do Jaú, Amazonas, Brazil [M. N. F. da Silva and J. L. Patton, unpubl. data]). Finally, we combine the inventories for each pair of cross-river sites along the Rio Juruá, so that both terra firme and várzea are represented, thus making the separate Rio Juruá inventories for this analysis more equivalent to those from other sites.

Despite the overall paucity of sample sites given the immense size of Amazonia, there is strong geographic structure to the data (figs. 161, 162). All sites fall into one of three major geographic clusters, with the three from Central America and northern South America strongly divergent from two geographic groups of Amazonian sites ($t = 18.523$, $p < 0.001$). The latter clearly divide into eastern and western units, bounded by the Rio Negro north of the Amazon-Solimões axis and an undefined region somewhere between the Rio Madeira and Rio Xingu to the south. Although substantial variation in species composition does exist among sites within each of these two Amazonian units, the differences between them are marked. Both geographic areas exhibit similar levels of within-area species compositions (mean Jaccard's coefficient for eastern Amazonia is 0.431; that for western sites is 0.449; $t = 1.356$, $p > 0.208$), but differ significantly between them (mean Jaccard's coefficient for comparisons between areas is 0.2263; $t = 6.938$, $p < 0.001$ in the comparison of between area and within eastern Amazonia; $t = 14.242$, $p < 0.001$, in comparison between area and within western Amazonia). Despite regional and habitat differences within the Rio Juruá, all of our sampled sites are contained within the western Amazonian geographic unit (fig. 162). A similar pattern of western and eastern community groupings, with a boundary approximating the Rio Negro–Rio Madeira axis, was also found for bats (Simmons and Voss, 1998) and squamate reptiles (da Silva and Sites, 1995). This same north-south axis was identified by Alfred Russel Wallace (1852) as a dividing line among Amazonian primate communities nearly one hundred and fifty years ago.

THE RIO JURUÁ, RIVERINE DIVERSIFICATION, AND AMAZONIAN BIOGEOGRAPHY

> During my residence in the Amazon district, I took every opportunity of determining the limits of species, and I soon found that the Amazon, the Rio Negro and the Madeira formed the limits beyond which certain species never passed. . . On approaching the sources of the rivers they cease to be a boundary, and most of the species are found on both sides of them. Thus several Guiana species come up to the Rio Negro and Amazon, but do not pass them; Brazilian species on the contrary reach but do not pass the Amazon to the north. Several Ecuador species from the east of the Andes reach down into the tongue of land between the Rio Negro and Upper Amazon, but pass neither of those rivers, and others from Peru are bounded on the north by the Upper Amazon, and on the east by the Madeira. Thus there are four districts, the Guiana, the Ecuador, the Peru and the Brazil districts, whose boundaries on one side are determined by the rivers I have mentioned. (Wallace, 1852: 110).

The earliest hypothesis of a biogeographic mechanism of species diversification for Amazonian organisms is credited to Alfred Russel Wallace in the quote above, based on his observations of primate distributions. There are two separate but fundamental evolutionary components in Wallace's statement. First, rivers mark the boundaries of geographic areas, within which there is a similar community of species but between which species compositions are different. The implication is that evolution proceeded separately in each area, with rivers serving as barriers between them. Second, the strength of any barrier may decrease toward the headwaters of a river, such that sharing of species in opposite-bank communities is more likely where the channel is narrower. Both of these predictions are supported by the recent analysis of Ayres and Clutton-Brock (1992), who

showed that primate community similarity on opposite sides of rivers within Amazonia decreased as a function of river size and that communities became progressively more similar towards the headwaters of the Amazon itself.

Wallace's hypothesis was based solely on distribution patterns, yet a clear corollary is that rivers within Amazonia not only separate distinct faunas but may have served also as barriers to gene flow and thus have promoted species divergence. This has been termed the ''Riverine Barrier Hypothesis'' in the recent literature, and it has been invoked as an alternative to the widely held ''Refuge Hypothesis,'' where divergence is hypothesized to have resulted from forest contraction coincident with Pleistocene glacial cycles (e.g., Haffer, 1969; Vanzolini and Williams, 1970). Empirical support for riverine divergence comes from the commonly observed pattern of organismal distribution, where the boundaries of closely related species or subspecies often coincide with the major rivers of Amazonia. One need only look at the distribution maps in Hershkovitz (1977) for tamarins and marmosets, those for various birds published by Haffer (1974, 1978) and Cracraft (1985), or for Amazonian lizard species (Ávila-Pires, 1995) for examples.

Despite the intuitive appeal of this hypothesis, given the obvious size and number of fluvial systems in lowland Amazonia, it has received only limited attention in the 150 years since the publication of Wallace's original observation. The most extensive literature on riverine effects is probably that based on avian distribution patterns, but the results have often been conflicting. Capparella (1988, 1991) has documented increased genetic differentiation among cross-river lineages of understory birds relative to differentiation along each bank. However, there has also been observed both an inconsistency of congruence between phenotypic diversity within lineages and rivers and the existence of congruent contact zones between phenotypically differentiated taxa in interfluvial regions rather than along rivers (Capparella, 1991; Haffer, 1993a, 1997a).

As with many hypotheses of species diversification and biogeography, the riverine hypothesis, even if appealing, has been difficult to test. For one, it is difficult to distinguish between rivers as primary barriers in the diversification process rather than the simple secondary meeting point of taxa that diverged elsewhere (see Simpson and Haffer, 1978; Haffer, 1993a, 1997b). A second problem is the way in which riverine effects have been typically measured. A recent approach has been to examine the degree of genetic differentiation between opposite-bank versus same-bank populations, using distance methodology derived from protein electrophoretic data (e.g., Capparella, 1988, 1991; Gascon et al., 1996, 1998). However, this type of analysis is potentially compromised by isolation-by-distance phenomena, and samples must be geographically placed so that genetic and geographic distances are not confounded. More importantly, these methods cannot distinguish between the alternative hypotheses of primary diversification versus secondary contact, in part because phenetic distance does not necessarily measure phyletic propinquity.

A major motivating force for our work on the Rio Juruá concerned the potential importance of the river as a barrier to terrestrial vertebrate taxa, primarily mammals, reptiles, and amphibians. The sample sites were selected with this goal in mind, and collections were made so that riverine effects could be examined, both at the level of community assemblages and for individual taxa by morphological and/or molecular methodologies. As we described in the section immediately above, we found little evidence that nonvolant mammal communities were structured by river bank, and thus there is no suggestion that the Rio Juruá has been an important barrier in the development of those communities. Rather, species communities group strongly into a combination of regional and ecological units, each of which includes both right and left bank samples. This is true even for the terra firme forest communities, which are separated by both the width of the river and an extensive lateral floodplain that may be many kilometers across. However, although riverine effects are not apparent at the level of species communities of marsupials and rodents, it is still possible that individual taxa are both bounded by the river and that their divergence can be ascribed to it.

PHYLOGEOGRAPHIC PATTERNS WITHIN THE RIO JURUÁ BASIN

Phylogeography, as defined by Avise and his coworkers (Avise et al., 1987; Avise, 1989), is the study of the principles and processes governing the geographic distribution of genealogical lineages, both at intraspecific and interspecific levels. Of fundamental importance is the expectation that monophyletic groups identified by phylogenetic reconstruction will usually arise from long-term extrinsic barriers to gene flow (such as rivers). The corollaries of this expectation are (1) that the degree of phylogeographic concordance among the gene genealogies of different organisms will increase as time since isolation increases, and (2) that the geographic placement of phylogeographic gaps will tend to be concordant across species. Thus, if independently evolving organisms exhibit the same phylogeographic structure, they then likely responded to the same historical event. The level of divergence exhibited by such groups need not be identical, as a number of factors contribute to the rate of divergence in any lineage other than time itself. These arguments have been reinforced by a number of theoretical studies based on coalescent models of isolation-by-distance. For example, Barton and Wilson (1995) have shown on theoretical grounds that the geographical distribution of mtDNA haplotype lineages is generated primarily by historical processes.

We have used a phylogeographic rather than distance approach to examine divergence patterns among the mammals of the Rio Juruá. As described in the individual taxon accounts, above, we have examined mtDNA cytochrome-b sequence data for nearly all species of marsupials and murid and echimyid rodents obtained by us from the Rio Juruá (11 of 13 marsupials, 16 of 18 murids, and 14 of 14 echimyids). Of these, we have data for individuals from at least two or more geographic sample regions for 28 species, including the tamarin *Saguinus fuscicollis*. We follow Avise et al. (1987; see also Avise, 1989) in defining four phylogeographic categories based on combinations of the degree of molecular sequence divergence and the relative amount of geographic structure exhibited by the haplotypes of each taxon (fig. 163). Some species may exhibit both deep divergences among haplotypes, with those strongly partitioned geographically (category I) or without such structure (category II). Alternatively, species can show little sequence differentiation, yet still have the variation present either partitioned geographically (category III) or not (category IV).

Several of the species or complexes of related species we have examined exhibit little or no differentiation along the Rio Juruá but may be strongly geographically structured across their larger distribution (such as *Metachirus nudicaudatus* [fig. 38] and the species pair *Oryzomys megacephalus* and O. *perenensis* [fig. 74]). Others (*Caluromys lanatus* and *Didelphis marsupialis* [fig. 28]) are relatively undifferentiated throughout their respective sample ranges within Amazonia. At least for *O. perenensis*, estimated gene flow rates are sufficient to mitigate against population subdivision by drift alone throughout the Rio Juruá basin (Patton et al., 1996a). This is also the case for *Oligoryzomys microtis* (Patton et al., 1996a) and presumably for the other undifferentiated taxa as well, although sample sizes are inadequate to estimate the extent of gene flow for these from our molecular data. With an increase in the level of molecular divergence, however, species become more structured geographically. For example, all species with average Kimura two-parameter distances among haplotypes of 5% or higher exhibit geographically restricted and reciprocally monophyletic clades within the Rio Juruá basin, as do some with lower average divergences. The levels of divergence in this group extend above 11% (for clades of *Isothrix bistriata*), and encompass the amount of divergence between pairs of related species distributed within the river basin (e.g., *Dactylomys boliviensis* and *D. dactylinus* [9.5%], and *Proechimys gardneri* and *P. pattoni* [13.7%]). These Category I species are thus divided into geographic segments, each of which has been substantially isolated with respect to historical and present day gene flow.

Phylogeographic analysis can do more than simply identify taxa that are structured geographically. It can also distinguish between alternative historical hypotheses underlying patterns of differentiation (Harrison,

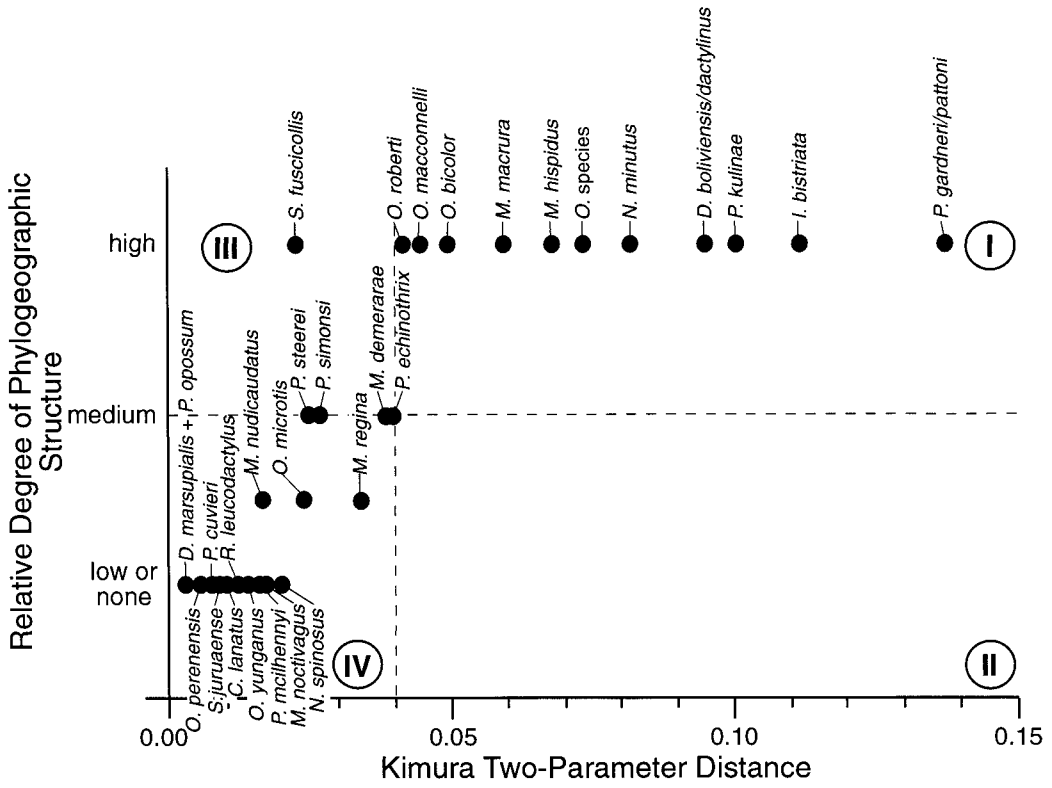

Fig. 163. The relationship between average sequence divergence (Kimura two-parameter distances) for the mitochondrial cytochrome-b gene and the relative degree of phylogeographic partitioning in 30 species or species pairs of nonvolant mammals of the Rio Juruá (following Avise et al., 1987). A high degree of phylogeographic structure indicates that haplotype lineages are confined to particular sections along the river, either left versus right bank or some pattern of regional partitioning. Medium structure is when some haplotype lineages are confined to single geographic areas while others are not. Finally, low or no structure characterizes those taxa where there is no relationship between haplotype lineages and geography. The four phylogeographic categories of Avise et al. (1987; Avise, 1989) are indicated with Roman numerals.

1991; Lynch, 1988; Patton and Smith, 1992; Patton et al., 1994; Patton and da Silva, 1998). As examples, three different hypotheses for riverine divergence can be formulated (fig. 164). In the first of these (fig. 164A), a river has been imposed on an existing taxon range, dividing it into two parts. If the river has formed a complete barrier, with time opposite bank populations will become comprised of reciprocally monophyly haplotype lineages which will remain sisters with regard to any haplotypes outside of the geographic area of interest. This outcome represents primary riverine diversification, which can be distinguished phylogenetically from secondary contact resulting from range expansions where the river forms only a common meeting place (fig. 164B). Phylogeography may also uncover instances of clear dispersal, with over water transfer from established populations on the opposite side (fig. 164C). We offer these as exemplars only, stressing that, in the early stages of divergence, gene genealogies may not be sufficiently robust to falsify one or more competing historical hypotheses. Given adequate time, however, hypotheses such as primary diversification versus secondary contact may be distinguishable by phylogeographic methodologies. The importance of this distinction in evaluating the riverine barrier hypothesis more generally was presented by Myers

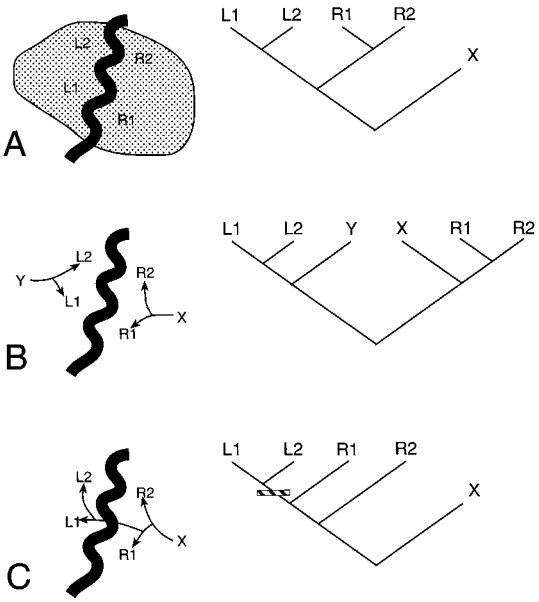

Fig. 164. Three alternative phylogeographic hypotheses. **A**: Primary Diversification: reciprocally monophyletic and sister clades bounded by a river that imposed itself on an existing species range. **B**: Secondary Contact: reciprocally monophyletic, but nonsister clades, bounded by a river that served as the secondary meeting point of clades that evolved elsewhere. **C**: Dispersal: paraphyletic relationship of right bank haplotypes relative to left bank ones due to one episode of cross-river transfer. See text for further explanation.

(1982; see also Patton et al., 1994; Patton and da Silva, 1998).

We have, therefore, used this type of phylogenetic approach to analyze divergence patterns in mtDNA cytochrome-b sequences for the nonvolant mammals of the Rio Juruá, with the goal of establishing the process (or processes) by which that divergence occurred. Data for four species have already been published, including those of the spiny tree rat *Mesomys hispidus* (Patton et al., 1994), the rice rats *Oligoryzomys microtis* and *Oryrzomys perenensis* (Patton et al., 1996a), and the saddle-back tamarin *Saguinus fuscicollis* (Peres et al., 1996). Those for two additional species, the terrestrial spiny rats *Proechimys simonsi* and *P. steerei*, are in preparation by M. D. Matocq, M. N. F. da Silva, and J. L. Patton. Each of these examples offer somewhat different patterns, but all provide important insights into the general divergence patterns and processes for the nonvolant mammals of the Rio Juruá, and elsewhere within Amazonia.

RIVERINE PATTERNS: Only one species among those examined exhibits a clear pattern of haplotype distribution that matches both expectations of the riverine divergence hypothesis; that is, both increasing differentiation from the headwaters towards the mouth along each bank and cross-river gene flow in upriver areas. This is the saddle-back tamarin, *Saguinus fuscicollis* (see Peres et al., 1996). With another two possible exceptions, all remaining species show varying degrees of within-locality haplotype uniqueness coupled with clear evidence of present, or past, cross-river transfer.

The level of cytochrome-b sequence differentiation among samples of tamarins is limited (an average of 2.3% among the eight haplotypes recovered), but the pattern of divergence matched both predictions of Wallace's model. Molecularly differentiated populations were separated on opposite sides of the river, concordant with the morphologically based subspecies *S. f. fuscicollis* and *S. f. melanoleucus* (see Hershkovitz, 1977, for complete taxon descriptions and distributions), but haplotypes were shared in opposite-bank samples in the Headwaters Region (Peres et al., 1996). This pattern of haplotype distribution, coupled with demonstrable morphological intermediacy of individual tamarins taken or seen on the left bank in the Headwaters Region (see Peres et al., 1996) supports an hypothesis of cross-river transfer. Saddle-back tamarins are terra firme specialists, so populations along the middle and lower sections of the river are separated not only by the width of the water but also by the extensive lateral expanse of floodplain várzea forest. The phylogeographic pattern of haplotype distribution is thus expected based on the ecological distribution of the species. Nevertheless, the Rio Juruá has apparently not served as a primary barrier in the evolutionary development of the subspecies occurring on opposite banks of the river. Phylogenetic analysis of the entire species complex (Jacobs et al., 1995) does not support a sister relationship between the two taxa interacting in the Rio Juruá basin (*fus-*

cicollis and *melanoleucus*), as would be required if the river were a primary barrier (that is, the phyletic pattern is that of Fig. 164B, not 164A; see Patton and da Silva, 1998).

Two other possible examples of riverine diversification among our samples are that of the scansorial murid *Oecomys* species, a member of the *O. bicolor* species complex (fig. 86), and the terrestrial echimyid *Proechimys echinothrix* (fig. 142). Only three individuals of *O.* species were obtained along the river, but each came from separate localities, two on the left bank and one on the right. The left bank specimens are nearly identical to one another (0.24% sequence divergence) although their respective localities are several hundred kilometers distant (fig. 80). These are, however, deeply divergent from the single individual taken at a right bank locality (7.29%; see fig. 86). In the case of *P. echinothrix*, samples are likewise limited, but those from the right bank locality of Vai-Quem-Quer (locality **15**) differ from those of two left bank localities (Barro Vermelho [locality **12**] and Vira-Volta [locality **14**]) by more than 4% (fig. 145). No other taxon among our sample exhibits a pattern of differentiation concordant with river bank, although there are many examples of taxa comprised of deeply divergent and reciprocally monophyletic clades (fig. 162).

Unlike the tamarins, each of the five murid and echimyid species for which extensive molecular data are available exhibits a substantial number of haplotypes shared among localities within and among the four sampled geographic regions along the river, including numerous examples of cross-river sharing. We have summarized these examples by mapping the distribution of individual haplotypes in figs. 165 and 166. Despite clear examples of cross-river sharing of haplotypes in each species, different general patterns emerge. For example, *Mesomys hispidus* (fig. 166A) exhibits a reverse riverine pattern, with each Headwaters locality is comprised of unique haplotypes, but with some sharing among the mid-river localities and extensive sharing of the same haplotypes among all Mouth localities (see discussion in Patton et al., 1994). Since this species is an arboreal member of both terra firme and várzea forests, the distribution of haplotypes (and the degree of cross-river exchange) is perhaps most generally related to the amount and rapidity of land transfer due to the dynamic nature of channel meanders, which increases successively downriver. In contrast, haplotype sharing among localities along both sides of the river, as well as across it at nearly all points, characterizes both *Oligoryzomys microtis* and *Oryzomys perenensis* (fig. 165A, B). In *O. perenensis*, for example, although unique haplotypes are found at nearly all localities throughout the river basin, others are extremely broadly distributed, and one is present at 14 of 15 sampled sites (see also Patton et al., 1996a). Finally, the two species of terrestrial spiny rats (fig. 166B, C), one a terra firme and the other a várzea specialist, also offer striking contrasts in their patterns of haplotype sharing despite similar geographic distributions and levels of haplotype diversity (table 83). In both species

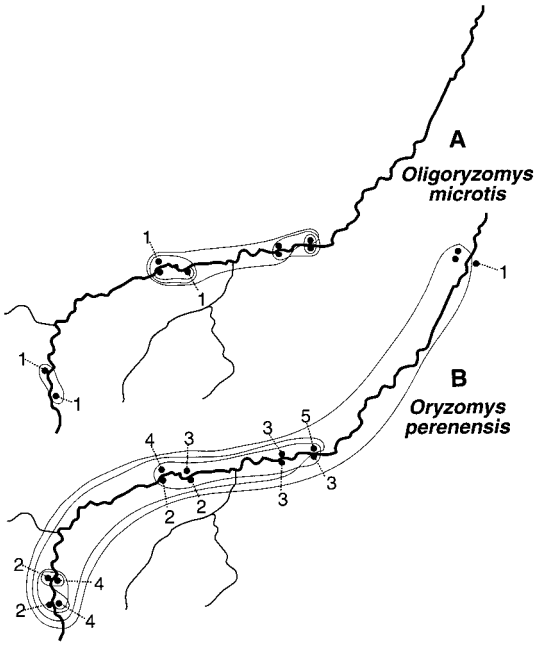

Fig. 165. Sample localities and distribution of haplotypes of the cytochrome-b gene for the pygmy rice rat *Oligoryzomys microtis* (above) and rice rat *Oryzomys megacephalus* (below) along the Rio Juruá. Single haplotypes shared among localities are indicated by ellipses connecting them. The number of haplotypes unique to each locality is also indicated.

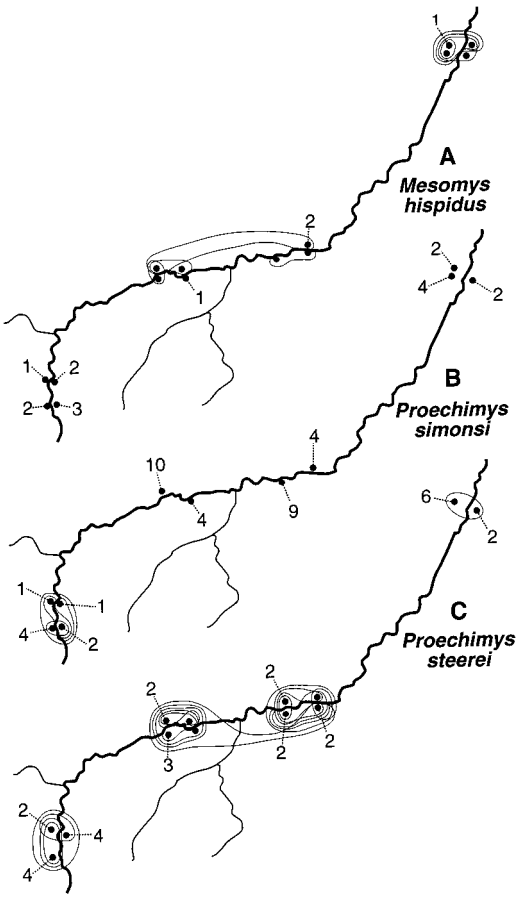

Fig. 166. Sample localities and distribution of haplotypes of the cytochrome-b gene for the spiny tree rat *Mesomys hispidus* (above) and two species of terrestrial spiny rats *Proechimys simonsi* (middle) and *P. steerei* (below) along the Rio Juruá. Single haplotypes shared among localities are indicated by ellipses connecting them. The number of haplotypes unique to each locality is also indicated.

haplotypes are shared across the river in the Headwaters Region, in adherence to expectations of the riverine barrier hypothesis, yet the pattern of sharing differs substantially between them elsewhere along the river. The várzea specialist, *P. steerei*, exhibits extensive cross-river, as well as along-river, sharing of a substantial proportion of its haplotypes within each geographic sampling region, and even among regions (fig. 166B). In contrast, all haplotypes of the terra firme *P. simonsi* are unique to specific localities, except in the Headwaters where there is substantial cross- and along-river sharing (fig. 166C).

Evidence for haplotype transfer across the river comes both from the current distribution of single haplotypes, as described above and mapped in figs. 165 and 166, as well as from phylogenetic analyses. Distinct but genealogically related haplotypes now distributed on opposite sides must necessarily represent the results of historical cross-river transfers. The distribution of single haplotypes, as described above, provides evidence of relatively recent, and possibly even ongoing dispersal movements across and along the river, while genealogical evidence suggests deeper historical dispersal events. We employed the coalescence methodology of Slatkin and Maddison (1989, 1990) to estimate the numbers of both types of cross-river haplotype transfers (see Patton et al., 1994, as an example of this approach for *Mesomys* and fig. 167 for *P. simonsi* and *P. steerei*; table 83).

The two species of terrestrial spiny rats exhibit essentially the same levels of haplotype diversity (table 83) yet offer dramatically different patterns of cross-river haplotype sharing, in the present (as noted above) and throughout their respective histories within the river basin. Both species contain the same number of total haplotypes in samples collected along the entire length of the river. Only 10 instances of cross-river haplotype transfer are estimated for *P. simonsi*, with most (7) of these historical rather than recent (fig. 167A). Moreover, cross-river haplotype sharing is limited to the Headwaters region despite the fact that the haplotypes present in this region are mostly basal in the tree. There are also five instances in *P. simonsi* of monophyletic assemblages of haplotypes restricted to single localities (Condor [locality **6**], Altamira [**9**], and Barro Vermelho [**12**]) or regions (Mouth Region). These data clearly suggest that most local populations, with the exception of those in the Headwaters, are not in continual genetic contact, even though the existence of two divergent monophyletic haplotypes clades at Altamira and the monophyletic assemblage in the Mouth localities, supports at least two important episodes of historical cross-river transfer. In contrast,

TABLE 83
Cytochrome-b Haplotype Diversity and Distribution for Five Species of Rodents Sampled Along the Rio Juruá, Western Brazil

Variable	*Oligoryzomys microtis*	*Oryzomys perenensis*	*Mesomys hispidus*	*Proechimys simonsi*	*Proechimys steerei*
No. individuals	76	164	95	150	205
No. localities	9	15	15	11	13
No. haplotypes	11	47	20	47	48
No. base pairs	414	414	399	390	390
No. unique/locality	4 (36.4%)	37 (78.7%)	12 (60.0%)	43 (91.5%)	30 (62.5%)
No. shared within regions	5 (45.5%)	3 (6.4%)	7 (35.0%)	4 (8.5%)	16 (33.3%)
Same side	1	1	3	2	4
Opposite side	3	1	1	1	5
Both sides	1	1	3	1	7
No. shared across regions	2 (18.2%)	7 (14.9%)	1 (5.0%)	0 (0.0%)	2 (4.2%)
Same side	0	0	1	0	0
Opposite sides	0	3	0	0	1
Both sides	2	4	0	0	1
Total transfers[a]	8/21 (38.1%)	21/82 (25.6%)	11/39 (28.2%)	10/92 (10.9%)	27/97 (27.8%)
Terminal	6/11 (54.5%)	9/47 (19.1%)	4/20 (20.0%)	3/47 (6.4%)	14/48 (29.2%)
Internal	2/10 (20.0%)	12/35 (34.3%)	7/19 (36.8%)	7/45 (15.6%)	13/49 (26.5%)

[a] Number of phyletically determined across river transfers and the number of possible transfers (i.e., terminal and internal nodes in the tree).

nearly three times as many (27) total haplotype transfers are recorded for *P. steerei*, with an equal numbers attributable to recent/current cross-river as to historical contact (fig. 167B). Given the differences between these two species in habitat preferences and life history (see accounts, above, and tables 63 and 75), these differences in both recent and historical cross-river haplotype transfers are to be expected. A várzea specialist, such as *P. steerei*, is likely to exhibit considerable contact between cross-river populations simply as a result of the continual land shifts accompanying lateral channel migration. The importance of the várzea habitat in this context is underscored by the patterns exhibited by both species of rice rats, which also show extensive cross-river sharing at all points of their sampled ranges along the river (fig. 165; discussion in Patton et al., 1996a). The trees we have chosen to illustrate in fig. 167 are maximum likelihood constructions. Somewhat different topologies are generated by maximum parsimony or other tree-building algorithms, but the relative numbers of historical versus "current" haplotype dispersal events remains the same.

It is possible, therefore, that riverine differentiation will eventually characterize some species, given sufficient time, no matter whether they dispersed into the river basin or were already present at the time the Rio Juruá was initially formed. This process is already apparent for *P. simonsi*, which shows both haplotype lineages (fig. 167A) and evident, even if minimal, morphometric divergence (fig. 151) associated with river bank. However, it is equally apparent that riverine divergence is not to be expected for all taxa. Certainly those whose biology dictates the habitat and reproductive potential typical for *Oryzomys perenensis*, for example, are likely to remain relatively unaffected by the presence of a river, such as the Rio Juruá.

NONRIVERINE PATTERNS: The first taxon for which we examined the pattern of haplotype divergence along the Rio Juruá was the spiny tree rat, *Mesomys hispidus* (Patton et al., 1994). In this case, while the mtDNA gene genealogy did identify two deeply divergent clades (6.8% divergence, on average), these corresponded to upriver versus downriver clades, not those on opposite banks (fig. 166A). One occurs through all sites of the Headwaters and Upper Central regions; the other overlaps with the first at one locality in

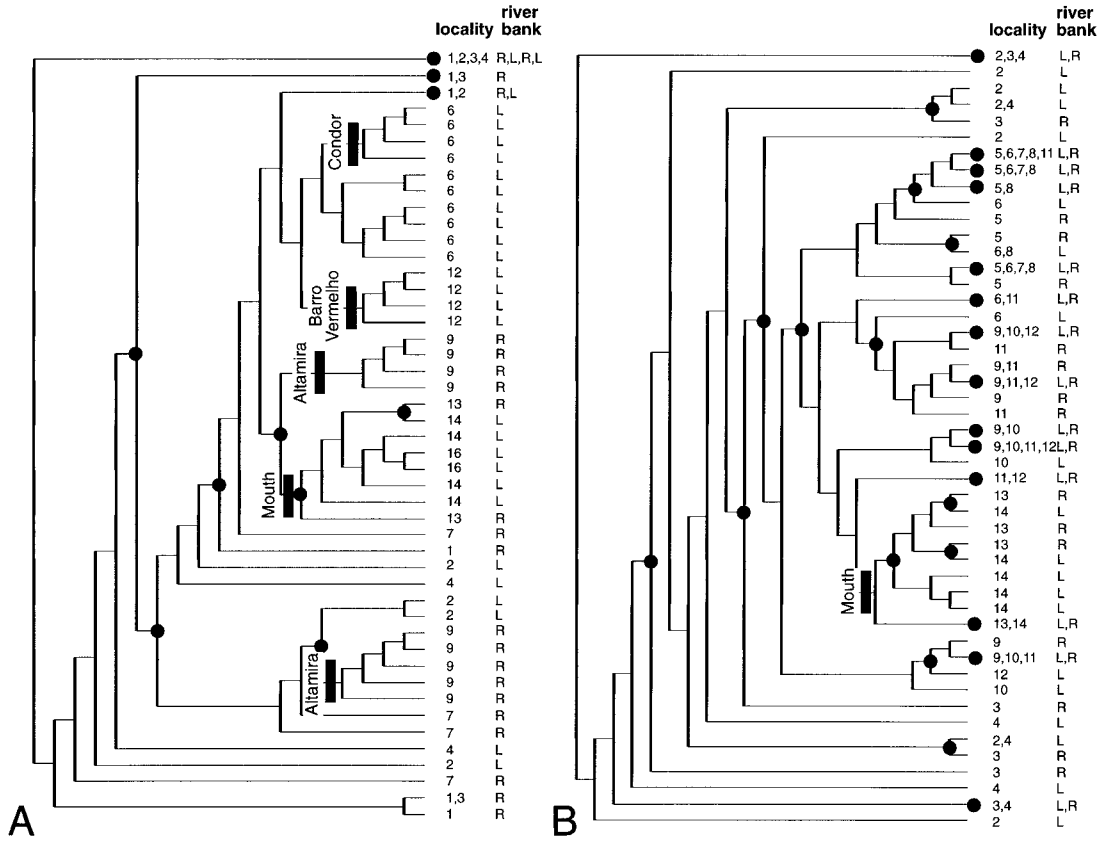

Fig. 167. (**A**) A maximum-likelihood tree of 47 cytochrome-b haplotypes of the terrestrial spiny rat, *Proechimys simonsi*, recovered from 150 individuals from 11 localities along the Rio Juruá. (**B**) A maximum-likelihood tree of 48 cytochrome-b haplotypes of the terrestrial spiny rat, *Proechimys steerei*, recovered from 205 individuals from 13 localities along the Rio Juruá. The locality (or localities) and river bank (R = right, L = left) for each haplotype are indicated. The solid circles indicate cases where individual haplotypes had to be transferred across the river given these particular tree topologies; those in a terminal position represent single haplotypes presently found on both banks, those at internal nodes hypothesize historical transfers to account for the genealogical distribution.

the Lower Central Region (Barro Vermelho, locality **12**) and otherwise occurs at all localities in the Lower Central and Mouth regions. The upriver versus downriver clade structure for this species was strongly supported in relation to alternative hypotheses of cross-river panmixia or riverine barrier by log-likelihood analysis (Patton et al., 1994).

The phylogeographic pattern exhibited by *M. hispidus* was an unexpected discovery. However, and equally unexpectedly, it is a pattern shared by all category I nonvolant mammals of the Rio Juruá (fig. 163), with the exception of *Oecomys* species. Four pairs of taxa exhibit a phylogeographic break between the Upper and Lower Central regional sampling sites, four between the Upper Central and Mouth, one between the Headwaters and Upper Central, and the last (*Proechimys pattoni* and *P. gardneri*) between either the Headwaters and Upper Central or the Upper and Lower Central (table 84). Gene genealogies of two taxa that include arboreal (*Mesomys hispidus*) and terrestrial (*Neacomys minutus*) species illustrate the phylogeographic break between the Upper and Lower Central regions (fig. 168). For *N. minutus* the break is complete, with no mixture of shared haplotypes between regions; for *Mesomys*, haplotypes of both clades are present at the

TABLE 84
Position of the Phylogeographic Break for the 10 Category I Taxon Pairs Relative to Sample Regions Along the Rio Juruá (Defined in fig. 1)

Taxon pair	Geographic position of phylogeographic break
Dactylomys boliviensis vs. *D. dactylinus*[a]	Headwaters–Upper Central
Proechimys pattoni vs. *P. gardneri*[b]	Headwaters–Lower Central
Neacomys minutus	Upper Central–Lower Central
Oecomys roberti	Upper Central–Lower Central
Mesomys hispidus[c]	Upper Central–Lower Central
Proechimys kulinae	Upper Central–Lower Central
Oecomys bicolor	Lower Central–Mouth
Oryzomys macconnelli	Lower Central–Mouth
Isothrix bistriata	Lower Central–Mouth
Makalata macrura	Lower Central–Mouth

[a] Position based on call structure; molecular samples are available only from Headwaters and Mouth regions.

[b] Position unclear, as neither species was collected in the Upper Central Region.

[c] Haplotype clades overlap at Barro Vermelho (locality **12**) in the Lower Central Region.

single Lower Central locality of Barro Vermelho (locality **12**; see Patton et al., 1994). Thus, 10 of the 11 category I species or species pairs (fig. 163) are divided into reciprocally monophyletic geographic segments, each of which has been substantially isolated with respect to gene flow for a considerable length of time, and with similar geographic distributions to those depicted in fig. 168 (for example, see the trees for *Oecomys bicolor* [fig. 86], *Oecomys roberti* [fig. 87], and *Proechimys kulinae* [fig. 142]). Accepting the principle of phylogeography (Avise, 1989; Riddle, 1996) that populations delineated by large phylogeographic gaps identify stable biogeographic barriers, if divergences for this set of taxa cannot be linked to the Rio Juruá itself, what then might have been a common event in their past?

LANDFORM EVOLUTION AND AMAZONIAN DIVERSIFICATION

Shared distribution patterns among diverse clades of organisms are more parsimoniously explained by the occurrence of extrinsic geological or climatic events, which affected all groups in the same way, than by the intrinsic characteristics of each taxon independently (Platnick and Nelson, 1978). Concordant distributions, or generalized tracks (Rosen, 1975), may thus be used as evidence to infer the biogeographical history of an area of interest.

The central portions of the Rio Juruá mark the phytogeographic transitional boundary between *floresta tropical densa* (downriver region) and *floresta tropical aberta* (upriver region), major terra firme plant formations that sit on different underlying soil formations (fig. 168; Projeto RadamBrasil, 1977). Positioned underneath this transitional area is a geological feature, the Iquitos Arch, a Precambrian zone of prior uplift within the western Amazon (Putzer, 1984), one of several deep basin features that generally delimit broad phytogeographic units across Amazonia (Daly and Prance, 1989). Although this feature is not part of the contemporary surface topography of western Amazonia, it marks the boundary between the pre-Pleistocene Acre and Central Amazon fluvial deposition systems (Räsänen et al., 1987, 1990, 1992). The Acre Basin, at least, apparently underwent impressive successive subsidence coincidental with the last major episode of Andean uplift, which began in the late Miocene and extended through the Pliocene into the Pleistocene (Lundberg et al., 1998). Our Upper Central Regional localities are on the upriver side of the underlying Iquitos Arch; those of the Lower Central Region are just downriver of the point where the Arch rises closest to the current surface (fig. 169).

The topographic and consequent ecological impact of landform changes resulting from Andean tectonic events are not known, nor is it understood whether, much less how, such events might be related causally to the phylogeographic patterns we observe. It is clear, nevertheless, that the arches have been undergoing active deformation since the Miocene due to Andean orogenic events, with the result that the structural character of the entire Amazon Basin has been altered (Mertes et al., 1996; Lundberg et al., 1998). Hence, the concordance of phylogeographic breaks with geological structures, such as the Iquitos Arch and the Acre and Central Am-

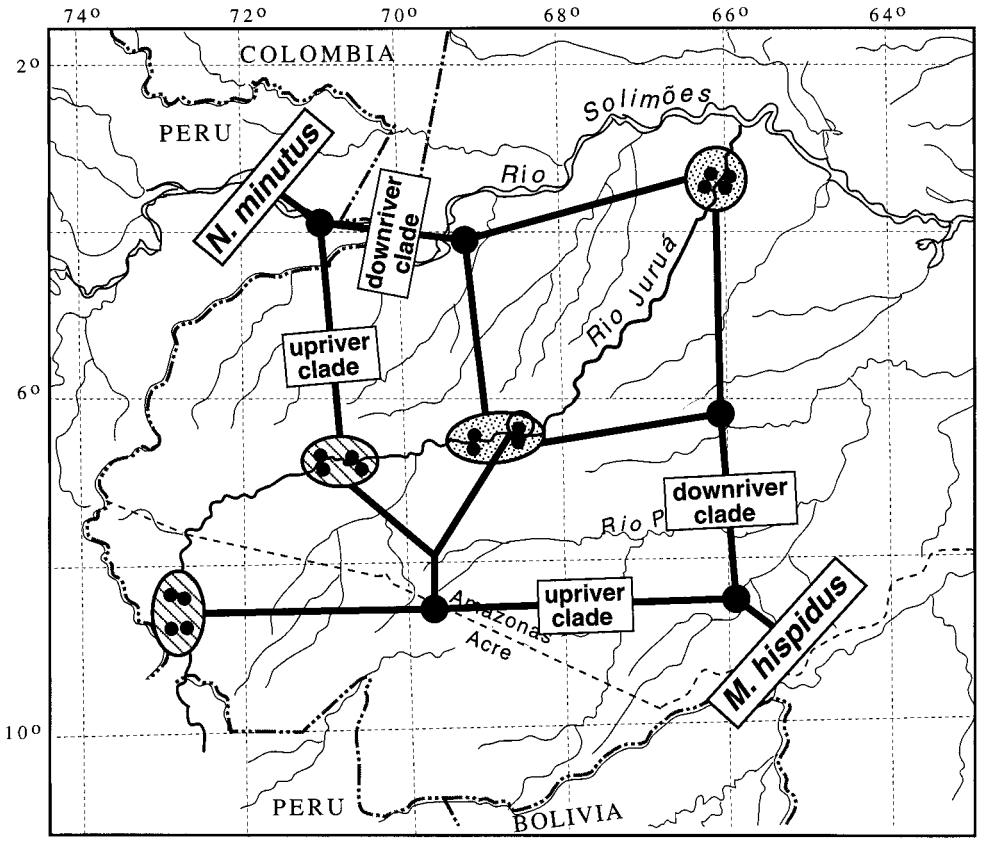

Fig. 168. Generalized gene genealogies of *Neacomys minutus* and *Mesomys hispidus*, two phylogeographic category I species of the Rio Juruá illustrating common patterns in their respective distributions of reciprocally monophyletic cytochrome-b clades. In both cases, as well as in nine other species or species-pairs, monophyletic clades are split into upriver (Headwaters and Upper Central regions) and downriver (Lower Central and Mouth regions), although overlap may be present in either the Upper or Lower Central regions, as is true for *M. hispidus*.

azon basins, are suggestive of a relationship between landform evolution in western Amazonia and these phylogeographic patterns. This relationship may have been a direct one, wherein lithospheric flexure due to tectonic loading of the Andes resulted in positive relief of the Iquitos Arch and thus the physical separation of faunas in the Acre and Central Amazon basins. Divergence under this scenario would have been strictly allopatric. Alternatively, the Iquitos Arch may only have affected the direction and extent of surface drainage systems, and thus soil formation, resulting in the present-day differences in major soil types and vegetation through the Rio Juruá basin. Consequent habitat mosaics and transitions could thus have provided the selection gradients needed for parapatric divergence (Endler, 1982; see Smith et al., 1997, and Orr and Smith, 1998, for recent discussions of the role of ecotones in rainforest diversification). While these, or other possible hypotheses remain to be tested, it is clear that the potential importance of an active tectonic history within Amazonia has been little appreciated by most students of the organismal diversification of the region until quite recently. Its importance cannot be underestimated, as emphasized by following quote from Räsänen et al. (1990: 330–331):

> The late Cenozoic foreland dynamics partitioning the western Amazon lowlands into more distinct intraforeland basins is the latest phase in the relief evolution which changed the Tertiary Neotropical low-

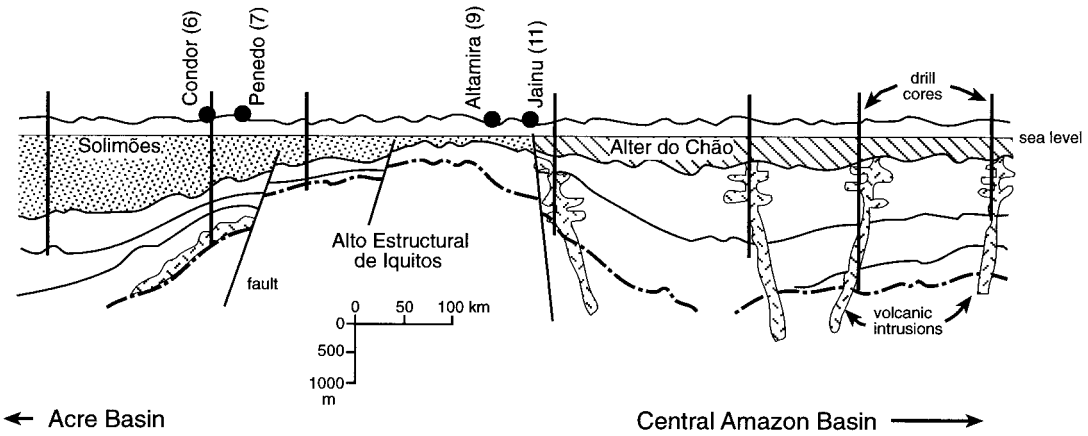

Fig. 169. Geological cross-section through the central portion of the Rio Juruá illustrating the position of the underlying structural Iquitos Arch relative to Upper Central and Lower Central sample sites, the positional shift of major soils from the downriver Alter do Chãu to upriver Solimes formations, and position and depths of the upper Acre Subbasin and lower Central Amazon Subbasin. The geographic position of drill core sites from the Brazilian oil consortium, Petrabras, are indicated. Redrawn from Fig. 10 in volume 15 of the Projeto RadamBrasil (1977).

> lands into the present Andes . . . . Instead of reflecting locations of isolated Pleistocene broad-leaved forests (climatic refuges), modern species distributions in the western Amazon may be a result of historical species dynamics controlled by landscape evolution. Owing to late Cenozoic palaeogeographical changes in relief evolution, the forest biota of the western Amazon have probably alternated between allopatry and sympatry, commonness and rarity, and continuous distribution and fragmentation . . . .

The linkage between late Cenozoic landform changes and the diversification of nonvolant mammals within the Rio Juruá basin, and elsewhere within Amazonia, is strengthened by estimates for the timing of lineage splits generated from the molecular sequence data. Although any such estimates are necessarily approximate, and with large errors (Hillis et al., 1996), divergence calculations based on third position transversions for the cytochrome-b gene (following Irwin et al., 1991, and Smith and Patton, 1993) for the 10 category I taxon pairs range from somewhat less than 1 to at least 3 million years (table 85; see also da Silva and Patton, 1993, and Patton and da Silva, 1998). Even given the uncertainties regarding rates of molecular evolution and the likely episodic time kept by any molecular clock, the extensive divergence values between most category I taxa (table 85) suggest vicariant events much more ancient than have been commonly invoked for forest refuge formation of the late Pleistocene (Haffer, 1969; but see Haffer, 1993b). These deep divergences, and the presence of regionally sharply defined and reciprocally monophyletic haplotype lineages in many, even if not all, small mammals offer no support for either the hypothesis that a freshwater lake covered most of lowland Amazonia in the late Pleistocene/early Holocene (Campbell, 1984, 1990; Frailey et al., 1988) or the widely held view that divergences within Amazonia resulted from late Pleistocene forest fragmentation (Haffer, 1969; Vanzolini and Williams, 1970; see da Silva and Patton, 1998, Patton and da Silva, 1998).

The hypothesis of a linkage between landform change and lineage diversification can be tested, at least in part, by examining the pattern of phylogeographic differentiation at other points where the Iquitos Arch underlies major drainages to the north and south of the Rio Juruá; for example, along the upper Rio Solimões downriver from Tabatinga (Projeto RadamBrasil, 1977) and the Rio Purus downriver from Boca do Acre (Projeto RadamBrasil, 1978). If similar patterns of differentiation exist in these areas, then the positions of paleobasins may signal present-day centers of endemism and diversity more

TABLE 85
Estimated Divergence Times (Myr) for the Major mtDNA Clades of Ten Taxon Pairs Within the Rio Juruá
Based on the average number of 3rd positon transversions (TV) between all pairs of haplotypes from the different clades. Divergence time estimated at a rate of 0.5%/Myr for artiodactyls (Irwin et al., 1991) and 1.7%/Myr for murid rodents (Smith and Patton, 1993).

Taxon pair	Mean TV	Mean no. codons	Estimated divergence time (Myr)	
			0.5%	1.7%
Neacomys minutus: upriver vs. downriver	15.75	267	11.798	3.469
Oecomys bicolor: upriver vs. downriver	4.5	267	3.371	0.721
Oecomys roberti: upriver vs. downriver	4.5	267	3.371	0.721
Oryzomys macconnelli: upriver vs. downriver	7.0	267	5.243	1.542
Dactylomys bolivianus vs. *D. dactylinus*	8.0	264	6.061	1.783
Isothrix bistriata: upriver vs. downriver	9.67	231	8.372	2.462
Makalata macrura: upriver vs. downriver	6.5	264	4.924	1.448
Mesomys hispidus: upriver vs. downriver	4.4	264	3.333	0.980
Proechimys gardneri vs. *P. pattoni*	6.0	210	5.714	1.681
Proechimys kulinae: upriver vs. downriver	9.0	264	6.818	2.005
Mean ± standard error	7.53 ± 1.09	256.5 ± 6.21	5.901 ± 0.843	1.681 ± 0.265

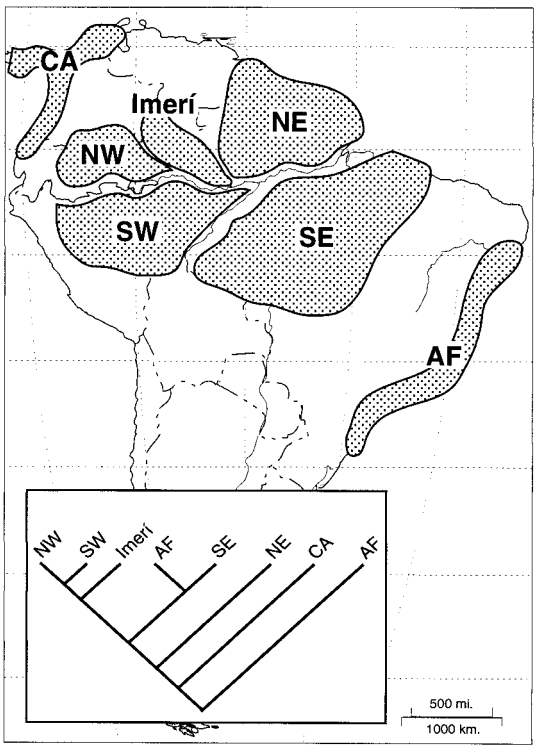

Fig. 170. Hypothesis of area relationships for lowland tropical forests of South America based on analyses of avian phyletic and distributional data (from Cracraft and Prum, 1988).

so than the putative Pleistocene refugia suggested by other workers (review in Brown, 1987). This perspective reinforces the recent view (Bush, 1994) that Amazonian speciation, and thus geographic patterns of species diversity, cannot be explained entirely by any single model of vicariance or climatic change. Rather, it is quite likely that pre-Quaternary events have established the major regional divisions of species complexes, with subsequent geographic differentiation, and particularly the redistribution of extant species, due to forest refuge formation (Haffer, 1969), distributional shifts due to intrinsic tolerances of individual species (Colinvaux, 1996; Colinvaux et al., 1996), floodplain dynamics (Salo 1987, 1988), and/or ecological heterogeneity (Tuomisto et al. 1995), superimposed upon these earlier patterns.

PHYLOGEOGRAPHIC PATTERNS WITHIN AMAZONIA

Both the geographic distribution of taxa comprising a biota and their phylogenetic relationships are strongly effected by the history of the areas where they evolved. Hence, an understanding of distributions and phyletic patterns is basic to any effort to determine the processes by which regional biotic diversification has taken place. In this section, we use our limited molecular phylogeographic

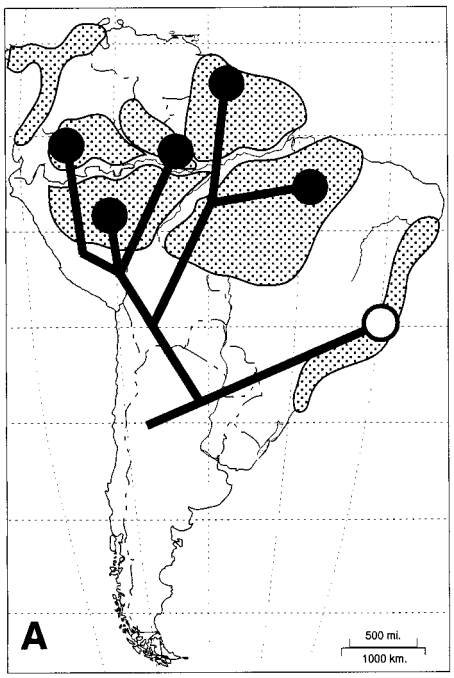

Didelphis marsupialis / aurita

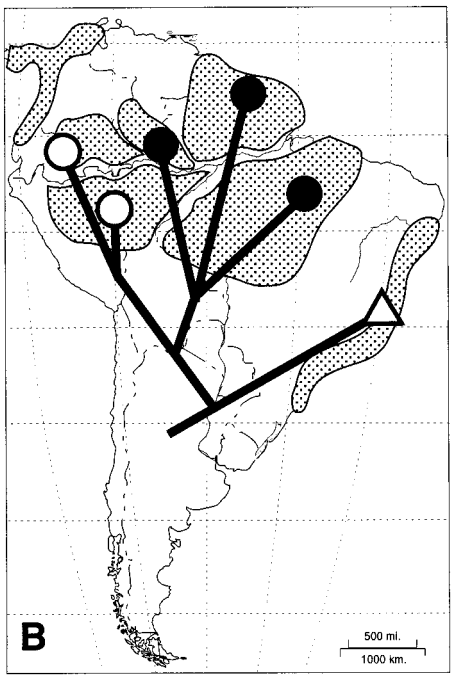

Oryzomys perenensis / megacephalus / laticeps

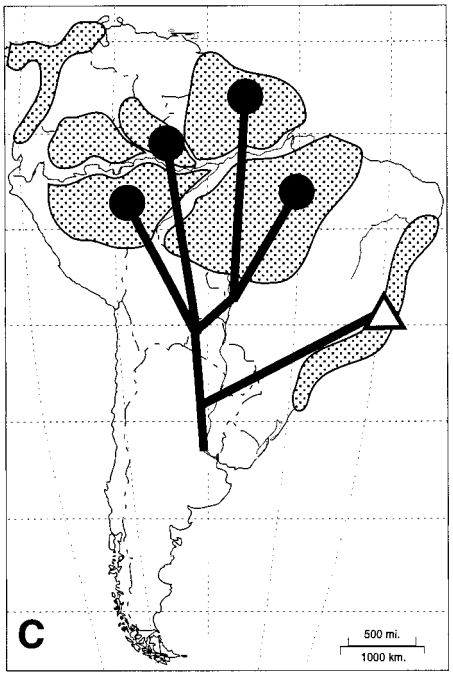

Microureus demerarae / limae

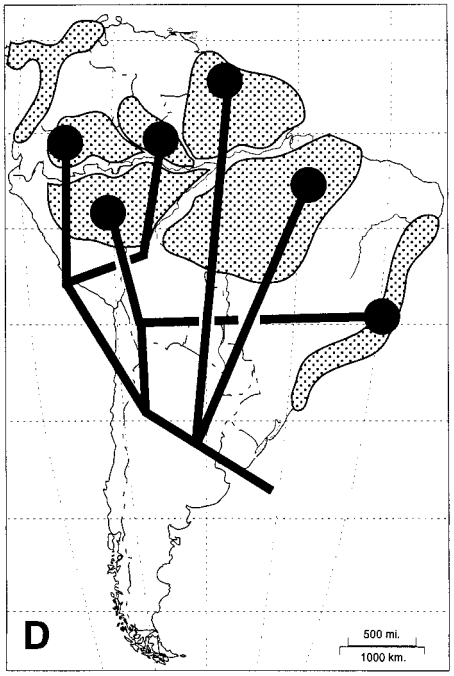

Metachirus nudicaudatus

data for small-bodied, nonvolant mammals to examine patterns of area relationships within greater Amazonia. We do this only to suggest future avenues of needed research, and fully recognize that the density and extent of geographic sampling for most taxa is currently inadequate for anything but gross approximations to actual patterns. We also stress that the uncertainly of both the alpha-taxonomy and distributional limits of many Amazonian small mammals potentially compromises the patterns apparent in our data. We have presented some of these patterns in previous publications (e.g., da Silva and Patton, 1993, 1998; Patton et al., 1997; and Patton and da Silva, 1998). However, the data base we summarize here is of a larger extent, relative to the number of taxa sampled and the number of localities represented for each taxon.

Da Silva and Patton (1998) provide a generalized synopsis of geographic areas of sharp molecular transition within Amazonia where reciprocally monophyletic clades of diverse marsupials and rodent abut. The region where the sharpest phylogeographic break occurs is along the lower Rio Negro northwest of Manaus, followed by the division through the central Rio Juruá we describe above as well as along the upper Rio Solimões. The average Kimura two-parameter distances for paired taxa across each of these regions is 9.72%, 7.92%, and 7.73%, respectively. Interestingly, divergence across the lower Rio Amazonas downriver from Manaus showed the least degree of differentiation, with an average of only 3.28%. The lessened degree of differentiation in paired taxon comparisons across the lower Amazon mirrors the higher similarity in primate community structure on opposite banks in this region as opposed to that upriver from Manaus (Ayres and Clutton-Brock, 1992). Clearly, however, there is great differentiation among regional areas occupied by a diverse set of mammalian taxa within Amazonia.

Among the first phylogenetic analyses of relationships among elements of the lowland Amazonian fauna was that for birds (Cracraft, 1985, 1988; Cracraft and Prum, 1988). These authors defined regional areas within Amazonia and related these to the extralimital lowland tropical forests of Central America, northwestern South America, and the Atlantic coast of Brazil. They based phylogenies on cladistic analyses of plumage characters, and combined cladograms to infer the history of areas of endemism (fig. 170). In a more recent paper, Bates et al. (1998) used raw distributional data to address the same question. Greater Amazonia was divided into five major geographic areas: NW (also termed Napo)—roughly that region north of the Río Marañón in northern Perú and extending through eastern Ecuador to southeastern Colombia; Imerí—the upper Rio Negro of southern Venezuela south to include that region between the lower Rio Negro and Rio Solimões; NE (or Guyanan)—the region east of the Rio Negro and north of the Rio Amazonas; SW (or Inambarí)—that portion of Perú, western Brazil, and northern Bolivia south of the Río Marañón–Rio Solimões axis and west of the Rio Madeira; and SE (or Belém-Pará)—that region of Brazil south of the Rio Amazonas and east of the Rio Madeira (see fig. 170). Bates et al. (1998) further subdivide the SE section. The SE, SW, NE, and combined NW-Imerí regions correspond generally to the original four Amazonian ''districts'' defined by Wallace (1852).

The hypothesis of area relationships developed by Cracraft and his colleagues (fig. 170) argues that the geographic subdivisions of Amazonia form a monophyletic assemblage of areas. Species diversification within Amazonia has thus been substantially in situ, with little or no historical influence from

←

Fig. 171. Phylogeographic patterns of four taxa of small-bodied, nonvolant mammalian taxa codistributed in Amazonia and the Atlantic Forest based on the mtDNA sequence data summarized in the individual species accounts. The avian faunal areas of fig. 170 are indicated and the topologies are based on haplotypes from each of the areas for which data are available. Symbols at the tips of each branch indicate the same, or different, species, either by current taxonomy or by the arguments made herein.

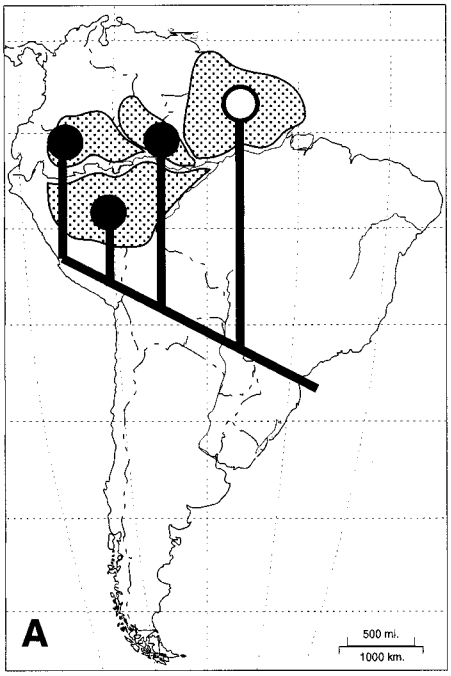

Isothrix bistriata / pagurus

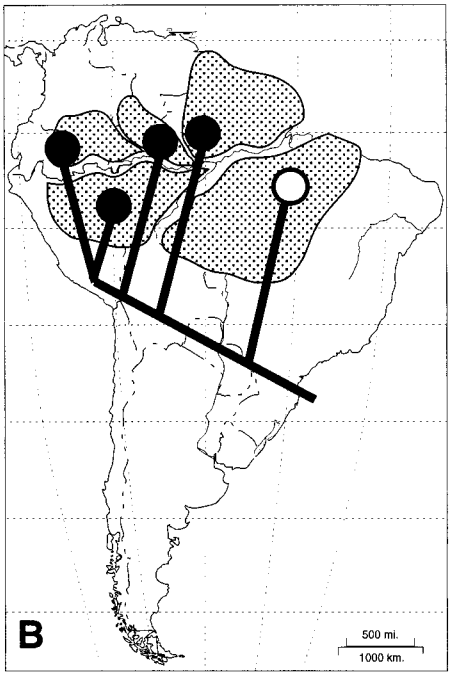

Makalata macrura / didelphoides

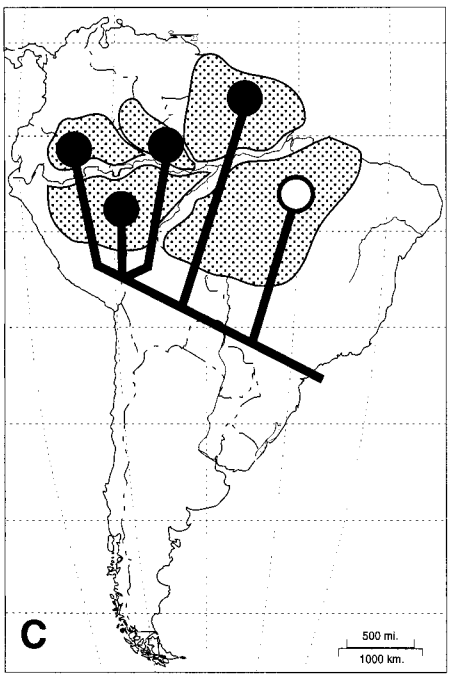

Mesomys hispidus / stimulax

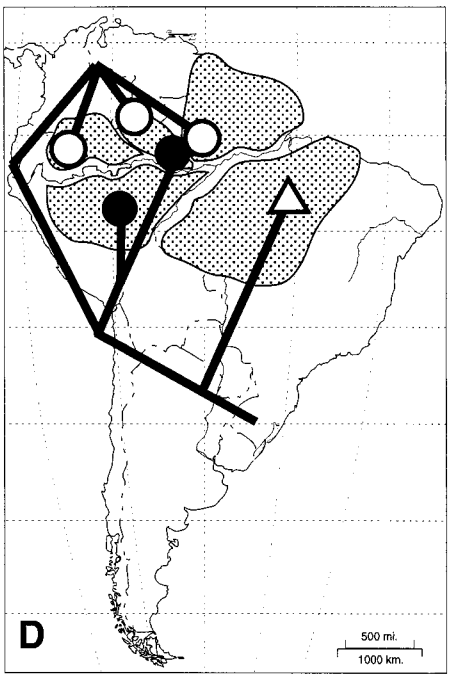

Proechimys goeldii - group

Central America and only marginal contact with the Mata Atlântica. Elements of the southeastern Brazilian Mata Atlântica fauna are generally the most divergent, such that coastal Brazil is the geographic sister area to all other lowland tropical forested regions. Examples are apparent, however, where Mata Atlântica taxa exhibit a sister relationship with an Amazonian area, in all cases with SE Amazonia (Belém-Pará).

We use this hypothesis of relationships among lowland tropical forest regions as a model with which to compare our data for Amazonian small mammals (figs. 171 and 172). In so doing, however, we emphasize that we have not equally sampled all geographic regions, especially the NE and SE. Consequently, the topologies of haplotype trees will possibly change as new localities are added for each geographic area. We also consider area relationships only within Amazonia and between that vast region and the Mata Atlântica, since we lack data for most taxa from localities in northwestern South America or Central America.

Resolution of area relationships is limited for many of the nonvolant small mammal species that we summarize in the accounts above. Nevertheless, reciprocal haplotype monophyly typically characterizes the geographic areas where data are available (see the haplotype trees for each taxon presented in the ''Species Accounts,'' above), and the patterns of area relationships are largely congruent with those presented for birds by Cracraft and colleagues. Where we have examined taxa that are distributed both within Amazonia and the Mata Atlântica, the latter area is usually the geographic outgroup to an assemblage of Amazonian forms (fig. 171A-C). Only in the case of *Metachirus nudicaudatus* is this pattern not apparent (fig. 171D). For both the *Oryzomys megacephalus* complex (fig. 171B) and the cluster of taxa (species or subspecies) in what is now the single species *Micoureus demerarae* (fig. 171C), the Amazonian taxa also form a monophyletic assemblage relative to their Mata Atlântica counterparts. Relationships among the geographic areas within Amazonia also display a rather uniform pattern. Most taxa divide within Amazonia into western and eastern groups of areas bounded by the north-south axis formed by the rios Negro and Madeira (figs. 171A, C, and D; fig. 172A–C). Alternative patterns of area relationships are only found in two examples: in the *Oryzomys megacephalus* complex, where samples from the Imerí region share a phyletic sister relationship with NE and SE Amazonia (fig. 171B), and in the *Proechimys goeldii*- group, where areas largely divide into north-south regions along the Rio Amazonas–Rio Solimões axis. How stable these patterns are, in fact, must await additional sampling, both of new geographic areas for the taxa examined herein as well as by adding additional species complexes of mammals and other organisms.

CONCLUDING REMARKS

The Amazonian fauna, mammalian or otherwise, is diverse and complex, with a long and convoluted history. After nearly two centuries of scientific inquiry, we are only now beginning to appreciate the true nature of diversity of small-bodied mammals over much of Amazonia, and we are only now beginning to develop hypotheses of species boundaries, of geographic distributions, and of phyletic relationships for much of this fauna. Sadly, we are achieving this level of appreciation only at a time when the natural

←

Fig. 172. Phylogeographic patterns of four taxa of small-bodied, nonvolant mammalian taxa with distributions limited to various areas within Amazonia and based on the mtDNA sequence data summarized in the individual species accounts. Again, the avian faunas areas of fig. 170 are indicated, and the topologies are based on haplotypes from each of the areas for which data are available. Symbols at the tips of each branch indicate the same, or different species, either by current taxonomy or by the arguments made herein.

systems of Amazonia are increasingly stressed by human encroachment, and thus when detailed knowledge of the ecology and evolution of the biota is in greatest need.

In closing this contribution, we paraphrase the final statement of Musser et al. (1998) in their review of the *Oryzomys ''capito''* complex. We are impressed with how much still needs to be learned about Neotropical mammals, especially the small-bodied nonvolant taxa. Our report represents only the beginning, an understanding in the museum and laboratory of the first lesson in the forest. We have posed as many questions as we have provided answers, which is how science should proceed. We can only hope, therefore, that our work will spur a new wave of exploration of Amazonia, the most biological diverse region in the world, even if the result is only to prove our ideas wrong. Nevertheless, we remain impressed with the prescience of Alfred Russel Wallace, who saw the forest as well as the trees in his description of faunal areas within Amazonia, and, as a result, developed the first testable hypothesis for the diversification of this fauna.

REFERENCES

Ab'Saber, A. N.
1977. Os domínos morfoclimáticos na América do sul. Primeira aproximação. Geomorfologia (São Paulo) 53: 1–23.

Adler, G. H.
1995. Fruit and seed exploitation by Central American spiny rats, *Proechimys semispinosus*. Studies Neotrop. Fauna Environ. 30: 237–244.

Aguilera, M., and M. Corti
1994. Craniometric differentiation and chromosomal speciation of the genus *Proechimys* (Rodentia: Echimyidae). Z. Säugetierkd. 59: 366–377.

Aguilera, M., and A. Pérez-Zapata
1989. Cariologia de *Holochilus venezuelae* (Rodentia, Cricetidae). Acta Cient. Venez. Genetica 40: 198–207.

Aguilera, M., A. Pérez-Zapata, N. Sanginés, and A. Martino
1993. Citogenetica evolutiva en dos generos de Roedores suramericanos: *Holochilus* y *Proechimys*. Biol. Soc. Zool. Uruguay 8: 49–61.

Allen, J. A.
1900. Descriptions of new American marsupials. Bull. Am. Mus. Nat. Hist. 13: 191–199.

Anderson, S.
1997. Mammals of Bolivia, taxonomy and distribution. Bull. Am. Mus. Nat. Hist. 231: 652 pp.

Aniskin, V. M.
1993. Three new karyotypes of prickly chinchillas of the family Echimyidae (Rodentia). Genetika 29: 1500–1507. [In Russian].

Aniskin, V. M., V. M. Malygin, A. A. Varshavski, and S. I. Isayev
1990. Karyological interrelations of three chromosomes forms of spiny rats of the genus *Proechimys* (Rodentia, Echimyidae). Genetika 27: 1066–1075. [In Russian].
1991. Chromosomes differentiation of spiny rats of the genus *Proechimys* (Rodentia, Echimyidae). Ibid. 27: 1431–1439. [In Russian].

Atramentowicz, M.
1986. Dynamique de population chez trois marsupiaux didelphidés de Guyane. Biotropica 18: 136–149.

Ávila-Pires, T.C.S.
1995. Lizards of Brazilian Amazonia (Reptilia: Squamata). Zool. Verh. (Leiden) 299: 637 pp.

Avise, J. C.
1989. Gene trees and organismal histories: a phylogenetic approach to population biology. Evolution 43: 1192–1208.

Avise, J. C., J. Arnold, R. M. Ball, E. Bermingham, T. Lamb, J. E. Neigel, C. A. Reeb, and N. C. Saunders
1987. Intraspecific phylogeography: the mitochondrial bridge between population genetics and systematics. Annu. Rev. Ecol. Syst. 18: 489–522.

Ayres, J. M., and T. H. Clutton-Brock
1992. River boundaries and species range size in Amazonian primates. Am. Nat. 140: 531–537.

Barros, M. A., O. A. Reig, and A. Pérez-Zapata
1992. Cytogenetics and karyosystematics of South American oryzomyine rodents (Cricetidae: Sigmodontinae). IV. Karyotypes of Venezuelan, Trinidadian, and Argentinian water rats of the genus *Nectomys*. Cytogenet. Cell Genet. 59: 34–38.

Barton, N. H., and I. Wilson
1995. Genealogies and geography. Philos. Trans. R. Soc. London Ser. B Biol. Sci. 349: 49–59.
Bates, J. M., S. J. Hackett, and J. Cracraft
1998. Area-relationships in the neotropical lowlands: An hypothesis based on raw distributions of Passerine birds. J. Biogeogr. 25: 783–793.
Blair, W. F.
1939. Some effects of stream-valley flooding on mammalian populations in eastern Oklahoma. J. Mammal. 20: 304–306.
Bodmer, R. E.
1990. Responses of ungulates to seasonal inundations in the Amazon floodplain. J. Trop. Ecol. 6: 191–201.
Bonvicino, C. R., P. S. D'Andrea, R. Cerqueira, and H. N. Seuánez
1996. The chromosomes of *Nectomys* (Rodentia, Cricetidae) with 2n = 52, 2n = 56, and interspecific hybrids (2n = 54). Cytogenet. Cell Genet. 73: 190–193.
Brown, K. S., Jr.
1982. Historical and ecological factors in the biogeography of aposematic neotropical butterflies. Am. Zool. 22: 453–471.
1987. Conclusions, synthesis, and alternative hypotheses. *In* T. C. Whitmore and G. T. Prance (eds.), Biogeography and Quaternary history of tropical America. Monogr. Biogeogr. 3: 175–196. New York: Oxford Univ. Press.
Bush, M. B.
1994. Amazonian speciation: a necessarily complex model. J. Biogeogr. 21: 5–17.
Cabrera, A.
1916. El tipo de *Philander laniger* Desm. en el Museo de Ciencias Naturales de Madrid. Bol. R. Soc. Esp. Hist. Nat. 16: 514–517.
1957 (1958). Catálogo de los mamíferos de América del Sur. Rev. Mus. Argent. Cien. Nat. ''Bernardino Rivadavia'' Cienc. Zool. 4(1): 1–308.
1961. Catálogo de los mamíferos de América del Sur. Ibid. 4(2): 309–732.
Campbell, K. E., Jr.
1984. Holocene flooding and species diversity in southwestern Amazonia. Quart. Res. 21: 369–375.
1990. The geological basis of biogeographic patterns in Amazonia. *In* G. Peters and R. Hutterer (eds.), Vertebrates in the tropics: 33–43. Bonn: Alexander K. Zool. Res. Inst. Zool. Mus.
Campbell, D. G., J. L. Stone, and A. Rosas, Jr.
1992. A comparison of the phygosociology and dynamics of three floodplain (várzea) forests of known ages, Rio Juruá, western Brazilian Amazon. Bot. J. Linn. Soc. 108: 213–237.
Capparella, A. P.
1988. Genetic variation in neotropical birds: implications for the speciation process. Acta Congr. Int. Ornithol. 19: 1658–1664.
1991. Neotropical avian diversity and riverine barriers. Ibid. 20: 307–316.
Carleton, M. D., and G. G. Musser
1989. Systematic studies of oryzomyine rodents (Muridae, Sigmodontinae): a synopsis of *Microryzomys*. Bull. Am. Mus. Nat. Hist. 191: 83 pp.
Carvalho, C. T.
1957. Alguns mamíferos do Acre ocidental. Bol. Mus. Para. Emilia Goeldi 6: 1–22.
Catzeflis, F., C. Richard-Hansen, C. Fournier-Chambrillon, A. Lavergne, and J.-C. Vié
1997. Biométrie, reproduction et sympatrie chez *Didelphis marsupialis* et *D. albiventris* en Guyane Française (Didelphidae: Marsupialia). Mammalia 61: 231–243.
Cerqueira, R.
1985. The distribution of *Didelphis* in South America (Polyprotodontia, Didelphidae). J. Biogeogr. 12:135–145.
Charles-Dominique, P.
1983. Ecology and social adaptations of didelphid marsupials: Comparisons with eutherians of similar ecology. *In* J. F. Eisenberg and D. G. Kleiman (eds.), Advances in the study of mammalian behavior: 395–422. Philadelphia: Am. Soc. Mammal.
Charles-Dominique, P., M. Atramentowicz, M. Charles-Dominique, H. Gérard, A. Hladik, C. M. Hladik, and M. F. Prévost
1981. Les mammifères frugivores arboricoles nocturnes d'une forêt guyanaise: interrelations plantes-animaux. Rev. Ecol. Terre Vie 35: 341–435.
Cody, M. L.
1996. Introduction to neotropical diversity. *In* A. C. Gibson (ed.), Neotropical biodiversity and conservation. Occas. Publ. Mildred E. Mathias Bot. Gard. 1: 1–20.
Colinvaux, P. A.
1996. Quaternary environmental history and forest history in the Neotropics. *In* J. B. C. Jackson, A. F. Budd, and A. G. Coates (eds.), Evolution and environment in tropical America: 359–405. Chicago: Univ. Chicago Press.

Colinvaux, P. A., P. E. De Oliveira, J. E. Moreno, M. C. Miller, and M. B. Bush
1996. A long pollen record from lowland Amazonia: forest and cooling in glacial times. Science 274: 85–88.
Colwell, R. K., and J. A. Coddington
1994. Estimating terrestrial biodiversity through extrapolation. Philos. Trans. R. Soc. London Ser. B Biol. Sci. 345: 101–118.
Cracraft, J.
1985. Historical biogeography and patterns of differentiation within the South American areas of endemism. *In* P. A. Buckley et al. (eds.), Neotropical ornithology: 49–84. Washington, D.C.: Am. Ornithol. Union.
1988. Deep-history biogeography: retrieving the historical pattern of evolving continental biotas. Syst. Zool. 37: 221–236.
Cracraft, J., and R. O. Prum
1988. Patterns and processes of diversification: speciation and historical congruence in some neotropical birds. Evolution 42: 603–620.
Daly, D. C., and G. T. Prance
1989. Brazilian Amazon. *In* D. G. Campbell and H. D. Hammond (eds.), Floristic inventory of tropical countries: the status of plant systematics, collections, and vegetation, plus recommendations for the future: 401–426. New York: New York Botanical Garden.
da Silva, M. N. F.
1995. Systematics and phylogeography of Amazonian spiny rats of the genus *Proechimys* (Rodentia: Echimyidae). Ph.D. Diss., Univ. California, Berkeley.
1998. Four new species of spiny rats of the genus *Proechimys* (Rodentia: Echimyidae) from the western Amazon of Brazil. Proc. Biol. Soc. Washington 111: 436–471.
da Silva, M. N. F., and J. L. Patton
1993. Amazonian phylogeography: mtDNA sequence variation in arboreal echimyid rodents (Caviomorpha). Mol. Phylgenet. Evol. 2: 243–255.
1998. Molecular phylogeography and the evolution and conservation of Amazonian mammals. Mol. Ecol. 7: 475–486.
da Silva, N. J., Jr., and J. W. Sites, Jr.
1995. Patterns of diversity of neotropical squamate reptile species with emphasis on the Brazilian Amazon and the conservation potential of Indigenous reserves. Conserv. Biol. 9: 873–901.
Davis, D. E.
1947. Notes on the life histories of some Brazilian mammals. Bol. Mus. Nac., nov. ser., Zool. 76: 1–8.
Didier, R.
1962. Note sur l'os penien de quelques rongeurs de l'Amerique du Sud. Mammalia 26: 408–430.
dos Reis, S. F., L. M. Pessôa, and R. E. Strauss
1990. Applications of size-free canonical-discriminant analysis to studies of geographic differentiation. Rev. Bras. Genet. 13: 509–520.
Duellman, W. E., and J. E. Koechlin
1991. The Reserva Cuzco Amazónico, Peru: Biological investigations, conservation, and ecotourism. Occas. Pap. Mus. Nat. Hist., Univ. Kansas 142: 1–38.
Dumont, J. F., S. Lamotte, and F. Kahn
1990. Wetland and upland forest ecosystems in Peruvian Amazonia: plant species diversity in the light of some geological and botanical evidence. For. Ecol. Manag. 33/34: 125–139.
Eisenberg, J. F.
1989. Mammals of the Neotropics, vol. 1: The northern Neotropics: Panamá, Colombia, Venezuela, Guyana, Suriname, French Guiana. Chicago: Univ. Chicago Press.
Eisenberg, J. F., and D. E. Wilson
1981. Relative brain size and demographic strategies in didelphid marsupials. Am. Nat. 118: 1–15.
Ellerman, J. R.
1940. The families and genera of living rodents. Vol. 1. London: British Museum (Natural. History).
Emmons, L. H.
1981. Morphological, ecological and behavioral adaptations for arboreal browsing in *Dactylomys dactylinus* (Rodentia, Echimyidae). J. Mammal. 62: 183–189.
1982. Ecology of *Proechimys* (Rodentia, Echimyidae) in south-eastern Peru. Trop. Ecol. 23: 280–290.
1984. Geographic variation in densities and diversities of non-flying mammals in Amazonia. Biotropica 16: 210–222.
1993. On the identity of *Echimys didelphoides* Desmarest, 1817 (Mammalia: Rodentia: Echimyidae). Proc. Biol. Soc. Washington 106: 1–4.
1994. New locality records of *Mesomys* (Rodentia: Echimyidae). Mammalia 58: 148–149.
Emmons, L. H., and F. Feer
1997. Neotropical rainforest mammals, a field

guide, 2nd edition. Chicago: Univ. Chicago Press.
Endler, J. A.
1982. Pleistocene forest refuges: fact or fancy? *In* G. T. Prance (ed.), Biological diversification in the tropics: 641–657. New York: Columbia Univ. Press.
Ernest, K. A.
1986. *Nectomys squamipes*. Mammalian Species, 265: 1–5.
Excoffier, L., P. E. Smouse, and J. M. Quattro
1992. Analysis of molecular variance inferred from metric distances among DNA haplotypes: application to human mitochondrial DNA restriction data. Genetics 131: 479–491.
Felsenstein, J.
1993. PHYLIP (Phylogeny Inference Package), version 3.5c. Seattle: Univ. Washington.
Fleming, T. H.
1972. Aspects of the population dynamics of three species of opossum in the Panama Canal Zone. J. Mammal. 53: 619–623.
Forget, P.-M.
1991. Scatterhoarding of *Astrocaryum paramaca* by *Proechimys* in French Guiana: comparison with *Myoprocta exilis*. Trop. Ecol. 32: 155–167.
Foster, R.
1990. The floristic composition of the Rio Manu floodplain forest. *In* A. H. Gentry (ed.), Four neotropical rainforests: 99–111. New Haven, CT: Yale Univ. Press.
Frailey, C. D., E. L. Lavina, A. Rancy, and J. Fereira de Souza Filho
1988. A proposed Pleistocene/Holocene lake in the Amazon Basin and its significance to Amazonian geology and biogeography. Acta Amazonica 18: 119–143.
Gardner, A. L.
1973. The systematics of the genus *Didelphis* (Marsupialia: Didelphidae) in North and Middle America. Spec. Publ. Mus. Texas Tech Univ. 4: 81 pp.
1982. Virginia opossum. *In* J. A. Hapman and G. A. Feldhamer (eds.), Wild mammals of North America: 3–36. Baltimore, MD: Johns Hopkins Univ. Press.
1989. Two new mammals from southern Venezuela and comments on the affinities of the highland fauna of Cerra de la Neblina. *In* K. H. Redford and J. F. Eisenberg (eds.), Advances in Neotropical mammalogy: 411–424. Gainesville, FL: Sandhill Crane Press.
1993. Order Didelphimorphia. *In* D. E. Wilson and D. M. Reeder (eds.), Mammal species of the world, 2nd ed., pp. 15–23. Washington, DC: Smithson. Inst. Press.
Gardner, A. L., and G. K. Creighton
1989. A new generic name for Tate's (1933) *microtarsus* group of South American mouse opossums (Marsupialia: Didelphidae). Proc. Biol. Soc. Washington 102: 3–7.
Gardner, A. L., and L. H. Emmons
1984. Species groups in *Proechimys* (Rodentia, Echimyidae) as indicated by karyology and bullar morphology. J. Mammal. 65: 10–25.
Gardner, A. L., and J. L. Patton
1972. New species of *Philander* (Marsupialia: Didelphidae) and *Mimon* (Chiroptera: Phyllostomidae) from Peru. Occas. Pap. Mus. Zool. Louisiana State Univ. 43: 12 pp.
1976. Karyotypic variation in oryzomyine rodents (Cricetinae) with comments on chromosomal evolution in the neotropical cricetine complex. Ibid. 49: 48 pp.
Gascon, C., S. C. Lougheed, and J. P. Bogart
1996. Genetic and morphological variation in *Vanzolinius discodactylus*: a test of the river hypothesis of speciation. Biotropica 28: 376–387.
1998. Patterns of genetic population differentiation in four species of Amazonian frogs: a test of the riverine barrier hypothesis. Biotropica 30: 104–119.
Gibbs, R. J.
1967. The geochemistry of the Amazon river system. I. The factors that control the salinity and the composition of suspended soils. Geol. Soc. Am. Bull. 78: 1203–1232.
Haffer, J.
1969. Speciation in Amazonian forest birds. Science 165: 131–137.
1974. Avian speciation in tropical South America. Publ. Nuttall Ornithol. Club 14: 1–390.
1975. Avifauna of northwestern Colombia, South America. Bonn. Zool. Monogr. 7: 182 pp.
1978. Distribution of Amazon forest birds. Bonn. Zool. Beitr. 29: 38–78.
1993a. On the ''river effect'' in some forest birds of southern Amazonia. Bol. Mus. Para. Emilio Goeldi Ser. Zool. 8: 217–245.
1993b. Time's cycle and Time's arrow in the

history of Amazonia. Biogeographica 69: 15–45.
1997a. Contact zones between birds of southern Amazonia. Ornithol. Monogr. 48: 281–305.
1997b. Alternative models of vertebrate speciation in Amazonia: an overview. Biodivers. Conserv. 6: 451–476.

Hall, E. R.
1981. The mammals of North America, 2nd ed., 2 vols. New York: Wiley.

Handley, C. O., Jr., and R. H. Pine
1984. A review of the Amazonian short-tailed opossum *Monodelphis emiliae* (Thomas). Mammalia 48: 239–245.

Harder, J. D.
1992. Reproductive biology of South American marsupials. *In* W. G. Hamlett (ed.), Reproductive biology of South American vertebrates: 211–228. New York: Springer.

Harrison, R.
1991. Molecular changes at speciation. Annu. Rev. Ecol. Syst. 22: 281–308.

Henry, O.
1994. Saisons de reproduction chez trois Rongeurs et un Artiodactyle en Guyane française, en fonction des facteurs de milieu et de l'alimentation. Mammalia 58: 183–200.

Hershkovitz, P.
1940. A new spiny mouse of the genus *Neacomys* from eastern Ecuador. Occas. Pap. Mus. Zool. 419: 1–4.
1944. A systematic review of the neotropical water rats of the genus *Nectomys* (Cricetinae). Misc. Publ. Mus. Zool. Univ. Michigan 58: 101 pp. + folding map.
1948. Mammals of northern Colombia. Preliminary report no. 2: Spiny rats (Echimyidae), with supplemental notes on related forms. Proc. U.S. Nat. Mus. 97: 125–140.
1955. South American marsh rats, genus *Holochilus*, with a summary of sigmodont rodents. Fieldiana: Zool. 37: 639–673.
1959. Nomenclature and taxonomy of the Neoropical mammals described by Olfers, 1818. J. Mammal. 40: 337–353.
1960. Mammals of northern Colombia, preliminary report No. 8: Arboreal rice rats, a systematic revision of the subgenus *Oecomys*, genus *Oryzomys*. Proc. U.S. Natl. Mus. 110: 513–568.
1977. Living New World monkeys (Platyrrhini) with an introduction to primates, vol. 1. Chicago: Univ. Chicago Press.
1983. Two new species of night monkeys, genus *Aotus* (Cebidae, Platyrrhini): a preliminary report on *Aotus* taxonomy. Am. J. Primatol. 4: 209–243.
1992. The South American gracile mouse opossums, genus *Gracilinanus* Gardner and Creighton, 1989 (Marmosidae, Marsupialia): a taxonomic review with notes on general morphology and relationships. Fieldiana Zool., n. ser. 70: 56 pp.
1997. Composition of the Family Didelphidae Gray, 1821 (Didelphoidea: Marsupialia), with a review of the morphology and behavior of the included four-eyed pouched opossums of the genus *Philander* Tiedemann, 1808. Ibid. 86: 103 pp.

Heyer, W. R.
1997. Geographic variation in the frog genus *Vanzolinius* (Anura: Leptodactylidae). Proc. Biol. Soc. Washington 110: 338–365.

Hillis, D. M., and J. J. Bull
1993. An empirical test of bootstrapping as a method for assessing confidence in phylogenetic analysis. Syst. Biol. 42: 182–192.

Hillis, D. M., B. K. Mable, and C. Moritz
1996. Applications of molecular systematics: the state of the field and a look to the future. *In* D. M. Hillis, C. Moritz, and B. K. Mable (eds.), Molecular systematics, 2nd ed.: 515–543. Sunderland, MA: Sinauer Associates

Hoffmann, R. S., C. G. Anderson, R. W. Thorington, Jr., and L. R. Heaney
1993. Family Sciuridae. *In* D. E. Wilson and D. M. Reeder (eds.), Mammal species of the world, 2nd ed.: 419–465. Washington, DC: Smithson. Inst. Press.

Hoffmeister, D. F.
1951. A taxonomic and evolutionary study of the piñon mouse, *Peromyscus truei*. Illinois Biol. Monogr. 21: 1–104.

Holdridge, L. R.
1967. Life zone ecology, rev. ed. San José, Costa Rica: Trop. Sci. Ctr.

Hutterer, R., M. Verhaagh, J. Diller, and R. Podloucky
1995. An inventory of mammals observed at Panguana Biological Station, Amazonian Peru. Ecotropica 1: 3–20.

Ihering, H. von
1904. O Rio Juruá. Rev. Mus. Paulista 6: 385–460.

Irwin, D. M., T. D. Kocher, and A. C. Wilson
1991. Evolution of the cytochrome *b* gene in mammals. J. Mol. Evol. 32: 128–144.

Jacobs, S. C., A. Larson, and J. M. Cheverud
1995. Phylogenetic relationships and orthogenetic evolution of coat color among tamarins (genus *Saguinus*). Syst. Biol. 44: 515–532.
Joseph, L., C. Moritz, and A. Hugall
1995. Molecular support for vicariance as a source of diversity in rainforest. Proc. R. Soc. London Ser. B Biol. Sci. 260: 177–182.
Julien-LaFerriere, D., and M. Atramentowicz
1990. Feeding and reproduction of three didelphid marsupials in two neotropical forests (French Guiana). Biotropica 22: 404–415.
Kay, R. F., R. H. Madden, C. Van Schaik, and D. Higdon
1997. Primate species richness is determined by plant productivity: Implications for conservation. Proc. Natl. Acad. Sci. U.S.A. 94: 13023–13027.
Kimura, M.
1980. A single method for estimating evolutionary rate of base substitutions through comparative studies of nucleotide sequences. J. Mol. Evol. 16: 111–120.
Klinge, H., W. J. Junk, and C. J. Revilla
1990. Status and distribution of forested wetlands in tropical South America. Forest Ecol. Management 33/34: 81–101.
Kumar, S., K. Tamura, and M. Nei
1993. MEGA: Molecular Evolutionary Genetics Analysis, version 1.02. University Park: Pennsylvania State Univ.
Lara, M. C., M. A. Bogan, and R. Cerqueira
1992. Sex and age components of variation in *Proechimys cuvieri* (Rodentia: Echimyidae) from northern Brazil. Proc. Biol. Soc. Washington 105: 882–893.
Lara, M. C., J. L. Patton, and M. N. F. da Silva
1996. The simultaneous diversification of South American echimyid rodents (Hystricognathi) based on complete cytochrome b sequences. Mol. Phylogenet. Evol. 5: 403–413.
Lavergne, A., O. Verneau, J. L. Patton, and F. M. Catzeflis
1997. Molecular discrimination of two sympatric species of opossum (genus *Didelphis*: Didelphidae) in French Guiana. Mol. Ecol. 6: 889–891.
Lawrence, B.
1941. *Neacomys* from northwestern South America. J. Mammal. 22: 418–427.
Lawrence, M. A.
1988. The identity of *Sciurus duida* J. A. Allen (Rodentia: Sciuridae). Am. Mus. Novitates 2919: 8 pp.
Leal-Mesquita, E. R. R. B. P.
1991. Estudos citogenéticos em dez espécies de roedores Brasileiros da família Echimyidae. MA thesis, Univ. São Paulo, Brazil.
Lönnberg, E.
1921. A second contribution to the mammalogy of Ecuador with some remarks on Caenolestes. Ark. Zool. 14:1–104.
Lundberg, J. G., L. G. Marshall, J. Guerrero, B. Horton, M. C. Malabarba, and F. Wesselingh
1998. The stage for neotropical fish diversification: a history of tropical South American rivers. *In* L. R. Malabarba, R. E. Reis, R. P. Vari, C. A. S. Lucena, and Z. M. S. Lucena (eds.), Phylogeny and classification of neotropical fishes: 13–48. Porto Alegre, Brazil: Mus. Ciênc. Tec., PUCRS. Porto Alegre, Brazil.
Lynch, J. D.
1988. Refugia. *In* A. A. Myers and P. S. Giller (eds.), Analytical biogeography: 311–342. London: Chapman and Hall.
Maddison, D. R.
1991. The discovery and importance of multiple islands of most-parsimonious trees. Syst. Zool. 40: 315–328.
Maia, V., Y. Yonenaga-Yasuda, J. R. O. Freitas, et al.
1984. Supernumerary chromosomes in *Nectomys squamipes* (Cricetidae-Rodentia). Genetica 63: 121–128.
Majer, J. D., and J. H. C. Delabie
1994. Comparison of the ant communities of annually inundated and terra firme forests at Trombetas in the Brazilian Amazon. Insectes Soc. 41: 343–359.
Malcolm, J. R.
1990. Estimation of mammalian densities in continuous forest north of Manaus. *In* A. H. Gentry (ed.), Four neotropical rainforests: 339–368. New Haven: Yale Univ. Press.
1991a. Comparative abundances of neotropical small mammals by trap height. J. Mammal. 72: 188–192.
1991b. The small mammals of tropical forest fragments: patterns and process. Ph.D. Disse., Univ. Florida, Gainesville.
1992. Use of tooth impressions to age and identify live *Proechimys guyannensis* and *P. cuvieri* (Rodentia: Echimyidae). J. Zool. 227: 537–546.
1995. Forest structure and the abundance and

diversity of neotropical small mammals. *In* M. D. Lowman and N. M. Nadkarni (eds.), Forest canopies: 179–197. New York: Academic Press.

Malygin, V. M., and M. Rosmiarek
1996. Morphological difference of two karyotypes of spiny cricetine genus *Neacomys* from the Peruvian Amazonia (Rodentia, Mammalia). Doklady Akad. Nauk 351(5): 712–714.

Malygin, V. M., V. M. Aniskin, S. I. Isaev, and A. N. Milishnikov
1994. *Amphinectomys savamis* Malygin gen. et sp. n., a new genus and a new species of water rat (Cricetidae, Rodentia) from Peruvian Amazonia. Zool. Zh. 73(7–8): 195–208.

Mares, M. A.
1992. Neotropical mammals and the myth of Amazonian biodiversity. Science 255: 976–979.

Martius, C.
1994. Diversity and ecology of termites in Amazonian forests. Pedobiologia 38: 407–428.

Massoia, E.
1981. El estado sistemático y zoogeografía de *Mus brasiliensis* Desmarest y *Holochilus sciureus* Wagner (Mammalia, Rodentia, Cricetidae). Physis Secc. C, Cont. Org. Terr. 39(97): 31–34.

Matschie, P.
1916. Bermerkungen über die Gattung *Didelphis* L. Sitzungsber. Ges. Naturf. Freunde Berlin 1916: 259–272 + 2 pls.

Mertes, L. A. K., T. Dunne, and L. A. Martinelli
1996. Channel-floodplain geomorphology along the Solimões-Amazon River, Brazil. Geol. Soc. Am. Bull. 108: 1089–1107.

Mills, L. S., and F. W. Allendorf
1996. The one-migrant-per-generation rule in conservation and management. Conserv. Biol. 10: 1509–1518.

Moojen, J.
1948. Speciation in the Brazilian spiny rats (genus *Proechimys*, family Echimyidae). Univ. Kans. Publ. Mus. Nat. Hist. 1: 301–406.

Musser, G. G., and M. D. Carleton
1993. Family Muridae. *In* D. E. Wilson and D. M. Reeder (eds.), Mammal species of the world, 2nd ed.: 501–755. Washington, D.C.: Smithson. Inst. Press.

Musser, G. G., E. M. Brothers, M. D. Carleton, and A. L. Gardner
1998. Systematic studies of oryzomine rodents (Muridae, Sigmodontinae): diagnoses and distributions of species formerly assigned to *Oryzomys* ''*capito*''. Bull. Am. Nat. Hist. 236: 376 pp.

Mustrangi, M. A., and J. L. Patton
1997. Phylogeography and systematics of the slender mouse opossum *Marmosops* (Marsupialia, Didelphidae). Univ. California Publ. Zool. 130: 86 pp.

Myers, P.
1982. Origins and affinities of the mammal fauna of Paraguay. *In* M. A. Mares and H. H. Genoways (eds.), Mammalian biology in South America. Univ. Pittsburgh, Pymatuning Lab. Ecol. Spec. Publ. Ser. 6: 85–93.
1989. A preliminary revision of the *varius* group of *Akodon*. *In* K. Redford and J. F. Eisenberg (eds.), Advances in Neotropical mammalogy: 5–54. Gainesville, FL: Sandhill Crane Press.

Myers, P., and M. D. Carleton
1981. The species of *Oryzomys* (*Oligoryzomys*) in Paraguay and the identity of Azara's ''Rat sixieme ou rat a tarse noir.'' Misc. Publ. Mus. Zool. Univ. Michigan 161: 1–41.

Myers, P., J. L. Patton, and M. F. Smith
1990. A review of the *boliviensis* group of *Akodon* (Muridae: Sigmodontinae), with emphasis on Peru and Bolivia. Misc. Publ. Mus. Zool. Univ. Mich. 177: 1–104.

Nachman, M.
1992. Geographic patterns of chromosomal variation in South American marsh rats, *Holochilus brasiliensis* and *H. vulpinus*. Cytogenet. Cell Genet. 61: 10–16.

O'Connell, M.
1979. Ecology of didelphid marsupials from northern Venezuela. *In* J. F. Eisenberg (ed.), Vertebrate ecology in the norther Neotropics: 73–87. Washington, D.C.: Smithson. Inst. Press.

Olalla, A. M.
1938. I. Un viaje a pesquizas zoológicas hacia el Rio Juruá, Estado del Amazonas, Brasil – 1936. II., Notas de campo: observaciones biológicas. Rev. Mus. Paulista 22: 235–297.

Olson, D. M., and E. Dinerstein
1998. The Global 200: A representation approach to conserving the earth's most biologically valuable ecoregions. Conserv. Biol. 12: 502–515.

Orr, M. R., and T. B. Smith
1998. Ecology and speciation. Trends Ecol. Evol. 13: 502–506.

Pacheco, V., and E. Vivar
1996. Annotated checklist of the non-flying mammals at Pakitza, Manu Reserve Zone, Manu National Park, Perú. *In* D. E. Wilson and A. Sandoval (eds.), Manu: the biodiversity of southeastern Peru: 577–592. Lima, Perú: Editorial Horizonte.

Pacheco, V., B. D. Patterson, J. L. Patton, L. H. Emmons, S. Solari, and C. Ascorra
1993. List of mammal species known to occur in Manu Biosphere Reserve, Peru. Publ. Mus. Hist. Nat. Univ. Nac. Mayor San Marcos, ser. A, Zool. 44: 12 pp.

Palma, R. E., and T. L. Yates
1996. The chromosomes of Bolivian didelphid marsupials. Occas. Pap. Mus. Texas Tech Univ. 162: 20 pp.

Patterson, B., and R. Pascual
1968. New echimyid rodent from the Oligocene of Patagonia, and a synopsis of the family. Breviora 301: 1–14.

Patterson, B. D.
1992. Mammals in the Royal Natural History Museum, Stockholm, collected in Brazil by A. M. Olalla during 1934–1938. Fieldiana Zool., n. ser., 66: 42 pp.

Patton, J. L.
1967. Chromosome studies of certain pocket mice, genus *Perognathus* (Rodentia: Heteromyidae). J. Mammal. 48: 27–37.
1984. Systematic status of the large squirrels (subgenus *Urosciurus*) of the western Amazon basin. Stud. Neotrop. Fauna Environ. 19: 53–72.
1987. Species groups of spiny rats, genus *Proechimys* (Rodentia: Echimyidae). Fieldiana Zool., n. ser., 39: 305–345.

Patton, J. L., and M. N. F. da Silva
1995. A review of the spiny mouse genus *Scolomys* (Rodentia: Muridae: Sigmodontinae) with the description of a new species from the western Amazon of Brazil. Proc. Biol. Soc. Washington 108: 319–337.
1997. Definition of species of pouched four-eyed opossums (Didelphidae, *Philander*). J. Mammal. 78: 90–102.
1998. Rivers, refuges, and ridges: the geography of speciation of Amazonian mammals. *In* D. Howard and S. Berlocher (eds.), Endless forms: modes and mechanisms of speciation: 202–213. Oxford: Oxford Univ. Press.

Patton, J. L., and L. H. Emmons
1985. A review of the genus *Isothrix* (Rodentia, Echimyidae). Am. Mus. Novitates 2817: 14 pp.

Patton, J. L., and A. L. Gardner
1972. Notes on the systematics of *Proechimys* (Rodentia: Echimyidae), with emphasis on Peruvian forms. Occas. Pap. Mus. Zool. Louisiana State Univ. 44: 30 pp.

Patton, J. L., and O. A. Reig
1989. Genetic differentiation among echimyid rodents, with an emphasis on spiny rats, genus *Proechimys*. *In* K. Redford and J. F. Eisenberg (eds.), Advances in Neotropical mammalogy: 75–96. Gainesville, FL: Sandhill Crane Press.

Patton, J. L., and M. A. Rogers
1983. Systematic implications of non-geographic variation in the spiny rat genus *Proechimys* (Echimyidae). Z. Säugetierkd. 48: 363–370.

Patton, J. L., and M. F. Smith
1990. The evolutionary dynamics of the pocket gopher *Thomomys bottae*, with emphasis on California populations. Univ. California Publ. Zool. 123: 161 pp.
1992. mtDNA phylogeny of Andean mice: a test of diversification across ecological gradients. Evolution 46: 174–183.

Patton, J. L., B. Berlin, and E. A. Berlin
1982. Aboriginal perspectives of a mammal community in Amazonian Peru: knowledge and utilization patterns among the Aguaruna Jívaro. *In* M. A. Mares and H. H. Genoways (eds.), Mammalian biology in South America. Univ. Pittsburgh, Pymatuning Lab. Ecol. Spec. Publ. Ser. 6: 111–128.

Patton, J. L., M. N. F. da Silva, and J. R. Malcolm
1994. Gene genealogy and differentiation among arboreal spiny rats (Rodentia: Echimyidae) of the Amazon Basin: a test of the riverine barrier hypothesis. Evolution 48: 1314–1323.
1996a. Hierarchical genetic structure and gene flow in three sympatric species of Amazonian rodents. Mol. Ecol. 5: 229–238.

Patton, J. L., S. dos Reis, and M. N. F. da Silva
1996b. A molecular view of relationships among didelphid marsupials: sequence variation in the mitochondrial cytochrome b gene. J. Mamm. Evol. 3: 3–29.

Patton, J. L., M. N. F. da Silva, M. C. Lara, and M. A. Mustrangi
1997. Diversity, differentiation, and the historical biogeography of nonvolant small mammals of the neotropical forests. *In* W. F. Laurance and R. O. Bier-

regaard, Jr. (eds.), Tropical forest remnants: ecology, management, and conservation of fragmented communities: 455–465. Chicago: Univ. Chicago Press.

Peres, C. A.
1993. Notes on the primates of the Juruá River, western Brazilian Amazonia. Folia Primatol. 61: 97–103.
1997. Primate community structure at twenty western Amazonian flooded and unflooded forests. J. Trop. Ecol. 13: 381–405.
1999. The structure of nonvolant mammal communities in different Amazonian forest types. *In* J. F. Eisenberg and K. H. Redford (ed.), Mammals of the Neotropics, Vol. 3: 564–581. Chicago: Univ. Chicago Press.

Peres, C. A., J. L. Patton, and M. N. F. da Silva
1996. Riverine barriers and gene flow in Amazonian saddle-back tamarins. Folia Primatol. 67: 113–124.

Pine, R. H.
1973. Mammals (exclusive of bats) of Belém, Pará, Brazil. Acta Amazonica 3: 47–79.
1981. Reviews of the mouse opossums *Marmosa parvidens* Tate and *Marmosa invicta* Goldman (Mammalia: Marsupialia: Didelphidae), with description of a new species. Mammalia 45: 55–70.

Pires, J. M., and G. T. Prance
1985. The vegetation types of the Brazilian Amazon. *In* G. T. Prance and T. E. Lovejoy (eds.), Amazonia: 109–145. Oxford: Pergamon Press.

Platnick, N. I., and G. Nelson
1978. A method for analysis of historical biogeography. Syst. Zool. 27: 1–16.

Projeto RadamBrasil
1977. Levantamento de Recursos naturais: Folha SB.19 Juruá. Departamento Nacional da Produção Mineral, Rio de Janeiro, Brazil.
1978. Ibid.: Folha SC.20 Porto Velho.

Puhakka, M., and R. Kalliola
1995. Floodplain vegetation mosaics in western Amazonia. Biogeographica 71: 1–14.

Putzer, H.
1984. The geological evolution of the Amazon basin and its miner resources. *In* H. Sioli (ed.), The Amazon, limnology and landscape ecology of a mighty tropical river and its basin: 15–46. Dordrecht, Netherlands: Dr. W. Junk Publishers.

Räsänen, M., J. Salo, and R. J. Kalliola
1987. Fluvial perturbance in the western Amazon basin: regulation by long-term sub-Andean tectonics. Science 238: 1398–1401.

Räsänen, M. R., J. S. Salo, H. Jungner, and L. R. Pittman
1990. Evolution of the western Amazon lowland relief: impact of Andean foreland dynamics. Terra Res. 2: 320–332.

Räsänen, M., R. Neller, J. Salo, and H. Jungner
1992. Recent and ancient fluvial deposition systems in the Amazonian foreland basin, Peru. Geol. Mag. 129: 293–306.

Redford, K. H., and J. F. Eisenberg
1992. Mammals of the Neotropics, vol. 2. The southern cone. Chicago: Univ. Chicago Press.

Reig, O. A.
1986. Diversity patterns and differentiation of high Andean rodents. *In* F. Vuilleumier and M. Monasterio (eds.), High altitude tropical biogeography: 404–440. New York: Oxford Univ. Press.

Reig, O. A., and M. Useche
1976. Diversidad cariotipica y sistematica en poblaciones Venezolanas de *Proechimys* (Rodentia, Echimyidae), con datos adicionales sobre poblaciones de Peru y Colombia. Acta Cient. Venez. 27: 132–140.

Reig, O. A., J.A.W. Kirsch, and L. G. Marshall
1987. Systematic relationships of the living and Neocenozoic American ''opossum-like'' marsupials (suborder Didelphimorphia), with comments on the classification of these and of the Cretaceous and Paleogene New World and European metatherians. *In* M. Archer (ed.), Possums and opossums: studies in evolution: 1–89. Chipping Norton, Australia: Currey Beatty.

Reig, O. A., M. Tranier, and M. A. Barros
1979. Sur l'identification chromosomique de *Proechimys guyannensis* (E. Geoffroy, 1803) et de *Proechimys cuvieri* Petter, 1978 (Rodentia, Echimyidae). Mammalia 43: 501–505.

Reig, O. A., M. Aguilera, M. A. Barros, and M. Useche
1980. Chromosomal speciation in a Rassenkries of Venezuelan spiny rats (genus *Proechimys*, Rodentia, Echimyidae). *In* N. N. Vorontsov and J. M. Van Brink (eds.), Amican genetics and evolution: 291–312. The Hague, Netherlands: Dr. W. Junk Publishers.

Reig, O. A., A. L. Gardner, N. O. Bianchi, and J. L. Patton
1977. The chromosomes of the Didelphidae (Marsupialia) and their evolutionary significance. Biol. J. Linn. Soc. 9: 191–216.
Renfree, M.
1993. Ontogeny, genetic control, and phylogeny of female reproduction in monotremes and therian mammals. *In* F. S. Szalay, M. J. Novacek, and M .C. McKenna (eds.), Mammal phylogeny. Mesozoic differentiation, multituberculates, monotremes, early therians, and marsupials: 4–20. New York: Springer.
Ricklefs, R. E., and D. Schluter
1993. Species diversity: regional and historical influences. *In* R. E. Ricklefs and D. Schulter (eds.), Species diversity in ecological communities. historical and geographical perspectives: 350–363. Chicago: Univ. Chicago Press.
Riddle, B. R.
1996. The molecular phylogeographic bridge between deep and shallow history in continental biotas. Trends Ecol. Evol. 11: 207–211.
Ridgway, R.
1912. Color standards and color nomenclature. Washington, DC. 44 pp.
Rosen, D. E.
1975. A vicariance model for Caribbean biogeography. Syst. Zool. 24: 431–464.
Salo, J.
1987. Pleistocene forest refuges in the Amazon: evaluation of the biostratigraphical, lithostratigraphical and geomorphological data. Ann. Zool. Fenn. 24: 203–211.
1988. Rainforest diversification in the western Amazon basin: the role of river dynamics. Univ. Turku, Biol. Dept. Rep 16, 18pp.
Salo, J., R. Kalliola, I. Hakkinen, et al.
1986. River dynamics and the diversity of Amazon lowland forest. Nature 322: 254–258.
Sangines, N., and M. Aguilera
1991. Chromosome polymorphism in *Holochilus venezuelae* (Rodentia: Cricetidae): C- and G-bands. Genome 34: 13–18.
SAS Institute, Inc.
1988. SAS user's guide: statistics. Cary, NC.
Silva, A. S., P. L. Lisboa, and U. N. Maciel
1992. Diversidade florística e estructural em floresta densa da Bacia do Rio Juruá—AM. Bol. Mus. Para. Emilio Goeldi, Ser. Bot. 8: 203–258.
Silva, M. J. da J., and Y. Yonenaga-Yassuda
1997. New karyotypes of two related species of *Oligoryzomys* genus (Cricetidae, Rodentia) involving centric fusion with loss of NORs and distribution of telomeric $(TTAGGG)_n$ sequences. Hereditas 127: 217–239.
Simmons, N. B., and R. S. Voss
1998. The mammals of Paracou, French Guiana: a neotropical lowland rainforest fauna. Part 1. Bats. Bull. Am. Mus. Nat. Hist. 237: 219 pp.
Simpson, B. B., and J. Haffer
1978. Speciation patterns in the Amazonian forest biota. Annu. Rev. Ecol. Syst. 9: 497–518.
Slatkin, M.
1993. Isolation by distance in equilibrium and non-equilibrium populations. Evolution 47: 264–279.
Slatkin, M., and W. P. Maddison
1989. A cladistic measure of gene flow inferred from the phylogenies of alleles. Genetics 123: 603–613.
1990. Detecting isolation by distance using phylogenies of genes. Genetics 126: 249–260.
Smith, M. F., and J. L. Patton
1991. Variation in mitochondrial cytochrome b sequence in natural populations of South American akodontine rodents (Muridae: Sigmodontinae). Mol. Biol. Evol. 8: 85–103.
1993. The diversification of South American murid rodents: evidence from mitochondrial DNA sequence data for the akodontine tribe. Biol. J. Linn. Soc. 50: 149–177.
Smith, T. B., R. K. Wayne, D. J. Ginman, and M. W. Bruford
1997. A role for ecotones in generating rainforest biodiversity. Science 276: 1855–1857.
Stephens, L., and M. A. Traylor, Jr.
1983. Ornithological gazetteer of Peru. Cambridge, MA: Harvard Univ. Mus. Comp. Zool. Vi + 271 pp.
Svartman, M.
1998. Evolução cariotípica de marsupiais de família Didelphidae. Ph.D. Disser., Univ. São Paulo, Brazil. 124 pp.
Swofford, D. L.
1998. PAUP: Phylogenetic Analysis Using Parsimony, beta test version 4.0b1. Sunderland, MA: Sinauer Associates.

Tate, G. H. H.
1933. A systematic revision of the marsupial genus *Marmosa*, with a discussion of the adaptive radiation of the murine opossums (*Marmosa*). Bull. Am. Mus. Nat. Hist. 66: 1–250.
1939. Mammals of the Guiana region. Ibid. 76: 151–229.
Terborgh, J., and K. Petren
1991. Development of structure through succession in an Amazonian floodplain forest. *In* S. S. Bell, E. D. McCoy, and H. R. Mushinsky (eds.), Habitat structure: the physical arrangement of objects in space: 28–34. London: Chapman and Hall.
Terborgh, J. W., S. K. Robinson, T. A. Parker III, C. A. Munn, and N. Pierpont
1990. Structure and organization of an Amazonian forest bird community. Ecol. Monogr. 60: 213–238.
Thomas, O.
1882. On a collection of rodents from north Peru. Proc. Zool. Soc. London 1882: 98–111 + 4 pl.
1911. The mammals of the tenth edition of Linnaeus; an attempt to fix the types of the genera and the exact bases and localities of the species. Proc. Zool. Soc. London 1911: 120–158.
1912. On small mammals from the Lower Amazon. Ann. Mag. Nat. Hist., ser. 8, 9: 84–90.
1924. On a collection of mammals made by Mr. Latham Rutter in the Peruvian Amazons. Ibid., ser. 9, 13: 530–538.
1926. On some mammals from the Middle Amazons. Ibid., ser. 9, 17: 635–639.
1928. The Godman-Thomas expedition to Peru. VII. The mammals of the Rio Ucayali. Ibid., ser. 10, 2: 249–265.
Thorpe, R.
1983. A review of the numerical methods for recognizing and analysing racial differentiation. *In* J. Felsenstein (ed.), Numerical taxonomy. NATO ASI Ser. G Ecol. Sci., 1: 404–423.
1987. Geographic variation: a synthesis of cause, data, pattern and consequence in relation to subspecies, multivariate analysis and phylogeny. Bull. Zool. 54: 3–11.
Thorpe, R., and M. Baez
1987. Geographic variation within an island: univariate and multi-variate contouring of scalation, size, and shape of the lizard *Gallotia galloti*. Evolution 41: 256–268.
Tosi, J.
1960. Zonas de vida natural en el Perú, memoria explicativa sobre el mapa ecológico de Perú. Bol. Tec. 5, Zona Andina, Proyecto 39. Inst. Interam. Cienc. Agrí. OEA Zona Andina Bol. Téc. 5: vi + 271 pp.
Tribe, C. J.
1996. The neotropical rodent genus *Rhipidomys* (Cricetidae: Sigmodontinae)—a taxonomic revision. Ph.D. Diss., Univ. College, London, 316 pp.
Tuomisto, H., A. Linna, and R. Kalliola
1994. Use of digitally processed satellite images in studies of tropical rain forest vegetation. Int. J. Remote Sens. 15(8): 1595–1610.
Tuomisto H., K. Ruokolainen, R. Kalliola, A. Linna, W. Danjoy, and Z. Rodriguez
1995. Dissecting Amazonian biodiversity. Science 269: 63–66.
Tyndal-Biscoe, C. H., and R. B. MacKenzie
1976. Reproduction in *Didelphis marsupialis* and *D. albiventris* in Colombia. J. Mammal. 57: 249–265.
Vanzolini, P. E., and E. E. Williams
1970. South American anoles: geographic differentiation and evolution of the *Anolis chrysolepis* species group (Sauria, Iguanidae). Arq. Zool. (São Paulo) 19: 1–298.
Vié, J. C., V. Volobouev, J. L. Patton, and L. Granjon
1997. A new species of *Isothrix* (Rodentia: Echimyidae) from French Guiana. Mammalia 60: 393–406.
Vieira, C. O. C.
1948. Nova contribuição ao conhecimento dos mamíferos do rio Juruá. Bol. Mus. Para. Emilio Goeldi 10: 239–274.
Voss, R. S.
1988. Systematics and ecology of ichthyomyine rodents (Muroidea): patterns of morphological evolution in a small adaptive radiation. Bull. Am. Mus. Nat. Hist. 188 (2): 259–493.
1991. An introduction to the neotropical muroid rodent genus *Zygodontomys*. Ibid. 210: 109 pp.
1993. A revision of the Brazilian muroid rodent genus *Delomys* with remarks on ''Thomasomyine'' characters. Am. Mus. Novitates 3073: 44 pp.
Voss, R. S., and M. D. Carleton
1993. A new genus for *Hesperomys molitor* Winge and *Holochilus magnus* Hershkovitz (Mammalia, Muridae) with an

analysis of its phylogenetic relationships. Am. Mus. Novitates 3085: 39 pp.

Voss, R. S., and L. H. Emmons
1996. Mammalian diversity in neotropical lowland rainforests: a preliminary assessment. Bull. Am. Mus. Nat. Hist. 230: 115 pp.

Voss, R. S., L. F. Marcus, and P. Escalante-P.
1990. Morphological evolution in muroid rodents I. Conservative patterns of craniometric covariance and their ontogenetic basis in the neotropical genus *Zygodontomys*. Evolution 44: 1568–1587.

Wallace, A. R.
1852. On the monkeys of the Amazon. Proc. Zool. Soc. London 20: 107–110.

Wilson, E. O.
1987. The arboreal ant fauna of Peruvian Amazon forests: a first assessment. Biotropica 19: 245–251.

Wilson, D. E., and D. M. Reeder
1993. Mammal species of the world, 2nd ed. Washington, D.C.: Smithson. Inst. Press.

Woodman, N., R. M. Timm, R. Arana C., V. Pacheco, C. A. Schmidt, E. D. Hooper, and C. Pacheco A.
1991. Annotated checklist of the mammals of Cuzco Amazónico, Peru. Occas. Pap. Mus. Nat. Hist. Univ. Kansas 145: 12 pp.

Woodman, N., N. A. Slade, R. M. Timm, and C. A. Schmidt
1995. Mammalian community structure in lowland tropical Perú, as determined by removal trapping. Zool. J. Linn. Soc. 113: 1–20.

Woods, C. A.
1993. Suborder Hystricognathi. *In* D. E. Wilson and D. M. Reeder (eds.), Mammal species of the world, 2nd ed.: 771–806. Washington, D.C.: Smithson. Inst. Press.

Worbes, M., H. Klinge, J. D. Revilla, and C. Martius
1992.
On the dynamics, floristic subdivision and geographical distribution of várzea forests in Central Amazonia. J. Veg. Sci. 3: 553–564.

Zanchin, N. I. T., A. Langguth, and M. S. Mattevi
1992. Karyotypes of Brazilian species of *Rhipidomys* (Rodentia, Cricetidae). J. Mammal. 73: 120–122.

APPENDIX A

Marsupial and Rodent Taxa (Murids and Echimyids Only) Collected at Each of the 16 Primary Localities Along the Rio Juruá, Grouped by the Four Sampling Regions (see fig. 1)

Taxa are recorded by habitat (seasonally flooded forest, or várzea; non-flooded upland forest, or terra firme; and miscellaneous, which includes all second growth, edge, garden, inundated grass and shrubland, and other local habitats as identified in the descriptions of each locality [see text]). For the four localities of the Mouth Region, the "miscellaneous" category includes only those trap stations on the edge of terra firme and flooded várzea.

Terra firme		Várzea		Miscellaneous	
Terrestrial	Canopy	Terrestrial	Canopy	Terrestrial	Canopy
HEADWATERS REGION					
Igarapé Porongaba, right bank (locality **1**)					
Marsupialia					
Didelphis marsupialis	*Caluromys lanatus*			*Didelphis marsupialis*	*Marmosops impavidus*
Marmosops impavidus	*Micoureus demerarae*			*Metachirus nudicaudatus*	*Marmosops noctivagus*
Marmosops noctivagus	*Micoureus regina*			*Philander mcilhennyi*	*Marmosops neblina*
Metachirus nudicaudatus				*Philander opossum*	*Micoureus demerarae*
Monodelphis emiliae					
Philander mcilhennyi					
Rodentia: Muridae					
Oryzomys perenensis	*Oecomys bicolor*			*Neacomys spinosus*	*Oecomys bicolor*
Oryzomys nitidus				*Oligoryzomys microtis*	
Oryzomys yunganus				*Oryzomys perenensis*	
Rodentia: Echimyidae					
Proechimys brevicauda	*Mesomys hispidus*			*Proechimys brevicauda*	*Dactylomys bolivianus*
Proechimys cuvieri				*Proechimys cuvieri*	*Isothrix bistriata*
Proechimys pattoni				*Proechimys pattoni*	*Mesomys hispidus*
Proechimys simonsi				*Proechimys simonsi*	
Opposite Igarapé Porongaba, left bank (locality **2**)					
		Marsupialia			
		Metachirus nudicaudatus	*Caluromys lanatus*	*Didelphis marsupialis*	
		Philander mcilhennyi	*Micoureus demerarae*	*Marmosops noctivagus*	
			Micoureus regina	*Philander mcilhennyi*	
		Rodentia: Muridae			
		Neacomys spinosus	*Oecomys bicolor*		

Terra firme		Várzea		Miscellaneous	
Terrestrial	Canopy	Terrestrial	Canopy	Terrestrial	Canopy
		Rodentia: Muridae (*continued*)			
		Neacomys musseri	*Rhipidomys gardneri*		
		Oecomys trinitatus			
		Oryzomys perenensis			
		Oryzomys yunganus			
		Rodentia: Echimyidae			
		Proechimys brevicauda	*Isothrix bistriata*	*Proechimys brevicauda*	*Isothrix bistriata*
		Proechimys cuvieri	*Mesomys hispidus*	*Proechimys simonsi*	
		Proechimys simonsi			
		Proechimys steerei			
		Nova Vida, right bank (locality **3**)			
		Marsupialia			
		Didelphis marsupialis	*Caluromys lanatus*		
		Marmosops neblina	*Micoureus demerarae*		
		Marmosops noctivagus	*Micoureus regina*		
		Metachirus nudicaudatus			
		Micoureus demerarae			
		Philander mcilhennyi			
		Philander opossum			
		Rodentia: Muridae			
		Oryzomys perenensis	*Oecomys bicolor*		
		Oryzomys yunganus			
		Rodentia: Echimyidae			
		Mesomys hispidus	*Isothrix bistriata*		
		Proechimys brevicauda	*Mesomys hispidus*		
		Proechimys cuvieri			
		Proechimys simonsi			
		Proechimys steerei			

Terra firme		Várzea		Miscellaneous	
Terrestrial	Canopy	Terrestrial	Canopy	Terrestrial	Canopy
Sobral, right bank (locality 4)					
Marsupialia					
Didelphis marsupialis	*Caluromys lanatus*	*Philander opossum*		*Metachirus nudicaudatus*	*Micoureus demerarae*
Metachirus nudicaudatus	*Micoureus regina*			*Philander mcilhennyi*	
Monodelphis emiliae				*Philander opossum*	
Philander mcilhennyi					
Rodentia: Muridae					
Neacomys spinosus				*Neacomys spinosus*	
Oecomys bicolor				*Oligoryzomys microtis*	
Oryzomys perenensis				*Oryzomys perenensis*	
Oryzomys yunganus					
Scolomys juruaense					
Rodentia: Echimyidae					
Proechimys brevicauda			*Mesomys hispidus*	*Proechimys brevicauda*	
Proechimys simonsi				*Proechimys cuvieri*	
Proechimys pattoni				*Proechimys simonsi*	
				Proechimys steerei	
UPPER CENTRAL REGION					
Sacado, right bank (locality 5)					
Marsupialia					
		Philander opossum	*Caluromys lanatus*		
			Micoureus regina		
Rodentia: Muridae					
		Neacomys minutus	*Oecomys bicolor*	*Oligoryzomys microtis*	
		Oecomys bicolor	*Oecomys roberti*	*Oryzomys perenensis*	
		Oecomys roberti			
		Oryzomys perenensis			

Terra firme		Várzea		Miscellaneous	
Terrestrial	Canopy	Terrestrial	Canopy	Terrestrial	Canopy
		Rodentia: Echimyidae			
		Proechimys steerei	*Isothrix bistriata*		
			Mesomys hispidus		
		Condor, left bank (locality **6**)			
		Marsupialia			
Didelphis marsupialis	*Micoureus demerarae*			*Marmosops noctivagus*	
Marmosops impavidus	*Micoureus regina*				
Marmosops noctivagus					
Metachirus nudicaudatus					
Monodelphis emiliae					
Philander mcilhennyi					
		Rodentia: Muridae			
Neacomys spinosus	*Rhipidomys leucodactylus*	*Oryzomys perenensis*		*Oecomys roberti*	
Nectomys apicalis		*Oryzomys yunganus*		*Oligoryzomys microtis*	
Oecomys species				*Oryzomys perenensis*	
Oryzomys macconnelli				*Oryzomys yunganus*	
Oryzomys perenensis					
Oryzomys yunganus					
Scolomys juruaense					
		Rodentia: Echimyidae			
Mesomys hispidus	*Mesomys hispidus*	*Proechimys steerei*		*Proechimys cuvieri*	
Proechimys cuvieri				*Proechimys simonsi*	
Proechimys simonsi				*Proechimys steerei*	
Proechimys echinothrix					
Proechimys kulinae					
Proechimys steerei					

Terra firme		Várzea		Miscellaneous	
Terrestrial	Canopy	Terrestrial	Canopy	Terrestrial	Canopy
Penedo, right bank (locality 7)					
Marsupialia					
Didelphis marsupialis	*Didelphis marsupialis*			*Didelphis marsupialis*	
Marmosops noctivagus	*Micoureus demerarae*			*Marmosops noctivagus*	
Metachirus nudicaudatus	*Micoureus regina*			*Marmosops neblina*	
Micoureus demerarae				*Micoureus demerarae*	
Monodelphis emiliae					
Philander mcilhennyi					
Rodentia: Muridae					
Neacomys spinosus	*Oecomys trinitatus*	*Oryzomys perenensis*		*Holochilus sciureus*	
Neacomys minutus	*Rhipidomys leucodactylus*	*Oryzomys yunganus*		*Nectomys apicalis*	
Oryzomys perenensis				*Oecomys roberti*	
Oryzomys yunganus				*Oecomys superans*	
Scolomys juruaense				*Oligoryzomys microtis*	
				Oryzomys perenensis	
				Oryzomys yunganus	
Rodentia: Echimyidae					
Proechimys cuvieri	*Mesomys hispidus*		*Isothrix bistriata*	*Proechimys cuvieri*	
Proechimys simonsi				*Proechimys simonsi*	
				Proechimys steerei	
Nova Empresa, left bank (locality 8)					
Marsupialia					
		Marmosops neblina	*Micoureus regina*		
		Philander opossum			
Rodentia: Muridae					
		Neacomys minutus	*Oecomys bicolor*		
		Oecomys roberti	*Oecomys roberti*		

Terra firme		Várzea		Miscellaneous	
Terrestrial	Canopy	Terrestrial	Canopy	Terrestrial	Canopy
		Rodentia: Muridae (*continued*)			
		Oryzomys perenensis			
		Oryzomys yunganus			
		Rodentia: Echimyidae			
		Proechimys steerei	*Isothrix bistriata*		
			Makalata macrura		
			Mesomys hispidus		
LOWER CENTRAL REGION					
Altamira, right bank (locality **9**; including Boa Esperança, locality **9a**)					
		Marsupialia			
Didelphis marsupialis	*Caluromys lanatus*	*Didelphis marsupialis*	*Marmosops neblina*	*Didelphis marsupialis*	
Philander mcilhennyi	*Micoureus demerarae*		*Micoureus demerarae*	*Marmosa murina*	
			Micoureus regina	*Marmosops impavidus*	
				Marmosops neblina	
				Metachirus nudicaudatus	
		Rodentia: Muridae			
Neacomys minutus		*Oryzomys perenensis*	*Oecomys roberti*	*Holochilus sciureus*	*Rhipidomys leucodactylus*
Oligoryzomys microtis		*Oryzomys yunganus*		*Nectomys apicalis*	
Oryzomys perenensis				*Oecomys superans*	
Oryzomys yunganus				*Oligoryzomys microtis*	
		Rodentia: Echimyidae			
Proechimys simonsi	*Mesomys hispidus*	*Proechimys steerei*		*Proechimys simonsi*	
Proechimys gardneri				*Proechimys gardneri*	
Proechimys steerei				*Proechimys steerei*	
Opposite Altamira, left bank (locality **10**)					
		Marsupialia			
		Marmosops neblina	*Caluromys lanatus*		
			Micoureus regina		

Terra firme		Várzea		Miscellaneous	
Terrestrial	Canopy	Terrestrial	Canopy	Terrestrial	Canopy
		Rodentia: Muridae			
		Oecomys roberti		*Nectomys apicalis*	
		Oryzomys perenensis		*Oligoryzomys microtis*	
		Oryzomys yunganus			
		Rodentia: Echimyidae			
		Makalata macrura	*Isothrix bistriata*		
		Proechimys steerei			
		Jainu, right bank (locality **11**)			
		Marsupialia			
		Didelphis marsupialis	*Micoureus regina*		
		Marmosops neblina			
		Rodentia: Muridae			
		Oecomys roberti	*Oecomys bicolor*	*Nectomys apicalis*	
		Oryzomys perenensis		*Oligoryzomys microtis*	
		Oryzomys yunganus			
		Rodentia: Echimyidae			
		Proechimys steerei	*Isothrix bistriata*		
			Mesomys hispidus		
		Barro Vermelho, left bank (locality **12**)			
		Marsupialia			
Marmosa murina	*Micoureus demerarae*		*Caluromys lanatus*		
Marmosops impavidus	*Micoureus regina*		*Didelphis marsupialis*		
Marmosops parvidens			*Micoureus demerarae*		
Metachirus nudicaudatus					
		Rodentia: Muridae			
Neacomys minutus	*Oecomys trinitatus*	*Neacomys minutus*	*Oecomys roberti*	*Oligoryzomys microtis*	
Nectomys apicalis		*Nectomys apicalis*	*Oecomys trinitatus*		
Oecomys trinitatus		*Oecomys bicolor*			

Terra firme		Várzea		Miscellaneous	
Terrestrial	Canopy	Terrestrial	Canopy	Terrestrial	Canopy
		Rodentia: Muridae (*continued*)			
Oryzomys macconnelli		*Oryzomys perenensis*			
Oryzomys perenensis		*Oryzomys yunganus*			
Scolomys juruaense					
		Rodentia: Echimyidae			
Proechimys cuvieri	*Mesomys hispidus*	*Proechimys steerei*		*Proechimys cuvieri*	
Proechimys simonsi					
Proechimys echinothrix					
Proechimys kulinae					
MOUTH REGION[a]					
Ilha Paxiuba, right bank (locality **13**)					
		Marsupialia			
				Metachirus nudicaudatus	*Caluromys lanatus*
					Micoureus demerarae
		Rodentia: Muridae			
				Oryzomys perenensis	*Oecomys bicolor*
		Rodentia: Echimyidae			
				Proechimys simonsi	*Mesomys hispidus*
				Proechimys steerei	
Colocação Vira-Volta, left bank (locality **14**)					
		Marsupialia			
Didelphis marsupialis	*Caluromys lanatus*			*Marmosops parvidens*	*Micoureus demerarae*
Marmosops impavidus	*Micoureus demerarae*				
Metachirus nudicaudatus					
		Rodentia: Muridae			
Neacomys minutus	*Oecomys bicolor*			*Oryzomys perenensis*	*Oecomys bicolor*
Oryzomys perenensis	*Oecomys trinitatus*				*Oecomys roberti*
Oryzomys yunganus	*Rhipidomys leucodactylus*				*Oecomys trinitatus*

Terra firme		Várzea		Miscellaneous	
Terrestrial	Canopy	Terrestrial	Canopy	Terrestrial	Canopy
		Rodentia: Echimyidae			
Proechimys simonsi	*Mesomys hispidus*			*Proechimys simonsi*	*Dactylomys dactylinus*
Proechimys echinothrix	*Mesomys occultus*			*Proechimys steerei*	*Isothrix bistriata*
					Mesomys hispidus
		Lago Vai-Quem-Quer, right bank (locality **15**)			
		Marsupialia			
Marmosops noctivagus	*Micoureus demerarae*			*Metachirus nudicaudatus*	
Marmosops parvidens					
Metachirus nudicaudatus					
		Rodentia: Muridae			
Oryzomys macconnelli	*Oecomys* species			*Oryzomys perenensis*	
Oryzomys perenensis	*Rhipidomys leucodactylus*				
		Rodentia: Echimyidae			
Proechimys simonsi	*Mesomys hispidus*			*Proechimys echinothrix*	*Isothrix bistriata*
Proechimys echinothrix				*Proechimys simonsi*	*Mesomys hispidus*
				Proechimys steerei	
		Ilhazinha, left bank (locality **16**)			
		Marsupialia			
				Didelphis marsupialis	*Didelphis marsupialis*
				Marmosops impavidus	*Marmosa murina*
				Marmosops parvidens	*Micoureus demerarae*
		Rodentia: Muridae			
				Neacomys minutus	
				Oryzomys perenensis	
		Rodentia: Echimyidae			
				Proechimys echinothrix	*Mesomys hispidus*
				Proechimys simonsi	
				Proechimys steerei	

[a] True várzea forest was not trapped at any sites in the Mouth Region because sampling was done during the wet season when that habitat was completely inundated.

APPENDIX B

Trap Results for the Standardized Lines at Each of the 16 Primary Localities

Numbers of each taxon collected are indicated, with the trap "nights" from table 1.

	Headwaters				Upper Central				Lower Central				Mouth			
Locality:	1	2	3	4	5	6	7	8	9/9a[a]	10	11	12	13	14	15	16
Habitat type:	TF	V	V	TF	V	TF	TF	V	TF/V	V	V	TF	Edge	TF	TF	Edge
No. trap nights:	2250	1920	2400	2370	2310	2550	2340	2026	2640	1620	1740	2970	1260	2310	2310	1260
Didelphimorphia																
Caluromys lanatus	1	1	4	4	1					1		1	1	3		
Didelphis marsupialis	2		2	2		1	6		7/1		1			1		6
Marmosa murina																1
Marmosops impavidus	1					1						1		1		1
Marmosops neblina			2					1		1	3					
Marmosops noctivagus	2		3			2	15									
Metachirus nudicaudatus	3	1	4	2		5	11					2	1	6	2	
Micoureus demerarae	1	1	4			4	7		4/2			3	2		1	11
Micoureus regina	3	4	2	1	8	1	7	12	/3	6	5	2		11		
Monodelphis emiliae	3			1		1	1									
Philander mcilhennyi	2	4	1	2		2	3		3/							
Philander opossum			1		1			1								
SUBTOTALS	18	11	23	12	10	17	50	14	14/6	8	9	9	4	22	3	19
Muridae																
Neacomys musseri		1														
Neacomys minutus					2		7	2	11/			2		8		1
Neacomys spinosus		1		2		1	22									
Nectomys apicalis						1										
Oecomys bicolor	3	6	2	1	14			9				1	1	2		
Oecomys roberti					14			14	/2	1	5	3		2		
Oecomys species						1										
Oecomys trinitatus		1					1					1		2		
Oligoryzomys microtis									1/							
Oryzomys macconnelli						19									3	
Oryzomys nitidus	3															
Oryzomys perenensis	26	46	27	12	50	9	23	31	7/9	7	11	20	1	28	4	19
Oryzomys yunganus	9	7	13	2		4	34	17	3/3	2	1	3		8		
Scolomys juruaense				5		5	5					7				
Rhipidomys gardneri		1														
Rhipidomys leucodactylus						3	1							2	1	
SUBTOTALS	41	63	42	22	80	43	93	73	22/14	10	17	37	2	52	8	20
Echimyidae																
Isothrix bistriata		1	1		4			2		11					1	
Makalata macrura								2		1						
Mesomys hispidus	3	4	7		8	7	8	9	7/		1	3	4	15	12	4
Mesomys occultus														3		
Proechimys brevicauda	21	7	15	11												
Proechimys cuvieri	7	1	4			5	10					1				
Proechimys echinothrix												6		13	28	1
Proechimys gardneri									17/							
Proechimys kulinae						23										
Proechimys pattoni	23			1												
Proechimys simonsi	44	8	13	31		49	52		32/			26	1	39	33	2
Proechimys steerei		1	8		69	1		129	1/10	21	13	3	46		1	15
SUBTOTALS	98	22	48	43	81	85	70	142	56/10	33	14	39	51	70	75	22
TOTALS	157	96	113	77	171	146	211	229	92/30	52	40	85	57	144	86	61

[a]Includes samples from both the terra firme site at Altamira (locality **9**) and the várzea site at Boa Esperança (locality **9a**).

APPENDIX C

Mammals Collected at Each Pair of Opposite-Bank Sites Along the Rio Juruá, 1991–1992

Primate data from Peres (1997). * designates sightings only, with no voucher specimens obtained. Localities identified by number as in figure 1.

		Locality						
		1/2	3/4	5/6	7/8	9/10	11/12	13/16[a]
				Didelphimorphia				
Caluromys	*lanatus*	X	X	X		X	X	X
Didelphis	*marsupialis*	X	X	X	X	X	X	X
Marmosa	*murina*					X	X	X
Marmosops	*impavidus*	X		X		X	X	X
	neblina	X	X		X	X	X	
	noctivagus	X	X	X	X			X
	parvidens						X	X
Metachirus	*nudicaudatus*	X	X	X	X	X	X	X
Micoureus	*demerarae*	X	X	X	X	X	X	X
	regina	X	X	X	X	X	X	
Monodelphis	*emiliae*	X	X	X	X			
Philander	*mcilhennyi*	X	X	X	X	X		
	opossum	X	X	X	X			
TOTALS		11	10	10	9	9	9	8
				Xenarthra				
Cabassous	*unicinctus*		X					
Choloepus	*hoffmanni*		X					
Cyclopes	*didactylus*	X	X		X			
Tamandua	*tetradactyla*				X			
TOTALS		1	3	0	2	0	0	0
				Primates				
Alouatta	*seniculus**	X	X	X	X	X	X	X
Aotus	*nigriceps*	X	X	X	X	X	X	X
Ateles	*paniscus**	X		X		X	X	X
Cacajao	*calvus**		X					X
Callicebus	*cupreus*	X	X	X	X	X	X	X
	torquatus				X	X	X	X
Callimico	*goeldii*	X						
Cebuella	*pygmaea*	X			X	X	X	
Cebus	*albifrons**	X	X	X	X	X	X	X
	*apella**	X	X	X	X	X	X	X
Lagothrix	*lagotricha*			X		X	X	X
Pithecia	*albicans**							X
	*irrorata**	X		X	X	X		
	*monachus**		X	X	X		X	X
Saguinus	*fuscicollis*	X	X	X	X		X	X
	imperator	X						
	mystax		X	X		X	X	X
Saimiri	*boliviensis*	X		X	X	X		X
	sciureus		X	X	X		X	X
TOTALS		12	10	13	12	12	13	15

APPENDIX C
(Continued)

		Locality						
		1/2	3/4	5/6	7/8	9/10	11/12	13/16[a]
				Carnivora				
Bassaricyon	*alleni*	X						
Puma	*concolor*				X			
Nasua	*nasua*	X			X			
Potos	*flavus*			X		X		
TOTALS		2	0	1	2	1	0	0
				Artiodactyla				
Mazama	*gouazoubira*	X				X		
TOTALS		1	0	0	0	1	0	0
				Perissodactyla				
Tapirus	*terrestris*					X		
TOTALS		0	0	0	0	1	0	0
				Rodentia: Sciuridae				
Microsciurus	*flaviventer*	X					X	
Sciurus	*igniventris*							X
	spadiceus	X		X				
	ignitus	X	X					
TOTALS		3	1	1	0	0	1	1
				Rodentia: Muridae				
Holochilus	*sciureus*				X	X		
Neacomys	*musseri*	X						
	minutus			X	X	X	X	X
	spinosus	X	X	X	X			
Nectomys	*apicalis*			X	X	X	X	
Oecomys	*bicolor*	X	X	X	X		X	X
	roberti			X	X	X	X	X
	species			X				X
	superans				X	X		
	trinitatus	X			X		X	X
Oligoryzomys	*microtis*	X	X	X	X	X	X	
Oryzomys	*macconnelli*			X			X	X
	perenensis	X	X	X	X	X	X	X
	nitidus	X						
	yunganus	X	X	X	X	X	X	X
Rhipidomys	*leucodactylus*			X	X	X		X
	gardneri	X						
Scolomys	*juruaense*		X	X	X		X	
TOTALS		9	6	12	13	9	10	9
				Rodentia: Erethizontidae				
Coendou	*bicolor*	X			X			
TOTALS		1	0	0	1	0	0	0
				Rodentia: Dasyproctidae				
Myoprocta	*pratti*	X				X		X
TOTALS		1	0	0	0	1	0	1

APPENDIX C
(Continued)

		Locality						
		1/2	3/4	5/6	7/8	9/10	11/12	13/16[a]
		Rodentia: Agoutidae						
Agouti	*paca*				X			
TOTALS		0	0	0	1	0	0	0
		Rodentia: Echimyidae						
Dactylomys	*bolivianus*	X						
	dactylinus							X
Isothrix	*bistriata*	X	X	X	X	X	X	X
Makalata	*macrura*				X	X		X
Mesomys	*hispidus*	X	X	X	X	X	X	X
	occultus							X
Proechimys	*brevicauda*	X	X					
	cuvieri	X	X	X	X		X	
	echinothrix						X	X
	gardneri					X		
	kulinae			X			X	
	pattoni	X	X					
	simonsi	X	X	X	X	X	X	X
	steerei	X	X	X	X	X	X	X
TOTALS		8	7	6	6	6	7	8
GRAND TOTALS		49	37	43	46	40	40	42
Marsupials, primates, murids, and echimyids		40	33	41	40	36	39	40
Marsupials, murids, and echimyids		28	23	28	28	24	26	25
Murids and echimyids		17	13	18	19	15	17	17

[a] The four localities in the Mouth Region are considered together, since the separate localities on each side were in close proximity (see table 1).